Synthesis of Substituted Quinolines & Furocoumarins: Some Naturally Occurring Coumestan Derivatives

A Dissertation Submitted to the

Indian Institute Technology Guwahati

As Partial Fulfillment for the Degree of

DOCTOR OF PHILOSOPHY

By

Simra Faraz

Roll No. 216122045

Department of Chemistry
Indian Institute of Technology Guwahati
Guwahati–781039, Assam
India

Dedicated to my beloved

Parents and Elder Brother

INDIAN INSTITUTE OF TECHNOLOGY GUWAHATI

Department of Chemistry

STATEMENT

I do hereby declare that the matter embodied in this thesis entitled **"*Synthesis of Substituted Quinolines & Furocoumarins: Some Naturally Occurring Coumestan Derivatives*"** is the result of investigations carried out by me at the Department of Chemistry, Indian Institute of Technology Guwahati, India, under the supervision of Professor Abu T. Khan.

In keeping with the general practice of reporting scientific observations, acknowledgement has been made wherever the work described is based on the investigators' findings.

IIT Guwahati
16th September 2024

Simra Faraz

Simra Faraz

Indian Institute of Technology Guwahati
Guwahati – 781039, India
Tel. No.: +91-361-2582305
Fax No.: +91-361-2582349
e-mail: atk@iitg.ac.in

Dr. Abu T. Khan
Professor of Chemistry

CERTIFICATE

This is to certify that Ms. Simra Faraz has worked in my research group since 15th October 2021 as a registered PhD student. Due to the COVID-19 pandemic, she was not permitted to join the institute, though she was admitted in July 2021.

I am forwarding her PhD thesis entitled "**Synthesis of Substituted Quinolines & Furocoumarins: Some Naturally Occurring Coumestan Derivatives**," which is being submitted for this institute's PhD (Science) Degree.

I certify that she has fulfilled all the requirements according to the rules and regulations of this Institute regarding the investigations embodied in her thesis, and this work has not been submitted elsewhere for a degree.

IIT Guwahati
18th September 2024

Prof. A. T. Khan
(Thesis Supervisor)

Acknowledgement

It is my great pleasure to take this opportunity to express my sincere thanks and gratitude to all the people who have helped and encouraged me during my Ph. D. studies. Nothing would have been possible in this thesis without every one of you. Thank you!

First and foremost, I would like to express my deepest gratitude and heartfelt thanks to my Thesis Supervisor, Professor Abu T. Khan, for his constant guidance and encouragement, thoughtful scientific ideas, enthusiasm, and inspiration to complete the thesis work. I am so grateful to him for giving me academic freedom to execute my research ideas embodied in the dissertation. His support and advice strengthen me professionally and personally, which I will treasure my whole life.

I also thank Professor Parameswar K. Iyer, the Chairman of the Doctoral Committee, for his endless support, guidance, and inspiration during my PhD tenure. I am highly indebted to all other Doctoral Committee Members, Professor Siddhartha Shankar Ghosh and Professor Lal Mohan Kundu, for their timely evaluation of my PhD work and for providing insightful suggestions, which helped greatly to improve my dissertation.

I also take this opportunity to express my deep gratitude to all the Department of Chemistry Faculty Members for their motivation and encouragement.

I express my sincere thanks to the staff members of the department as well as staff members of the central instrument facility centre for their help and cooperation. I especially thank Dr. Babulal Das for his help with the single crystal XRD collection and their interpretation, which are incorporated in the PhD thesis.

I am grateful to the Council of Scientific and Industrial Research, New Delhi, Government of India, for providing a research fellowship with Sanction No.: 09/0731(13234)/2022-EMR-I, dated 15.09.2021. I am extremely thankful to the Department of Chemistry, IIT Guwahati, for providing all the facilities that were made available for the thesis work. I duly acknowledged DST for providing the XRD facility and 500 MHz NMR under the DST-FIST programme to the Department of Chemistry and

MHRD for 400 MHz NMR. I must gratefully acknowledge DST, New Delhi, for sanctioning the research project to my Thesis Supervisor (Research Grant No.: CRG/2022/002751/OC) from where the procurement of chemicals, solvents, and other items was done for my day to day research work.

Besides, I have come across wonderful lab seniors like Dr. Saghir Ali, Dr. Santa Mondal, and Dr. Sabina Yashmin. I also feel lucky to have shared my moments with my labmates, Mr. Ujjwal Jyoti Goswami, Ms. Anjela Xalxo, Mr. Ahmad Ali, Mr. Mukesh Kumar, Mr. Anil Rangnath Pawar, Mr. Satyajit Singh, Mr. Eman Ali Sk., Ms. Nisha Rani, Ms. Halida Khatun, Mr. Afzal, and Mr. Devendra Kumar, Mr. Somesh Shekhar Chaugule, and Gyani Yumnum. You all have been fabulous and cooperative under all circumstances. I am also thankful to the postdoctoral fellows Dr. Md. Belal and Dr. Arnab Mandal. I also worked with some dedicated B. Tech., M. Sc., and summer trainees.

I would like to thank my friends, Dr. Huma Naz, Dr. Nehal Zehra, Dr. Kainat Aziz, Ms. Arpita Hajra, Ms. Deepanshi Nara, Ms. Afshaan Parveen, Ms. Maitery Yadav, Ms. Ritvika Kushwaha, Ms. Nandini Ray and Ms. Kirti Yadav for their support and joyful moments shared with them at IIT Guwahati.

Finally, my deepest gratitude goes to my family for their untiring love, affection, support, and blessings throughout my life. My deepest gratitude, especially to my mother, father, and brother, who stood up against all odds timings to support me. Their unwavering support, encouragement, and sacrifices have been the cornerstone of my journey throughout this thesis. Their endless love and belief in my abilities have been my guiding light, propelling me forward even in the most challenging times. Their enormous sacrifices, unconditional love, and support at every stage of life motivated me to overcome all the challenges, and I owe my entire life to them.

Furthermore, I would like to acknowledge the divine guidance and blessings of the Almighty, without whom none of this would have been possible. His grace has sustained me, granting me the strength and wisdom to overcome obstacles and persevere in my academic endeavours.

Lastly, I extend my heartfelt appreciation to all the individuals who have contributed to this thesis, directly or indirectly, through their support, advice, and valuable insights. Your contributions have enriched this work beyond measure.

Simra Faraz

SUMMARY OF THE THESIS

The thesis work, "***Synthesis of Substituted Quinolines & Furocoumarins: Synthesis of Some Naturally Occurring Coumestan Derivatives***," was carried out by me from 15th October 2021 to 31st May 2024.

The contents of the dissertation are divided into two parts, namely **Part A** and **Part B**, on two broad research topics. In **Part A**, the synthesis of various substituted quinolines will be highlighted. Similarly, the synthesis of furocoumarin derivatives, with special emphasis on synthesizing some naturally occurring coumestan derivatives, will be elaborated on in **Part B**.

Part A of the Thesis will be divided into two chapters, **Chapter I** and **Chapter II**. Likewise, **Part B** of the Thesis will also be organized into **Chapter I** and **Chapter II**.

Part A of **Chapter I** of the thesis will describe the motivation of the first research topic and the brief importance of quinoline and its derivatives, as well as the literature survey on the synthesis of substituted quinolines with special emphasis on synthesizing mono- and disubstituted quinoline derivatives. In addition, the outline of the first research will be elaborated on, along with the justifications for choosing the research problems.

Chapter II of **Part A** will present the results and discussions based on experimental works and findings towards synthesizing various substituted quinolines involving multi-component reactions (MCRs) strategies using arylamines as the key starting material. This chapter will be subdivided into four Sections: **Section A**, **Section B**, **Section C**, and **Section D**, respectively.

In **Section A**, metal-free, environmentally benign and regioselective synthesis of 4-aryl quinoline derivatives will be presented from aryl amine, aryl acetylene, and dimethyl sulfoxide in the presence of 20 mol% *p*-TSA•H_2O**,** as shown in Scheme 1**.**

The attractive feature of the protocol is that the solvent DMSO serves as a reactant-cum-solvent for providing the C2 carbon atom of the quinoline backbone.

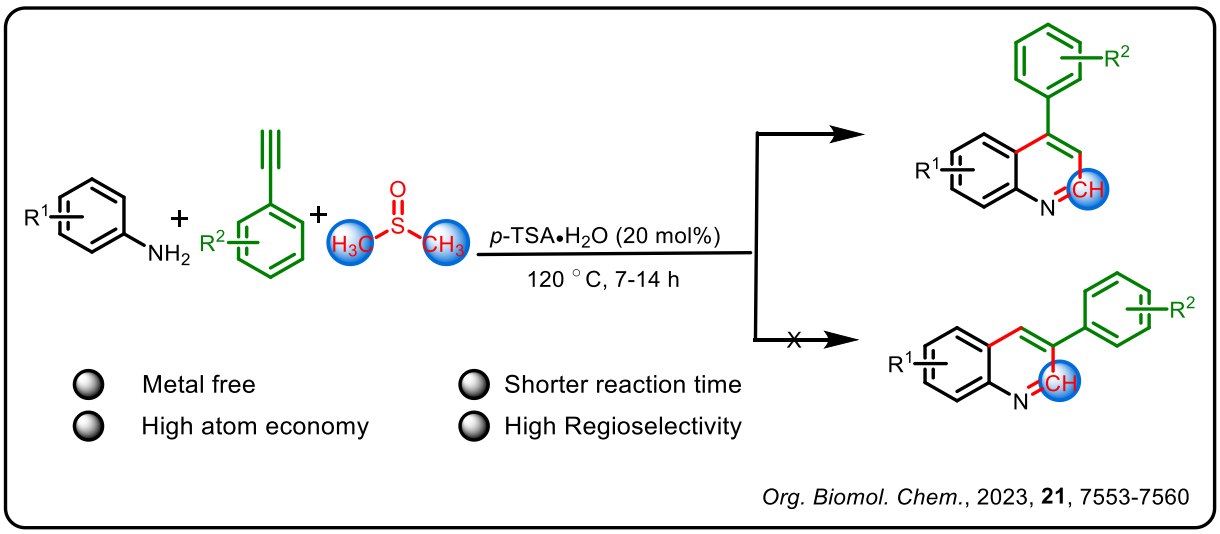

Scheme I. Synthesis of 4-arylquinoline derivatives from arylamine, arylacetylene, and DMSO.

In **Section B,** an efficient and expedient synthesis of 2,3-diarylquinoline derivatives will be presented from readily available aryl amines, aryl aldehydes, and styrene oxides using 20 mol% *p*-TSA•H_2O *via* one-pot three-component reaction, as depicted in **Scheme 2.**

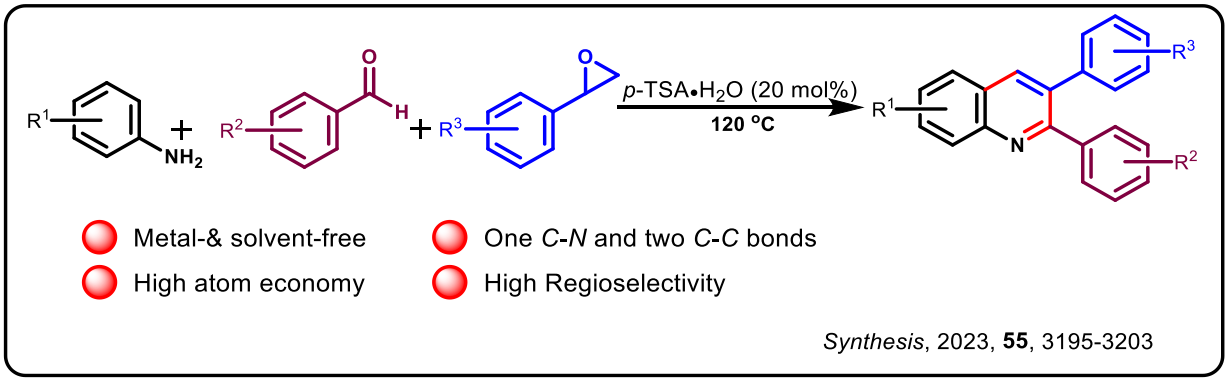

Scheme II. Synthesis of 2,3-diarylquinoline from aryl amines, aryl aldehydes, and styrene oxides.

In **Section D,** environmentally benign and greener synthesis of 2,4-diarylquinoline derivatives will be elaborated from commercially available starting material, aryl amines, benzaldehyde, and phenylacetylene in the presence of 30 mol% *p*-TSA•H_2O as shown in **Scheme 3.**

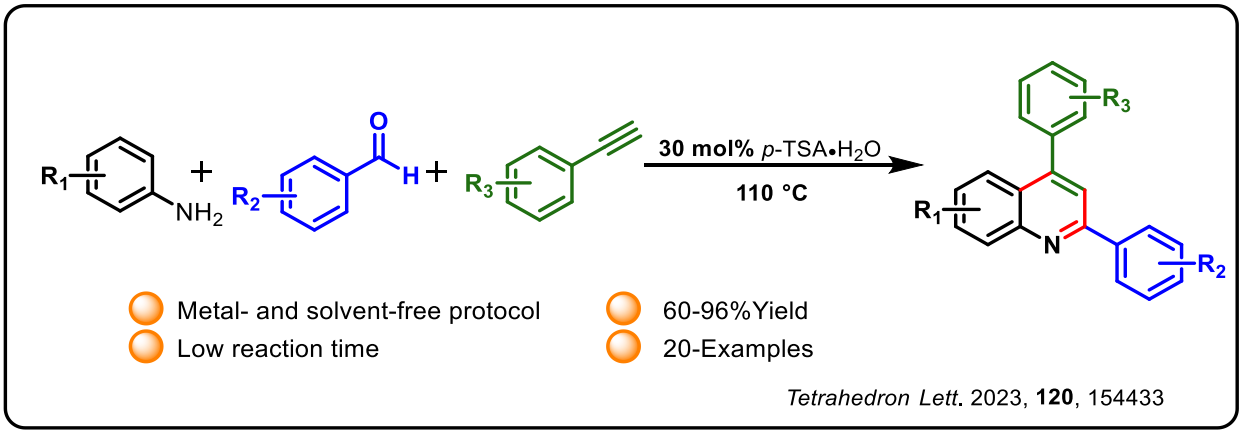

Scheme III. Synthesis of 2,4-diarylquinolines from aryl amines, benzaldehyde, and phenylacetylene.

In **Section D,** using a pseudo-three-component reaction, the environmentally acceptable and regioselective synthesis of 2-benzyl-3-aryl quinoline derivatives will be portrayed from aryl amine and styrene oxide in the presence of 20 mol% hydrated *p*-toluene sulfonic acid, as shown in **Scheme 4**. Not only that but also, the synthesis of 2,3-dialkyl quinoline derivatives by changing styrene oxide with alkyl epoxide under identical reaction conditions.

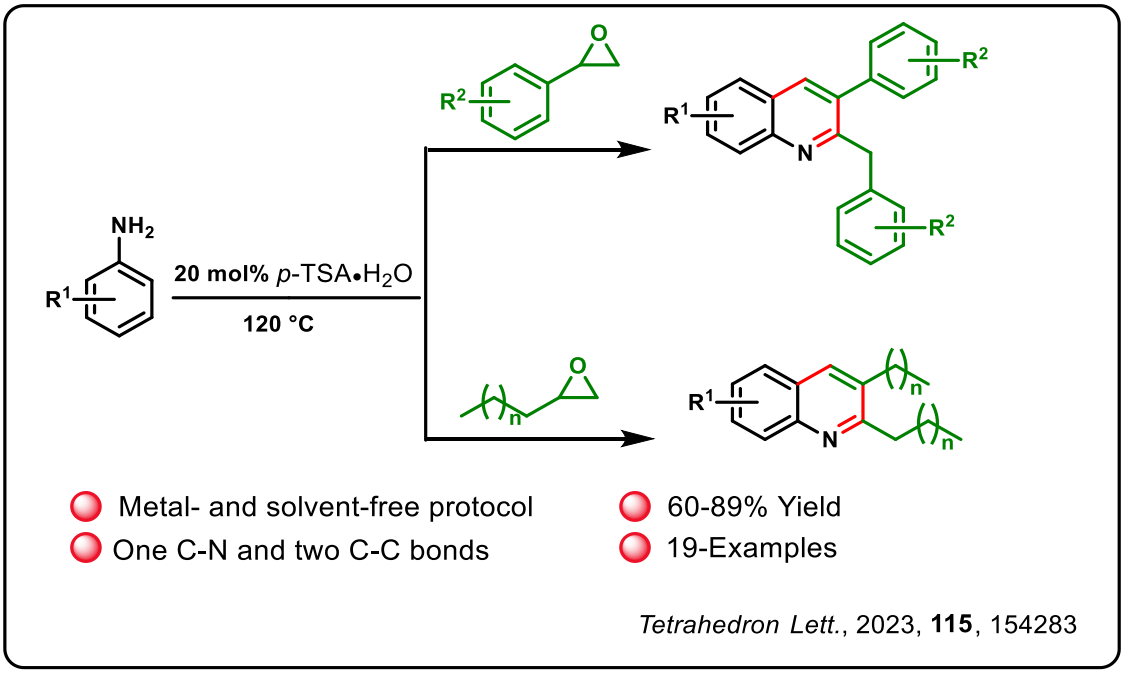

Scheme IV. Synthesis of 2-benzyl-3-arylquinoline from aryl amines and styrene oxides.

Finally, the conclusion will be drawn for **Part A** of the thesis on synthesizing of various substituted quinoline derivatives using hydrated *p*-toluene sulfonic acid is an effective acid catalyst.

Chapter I of **Part B** of the thesis will deal with the inspiration of the second research topic on the synthesis of furocoumarins and their importance, including biological importance, with special emphasis on some naturally occurring coumestan derivatives. In addition, a literature survey will be conducted on the synthesis of furocoumarin, which is mainly derived from 4-hydroxycoumarin and various substituted 4-hydroxycoumarin. Finally, the outline of the second research topic will be given based on the shortcomings of the earlier reported methods.

Chapter II of **Part B** of the thesis is subdivided into four sections: **Section A**, **Section B**, **Section C**, and **Section D,** respectively.

In **Section A** of **Part B,** the regioselective synthesis of 2-aryl-4*H*-furo[3,2-*c*] coumarin will be discussed from 4-hydroxycoumarins and styrene oxides in the presence of 20 mol% $FeCl_3$, as shown in **Scheme 5.**

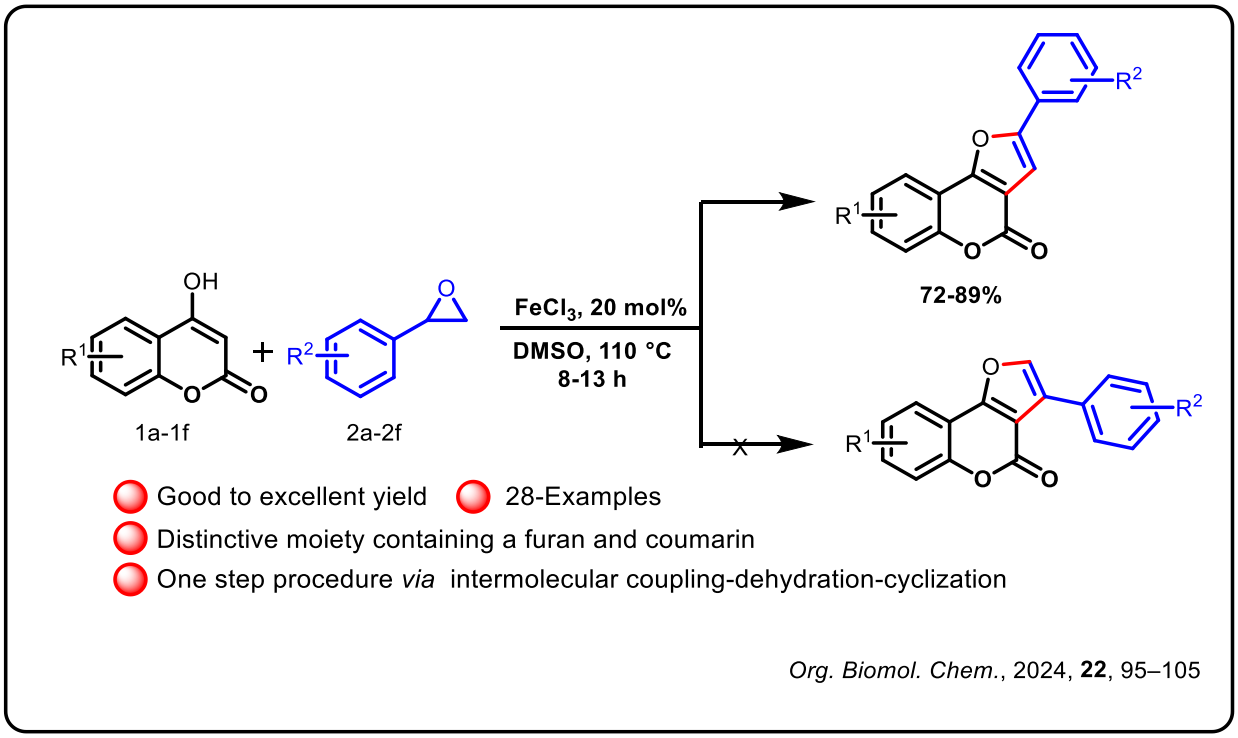

Scheme V. Synthesis of 2-aryl-4*H*-furo[3,2-*c*] coumarin from various 4-hydroxycoumarins and styrene oxides.

In **Section B,** the concise and elegant synthesis of 9-substituted tetrahydro coumestan derivatives will be presented from 4-hydroxycoumarin and cyclohexanones in the presence of $FeCl_3$ as a catalyst, as shown in **Scheme 6**. In addition, the synthesis of some naturally occurring coumestan derivatives will also be described from the corresponding tetrahydrocoumestan derivatives. The present synthetic approach provided an efficient and straightforward method for synthesising naturally occurring coumestan and its analogues.

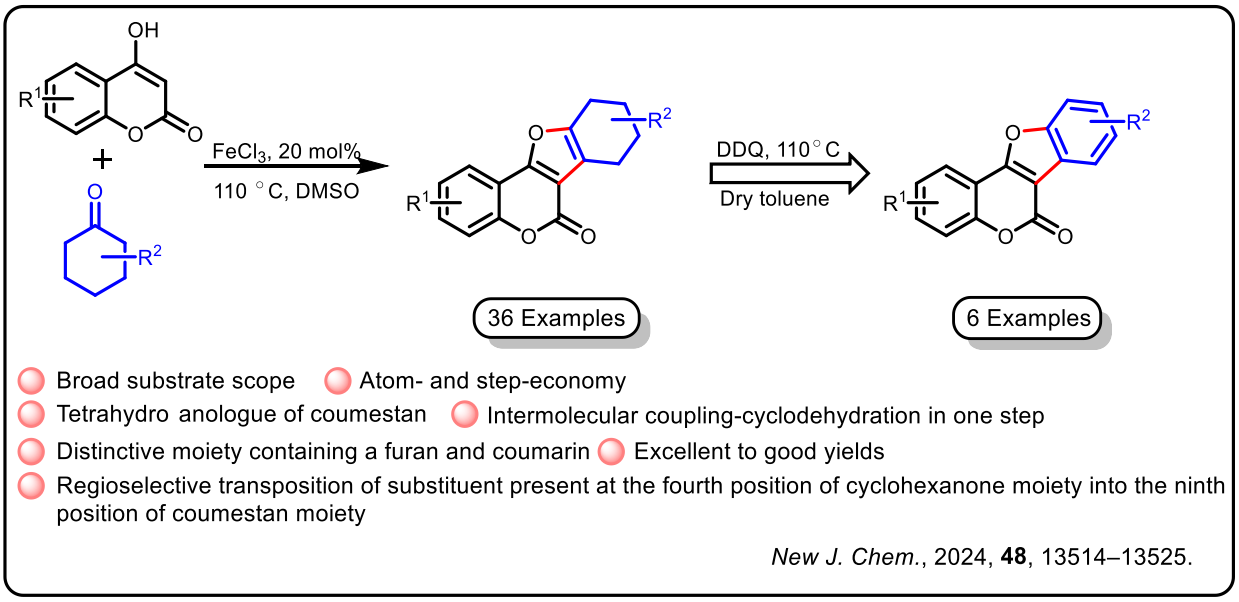

Scheme VI. Synthesis of tetrahydrocoumestan derivatives from various 4-hydroxycoumarins and cyclohexanones.

Section C of **Part B** will describe the synthesis of dinaphthofuran from β-tetralone and furocoumarin derivatives from 4-hydroxycoumarin in the presence of DMSO involving ferric(III) chloride catalyst through intermolecular cross-coupling and cyclization. In some cases, a dehydrogenated product was also obtained. In addition, highly functionalized furocoumarin derivatives will be synthesized from 4-hydroxycoumarins in a single step using a 20mol% ferric chloride catalyst in a dimethyl sulfoxide solvent. Notably, functionalized furocoumarins are formed through the dicoumarol intermediate by the insertion of methylene group at the 3-position of 4-hydroxycoumarin from DMSO. The intermediate dicoumarol undergoes concomitant ring-opening, cyclization, and dehydrogenation, providing furocoumarin derivatives in good yields. The reaction condition is mild and easily handled without the involvement of any oxidants, additives, and inert atmosphere. Later, the OH group in the furocoumarin derivative was further explored to synthesise the ether derivatives, which can be converted to new chemical entities. The salient feature of this protocol is that it has a wide substrate scope, good to excellent yield, polyfunctional moiety, and products have more than one pharmaceutically important motif.

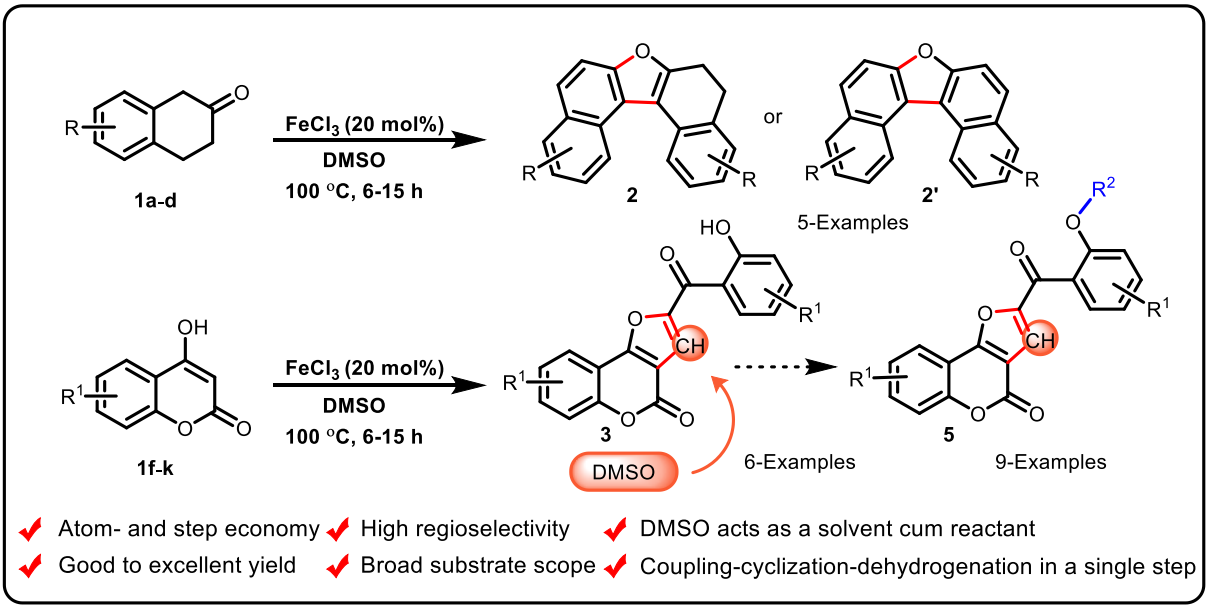

Scheme VII. Synthesis of dinaphthofurans and polyfunctional furocoumarins derivatives.

Section D illustrates the synthesis of 3-aryl-2*H*,5*H*-pyrano[3,2-*c*]chromen-5-ones (**3**) reported from 4-hydroxycoumarin, styrene oxide, and DMSO in the presence of *p*-TSA•H_2O at 110 °C using a three-component reaction in which the CH_2 of the pyrano moiety is inserted from DMSO. On the contrary, the reaction of 4-hydroxycoumarin and styrene oxide in the presence of DMSO under identical reaction conditions provided 2-aryl-4*H*-furo[3,2-*c*]chromen-4-one depending upon the substituent present either on the 4-hydroxycoumarins or styrene oxides. By changing the solvent DMSO from CH_3CN, the novel monomeric product 4-hydroxy-3-styryl-2*H*-chromen-2-one was obtained instead of the expected furocoumarins exclusively from 4-hydroxycoumarins and styrene oxides. Moreover, the novel monomeric product (*E*)-6-chloro-3-(4-fluorostyryl)-4-hydroxy-2*H*-chromen-2-one underwent unexpected cyclization to provide a more interesting tricyclic product.

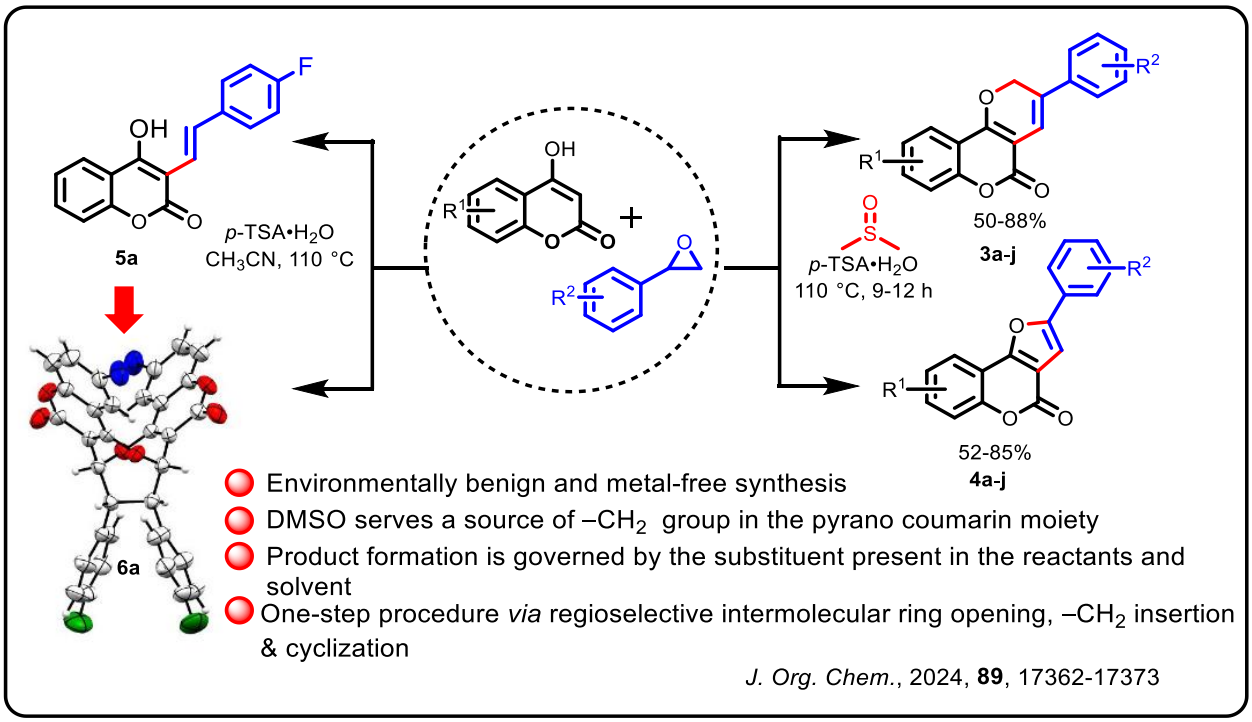

Scheme VIII. Synthesis of solvent and substituents dependent formation of furocoumarins and pyranocoumarins.

Finally, the conclusion of **Part B** of the thesis will be made on synthesizing furocoumarin derivatives.

CONTENTS OF THE THESIS

GENERAL REMARKS

The present investigations were conducted at the Department of Chemistry, India Institute of Technology Guwahati, Guwahati – 781039, Assam, India, from 15th October 2021 to 31st May 2024.

The analytical samples were routinely dried *in vacuo* at 50 °C. The TLC experiment used silica gel G (SRL) or GF 254 (SRL) as adsorbent. Column chromatography was done with silica gel (60-120 mesh, Merck or SRL) to purify the reaction mixture. After purification, the solvent was usually removed in a rotary evaporator using the Buchi R-114 V instrument. Melting points were determined on a Buchi-540 melting point apparatus. IR spectra were recorded on Perkin Elmer 281 IR spectrophotometer. ^{1}H spectra were recorded on 400 MHz, 500 MHz and 600 MHz Brukers spectrometers. Similarly, ^{13}C spectra were recorded on 100 MHz, 125 MHz, and 150 MHz NMR Bruker spectrometers. TMS as an internal reference; chemical shifts (δ scale) were reported in parts per million (ppm). ^{1}H NMR spectra are reported in order: multiplicity, coupling constant (*J* value) in Hertz (Hz), and no of protons; signals were characterized as s (singlet), d (doublet), t (triplet), m (multiplet), brs (broad singlet), dd (doublet of doublet), dt (doublet of triplet), dq (doublet of the quartet) and ddt (doublet of doublet and further split to triplet). HRMS spectra were recorded using ESI (TOF) mode, and crystal data was collected with Bruker Smart Apex-II CCD diffractometer using graphite monochromatic MoKα radiation (λ = 0.71073 Å) at 298 K.

ABBREVIATIONS

Ac	Acetyl
acac	Acetylacetonate
p-TSA•H_2O	*para*-toluene sulfonic acid monohydrate
Ac_2O	Acetic anhydride
AcOH	Acetic acid
Bn	Benzyl
Bu	Butyl
BuOH	Butanol
Bz	Benzoyl
CCDC	Cambridge Crystallographic Data Centre
DCE	1,2-Dichloroethane
DCM	Dichloromethane
DMF	*N*, *N*-Dimethylformamide
DMSO	Dimethyl Sulfoxide
ESI (TOF)	Electrospray Ionisation (Time-of-flight)
Et	Ethyl
EtOH	Ethanol
EWG	Electron-withdrawing Group
EDG	Electron-donating Group
mg	Milligram

h	Hour
HRMS	High-Resolution Mass Spectrometer
IR	Infrared spectroscopy
MCR	Multicomponent reaction
MeOH	Methanol
mp	Melting point
MS	Molecular Sieves
NMR	Nuclear Magnetic Resonance
ORTEP	Oak Ridge Thermal Ellipsoid Program
PPA	Polyphosphoric acid
Ph	Phenyl
ppm	Parts per million
rt	Room temperature
TEMPO	2,2,6,6-Tetramethyl pyridine-*N*-Oxide
TFA	Trifluoroacetic acid
THF	Tetrahydrofuran
TLC	Thin-Layer chromatography
TMS	Tetramethylsilane
XRD	X-ray Diffraction

Part A

Significance of Substituted Quinolines

Introduction to quinolines

Quinoline is an important nitrogen-containing heterocyclic compound present in alkaloids.[1] It was first extracted in 1834 from coal tar by German Chemist Friedlieb Ferdinand Runge. Later on, in 1842, it was isolated from the distillation of decomposed quinine and cinchonine antedates by French Chemist Charles Gerhardt. The chemical properties of quinoline are influenced by its aromatic nature and the presence of a nitrogen atom in the pyridine ring. It is a colourless to yellow liquid with a distinct, somewhat medicinal odour. It is a common scaffold in a wide range of biologically active natural products and has extensive applications in biology and pharmacology, as shown in Figure **1**.[2.] The natural and non-natural products with quinoline backbone displayed various biological activities, such as antimalarial,[3a] antiasthmatic,[3b] antituberculosis,[3c] antihypertensive,[3d] anticancer,[3e] and anti-HIV.[3f] Well-known antimalarial drugs such as chloroquine, hydroxychloroquine,[3a] and mefloquine[3b] are quinoline derivatives. Recently, researchers have found that quinoline analogues have potent activity against SARS-CoV-2 disease[4] caused by a novel coronavirus. Some of the related natural products have been marketed as potent drugs. In addition, analogues of quinoline have also been exploited in material science.[5a,b] Due to its potential applications in various scientific areas, organic chemists have put an enormous effort into developing various synthetic methodologies for the synthesis of quinoline derivatives. Besides biological and pharmacological properties, quinoline derivatives have also shown potential applications in agrochemicals.[6]

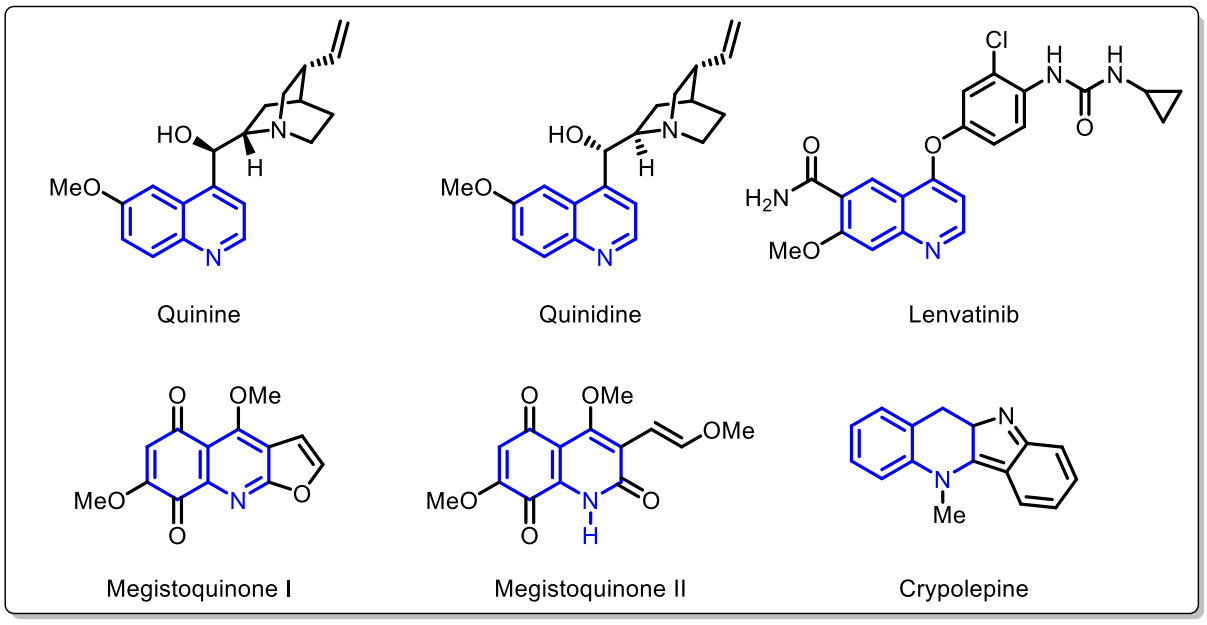

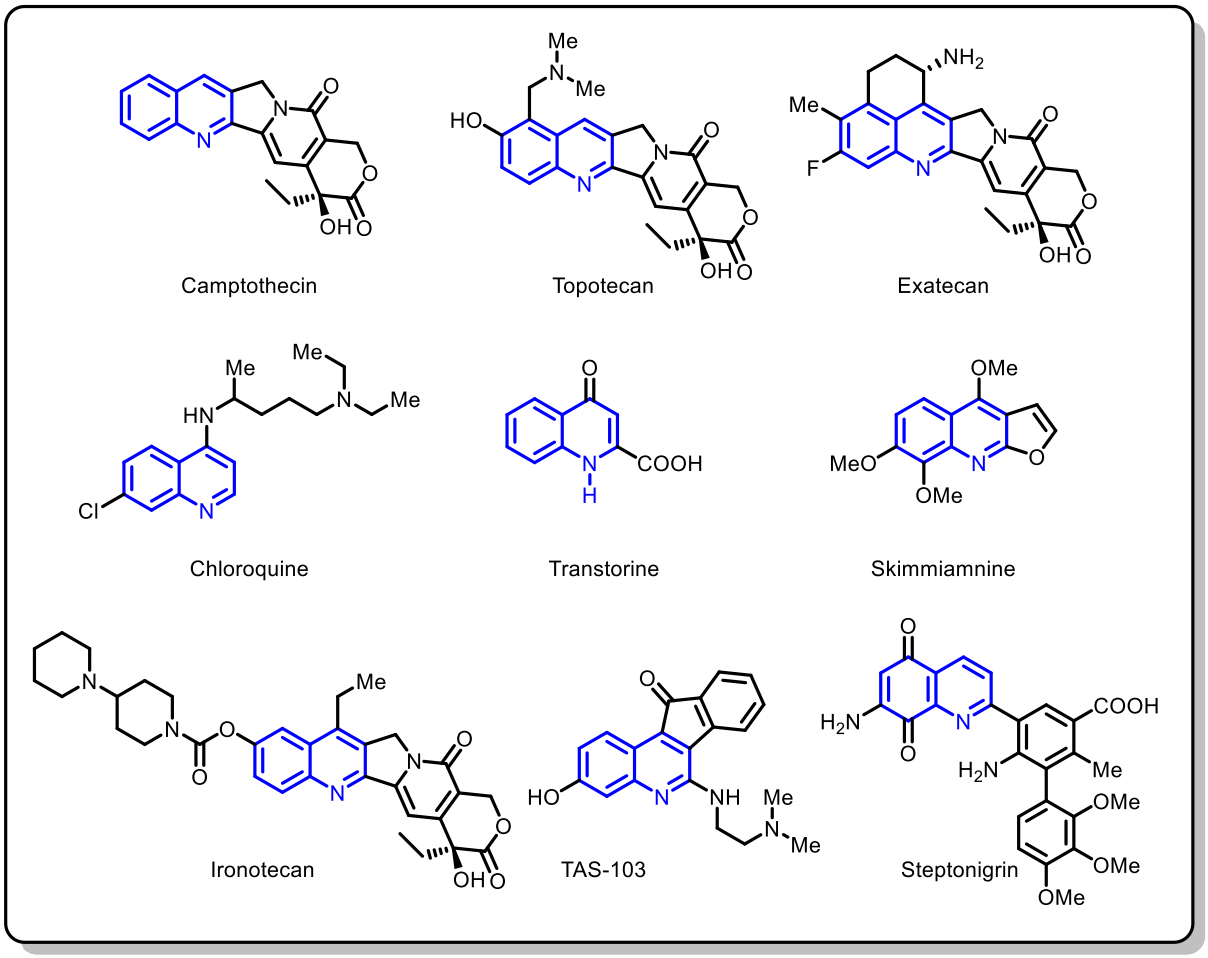

Figure 1. Biologically active natural and non-natural quinoline scaffolds.

Traditional methods for the synthesis of substituted quinolines and their analogues from aniline

Over the years, several traditional routes for the synthesis of quinoline and its derivatives have been developed. These are well-known in the literature, as shown in Figure **2**. These methods are the popular name reactions, such as Skraup,[7a] Doebner,[7b] Combes,[7c] Doebner-von-Miller,[7d] Povarov synthesis[7e] and Conard-Limpach.[7f] It is noteworthy to mention that aniline is the common starting material in all these methods.

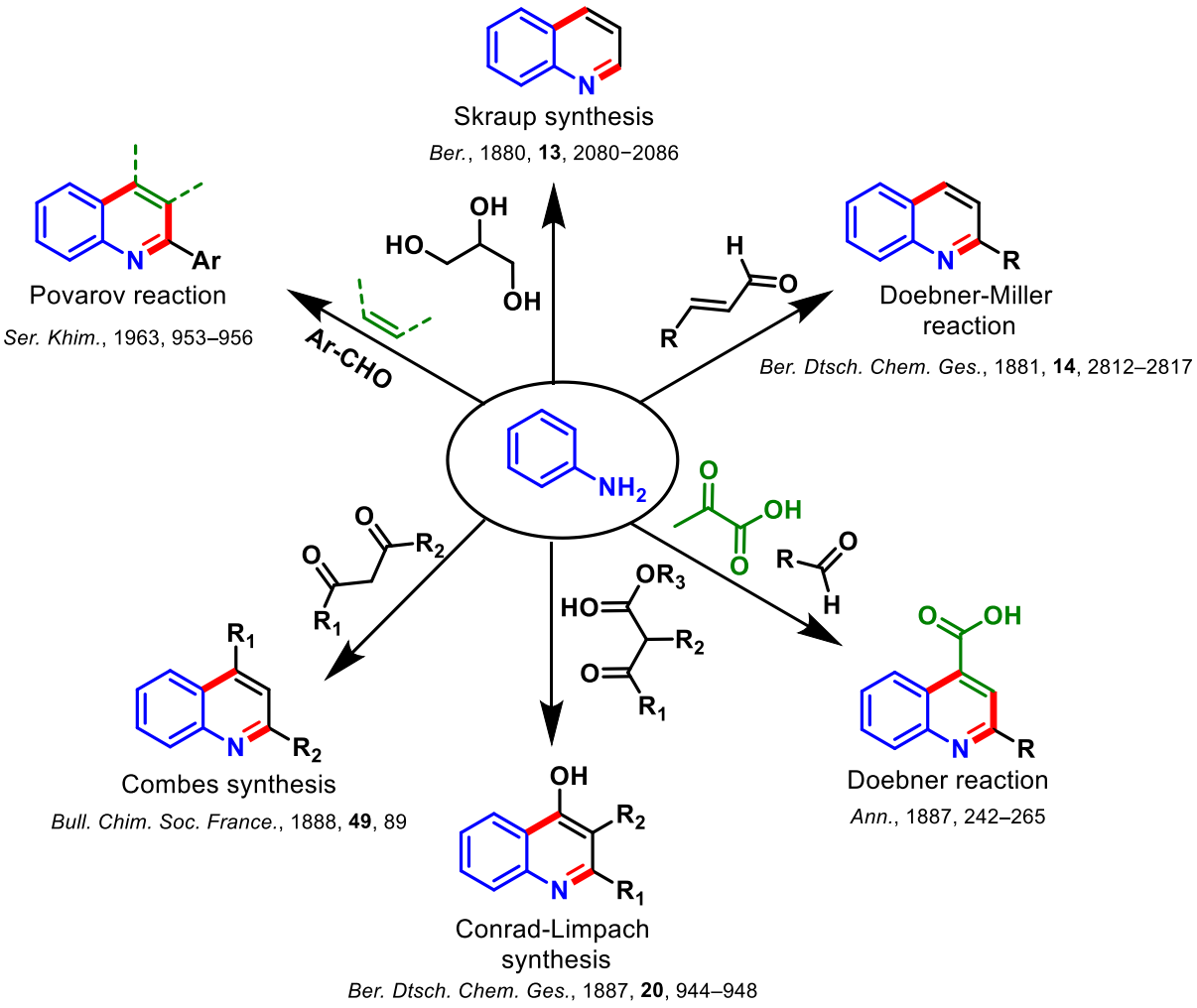

Figure 2. Traditional methods for synthesis of quinoline and its analogues from aniline.

Besides these methods in which aniline is a common starting material, some other reported methods show the synthesis of substituted quinolines, such as the Pfitzinger reaction, Friedländer synthesis, and Knorr synthesis, which have been shown below.

Pfitzinger reaction

In 1886, Pfitzinger et *al.*[8] successfully synthesized quinoline-4-carboxylic acids through base-catalyzed reactions involving isatin and carbonyl compounds. This reaction entails the base hydrolysis of isatin, yielding a keto-acid, which then undergoes further reaction with a carbonyl compound to yield the final product, as depicted in Scheme 1.

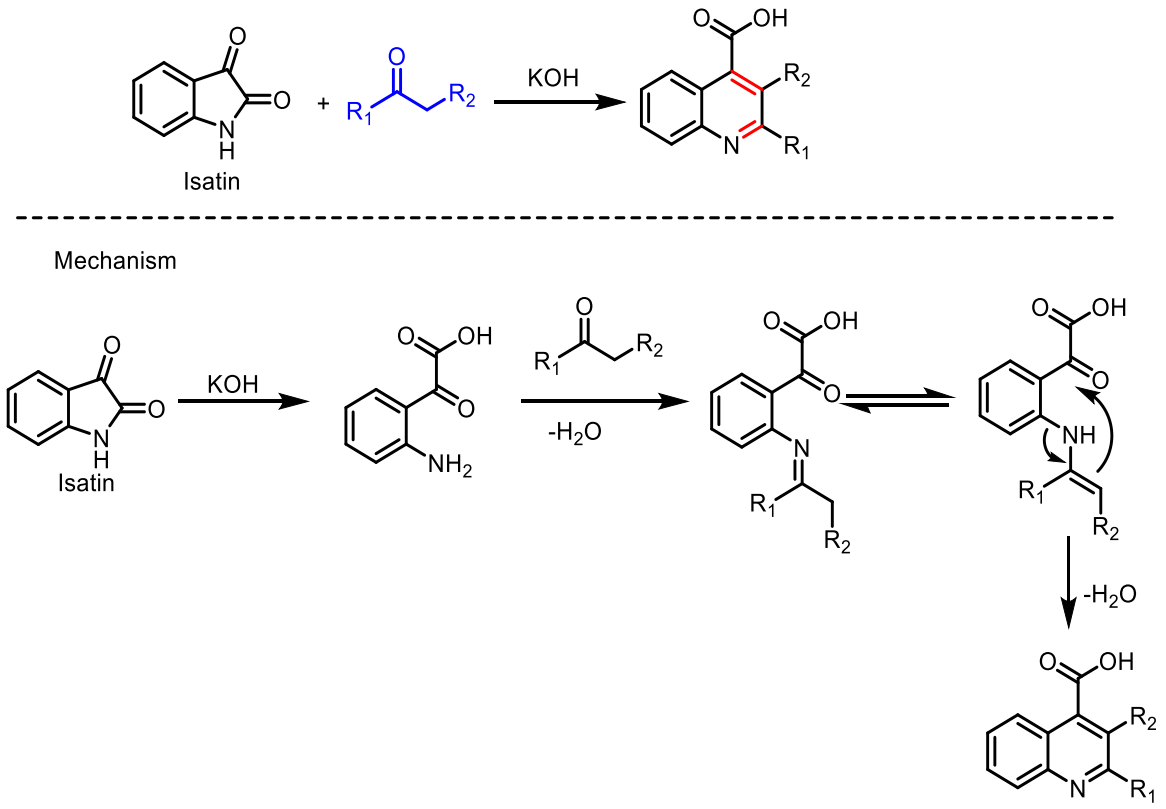

Scheme 1

Friedländer synthesis

In 1882, Friedlander and co-workers[9] demonstrated a straightforward and efficient approach for synthesizing 2,3-disubstituted quinoline derivatives via acid-catalyzed condensation reactions involving 2-amino benzaldehyde and a ketone, illustrated in Scheme 2.

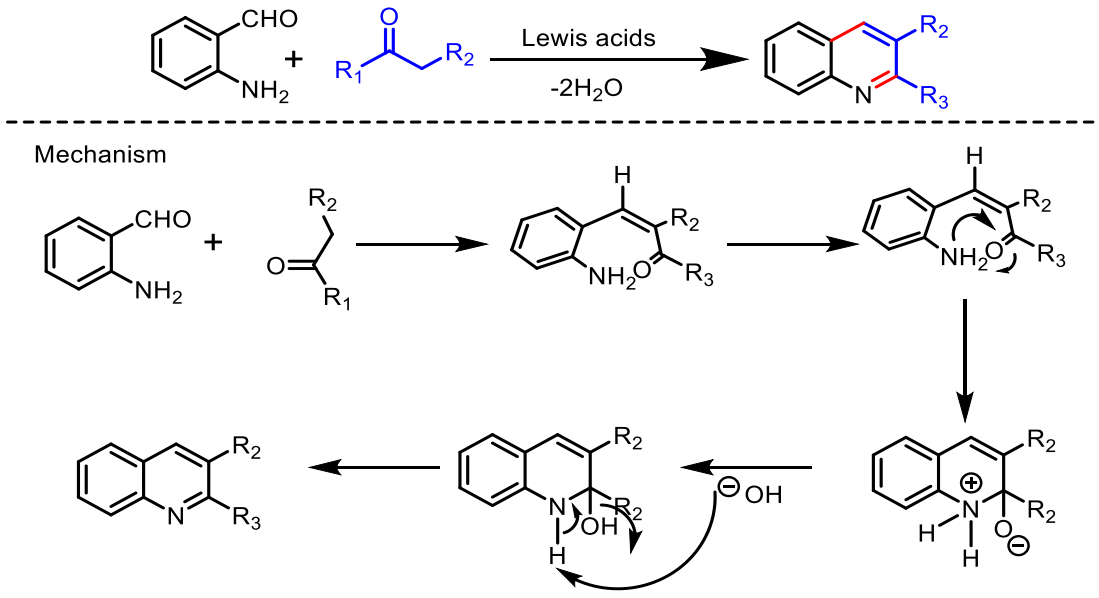

Scheme 2

Knorr Quinoline Synthesis

In 1886, Ludwig-Knorr[10] described an effective method for synthesizing 2-hydroxyquinoline through the intramolecular cyclization reaction of β-ketoanilide in the presence of concentrated sulfuric acid, as depicted in Scheme 3.

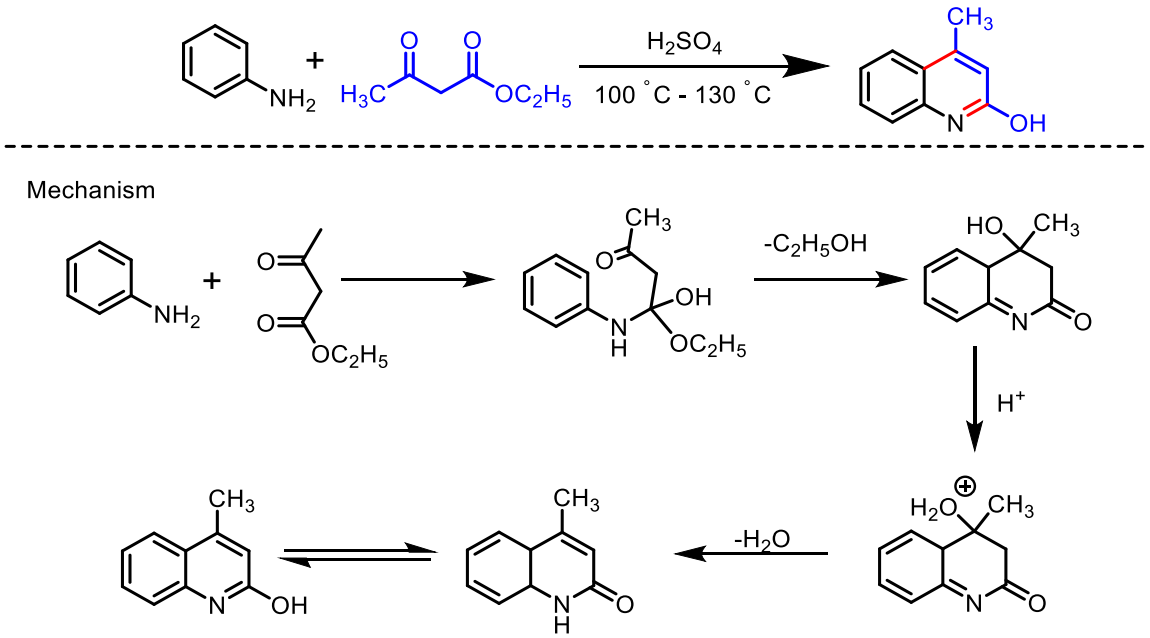

Scheme 3

Though this method has been useful for accessing 2,3-dialkylquinoline scaffolds, it suffers from some drawbacks, such as the requirement of harsh reaction conditions, cumbersome work-up procedure, and most importantly, less substrate scope and low yield.

Reported methods for synthesis of 4-arylquinoline derivatives

Over the past few years, significant efforts have been dedicated to developing various methods for synthesizing scaffolds of 4-arylquinoline. For the first time, Zhang *et a*l. demonstrated Cu-catalyzed quinazolines synthesis from amidines and DMSO through direct oxidative amination of N–H bonds and methyl C(sp^3)–H bonds.[11] Recently, Cheng and co-workers have shown the Pd-catalyzed synthesis of 4-aryl quinolines from *ortho*-vinyl anilines with DMSO in inert atmospheric conditions at 140 °C as depicted in Scheme 4.[11b]

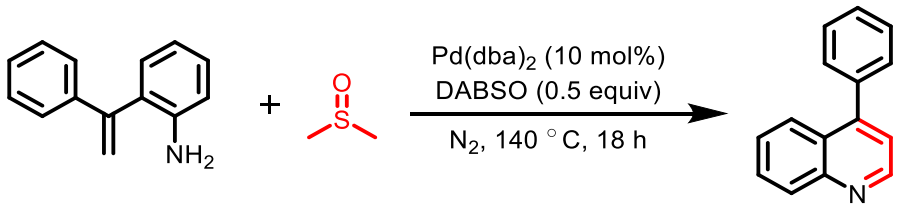

Scheme 4

Similarly, Singh *et al*. also reported the synthesis of 4-aryl quinoline from arylamine and acetophenone using DMSO as a source of CH_2 under inert atmospheric reaction conditions as shown in Scheme 5.[11c]

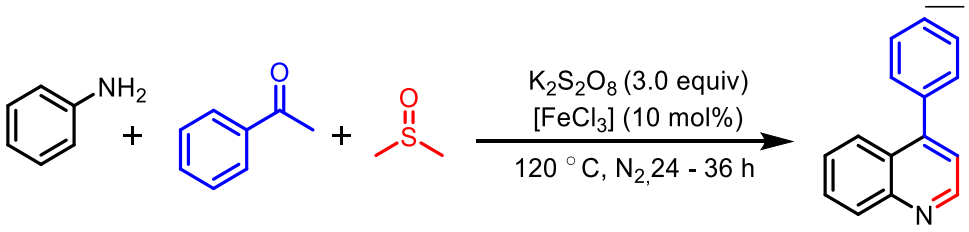

Scheme 5

These existing methods exhibit limited substrate compatibility and require stringent oxidative conditions, complicating selectivity, high temperatures (140 °C), and an inert atmosphere, adding operational complexity and costs due to the expensive metal catalyst.

Reported protocols for the synthesis of 2,3-diarylquinoline

A literature survey revealed few approaches to synthesizing 2,3-diarylquinoline derivatives. Vanella *et al*.[12a] proposed a two-step strategy for preparing analogues of 2,3-diarylquinoline (Scheme 6). In the first step, o-nitrobenzyl chloride reacts with α-diketone in the presence of tetrakis(dimethylamino)ethylene (TDAE) to yield α-hydroxyketone. The second step involves reducing the nitro group followed by cyclization to produce the desired scaffolds of 2,3-diphenylquinoline.

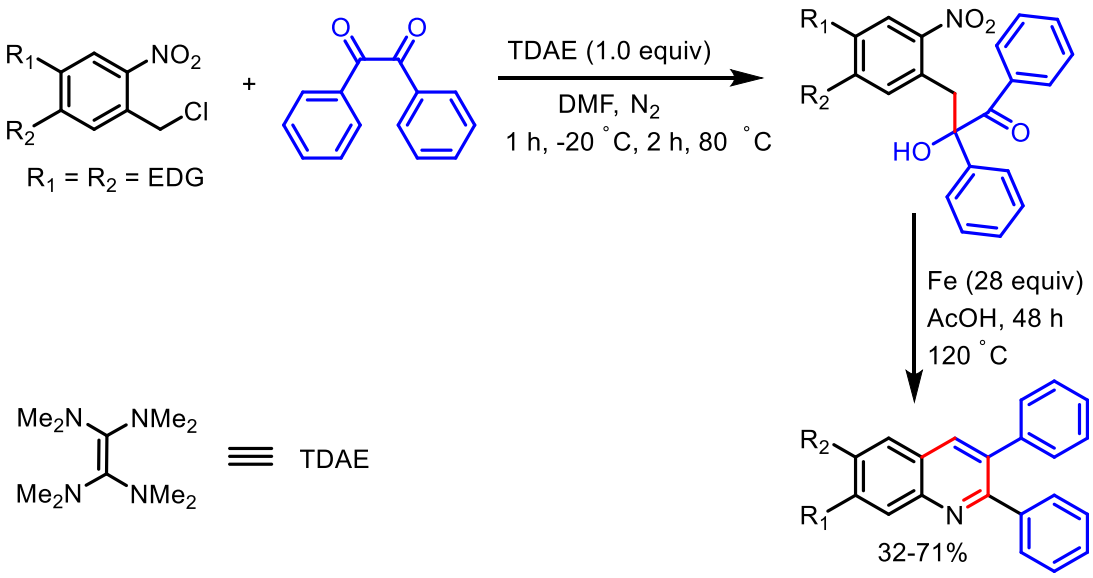

Scheme 6

Later on, Verma and co-workers[12b] showed a base-promoted, protection-free, and regioselective method for the synthesis of 2,3-diarylquinoline derivatives (Scheme 7). This reaction proceeds *via* [4+2] cycloaddition of *in-situ* generated azadiene from *o*-amino benzyl alcohol with internal alkynes.

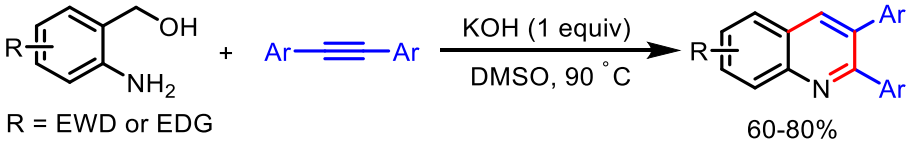

Scheme 7

In recent years, the synthesis of 2,3-diarylquinoline derivatives was reported from aniline and two different amino acids by Wu and co-workers [13] in the presence of catalytic amounts of iodine and hydrogen iodide, as demonstrated in Scheme 8.

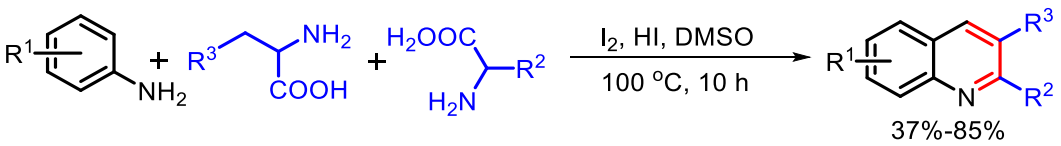

Scheme 8

Another important method for the synthesis of 2,3-diarylquinoline developed by Reddy and co-workers[14] which involves the reaction of 2-azido phenyl propargylic alcohol with a wide range of boronic acids in the presence of 10 mol% $Ni(acac)_2$ as a catalyst (Scheme 9).

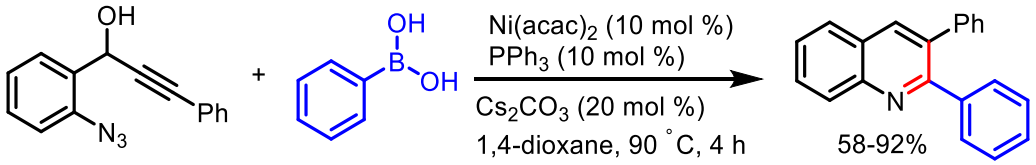

Scheme 9

Our research group[15] recently synthesized 2,3-diarylquinoline using 10 mol% $Cu(OTf)_2$ from aryl amines, styrene oxide, and benzaldehyde in DMSO as a solvent, as depicted in Scheme 10.

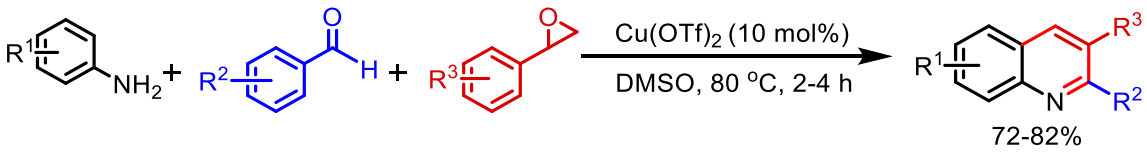

Scheme 10

Though this approach is good for providing 2,3-diarylquinoline derivatives, it has some drawbacks including the use of costly catalysts and ligands, the necessity for preparing 2-alkenylanilines, extended reaction times, the requirement for an argon inert atmosphere, and low yield.

Reported protocols for the synthesis of 2,4-diarylquinoline derivatives

Over the years, the synthesis of 2,4-diarylquinoline was explored by the A3-coupling reaction[16] of alkynes, aldehydes, and amines in the presence of mostly catalysts such as $Zn(OTf)_2$,[17] $FeCl_3$,[18] AuCl–AgOTf,[19] and $K_5WCo_{12}O_{40}$,[20] In 2015, Huang *et al*. reported a metal-free synthesis of 2,4-diarylquinoline from enamide and imine using an I_2 catalyst (Scheme 11).[21]

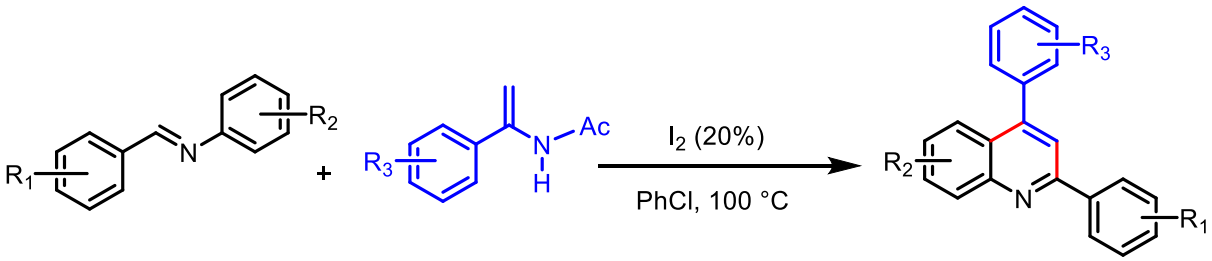

Scheme 11

Another important synthesis was demonstrated by Wakatsuki *et al*. used ruthenium as a catalyst for the synthesis of 2,4-diarylquinoline as shown in Scheme 12.[22]

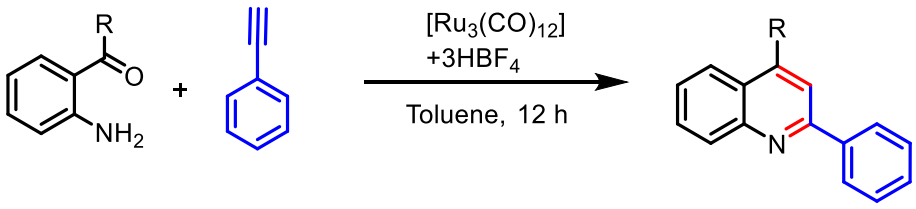

Scheme 12

Most of these methods involve metal catalysts, which undoubtedly bring high costs, heavy metal residues, and various side reactions. However, these methods have significant drawbacks. The use of metal catalysts introduces high costs and can lead to heavy metal residues in the final product, raising environmental and health concerns. Additionally, these reactions often result in side reactions, reducing the overall yield and selectivity. Therefore, the reliance on metal catalysts makes these methods less desirable for sustainable and efficient synthesis.

Reported protocols for the synthesis of 2-benzyl-3-phenylquinoline derivatives

A thorough examination of the literature revealed few methods for synthesizing 2-benzyl-3-phenylquin scaffolds. First, Beller and co-workers[23] introduced a protocol for synthesizing 2-benzyl-3-phenylquinolines from reactions of substituted anilines with aromatic olefins in the presence of cationic rhodium catalysts, such as $[Rh(cod)_2]BF_4$, and PPh_3 (Scheme 13). This method involves the amination of aromatic olefin followed by the formation of an enamine intermediate, which tautomerizes to the corresponding imine. At last, enamine reacts with imine followed by cyclization providing product 2-benzyl-3-phenylquinoline derivatives.

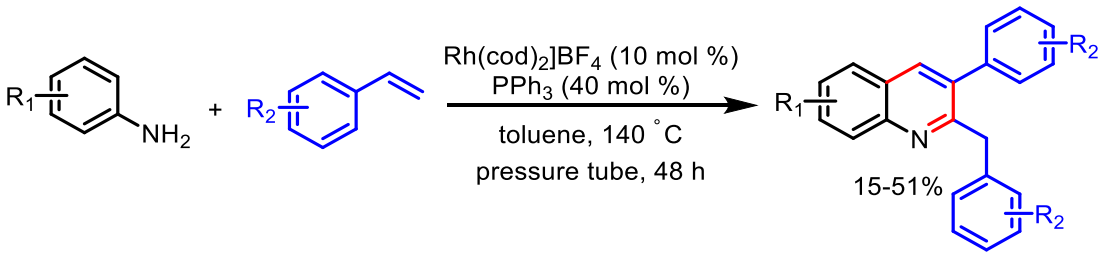

Scheme 13

Zhang *et al.*[24] showed a solvent-free and sulfamic acid-catalyzed reaction of substituted anilines with phenylacetaldehyde derivatives to synthesize 2-benzyl-3-phenylquinolines (Scheme 14). Other methods are also available for synthesizing 2-benzyl-3-phenylquinoline derivatives from substituted aryl amines and phenylacetaldehyde.[25a,b,c]

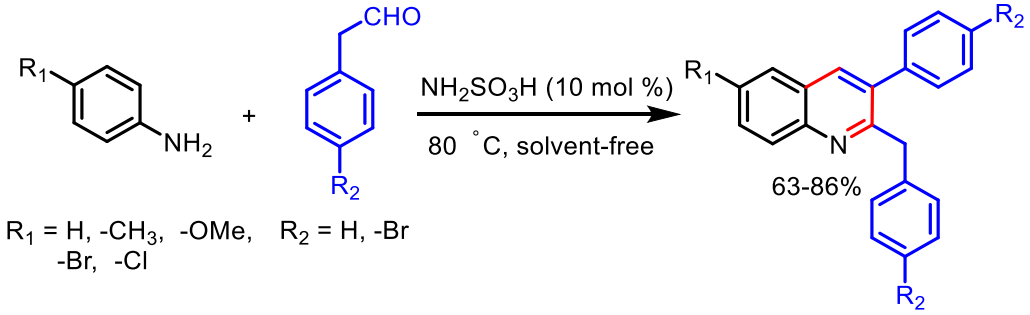

Scheme 14

Recently, Tepe's research group[26a] and our research group[26b] reported the synthesis of 2-benzyl-3-phenylquinolines using aniline and styrene oxide in the presence of 0.5 equivalent of scandium(III) triflate and 10 mol% $Yb(OTf)_3$ respectively as shown in Scheme 15.

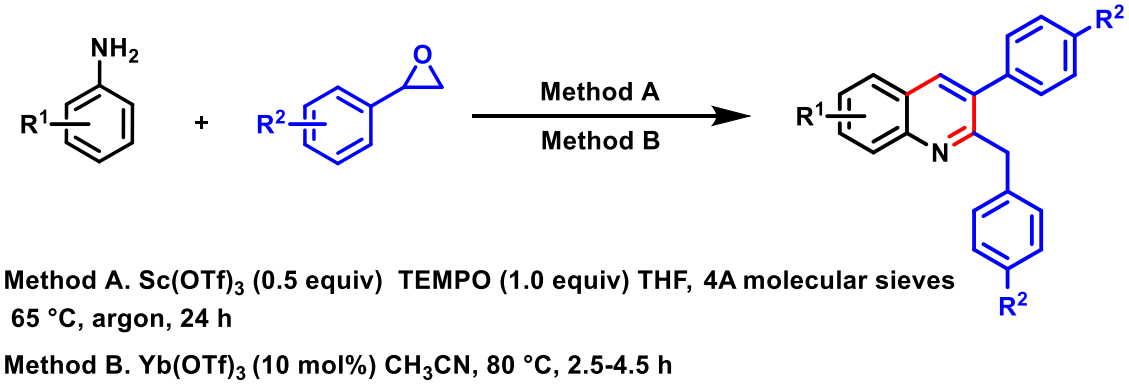

Scheme 15

The methods mentioned are environmentally unfriendly due to hazardous reagents, toxic by-products, and rare earth metal catalysts like scandium(III) triflate and $Yb(OTf)_3$. These metals are expensive and generate waste that poses significant disposal and environmental contamination issues.

Reason for choosing research topics

From the literature survey, it reveals that there is a large number of reported methods for the synthesis of substituted quinoline derivatives, such as 4-arylquinolines, 2,3-diaryl quinolines, 2,4-diarylquinolines, and 2-benzyl-3-phenylquinolines and 2,3-diarylquinolines. Although these existing methods for the synthesis of substituted quinoline scaffolds possess certain merits, they are plagued by numerous drawbacks that hinder their widespread applicability. These methods often rely on the use of hazardous acids and expensive catalysts, necessitate high reaction temperatures, and involve long reaction times. Furthermore, the work-up

procedures can be tedious, and the overall yields are often compromised, most importantly with a limited substrate scope.

In response to the growing demand for sustainable and greener practices in organic synthesis, there is a critical need to devise novel and efficient strategies to overcome these inherent challenges. The development of competent and versatile synthetic approaches is crucial not only for enhancing the efficiency of quinoline synthesis but also for mitigating the environmental impact associated with traditional methods.

To address these issues comprehensively, extensive efforts have been dedicated to pioneering new synthetic methodologies. These endeavors aim to streamline the synthetic routes by minimizing the use of hazardous reagents and optimizing reaction conditions to reduce energy consumption and waste generation.

The advancement in synthetic strategies also focuses on expanding the substrate scope, allowing for the synthesis of diverse substituted quinoline derivatives. This diversification not only broadens the applicability of these compounds in various fields such as medicinal chemistry and materials science but also fosters innovation in organic synthesis methodologies.

Here, by addressing the shortcomings of current synthetic methods and embracing sustainable practices, ongoing research endeavors strive to pave the way for the development of more efficient, environmentally friendly, and versatile strategies for the synthesis of as 4-arylquinolines, 2,3-diaryl quinolines, 2,4-diarylquinolines, and 2-benzyl-3-phenylquinolines scaffolds. These efforts are pivotal in meeting the evolving demands of modern organic synthesis and advancing the frontiers of chemical innovation.

These methods offer advantages such as easy handling, high regioselectivity, utilization of readily available starting materials, cost-effective and versatile metal triflates as catalysts, mild reaction conditions, short reaction times, and a broad substrate scope with high yields. Each of these methods will be discussed in successive Chapter II (**Section A**, **Section B**, **Section C**, **Section D**) of Part A in this thesis.

Despite the extensive repertoire of existing methods for synthesizing quinoline, the drive to simplify the synthesis of substituted quinolines remains vital. This review elucidates why developing simpler and more efficient synthetic routes for substituted quinolines is crucial despite the availability of established methodologies.

Challenges with Existing Methods

1. **Complexity and Cost**: Many traditional quinoline synthesis methods, such as the Skraup, Doebner–Miller, and Friedländer syntheses, often involve multiple steps, harsh reaction conditions, and expensive or hazardous reagents. These factors can impede large-scale production and increase costs.

2. **Low Yield and Selectivity**: Achieving high yield and selectivity, especially for substituted quinolines, can be challenging with conventional methods. Unwanted side reactions and low regioselectivity often complicate the purification process, resulting in lower overall efficiency.

3. **Environmental Impact**: Traditional synthesis routes frequently use toxic solvents and generate considerable waste, raising environmental and safety concerns. The push towards greener chemistry necessitates the development of more environmentally benign methods.

The continuous quest to simplify the synthesis of substituted quinolines is driven by the need for more efficient, cost-effective, and environmentally friendly production methods. Despite the availability of classical synthetic routes, the challenges associated with complexity, cost, and environmental impact underscore the necessity for ongoing innovation. Simplified synthesis enhances the practicality of producing these vital compounds and aligns with the broader goals of sustainable and green chemistry. Thus, developing easy and straightforward synthetic methods for substituted quinolines remains critical in chemical research and industrial applications.

We conceived the idea that organocatalysts are gaining importance as catalysts in various transformations.

Reason for Choosing *p*-Toluenesulfonic acid monohydrate (*p*-TSA·H_2O) as a catalyst:

p-Toluenesulfonic acid monohydrate (*p*-TSA·H_2O) is often considered one of the best catalysts for organic reactions in synthetic methodologies due to several reasons. First, *p*-TSA is a strong organic acid, which makes it an excellent proton donor. This strong acidity can catalyze a variety of reactions, such as esterifications, transesterifications, dehydration, and polymerizations. Additionally, *p*-TSA is highly soluble in organic solvents, which allows it to be used in a wide range of reaction media. Its solubility in both polar and non-polar solvents makes it versatile and easy to work with in different reaction conditions.[26c-e] Unlike mineral acids like HCl or H_2SO_4, *p*-TSA is non-volatile and more manageable in the laboratory, reducing the risk of handling issues and loss of catalyst due to evaporation. Furthermore, *p*-

TSA is thermally stable, allowing it to be used in reactions that require high temperatures without decomposition. This stability is advantageous for reactions that need prolonged heating. Despite being a strong acid, *p*-TSA is considered milder compared to some inorganic acids, reducing the risk of side reactions and degradation of sensitive functional groups in the substrate. Moreover, *p*-TSA·H_2O, being the hydrated form, can tolerate the presence of water in reactions, which is particularly useful in reactions where water is either a byproduct or where trace amounts of moisture cannot be avoided. After the reaction, *p*-TSA can often be easily removed from the reaction mixture by simple aqueous workup due to its high solubility in water, facilitating the purification of the desired product. In many reactions, *p*-TSA is effective in catalytic amounts, meaning only a small quantity is needed to achieve high yields. This efficiency is both cost-effective and beneficial in minimizing the amount of catalyst residues in the final product. Overall, the combination of strong acidity, solubility, non-volatility, thermal stability, mildness, water tolerance, ease of removal, and catalytic efficiency makes *p*-TSA·H_2O a highly effective and preferred catalyst in various organic synthetic methodologies.

Part A

Chapter II: Section A

Synthesis of 4-arylquinolines derivatives

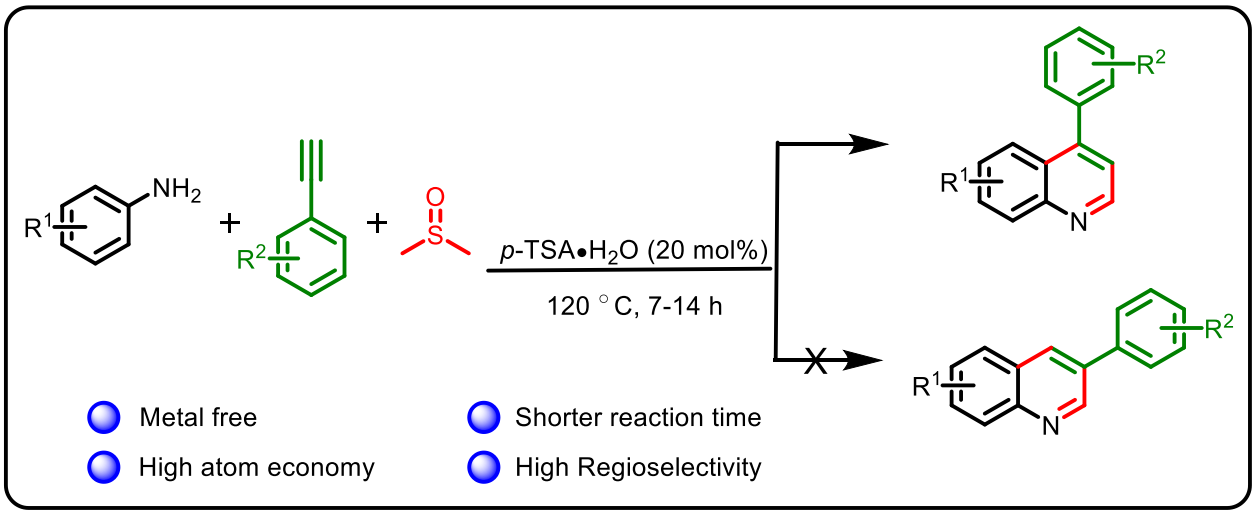

RESULT AND DISCUSSION

EXPERIMENTAL SECTION

Results and Discussion

Chapter I has already covered the significance of 4-arylquinolines and the synthetic approaches employed for their synthesis. Dimethyl sulfoxide (DMSO) is predominantly utilized as an aprotic polar solvent due to its minimal toxicity, stability, and outstanding solvent capabilities.[27a,b] Additionally, it plays a crucial role in organic synthesis owing to its versatile nature, serving as a key reagent as DMSO becomes the source for embedding Me,[28a] SO_2Me,[28b] CHO,[28c] SMe,[28d] and $MeSOCH_2$.[28e] It is also used in well-known reactions such as Swern oxidation,[29] Pfitzner-Moffatt,[30] and complex molecule synthesis.[31a,b] As a matter of fact, it has become the synthon in organic synthesis. In this section of Chapter II, a straightforward and highly efficient procedure for the synthesis of 4-aryl quinolines is demonstrated by employing readily available arylamine, arylacetylene, and DMSO in the presence of 20 mol% *p*-TSA·H_2O. In addition, the reaction proceeds effectively and efficiently without the involvement of any metal catalyst, ligand, or co-catalyst as additives and inert atmospheric reaction conditions.

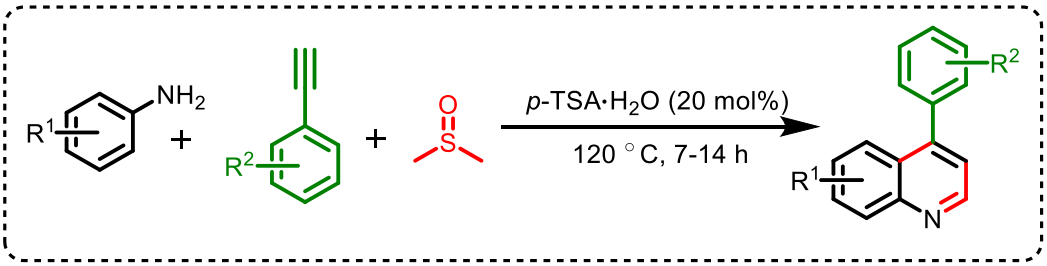

Scheme 16. Synthetic protocol for the synthesis of 4-aryl quinolines derivatives.

This study was begun by finding optimization reaction conditions. For this purpose, the model substrates chosen were *p*-anisidine (**1a**, 1.0 mmol) and phenylacetylene (**2a**, 1.0 mmol) to determine suitable reaction conditions. Initially, a reaction was scrutinized without a catalyst between *p*-anisidine **1a,** phenylacetylene **2a**, and DMSO at room temperature as well as slowly heating from temperature to 120 °C (Table 1, Entries 1 and 2). In both cases, the reaction did not provide the product as the starting material was recovered.hen the same reaction was examined with 5 mol% *p*-TSA•H_2O at room temperature and no reaction took place (Table 1, Entry 3). Next, when the reaction was carried out in the presence of 5 mol% *p*-TSA·H_2O at 100 °C, product **3a** was obtained in 31% yield (Table 1, Entry 4). To ascertain the structure of the desired product, the ^1H NMR and ^{13}C NMR spectral data of compound **3a** were recorded, and observed that the H-2

proton appears at δ 8.80 and H-3 at δ 7.29, and also in infrared (IR) spectrum as a characteristic absorption band in at 3397 and 3483 cm^{-1} has not appeared. (Incorporated in the experimental section). For a better understanding of the structure, the labelled structure of 4-substituted quinoline is shown below in Figure **3**. Significantly, the yield was increased from 31% to 53% as soon as the temperature was increased from 100 °C to 120 °C (Table 1, Entry 4–6,). However, by further increasing the reaction temperature at 130 °C and 140 °C, the yield of the desired product **3a** was not improved further, and a mixture of products formed during the reaction (Table 1, Entries 7 and 8).

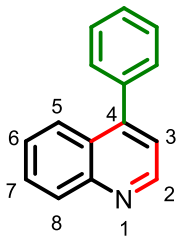

Figure 3. 4-Substituted quinoline with numbering of the position of the quinoline.

Table 1. Optimization of reaction conditions[a,b,c,d]

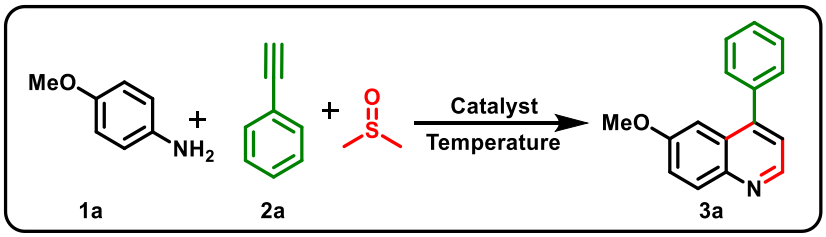

Entry	Catalyst	Mol (%)	Time (h)	Temp (°C)	Yield[b] (%)
1[c]	-	-	24	RT	ND
2	-	-	24	RT →120	ND
3[c]	*p*-TSA•H_2O	5	24	RT	ND
4	*p*-TSA•H_2O	5	15	100	31
5	*p*-TSA•H_2O	5	15	110	46
6	*p*-TSA•H_2O	5	15	120	53
7	*p*-TSA•H_2O	5	15	130	66

8	*p*-TSA•H_2O	5	15	140	28
9	*p*-TSA•H_2O	10	11	120	68
10	***p*-TSA•H_2O**	**20**	**8**	**120**	**88**
11	MsOH	20	10	120	29
12	TfOH	20	10	120	32
13	(±)CSA	20	10	120	62

[a]Reaction conditions: All the reactions were performed using *p*-anisidine (**1a**, 1.0 mmol), and phenylacetylene (**2a**, 1.0 mmol), in DMSO. [b]Isolated yield. [C]Reaction performed at room temperature. ND: No desired product.

To facilitate the process more efficiently, the amount of catalyst was increased from 5 to 10 mol %, and a 68% yield of product **3a** was obtained (Table 1, Entry 9). It was notably observed that below 100°C, DMSO does not readily form sulfenium ions, to facilitate the reaction more efficiently. Encouraged by this successful result, the amount of catalyst was increased to 20 mol% and surprisingly the yield increased significantly increased from 68% to 88% (Table 1, Entry 10).

Thereafter, the efficiency of several other non-metal acid catalysts was also examined such as MsOH, TfOH, and (±) CSA at 120 °C under similar reaction conditions and the yield was obtained 29%, 32%, and 62%, respectively (Table 1, Entries 11–13). Based on the above optimization results, it was concluded that *p*-TSA•H_2O is the most effective catalyst for this reaction at 120 °C in DMSO as a solvent cum source of CH_2.

Having optimized reaction conditions in hand, the generality and substrate scope were evaluated. Initially, various substituted arylacetylenes were examined with *p*-anisidine **1a** (Table 2). Electron donating groups on arylacetylene such as *ortho*-methyl **2b** and *para*-methyl **2c** positions provide the desired product **3b** and **3c** in 88% and 90%, respectively. Likewise, the arylacetylenes having electron-donating groups such as 4-ethyl **2d**, 4-*tert*-butyl **2e**, and 4-methoxy **2f** provided the corresponding products in good yields. Interestingly, the arylacetylenes containing electron-withdrawing groups like 4-fluoro **2g**, 4-bromo **2h**, 2-CF_3 **2i**, and 1,3-diethynyl **2j** groups were also found to be compatible under the present reaction conditions, and furnished the desired products **3g**, **3h**, **3i**, and **3j** in 83%, 82%, 78 %, and 83% yield, respectively.

Table 2. The reaction of arylamines **1a** and **1e** with various substituted arylacetylenes **2a-m**.[a,b]

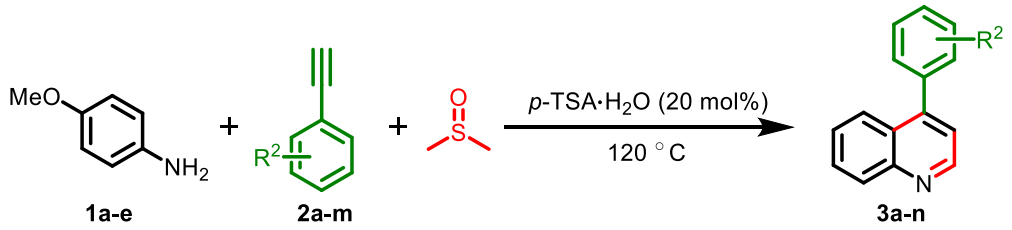

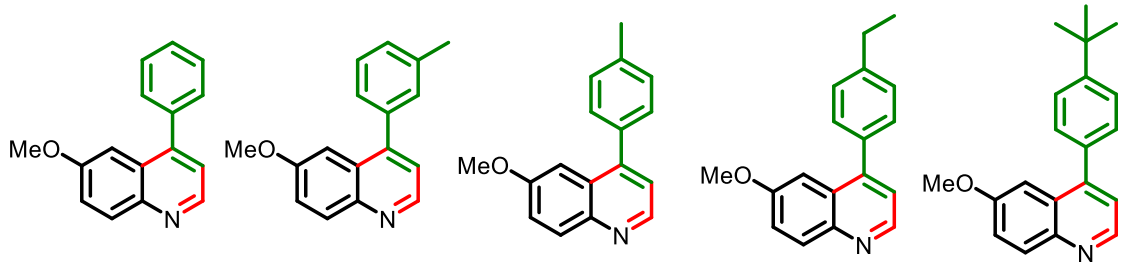

3a, 8 h, 88% **3b**, 8.5 h,88% **3c**, 8 h, 90% **3d**, 9.5 h, 85% **3e**, 8 h, 91%

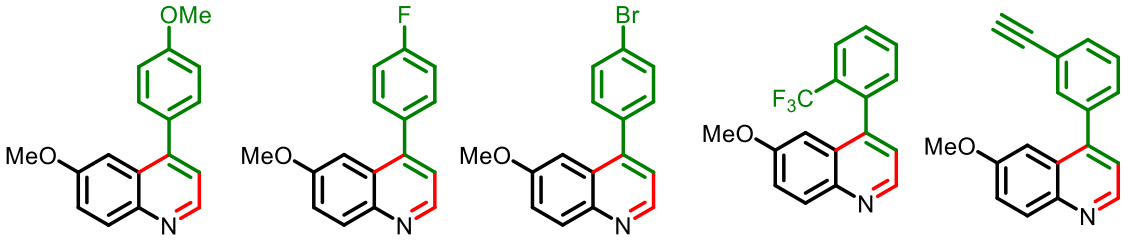

3f, 7 h, 88% **3g**, 9.5 h, 83% **3h**, 8 h, 82% **3i**, 8.5 h,78% ***3***j, 8.5 h, 83%

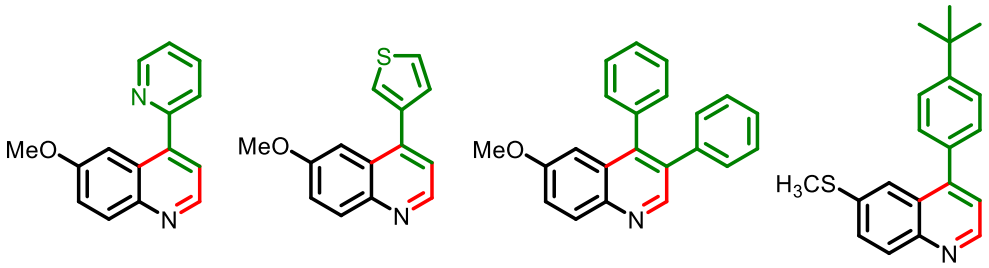

3k, 8 h, 78% **3l**, 9.5 h,80% **3m**, 10 h, 89% **3n**, 10.5 h, 83%

[a]Reaction conditions: All the reactions were performed using arylamine (**1a** and **1e**, 1.0 mmol), arylacetylene (**2a-m**, 1.0 mmol), in DMSO at 120 °C. [b]Isolated yield.

Heterocyclic arylacetylenes such as 2-ethynyl pyridine **2k** and 3-ethynyl thiophene **2l** underwent the reaction smoothly and provided the desired products **3k** and **3l** in 78% and 80% yield respectively. Noteworthy, the disubstituted arylacetylene namely 1,2-diphenylacetylene **2m** also reacted to give the desired product **3m** in 89% yield. To further explore the practicability, reactions were carried out between **1e** with **2e** and the desired product **3n** was isolated in 83%. The reaction

time and yield of the products are summarized in **Table 2**. Various aryl alkynes reacted effectively with arylamines **1a** and **1e,** irrespective of the position and electronic nature of the substituent groups on the arylacetylene. All substitution patterns on aromatic acetylene were well tolerated and evenly produced desired products. The practicability of this transformation was further enhanced as the desired product was isolated in 91% yield when the reaction was carried at a 5 mmol scale between *p*-anisidine **1a**, phenylacetylene **2a**, and DMSO under the same reaction condition.

Table 3. The reaction of various arylamines **1a-p** with phenylacetylenes **2a**.[a,b,c]

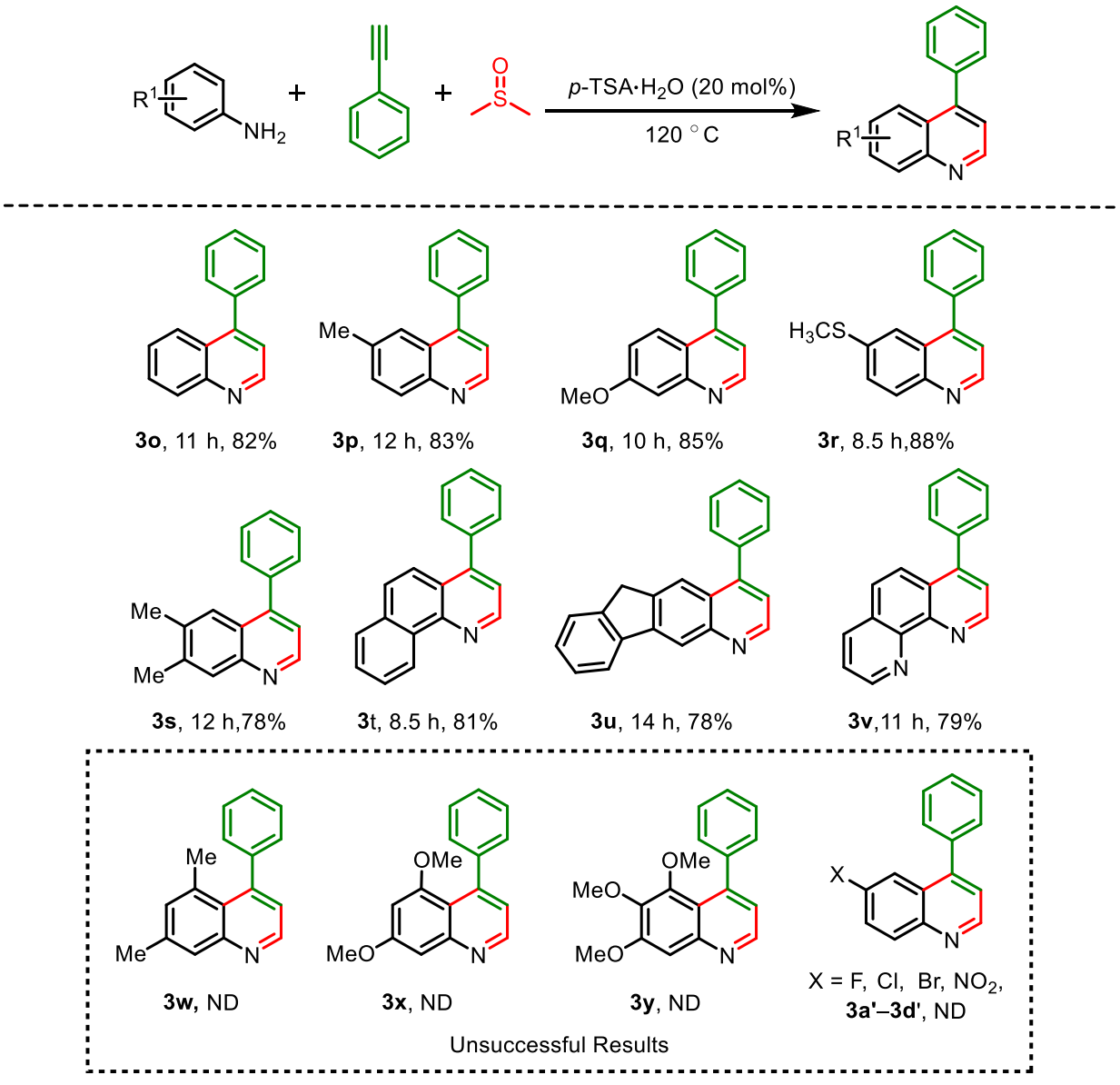

[a]Reaction conditions: All the reactions were performed using arylamines (**1a-p**, 1.0 mmol), phenylacetylene (**2a**, 1.0 mmol), in DMSO at 120 °C. [b]Isolated yield. [c]ND: No Desired Product.

Encouraged by the above results, the reaction of various arylamines **1b-j** was examined with phenylacetylene **2a**, as shown in Table 3. First, aniline **1b** and mono-substituted (4-Me, 3-OMe, and 4-SCH_3) regioselectively form 4-aryl quinoline **3o-3r** in 82-88% yield. Disubstituted aniline **1f** also reacts smoothly to afford the product **3s** in a 78% yield. Next, polycyclic amines **1g** and **1h** were reacted with **2a** to give the desired product **3t** and **3u** in 81% and 78% respectively. Likewise, 8-Aminoquinoline **1i** also favorably tolerated this procedure to yield the corresponding product **3v**. The limitation of the present protocol is that electron-rich aniline such as 3,5-dimethylaniline **1j**, 3,5-dimethoxy aniline **1k**, and 3,4,5-trimethoxyaniline **1l** did not provide the desired products (**3w–y**) under identical reaction conditions.

The reason for the failure of the reactions is a steric reason, i.e. due to the presence of substituents in the 3 position of aniline, phenylacetylene can not come close to forming Povarov-type reactions. Similarly, 4-substituted arylamines having electron-withdrawing groups such as F, Cl, Br, and NO_2 also did not give the expected desired products (**3a´-d'**) because it deactivates amino group to react with *in situ* generated sulfenium ion [**A**] to form intermediate [**C**].

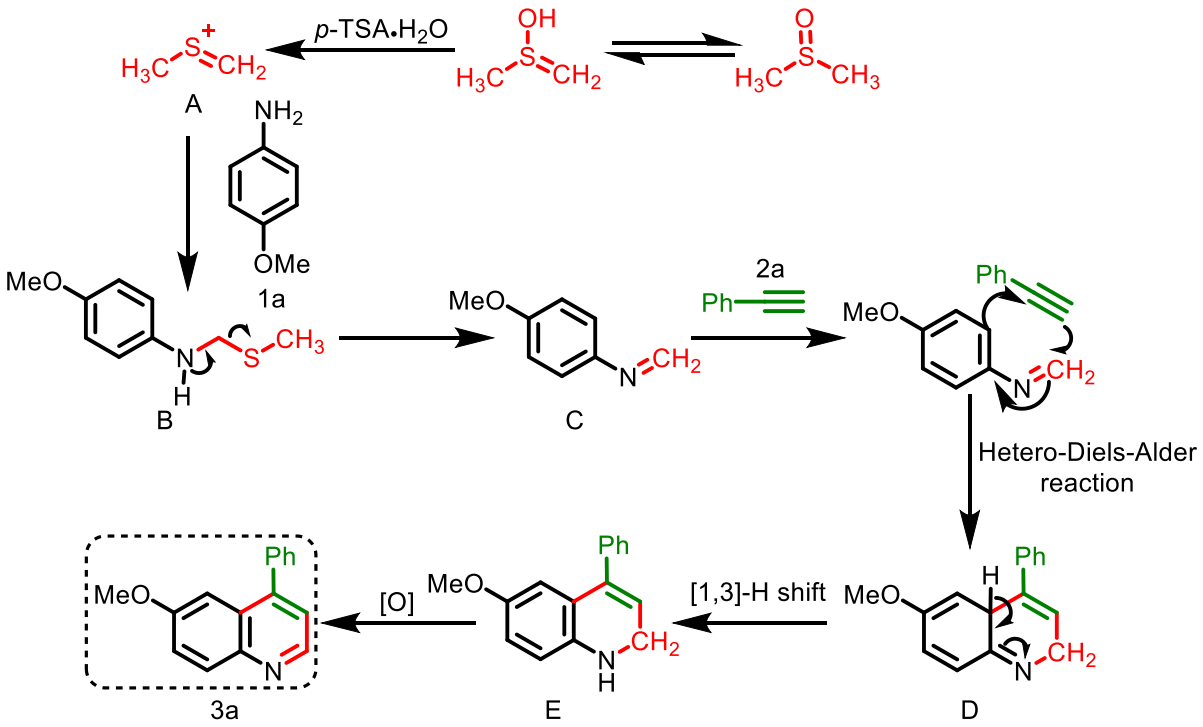

Scheme 17. A plausible mechanism for the formation of **3a.**

On the basis of preliminary experiments and the previous literature reports, the plausible reaction mechanism is shown in **Scheme 17**. The reactive sulfenium ion **A** is generated from DMSO in the

presence of *p*-TSA•H_2O.[32] The sulfenium ion **A** then reacts with *p*-anisidine **1a** to form another intermediate **B**, which undergoes the elimination of methanethiol to form iminium intermediate **C**.[33] The intermediate **C** reacts with phenylacetylene **2a** in a hetero-Diels-Alder manner to form the cyclized intermediate **D**. At last, the intermediate **D** undergoes [1,3]-H shifts to form the intermediate **E**, which upon aerial oxidation provides the desired product **3a.**

In summary, the synthesis of 4-aryl quinoline derivatives has been achieved regioselectively from arylamine, arylacetylene, and DMSO using a three-component reaction in an atom-economic manner and metal-free conditions. The substitution patterns on aromatic rings of arylamine and arylacetylene were well tolerated and evenly produced desired products in good to excellent yields. This method does not involve any ligand, co-catalyst, or inert atmospheric conditions. The reaction was accomplished through two *C-C* bonds and one *C-N* bond formation, along with the addition of methylene group from solvent DMSO. Importantly, this work provides an example of applying *p*-TSA•H_2O as a promising alternative catalyst to transition metal catalysts.

General Procedure for the Synthesis of 4-aryl quinolines Derivatives 3a-3v.

Arylamine (**1**, 1.0 mmol) and arylacetylene (**2**, 1.0 mmol) were dissolved in 2 mL of DMSO in the 25 mL round-bottomed flask. After that 20 mol% *p*-TSA•H_2O was added to the reaction mixture as a catalyst and kept in a pre-heated oil bath at 120 ^oC with constant stirring under an air atmosphere. The progress of the reaction was monitored by checking TLC from time to time. After the completion of the reaction, it was brought to room temperature, and the resulting mixture was diluted with 10 mL DCM. The organic layer was washed with brine solution (5 mL x 2). After that dried with anhydrous sodium sulfate, the solvent was removed in the rotary evaporator and the crude residue was purified through a silica gel (60−120 mesh) column chromatography.

6-Methoxy-4-phenylquinoline (3a) White solid (207.05 mg, 88%); mp 138-140 ^oC. ^1H NMR

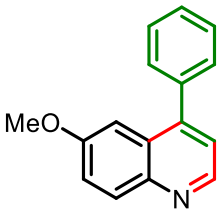

NMR (600 MHz, $CDCl_3$) δ 8.80 (d, *J* = 4.1 Hz, H-2), 8.08 (d, *J* = 9.2 Hz, H-8), 7.49 – 7.55 (m, 5H), 7.39 (dd, J_1 = 9.2, J_2 =2.7 Hz, H-7), 7.29 (d, *J* = 4.3 Hz, H-3), 7.19 (d, *J* = 2.6 Hz, H-5), 3.79; ^{13}C NMR (150 MHz, $CDCl_3$) δ 158.0, 147.6, 147.2, 144.9, 138.5, 131.4, 129.4 (2C), 128.8 (2C), 128.5, 127.8, 121.9, 121.8, 103.8, 55.5; IR (KBr)ν_{max}/cm^{-1} 3021 (C–H), 2926 (C–H), 1622 (C=C), 1372 (C–O); HRMS (ESI) Calcd For $C_{16}H_{14}NO$ 236.1070 ($M+H^+$); Found 236.1070.

6-Methoxy-4-(m-*tolyl*)quinoline (3b) Light yellow liquid (219.39 mg, 88%). ^1H NMR (600 MHz,

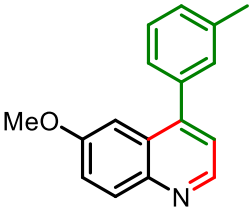

$CDCl_3$) δ 8.78 (d, *J* = 4.4 Hz, 1H), 8.07 (d, *J* = 9.2 Hz, 1H), 7.42 (t, *J* = 7.5 Hz, 1H), 7.38 (dd, *J* = 9.2, 2.7 Hz, 1H), 7.29 – 7.33 (m, 3H), 7.27 (d, *J* = 4.4 Hz, 1H), 7.21 (d, *J* = 2.6 Hz, 1H), 3.79 (s, 3H), 2.46 (s, 3H); ^{13}C NMR (150 MHz, $CDCl_3$) δ 157.9, 147.6, 147.4, 144.9, 138.5, 138.4, 131.3, 130.1, 129.2, 128.6, 127.8, 126.5, 121.8, 121.7, 103.9, 55.5, 21.6; IR (KBr)ν_{max}/cm^{-1} 3023 (C–H), 2926 (C–H), 1622 (C=C), 1300 (C–O); HRMS (ESI) Calcd For $C_{17}H_{16}NO$ 250.1227 ($M+H^+$); Found 250.1227.

6-Methoxy-4-(*p*-tolyl)quinoline (3c) Yellow liquid (224.37 mg, 90%). ^1H NMR (600 MHz,

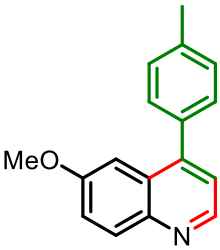

$CDCl_3$) δ 8.78 (d, *J* = 4.2 Hz, 1H, H-2), 8.08 (d, *J* = 9.2 Hz, 1H, H-8), 7.42 (d, *J* = 7.8 Hz, 2H), 7.38 (dd, *J* = 9.2, 2.5 Hz, 1H, H-7), 7.34 (d, *J* = 7.7 Hz, 2H), 7.27 (d, *J* = 4.3 Hz, 1H, H-3), 7.23 (d, *J* = 2.4 Hz, 1H, H-5), 3.79 (s, 3H), 2.47 (s, 3H); ^{13}C NMR (150 MHz, $CDCl_3$) δ 157.9, 147.5, 147.4, 144.8, 138.3, 135.5, 131.2, 129.5 (2C), 129.3 (2C), 127.9, 121.9, 121.8, 103.8, 55.5, 21.4;

IR (KBr)ν_{max}/cm^{-1} 2926 (C–H), 1620 (C=C), 1362 (C–O); HRMS (ESI) Calcd For $C_{17}H_{16}NO$ 250.1227 (M+H$^+$); Found 250.1229.

4-(4-Ethylphenyl)-6-methoxyquinoline (3d) White Liquid (223.83 mg, 85%). ^{1}H NMR (500 MHz, $CDCl_3$) δ 8.77 (d, *J* = 4.4 Hz, 1H, H-2), 8.07 (d, *J* = 9.2 Hz, 1H, H-8), 7.44 (d, *J* = 7.9 Hz, 2H), 7.35 – 7.39 (m, 3H), 7.26 (d, *J* = 4.5 Hz, 1H, H-3), 7.25 (d, *J* = 2.6 Hz, 1H, H-5), 3.79 (s, 3H), 2.76 (q, *J* = 7.6 Hz, 2H), 1.33 (t, *J* = 7.6 Hz, 3H); ^{13}C NMR (125 MHz, $CDCl_3$) δ 157.9, 147.6, 147.3, 144.9, 144.6, 135.7, 131.3, 129.4, 128.2, 127.9, 121.7, 121.7, 104.0, 55.5, 28.7, 15.5; IR (KBr)ν_{max}/cm^{-1} 3022 (C–H), 2926 (C–H), 1622 (C=C), 1312 (C–O); HRMS (ESI) Calcd For $C_{18}H_{18}NO$ 264.1383 (M+H$^+$); Found 264.1383.

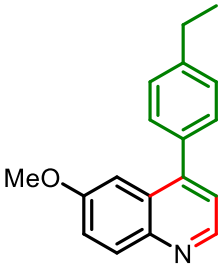

4-(4-(*tert*-Butyl)phenyl)-6-methoxyquinoline (3e) Yellow liquid (265.16 mg, 91%). ^{1}H NMR (600 MHz, $CDCl_3$) δ 8.80 (d, *J* = 4.2 Hz, 1H), 8.11 (d, *J* = 9.2 Hz, 1H), 7.57 (d, *J* = 8.0 Hz, 2H), 7.49 (d, *J* = 8.0 Hz, 2H), 7.41 (dd, *J* = 9.2, 2.0 Hz, 1H), 7.31 (dd, *J* = 9.3, 3.2 Hz, 2H), 3.83 (s, 3H), 1.44 (s, 9H); ^{13}C NMR (100 MHz, $CDCl_3$) δ 157.8, 151.5, 147.5, 147.2, 144.8, 135.4, 131.2, 129.1, 127.8, 125.6, 121.8, 121.6, 104.1, 55.5, 34.8, 31.4; IR (KBr)ν_{max}/cm^{-1} 2957 (C–H), 1616 (C=C), 1363 (C–O); HRMS (ESI) Calcd For $C_{20}H_{22}NO$ 292.1696 (M+H$^+$); Found 292.1695.

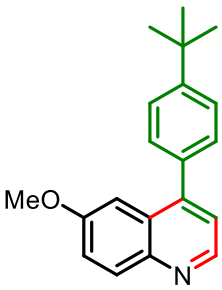

6-Methoxy-4-(4-methoxyphenyl)quinoline (3f) Light brown liquid (233.47 mg, 88%). ^{1}H NMR (500 MHz, $CDCl_3$) δ 8.77 (d, *J* = 4.4 Hz, 1H), 8.06 (d, *J* = 9.2 Hz, 1H), 7.46 (d, *J* = 8.6 Hz, 2H), 7.37 (dd, *J* = 9.2, 2.7 Hz, 1H), 7.25 (dd, *J* = 10.9, 3.6 Hz, 2H), 7.06 (d, *J* = 8.6 Hz, 2H), 3.90 (s, 3H), 3.80 (s, 3H); ^{13}C NMR (125 MHz, $CDCl_3$) δ 159.9, 157.9, 147.6, 147.0, 144.9, 131.3, 130.6, 128.0, 121.8, 121.7, 116.5, 114.2, 103.9, 55.5, 55.5; IR (KBr)ν_{max}/cm^{-1} 3022 (C–H), 2922 (C–H), 1622 (C=C), 1372 (C–O); HRMS (ESI) Calcd For $C_{17}H_{16}NO_2$ 266.1176 (M+H$^+$); Found 266.1173.

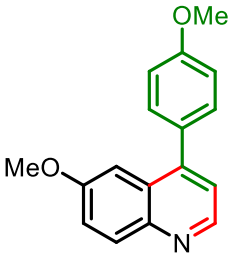

4-(4-Fluorophenyl)-6-methoxyquinoline (3g) White solid (210.21 mg, 83%); mp 98-100 °C. ^{1}H NMR (400 MHz, $CDCl_3$) δ 8.79 (d, *J* = 4.4 Hz, 1H), 8.08 (d, *J* = 9.2 Hz, 1H), 7.47 – 7.51 (m, 2H), 7.39 (dd, *J* = 9.2, 2.7 Hz, 1H), 7.21 – 7.25 (m, 3H), 7.12 (d, *J* = 2.7 Hz, 1H), 3.80 (s, 3H); ^{13}C NMR (100 MHz, $CDCl_3$) δ 162.9 ($J_{C\text{-}F}$ = 246.4 Hz),158.1, 147.6, 146.1, 145.0, 134.4 ($J_{C\text{-}F}$ = 3.4 Hz), 131.5, 131.1 ($J_{C\text{-}F}$ = 8.1 Hz), 127.8, 121.9, 121.8, 115.9 ($J_{C\text{-}F}$ = 21.4 Hz), 103.6, 55.6; ^{19}F NMR

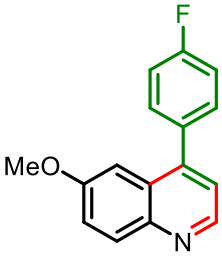

(565 MHz, $CDCl_3$) δ -113.36; IR (KBr)ν_{max}/cm^{-1} 2937 (C–H), 1611 (C=C), 1361 (C–O); HRMS (ESI) Calcd For $C_{16}H_{13}FNO$ 254.0976 ($M+H^+$); Found 254.0981.

4-(4-Bromophenyl)-6-methoxyquinoline (3h) White solid (257.48 mg, 82%). mp 95-96 ºC ^1H

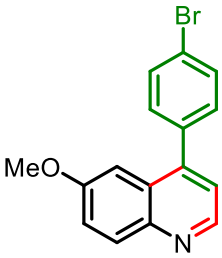

NMR (600 MHz, $CDCl_3$) δ 8.78 (d, *J* = 4.3 Hz, 1H), 8.07 (d, *J* = 9.2 Hz, 1H), 7.66 (d, *J* = 8.1 Hz, 2H), 7.39 (d, *J* = 7.9 Hz, 3H), 7.24 (d, *J* = 4.3 Hz, 1H), 7.10 (d, *J* = 2.2 Hz, 1H), 3.79 (s, 3H); ^{13}C NMR (150 MHz, $CDCl_3$) δ 158.1, 147.5, 145.8, 144.9, 137.3, 132.0, 131.5, 131.0, 127.5, 122.8, 122.1, 121.6, 103.3, 55.6; IR (KBr)ν_{max}/cm^{-1} 2936 (C–H), 1612 (C=C), 1362 (C–O); HRMS (ESI) Calcd For $C_{16}H_{13}BrNO$ 314.0176 ($M+H^+$); Found 314.1073.

6-Methoxy-4-(2-(trifluoromethyl)phenyl)quinoline (3i) Light brown Liquid (236.55 mg, 78%).

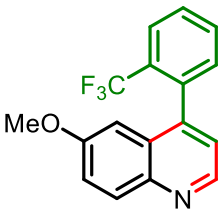

^1H NMR (400 MHz, $CDCl_3$) δ 8.80 (d, *J* = 4.3 Hz, 1H), 8.07 (d, *J* = 9.2 Hz, 1H), 7.87 (d, *J* = 7.6 Hz, 1H), 7.62 – 7.68 (m, 2H), 7.34 – 7.39 (m, 2H), 7.25 (d, *J* = 4.3 Hz, 1H), 6.57 (d, *J* = 3.0 Hz, 1H), 3.70 (s, 3H); ^{13}C NMR (100 MHz, $CDCl_3$) δ 157.9, 147.0, 144.4 (J_{C-F} = 5.4 Hz), 136.7 (J_{C-F} = 2 Hz Hz), 131.7, 131.6, 131.2, 128.7, 126.6(J_{C-F} = 5 Hz), 122.1, 121.9, 122.0(J_{C-F} = 106 Hz), 114.6, 104.1, 55.5; ^{19}F NMR (377 MHz, $CDCl_3$) δ -58.35; IR (KBr)ν_{max}/cm^{-1} 3022 (C–H), 2921 (C–H), 1622 (C=C), 1301 (C–O); HRMS (ESI) Calcd For $C_{17}H_{13}F_3NO$ 304.0944 ($M+H^+$); Found 304.0943.

4-(3-Ethynylphenyl)-6-methoxyquinoline (3j) White Liquid (215.21 mg, 83%). ^1H NMR (600

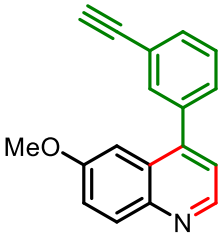

MHz, $CDCl_3$) δ 8.80 (d, *J* = 4.3 Hz, 1H), 8.08 (d, *J* = 9.2 Hz, 1H), 7.65 (s, 1H), 7.61 – 7.62 (m, 1H), 7.50 (d, *J* = 4.9 Hz, 2H), 7.39 (dd, *J* = 9.2, 2.6 Hz, 1H), 7.27 (d, *J* = 4.7 Hz, 1H), 7.11 (d, *J* = 2.5 Hz, 1H), 3.80 (s, 3H), 3.14 (s, 1H); ^{13}C NMR (150 MHz, $CDCl_3$) δ 158.1, 147.6, 146.1, 144.9, 138.7, 133.0, 132.1, 131.4, 129.8, 128.8, 127.6, 122.9, 122.0, 121.7, 103.5, 83.1, 78.1, 55.6; IR (KBr)ν_{max}/cm^{-1} 3018(C–H), 2899(C–H), 1603(C=C), 1311 (C–O); HRMS (ESI) Calcd For $C_{18}H_{14}NO$ 260.1070 ($M+H^+$); Found 260.1073.

6-Methoxy-4-(pyridin-2-yl)quinoline (3k) Light brown Liquid (174.92 mg, 78%). ^1H NMR (600

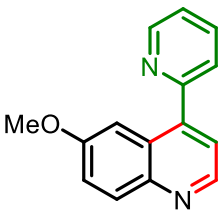

MHz, $CDCl_3$) δ 9.36 (s, 1H), 8.76 (d, *J* = 4.6 Hz, 1H), 8.66 (s, 1H), 8.03 (d, *J* = 9.1 Hz, 1H), 7.87 (d, *J* = 7.9 Hz, 1H), 7.80 – 7.83 (m, 1H), 7.38 (dd, *J* = 9.1, 2.3 Hz, 1H), 7.29 – 7.31 (m, 1H), 7.16 (d, *J* = 2.3 Hz, 1H), 3.93 (s, 3H); ^{13}C NMR (150 MHz, $CDCl_3$) δ 158.2, 155.1, 150.2, 146.8, 144.5, 137.1, 132.8,

132.2, 130.7, 129.0, 122.9, 120.9, 120.9, 105.8, 55.6; IR (KBr)ν_{max}/cm^{-1} 3021 (C–H), 2926 (C–H), 1622 (C=C), 1372 (C–O); HRMS (ESI) Calcd For $C_{14}H_{13}N_2O$ 225.1023 (M+H$^+$); Found 225.1024.

6-Methoxy-4-(thiophen-3-yl)quinoline (3l) Light brown Liquid (193.04 mg, 80%). ^{1}H NMR

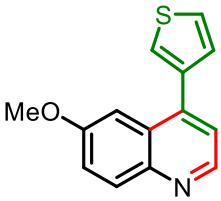

(600 MHz, $CDCl_3$) δ 8.67 (d, *J* = 4.3 Hz, 1H, H-2), 7.97 (d, *J* = 9.1 Hz, 1H, H-8), 7.43 (d, *J* = 4.0 Hz, 2H, H-4′ & H-5′), 7.30 (dd, *J* = 9.2, 2.2 Hz, 2H, H-7), 7.24 (d, *J* = 4.3 Hz, 1H, H-3), 7.16 (s, 1H, H-2′), 3.75 (s, 3H); ^{13}C NMR (150 MHz, $CDCl_3$) δ 158.1, 147.6, 144.9, 142.03, 139.0, 131.4, 128.7, 127.9, 126.5, 124.7, 121.9, 121.6, 103.7, 55.6; IR (KBr)ν_{max}/cm^{-1} 3018 (C–H), 2926 (C–H), 1619 (C=C), 1299 (C–O); HRMS (ESI) Calcd For $C_{14}H_{12}NOS$ 242.0635 (M+H$^+$); Found 242.0633.

6-Methoxy-3,4-diphenylquinoline (3m) Brown liquid (277.12 mg, 89%). ^{1}H NMR (600 MHz,

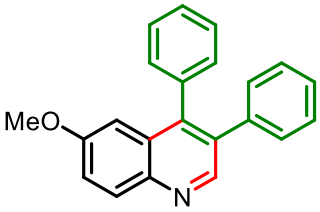

$CDCl_3$) δ 8.85 (s, 1H), 8.09 (d, *J* = 9.2 Hz, 1H), 7.33 – 7.39 (m, 4H), 7.20 – 7.23 (m, 5H), 7.16 (d, *J* = 7.6 Hz, 2H), 6.95 (d, *J* = 2.4 Hz, 1H), 3.73 (s, 3H); ^{13}C NMR (150 MHz, $CDCl_3$) δ 158.2, 149.5, 144.4, 143.8, 138.4, 136.7, 133.5, 131.7, 131.0, 130.5, 130.2, 128.3, 128.1, 127.8, 127.1, 121.5, 104.7, 55.5; IR (KBr)ν_{max}/cm^{-1} 3029 (C–H), 2916 (C–H), 1622 (C=C), 1372 (C–O); HRMS (ESI) Calcd For $C_{20}H_{18}NO$ 314.1383 (M+H$^+$); Found 314.1390.

4-(4-(*tert*-Butyl)phenyl)-6-(methylthio)quinoline (3n) Dark brown liquid (255.18 mg, 83%). ^{1}H

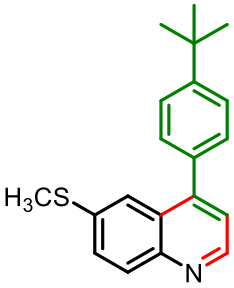

NMR (500 MHz, $CDCl_3$) δ 8.84 (d, *J* = 4.4 Hz, 1H), 8.06 (d, *J* = 8.9 Hz, 1H), 7.77 (d, *J* = 2.0 Hz, 1H), 7.62 (dd, *J* = 8.9, 2.1 Hz, 1H), 7.55 (d, *J* = 8.2 Hz, 2H), 7.45 (d, *J* = 8.2 Hz, 2H), 7.31 (d, *J* = 4.4 Hz, 1H), 2.49 (s, 3H), 1.41 (s, 9H); ^{13}C NMR (125 MHz, $CDCl_3$) δ 151.8, 149.3, 147.3, 147.1, 137.3, 134.9, 130.2, 129.3, 128.8, 127.3, 125.7, 122.0, 121.8, 34.9, 31.5, 16.0; IR (KBr)ν_{max}/cm^{-1} 3022 (C–H), 2889 (C–H), 1615 (C=C); HRMS (ESI) Calcd For $C_{20}H_{22}NS$ 308.1468 (M+H$^+$); Found 308.1468.

4-Phenylquinoline (3o) White liquid (168.16 mg, 82%). ^{1}H NMR (600 MHz, $CDCl_3$) δ 8.96 (d, *J*

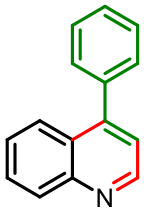

= 4.3 Hz, 1H), 8.19 (d, *J* = 8.4 Hz, 1H), 7.93 (d, *J* = 8.4 Hz, 1H), 7.73 – 7.75 (m, 1H), 7.53 (dt, *J* = 13.1, 7.1 Hz, 6H), 7.36 (d, *J* = 4.3 Hz, 1H); ^{13}C NMR (150 MHz, $CDCl_3$) δ 149.9, 148.9, 148.5, 138.0, 129.7, 129.6, 129.6, 128.7, 128.6, 126.9, 126.8, 126.0, 121.5; IR (KBr)ν_{max}/cm^{-1} 3022 (C–H), 2889 (C–H), 1615 (C=C), 1301 (C–O); HRMS (ESI) Calcd For $C_{15}H_{12}N$ 206.0965 (M+H$^+$); Found 206.0965.

6-Methyl-4-phenylquinoline (3p) White semisolid (182.00 mg, 83%). ^{1}H NMR (600 MHz, $CDCl_3$) δ 8.87 (d, *J* = 4.3 Hz, 1H), 8.07 (d, *J* = 8.6 Hz, 1H), 7.66 (s, 1H), 7.54 (dd, *J* = 16.9, 7.9 Hz, 3H), 7.50 – 7.51 (m, 3H), 7.29 (d, *J* = 4.3 Hz, 1H), 2.47 (s, 3H); ^{13}C NMR (150 MHz, $CDCl_3$) δ 149.1, 147.9, 147.3, 138.3, 136.6, 131.7, 129.6, 128.6, 128.5, 128.4, 126.8, 124.6, 121.5, 21.9; IR (KBr)ν_{max}/cm^{-1} 3026 (C–H), 2912 (C–H), 1622 (C=C), 1362 (C–O); HRMS (ESI) Calcd For $C_{16}H_{14}N$ 220.1121 ($M+H^+$); Found 220.1120.

7-Methoxy-4-phenylquinoline (3q) Light brown Liquid (199.82 mg, 85%). ^{1}H NMR (600 MHz, $CDCl_3$) δ 8.80 (d, *J* = 4.3 Hz, 1H), 8.08 (d, *J* = 9.2 Hz, 1H), 7.49 – 7.54 (m, 5H), 7.39 (dd, *J* = 9.2, 2.3 Hz, 1H), 7.29 (d, *J* = 4.3 Hz, 1H), 7.19 (d, *J* = 2.3 Hz, 1H), 3.79 (s, 3H); ^{13}C NMR (100 MHz, $CDCl_3$) δ 158.0, 153.6, 147.6, 138.4, 131.3, 129.4, 128.8, 128.6, 128.5, 126.3, 121.9, 121.8, 103.8, 55.5; IR (KBr)ν_{max}/cm^{-1} 3033 (C–H), 2926 (C–H), 1622 (C=C), 1372 (C–O); HRMS (ESI) Calcd For $C_{16}H_{14}NO$ 236.1070 ($M+H^+$); Found 236.1072.

6-(Methylthio)-4-phenylquinoline (3r) Light brown Liquid (221.17 mg, 88%). ^{1}H NMR (600 MHz, $CDCl_3$) δ 8.85 (d, *J* = 4.4 Hz, 1H), 8.07 (d, *J* = 8.8 Hz, 1H), 7.67 (d, *J* = 1.8 Hz, 1H), 7.61 (dd, *J* = 8.9, 2.0 Hz, 1H), 7.50 – 7.55 (m, 5H), 7.31 (d, *J* = 4.4 Hz, 1H), 2.46 (s, 3H); ^{13}C NMR (150 MHz, $CDCl_3$) δ 149.2, 147.3, 147.0, 137.9, 137.6, 130.2, 129.5, 128.8, 128.8, 128.6, 127.2, 122.0, 121.2, 15.8; IR (KBr)ν_{max}/cm^{-1} 3018 (C–H), 2912 (C–H), 1621 (C=C), 1372 (C–O); HRMS (ESI) Calcd For $C_{16}H_{14}NS$ 252.0842 ($M+H^+$); Found 252.0815.

6,7-Dimethyl-4-phenylquinoline (3s) White liquid (181.98 mg, 78%). ^{1}H NMR (600 MHz, $CDCl_3$) δ 8.85 (d, *J* = 4.4 Hz, 1H), 7.95 (s, 1H), 7.64 (s, 1H), 7.50 – 7.55 (m, 5H), 7.25 (s, 1H), 2.49 (s, 3H), 2.38 (s, 3H); ^{13}C NMR (151 MHz, $CDCl_3$) δ 148.7, 148.1, 147.4, 140.1, 138.4, 136.9, 129.6, 128.8, 128.7, 128.5, 125.4, 125.1, 120.8, 20.4, 20.4; IR (KBr)ν_{max}/cm^{-1} 3013 (C–H), 2908 (C–H), 1615 (C=C), 1372 (C–O); HRMS (ESI) Calcd For $C_{17}H_{16}N$ 243.3215 ($M+H^+$); Found 243.3230.

4-Phenylbenzo[*h*]quinoline (3t) White solid (206.63 mg, 81%). mp 110-112 °C ^{1}H NMR (600 MHz, $CDCl_3$) δ 9.75 (d, *J* = 8.0 Hz, 2H), 8.63 (s, 1H), 7.94 (d, *J* = 7.7 Hz, 2H), 7.81 – 7.86 (m, 6H), 7.76 (t, *J* = 7.4 Hz, 2H); ^{13}C NMR (150 MHz, $CDCl_3$) δ 146.0, 134.6, 134.0, 132.1, 131.0, 129.7, 129.7, 128.7, 128.0, 127.8, 127.7, 127.4, 127.2, 125.6, 125.5, 125.3, 124.8; IR (KBr)ν_{max}/cm^{-1} 3012 (C–H), 2911 (C–H), 1622 (C=C), 1372 (C–O); HRMS (ESI) Calcd For $C_{19}H_{14}N$ 256.1121 ($M+H^+$); Found 256.1156.

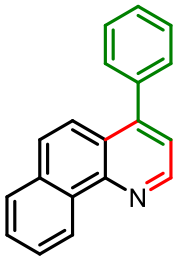

4-Phenyl-6*H*-indeno[2,1-*g*]quinoline (3u) Light brown liquid (267.86 mg, 78%). ^{1}H NMR (600 MHz, $CDCl_3$) δ 8.88 (d, *J* = 4.2 Hz, 1H), 8.26 (d, *J* = 8.6 Hz, 1H), 8.20 (d, *J* = 8.5 Hz, 1H), 7.83 (d, *J* = 7.5 Hz, 1H), 7.56 (p, *J* = 8.3, 7.8 Hz, 4H), 7.41 (d, *J* = 6.8 Hz, 2H), 7.37 (t, *J* = 7.4 Hz, 1H), 7.32 (d, *J* = 7.5 Hz, 1H), 7.28 (d, *J* = 4.2 Hz, 1H), 3.32 (s, 2H); ^{13}C NMR (150 MHz, $CDCl_3$) δ 148.4, 144.1, 141.0, 140.9, 140.8, 139.4, 130.2, 128.8, 128.6, 128.5, 127.5, 126.8, 126.8, 125.1, 124.5, 123.0, 122.3, 119.7, 118.5, 39.2; IR (KBr)ν_{max}/cm^{-1} 3020 (C–H), 2906 (C–H), 1622 (C=C), 1372 (C–O); HRMS (ESI) Calcd For $C_{22}H_{16}N$ 294.1278 ($M+H^+$); Found 294.1279.

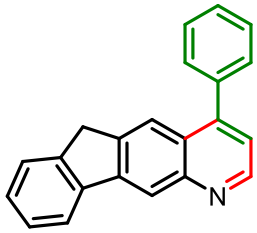

4-Phenyl-1,10-phenanthroline (3v) White solid (202.47 mg, 79%). mp 106-108 °C ^{1}H NMR (600 MHz, $CDCl_3$) δ 8.42 (d, *J* = 12.6 Hz, 2H), 8.33 (s, 1H), 7.99 – 8.02 (m, 4H), 7.95 (d, *J* = 9.0 Hz, 1H), 7.46 – 7.49 (m, 3H), 7.39 (dd, *J* = 8.5, 1.4 Hz, 1H); ^{13}C NMR (150 MHz, $CDCl_3$) δ 132.3, 131.8, 131.8, 131.2, 130.0, 129.8, 128.3, 128.3, 128.2, 126.7, 126.6, 126.4, 126.3, 126.1, 125.8, 125.5; IR (KBr)ν_{max}/cm^{-1} 3011 (C–H), 2906 (C–H), 1622 (C=C), 1372 (C–O); HRMS (ESI) Calcd For $C_{18}H_{13}N_2$ 257.1074 ($M+H^+$); Found 257.0742.

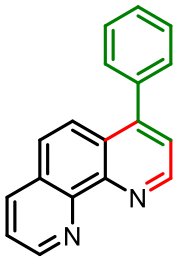

^{1}H NMR Spectrum of 6-Methoxy-4-phenylquinoline (3a)

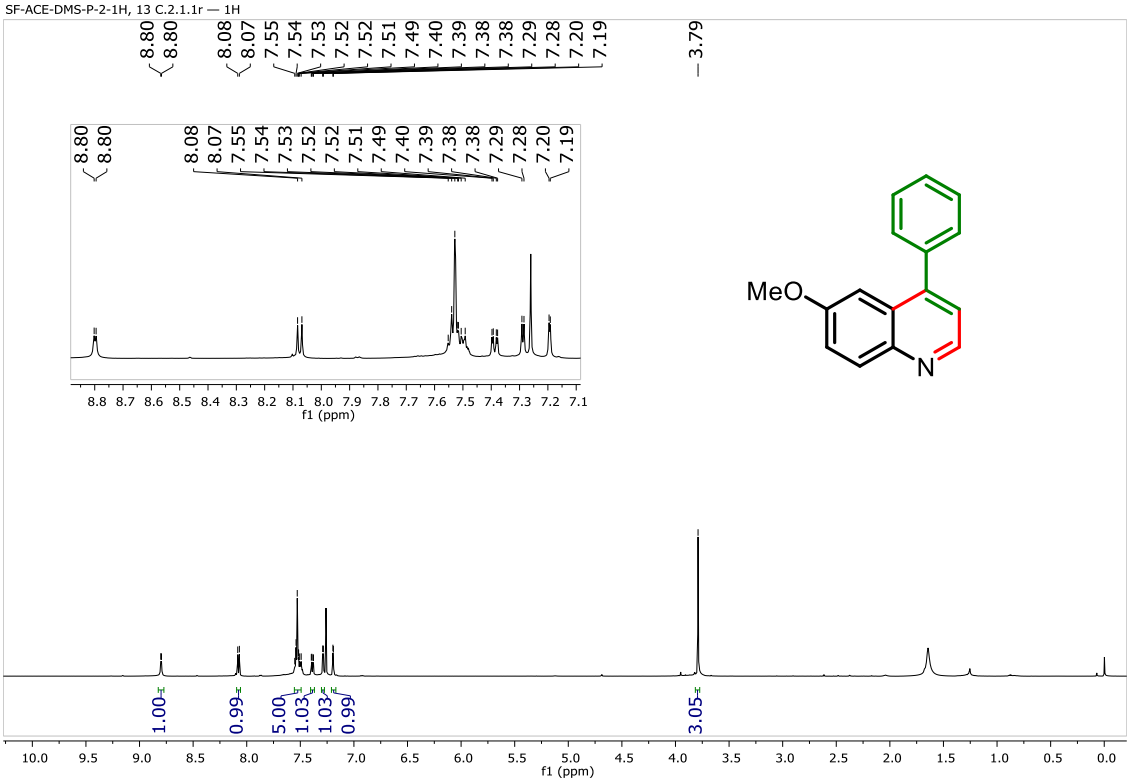

^{13}C NMR Spectrum of 6-Methoxy-4-phenylquinoline (3a)

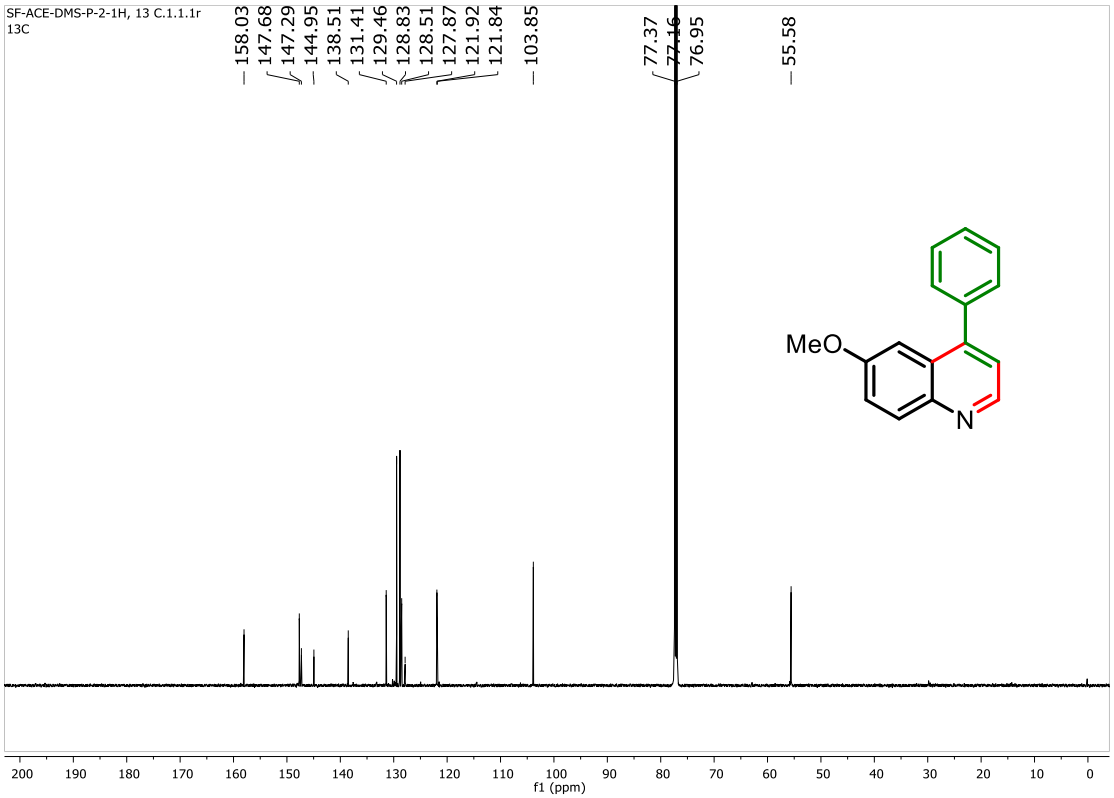

HRMS Spectrum of 6-Methoxy-4-phenylquinoline (3a)

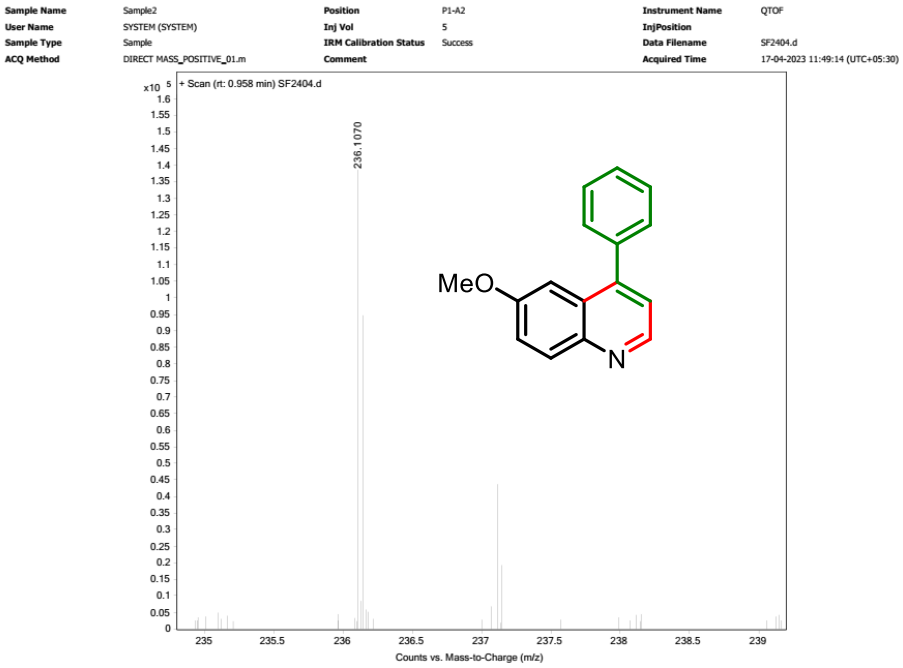

^{1}H NMR Spectrum of 4-Phenylquinoline(3o)

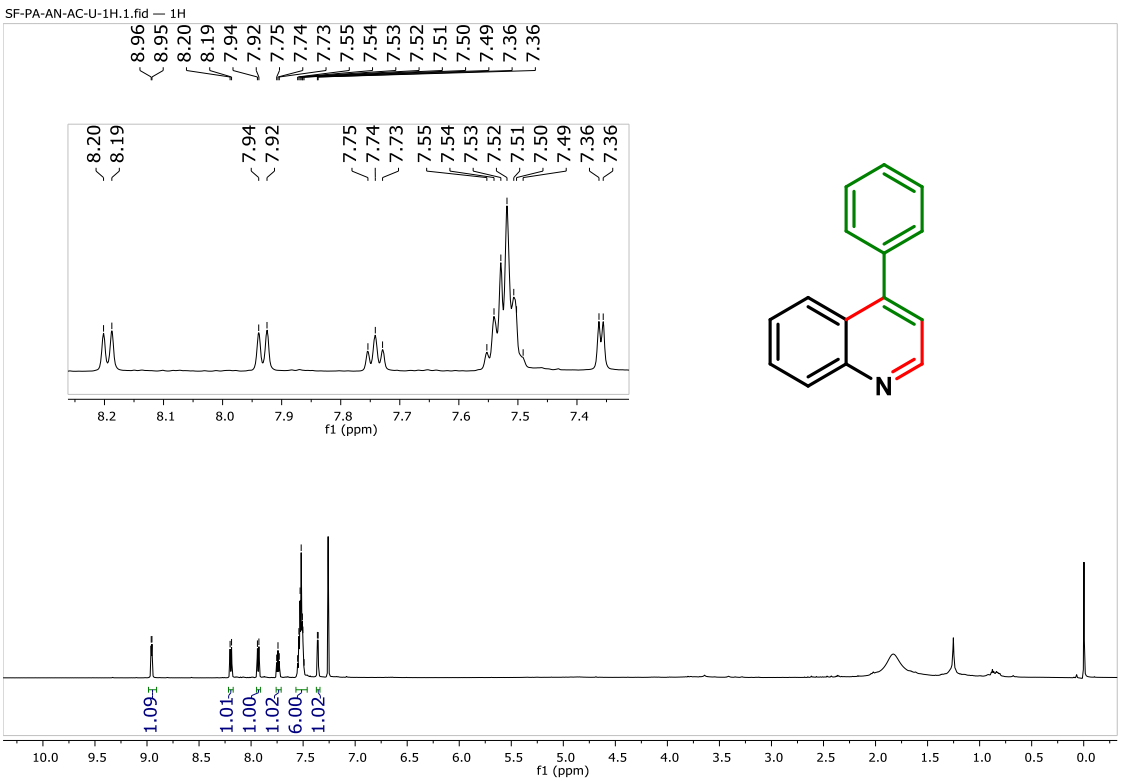

^{13}C NMR Spectrum of 4-Phenylquinoline(3o)

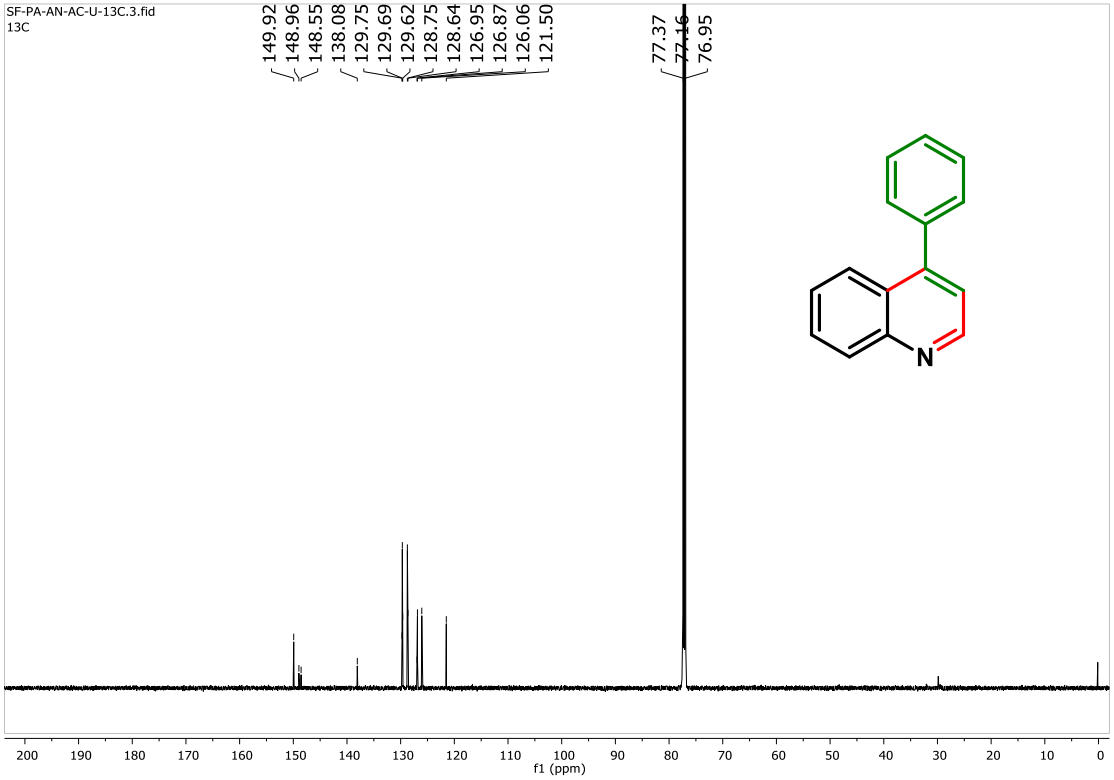

HRMS Spectrum of 4-Phenylquinoline(3o)

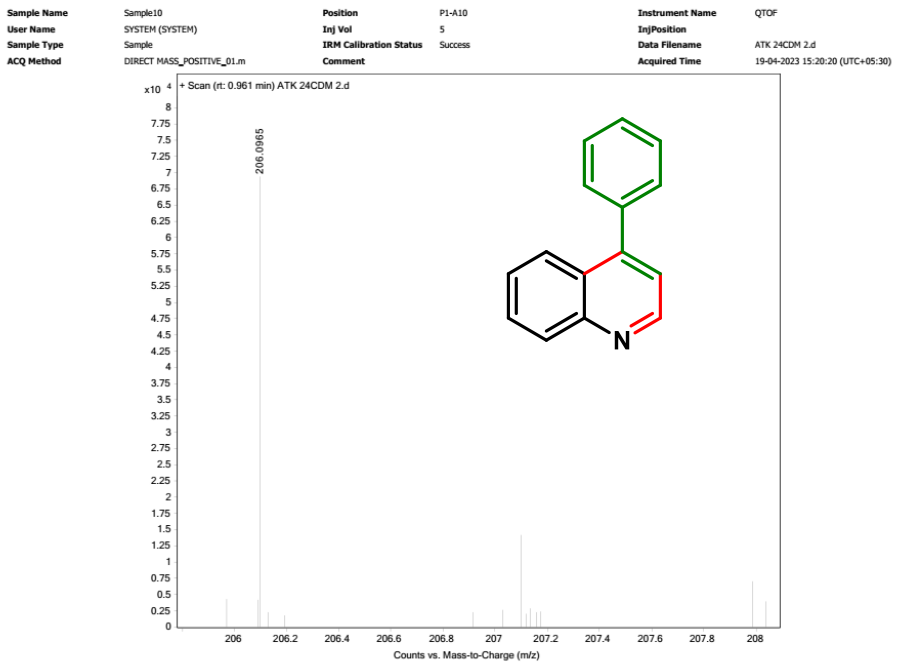

Part A

Chapter II: Section B

Synthesis of 2,3-diarylquinoline derivatives

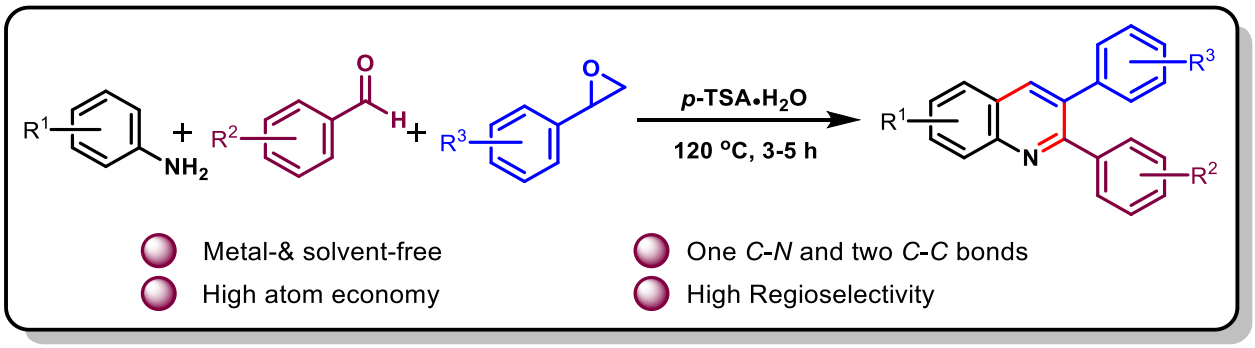

RESULT AND DISCUSSION

EXPERIMENTAL SECTION

Results and Discussion

In Chapter I, the importance and synthetic methodologies utilized for the synthesis of 2,3-diarylquinoline have been thoroughly elucidated. In recent times, the multicomponent reactions approach has emerged as an important synthetic tool in modern organic chemistry for the total synthesis of natural products and synthetic building blocks.[34] Considering the aforementioned advantages of MCRs, we explored this tool for synthesising 2,3-diarylquinoline derivatives. This part of the chapter emphasizes an environmentally benign synthesis of 2,3-diarylylquinoline *via* a one-pot three-component reaction from aryl amines, benzaldehyde, and styrene oxide in the presence of 20 mol% *p*-TSA•H_2O at 120 °C under mild reaction conditions (Scheme 18). The salient features of this protocol are easy handling, broad substrate scope, shorter reaction time, high atom economy and regioselectivity, good yields, and the formation of one *C–N* and two *C–C* bonds take place in a single step.

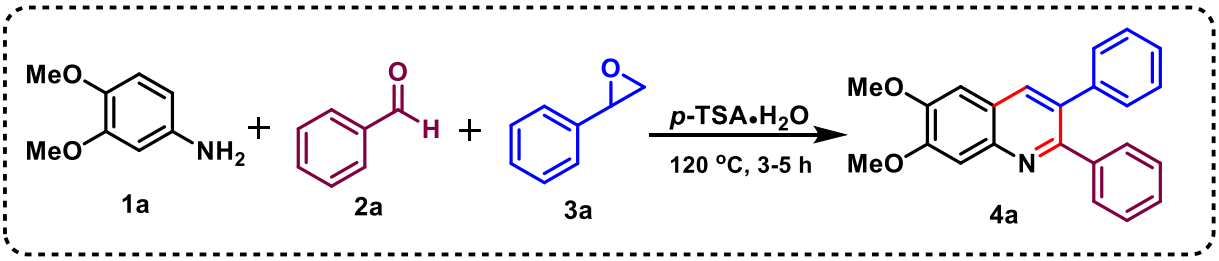

Scheme 18. Synthetic approach for the synthesis of 2,3-diarylquinolines derivatives.

The optimization studies were examined with 3,4-dimethoxy aniline (**1a**, 1.0 mmol), benzaldehyde (**2a**, 1.0 mmol), and styrene oxide (**3a**, 1.0 mmol), as demonstrated in Table 4. Initially, the reaction was carried out without a catalyst at room temperature and 120 °C. No desired product **4a** is obtained in both cases (Table 4, Entries 1 and 2). Next, the reaction was examined with 5 mol% of *p*-TSA•H_2O at room temperature. Unfortunately, the reaction did not proceed (Table 4, Entry 3). Interestingly, when the same reaction was performed at 60 °C, 80 °C, and 100 °C, the desired product was obtained in 30%, 42%, and 49% respectively (Table 4, Entries 4, 5, and 6). From the spectral analysis of compound **4a** by IR, ^{1}H NMR, ^{13}C NMR, and HRMS (experimental section), it was found to be 6,7-dimethoxy-2,3-diphenylquinoline **4a**. As the temperature was increased to 120 °C, the desired product **4a** was isolated in 68 % yield in 5 h (Table 4, Entry 7). The reaction provides better yield at 120 °C as the catalyst *p*-TSA•H_2O is melted at this temperature, and it acts as solvent cum catalyst. Further, the same reaction is scrutinized with 10 mol% catalysts to make the process more efficient and yield increase (Table 4, Entry 8). Subsequently, the reaction was scrutinized with 20 mol% catalysts,

and the yield was further improved to 88% in 3 h (Table 4, Entry 9). It was observed that reaction time was also reduced. To examine the effectiveness of other catalysts, we also examined the same reaction with no-metal catalyst I_2, MsOH, and (±)-CSA, respectively. The corresponding yields were obtained 69%, 35%, and 38% (Table 4, Entries 10, 11, & 12). In order to further increase the yield of the desired product as well as to find out the solvent effect, reactions were performed in the presence of different solvents such as DMSO, DMF, and toluene. For these reactions, the desired product **4a** was isolated in 68%, 63%, and 55%, respectively (Table 4, Entries 13, 14, & 15).

Table 4. Optimization of reaction conditions[a,b]

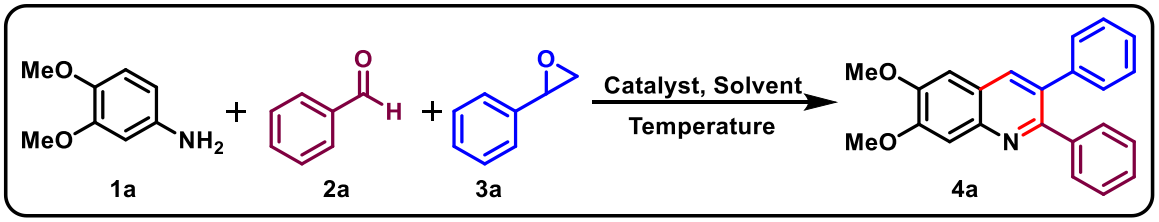

Entry	Catalysts	Mol%	Temp (°C)	Solvent	Time (h)	Yield[b] (%)
1[c]	-	-	RT	-	10	ND
2	-	-	120	-	10	ND
3[c]	*p*-TSA.H_2O	5	RT	-	10	ND
4	*p*-TSA.H_2O	5	60	-	6	30
5	*p*-TSA.H_2O	5	80	-	5	42
6	*p*-TSA.H_2O	5	100	-	4	49
7	*p*-TSA.H_2O	5	120	-	5	68
8	*p*-TSA.H_2O	10	120	-	3	73
9	***p*-TSA.H_2O**	**20**	**120**	**-**	**3**	**88**
10	I_2	20	120	-	8	69
11	MsOH	20	120	-	6	35
12	(±)-CSA	20	120	-	6	38
13	*p*-TSA.H_2O	20	120	DMSO	3	68
14	*p*-TSA.H_2O	20	120	DMF	3	63
15	*p*-TSA.H_2O	20	120	Toluene	3	55

[a]Reaction conditions: All the reactions were performed using 3,4-dimethoxy aniline (**1a**, 1.0 mmol), benzaldehyde (**2a**, 1.0 mmol), and styrene oxide (**3a**, 1.0 mmol). [b]Isolate yield. [C]Reaction performed at the room temperature. ND: No desired product was obtained.

After screening all the parameters, it was concluded that *p*-TSA**.**H_2O is the most effective catalyst for this reaction at 120 °C in solvent-free conditions. Notably, it was observed that the efficiency of *p*-TSA**.**H_2O as a catalyst decreases when a solvent is used in a reaction. *p*-TSA**.**H_2O as a catalyst is more efficient in solvent-free conditions.

With the optimized reaction condition in hand, we explored the feasibility and impact of substituent variation on aryl amines with benzaldehyde and styrene oxide. The successful result showed that the reaction goes smoothly, providing desired products in high to moderate yields with high regioselectivity. The number of substituents, electronic, and steric effects of the substituent on the arylamines did not influence the efficiency of the reaction such as disubstituted arylamines **1a**, **1b**, and **1c** gave the desired product **4a**, **4b**, and **4c** in 88%, 75%, and 85% yield, respectively. To further evaluate the scope of this method, trisubstituted aniline was scrutinized. As expected trisubstituted arylamine **1d** also behaves very well and provides the desired product **4d** in 88% yield. Subsequently, the scope of the reaction was further explored using a variety of substituted benzaldehyde and styrene oxide. For example, benzaldehyde having electron-withdrawing substituent **2b**, **2c**, **2d**, **2e**, and **2f** react with *p*-anisidine **1e** and styrene oxide **3a,** give expected product **4e**, **4f**, **4g**, **4h**, and **4i** in 80%, 78%, 81%, 80%, and 75%, respectively. Similarly, electron-rich benzaldehyde **2g**, **2h**, **2i**, and **2j** provide the corresponding products **4j**, **4k**, **4l**, and **4m** in 78%, 85%, 82%, and 85% yield. Furthermore, 2-naphthaldehyde **2k** was also found to be compatible under present conditions and furnished the desired product **4n** in 75% yield. Interestingly, substituted styrene oxide **3b** (4-Cl) and **3c** (4-Br) proceeded smoothly with *p*-anisidine and 4-methylbenzaldehyde under the given condition to give the expected products **4o** and **4p** in 79% and 80%, respectively. Electron-rich styrene oxide (4-Me) **3d** also behaves very well with *p*-anisidine **1e** and 4-bromobenzaldehyde **2f** to give the desired product **4q** in 79% yield. It was worth mentioning that 4-(methylthio)aniline **1f** reacts very well with 4-chlorobenzaldehyde **2d** and 3-bromobenzaldehyde **2e** to give the corresponding product in 78% and 85% yield respectively.

It is important to mention that the presence of electron-withdrawing substituents such as F, Cl, Br, and NO_2 on arylamines gave no desired product as expected under similar reaction conditions because of less electron density at the *ortho*-position of the intermediate [**A**]. Similarly, the reaction was unsuccessful in obtaining the desired product with 4-fluoro styrene oxide **3e** due to less electrophilicity. Unfortunately, *ortho*-methyl styrene oxide **3f** and *meta*-

methyl styrene oxide **3g** also did not give the expected product because of steric hindrance during the cyclization process as shown in Table 5.

Table 5. Substrate scope with different arylamines **1a-i** and benzaldehyde **2a** and styrene oxide **3a**.[a,b]

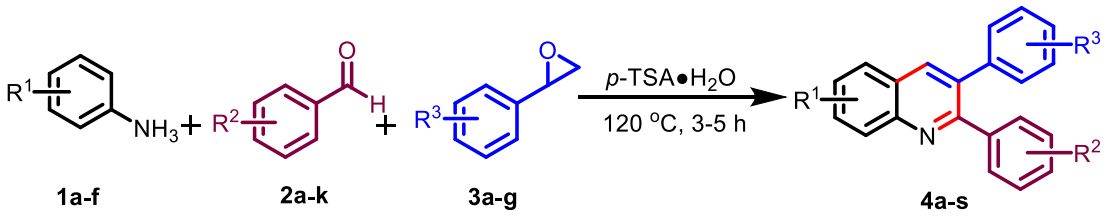

1a-f **2a-k** **3a-g** **4a-s**

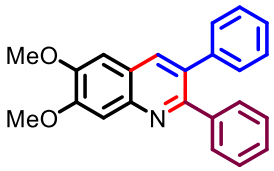

4a, 5 h, 88%

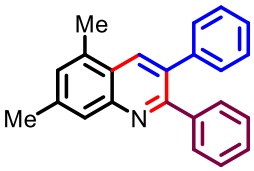

4b, 4.5 h, 75%

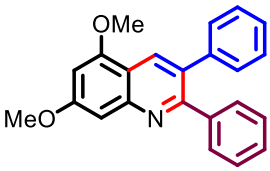

4c, 3.5 h, 85%

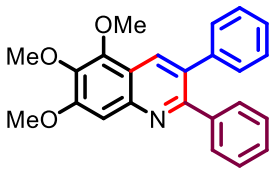

4d, 3 h, 88%

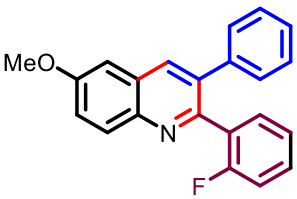

4e, 4 h, 80%

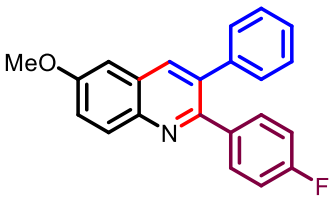

4f, 4.5 h, 78%

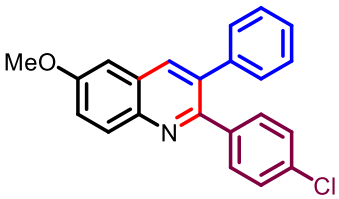

4g, 4.5 h, 81%

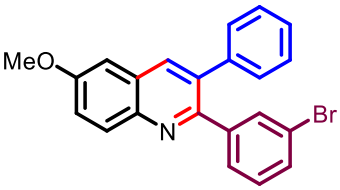

4h, 5 h, 80%

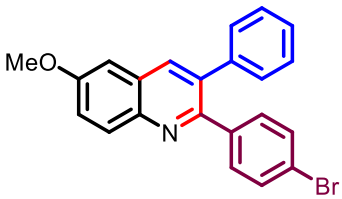

4i, 3 h, 75%

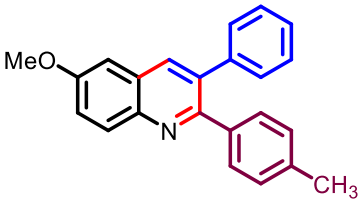

4j, 4 h, 78%

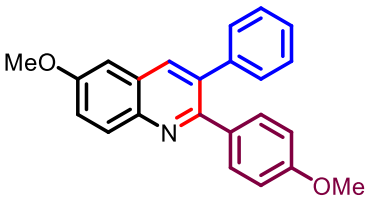

4k, 5 h, 85%

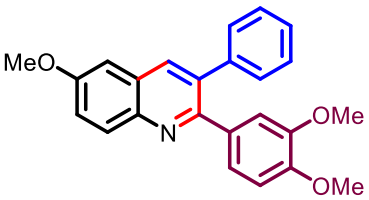

4l, 5 h, 82%

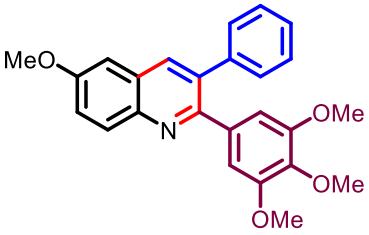

4m, 4.5 h, 85%

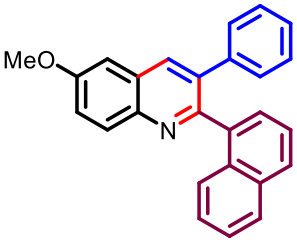

4n, 5 h, 75%

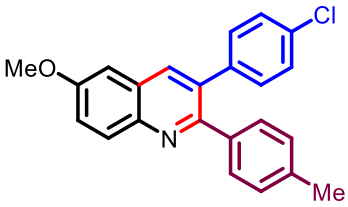

4o, 4.5 h, 79%

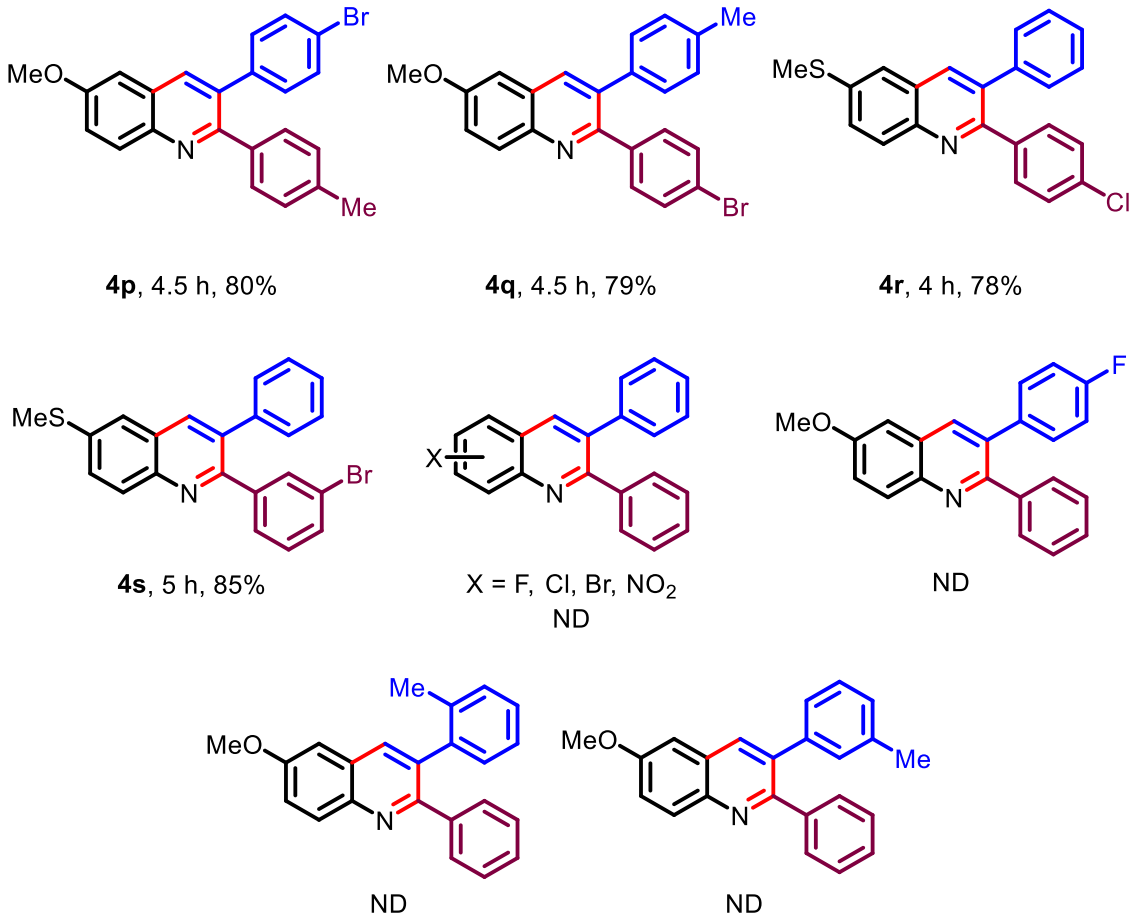

[a]Reaction conditions: All the reactions were performed using substituted anilines (**1a-f**, 1.0 mmol), benzaldehyde (**2a-k**, 1.0 mmol), and styrene oxide (**3a-g**, 1.0 mmol) in the presence of *p*-TSA•H_2O at 120 °C. [b]Isolated yield. ND: No desired product.

Table 6. Reaction between *p*-anisidine, **1e** and styrene oxide with aliphatic aldehyde[a,b]

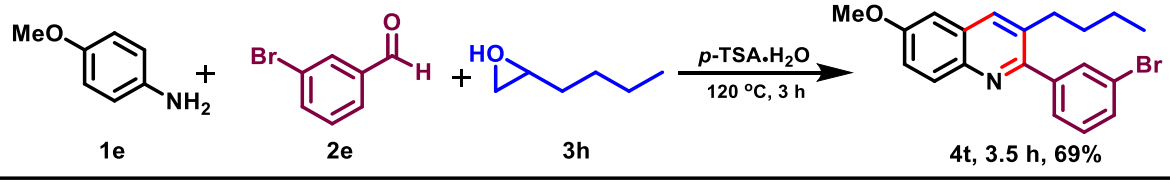

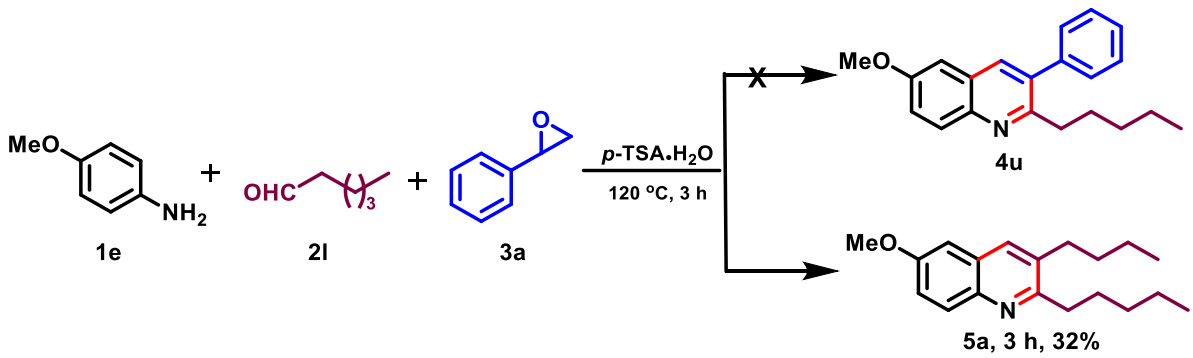

[a]Reaction conditions: All the reactions were performed using *p*-anisidine (**1e**, 1.0 mmol), 3-bromobenzaldehyde(**2e**), aliphatic aldehyde (**2l**, 1.0 mmol), and epoxide (**3h**), styrene oxide (**3a**, 1.0 mmol) in the presence of *p*-TSA•H_2O at 120 °C. [b]Isolated yield.

Next, we decided to apply the same reaction conditions for the 1,2-epoxyhexane **3h** with *p*-anisidine **1e** and 3-bromobenzaldehyde **2e**. Surprisingly, the reaction between **3h** with **1e** and **2e** gave the expected product 2-aryl-3-alkylquinoline **4t** in 69%. Encouraged by the successful result mentioned above, we further checked the practicality of the reaction with aliphatic aldehyde **2l** with *p*-anisidine **1e** and styrene oxide **3a**. Unfortunately, this time we obtained 2,3-dialkyquinoline **5a** in place of 2-alkyl-3-arylquinoline **4u** as shown in Table 6.

To understand the reaction pathway, we carried out two control experiments (Scheme 19). Where first the reactants *p*-anisidine and 4-methoxybenzaldehyde were stirred for 1 h in the presence of *p*-TSA•H_2O at 120 °C After 1 hr, the styrene oxide was added, and the desired product **4k** was isolated in 86% yield. However, in the second case, the reaction was performed with a different sequence of adding the reagents, the product 2-benzyl-3-phenylquinoline **6a** was obtained in 42% yield instead of **4k** along with the imine **7a** of 45% yield. From these two experiments, we conclude that imine formation occurs first and then reacts with the styrene oxide.

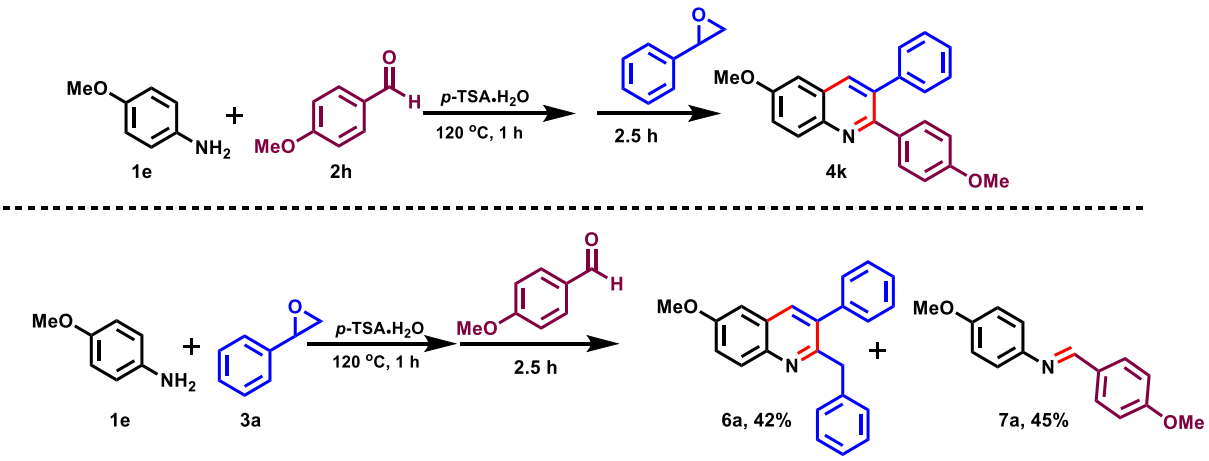

Scheme 19. Control experiment.

Based on control experimental results and the previous literature report,[15] a plausible reaction mechanism is shown in (Scheme 20). First, Imine **A** (Schiff base) is formed by reacting 3,4-dimethoxy aniline **1a** with benzaldehyde **2a**. Then, imine **A** reacts with styrene oxide **3a** in the presence of *p*-TSA•H_2O to give intermediate **B** which undergoes aromatization to give intermediate **C**. Elimination of water takes place from intermediate **C** to form the next intermediate **D**. The intermediate **D** undergoes 6π electrocyclization to form intermediate **E**.

Next [1,5] H shift takes place to form dihydroquinoline **F**. At last, intermediate **F** undergoes aerial oxidation to form desired product **4a**. Mechanistic studies show that an *in situ* formed imine intermediate may be a key intermediate for the reaction.

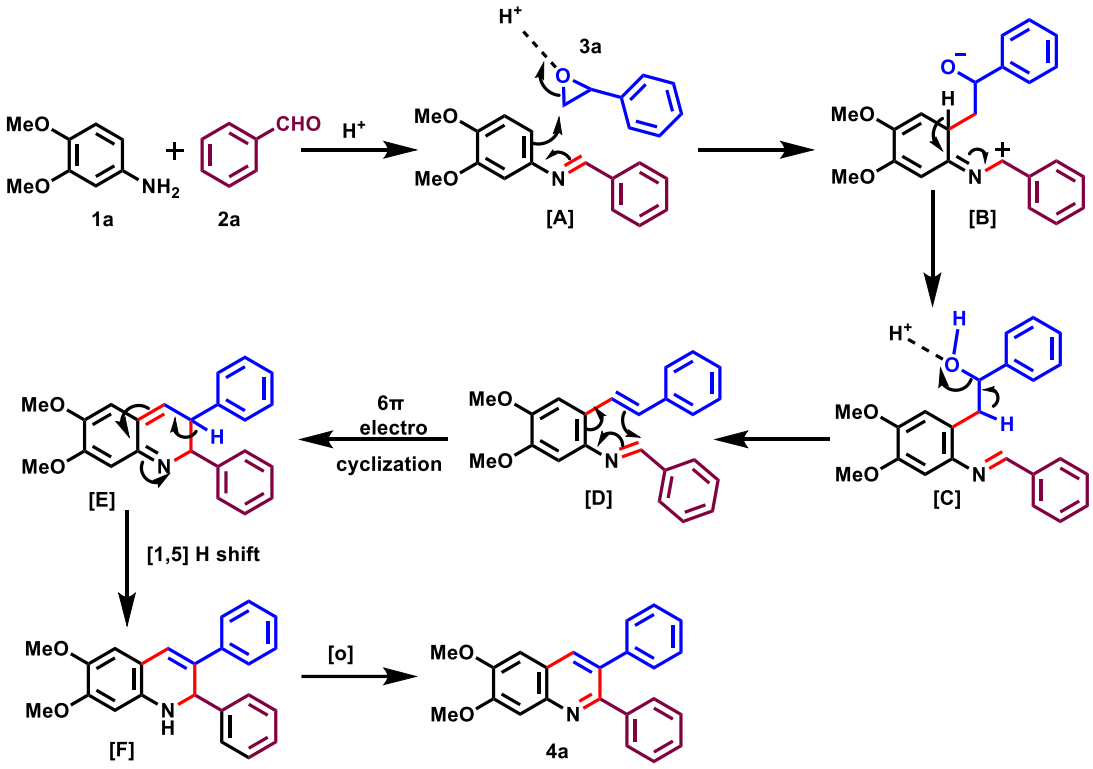

Scheme 20. The plausible mechanism for the formation of the desired product.

In conclusion, a reliable, straightforward, and operationally simple method for the synthesis of 2,3-diarylquinoline from the readily available starting material in the presence of low-cost catalyst *p*-TSA•H_2O has been developed. This protocol does not require any metal or harsh reaction conditions, providing a green alternative synthetic pathway for the synthesis of 2,3-diarylquinoline compared to existing methods.

Experimental Section

General procedure for the synthesis of 2,3-diarylquinoline derivatives.

Arylamine (**1**, 1.0 mmol), substituted benzaldehyde (**2**, 1.0 mmol), and substituted styrene oxide (**3**, 1.0 mmol) are mixed in the round-bottomed flask. *p*-TSA**.**H_2O (20 mol%) as a catalyst was added to the reaction mixture and kept in a pre-heated oil bath at 120 ^oC with constant stirring under an air atmosphere. The progress of the reaction was monitored by checking TLC. After the completion of the reaction, it was brought to room temperature. 0.1% aqueous solution of $NaCHO_3$ (5 ml) was added to the reaction mixture. Then it was extracted with ethyl acetate (5 mL x 2) and the organic layer was washed with a brine solution (5 mL x 2). Then dried with anhydrous sodium sulfate. After that, the solvent was removed in the rotary evaporator and the crude residue was purified by column chromatography using silica gel (60-120 mesh).

6,7-Dimethoxy-2,3-diphenylquinoline (4a) white solid (279.95 mg, 82%); mp 118-120 ^oC**.** ^1H NMR (600 MHz, $CDCl_3$) δ 8.09 (d, *J* = 7.6 Hz, 1H), 8.03 (s, 1H), 7.61 – 7.55 (m, 2H), 7.47 (t, *J* = 7.6 Hz, 1H), 7.42 – 7.41 (m, 2H), 7.28 – 7.27 (m, 3H), 7.23 (d, *J* = 7.5 Hz, 2H), 7.10 (s, 1H), 4.05 (s, 3H), 4.04 (s, 3H); ^{13}C NMR (150 MHz, $CDCl_3$) δ 156.2, 152.8, 150.2, 144.4, 140.7, 140.4, 136.1, 132.9, 130.1, 129.9, 128.30, 128.0, 127.8, 127.0, 122.9, 108.1, 104.8, 56.3, 56.2; IR (KBr)ν_{max}/cm^{-1} 3012 (Ar–H), 2924 (C–H), 1619 (C=C), 1231 (C–O); HRMS (ESI) Calcd For $C_{23}H_{20}NO_2$ 342.1489 $(M+H^+)$; Found 342.1489.

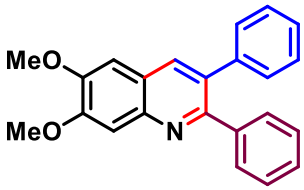

5,7-Dimethyl-2,3-diphenylquinoline (4b) Whitish yellow solid (232.05 mg, 75%); mp 110-113 ^oC. ^1H NMR (400 MHz, $CDCl_3$) δ 8.16 (d, *J* = 0.7 Hz, 1H), 7.77 (s, 1H), 7.36 (dd, *J* = 6.7, 3.0 Hz, 2H), 7.21 (dd, *J* = 5.3, 1.9 Hz, 3H), 7.19 – 7.16 (m, 5H), 7.15 (s, 1H), 2.59 (s, 3H), 2.45 (s, 3H); ^{13}C NMR (100 MHz, $CDCl_3$) δ 157.8, 148.0, 140.6, 140.6, 139.6, 134.2, 134.1, 133.3, 130.1, 129.9, 129.6, 128.3, 128.0, 127.9, 127.1, 126.7, 124.7, 22.0, 18.6; IR (KBr)ν_{max}/cm^{-1} 3032 (Ar–H), 2922 (C=H), 1605 (C–C); HRMS (ESI) Calcd For $C_{23}H_{20}N$ 310.1590 $(M+H^+)$; Found 310.1608.

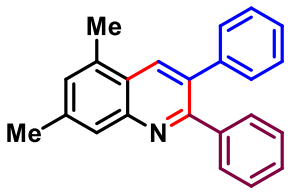

5,7-Dimethoxy-2,3-diphenylquinoline (4c) Yellowish white solid (290.19 mg, 85%); mp 113-115 °C. ^{1}H NMR (600 MHz, $CDCl_3$) δ 8.46 (s, 1H), 7.43 (dd, *J* = 6.4, 3.0 Hz, 2H),), 7.26 (dd, *J* = 6.4, 3.1 Hz, 6H), 7.23 (d, *J* = 7.9 Hz, 2H), 7.13 (d, *J* = 1.26 Hz, 1H), 6.53 (d, *J* = 1.9 Hz, 1H), 3.98 (s, 3H), 3.95 (s, 3H); ^{13}C NMR (150 MHz, $CDCl_3$) δ 161.6, 158.9 156.1, 149.4, 140.8, 140.5, 132.7, 131.6, 130.1, 129.9, 128.2, 128.0, 127.9, 126.9, 115.8, 99.8, 98.4, 55.9, 55.8; IR (KBr)ν_{max}/cm^{-1} 3018 (Ar–H), 2928 (C–H), 1620 (C=C), 1211 (C–O); HRMS (ESI) Calcd For $C_{23}H_{20}NO_2$ 342.1489 (M+H$^+$); Found 342.1489.

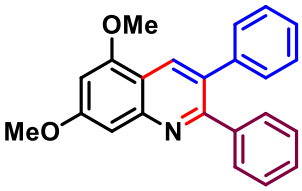

5,6,7-Trimethoxy-2,3-diphenylquinoline (4d) White solid (326.86 mg, 88%); mp 113-115 °C. ^{1}H NMR (600 MHz, $CDCl_3$) δ 8.36 (s, 1H), 7.42 – 7.40 (m, 2H), 7.36 (s, 1H), 7.30 – 7.27 (m, 6H), 7.24 (d, *J* = 7.7 Hz, 2H), 4.09 (s, 3H), 4.03 (s, 3H), 4.01 (s, 3H); ^{13}C NMR (150 MHz, $CDCl_3$) δ 157.8, 156.2, 147.0, 145.2, 141.1, 140.7, 140.5, 132.4, 132.1, 130.0, 130.0, 128.3, 128.0, 127.9, 127.0, 118.4, 104.3, 61.7, 61.4, 56.3; IR (KBr)ν_{max}/cm^{-1} 3024 (Ar–H), 2935 (C–H), 1610 (C=C), 1225 (C–O); HRMS (ESI) Calcd For $C_{24}H_{22}NO_3$ 372.1595 (M+H+); Found 372.1613.

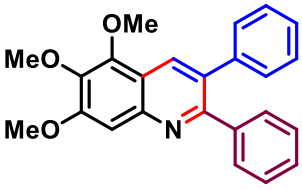

2-(2-Fluorophenyl)-6-methoxy-3-phenylquinoline (4e) Black solid (263.49 mg, 80%); mp 84-86 °C. ^{1}H NMR (400 MHz, $CDCl_3$) δ 8.05 – 8.03 (m, 2H), 7.48 (td, *J* = 7.4, 1.8 Hz, 1H), 7.34 (dd, *J* = 9.3, 2.8 Hz, 1H), 7.22 – 7.18 (m, 6H), 7.13 (dd, *J* = 7.5, 1.0 Hz, 1H), 7.09 (d, *J* = 2.8 Hz, 1H), 6.82 (t, *J* = 9.1 Hz, 1H), 3.91 (s, 3H); ^{13}C NMR (100 MHz, $CDCl_3$) δ 161.0, 158.4, 151.8, 143.4, 139.6, 136.0, 135.7, 131.8, 131.0, 130.2, 129.2, 128.7, 128.1, 127.3, 124.3, 122.6, 115.7, 115.5, 104.9, 55.7; IR (KBr)ν_{max}/cm^{-1} 3028 (Ar–H), 2920 (C–H), 1622 (C=C), 1232 (C–O); HRMS (ESI) Calcd For $C_{22}H_{17}FNO$ 330.1289 (M+H$^+$); Found 330.1306.

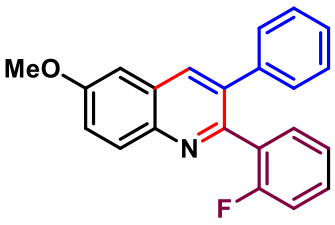

2-(4-Fluorophenyl)-6-methoxy-3-phenylquinoline (4f) Black solid (256.91 mg, 78%); mp 84-86 °C. ^{1}H NMR (400 MHz, $CDCl_3$) δ 8.07 (d, *J* = 9.2 Hz, 2H), 7.40 (ddd, *J* = 8.6, 5.3, 2.6 Hz, 3H), 7.31 (dd, *J* = 5.0, 1.9 Hz, 3H), 7.23 (dd, *J* = 6.9, 2.8 Hz, 2H), 7.12 (d, *J* = 2.8 Hz, 1H), 6.95 (t, *J* = 8.8 Hz, 2H), 3.96 (s, 3H); ^{13}C NMR (100 MHz, $CDCl_3$) δ 158.2, 154.9, 143.3, 140.1, 136.6, 134.7, 131.9, 131.9, 130.9, 129.8, 128.4,

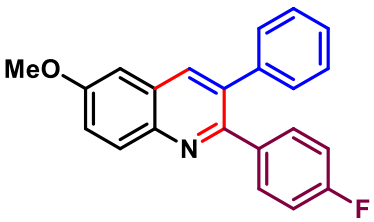

128.3, 127.4, 122.7, 115.1, 114.9, 104.9, 55.7; IR (KBr)ν_{max}/cm^{-1} 3022 (Ar–H), 2926 (C–H), 1623 (C=C), 1230 (C–O); HRMS (ESI) Calcd For $C_{22}H_{17}FNO$ 330.1289 ($M+H^+$); Found 330.1317.

2-(4-Chlorophenyl)-6-methoxy-3-phenylquinoline (4g) Brown solid (280.11 mg, 81%); mp 148-150 °C. ^{1}H NMR (400 MHz, $CDCl_3$) δ 8.07 (d, *J* = 8.6 Hz, 2H), 7.41 – 7.38 (m, 2H), 7.37 – 7.36 (m, 1H), 7.32 (dd, *J* = 5.0, 1.8 Hz, 2H), 7.26 – 7.22 (m, 5H), 7.12 (d, *J* = 2.8 Hz, 1H), 3.96 (s, 3H); ^{13}C NMR (100 MHz, $CDCl_3$) δ 158.3, 154.6, 143.6, 140.0, 139.1, 136.7, 134.7, 134.0, 131.5, 131.0, 129.8, 128.5, 128.4, 128.2, 127.4, 122.7, 104.9, 55.7; IR (KBr)ν_{max}/cm^{-1} 3025 (Ar–H), 2926 (C–H), 1623 (C=C), 1232 (C–O); HRMS (ESI) Calcd For $C_{22}H_{17}ClNO$ 346.0993 ($M+H^+$); Found 346.0993.

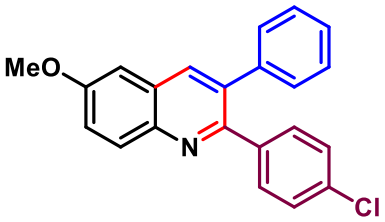

2-(3-Bromophenyl)-6-methoxy-3-phenylquinoline (4h) Brown liquid (312.22 mg, 80%). ^{1}H NMR (500 MHz, $CDCl_3$) δ 8.10 – 8.07 (m, 2H), 7.72 (t, *J* = 1.9 Hz, 1H), 7.42 – 7.39 (m, 2H), 7.32 (dd, *J* = 5.3, 1.8 Hz, 3H), 7.25 – 7.22 (m, 3H), 7.13 (d, *J* = 2.6 Hz, 1H), 7.07 (t, *J* = 7.8 Hz, 1H), 3.96 (s, 3H); ^{13}C NMR (125 MHz, $CDCl_3$) δ 158.4, 154.2, 143.5, 142.6, 139.8, 136.7, 134.8, 133.1, 131.0, 130.9, 129.8, 129.3, 128.8, 128.5, 128.5, 122.8, 122.3, 104.9, 55.7; IR (KBr)ν_{max}/cm^{-1} 3066 (Ar–H), 2929 (C–H), 1622 (C=C), 1245 (C–O); HRMS (ESI) Calcd For $C_{22}H_{17}BrNO$ 390.0494 ($M+H^+$); Found 390.0524.

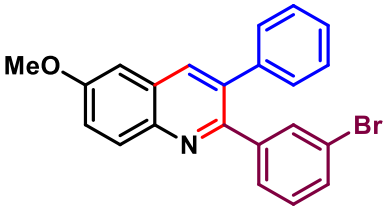

2-(4-Bromophenyl)-6-methoxy-3-phenylquinoline (4i) Brown solid (292.71 mg, 75%); mp 140-144 °C. ^{1}H NMR (400 MHz, $CDCl_3$) δ 8.07 (d, *J* = 8.6 Hz, 2H), 7.41 – 7.39 (m, 3H), 7.32 (dd, *J* = 5.0, 1.8 Hz, 5H), 7.24 – 7.23 (m, 2H), 7.12 (d, *J* = 2.8 Hz, 1H), 3.96 (s, 3H); ^{13}C NMR (100 MHz, $CDCl_3$) δ 158.3, 154.6, 143.6, 139.9, 139.5, 136.7, 134.6, 131.8, 131.2, 131.0, 129.8, 128.5, 128.4, 127.5, 122.7, 122.4, 104.9, 55.7; IR (KBr)νmax/cm^{-1} 3021 (Ar–H), 2925 (C–H), 1622 (C=C), 1233 (C–O); HRMS (ESI) Calcd For $C_{22}H_{17}BrNO$ 390.0494 ($M+H^+$); Found 390.0482.

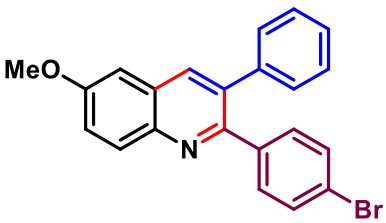

6-Methoxy-3-phenyl-2-(*p*-tolyl)quinoline (4j) Yellow liquid (253.81 mg, 78%). ^{1}H NMR (400 MHz, $CDCl_3$) δ 8.08 (d, *J* = 9.2 Hz, 1H), 8.04 (s, 1H), 7.38 (dd, *J* = 9.2, 2.8 Hz, 1H), 7.33 – 7.28 (m, 5H), 7.26 – 7.24 (m, 2H), 7.11 (d, *J* = 2.8 Hz, 1H), 7.07 (d, *J* = 7.9 Hz, 2H), 3.95 (s, 3H), 2.32 (s, 3H); ^{13}C NMR (100 MHz, $CDCl_3$) δ 158.0, 156.0, 143.5, 140.4, 137.7, 137.6, 136.5, 134.8, 130.9, 130.0, 129.8, 128.7, 128.3, 128.2, 127.2, 122.4, 104.9, 55.7, 21.3; IR (KBr)ν_{max}/cm^{-1} 3025 (Ar–H), 2923 (C–H), 1622 (C=C), 1232 (C–O); HRMS (ESI) Calcd For $C_{23}H_{20}NO$ 326.1545 ($M+H^+$); Found 326.1563.

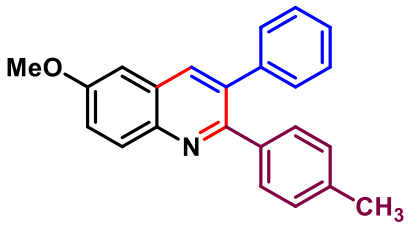

6-Methoxy-2-(4-methoxyphenyl)-3-phenylquinoline (4k) Brown liquid (290.19 mg, 85%). ^{1}H NMR (600 MHz, $CDCl_3$) δ 8.06 (d, *J* = 8.9 Hz, 1H), 8.01 (s, 1H), 7.36 – 7.33 (m, 3H), 7.27 (q, *J* = 5.7 Hz, 3H), 7.22 (d, *J* = 5.7 Hz, 2H), 7.08 (d, *J* = 2.0 Hz, 1H), 6.76 (d, *J* = 8.5 Hz, 2H), 3.92 (s, 3H), 3.76 (s, 3H); ^{13}C NMR (150 MHz, $CDCl_3$) δ 159.5, 158.0, 155.5, 143.4, 140.4, 136.7, 134.8, 131.5, 130.7, 129.8, 129.4, 128.4, 128.1, 127.2, 122.5, 113.5, 104.9, 55.7, 55.39; IR (KBr)ν_{max}/cm^{-1} 3018 (Ar–H), 2929 (C–H), 1619 (C=C), 1232 (C–O); HRMS (ESI) Calcd For $C_{23}H_{20}NO_2$ 342.1494 ($M+H^+$); Found 342.1490.

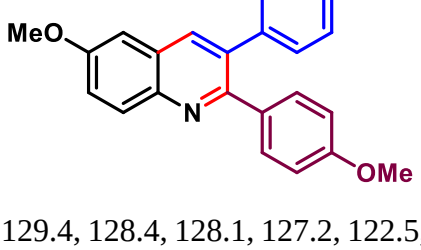

2-(3,4-Dimethoxyphenyl)-6-methoxy-3-phenylquinoline (4l) Brown liquid (304.57 mg, 82%). ^{1}H NMR (500 MHz, $CDCl_3$) δ 8.08 (d, *J* = 9.2 Hz, 1H), 8.04 (s, 1H), 7.38 (dd, *J* = 9.2, 2.5 Hz, 1H), 7.31 (t, *J* = 7.8 Hz, 2H), 7.29 – 7.27 (m, 2H), 7.12 – 7.10 (m, 2H), 6.90 (s, 1H), 6.80 (d, *J* = 8.3 Hz, 1H), 3.96 (s, 3H), 3.87 (s, 3H), 3.61 (s, 3H); ^{13}C NMR (125 MHz, $CDCl_3$) δ 158.0, 155.5, 149.0, 148.3, 143.6, 140.8, 136.6, 134.8, 133.1, 130.9, 129.8, 128.4, 128.2, 127.2, 123.0, 122.4, 113.7, 110.9, 105.0, 56.0, 55.7, 55.7; IR (KBr)ν_{max}/cm^{-1} 3011 (Ar–H), 2929 (C–H), 1623 (C=C), 1233 (C–O); HRMS (ESI) Calcd For $C_{24}H_{22}NO_3$ 372.1600 ($M+H^+$); Found 372.1605.

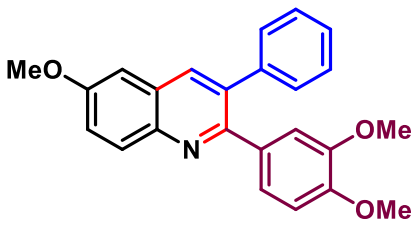

6-Methoxy-3-phenyl-2-(3,4,5-trimethoxyphenyl)quinoline (4m) Brown liquid (341.24 mg, 85%). ^{1}H NMR (600 MHz, $CDCl_3$) δ 8.09 (d, *J* = 9.2 Hz, 1H), 8.06 (s, 1H), 7.40 – 7.38 (m, 1H), 7.34 – 7.27 (m, 5H), 7.12 – 7.12 (m, 1H), 6.67 (s, 2H), 3.96 (s, 3H), 3.82 (s, 3H), 3.64 (s, 6H); ^{13}C NMR (150 MHz, $CDCl_3$) δ 158.2, 155.4, 152.7, 143.5, 140.6, 138.0, 136.6, 135.6, 134.8, 130.9, 129.7, 128.4, 128.3, 127.2, 122.6, 107.7, 104.9, 61.0, 55.9, 55.7; IR (KBr)ν_{max}/cm^{-1} 3014 (Ar–H), 2934 (C–H), 1590 (C=C), 1241 (C–O); HRMS (ESI) Calcd For $C_{25}H_{24}NO_4$ 402.1705 ($M+H^+$); Found 402.1696.

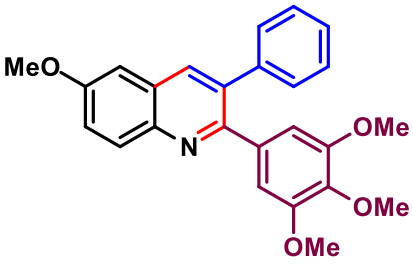

6-Methoxy-2-(naphthalen-1-yl)-3-phenylquinoline(4n) White semi-solid (271.08 mg, 75%). ^{1}H NMR (600 MHz, $CDCl_3$) δ 8.61 (s, 1H), 8.38 (d, *J* = 8.5 Hz, 1H), 8.20 (d, *J* = 9.1 Hz, 1H), 8.02 – 7.89 (m, 5H), 7.63 – 7.58 (m, 3H), 7.54 – 7.51 (m, 3H), 7.42 (dd, *J* = 9.5, 2.4 Hz, 1H), 7.22 – 7.20 (m, 1H), 3.82 (s, 3H); ^{13}C NMR (150 MHz, $CDCl_3$) δ 158.0, 154.5, 148.0, 145.1, 138.9, 137.1, 133.8, 133.7, 131.7, 129.5, 128.8, 128.6, 128.5, 127.8, 126.8, 126.8, 126.6, 126.4, 125.1, 122.0, 119.9, 103.9, 55.6; IR (KBr)ν_{max}/cm^{-1} 3027 (Ar–H), 2926 (C–H), 1622 (C=C), 1372 (C–O); HRMS (ESI) Calcd For $C_{26}H_{20}NO$ 362.1544 ($M+H^+$); Found 362.1554.

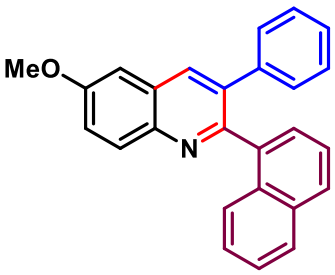

3-(4-Chlorophenyl)-6-methoxy-2-(*p*-tolyl)quinoline (4o) Brown liquid (284.28 mg, 79%). ^{1}H NMR (600 MHz, $CDCl_3$) δ 8.08 (d, *J* = 9.2 Hz, 1H), 8.01 (s, 1H), 7.39 (dd, *J* = 9.1, 2.4 Hz, 1H), 7.30 (d, *J* = 7.9 Hz, 2H), 7.27 (d, *J* = 8.9 Hz, 2H), 7.18 (d, *J* = 8.3 Hz, 2H), 7.10 (dd, *J* = 13.2, 5.1 Hz, 3H), 3.95 (s, 3H), 2.34 (s, 3H); ^{13}C NMR (150 MHz, $CDCl_3$) δ 158.1, 155.8, 143.7, 138.9, 137.9, 137.4, 136.4, 133.6, 133.3, 131.1, 131.0, 129.9, 128.9, 128.5, 128.1, 122.7, 104.9, 55.7, 21.4; IR (KBr)ν_{max}/cm^{-1} 3014(Ar–H), 2922(C–H), 1623 (C=C), 1222 (C–O); HRMS (ESI) Calcd For $C_{23}H_{19}ClNO$ 360.1155 ($M+H^+$); Found 360.1142.

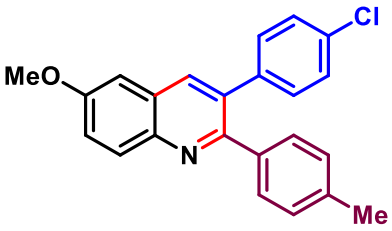

3-(4-Bromophenyl)-6-methoxy-2-(*p*-tolyl)quinoline (4p) Brown liquid (323.44 mg, 80%). ^{1}H NMR (600 MHz, $CDCl_3$) δ 8.08 (d, *J* = 9.2 Hz, 1H), 8.01 (s, 1H), 7.42 (d, *J* = 8.3 Hz, 2H), 7.39 (dd, *J* = 9.2, 2.5 Hz, 1H), 7.30 (d, *J* = 7.9 Hz, 2H), 7.11 (dd, *J* = 17.2, 8.0 Hz, 5H), 3.95 (s, 3H), 2.34 (s, 3H); ^{13}C NMR (150 MHz, $CDCl_3$) δ 158.1, 155.7, 143.7, 139.4, 137.9, 136.4, 133.6, 131.7, 131.5, 131.4, 131.0, 129.9, 129.2, 128.9, 122.7, 121.5, 104.9, 55.7, 21.4; IR (KBr)ν_{max}/cm^{-1} 3022 (Ar–H), 2924 (C–H), 1620 (C=C), 1241 (C–O); HRMS (ESI) Calcd For $C_{23}H_{19}BrNO$ 404.0650 ($M+H^+$); Found 404.0641.

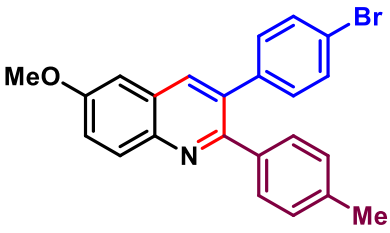

2-(4-Bromophenyl)-6-methoxy-3-(*p*-tolyl)quinoline (4q) Brown liquid (319.40 mg, 79%). ^{1}H NMR (400 MHz, $CDCl_3$) δ 8.09 – 8.05 (m, 2H), 7.74 (s, 1H), 7.41 – 7.38 (m, 2H), 7.21 (d, *J* = 7.8 Hz, 1H), 7.12 (d, *J* = 3.7 Hz, 5H), 7.0l7 (t, *J* = 7.9 Hz, 1H), 3.96 (s, 3H), 2.37 (s, 3H); ^{13}C NMR (150 MHz, $CDCl_3$) δ 158.1, 155.8, 143.7, 138.98, 137.9, 137.4, 136.5, 133.6, 133.3, 131.1, 131.0, 129.9, 128.9, 128.5, 128.1, 122.71, 104.9, 55.7, 21.4; IR (KBr)ν_{max}/cm^{-1} 3023(Ar–H), 2924 (C–H), 1620 (C=C), 1241 (C–O); HRMS (ESI) Calcd For $C_{23}H_{19}BrNO$ 404.0645 ($M+H^+$); Found 404.0639.

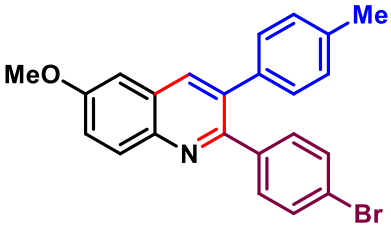

2-(4-Chlorophenyl)-6-(methylthio)-3-phenylquinoline (4r) Light yellow Solid (282.26 mg, 78%); mp 170-172 ^{o}C. ^{1}H NMR (600 MHz, $CDCl_3$) δ 8.06 – 8.04 (m, 2H), 7.61 (dd, *J* = 8.8, 2.1 Hz, 1H), 7.56 (d, *J* = 1.9 Hz, 1H), 7.38 (d, *J* = 8.5 Hz, 2H), 7.32 (dd, *J* = 4.9, 1.7 Hz, 3H), 7.25 – 7.22 (m, 4H), 2.61 (s, 3H); ^{13}C NMR (150MHz, $CDCl_3$) δ 156.1, 145.6, 139.7, 138.9, 138.1, 136.5, 135.0, 134.2, 131.5, 129.8, 129.6, 129.3, 128.5, 128.2, 127.8, 127.5, 122.0, 15.7; IR (KBr)ν_{max}/cm^{-1} 3023(Ar–H), 2924 (C–H), 1620 (C=C), 1241 (C–O); HRMS (ESI) Calcd For $C_{22}H_{17}ClNS$ 362.0765 ($M+H^+$); Found 362.0760.

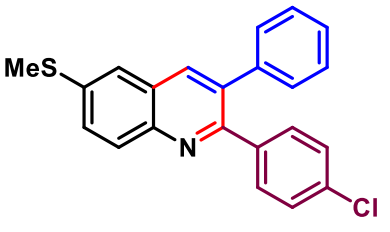

2-(3-Bromophenyl)-6-(methylthio)-3-phenylquinoline (4s) Light yellow liquid (345.38 mg, 85%). ^{1}H NMR (400 MHz, $CDCl_3$) δ 8.07 (d, *J* = 7.0 Hz, 2H), 7.73 (s, 1H), 7.62 (dd, *J* = 8.9, 1.8 Hz, 1H), 7.57 (d, *J* = 1.9 Hz, 1H), 7.41 (d, *J* = 7.3 Hz, 1H), 7.33 – 7.32 (m, 3H), 7.24 – 7.21 (m, 3H), 7.07 (t, *J* = 7.8 Hz, 1H), 2.62 (s, 3H); ^{13}C NMR (125 MHz, $CDCl_3$) δ 155.8, 145.6, 142.4, 139.5, 138.3, 136.5, 135.1,

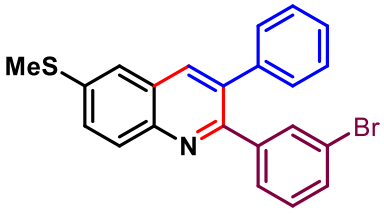

133.0, 131.1, 129.8, 129.7, 129.4, 129.3, 128.8, 128.5, 127.9, 127.6, 122.3, 122.0, 15.7; IR (KBr)ν_{max}/cm^{-1} 3020(Ar–H), 2924 (C–H), 1620 (C=C), 1241 (C–O); HRMS (ESI) Calcd For $C_{22}H_{17}BrNS$ 406.0260 (M+H$^+$); Found 406.0251.

2-(3-Bromophenyl)-3-butyl-6-methoxyquinoline (4t) Light Brown liquid (255.50 mg, 69%). ^{1}H NMR (600 MHz, $CDCl_3$) δ 8.00 (d, *J* = 9.2 Hz, 1H), 7.94 (s, 1H), 7.70 (t, *J* = 1.6 Hz, 1H), 7.56 (d, *J* = 8.0 Hz, 1H), 7.46 (d, *J* = 7.6 Hz, 1H), 7.35 – 7.32 (m, 2H), 7.06 (d, *J* = 2.7 Hz, 1H), 3.94 (s, 3H), 2.74 – 2.72 (m, 2H), 1.53 (p, *J* = 7.7 Hz, 2H), 1.30 – 1.25 (m, 2H), 0.84 (t, *J* = 7.4 Hz, 3H); ^{13}C NMR (150 MHz, $CDCl_3$) δ 158.1, 156.6, 143.0, 142.5, 135.0, 134.1, 132.1, 131.1, 130.7, 129.8, 128.9, 127.6, 122.5, 121.9, 104.4, 55.6, 32.9, 32.4, 22.4, 13.9; IR (KBr)ν_{max}/cm^{-1} 3014(Ar–H), 2922(C–H), 1623 (C=C), 1222 (C–O); HRMS (ESI) Calcd For $C_{20}H_{21}BrNO$ 370.0802 (M+H$^+$); Found 370.0803.

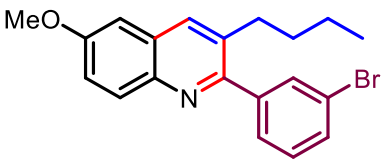

3-Butyl-6-methoxy-2-pentylquinoline (5a) Black liquid (91.33 mg, 32%). ^{1}H NMR (600 MHz, $CDCl_3$) δ 7.90 (d, *J* = 9.1 Hz, 1H), 7.75 (s, 1H), 7.27 (d, *J* = 2.8 Hz, 1H), 7.00 (d, *J* = 2.7 Hz, 1H), 3.91 (s, 3H), 2.94 – 2.91 (m, 2H), 2.78 – 2.75 (m, 2H), 1.79 – 1.74 (m, 2H), 1.69 – 1.64 (m, 2H), 1.45 (dt, *J* = 14.6, 7.3 Hz, 4H), 1.40 – 1.37 (m, 2H), 0.99 (t, *J* = 7.4 Hz, 3H), 0.92 (t, *J* = 7.2 Hz, 3H); ^{13}C NMR (150 MHz, $CDCl_3$) δ 159.8, 157.2, 142.6, 134.5, 134.0, 130.0, 128.1, 120.9, 104.7, 55.6, 35.7, 32.8, 32.3, 32.2, 29.7, 22.8, 22.7, 14.2, 14.1; IR (KBr)ν_{max}/cm^{-1} 3025 (C–H), 2952 (C–H), 1623 (C=C) 1233 (C–O); HRMS (ESI) Calcd For $C_{19}H_{28}NO$: 286.2166 (M+H$^+$); Found 286.2182.

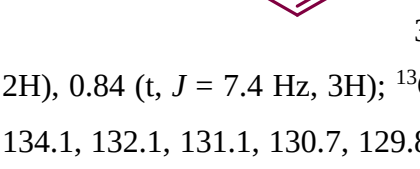

2-Benzyl-6-methoxy-3-phenylquinoline (6a) Light Brown liquid (136.5 mg, 42%). ^{1}H NMR (600 MHz, $CDCl_3$) δ 8.05 (d, *J* = 9.2 Hz, 1H), 7.86 (s, 1H), 7.38 (td, *J* = 5.0, 2.5 Hz, 4H), 7.20 – 7.19 (m, 2H), 7.13 – 7.08 (m, 3H), 7.05 (d, *J* = 2.7 Hz, 1H), 6.93 (d, *J* = 6.8 Hz, 2H), 4.29 (s, 2H), 3.93 (s, 3H); ^{13}C NMR (150 MHz, $CDCl_3$) δ 157.8, 156.6, 143.4, 139.9, 139.7, 136.4, 135.9, 130.4, 129.5, 128.9, 128.3, 128.1, 127.9, 127.6, 125.9, 122.1, 105.0, 55.7, 42.6; IR (KBr)ν_{max}/cm^{-1} 2924 (C–H), 1621 (C=C), 1228 (C–O); HRMS (ESI) Calcd For $C_{23}H_{20}NO$ 326.1539 (M+H$^+$); Found 326.1552.

^{1}H NMR Spectrum of 6,7-Dimethoxy-2,3-diphenylquinoline (4a)

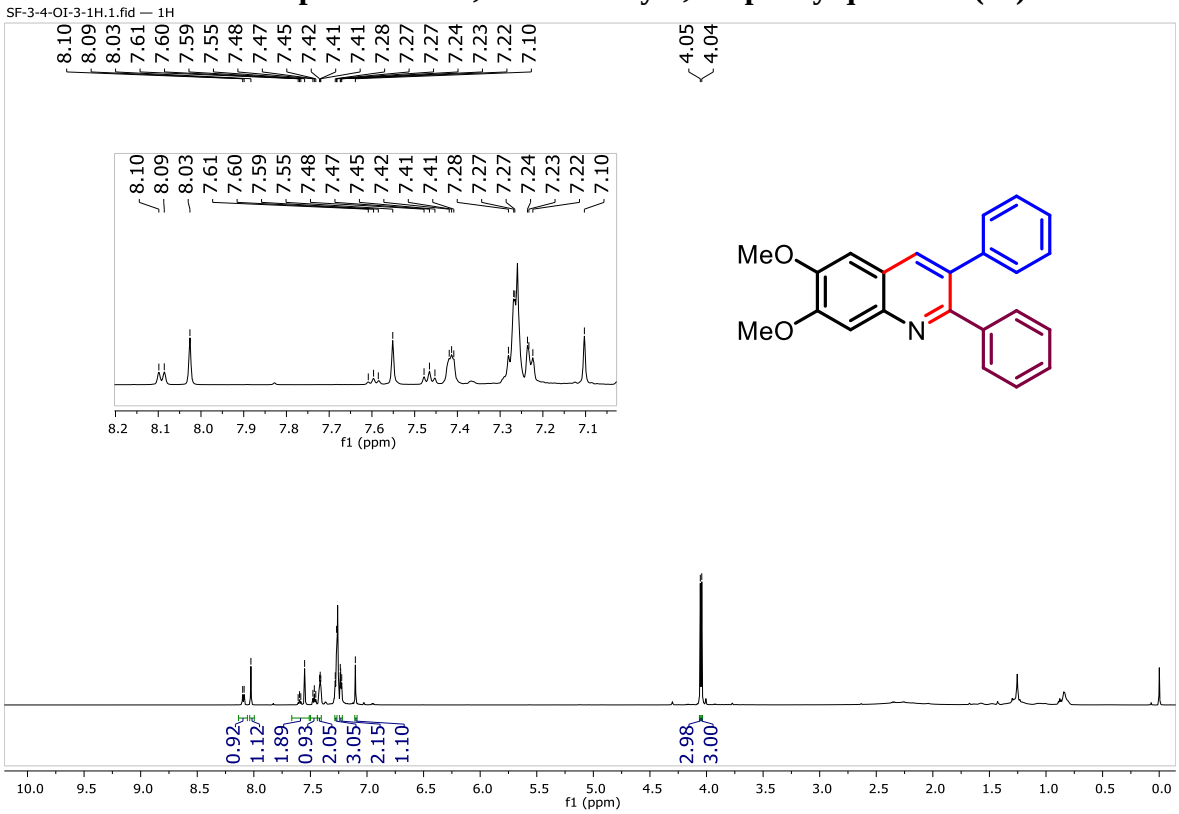

^{13}C NMR Spectrum of 6,7-Dimethoxy-2,3-diphenylquinoline (4a)

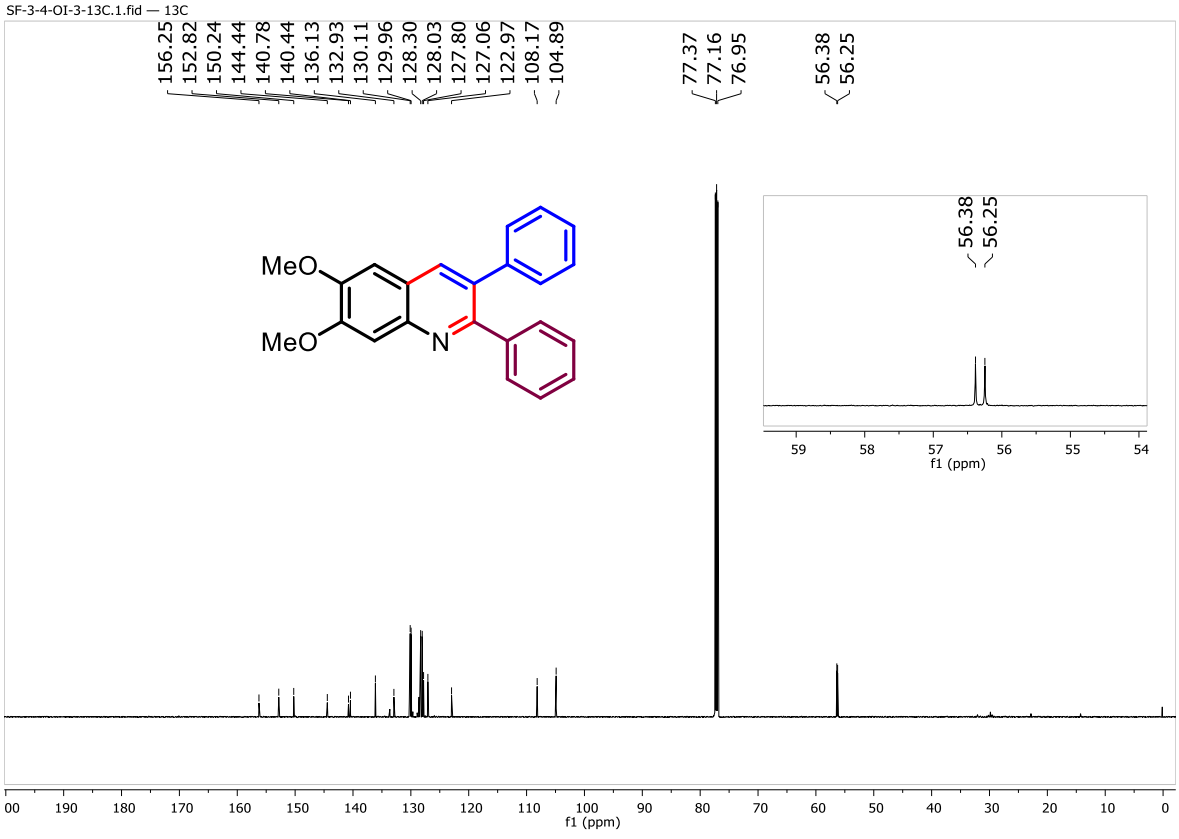

HRMS Spectrum of 6,7-Dimethoxy-2,3-diphenylquinoline (4a)

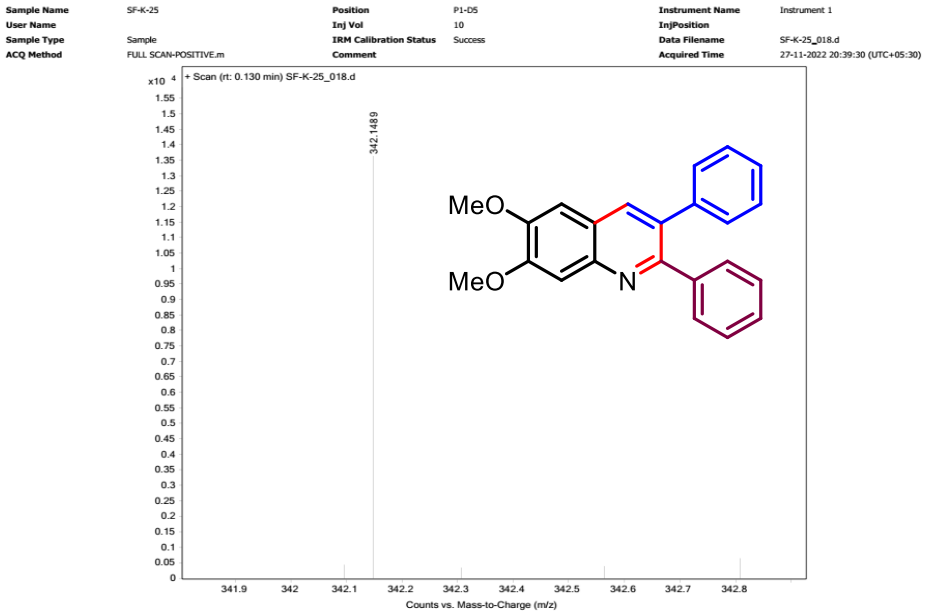

^{1}H NMR Spectrum of 2-(3-Bromophenyl)-3-butyl-6-methoxyquinoline (4t)

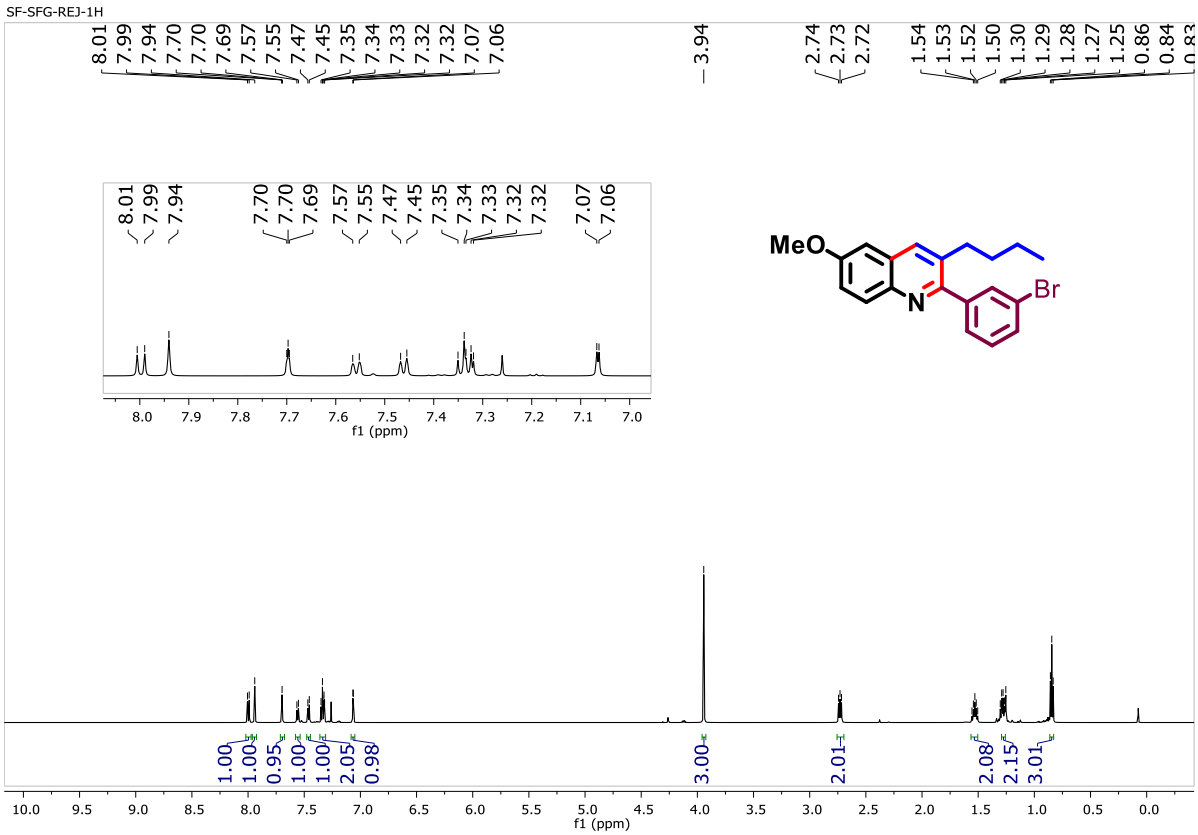

^{13}C NMR Spectrum of 2-(3-Bromophenyl)-3-butyl-6-methoxyquinoline (4t)

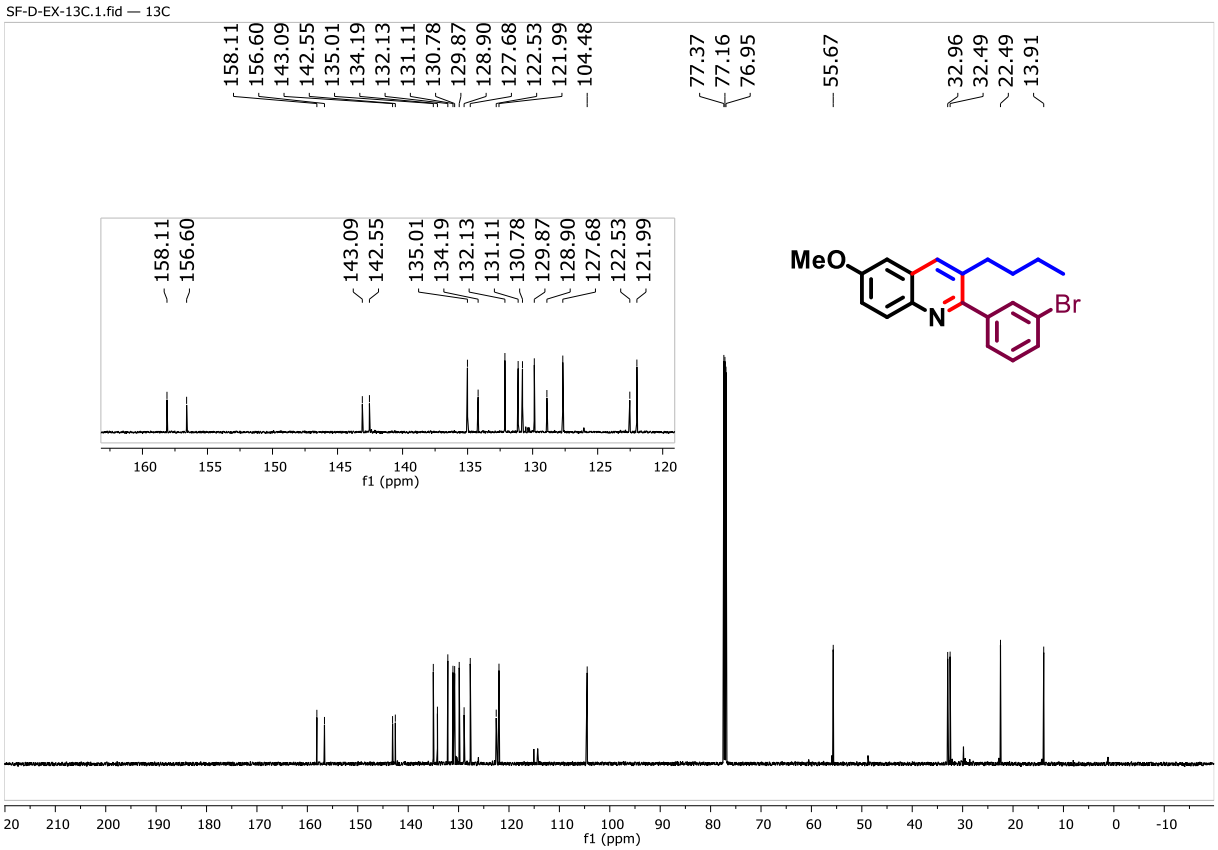

HRMS Spectrum of 2-(3-Bromophenyl)-3-butyl-6-methoxyquinoline (4t)

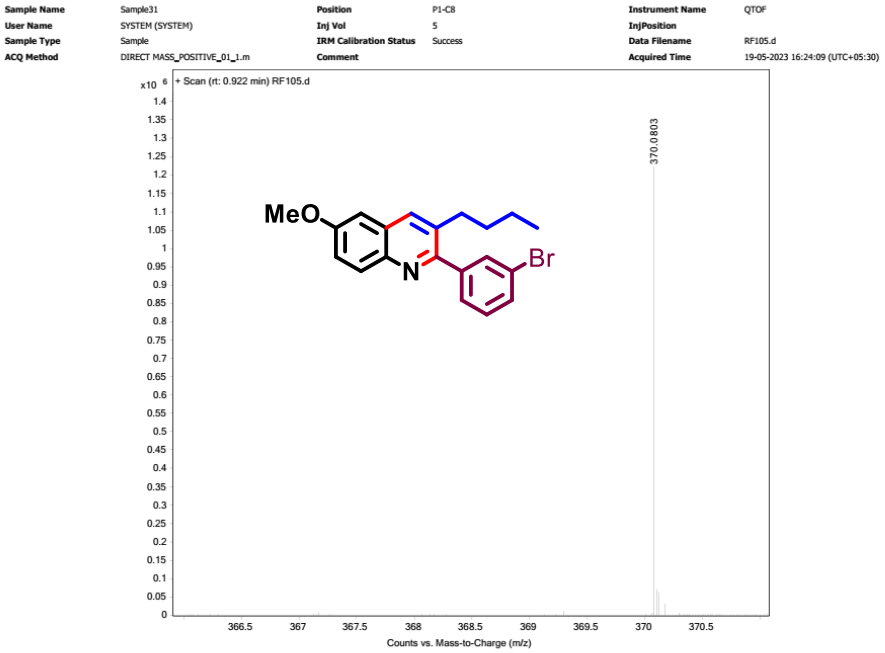

^{1}H NMR Spectrum of 3-Butyl-6-methoxy-2-pentylquinoline (5a)

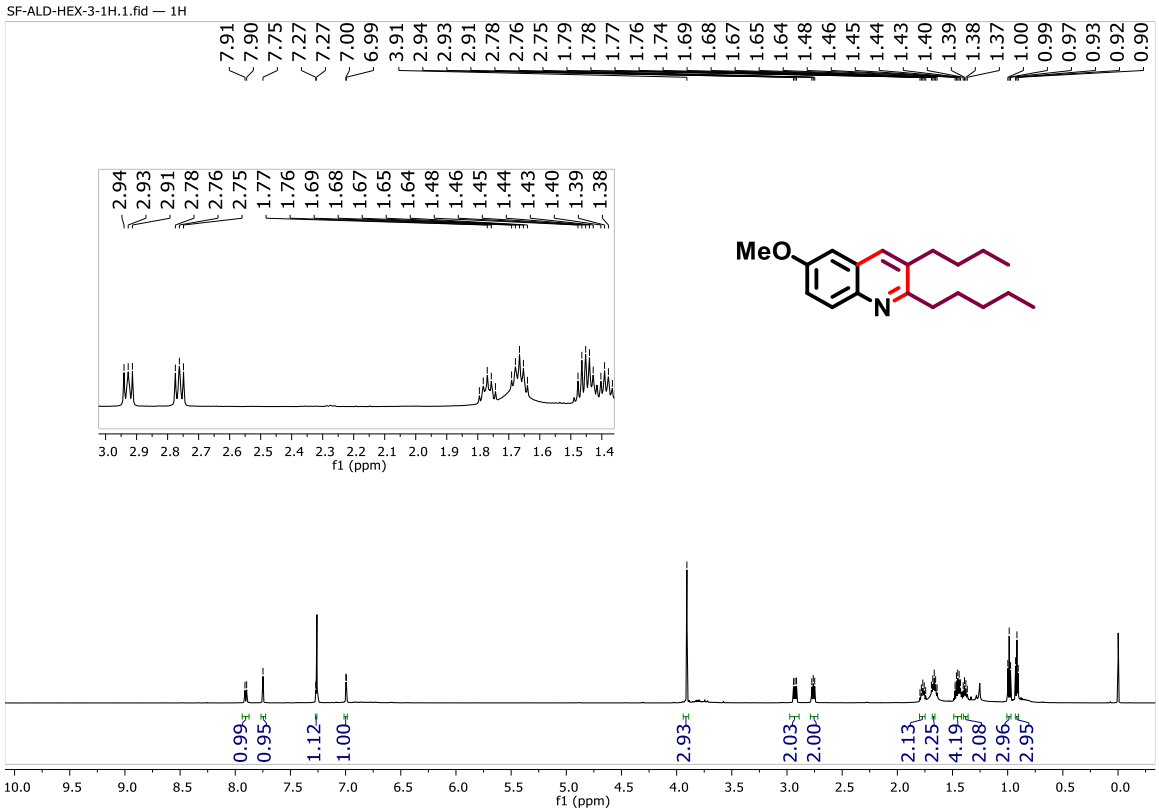

^{13}C NMR Spectrum of 3-Butyl-6-methoxy-2-pentylquinoline (5a)

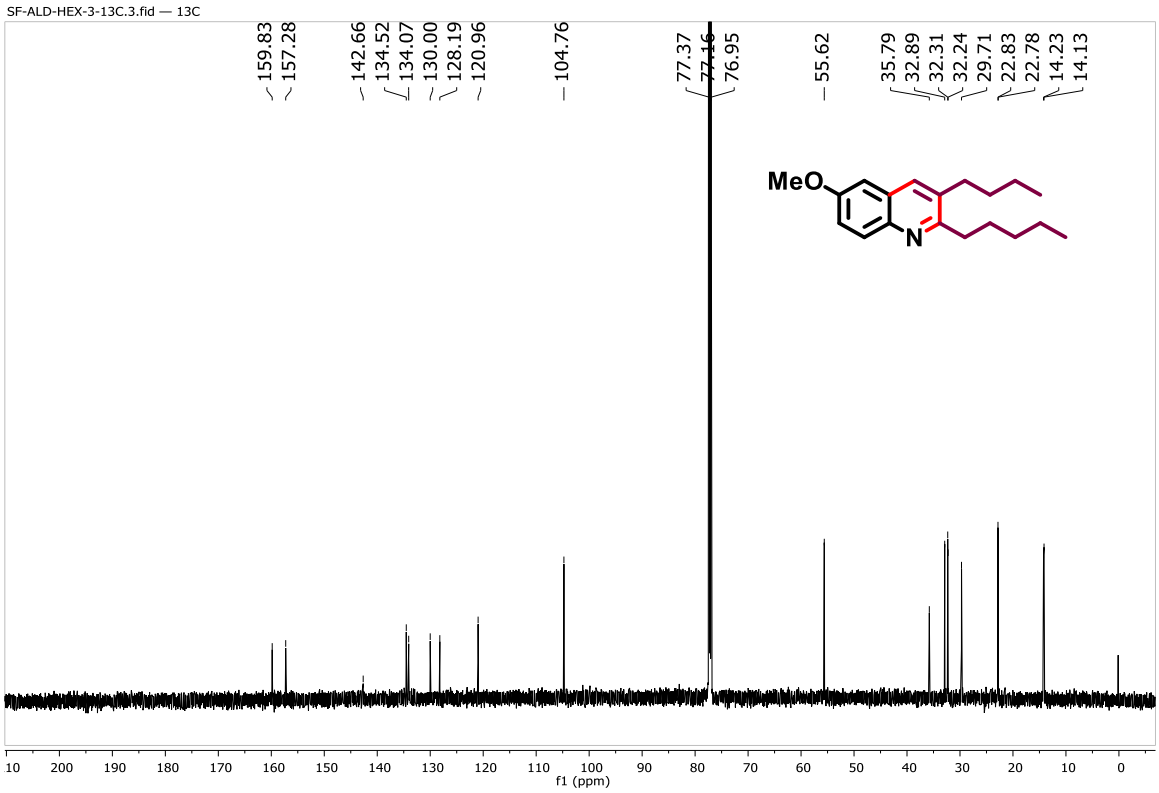

HRMS Spectrum of 3-Butyl-6-methoxy-2-pentylquinoline (5a)

Sample Name	2 AF	**Position**	P2-C8	**Instrument Name**	Instrument 1
User Name		**Inj Vol**	10	**InjPosition**	
Sample Type	Sample	**IRM Calibration Status**	Success	**Data Filename**	10DO_F.027.d
ACQ Method	FULL SCAN-POSITIVE.m	**Comment**		**Acquired Time**	08-04-2022 23:18:41 (UTC+05:30)

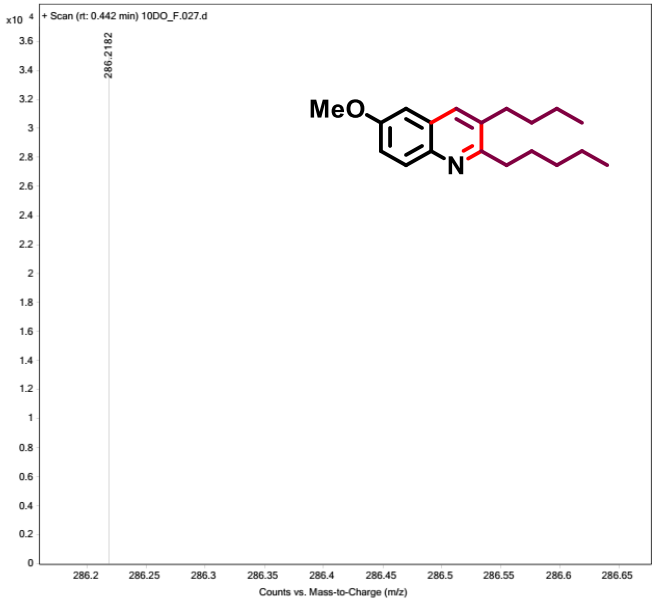

Part A

Chapter II: Section C

Synthesis of 2,4-diarylquinolines derivatives

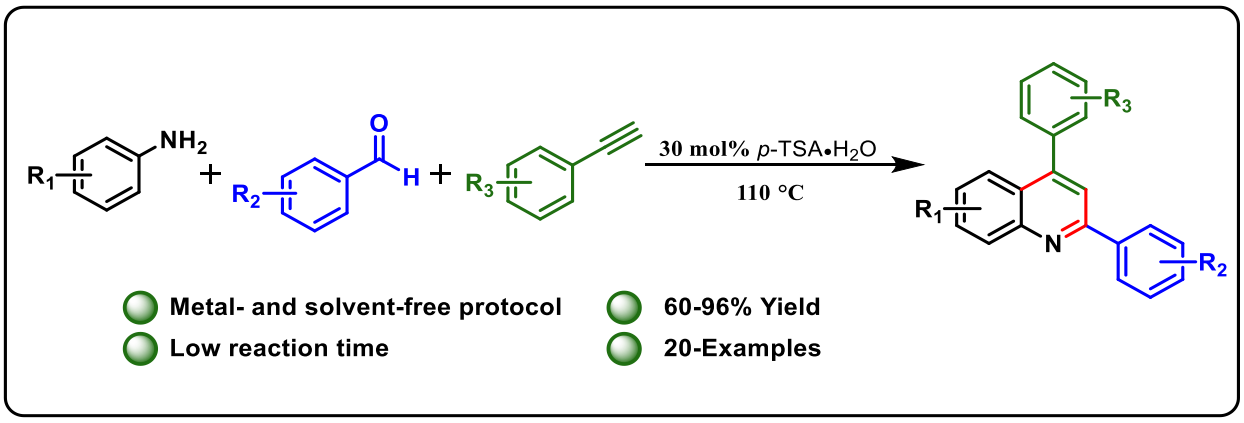

RESULT AND DISCUSSION

EXPERIMENTAL SECTION

Results and Discussion

Chapter I has already discussed the importance and synthetic approaches concerning the synthesis of 2,4-diarylquinolines scaffolds. This part of the chapter focuses on the synthesis of 2,4-diarylquinolines from a commercially available starting material arylamine, aryl aldehyde, and arylacetylene using 30 mol% *p*-toluenesulfonic acid monohydrate (*p*-TSA·H_2O) as a catalyst at 110 °C temperature under solvent-free conditions via a one-pot three-component reaction. (Scheme 21). The advantages of the present protocol are the nonrequirement of a metal catalyst, solvent, additive, & inert atmospheric reaction conditions, and easy separation. This method provides a good to excellent yield, broad substrate scope, shorter reaction time, and formation of one *C–N* and two *C–C* bonds in a single step.

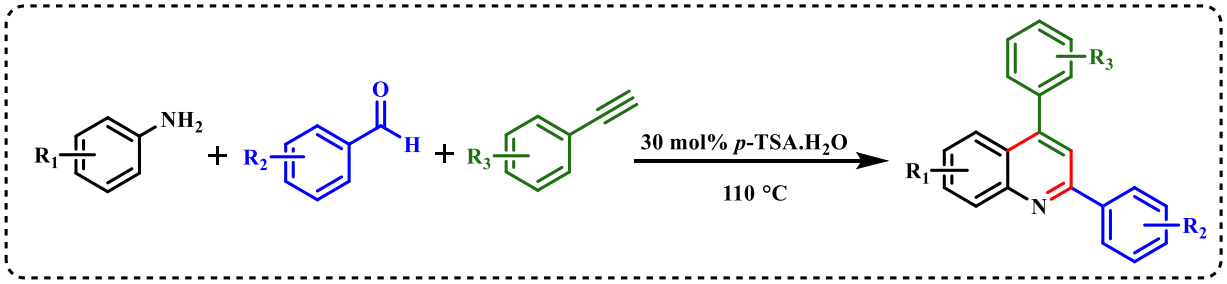

Scheme 21. Synthetic approach for synthesis of 2,4-diarylquinoline derivatives.

The study began by establishing suitable reaction conditions. For this, we have chosen *p*-anisidine (**1a**, 1.0 mmol), benzaldehyde (**2a**, 1.0 mmol), and phenylacetylene (**3a**, 1.0 mmol) as the model substrates. The results are summarized in Table 7. Initially, a reaction was examined with the model substrates without a catalyst at room temperature for 12 h followed by heating gradually up to 120 °C in a preheated oil bath for another 12 h. Unfortunately, no desired product was obtained (Table 7, Entry 1). Next, a similar reaction was examined in the presence of 10 mol% *p*-TSA**.**H_2O at room temperature. Again, no desired product was isolated (Table 7, Entry 2). After that the reaction was performed in the presence of 10 mol% catalysts at 80 °C for 4 h, and the desired product **4a** was isolated in 60% (Table 7, Entry 3). Then, two different reactions were performed using 20 mol% and 30 mol% catalysts at the same temperature, respectively. The yield was increased from 60% to 75% with an increase in the amount of the catalyst (Table 7, Entries 3-5). However, a further increase in the catalyst did not improve the outcome (Table 7, Entry 6). One step ahead, we tried to optimize the reaction temperature. So different reactions were scrutinized at 90 °C, 100 °C, and 110 °C because at the higher temperature, the catalyst will be melted (Table 7, Entries 7-9). The best result was

obtained at 110 °C with a 92% yield among three different reaction conditions. From these observations, it was observed that not only the yield was improved, but also reaction time was reduced significantly. Further, increasing the reaction temperature, the yield was not improved (Table 7, Entry 10). To check the efficacy of other catalysts, various reactions were performed using different Lewis acid catalysts such as TfOH, (±)-CSA, and acetic acid (Table 7, Entries 11, 12 & 13). Unfortunately, the yield of the desired product was not satisfactory for each case. From all these observations, we conclude that the 30 mol% of catalyst and 110 °C temperature are optimum reaction conditions for forming the expected product.

Table 7. Optimization of reaction conditions for the synthesis of 2,4-diarylquinoline.[a,b]

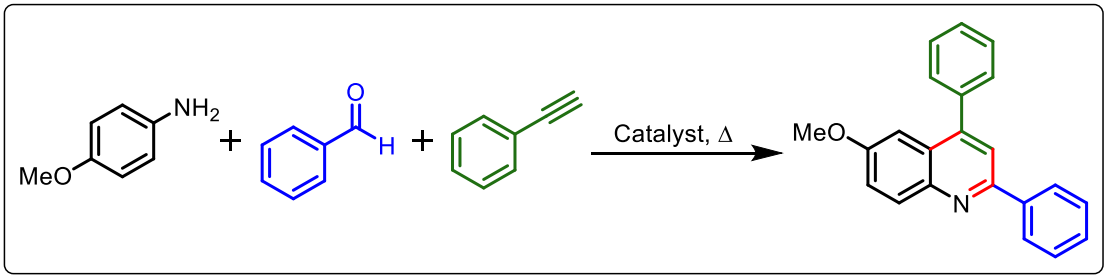

Entry	Catalyst	Mol %	Temp (°C)	Time (h)	Yield (%)[b]
1	*p*-TSA.H_2O	-	RT→120	24	NR
2	*p*-TSA. H_2O	10	RT	12	NR
3	*p*-TSA. H_2O	10	80	4	60
4	*p*-TSA. H_2O	20	80	3.5	68
5	*p*-TSA. H_2O	30	80	2.5	75
6	*p*-TSA. H_2O	40	80	2.5	76
7	*p*-TSA. H_2O	30	90	2	80
8	*p*-TSA. H_2O	30	100	2	85
9	***p*-TSA. H_2O**	**30**	**110**	**1**	**92**
10	*p*-TSA. H_2O	30	120	1	90
11	TfOH	30	120	1	28
12	(±)-CSA	30	120	1	25
13	Acetic Acid	30	120	1	29

[a]Reaction conditions: All reactions are carried out using *p*-anisidine (**1a**, 1.0 mmol), benzaldehyde (**2a**, 1.0 mmol), and Phenyl acetylene (**3a**, 1.0 mmol). [b]Isolate yield. RT: Room Temperature. ND: No desired product was obtained.

After getting the optimized reaction conditions in hand, we explored the present protocol with various arylamines, aryl aldehydes, and substituted phenylacetylene derivatives (Table 8). First, the reaction of *p*-anisidine **1a** and benzaldehyde **2a** was examined with 4-(*tert*-butyl)phenylacetylene **3b**, and the desired product **4b** was isolated in 86% yield. Likewise, various reactions were carried out with the aryl aldehydes having electron-withdrawing groups at the different positions in the aromatic ring. The reaction of *p*-anisidine **1a** and aryl acetylene with 2-fluoro **2b**, 4-fluoro **2c**, 2-chloro **2d**, 3-chloro **2e**, and 4-chloro-benzaldehyde **2f** provided corresponding expected product 2,4-diarylquinoline **4c**-**g** in 75-85% yields. Similarly, the desired products **4h**, **4i**, and **4j** were isolated from the reaction of *p*-anisidine **1a** and phenylacetylene **3a** with 2-bromo- **2g**, 3-bromo-**2h**, and 4-bromobenzaldehyde **2i**, respectively. The protocol was further extended with *p*-anisidine **1a,** 3-bromobenzaldehyde **2h**, and various arylacetylene having electron-donating and electron-withdrawing groups such as 4-methyl **3c**, 4-ethyl **3d**, 4-*tert*-butyl **3b**, 4-methoxy **3e**, and 4-fluoro phenylacetylene **3f**. They all produced the expected products **4k**-**4o** in very good to excellent yields. 2,4-Dimethoxybenzaldehyde **2j**, and naphthalene-1-carboxaldehyde **2k** have been successfully utilized to get the corresponding quinoline derivatives **4p** and **4q**, respectively. Apart from *p*-anisidine, the present protocol was studied with other electron-rich aniline derivatives such as *o*-anisidine **1b**, 4-methyl aniline 1c, 3,4-dimethylaniline 1d, and the desired 2,4-diaryl quinolines **4r**-**4t** was isolated in fair to good yield. It is worth mentioning that most of the synthesized compounds summarized in Table 8 have not been previously reported in the literature. Unfortunately, the reactions with arylamines containing electron-withdrawing groups such as halogen, $-NO_2$, and $-CF_3$ failed to deliver the desired product.

To verify the practicability of reaction behaviour with aliphatic aldehydes, a reaction was examined with *p*-anisidine **1a**, phenylacetylene **3a**, and butyraldehyde **2l** under the same reaction conditions. Surprisingly, the obtained product was 3-ethyl-6-methoxy-2-propylquinoline (**4v**) instead of the expected 6-methoxy-4-phenyl-2-propylquinoline as shown in Scheme 22. The reaction of arylamine with arylaldehyde produces emine which subsequently converts to enamine. This consequently leads to the formation of 2,3-disubstituted quinoline rather than 2,4-diarylquinoline. This observation shows that aryl acetylene does not participate in the reaction in the presence of aliphatic aldehyde to form 2-alkyl-4-aryl-quinoline (**4v**).

Table 8. Scope of various 2,4-diarylquinoline from different arylamines, arylaldehyde, and substituted phenylacetylene.[a,b]

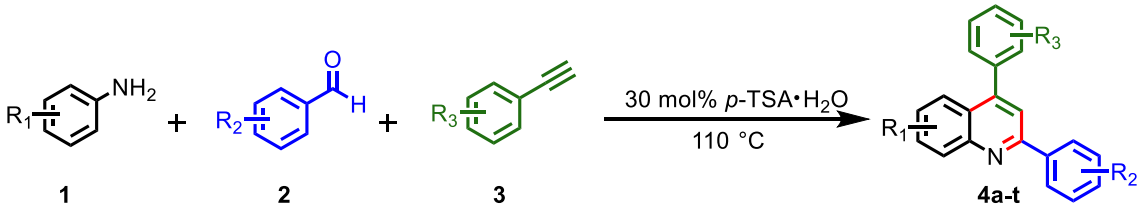

1 2 3 4a-t

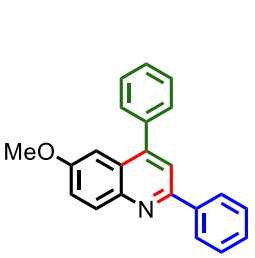

4a, 1.0 h, 92%

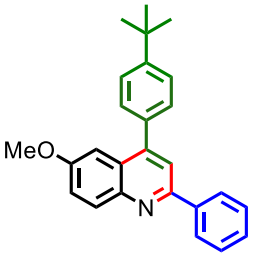

4b, 0.5 h, 86%

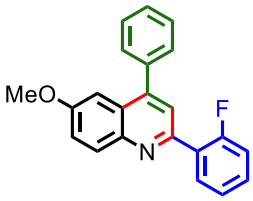

4c, 1.0 h, 79%

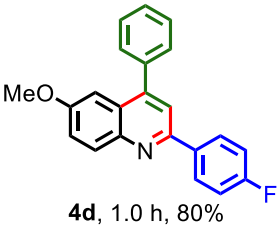

4d, 1.0 h, 80%

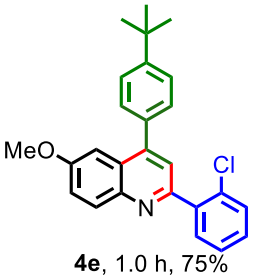

4e, 1.0 h, 75%

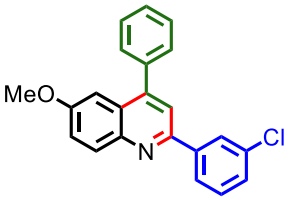

4f, 1.0 h, 85%

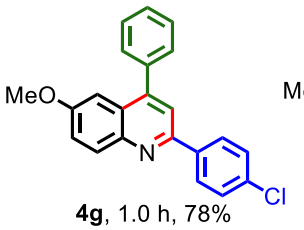

4g, 1.0 h, 78%

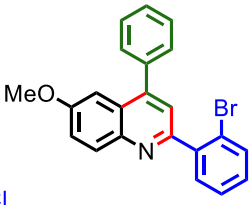

4h, 1.0 h, 80%

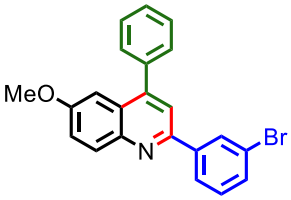

4i, 0.5 h, 82%

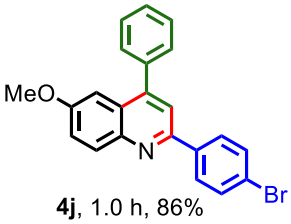

4j, 1.0 h, 86%

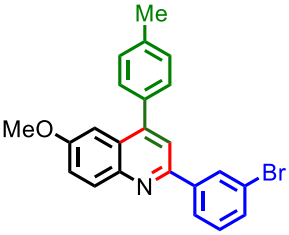

4k, 1.0 h, 82%

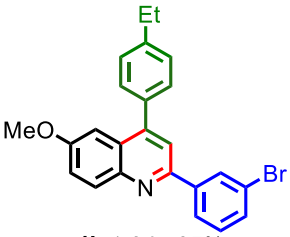

4l, 1.0 h, 85%

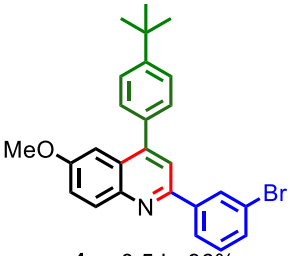

4m, 0.5 h, 96%

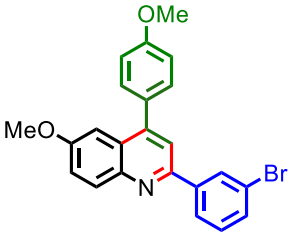

4n, 1.0 h, 86%

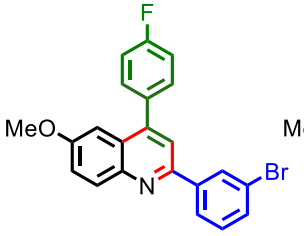

4o, 1.0 h, 80%

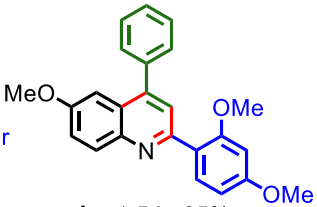

4p, 1.5 h, 85%

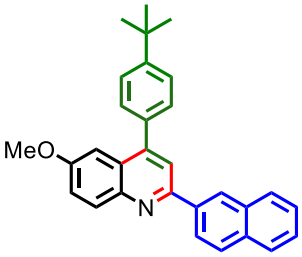

4q, 2.0 h, 88%

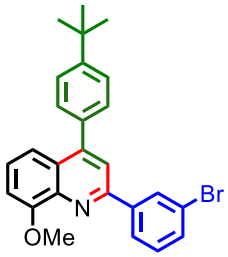

4r, 2.0 h, 70%

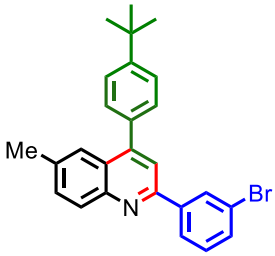

4s, 1.5 h, 68%

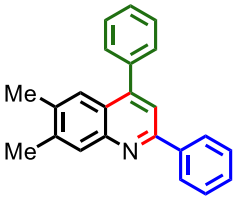

4t, 1.5 h, 60%

[a]Reaction conditions: All reactions are carried out using arylamines (**1a-d**, 1.0 mmol), arylaldehydee (**2a-k**, 1.0 mmol), and arylacetylene (**3a-f**, 1.0 mmol) in the presence of *p*-TSA**.**H_2O at 110 °C. [b]Isolated yields.

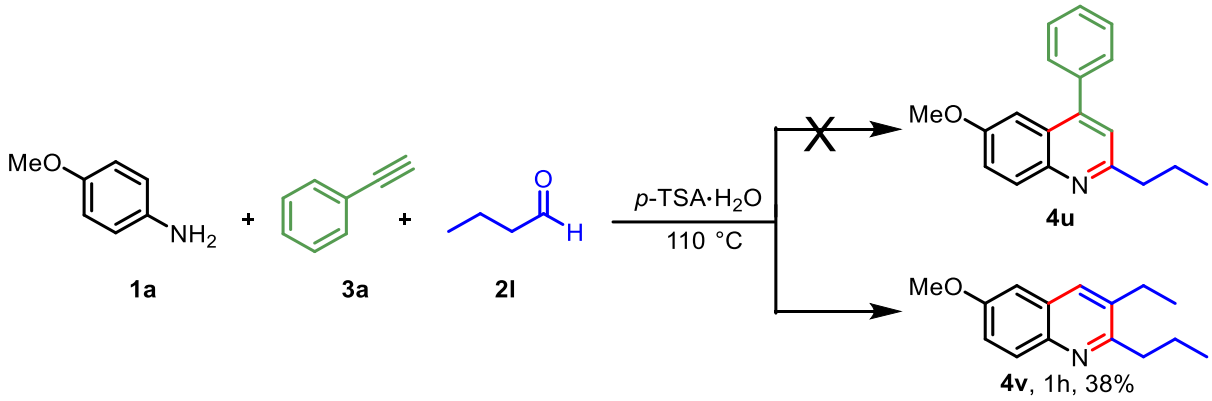

Scheme 22. Reaction with *p*-anisidine **1a**, aliphatic aldehyde **2l**, and phenylacetylene **3a**.

A plausible mechanism of this reaction is demonstrated in Scheme 23. Initially, *p*-anisidine **1a** reacts with benzaldehyde **2a** in the presence of *p*-TSA**.**H_2O to form imine **A**. Then, imine **A** and phenylacetylene **3a** undergo a Povarov reaction[35a-e] to form intermediate **B**. Next, intermediate **B** undergoes [1,3]-H shift to form the next intermediate **C**. Ultimately, aerial oxidation of intermediate **C** furnishes the desired product **4a**.

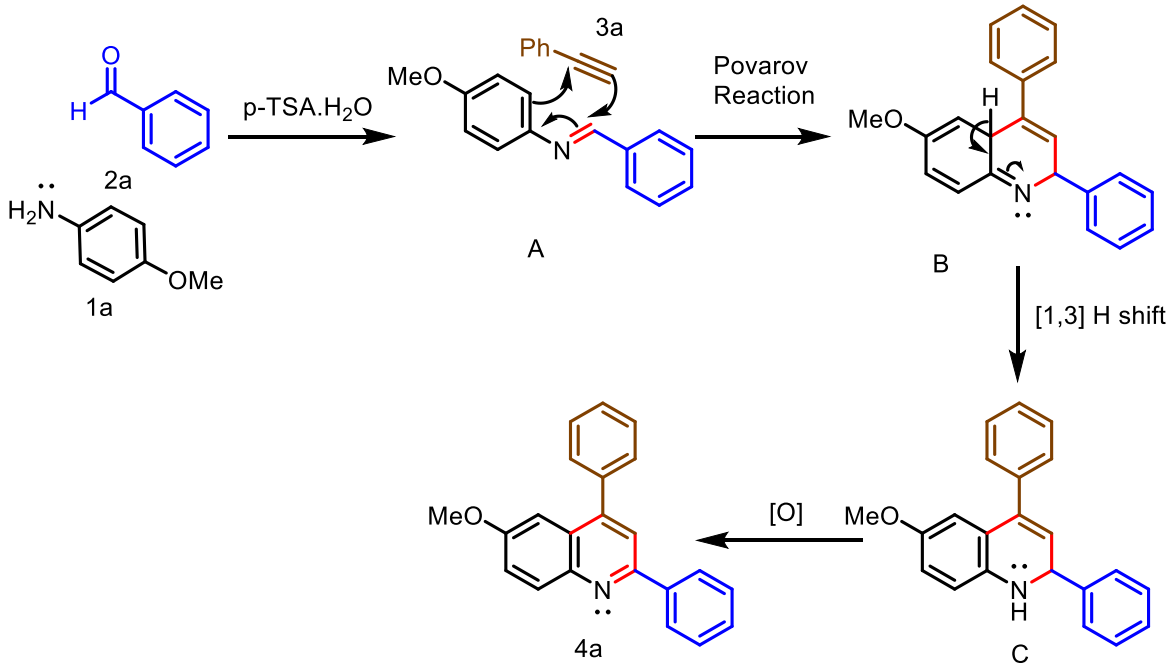

Scheme 23. A plausible mechanism for the formation of a product **4a.**

In summary, we have developed an environmentally benign protocol for the synthesis of 2,4-diarylquinolines involving a three-component neat reaction of arylamines, arylaldehyde, and arylacetylene using 30 mol% of *p*-TSA**.**H_2O at 110 °C. The perks of this reaction are high

regioselectivity, metal- and solvent-free reaction conditions, very good to excellent yield, broad substrate scope, short reaction time, and the formation of one *C-N* and two *C-C* bonds in a single step.

Experimental Section

General Procedure for the Synthesis of 2,4-diarylquinoline Derivatives

Arylamine (**1**, 1.0 mmol), substituted benzaldehyde (**2**, 1.0 mmol), and substituted phenyl acetylene (**3**, 1.0 mmol) are mixed in the round-bottomed flask. *p*-TSA•H_2O (30 mol%) was added to the reaction mixture as a catalyst and kept in a pre-heated oil bath at 110 ^oC with constant stirring under an air atmosphere. The progress of the reaction was monitored by checking TLC from time to time. After the completion of the reaction, the sticky reaction mixture was brought to room temperature. Then, 1 mL of ethyl acetate was added to it and scratched to remove the stickiness of the mixture until it dissolved properly. After that another 5 mL of ethyl acetate was added to it, followed by the addition of 5 mL of water. The organic layer was collected using a separatory funnel and dried with anhydrous sodium sulfate. The solvent was then removed from the rotary evaporator. Finally, the crude residue was purified by column chromatography (silica gel 60-120 mesh) using (9.8: 0.2, v/v) n-hexane and ethyl acetated mixture to obtain the final product (**4**).

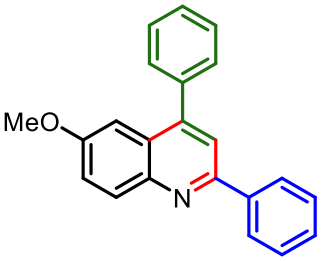

6-Methoxy-2,4-diphenylquinoline (4a) White solid (286.25 mg, 92%); mp 118-120 °C. ^1H NMR (600 MHz, $CDCl_3$) δ 8.17–8.15 (m, 3H), 7.78 (s, 1H), 7.57 (q, *J* = 7.2 Hz, 4H), 7.52 (t, *J* = 7.3 Hz, 3H), 7.45 (d, *J* = 7.3 Hz, 1H), 7.40 (dd, *J* = 9.2, 2.6 Hz, 1H), 7.20 (d, *J* = 2.5 Hz, 1H), 3.81 (s, 3H); ^{13}C NMR (150 MHz, $CDCl_3$) δ 157.9, 154.8, 147.9, 145.0, 139.8, 138.8, 131.7, 129.5, 129.1, 128.9, 128.8, 128.4, 127.4, 126.8, 121.9, 119.8, 103.8, 55.6; IR (KBr)ν_{max}/cm-^{1} 3025 (C-H), 2962 (C-

H), 1620 (C=C), 1361 (C-O); HRMS (ESI) Calcd For $C_{26}H_{26}NO$ 312.1383 ($M+H^+$); Found 312.1401.

4-(4-(*tert*-Butyl)phenyl)-6-methoxy-2-phenylquinoline (4b) White solid (316.05 mg, 86%);

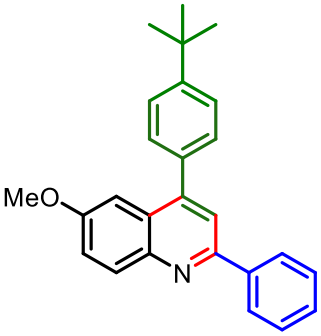

mp 140-142 °C. ^{1}H NMR (500 MHz, $CDCl_3$) δ 8.17 – 8.15 (m, 3H), 7.78 (s, 1H), 7.59 – 7.57 (m, 2H), 7.55 – 7.50 (m, 4H), 7.45 (d, *J* = 7.4 Hz, 1H), 7.41 (dd, *J* = 9.2, 2.7 Hz, 1H), 7.29 (d, *J* = 2.5 Hz, 1H), 3.84 (s, 3H), 1.44 (s, 9H); ^{13}C NMR (100 MHz, $CDCl_3$) δ 157.8, 154.8, 151.5, 147.8, 145.0, 139.9, 135.8, 131.7, 129.2, 129.0, 128.9, 127.4, 126.8, 125.7, 121.7, 119.9, 104.1, 55.6, 34.8, 31.5; IR (KBr)ν_{max}/cm^{-1} 3027 (C-H), 2922 (C-H), 1622 (C=C), 1370 (C-O); HRMS (ESI) Calcd For $C_{26}H_{26}NO$ 368.2009 ($M+H^+$); Found 368.2012.

2-(2-Fluorophenyl)-6-methoxy-4-phenylquinoline (4c) Colorless liquid (260.20 mg, 79%).

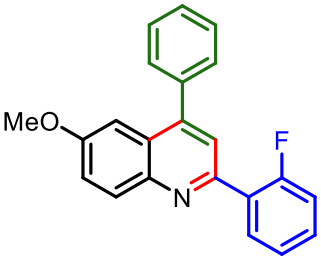

^{1}H NMR (400 MHz, $CDCl_3$) δ 8.17 (d, *J* = 9.2 Hz, 1H), 8.12 (td, *J* = 7.8, 1.9 Hz, 1H), 7.81 (d, *J* = 2.7 Hz, 1H), 7.61 – 7.53 (m, 4H), 7.55 – 7.53 (m, 1H), 7.44 – 7.38 (m, 2H), 7.34 – 7.30 (m, 1H), 7.24 (d, *J* = 2.8 Hz, 1H), 7.19 (ddd, *J* = 11.2, 8.2, 1.1 Hz, 1H), 3.80 (s, 3H); ^{13}C NMR (100 MHz, $CDCl_3$) δ 160.8 (d, *J* = 247.9 Hz), 158.1, 151.2, 147.2, 145.0, 138.6, 131.6, 131.4 (d, *J* = 3.1 Hz), 130.6 (d, *J* = 8.4 Hz), 129.5, 128.7, 128.4, 128.1 (d, *J* = 11.9 Hz), 126.8, 124.7 (d, *J* = 3.5 Hz), 123.1 (d, *J* = 7.9 Hz), 122.0, 116.3 (d, *J* = 22.7 Hz), 103.6, 55.5; ^{19}F NMR (377 MHz, $CDCl_3$) δ -117.08; IR (KBr)ν_{max}/cm^{-1} 3028(C-H), 2920 (C-H), 1622 (C=C), 1232 (C-O); HRMS (ESI) Calcd For $C_{22}H_{17}FNO$ 330.1289 ($M+H^+$); Found 330.1319.

2-(4-Fluorophenyl)-6-methoxy-4-phenylquinoline (4d) Light yellow liquid (263.36 mg, 80%).

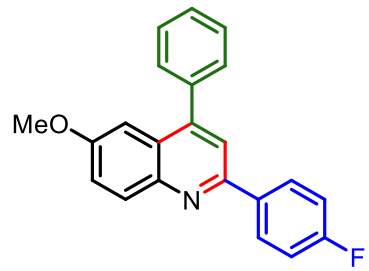

^{1}H NMR (400 MHz, $CDCl_3$) δ 8.17 – 8.11 (m, 3H), 7.72 (s, 1H), 7.57– 7.56 (m, 4H), 7.55 – 7.51 (m, 1H), 7.40 (dd, *J* = 9.2, 2.8 Hz, 1H), 7.21 – 7.17 (m, 3H), 3.80 (s, 3H); ^{13}C NMR (100 MHz, $CDCl_3$) δ 163.7 (d, *J* = 246.9 Hz), 157.9, 153.6, 148.0, 144.9, 138.7, 136.0 (d, *J* = 3.04 Hz), 131.6, 129.4, 129.2 (d, *J* = 8.3 Hz), 128.8, 128.5, 126.6, 122.0, 119.4, 115.8 (d, J = 21.41 Hz), 103.8, 55.5; ^{19}F NMR (377 MHz, $CDCl_3$) δ -113.08; IR (KBr)ν_{max}/cm^{-1} 3022 (C-H), 2926 (C-H), 1623 (C=C), 1230 (C-O); HRMS (ESI) Calcd For $C_{22}H_{17}FNO$ 330.1289 ($M+H^+$); Found 330.1317.

4-(4-(*tert*-Butyl)phenyl)-2-(2-chlorophenyl)-6-methoxyquinoline (4e) White solid (301.45 mg, 75%); mp 113-115 °C. ^{1}H NMR (400 MHz, $CDCl_3$) δ 8.15 (d, *J* = 9.2 Hz, 1H), 7.73 (dd, *J* = 9.4, 1.92, Hz, 1H), 7.66 (s, 1H), 7.56 – 7.54 (m, 3H), 7.51 – 7.49 (m, 1H), 7.43 (d, *J* = 2.8 Hz, 1H), 7.41 (d, *J* = 2.3 Hz, 1H), 7.39 – 7.37 (m, 1H), 7.36 – 7.34 (m, 2H), 3.85 (s, 3H), 1.42 (s, 9H); ^{13}C NMR (100 MHz, $CDCl_3$) δ 158.1, 154.6, 151.5, 146.7, 144.8, 139.8, 135.5, 132.5, 131.8, 131.6, 130.1, 129.7, 129.2, 127.2, 126.8, 125.7, 123.5, 121.7, 104.1, 55.7, 34.8, 31.5; IR (KBr)ν_{max}/cm^{-1} 3025 (C-H), 2928 (C-H), 1622 (C=C), 1260 (C-O); HRMS (ESI) Calcd For $C_{26}H_{25}ClNO$ 402.1619 ($M+H^+$); Found 402.1612.

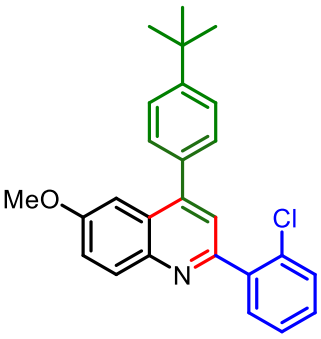

2-(3-Chlorophenyl)-6-methoxy-4-phenylquinoline (4f) White solid (293.95 mg, 85%); mp 119-121 °C. ^{1}H NMR (400 MHz, $CDCl_3$) δ 8.20 – 8.19 (m, 1H), 8.14 (d, *J* = 9.2 Hz, 1H), 8.05 – 8.02 (m, 1H), 7.73 (s, 1H), 7.58 – 7.56 (m, 4H), 7.54 – 7.52 (m, 1H), 7.43 – 7.39 (m, 3H), 7.20 (d, *J* = 2.6 Hz, 1H), 3.80 (s, 3H); ^{13}C NMR (100 MHz, $CDCl_3$) δ 158.1, 153.0, 148.1, 144.9, 141.6, 138.6, 135.0, 131.7, 130.1, 129.4, 129.0, 128.8, 128.5, 127.5, 127.0, 125.4, 122.2, 119.4, 103.7, 55.5; IR (KBr)ν_{max}/cm^{-1} 3025 (C-H), 2926 (C-H), 1622 (C=C), 1262 (C-O); HRMS (ESI) Calcd For $C_{22}H_{17}ClNO$ 346.0993 ($M+H^+$); Found 346.0993.

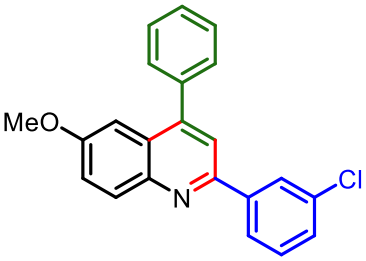

2-(4-Chlorophenyl)-6-methoxy-4-phenylquinoline (4g) Colorless liquid (269.73 mg, 78%). ^{1}H NMR (400 MHz, $CDCl_3$) δ 8.13 – 8.10 (m, 3H), 7.73 (s, 1H), 7.57 – 7.56 (m, 4H), 7.54 – 7.51 (m, 1 H), 7.49 – 7.47 (m, 2H), 7.42 –7.39 (m, 1H), 7.18 (d, J = 2.8 Hz,1H), 3.80 (s, 3H); ^{13}C NMR (100 MHz, $CDCl_3$) δ 158.0, 153.4, 148.1, 144.9, 138.7, 138.2, 135.2, 131.6, 129.4, 129.1, 128.8, 128.6, 128.5, 126.8, 122.2, 119.4, 103.8, 55.6; IR (KBr)ν_{max}/cm^{-1} 3025 (C-H), 2926 (C-H), 1623 (C=C), 1232 (C-O); HRMS (ESI) Calcd For $C_{22}H_{17}ClNO$ 346.0993 ($M+H^+$); Found 346.0993.

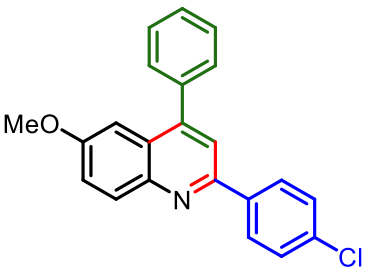

2-(2-Bromophenyl)-6-methoxy-4-phenylquinoline (4h) Brownish liquid (312.22 mg, 80%). ^{1}H NMR (400 MHz, $CDCl_3$) δ 8.15 (d, *J* = 9.2 Hz, 1H), 7.71 – 7.68 (m, 2H), 7.63 (s, 1H), 7.61 – 7.59 (m, 2H), 7.57 – 7.53 (m, 2H), 7.52 – 7.49 (m, 1H), 7.46 (dd, J = 7.5, 1.2 Hz, 1H), 7.41 (dd, *J* = 9.2, 2.9 Hz, 1H), 7.29 (dd, *J* = 8.0, 1.7 Hz, 1H), 7.27 (d, J = 2.72 Hz, 1H), 3.81 (s, 3H); ^{13}C NMR (100 MHz, $CDCl_3$) δ 156.3, 154.0, 144.7, 142.7, 139.7, 136.5, 131.4, 129.6, 127.9, 127.5, 126.8, 126.5,

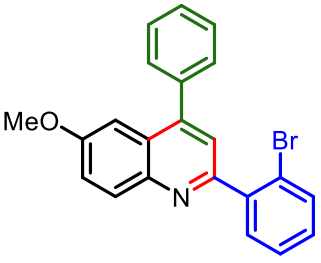

125.8, 124.7, 121.4, 120.1, 120.0, 101.8, 53.6; IR (KBr)ν_{max}/cm^{-1} 3021 (C-H), 2925 (C-H), 1622 (C=C), 1233 (C-O); HRMS (ESI) Calcd For $C_{22}H_{17}BrNO$ 390.0488 (M+H$^+$); Found 390.0519.

2-(3-Bromophenyl)-6-methoxy-4-phenylquinoline (4i) White solid (320.02 mg, 82%); mp 153 °C. ^{1}H NMR (400 MHz, $CDCl_3$) δ 8.35 – 8.34 (m, 1H), 8.14 (d, *J* = 9.2 Hz, 1H), 8.09 – 8.06 (m, 1H), 7.73 (s, 1H), 7.57 – 7.56 (m, 4H), 7.55 – 7.52 (m, 2H), 7.42 – 7.35 (m, 2H), 7.19 (d, *J* = 2.8 Hz, 1H), 3.80 (s, 3H); ^{13}C NMR (100 MHz, $CDCl_3$) δ 158.1, 152.9, 148.1, 144.9, 141.8, 138.6, 131.9, 131.7, 130.4, 130.4, 129.4, 128.8, 128.5, 127.0, 125.9, 123.2, 122.2, 119.4, 103.75, 55.5; IR (KBr)ν_{max}/cm^{-1} 3029 (C-H), 2922 (C-H), 1620 (C=C), 1260 (C-O); HRMS (ESI) Calcd For $C_{22}H_{17}BrNO$ 390.0488 (M+H$^+$); Found 390.0521.

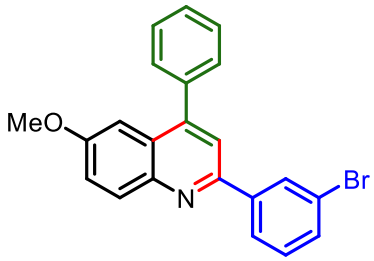

2-(4-Bromophenyl)-6-methoxy-4-phenylquinoline (4j) Brown solid (335.63 mg, 86%); mp 119 °C. ^{1}H NMR (400 MHz, $CDCl_3$) δ 8.12 (d, *J* = 9.2 Hz, 1H), 8.06 – 8.03 (m, 1H), 8.04 (d, *J* = 1.9 Hz, 1H), 7.72 (s, 1H), 7.64 – 7.61 (m, 2H), 7.57 – 7.56 (m, 4H), 7.54 – 7.53 (m, 1H), 7.40 (dd, *J* = 9.3, 2.9 Hz, 1H), 7.18 (d, *J* = 2.8 Hz, 1H), 3.79 (s, 3H); ^{13}C NMR (100 MHz, $CDCl_3$) δ 157.0, 152.3, 147.0, 143.9, 137.6, 131.5, 131.0, 130.6, 128.4, 127.9, 127.8, 127.5, 125.8, 122.5, 121.1, 118.2, 102.7, 54.5; IR (KBr)ν_{max}/cm^{-1} 3029 (C-H), 2925 (C-H), 1622 (C=C), 1262(C-O); HRMS (ESI) Calcd For $C_{22}H_{17}BrNO$ 390.0488 (M+H$^+$); Found 390.0523.

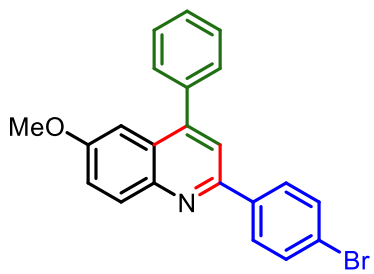

2-(3-Bromophenyl)-6-methoxy-4-(*p*-tolyl)quinoline (4k) White liquid (331.52 mg, 82%). ^{1}H NMR (500 MHz, $CDCl_3$) δ 8.34 (t, *J* = 1.7 Hz, 1H), 8.13 (d, *J* = 9.2 Hz, 1H), 8.07 (d, *J* = 7.9 Hz, 1H), 7.71 (s, 1H), 7.56 (d, *J* = 8.8 Hz, 1H), 7.47 (d, *J* = 8.0 Hz, 2H), 7.41 – 7.35 (m, 4H), 7.23 (d, *J* = 2.7 Hz, 1H), 3.81 (s, 3H), 2.49 (s, 3H); ^{13}C NMR (100 MHz, $CDCl_3$) δ 158.1, 152.9, 148.2, 144.9, 141.9, 138.5, 135.6, 131.9, 131.7, 130.4, 130.3, 129.5, 129.3, 127.1, 125.8, 123.2, 122.2, 119.4, 103.7, 55.6, 21.4; IR (KBr)ν_{max}/cm^{-1} 3027 (C-H), 2926 (C-H), 1620 (C=C), 1262 (C-O); HRMS (ESI) Calcd For $C_{23}H_{19}BrNO$ 404.0645 (M+H$^+$); Found 404.0653.

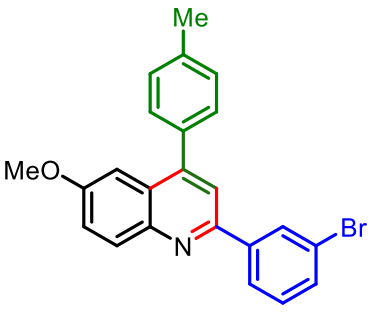

2-(3-Bromophenyl)-4-(4-ethylphenyl)-6-methoxyquinoline (4l) Light brown liquid (355.58 mg, 85%). ^{1}H NMR (500 MHz, $CDCl_3$) δ 8.16 – 8.13 (m, 3H), 7.77 (s, 1H), 7.52 – 7.50 (m, 4H), 7.44 (d, *J* = 7.3 Hz, 1H), 7.41 – 7.38 (m, 2H), 7.25 (d, *J* = 2.8 Hz, 1H), 3.82 (s, 3H), 2.79 (q, *J* = 7.6 Hz, 2H), 1.35 (t, *J* = 7.6 Hz, 3H); ^{13}C NMR (100 MHz, $CDCl_3$) δ 157.8, 154.8, 147.9, 145.0, 144.6, 139.9, 136.1, 131.7, 129.4, 129.0, 128.9, 128.3, 127.4, 126.8, 121.8, 119.8, 115.0, 114.2, 103.9, 55.6, 28.8, 15.6; IR (KBr)ν_{max}/cm^{-1} 3025 (C-H), 2922 (C-H), 1620 (C=C), 1265 (C-O); HRMS (ESI) Calcd For $C_{24}H_{21}BrNO$ 418.0801 ($M+H^+$); Found 418.0803.

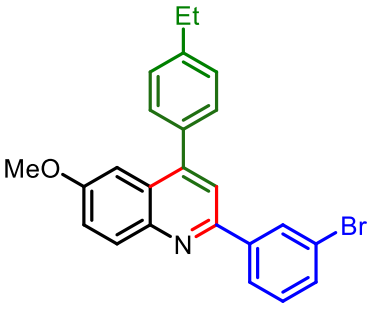

2-(3-Bromophenyl)-4-(4-(*tert*-butyl)phenyl)-6-methoxyquinoline (4m) White solid (446.38 mg, 100%); mp 149 °C. ^{1}H NMR (500 MHz, $CDCl_3$) δ 8.34 – 8.33 (m, 1H), 8.14 (d, *J* = 9.2 Hz, 1H), 8.08 (d, *J* = 7.8 Hz, 1H), 7.73 (s, 1H), 7.59 – 7.51 (m, 5H), 7.41 (dd, *J* = 9.2, 2.8 Hz, 1H), 7.37 (t, *J* = 7.9 Hz, 1H), 7.28 (d, *J* = 2.7 Hz, 1H), 3.84 (s, 3H), 1.43 (s, 9H); ^{13}C NMR (125 MHz, $CDCl_3$) δ 158.1, 153.0, 151.7, 148.2, 145.0, 142.0, 135.6, 131.9, 131.7, 130.4, 130.4, 129.2, 127.1, 125.9, 125.8, 123.2, 122.0, 119.5, 104.1, 55.7, 34.9, 31.5; IR (KBr)ν_{max}/cm^{-1} 3026 (C-H), 2922 (C-H), 1620 (C=C), 1262 (C-O); HRMS (ESI) Calcd For $C_{26}H_{25}BrNO$ 446.1114 ($M+H^+$); Found 446.1122.

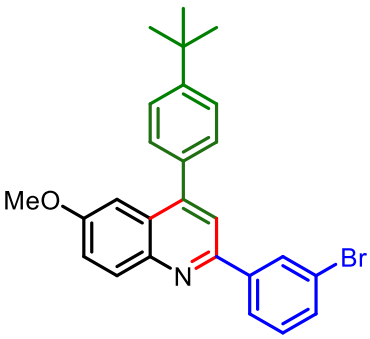

2-(3-Bromophenyl)-6-methoxy-4-(4-methoxyphenyl)phenylquinoline (4n) White solid (361.45 mg, 86%); mp 158 °C. ^{1}H NMR (400 MHz, $CDCl_3$) δ 8.33 (t, *J* = 1.8 Hz, 1H), 8.12 (d, *J* = 9.2 Hz, 1H), 8.07 (d, *J* = 7.8 Hz, 1H), 7.70 (s, 1H), 7.57 – 7.54 (m, 1H), 7.52 – 7.50 (m, 2H), 7.41 – 7.35 (m, 2H), 7.23 (d, *J* = 2.8 Hz, 1H), 7.09 (d, *J* = 8.7 Hz, 2H), 3.92 (s, 3H), 3.82 (s, 3H); ^{13}C NMR (100 MHz, $CDCl_3$) δ 159.9, 158.1, 153.0, 147.9, 145.0, 141.9, 131.9, 131.7, 130.9, 130.6, 130.4, 130.4, 127.2, 125.9, 123.2, 122.1, 119.4, 114.3, 103.8, 55.6, 55.5; IR (KBr)ν_{max}/cm^{-1} 3025 (C-H), 2926 (C-H), 1618 (C=C), 1268 (C-O); HRMS (ESI) Calcd For $C_{23}H_{19}BrNO_2$ 420.0594 ($M+H^+$); Found 420.0597.

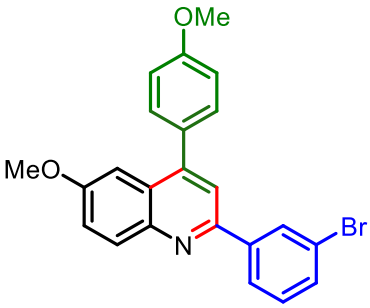

2-(3-Bromophenyl)-4-(4-fluorophenyl)-6-methoxyquinoline (4o) Black liquid (326.61 mg, 80%). ^{1}H NMR (400 MHz, $CDCl_3$) δ 8.19 (d, *J* = 9.2 Hz, 1H), 7.73 (td, *J* = 6.1, 5.7, 3.0 Hz, 2H), 7.64 (s, 1H), 7.62 – 7.59 (m, 2H), 7.51 – 7.45 (m, 2H), 7.35 – 7.28 (m, 3H), 7.24 (d, *J* = 2.8 Hz, 1H), 3.87 (s, 3H); ^{13}C NMR (100 MHz, $CDCl_3$) δ 163.0 (d, *J* = 246.57 Hz), 158.4, 155.9, 145.6, 144.7, 141.6, 134.5, (d, *J* = 3.4 Hz), 133.4, 131.8 (d, *J* = 1.57 Hz), 131.2(d, *J* = 8.11 Hz), 130.0, 127.8, 126.7, 123.4, 122.1, 122.0, 116.0, 115.8, 103.5, 55.6; ^{19}F NMR (377 MHz, $CDCl_3$) δ -113.24; IR (KBr)ν_{max}/cm^{-1} 3027 (C-H), 2926 (C-H), 1622 (C=C), 1372 (C-O); HRMS (ESI) Calcd For $C_{22}H_{16}BrFNO$ 408.0394 (M+H$^+$); Found 408.0394.

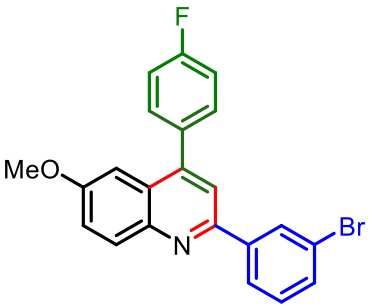

2-(2,4-Dimethoxyphenyl)-6-methoxy-4-phenylquinoline (4p) Light yellow liquid (315.71 mg, 85%). ^{1}H NMR (500 MHz, DMSO-*d*$_6$) δ 7.66 (d, *J* = 8.6 Hz, 1H), 7.48 (d, *J* = 8.0 Hz, 3H), 7.27 (d, *J* = 8.9 Hz, 2H), 7.12 (d, *J* = 7.8 Hz, 2H), 7.06 – 7.03 (m, 2H), 6.68 – 6.64 (m, 2H), 3.90 (s, 3H), 3.86 (s, 3H), 3.76 (s, 3H); ^{13}C NMR (125 MHz, DMSO-*d*$_6$) δ 187.5, 166.3, 163.7, 159.0, 145.6, 138.0, 130.1, 128.3, 125.7, 125.1, 124.4, 124.3, 122.8, 122.8, 118.3, 115.2, 114.9, 107.0, 98.4, 56.2, 56.0, 55.7; IR (KBr)ν_{max}/cm^{-1} 3027 (C-H), 2928 (C-H), 1628 (C=C), 1372 (C-O); HRMS (ESI) Calcd For $C_{24}H_{22}NO_3$ 372.1594 (M+H$^+$); Found 372.1623.

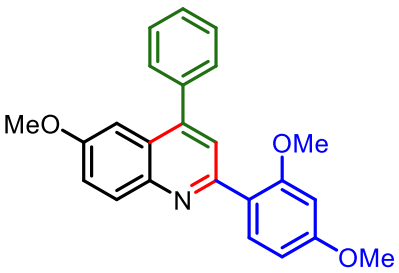

4-(4-(*tert*-Butyl)phenyl)-6-methoxy-2-(naphthalen-2-yl)quinoline (4q) White solid (367.45 mg, 88%); mp 120-122 °C. ^{1}H NMR (500 MHz, DMSO-*d*$_6$) δ 8.84 (s, 1H), 8.51 (d, *J* = 8.7 Hz, 1H), 8.15 – 8.13 (m, 2H), 8.08 – 8.05 (m, 2H), 7.97 (dd, *J* = 5.9, 3.4 Hz, 1H), 7.67 – 7.63 (m, 4H), 7.57 – 7.56 (m, 2H), 7.51 (dd, *J* = 9.1, 2.5 Hz, 1H), 7.27 (d, *J* = 2.5 Hz, 1H), 3.80 (s, 3H), 1.38 (s, 9H); ^{13}C NMR (100 MHz, DMSO-*d*$_6$) δ 157.8, 153.6, 151.4, 147.5, 144.5, 136.3, 135.2, 133.6, 133.4, 131.7, 129.5, 129.0, 128.5, 127.8, 127.1, 126.8, 126.7, 126.4, 126.0, 124.9, 122.0, 119.70, 104.1, 55.7, 34.8, 31.4; IR (KBr)ν_{max}/cm^{-1} 3036 (C-H), 2926 (C-H), 1662 (C=C), 1363 (C-O); HRMS (ESI) Calcd For $C_{30}H_{28}NO$ 418.2165 (M+H$^+$); Found 418.2171.

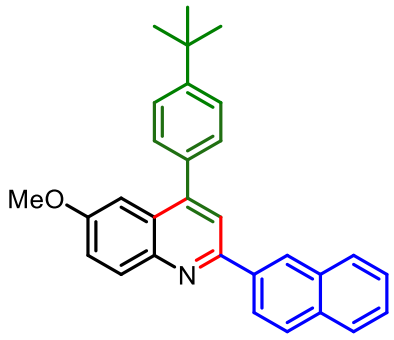

2-(3-Bromophenyl)-4-(4-(*tert*-butyl)phenyl)-8-methoxyquinoline (4r) Dark red liquid

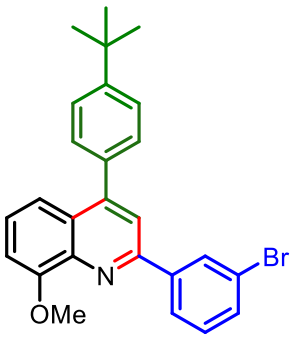

(312.46 mg, 70%); ^{1}H NMR (500 MHz, $CDCl_3$) δ 8.38 (t, *J* = 1.7 Hz, 1H), 8.13 (d, *J* = 7.9 Hz, 1H), 7.80 (s, 1H), 7.57 – 7.54 (m, 3H), 7.53 – 7.49 (m, 2H), 7.44 – 7.33 (m, 3H), 7.10 (d, *J* = 7.3 Hz, 1H), 4.13 (s, 3H), 1.42 (s, 9H); ^{13}C NMR (125 MHz, $CDCl_3$) δ 155.9, 154.2, 151.7, 149.6, 142.0, 140.8, 135.7, 132.2, 130.8, 130.3, 129.4, 127.3, 126.7, 126.3, 125.6, 123.2, 119.8, 117.8, 108.1, 56.3, 34.9, 31.5; IR (KBr)ν_{max}/cm^{-1} 3027 (C-H), 2959 (C-H), 16220 (C=C), 1368 (C-O); HRMS (ESI) Calcd For $C_{26}H_{25}BrNO$ 446.1114 ($M+H^+$); Found 446.1155.

2-(3-Bromophenyl)-4-(4-(*tert*-butyl)phenyl)-6-methylquinoline (4s) White solid (292.65 mg, 68%); mp 130-132 °C. ^{1}H NMR (400 MHz, $CDCl_3$) δ 8.38 (s, 1H), 8.12 (dd, *J* = 16.6, 8.2 Hz, 2H), 7.74 (s, 2H), 7.58 (t, *J* = 6.6 Hz, 4H), 7.51 (d, *J* = 8.1 Hz, 2H), 7.37 (t, *J* = 7.9 Hz, 1H), 2.50 (s, 3H), 1.45 (s, 9H); ^{13}C NMR (100 MHz, $CDCl_3$) δ 154.3, 151.6, 148.8, 147.4, 141.9, 136.6, 135.5, 132.0, 132.0, 130.6, 130.3, 129.9, 129.3, 126.0, 125.7, 124.6, 124.4, 123.2, 119.2, 34.8, 31.5, 21.9; IR (KBr)ν_{max}/cm^{-1} 3022 (C-H), 2926 (C-H), 1622 (C=C), 1262(C-O); HRMS (ESI) Calcd For $C_{26}H_{25}BrN$ 430.1165 ($M+H^+$); Found 430.1152.

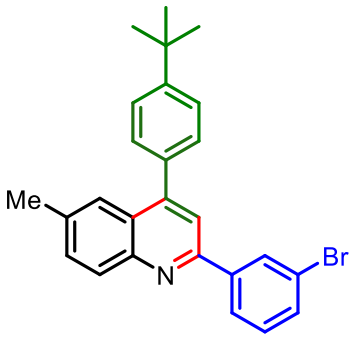

6,7-Dimethyl-2,4-diphenylquinoline (4t) Colourless liquid (185.65 mg, 60%). ^{1}H NMR (500 MHz, $CDCl_3$) δ 8.28 – 8.26 (m, 2H), 7.80 (s, 1H), 7.55 – 7.54 (m, 3H), 7.53 – 7.50 (m, 3H), 7.47 – 7.44 (m, 3H), 7.39 – 7.33 (m, 1H), 2.92 (s, 3H), 2.42 (s, 3H); ^{13}C NMR (125 MHz, $CDCl_3$) δ 154.2, 148.7, 146.4, 140.1, 139.3, 137.7, 135.8, 132.0, 129.7, 129.2, 128.8, 128.6, 128.2, 127.5, 125.8, 122.4, 118.8, 21.9, 18.4; IR (KBr)ν_{max}/cm^{-1} 3022 (C–H), 2926 (C–H), 1620 (C=C), 1372 (C-O); HRMS (ESI) Calcd For $C_{23}H_{19}N$ 310.1590 ($M+H^+$); Found 310.1596.

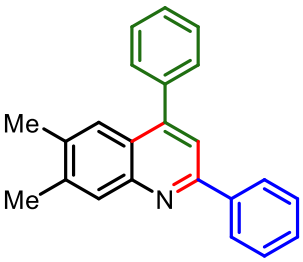

3-Ethyl-6-methoxy-2-propylquinoline (4v) Brownish liquid (87.13 mg, 38%). ^{1}H NMR (400 MHz, $CDCl_3$) δ 7.91 (d, *J* = 9.2 Hz, 1H), 7.77 (s, 1H), 7.27 (dd, *J* = 9.1, 2.9 Hz, 1H), 7.01 (d, *J* = 2.8 Hz, 1H), 3.91 (s, 3H), 2.94 – 2.90 (m, 2H), 2.81 (q, *J* = 7.5 Hz, 2H), 1.85 – 1.76 (m, 2H), 1.33 (t, *J* = 7.5 Hz, 3H), 1.05 (t, *J* = 7.4 Hz, 3H); ^{13}C NMR (100 MHz, $CDCl_3$) δ 159.5, 157.2, 142.5, 135.7, 133.1, 129.9, 128.2, 120.9,

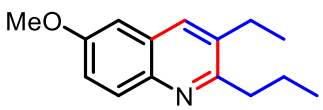

104.7, 55.6, 37.6, 25.3, 23.1, 14.6, 14.5; IR (KBr)ν_{max}/cm^{-1} 3034 (C-H), 2960 (C-H), 1619 (C=C) 1224 (C-O); HRMS (ESI) Calcd For $C_{15}H_{20}NO$ 230.1539 ($M+H^+$); Found 230.1540.

XRD for compound (4i): All the data for the structural analysis of compound **4i** has been deposited to the Cambridge Crystallographic Data Centre, CCDC No. 2218059.

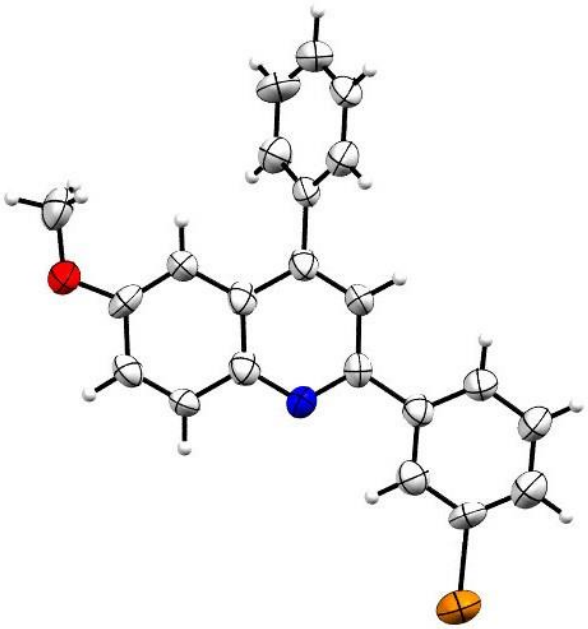

Figure 4. The ORTEP diagram of compound **4i**

Table 9. Crystal data and structure refinement for compound **4i**

Entry	Identification Code	Compound 4i
01	Empirical formula	C_{22} H_{16} Br N O
02	Formula weight	390.28
03	Temperature	296 K
04	Wavelength	0.71073
05	Radiation type	Mo K\a
06	Radiation system	Fine-focus sealed tube
07	Crystal system	Monoclinic
08	Space group	P 21/c
09	Cell length	a=7.6057(5) b=20.0110(12) c=11.6782(7)
10	Cell angle	α=90 β=99.698(2) γ=90
11	Cell volume	1751.99(19)
12	Density	1.434
13	Completeness to theta	99
14	Absorption correction	multi-scan

15	Refinement method	Full-matrix least-squares on F2
16	Index ranges	-9<=h<=9, -23<=k<=23, -13<=l<=13
17	Reflection number	2080
18	Theta range	24.999
19	Cell formula units Z	4
20	CCDC no	2218059

^{1}H NMR Spectrum of 6-Methoxy-2,4-diphenylquinoline (4a)

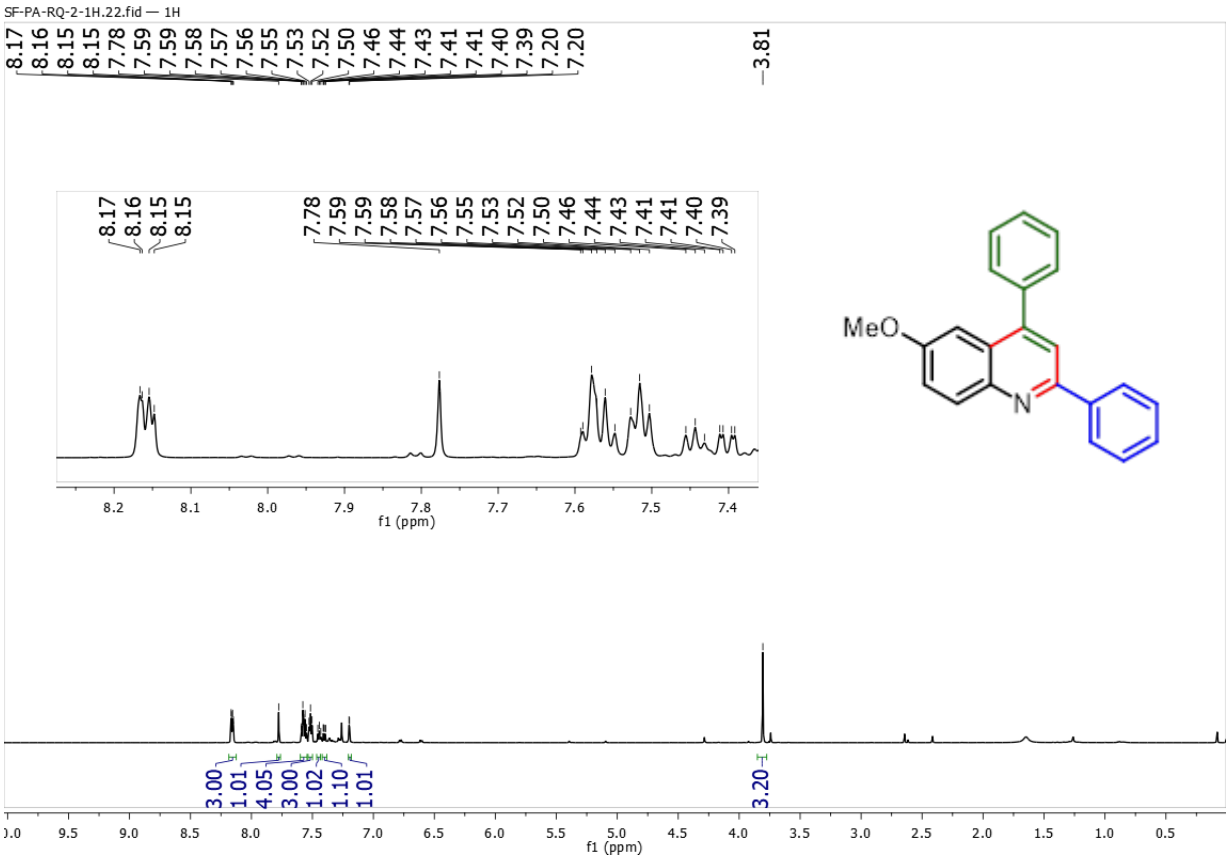

^{13}C NMR Spectrum of 6-Methoxy-2,4-diphenylquinoline (4a)

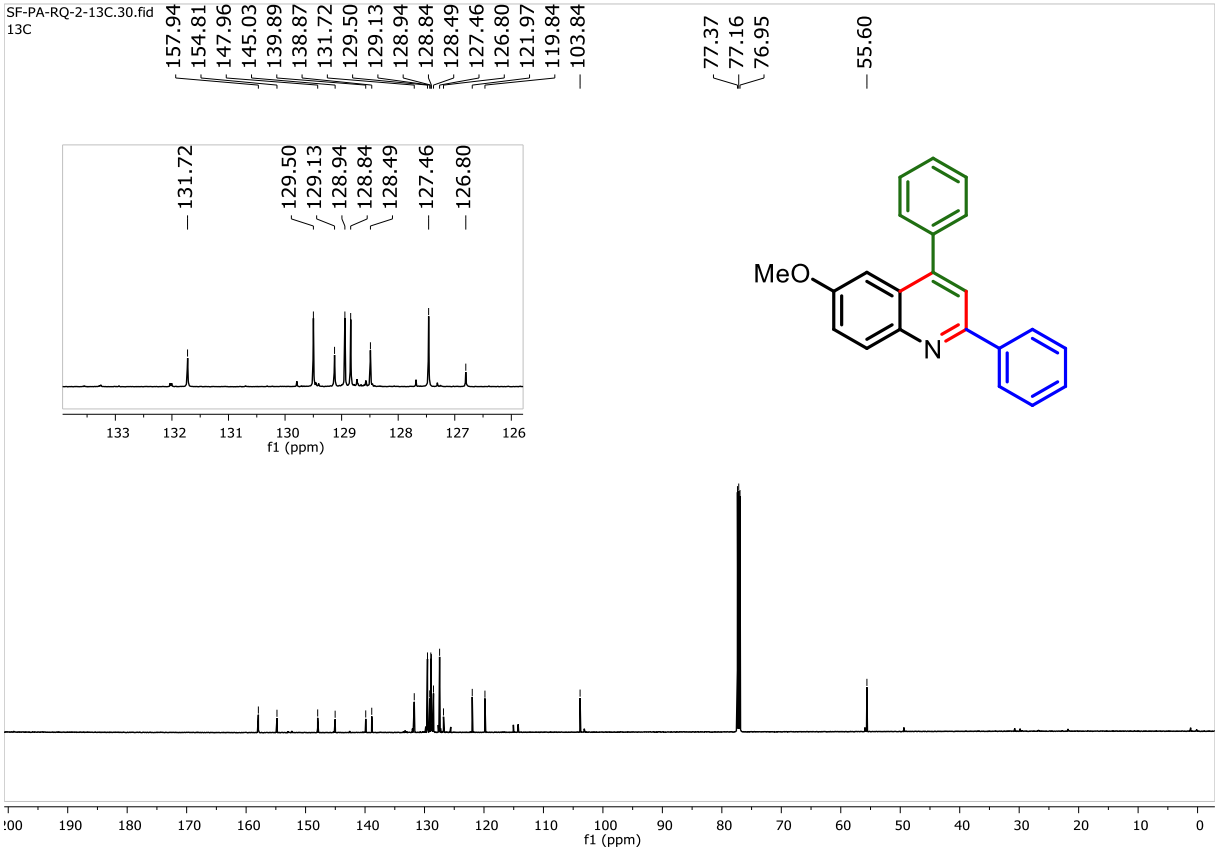

HRMS Spectrum of 6-Methoxy-2,4-diphenylquinoline (4a)

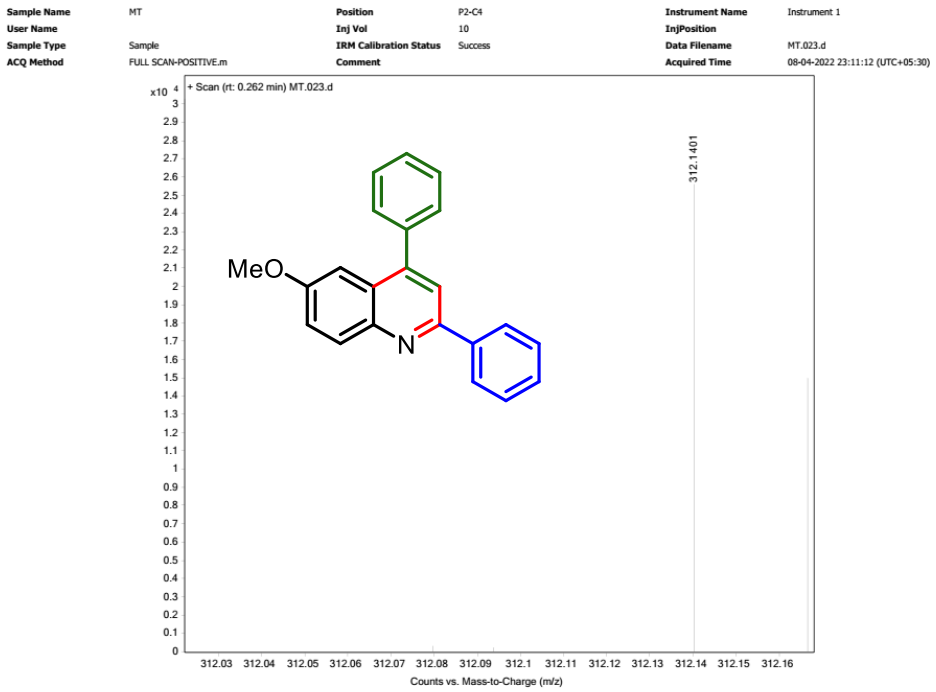

^{1}H NMR Spectrum of 3-Ethyl-6-methoxy-2-propylquinoline (4v)

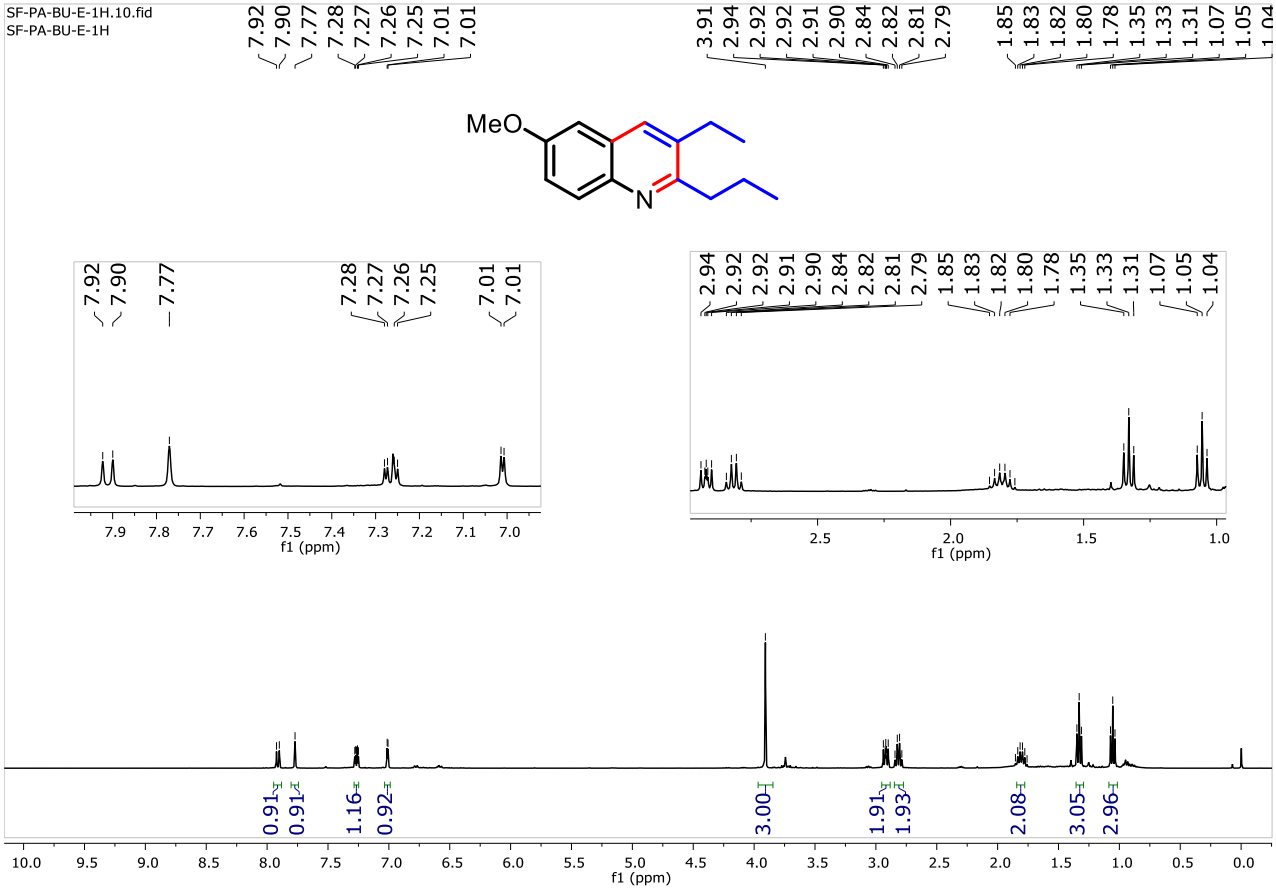

^{13}C NMR Spectrum of 3-Ethyl-6-methoxy-2-propylquinoline (4v)

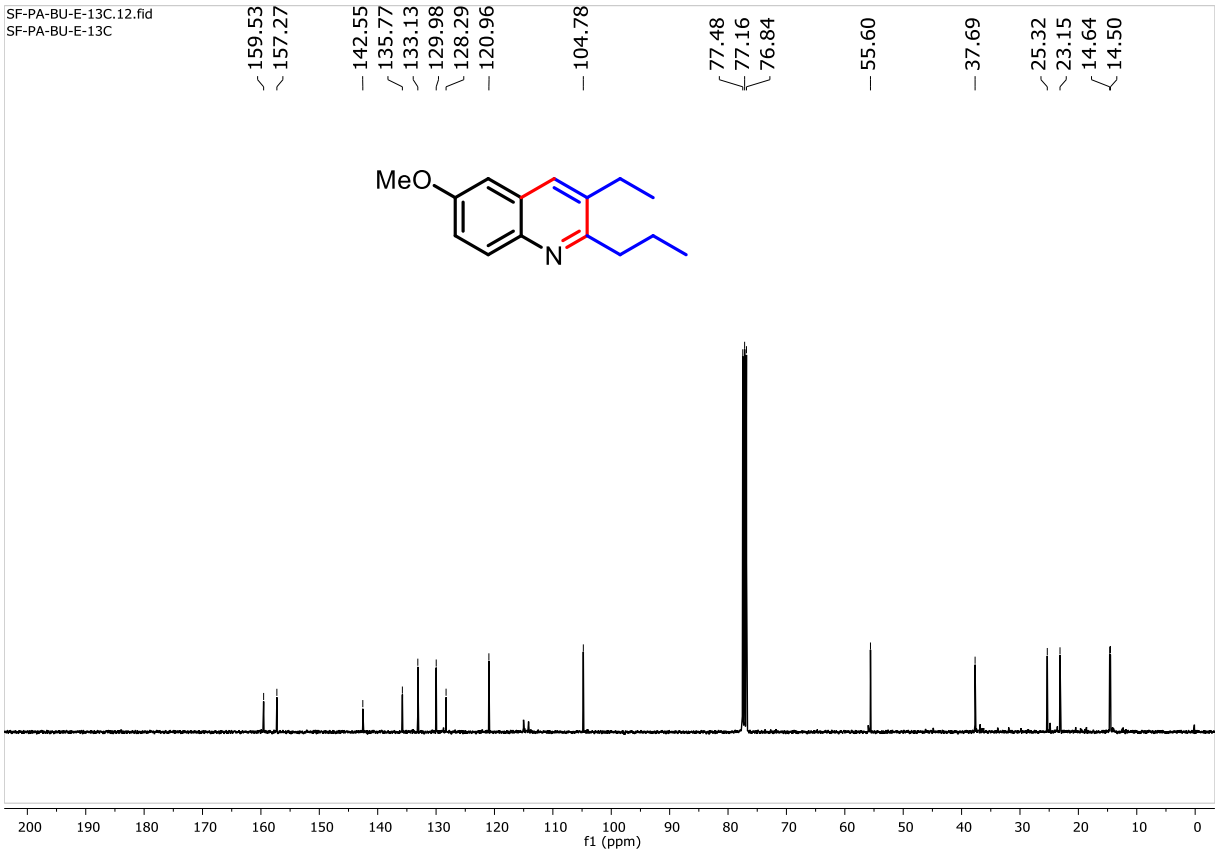

HRMS Spectrum of 3-Ethyl-6-methoxy-2-propylquinoline (4v)

Compounds

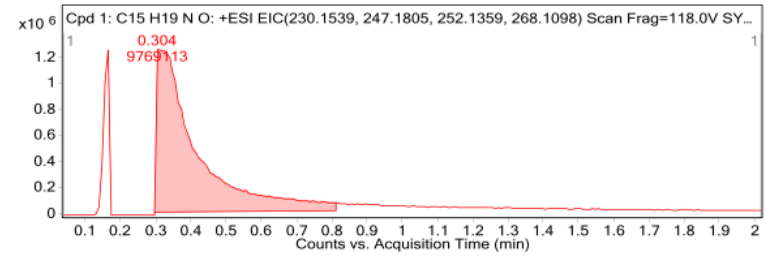

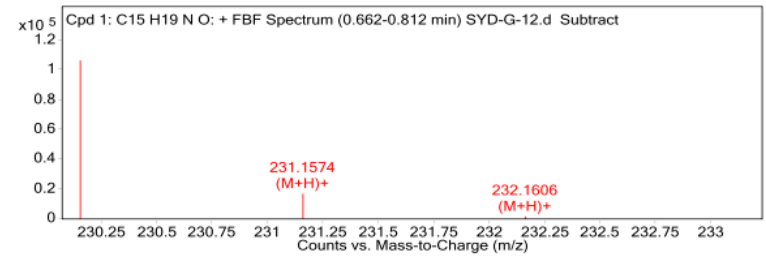

Peak List

m/z	z	Abund	Formula	Ion
230.154	1	106808.38	C15H20NO	(M+H)+
231.1574	1	16996.47	C15H20NO	(M+H)+
232.1606	1	1620.69	C15H20NO	(M+H)+
233.1525	1	126.17	C15H20NO	(M+H)+

Part A

Chapter II: Section D

Synthesis of 2-benzyl-3-arylquinoline derivatives

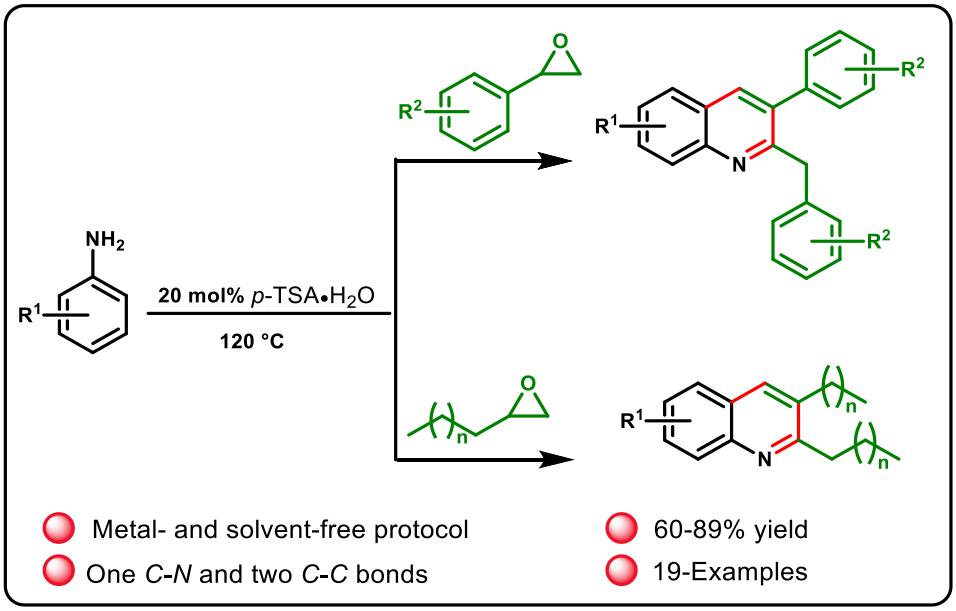

RESULT AND DISCUSSION

EXPERIMENTAL SECTION

Results and Discussion

The importance of 2-benyl-3-phenylquinoline and previously reported methods have already been overviewed in Chapter I. This section of the chapter demonstrated the regioselective synthesis of 2-benyl-3-phenylquinoline derivatives through a pseudo-three-component reaction from arylamines and styrene oxide (Scheme 24**)**. This particular transformation takes place without the use of metals and solvents, employing 20 mol% *p*-toluenesulfonic acids. Moreover, under similar reaction conditions, the synthesis of 2,3-dialkylquinoline derivative can also be accomplished using aliphatic epoxide. This methodology has several perks such as its short reaction time, high regioselectivity, easy to handle, broad substrate scope, good yields, metal- and solvent-free reaction conditions, and the formation of one *C–N* and two *C*–C bonds in a single step.

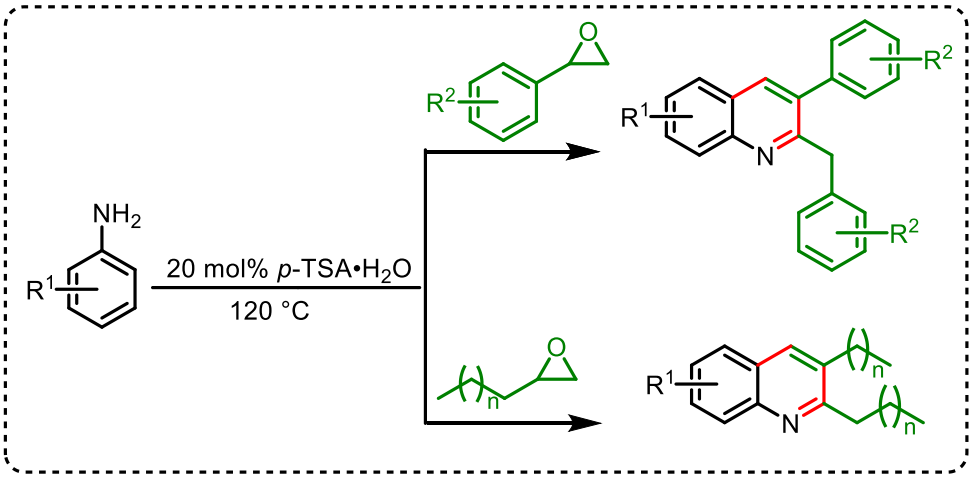

Scheme 24. Reactions between aryl amines and styrene oxide.

To determine the best reaction conditions, *m*-anisidine (**1a**) and styrene oxide (**2a**) were chosen as the model substrates. Then, various reactions were carried out with the model substrates, and their results are summarized in Table 10. Initially, the substrates **1a** (0.123 g, 1 mmol) and **2a** (0.240 g, 2.00 mmol) were taken in a 10 mL round-bottomed flask without adding solvent and catalyst, and it was stirred for 5 h at room temperature. Unfortunately, the reaction did not proceed. Then, the same reaction mixture was heated in a pre-heated oil bath at 120 °C for another 5 h (Table 10, Entry 1). Again, no reaction took place, and the starting materials were recovered. After that, a similar reaction was scrutinized in the presence of 5 mol% *p*-toluenesulfonic acid monohydrate (*p*-TSA·H_2O) at room temperature, but there was no progress in the reaction (Table 10, Entry 2). Subsequently, the reaction mixture was heated in a pre-heated oil bath at 80 °C with 5 mol% *p*-TSA·H_2O, and product **3a** was isolated after 3 h

with a 40 % yield (Table 10, Entry 3). It was characterized by IR, ^{1}H-NMR, ^{13}C-NMR-spectra, and HRMS. In the ^{1}H-NMR spectrum, it gives characteristics peaks at δ 4.26 ppm for two protons as a singlet for the benzylic proton and at δ 7.83 ppm as a singlet for 1H, which resembles 2-benzyl-7-methoxy-3-phenylquinoline. In addition, the characteristic δ values at 3.82, 3.09, and 2.76 ppm present in styrene oxide have disappeared. Moreover, the singlet hydrogen at δ 7.44 ppm in **3a** indicates the formation of 2-benzyl-7-methoxy-3-phenylquinoline instead of another regioisomer 2-benzyl-5-methoxy-3-phenylquinoline. The singlet hydrogen at δ 7.44 ppm in the ^{1}H NMR spectrum indicates that the product **3a** was formed since there are two singlet signals. From the previous reports, we concluded that the singlet appeared at δ 7.44 ppm is for H-8 and at δ 7.83 ppm is for H-4. The other possible isomer has only one proton that can appear as a singlet. All these data agree with the proposed structure of compound **3a**. Next, we proceeded further to optimize the reaction temperature. At first, we did the reaction at 100 °C using 5 mol % *p*-TSA·H_2O, and product **3a** was isolated in 50 % yield as shown in (Table 10, Entry 4). When the reaction was performed at 110 °C, desired product **3a** was obtained in 58 % (Table 10, Entry 5). The yield was further increased up to 69 % at 120 °C (Table 10, Entry 6).

Table 10. Optimization of 2-benzyl-3-phenylquinoline

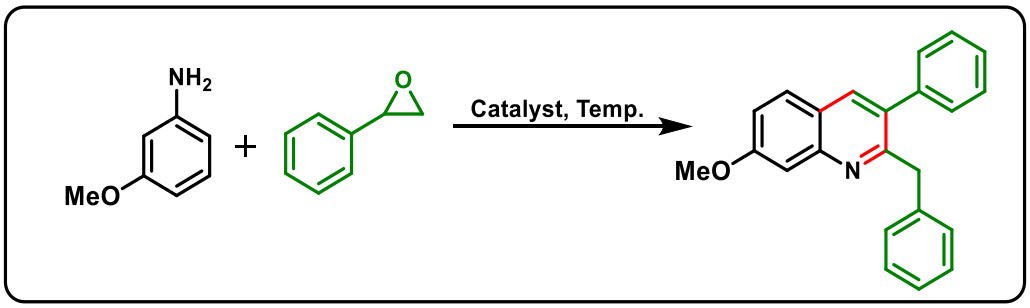

Entry	Catalyst	Mol %	Time (h)	Temp. (°C)	Yield[b] (%)
1	-	-	5	RT→120	NR
2	*p*-TSA.H_2O	5	5	RT	NR
3	*p*-TSA.H_2O	5	3	80	40
4	*p*-TSA.H_2O	5	3	100	50
5	*p*-TSA.H_2O	5	3	110	58
6	*p*-TSA.H_2O	5	3	120	69
7	*p*-TSA.H_2O	10	2	120	75

8	***p*-TSA.H_2O**	**20**	**1.5**	**120**	**89**
9	*p*-TSA.H_2O	30	1.5	120	87
10	*p*-TSA.H_2O	20	1.5	130	70
11	MsOH	20	1.5	120	26
12	TfOH	20	1.5	120	15
13	(±)-CSA	20	1.5	120	49

[a]Reaction conditions: All reactions were performed using *m*-anisidine (**1a**, 1.0 mmol), and styrene oxide (**2a**, 2.0 mmol). [b]Isolated yield. RT: Room Temperature. NR: No Reaction.

So, the next reaction was done at 120 °C using 10 mol% *p*-TSA•H_2O, and product **3a** obtained in 75 % yield relatively at a shorter time (Table 10, Entry 7). After that, the amount of the catalyst was increased to 20 mol% at the same temperature, which subsequently furnishes the product with a maximum yield of 89 % after 2 h (Table 10, Entry 8). However, further yield of the desired product did not improve by increasing the amount of catalyst (Table 10, Entry 9). Another reaction was performed using 20 mol% *p*-TSA•H_2O at 130 °C, to further check the role of reaction temperature (Table 10, Entry 10). Unfortunately, the yield was decreased to 70 %, which may be due to the decomposition of the product at a higher temperature. Then few other reactions were examined using different sulfonic acid catalysts, MsOH, TfOH, and (±)-CSA, respectively, in 20 mol% amounts (Table 10, Entry 11, 12 & 13) respectively. The isolated yield for those reactions was not satisfactory. From all the optimization reactions, we concluded that the best condition for the synthesis of 2-benzyl-3-phenylquinoline from aryl amines and styrene oxide is 20 mol% *p*-TSA·H_2O at 120 °C.

After having the optimized reaction conditions in hand, we investigated the scope, practicability, and generality of the present protocol using various other arylamines **1a-l** and different substituted styrene oxides **2a-b**, which are summarized in (Table 11). The reactions of styrene oxide **2a** with mono-substituted aryl amines **1a-e** provided various 2-benzyl-3-phenylquinoline derivatives **3a-e** in 65-89% yield. Similarly, reactions with disubstituted arylamines **1f-j** and styrene oxide **2a** underwent smoothly to provide expected quinolines **3f-j** in 70-85% yield. Trisubstituted arylamines **1k** with styrene oxide **2a** also gave 3k product in 84% yield. The reaction of 4-chlorostyrene oxide **2b** and *p*-anisidine **1b** proceeded very well and furnished the anticipated quinoline **3l** in 70% yield. Surprisingly, bicyclic amines like 1-Napthylamine **1l** also provided the desired product 2-benzyl-3-phenylbenzo[*h*]quinoline **3m** in 64% yield (Table 12). Subsequently, styrene oxide was examined with bicyclic 5-aminoindan

1m and tricyclic 2-aminofluorene **1n**, successfully furnishing expected products **3n** and **3o** in 65% and 68% yield, respectively (Table 12). Unfortunately, the reaction did not proceed at all with the arylamines containing an electron-withdrawing group at the ortho, para, and meta positions.

Table 11. Substrate scope.[a,b]

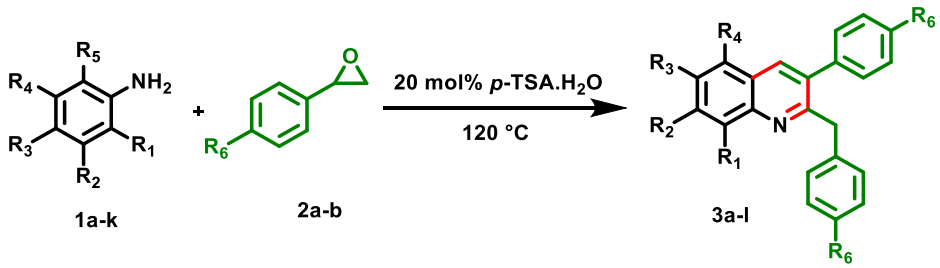

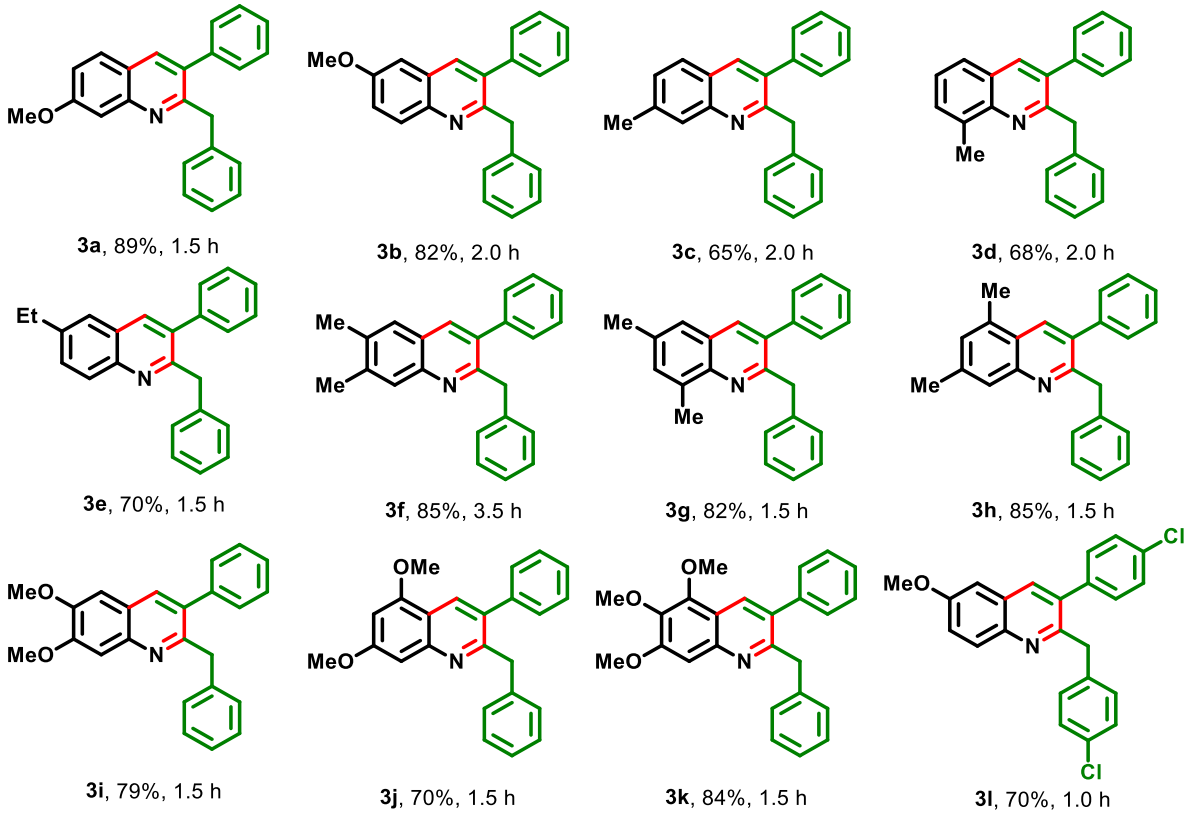

[a]Reaction conditions: All reactions are carried out using arylamines (**1a-k**, 1.0 mmol), with styrene oxide (**2a-b,** 2.0 mmol) in the presence of 20 mol% *p*-TSA**.**H_2O at 120 °C. [b]Isolated yields.

Delightfully, the procedure was extended further on a large-scale reaction using 24.4 mmol of *m*-anisidine **1a** and 48.7 mmol of styrene oxide **2a**, and desired product **3a** was isolated in 91% yield (7.23 g).

Inspired by the above results, we further explored the scope of this reaction with various aliphatic epoxide **2c-2f** as shown in (Table 13). The reaction of *p*-anisidine **1b** with 1,2-

epoxybutane (**2c**), 1,2-epoxyhexane (**2d**), 1,2-epoxydodecane (**2e**), and 1,2-epoxytetradecane (**2f**) also gave the desired products in 69% (**3p**), 65% (**3q**), 66% (**3r**) and 60% (**3s**) respectively.

Table 12. Substrate scope.[a,b]

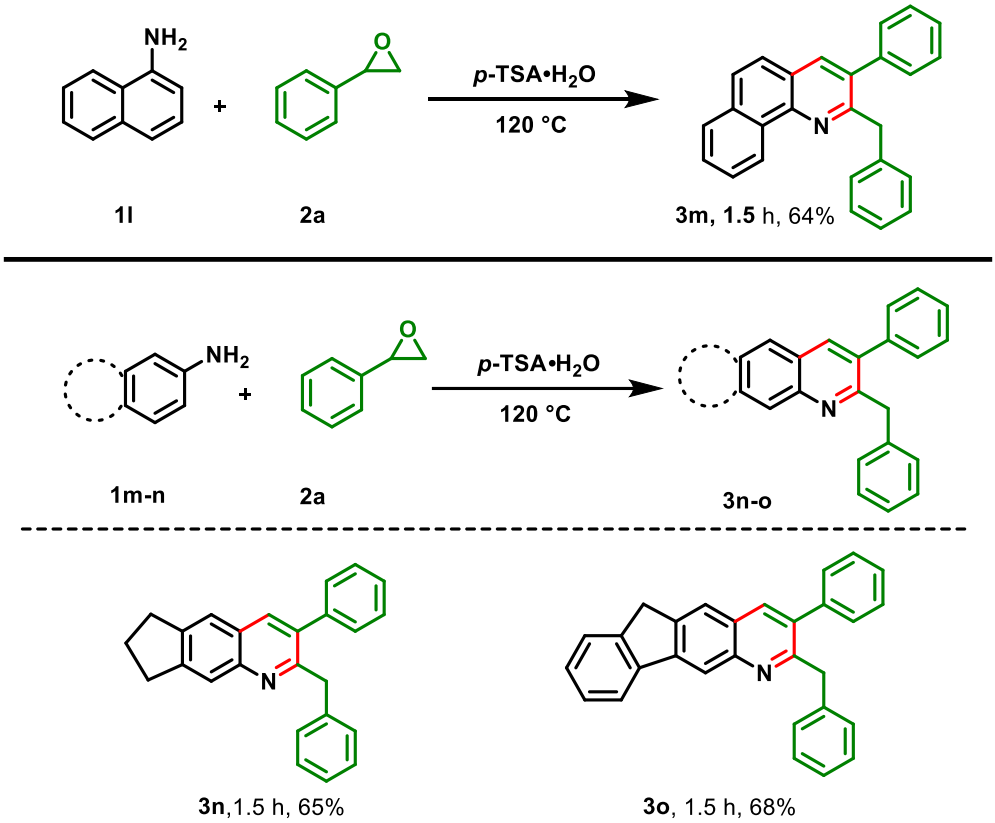

[a]Reaction conditions: All reactions are carried out using arylamines (**1l-o**, 1.0 mmol), with styrene oxide (**2a,** 2.0 mmol) in the presence of 20 mol% *p*-TSA**.**H_2O at 120 °C. [b]Isolated yields.

The probable mechanism for the formation of the desired product is shown in (Scheme 25) as follows: Initially, *m*-anisidine **1a** reacts with styrene oxide **2a** in the presence of *p*-toluenesulfonic acid monohydrate to form *ß*-amino alcohol **A** by ring-opening preferentially at the less hindered side[36] of the styrene oxide. Promptly, the enamine intermediate **B** is formed after the elimination of one molecule of water, which can readily tautomerize to its corresponding imine intermediate **C**. Subsequently, the imine intermediate **C** reacts with enamine **B** to provide the intermediate **D** *via* an intermolecular Mannich-type reaction as reported by Beller and co-workers[23]. After that, intermediate **D** undergoes intramolecular cyclization followed by aromatization to form an intermediate **F**. Then, the intermediate **F** is converted into the dihydroquinoline intermediate **G** after the elimination of one molecule of 3-methoxyaniline **1a**. Finally, upon aerial oxidation of the intermediate **G**, the desired product **3a** is obtained.

Table 13. Substrate scope.[a,b]

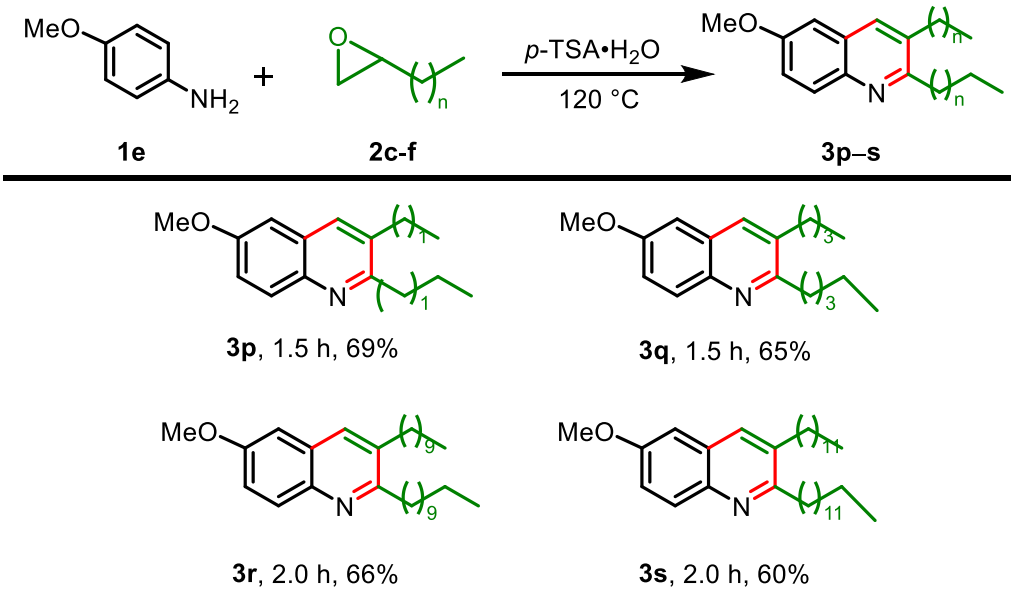

[a]Reaction conditions: All reactions are carried out using *p*-anisidine (**1b**, 1.0 mmol), with aliphatic epoxides (**2c-f**, 2.0 mmol) in the presence of 20 mol% *p*-TSA**.**H_2O at 120 °C. [b]Isolated yields.

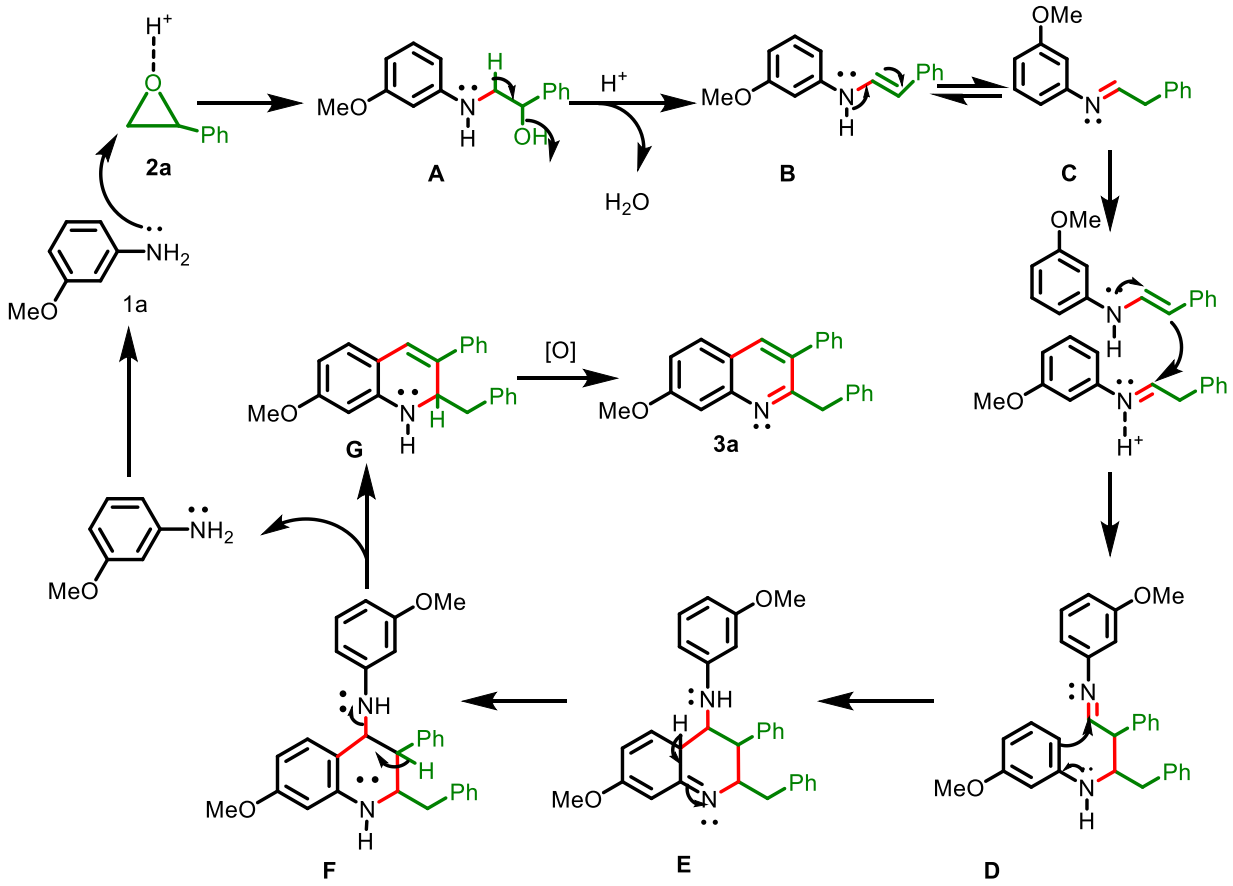

Scheme 25. A plausible mechanism for the formation of 2-benzyl-3-phenylquinoline **3a**.

In conclusion, we have developed a convenient solvent-free protocol for the synthesis of 2-benzyl-3-phenylquinoline *via* a pseudo-three-component reaction from arylamines and epoxides in the presence of 20 mol% *p*-TSA•H_2O at 120 °C under an open-air atmospheric condition. The salient features of this protocol are easy handling, metal- and solvent-free reaction conditions, good yield, use of cheaper catalysts, and shorter reaction time. Notably, it is the first metal- and solvent-free synthesis of 2-benzyl-3-phenylquinoline using arylamines and styrene oxide derivatives.

Experimental Section

General Procedure for the Synthesis of 2-Benzyl-3-phenylquinoline Derivatives

Arylamine (**1**, 1.0 mmol) and styrene oxide (**2**, 2.0 mmol) were taken in a 10 mL round-bottomed flask. *p*-TSA·H_2O (20 mol%) was added to the reaction mixture and kept in a pre-heated oil bath with constant stirring under an air atmosphere at 120 °C. The progress of the reaction was monitored by checking TLC. After the completion of the reaction, it was brought to room temperature. A workup was done using EtOAc and brine solution and dried with anhydrous sodium sulfate. After that, the solvent was removed in a rotary evaporator, and the crude residue was passed through a silica gel column (silica gel 60-120 mesh) to obtain the pure product.

2-Benzyl-7-methoxy-3-phenylquinoline (3a) Yellow liquid (289.61 mg, 89%). ^{1}H NMR (500

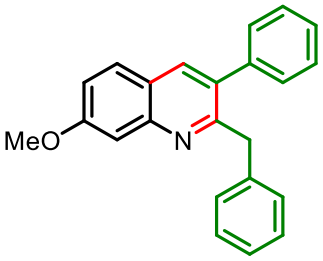

MHz, $CDCl_3$) δ 7.83 (s, 1H), 7.61 (d, *J* = 8.9 Hz, 1H), 7.44 (s, 1H), 7.32 – 7.30 (m, 3H), 7.16 – 7.13 (m, 3H), 7.06 (m, 3H), 6.90 (d, *J* = 7.1 Hz, 2H), 4.26 (s, 2H), 3.93 (s, 3H); ^{13}C NMR (100 MHz, $CDCl_3$) δ 160.8, 1159.2, 148.9, 140.2, 139.7, 136.8, 134.1, 129.8, 129.0, 128.5, 128.3, 128.2, 127.4, 125,9, 122.2, 119.2, 107.1, 55.7, 42.7; IR (KBr)ν_{max}/cm^{-1} 2924 (C–H), 1621 (C=C), 1228 (C–O); HRMS (ESI): *m/z* [M+H$^+$] Calcd for $C_{23}H_{20}NO$: 326.1539; Found: 326.1549.

2-Benzyl-6-methoxy-3-phenylquinoline (3b) Light Brown liquid (266.83 mg, 82%). ^{1}H NMR

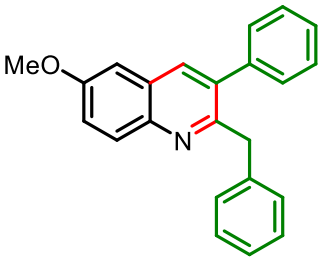

(600 MHz, $CDCl_3$) δ 8.04 (d, *J* = 9.2 Hz, 1H), 7.85 (s, 1H), 7.36 (d, *J* = 4.9 Hz, 4H), 7.21 – 7.18 (m, 2H), 7.09 (dd, *J* = 12.3, 7.1 Hz, 3H), 7.05 (s, 1H), 6.93 (d, *J* = 7.3 Hz, 2H), 4.28 (s, 2H), 3.92 (s, 3H); ^{13}C NMR (100 MHz, $CDCl_3$) δ 157.9, 156.6, 143.4, 139.9, 139.8, 136.5, 135.9, 130.5, 129.5, 128.9, 128.3, 128.2, 128.0, 127.6, 126.0, 122.2, 105.0, 55.7, 42.6; IR (KBr)ν_{max}/cm^{-1} 2924 (C–H), 1621 (C=C), 1228 (C–O); HRMS (ESI) Calcd For $C_{23}H_{20}NO$ 326.1539 (M+H$^+$); Found 326.1537.

2-Benzyl-7-methyl-3-phenylquinoline (3c) Dark Brown liquid (201.11 mg, 65%). ^{1}H NMR

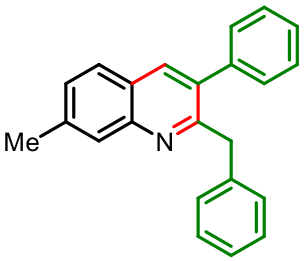

(400 MHz, $CDCl_3$) δ 7.94 (s, 1H), 7.91 (s, 1H), 7.69 (d, *J* = 9.0 Hz, 1H), 7.37 – 7.36 (m, 4H), 7.21 (dd, *J* = 6.6, 3.0 Hz, 2H), 7.10 (dt, *J* = 6.9, 2.0 Hz, 3H), 6.94 – 6.93 (m, 2H), 4.31 (s, 2H), 2.59 (s, 3H); ^{13}C NMR (100 MHz, $CDCl_3$) δ 159.0, 139.8, 139.5, 136.8, 135.3, 130.1, 129.9, 129.6, 128.9, 128.7, 128.3, 12.1, 128.0, 127.6, 127.2,

125.9, 125.0, 42.8, 22.0; IR (KBr)ν_{max}/cm^{-1} 3057 (C–H), 2921 (C–H), 1600 (C=C); HRMS (ESI): *m/z* [M+H$^+$] Calcd for $C_{23}H_{20}N$: 310.1590; Found: 310.1601.

2-Benzyl-8-methyl-3-phenylquinoline (3d) Brown liquid (210.39 mg, 68%). ^{1}H NMR (500 MHz, $CDCl_3$) δ 7.81 (s, 1H), 7.52 (d, *J* = 9.2 Hz, 1H), 7.45 (d, *J* = 6.9 Hz, 1H), 7.32 – 7.28 (m, 4H), 7.15 (dd, *J* = 6.5, 2.9 Hz, 2H), 6.99 – 6.95 (m, 3H), 6.98 (d, *J* = 8.0 Hz, 2H), 4.23 (s, 2H), 2.77 (s, 3H); ^{13}C NMR (100 MHz, $CDCl_3$) δ 157.8, 146.4, 140.1, 139.8, 137.1, 136.9, 135.6, 129.6, 129.4, 129.2, 128.3, 128.1, 127.6, 126.8, 126.1, 125.9, 125.5, 42.9, 18.1; IR (KBr)ν_{max}/cm^{-1} 3058 (C–H), 2922 (C–H), 1598 (C=C); HRMS (ESI): *m/z* [M+H$^+$] Calcd for $C_{23}H_{20}N$: 310.1590; Found: 310.1603.

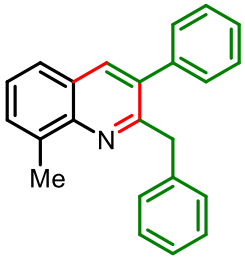

2-Benzyl-6-ethyl-3-phenylquinoline (3e) Reddish Brown liquid (226.40 mg, 70%). ^{1}H NMR (400 MHz, $CDCl_3$) δ 8.09 (d, *J* = 8.6 Hz, 1H), 7.90 (s, 1H), 7.60 (dd, *J* = 8.9, 2.2 Hz, 1H), 7.57 (s, 1H), 7.39 (dd, *J* = 5.0, 2.0 Hz, 3H), 7.21 – 7.17 (m, 2H), 7.12 – 7.07 (m, 3H), 6.93 (d, *J* = 7.4, 2H), 4.34 (s, 2H), 2.85(q, *J* = 7.6 Hz, 2H), 1.35 (t, *J* = 7.6 Hz, 3H); ^{13}C NMR (100 MHz, $CDCl_3$) δ 158.3, 146.06, 142.6, 139.9, 139.6, 136.6, 136.2, 130.8, 129.6, 129.0, 128.8, 128.3, 128.1, 127.6, 127.1, 126.0, 125.1, 42.8, 29.0, 15.6; IR (KBr)ν_{max}/cm^{-1} 3058 (C–H), 2963 (C–H), 1614 (C=C); HRMS (ESI): *m/z* [M+H$^+$] Calcd for $C_{24}H_{22}N$: 324.1747; Found: 324.1758.

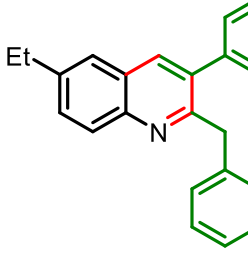

2-Benzyl-6,7-dimethyl-3-phenylquinoline (3f) Light Brown liquid (274.91 mg, 85%). ^{1}H NMR (400 MHz, $CDCl_3$) δ 7.92 (s, 1H), 7.83 (s, 1H), 7.52 (s, 1H), 7.35(dd, *J* = 4.9, 1.9 Hz, 3H), 7.18 (dd, *J* = 6.7, 2.9 Hz, 2H), 7.01 (td, *J* = 6.5, 6.1, 2.9 Hz, 3H), 6.92 (d, *J* = 7.6 Hz, 2H), 4.30 (s, 2H), 2.49 (s, 3H), 2.45 (s, 3H); ^{13}C NMR (100 MHz, $CDCl_3$) δ 158.1, 146.4, 140.1, 139.7, 136.4, 136.0, 135.4, 129.9, 129.6, 128.9, 128.4, 128.3, 128.1, 127.5, 126.7, 125.9, 125.6, 42.8, 20.6, 20.2; IR (KBr)ν_{max}/cm^{-1} 3024 (C–H), 2922 (C–H), 1600 (C=C); HRMS (ESI): *m/z* [M+H$^+$] Calcd for $C_{24}H_{22}N$: 324.1747; Found: 324.1759.

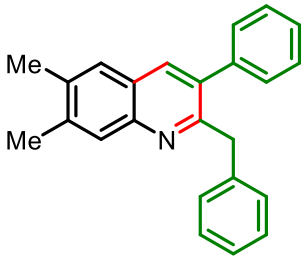

2-Benzyl-6,8-dimethyl-3-phenylquinoline (3g) Dark yellow liquid (265.21 mg, 82%). ^{1}H NMR (400 MHz, $CDCl_3$) δ 7.80 (s, 1H), 7.40 – 7.36 (m, 5H), 7.24 – 7.21 (m, 2H), 7.14 – 7.10 (m, 3H), 7.05 (d, *J* = 8.2 Hz, 2H), 4.29 (s, 2H), 2.80 (s, 3H), 2.46 (s, 3H); ^{13}C NMR (100 MHz, $CDCl_3$) δ 156.7, 145.0, 140.2, 140.0, 136.7, 136.3, 135.8, 135.6, 131.7, 129.6, 129.2, 128.3, 128.0, 127.5, 126.9, 125.9, 124.2, 42.2, 21.3, 17.7; IR (KBr)ν_{max}/cm^{-1} 3058(C–H), 2920 (C–H), 1625 (C=C); HRMS (ESI): *m/z* [M+H$^+$] Calcd for $C_{24}H_{22}N$: 324.1747; Found: 324.1758.

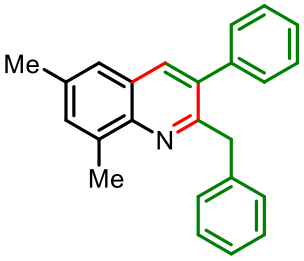

2-Benzyl-5,7-dimethyl-3-phenylquinoline (3h) Yellow liquid (274.91 mg, 85%). ^{1}H NMR (600 MHz, $CDCl_3$) δ 8.04 (s, 1H), 7.80 (s, 1H), 7.38 (d, *J* = 4.7 Hz, 3H), 7.21 (d, *J* = 4.6 Hz, 3H), 7.10 (q, *J* = 10.6, 8.7 Hz, 3H), 6.94 (d, *J* = 7.2 Hz, 2H), 4.31 (s, 2H), 2.61 (s, 3H), 2.54 (s, 3H); ^{13}C NMR (100 MHz, $CDCl_3$) δ 158.5, 147.9, 140.2, 139.6, 139.4, 134.8, 134.1, 133.5, 129.7, 129.2, 128.9, 128.3, 128.1, 127.5, 126.3, 125.9, 124.3, 42.8, 22.0, 18.6; IR (KBr)ν_{max}/cm^{-1} 3057(C–H), 2921 (C–H), 1621 (C=C); HRMS (ESI): *m/z* [M+H$^+$] Calcd for $C_{24}H_{22}N$: 324.1747; Found: 324.1758.

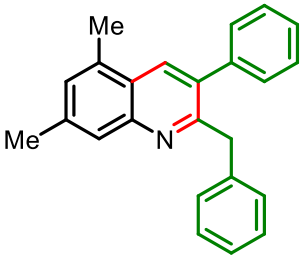

2-Benzyl-6,7-dimethoxy-3-phenylquinoline (3i) Light Brown liquid (280.78 mg, 79%). ^{1}H NMR (400 MHz, $CDCl_3$) δ 7.83 (s, 1H), 7.53 (s, 1H), 7.36 (t, *J* = 4.0 Hz, 3H), 7.23-7.19 (m, 2H), 7.15-7.08 (m, 3H), 7.03 (s, 1H), 6.95 (d, J = 6.5 Hz, 2H), 4.31 (s, 2H), 4.06 (s, 3H), 4.01 (s, 3H); ^{13}C NMR (100 MHz, $CDCl_3$) δ 156.5, 152.7, 149.9, 144.0, 139.9, 139.8, 135.7, 134.4, 129.6, 128.9, 128.2, 128.2, 127.5, 125.9, 122.5, 107.6, 104.9, 56.3, 56.2, 42.3; IR (KBr)ν_{max}/cm^{-1} 3026 (C–H), 2929 (C–H), 1621 (C=C); HRMS (ESI): *m/z* [M+H$^+$] Calcd for $C_{24}H_{22}NO_2$: 356.1645; Found: 356.1658.

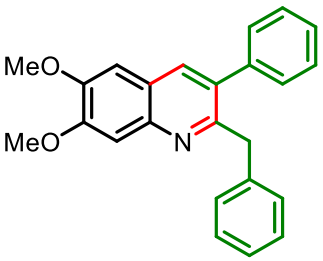

2-Benzyl-5,7-dimethoxy-3-phenylquinoline (3j) Yellow liquid (248.80 mg, 70%). ^{1}H NMR (600 MHz, $CDCl_3$) δ 8.25 (s, 1H), 7.35 (s, 3H), 7.20 (s, 2H), 7.10 (dd, *J* = 14.6, 6.4 Hz, 4H), 6.95 (d, *J* = 6.6 Hz, 2H), 6.51 (s, 1H), 4.29 (s, 2H), 3.97 (s, 4H), 3.94 (s, 4H); ^{13}C NMR (100 MHz, $CDCl_3$) δ 161.5, 159.5, 156.2, 147.1, 140.2, 139.7, 133.2, 132.0, 129.7, 128.9, 128.2, 128.2, 127.4, 126.0, 115.4, 99.4, 98.1, 55.9, 55.8, 42.7; IR (KBr)ν_{max}/cm^{-1} 3026 (C–H), 2935 (C–H), 1623 (C=C); HRMS (ESI): *m/z* [M+H$^+$] Calcd for $C_{24}H_{22}NO_2$: 356.1645; Found: 356.1645.

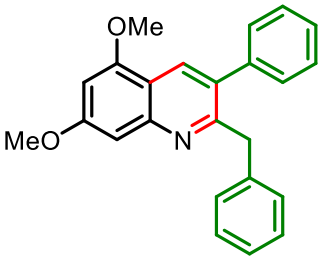

2-Benzyl-5,6,7-trimethoxy-3-phenylquinoline (3k) Dark orange liquid (323.78 mg, 84%). ^{1}H

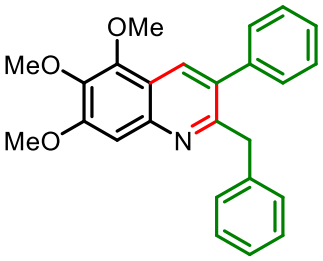

NMR (500 MHz; $CDCl_3$) δ 8.16 (s, 1H), 7.37 – 7.36 (m, 3H), 7.31 (s, 1H), 7.22 – 7.20 (m, 2H), 7.12 (t, *J* = 8.0 Hz, 3H), 6.94 (d, *J* = 6.9 Hz, 2H), 4.29 (s, 2H), 4.04 (s, 3H), 4.03 (s, 3H), 3.98 (s, 3H); ^{13}C NMR (100 MHz, $CDCl_3$) δ 158.3, 156.1, 147.0, 144.9, 140.8, 140.1, 139.6, 133.9, 131.6, 129.7, 128.9, 128.3, 128.2, 127.3, 125.9, 117.9, 103.8, 61.7, 61.4, 56.3, 42.5; IR (KBr)ν_{max}/cm^{-1} 3058 (C–H), 2937 (C–H), 1616 (C=C); HRMS (ESI): *m/z* [M+H$^+$] Calcd for For $C_{25}H_{24}NO_3$: 386.1751; Found: 386.1756.

2-(4-Chlorobenzyl)-3-(4-chlorophenyl)-6-methoxyquinoline (3l) Black liquid (276.00 mg,

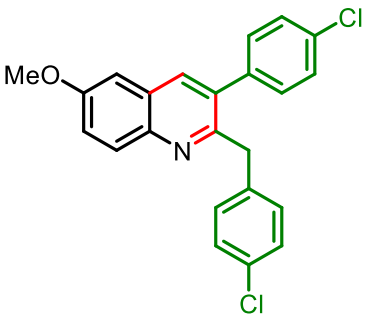

70%). ^{1}H NMR (400 MHz, $CDCl_3$) δ 8.04 (d, *J* = 9.3 Hz, 1H), 7.83 (s, 1H), 7.42 – 7.38 (m, 1H), 7.37 – 7.34 (m, 2H), 7.10 (d, *J* = 8.1 Hz, 4H), 7.05 (d, *J* = 2.8 Hz, 1H), 6.86 (d, *J* = 8.4 Hz, 2H), 4.22 (s, 2H), 3.93 (s, 3H); ^{13}C NMR (100 MHz, $CDCl_3$) δ 158.1, 155.7, 138.1, 137.9, 135.1, 134.0, 132.0, 131.5, 130.8, 130.2, 129.0, 128.8, 128.6, 128.4, 128.0, 122.7, 105.0, 55.8, 42.1; IR (KBr)ν_{max}/cm^{-1} 3028 (C–H), 2922 (C–H), 1623 (C=C) 1228 (C–O); HRMS (ESI): *m/z* [M+H$^+$] Calcd for $C_{23}H_{18}Cl_2NO$: 394.0760; Found: 394.0772.

2-Benzyl-3-phenylbenzo[*h*]quinoline (3m) Brown liquid (221.08 mg, 64%). ^{1}H NMR (400

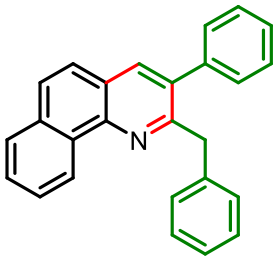

MHz, $CDCl_3$) δ 9.39 (d, *J* = 7.0 Hz, 1H), 7.98 (s, 1H), 7.89 (d, *J* = 8.1 Hz, 1H), 7.79 (d, *J* = 8.8 Hz, 1H), 7.78 – 7.70 (m, *2*H), 7.67 (d, *J* = 8.8 Hz, 1H), 7.43 (dd, *J* = 5.2, 1.9 Hz, 3H), 7.31 (dt, *J* = 6.6, 2.3 Hz, 3H), 7.22 – 7.13 (m, 5H), 4.42 (s, 2H); ^{13}C NMR (100 MHz, $CDCl_3$) δ 157.4, 145.3, 140.1, 140.0, 136.8, 136.3, 133.8, 131.6, 129.7, 129.2, 128.4, 128.2, 128.1, 127.9, 127.7, 127.5, 127.1, 126.0, 125.2, 124.8, 124.7, 42.7; IR (KBr)ν_{max}/cm^{-1} 3059 (C–H), 2922 (C–H), 1600 (C=C); HRMS (ESI): *m/z* [M+H$^+$] Calcd for $C_{26}H_{20}N$: 346.1590; Found: 346.1616.

2-Benzyl-3-phenyl-7,8-dihydro-6*H*-cyclopenta[*g*]-quinoline (3n) Dark grey solid (218.04

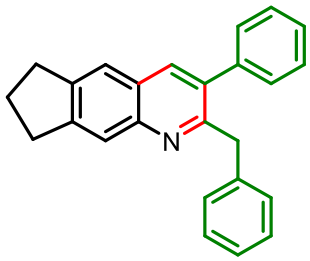

mg, 65%); mp 80-82 ^{o}C. ^{1}H NMR (400 MHz, $CDCl_3$) δ 7.96 (s, 1H), 7.87 (s, 1H), 7.58 (s, 1H), 7.36 (dd, *J* = 4.9 Hz, 3H), 7.22 – 7.17 (m, 2H), 7.13 – 7.06 (m, 3H), 6.94 (d, *J* = 7.8 Hz, 2H), 4.30 (s, 2H), 3.13 (t, *J* = 7.2 Hz, 2H), 3.07 (t, *J* = 7.3 Hz, 2H) 2.17 (p, *J* = 7.1 Hz, 2H); ^{13}C NMR (100 MHz, $CDCl_3$) δ 157.8, 147.8, 147.1, 144.1, 140.1, 139.8, 136.6, 135.1, 129.6, 128.9, 128.3, 128.1, 127.5, 126.2, 125.9, 123.3, 121.5, 42.8, 33.1,

32.7, 25.8; IR (KBr)ν_{max}/cm^{-1} 3022 (C–H), 2922 (C–H), 1599 (C=C); HRMS (ESI): *m/z* [M+H$^+$] Calcd for $C_{25}H_{22}N$: 336.1747; Found: 336.1757.

2-Benzyl-3-phenyl-6*H*-indeno[2,1-*g*]quinoline (3o) Dark Red liquid (260.76 mg, 68%). ^{1}H NMR (400 MHz, $CDCl_3$) δ 8.28 (s, 1H), 8.12 (s, 1H), 8.05 (s, 1H), 7.92 (d, *J* = 7.1 Hz, 1H), 7.60 (d, *J* = 7.3 Hz, 1H), 7.46 – 7.38 (m, 6H), 7.24 (d, *J* = 3.6 Hz, 1H), 7.15 – 7.10 (m, 3H), 7.00 – 6.97 (m, 2H), 4.34 (s, 2H), 4.17 (s, 2H); ^{13}C NMR (100 MHz, $CDCl_3$) δ 158.3, 145.4, 144.0, 141.1, 140.6, 139.9, 139.6, 137.2, 135.7, 129.6, 129.0, 128.4, 128.1, 127.7, 127.2, 126.5, 126.0, 125.5, 124.6, 120.9, 117.0, 42.8, 36.9; IR (KBr)ν_{max}/cm^{-1} 3090 (C–H), 2922 (C–H), 1600 (C=C); HRMS (ESI): *m/z* [M+H$^+$] Calcd for $C_{29}H_{21}N$: 383.1674; Found: 383.1653.

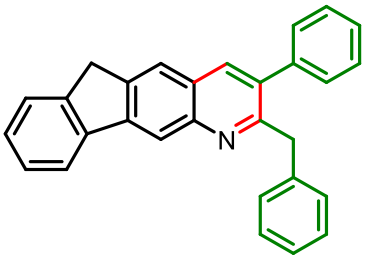

3-Ethyl-6-methoxy-2-propylquinoline (3p) Black liquid (158.23 mg, 69%). ^{1}H NMR (400 MHz, $CDCl_3$) δ 7.91 (d, *J* = 8.5 Hz, 1H), 7.77 (s, 1H), 7.26 (dd, *J* = 9.2, 2.8 Hz, 1H), 7.00 (d, *J* = 2.7 Hz, 1H), 3.90 (s, 3H), 2.98 (t, *J* = 7.5 Hz, 2H), 2.81 (q, *J* = 7.5 Hz, 2H), 1.81 (sext, *J* = 7.4 Hz, 2H), 1.33 (t, *J* = 7.5 Hz, 3H), 1.05 (t, *J* = 7.3 Hz, 3H); ^{13}C NMR (100 MHz, $CDCl_3$) δ 159.5, 157.3, 142.5, 135.8, 133.1, 130.0, 128.3, 121.0, 104.8, 55.6, 37.7, 25.3, 23.14, 14.6, 14.5; IR (KBr)ν_{max}/cm^{-1} 3034 (C–H), 2960 (C–H), 1619 (C=C) 1224 (C–O); HRMS (ESI): *m/z* [M+H$^+$] Calcd for $C_{15}H_{20}NO$: 230.1539; Found: 230.1548.

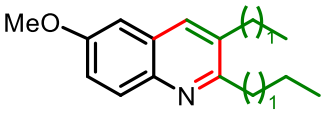

3-Butyl-6-methoxy-2-pentylquinoline (3q) Black liquid (185.52 mg, 65%). ^{1}H NMR (400 MHz, $CDCl_3$) δ 7.92 (d, *J* = 9.2 Hz, 1H), 7.75 (s, 1H), 7.26 (dd, *J* = 9.2, 2.8 Hz, 1H), 6.99 (d, *J* = 2.8 Hz, 1H), 3.90 (s, 3H), 2.98 (t, *J* = 8.0 Hz, 2H), 2.82 (t, *J* = 8.0 Hz, 2H), 1.77 (quint, *J* = 8.0 Hz, 2H), 1.67 (quint, *J* = 8.0 Hz, 2H), 1.48 – 1.38 (m, 6H), 0.99 (t, *J* = 7.3 Hz, 3H), 0.93 (d, *J* = 7.1 Hz, 3H); ^{13}C NMR (100 MHz, $CDCl_3$) δ 159.80, 157.25, 142.59, 134.50, 134.08, 129.94, 128.17, 120.97, 104.71, 55.59, 35.76, 32.86, 32.30, 32.22, 29.73, 22.81, 22.76, 14.22, 14.13; IR (KBr)ν_{max}/cm^{-1} 3025 (C–H), 2952 (C–H), 1623 (C=C) 1233 (C–O); HRMS (ESI): *m/z* [M+H$^+$] Calcd for $C_{19}H_{28}NO$: 286.2165; Found: 286.2169.

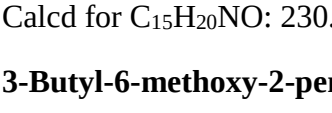

3-Decyl-6-methoxy-2-undecylquinoline (3r) Black liquid (299.48 mg, 66%). ^{1}H NMR (400 MHz, $CDCl_3$) δ 7.91 (d, *J* = 9.0 Hz, 1H), 7.74 (s, 1H), 7.26 (dd, *J* = 9.2, 2.8 Hz, 1H), 6.98 (d, *J* = 2.8 Hz, 1H), 3.89 (s, 3H), 2.92 (t, *J* = 7.3 Hz, 2H), 2.72 (t, *J* = 7.3 2H), 1.76 (quint, *J* = 7.9 Hz, 2H), 1.66 (quint, *J* = 7.8 Hz, 2H), 1.48 – 141 (m, 4H), 1.26 (d, *J* = 6.7 Hz, 26H), 0.90 – 0.86 (m,

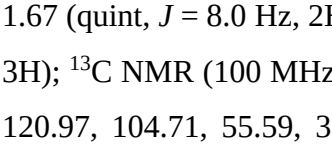

6H); ^{13}C NMR (100 MHz, $CDCl_3$) δ 159.8, 157.2, 142.5, 134.5, 134.1, 129.9, 128.2, 121.0, 104.7, 55.5, 35.7, 32.5, 32.0, 30.7, 30.1, 30.1, 29.9, 29.7, 29.6, 29.5, 29.5, 22.8, 14.2; IR (KBr)ν_{max}/cm^{-1} 3028 (C–H), 2921 (C–H), 1622 (C=C) 1274 (C–O); HRMS (ESI): *m/z* [M+H$^+$] Calcd for $C_{31}H_{52}NO$: 454.4043; Found: 454.4052.

3-Dodecyl-6-methoxy-2-tridecylquinoline (3s) Dark Black liquid (305.91 mg, 60%). ^{1}H

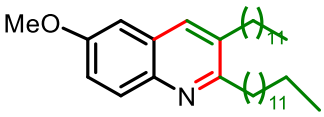

NMR (400 MHz, $CDCl_3$) δ 6.75 (q, *J* = 9.5 Hz, 3H), 6.51 (d, *J* = 9.1 Hz, 1H), 3.67 (s, 3H), 3.47 (d, *J* = 14.5 Hz, 1H), 3.20 (dd, *J* = 14.2, 2.3 Hz, 1H), 2.95 – 2.82 (m, 2H), 1.35 (dd, *J* = 11.9, 5.9 Hz, 6H), 1.19 (s, 36H), 0.81 (t, *J* = 6.8 Hz, 6H); ^{13}C NMR (100 MHz, $CDCl_3$) δ 153.2, 152.1, 144.0, 143.1, 130.0, 128.1, 118.2, 115.0, 114.7, 70.1, 68.6, 62.2, 60.3, 55.9, 55.7, 34.9, 34.8, 32.0, 30.0, 29.9, 29.8, 29.8, 29.8, 29.7, 29.5, 25.8, 25.6, 14.2; IR (KBr)ν_{max}/cm^{-1} 3150 (C–H), 1650 (C=C); HRMS (ESI): *m/z* [M+H$^+$] Calcd for $C_{35}H_{59}NO$: 510.4669; Found: 510.4678.

^{1}H NMR Spectrum of 2- Benzyl-7-methoxy-3-phenylquinoline (3a)

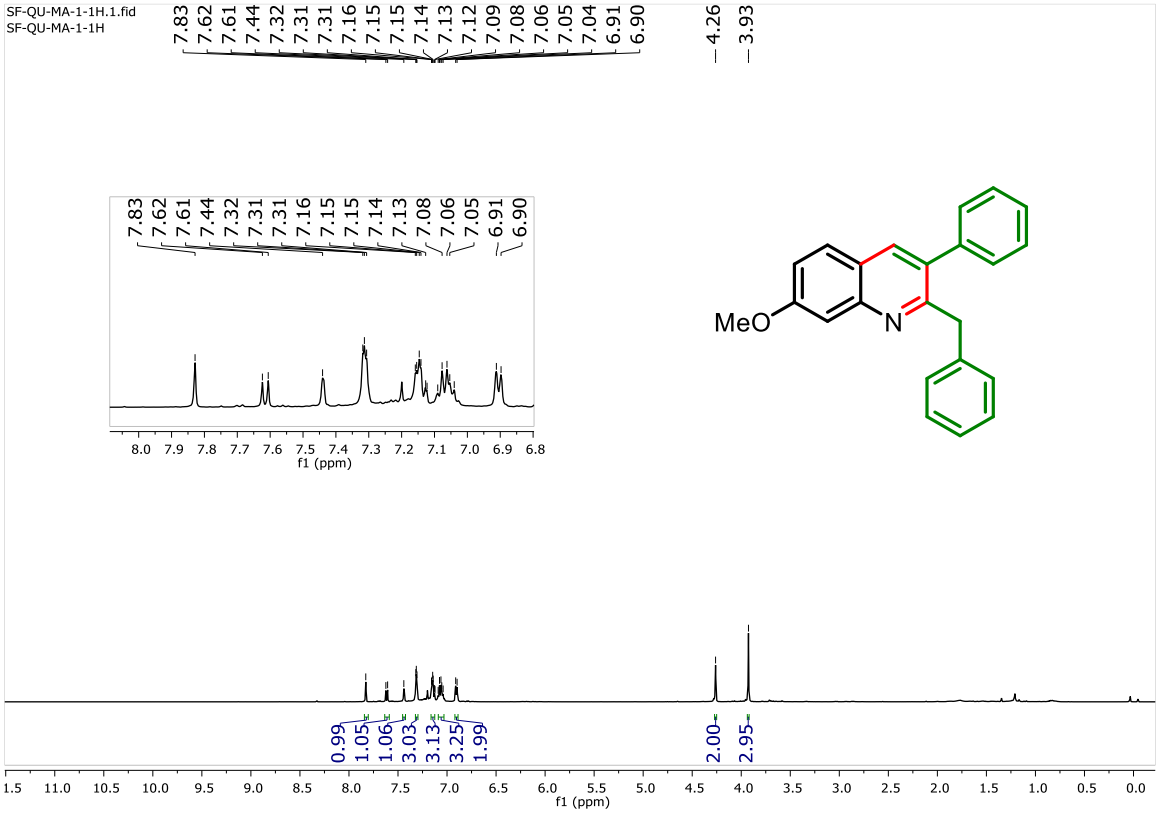

^{13}C NMR Spectrum of 2-Benzyl-7-methoxy-3-phenylquinoline (3a)

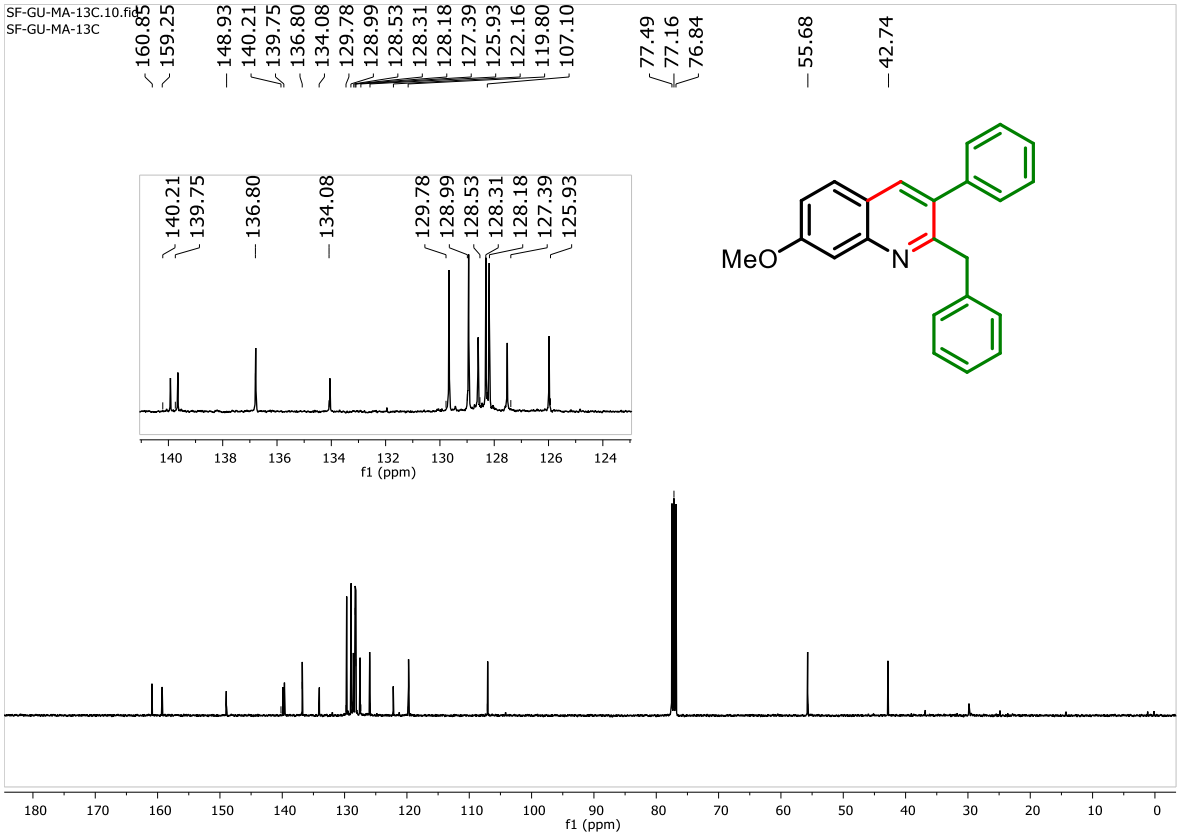

HRMS Spectrum of 2- Benzyl-7-methoxy-3-phenylquinoline (3a)

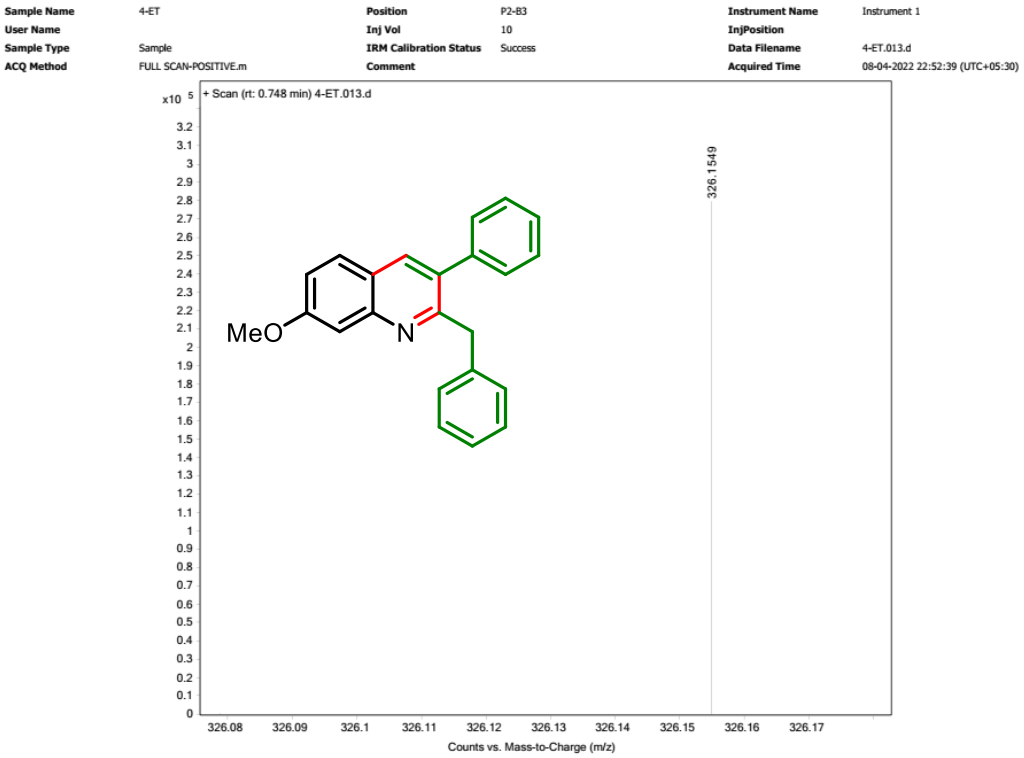

^{1}H NMR Spectrum of 2-Benzyl-3-phenylbenzo[*h*]quinoline (3m)

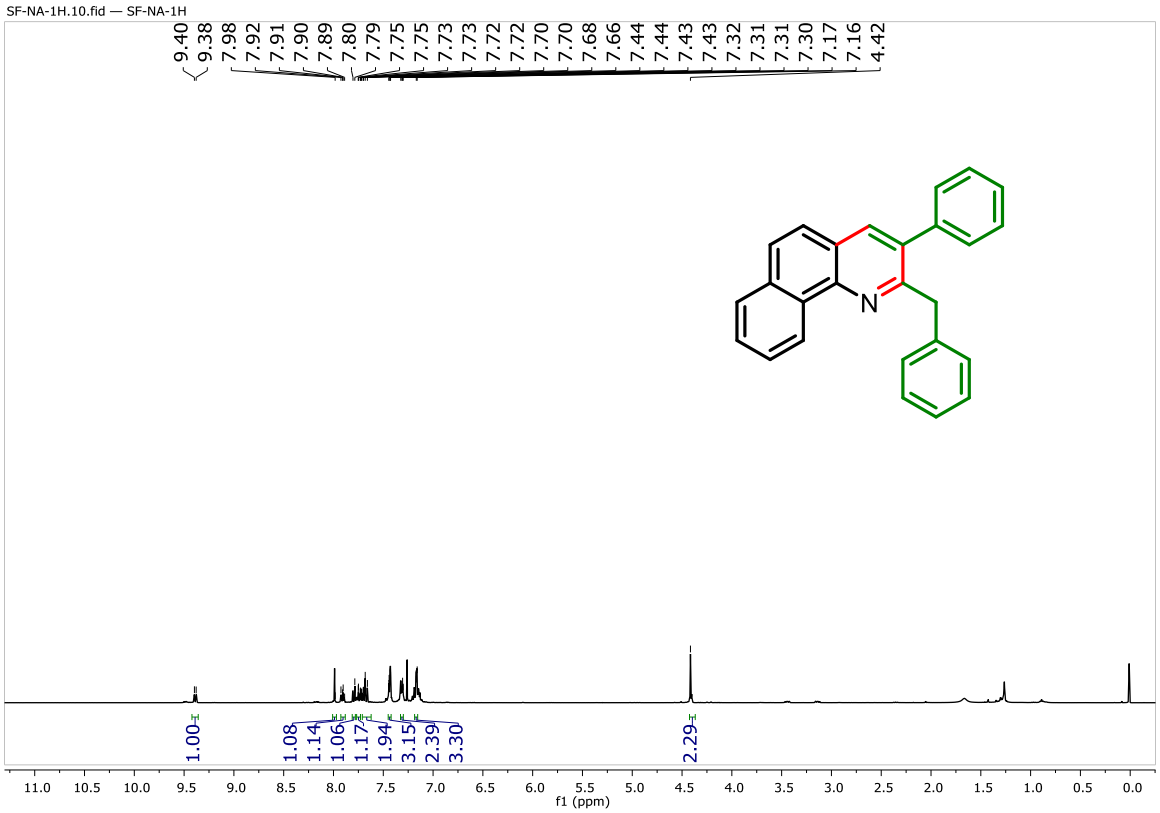

^{13}C NMR Spectrum of 2-Benzyl-3-phenylbenzo[*h*]quinoline (3m)

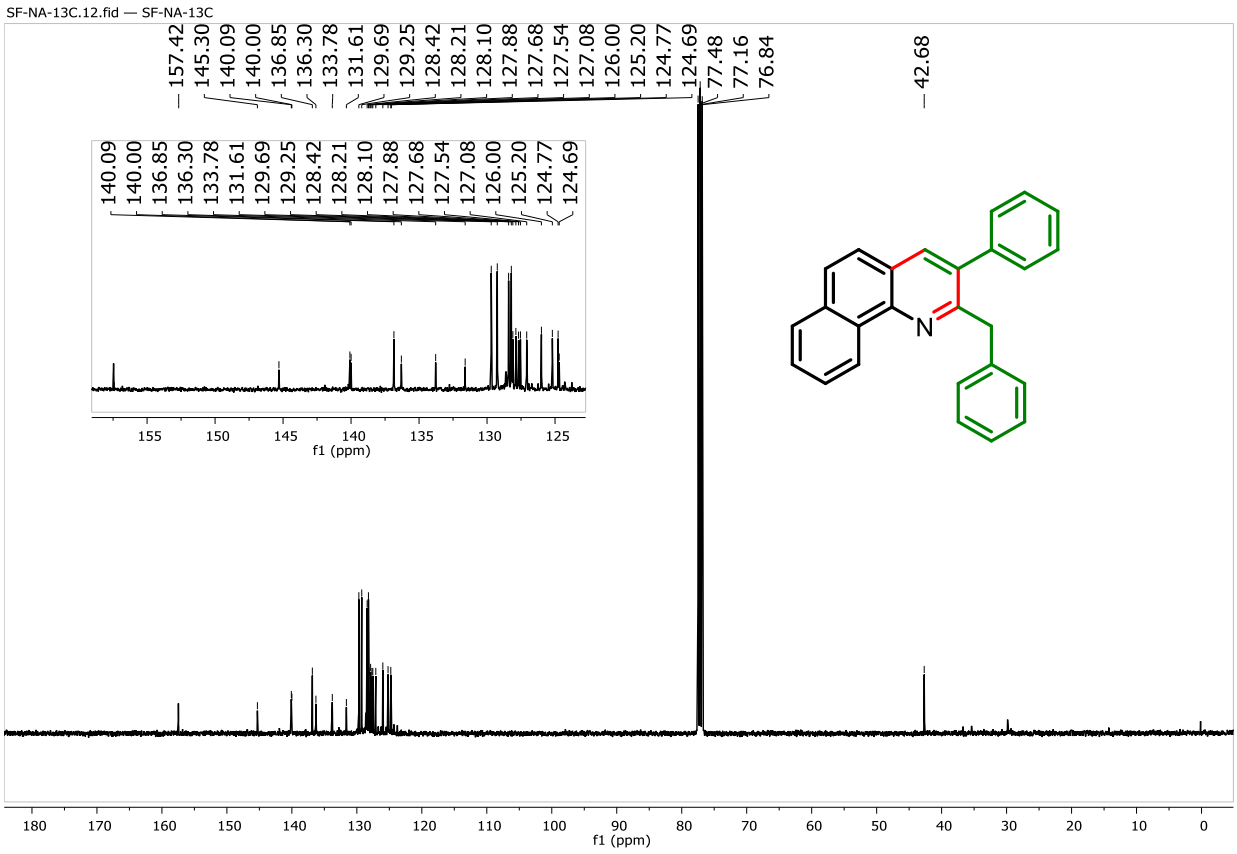

HRMS Spectrum of 2-Benzyl-3-phenylbenzo[*h*]quinoline (3m)

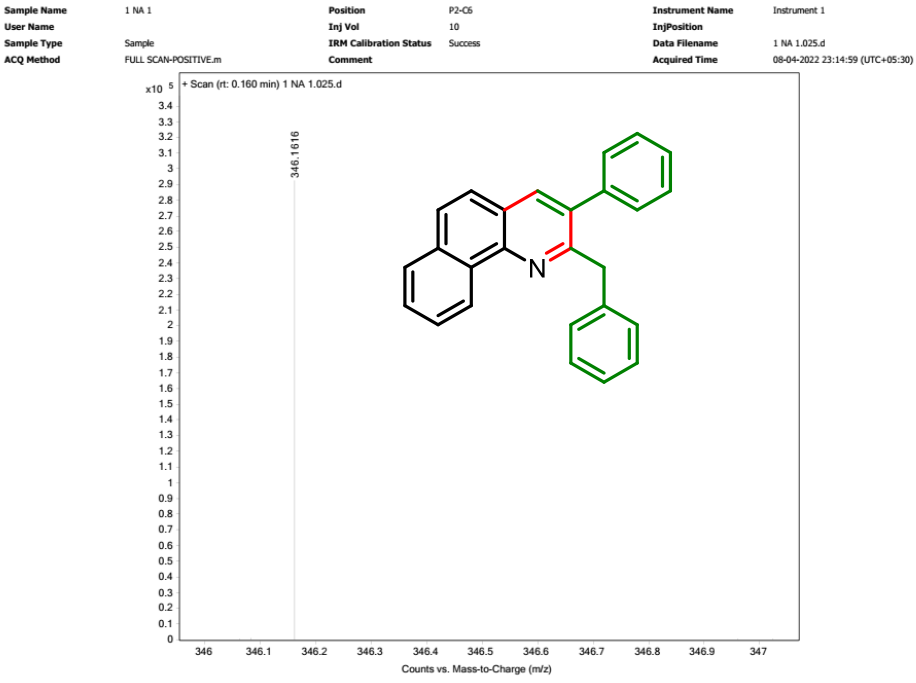

^{1}H NMR Spectrum of 3-Ethyl-6-methoxy-2-propylquinoline (3p)

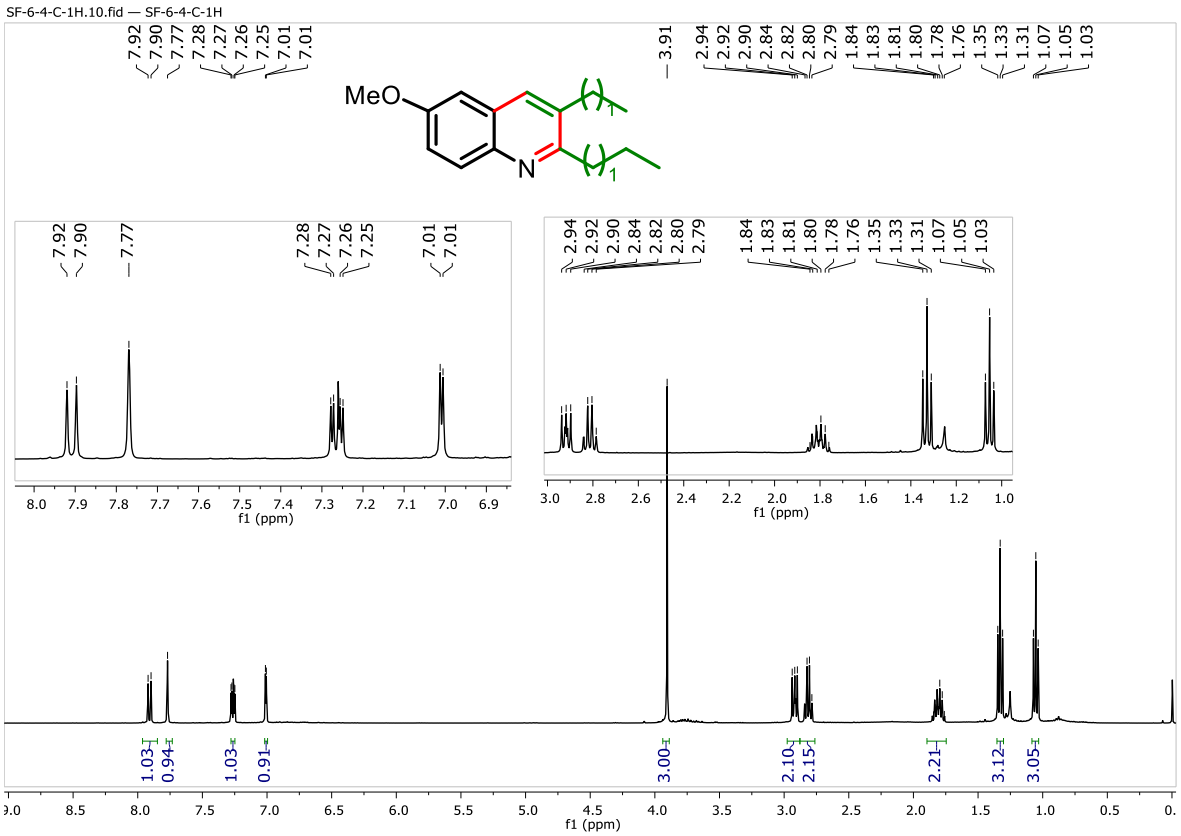

^{13}C NMR Spectrum of 3-Ethyl-6-methoxy-2-propylquinoline (3p)

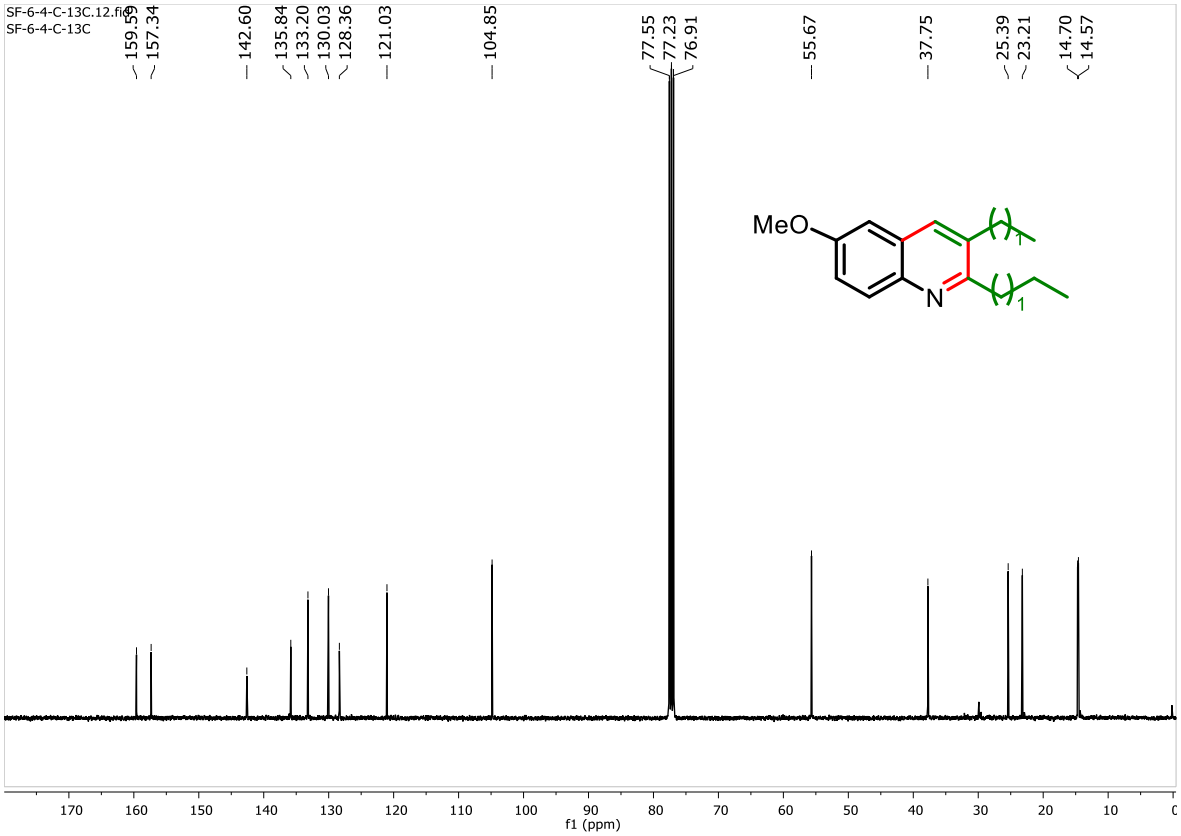

HRMS Spectrum of 3-Ethyl-6-methoxy-2-propylquinoline (3p)

Sample Name	SF 4E B	**Position**	P2-C3	**Instrument Name**	Instrument 1
User Name		**Inj Vol**	10	**InjPosition**	
Sample Type	Sample	**IRM Calibration Status**	Success	**Data Filename**	SF 4E B_021.d
ACQ Method	FULL SCAN-POSITIVE.m	**Comment**		**Acquired Time**	29-07-2022 23:49:36 (UTC+05:30)

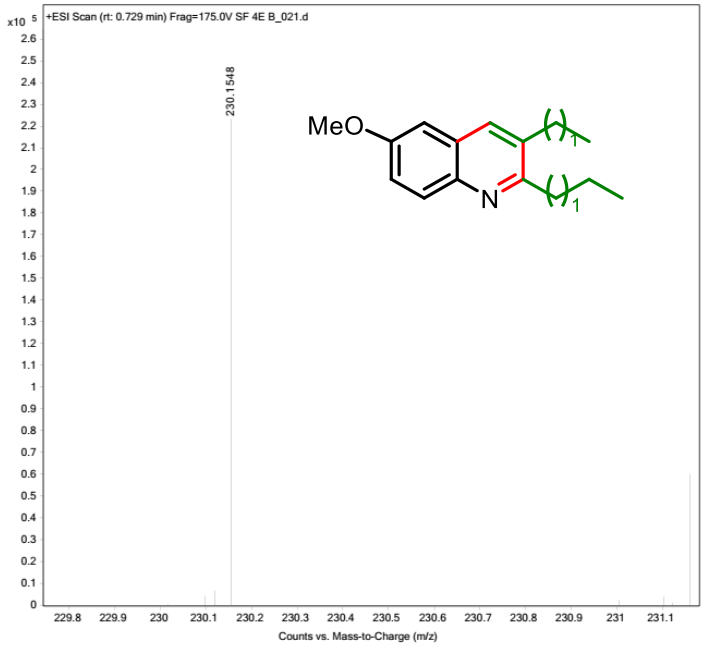

References:

1. V. R. Solomon, W. Haq, K. Srivastava, S. K. Puri and S. B. Katti, *J. Med. Chem.*, 2007, **50**, 394–398.
2. X.-F. Shang, S. L. Morris-Natschke, Y.-Q. Liu, X. Guo, X.-S. Xu, M. Goto, J.-C. Li, G.-Z. Yang and K.-H. Lee, *Med Res Rev*, 2018, **38**, 775–828.
3. (a) S. I. Pretorius, W. J. Breytenbach, C. de Kock, P. J. Smith and D. D. N'Da, *Bioorg. & Med. Chem.*, 2013, **21**, 269–277; (b) A. R. Chabukswar, B. S. Kuchekar, S. C. Jagdale, P. D. Lokhande, V. V. Chabukswar, S. U. Shisodia, R. H. Mahabal, A. M. Londhe and N. S. Ojha, *Arab. J. Chem.*, 2016, **9**, 704–712; (c) C.-X. Liu, X. Zhao, L. Wang and Z.-C. Yang, *Microb. Pathog.*, 2022, **165**, 105507; (d) H. Kumar, V. Devaraji, R. Joshi, M. Jadhao, P. Ahirkar, R. Prasath, P. Bhavana and S. K. Ghosh, *RSC Adv.*, 2015, **5**, 65496–65513; (e) M. F. A. Mohamed and G. E.-D. A. Abuo-Rahma, *RSC Adv.*, 2020, **10**, 31139–31155; (f) S. Hu, J. Chen, J.-X. Cao, S.-S. Zhang, S.-X. Gu and F.-E. Chen, *Bioorg. Chem.*, 2023, **136**, 106549.
4. L. Herrmann, F. Hahn, C. Wangen, M. Marschall and S. B. Tsogoeva, *Chem. Eur. J.*, 2022, **28**, e202103861.
5. A. K. Agrawal and S. A. Jenekhe, *Macromolecules*, 1991, **24**, 6806–6808; (b) X. Zhang, A. S. Shetty and S. A. Jenekhe, *Macromolecules*, 1999, **32**, 7422–7429.
6. Q. Cai, H. Song, Y. Zhang, Z. Zhu, J. Zhang and J. Chen, *J. Agric. Food Chem.*, 2024, **72**, 12373–12386.
7. (a) S. Kraup, *Ber*., 1880, **13**, 2080−2086; (b) O. Doebner, *Ann.*, 1887, 242–265; (c) A. Combes, *Bull. Chim. Soc. France*., 1888, **49**: 89; (d) O. Doebner and W. V. Miller, *Ber. Dtsch. Chem. Ges.*, 1881, **14**, 2812–2817. (e) L. S. Povarov, B. M. Izv. Mikhailov, *Akad. Nauk SSR, Ser. Khim*., 1963, 953–956; (f) M. Conrad and L. Limpach, *Ber. Dtsch. Chem. Ges.*, 1887, **20**, 944–948.
8. W. Pfitzinger, *J. Prakt. Chem.*, 1886, **33**, 100.
9. P. Friedlander, *Chemische Berichte*, 1882, **15**, 2572−2575.
10. L. Knorr, *Ann*, 1886, **236**, 69.
11. (a) Y. Lv, Y. Li, T. Xiong, W. Pu, H. Zhang, K. Sun, Q. Liu and Q. Zhang, *Chem. Commun.*, 2013, **49**, 6439–6441; (b) J. Yuan, J.-T. Yu, Y. Jiang and J. Cheng, *Org. Biomol. Chem.*, 2017, **15**, 1334–1337; (c) S. D. Jadhav and A. Singh, *Org. Lett.*, 2017, **19**, 5673–5676.

12. (a) T. Juspin, T. Terme and P. Vanelle, *Synlett*, 2009, **9**, 1485–1489; (b) R. K. Saunthwal, M. Patel and A. K. Verma, *Org. Lett*., 2016, **18**, 2200–2203.
13. J. C. Xiang, Z. X. Wang, Y. Cheng, S. Q. Xia, M. Wang, B. C. Tang, Y. D. Wu and A. X. Wu, *J. Org. Chem*., 2017, **82**, 9210–9216.
14. G. R. Kumar, R. Kumar, M. Rajesha and M. S. Reddy, *Chem. Commun*., 2018, **54**, 759–762.
15. S. Ali and A. T. Khan, *Org. Biomol. Chem.*, 2021, **19**, 3255–3262.
16. Y. Volkova, S. Baranin and I. Zavarzin, *Adv. Synth. Catal.*, 2021, **363**, 40–61.
17. P. B. Sarode, S. P. Bahekar and H. S. Chandak, *Tetrahedron Lett.*, 2016, **57**, 5753–5756.
18. X. Mi, J. Chen and L. Xu, *Eur. J. Org. Chem.*, 2015, 1415–1418.
19. Y. Kuninobu, Y. Inoue and K. Takai, *Chem. Lett.*, 2007, **36**, 1422–1423.
20. S. Anvar, I. Mohammadpoor-Baltork, S. Tangestaninejad, M. Moghadam, V. Mirkhani, A. R. Khosropour and R. Kia, *RSC Adv.*, 2012, **2**, 8713–8720.
21. Ya Li, X. Zhou, Z. Wu, J. Cao, C. Ma, Y. He G. Huang, *RSC Adv.*, 2015, **5**, 88214–88217.
22. M. Tokunaga, M. Eckert, Y. Wakatsuki, *Angew. Chem. Int. Ed.* 1999, **38**, 3222–3225.
23. M. Beller, O. R. Thiel, H. Trauthwein and C. G. Hartung, *Chem. Eur. J*., 2000, ***6***, 2513–2521.
24. M. Zhang, B. Xiong, W. Yang, D. N. T. Kumar and Y. Q. Din, *Monatsh Chem*., 2012, **143**, 471–478.
25. (a) M. Zhang, B. Xiong, T. Wang, Y.Q. Ding, L. Wang, *Heterocycles*, 2011, **83**, 2289; (b) M. Zhang, B. Xiong, W. Yang, D.N.T. Kumar, Y.Q. Ding, *Monatsh. Chem.* 2012, **143,** 471; (c) J. B. Bharate, S. B. Bharate and R. A. Vishwakarma, *ACS Comb. Sci.*, 2014, **16**, 624–630.
26. (a) M. S. A. Mehedi and J. J. Tepe, *J. Org. Chem.*, 2020, **85**, 6741–6746; (b) S. Ali and A. T. Khan, *Tetrahedron Lett.*, 2021, **70**, 152981; (c) Baghernejad, *Chem. Inform.*, 2012, **43**, chin.201207239; (d) B. Baghernejad, *Curr. Org. Chem.*, **15**, 3091–3097; (e) S. Das, S. Paul, B. Mitra, G. Chandra Pariyar and P. Ghosh, *ChemistrySelect*, 2024, **9**, e202401822.
27. (a) K. Capriotti and J. A. Capriotti, *J Clin Aesthet Dermatol*, 2012, **5**, 24–26; (b) D. Martin, A. Weise and H.-J. Niclas, *Angew. Chem. Int. Ed. Engl.*, 1967, **6**, 318–334

28. (a) X. Ren, J. Chen, F. Chen and J. Cheng, *Chem. Commun.*, 2011, **47**, 6725–6727; (b) X. Gao, X. Pan, J. Gao, H. Huang, G. Yuan and Y. Li, *Chem. Commun.*, 2014, **51**, 210–212; (c) H. Cao, S. Lei, N. Li, L. Chen, J. Liu, H. Cai, S. Qiu and J. Tan, *Chem. Commun.*, 2015, **51**,1823–1825; (d) L. Chu, X. Yue, and F.-L. Qing, *Org. Lett.*, 2010, **12**, 1644–1647; (e) T. Jia, A. Bellomo, K. E. Baina, S. D. Dreher and P. J. Walsh, *J. Am. Chem. Soc.*, 2013, **135**, 3740–3743.
29. K. Omura and D. Swern, *Tetrahedron*, 1978, **34**, 1651–1660.
30. K. E. Pfitzner and J. G. Moffatt, *J. Am. Chem. Soc.*, 1963, **85**, 3027–3028.
31. (a) S. Yashmin, R. Ali, S. Mondal and A. T. Khan, *Chem. Commun.*, 2022, **58**, 5853–5856; (b) S. Yashmin, S. Mondal, R. Das, P. Banerjee and A. T. Khan, *Org. Biomol. Chem.*, 2022, **20**, 7302–7315.
32. T.-S. Jiang, X. Wang and X. Zhang, *Tetrahedron Lett.*, 2018, **59**, 2979–2982.
33. M. Phanindrudu, S. B. Wakade, D. K. Tiwari, P. R. Likhar and D. K. Tiwari, *J. Org. Chem.*, 2018, **83**, 9137–9143.
34. B. Trost, *Science*, 1991, **254**, 1471–1477; (b) B. M. Trost, *Angew. Chem.*, 1995, **107**, 285–307.
35. (a) Y. Li, X. Cao, Y. Liu and J.-P. Wan, *Org. Biomol. Chem.*, 2017, **15**, 9585–9589; (b) K. Cao, F.-M. Zhang, Y.-Qi. Tu, X.-T. Zhuo, C.-A. Fan, *Chem. Eur. J.* 2009, **15**, 6332–6334; (c) J. Tang, L. Wang, D. Mao, W. Wang, L. Zhang, S. Wu, Y. Xie, *Tetrahedron*, 2011, **67**, 8465–8469; (d) B. Chakraborty, A. Kar, R. Chanda, U. Jana, *J Org Chem.* **85,** 9281–9289; (e) L. S. Povarov, B. M. Mikhailov, Izv. Akad. Nauk SSR, *Ser. Khim.* 1963, 953–956.
36. M. Zhang, B. Xiong, T. Wang, Y.Q. Ding, L. Wang, *Heterocycles*, 2011, **83,** 2289.

Part B

Chapter I

Significance of substituted furocoumarins

Introduction

The furo[3,2-*c*]coumarin backbone is present in many bioactive natural products. Among numerous heterocyclic fused coumarins, furocoumarins have received significant attention due to their essential medicinal values.[1a] Furcoumarins represent a class of compounds with diverse biological activities and potential applications in pharmaceuticals and agriculture.[1b] Their structural versatility and pharmacological properties continue to attract attention in medicinal chemistry and natural product research. For instance, Coumestrol and 4'-*O*-methylcoumestrol are natural products isolated from soy products[2a] and Forage Crops,[2b] These are naturally occurring biologically active secondary metabolites.[3a,b] They exhibit numerous pharmacological activities such as antimicrobial,[4a] anti-cancer,[4b] anti-diabetic,[4c] antioxidant,[4d] and anti-obesity,[4e] anti-inflammatory,[4f] anti-osteoporotic,[4g] estrogenic,[4h] neuroprotective,[4i] and immuno-suppressive.[4j] Most important, the biological activities associated with these furocoumarins is their ability to cross-link DNA via intercalation of the furocoumarins between the base pairs of the nucleic acid and [2+2] photocycloaddition with the pyrimidine bases, particularly thymine.[5] Some promising coumestans derivatives are coumestrol, wedelolactone, psoralidin, and glycyrol.[6]

Pyranocoumarins are a class of organic compounds characterized by their fused ring structure, combining a coumarin core with a pyran ring. This structural arrangement gives them distinct chemical properties and biological activities.[7] It is also one of the most important heterocyclic backbones, and it displays a wide range of biological activities such as COX-2 inhibitors,[8a] anti-MCF-7 breast cancer cell growth,[8b] anti-lung tumor cell growth,[8c] cytotoxic activity,[8d] antibacterial,[8e] and antinflamatory[8f] as depicted in Figure 1.

Dinaphthofurans compounds with a fused ring structure combining two naphthalene rings and a furan ring. They exhibit diverse biological activities such as antimicrobial, anticancer, and antioxidant properties, making them promising candidates for drug discovery.[9] Their synthesis and modification challenge organic chemists while offering potential advancements in chemical methodologies. Found naturally in plants,[10] dinaphthofurans contribute to understanding biosynthesis and ecological roles. Their interdisciplinary importance spans chemistry, biology, and medicine, driving research toward developing new pharmaceuticals and expanding scientific knowledge of their therapeutic potential. Dinaphthofurans thus hold significant promise in both scientific research and potential medical applications.[11]

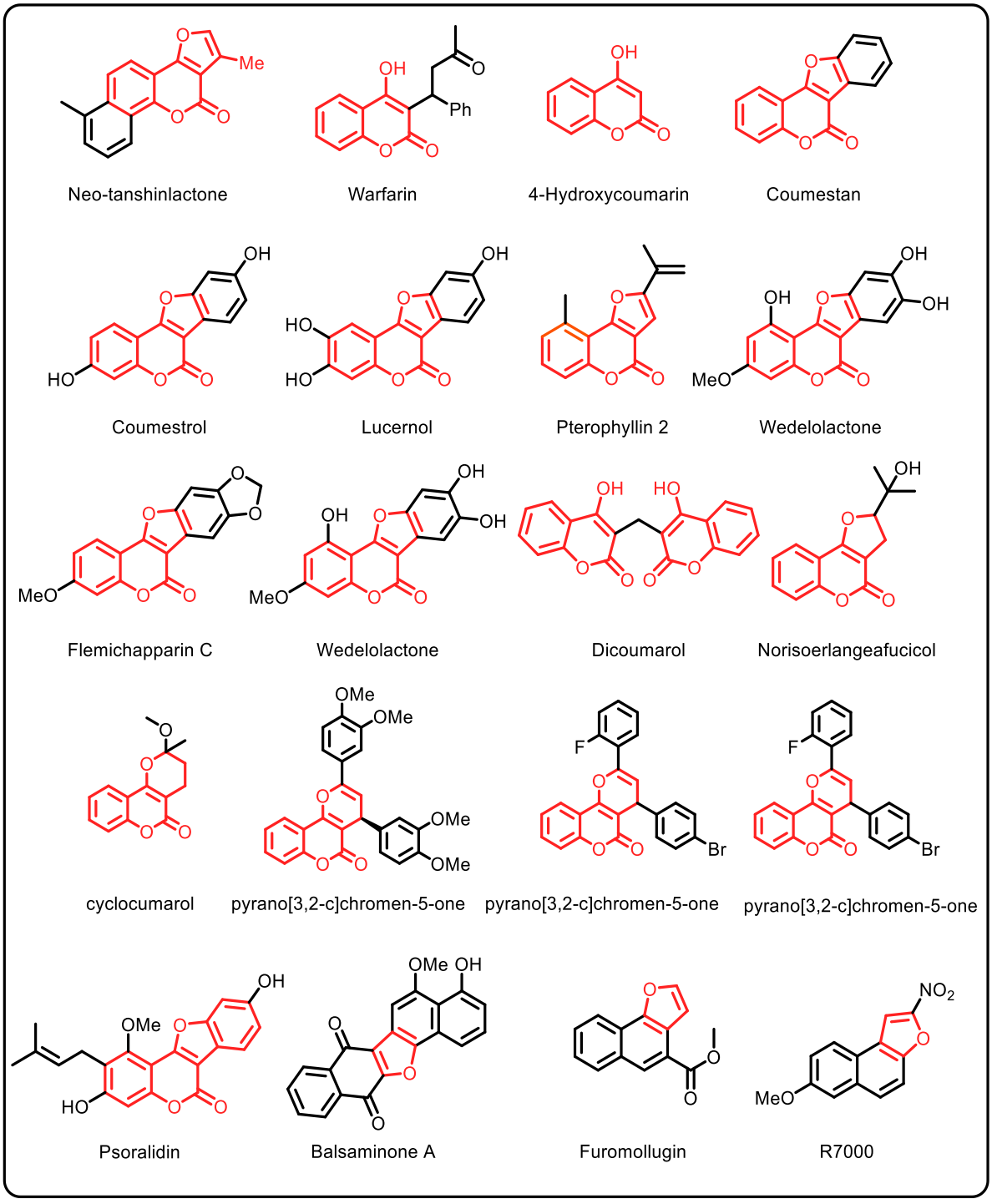

Figure 1. Biologically active natural and non-natural furocoumarin, pyranocoumarin, and Dinaphthofurans scaffolds.

Literature Survey on Furocoumarins

Synthesis of Furocoumarins

The synthesis of furocoumarins was a significant milestone in the field of natural product chemistry.

Psoralen Synthesis

By utilizing the 7-hydroxy derivative of 2,3-dihydrobenzofuran (coumarin), which had been subjected to substitution at the 6-position, the coumarin system had been synthesized through a Gattermann–Koch reaction followed by a Perkin condensation with acetic anhydride.[12] The process was completed by the dehydrogenation of the five-membered ring to produce the furan ring as shown in Scheme 1.

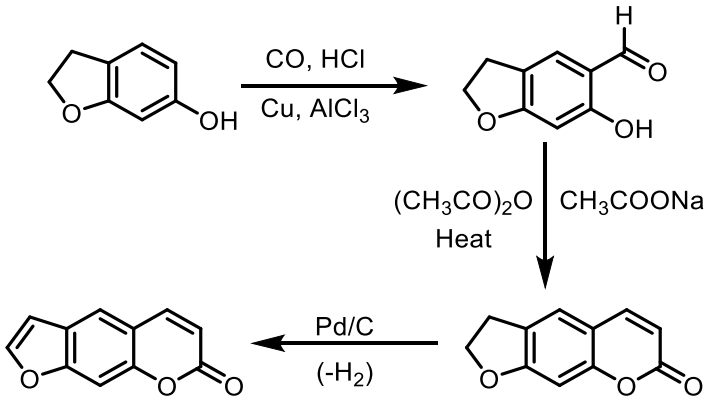

Scheme 1. Synthesis of Psoralen

Angelicin Synthesis The iodination of commercially available umbelliferone (7-hydroxycoumarin) produced 7-hydroxy-8-iodocoumarin.

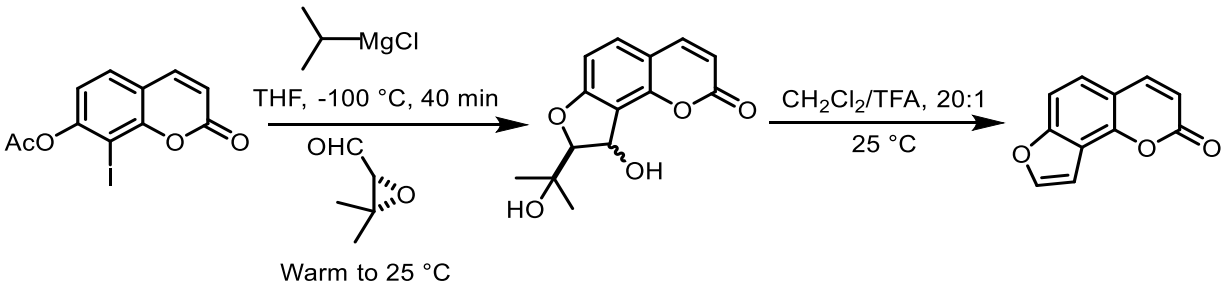

Scheme 2. Synthesis of Angelicin

This compound had then undergone acetylation at the hydroxyl group to form 7-acetoxy-8-iodocoumarin. The resulting compound was subsequently reacted with an isopropyl Grignard reagent and commercially available epoxy aldehydes to synthesize vaginol or vaginidiol.

Finally, vaginol had been fragmented into angelicin through an acid-catalyzed reaction with dichloromethane in trifluoroacetic acid, demonstrated in **Scheme 2**.[13]

Synthesis of substituted furocoumarins

The Gogoi group[14] demonstrated that propargyl bromide served as a coupling partner in the debromination reaction with 4-hydroxycoumarin, leading to the formation of methyl-substituted furo[3,2-*c*]coumarin. This one-pot reaction was catalyzed by $[RuCl_2(p\text{-cymene})]_2$ in the presence of CsOAc and conducted in tAmOH (**Scheme 3**).

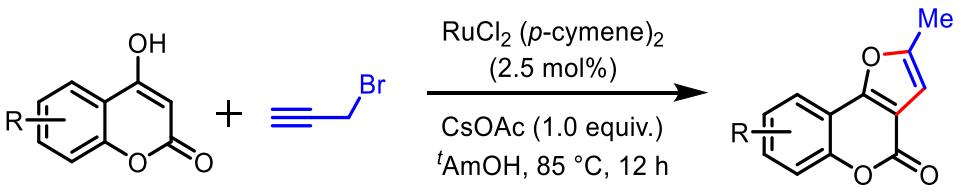

Scheme 3

Kim and co-workers[15] had broadened the range of substrates to include terminal propargyl alcohols by using $Bi(OTf)_3$ as the catalyst and diglyme as the solvent. This approach allowed them to obtain the furo[3,2-*c*]coumarins via an initial propargylation of 4-hydroxycoumarins, followed by intramolecular cyclization of the resulting propargylated coumarins as illustrated in **Scheme 4**.

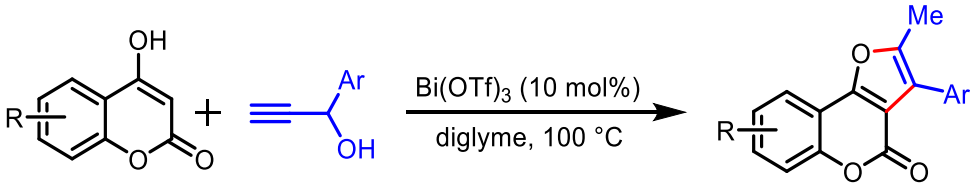

Scheme 4

In 2022, Pelipko and colleagues[16] developed a method for the synthesis of two furo[3,2-c]coumarin-3-carboxylates in anhydrous MeOH through a simple reaction of 4-hydroxycoumarin with readily accessible alkyl 3-bromo-3-nitroacrylates, catalyzed by 1.0 equiv. AcOK (Scheme 5).

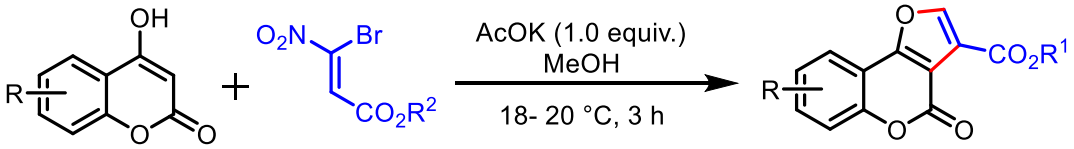

Scheme 5

Reported protocols for the synthesis of 2-aryl-4*H*-furo[3,2-*c*] coumarin derivatives

In the year 2007, Hu and his co-workers[17] demonstrated a method for the synthesis of furocoumarins. Their innovative approach involves a meticulously designed one-pot reaction process. Specifically, this methodology entails a cascade reaction mechanism that integrates sequential addition, cyclization, and oxidation steps, starting from the compound 3-(phenylethynyl)-4*H*-chromen-4-one (Scheme 6).

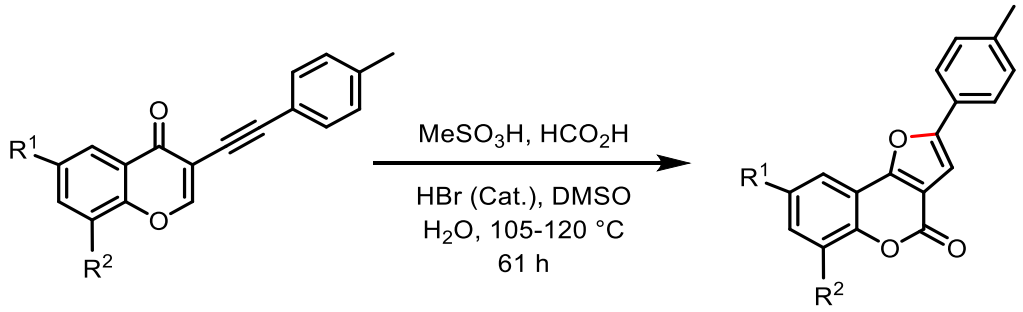

Scheme 6

In 2010, Xu *et al.*[18] illustrated a novel synthetic strategy for the formation of furocoumarins through a well-orchestrated sequence of chemical reactions. Their approach features a two-step process involving a Pd/Cu-catalyzed alkynylation followed by an intramolecular hydroalkoxylation. This method effectively combines these catalytic transformations to produce furocoumarins with high efficiency (Scheme 7).

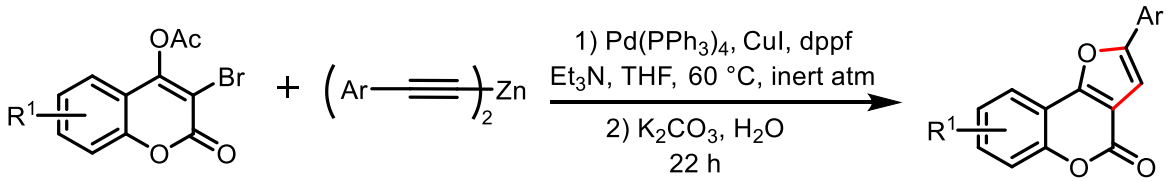

Scheme 7

In 2017, Li, Wang, and their colleagues[19] demonstrated a novel method for synthesizing 4*H*-furo[3,2-*c*]chromen-4-one derivatives through the tandem cyclization of a hypervalent iodine reagent (HIR) derived from 4-hydroxycoumarin and propiolic acids.

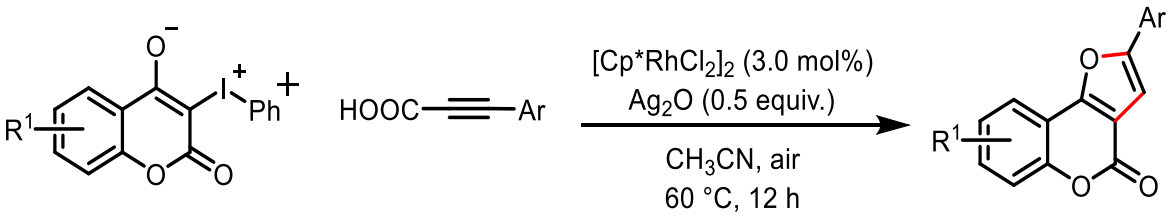

Scheme 8

This process, which employs Rh-catalyzed decarboxylation in conjunction with Ag_2O as a co-catalyst, is illustrated in Scheme 8.

In the same year, Hajra *et al.*[20] reported a method for synthesizing furocoumarin derivatives through an intermolecular coupling reaction between 4-hydroxycoumarins and alkynes. This process is catalyzed by a combination of $FeCl_3$ and ZnI_2, where ZnI_2 serves as a crucial additive (Scheme 9).

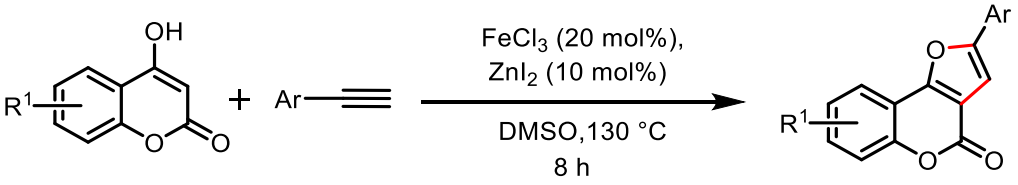

Scheme 9

Other notable methods for furocoumarin synthesis include the following approaches: In 2019, Chem and colleagues developed a tandem reaction method for producing 2,3-di-substituted furocoumarins from a combination of arylglyoxal, 4-hydroxycoumarin, and allyltrimethylsilane.[21] Furthermore, in 2022, Choudhary *et al.* reported a three-component reaction catalyzed by $Sc(OTf)_3$ for the efficient synthesis of furocoumarins.[22]

Although the earlier synthetic approaches to furocoumarins are both unique and elegant, they have several drawbacks. Challenges include the labour-intensive procedures for creating pre-functionalized substrates, the higher cost of aryl acetylenes compared to alternatives like styrene oxide, the requirement for additional additives, harsh or inert atmospheric conditions for the reactions, and the use of expensive transition metal catalysts. Consequently, there is significant potential for developing a new synthetic method that is more efficient, convenient, reliable, and straightforward, intending to generate a variety of furocoumarin derivatives in a step-economical manner.

Reported protocols for the synthesis of tetrahydro coumestan scaffolds

The first reported synthesis of tetrahydro coumestan derivatives was reported by Lee *et al.* in 2000.[23] Their approach involved the reaction of 4-hydroxycoumarin with vinyl sulfide (Scheme 10).

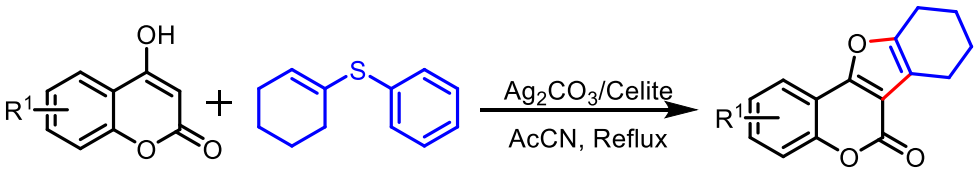

Scheme 10

In 2014, Zhang *et al.*[24] demonstrated a novel method for synthesizing tetrahydro coumestan by employing 2-bromocyclohexanone under microwave irradiation conditions as illustrated in Scheme 11.

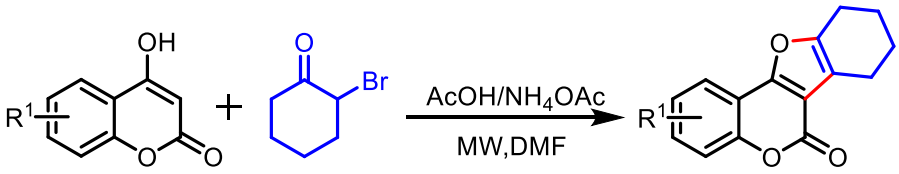

Scheme 11

Later, Le and co-workers[25] demonstrated the synthesis of one derivative of tetrahydro coumestan derivative from 4-hydroxycoumarin and cyclohexanone molecular I_2 catalysts in mesitylene as depicted in scheme 12.

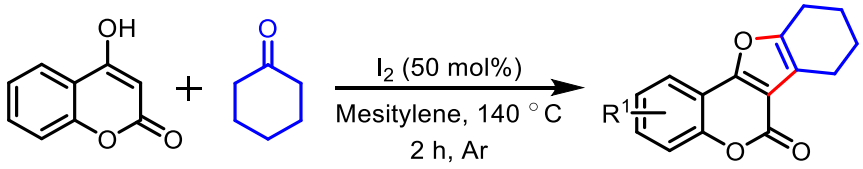

Scheme 12

Reported methods for the synthesis of coumestan scaffolds

Due to their significant biological importance, a wide range of synthetic approaches for furocoumarins have been developed, as illustrated in Scheme 13.

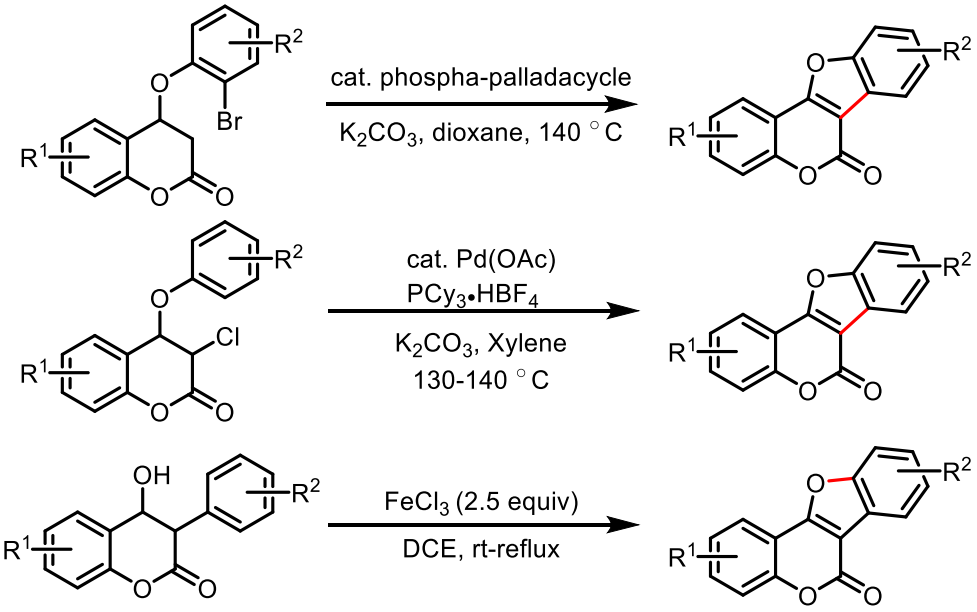

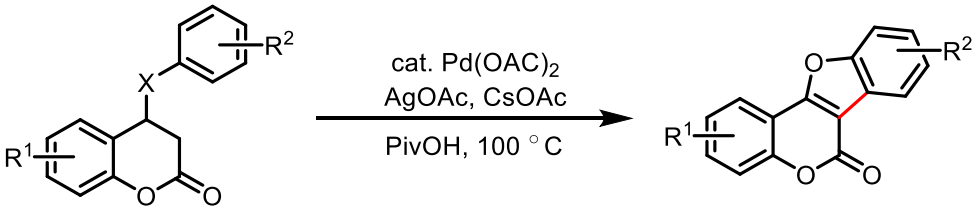

Scheme 13

These methods generally involve coupling reactions where either a substituent at the C-3 position of coumarin is combined with a 4-aryloxy coumarin or a C-3 substituted phenyl ring is coupled with the 4-OH group of coumarin. Among these approaches, notable strategies include [3,3]-sigmatropic rearrangement-based cyclization and elimination, $PtCl_2$-catalyzed cycloisomerization, and Pd-catalyzed C-S activation involving aryl boronic acids for [3+3] annulation reactions.[26a-h]

Reported Strategies for the synthesis of dinaphthofurans scaffolds

From the literature, it is evident that Yorimitsu and co-workers[27] showed how iodoarenes are first converted into biaryls and then how these biaryls can be further transformed into dinaphthofurans as depicted in the Scheme. In 2014, Tsubaki and his team[28] demonstrated the synthesis of oligonaphthofurans, a fan-shaped molecule that exhibits an effective spreading of the π-resonance system (Scheme 14).

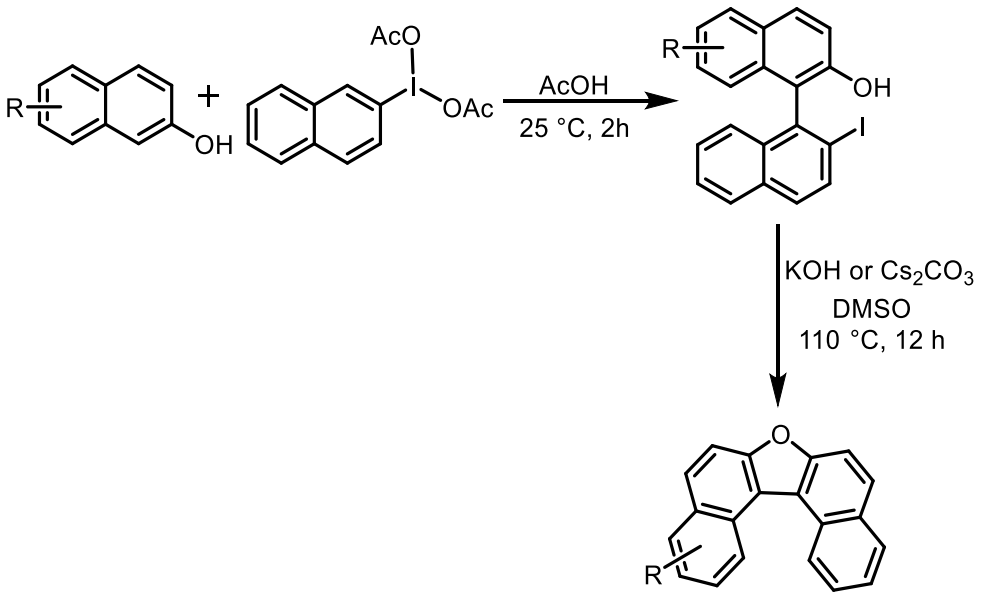

Scheme 14

Literature survey on the synthesis of polyfunctional furocoumarins

In 2012, Bandyopadhyaya *et al*. reported the synthesis of furo[3,2-*c*]coumarin from 3-halochromone and 2-aminochromone as a mask 4-hydroxycoumarin.[29] In 2013, the synthesis of furo[3,2-c]coumarin was accomplished from 3-halo chromones with 4-hydroxycoumarin,[30] as presented in Scheme 15.

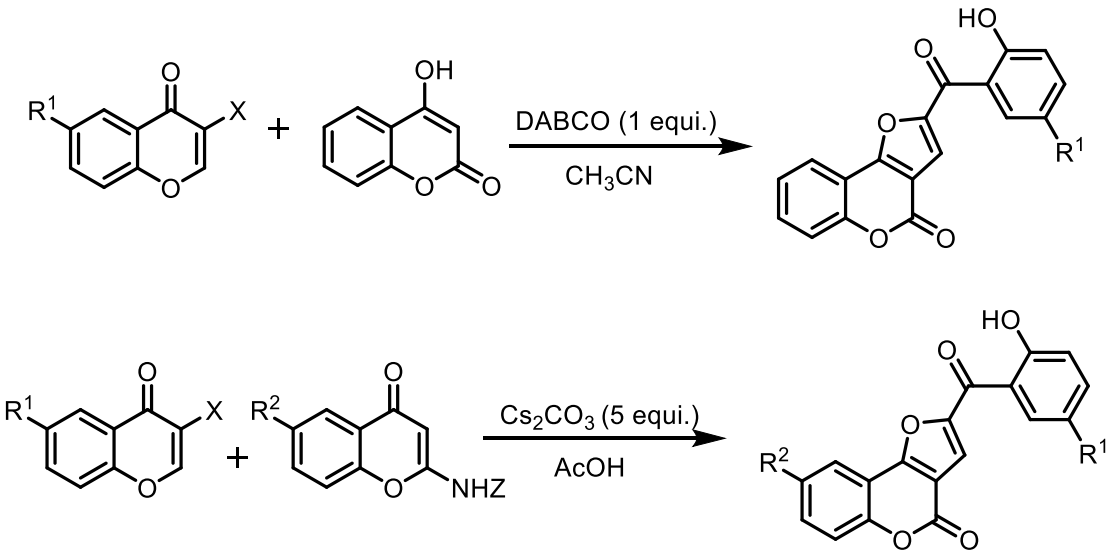

Scheme 15

So far, there are only a few established methods for synthesizing angularly fused furan analogs and furocoumarins. Although these methods can generate dinaphthofuran and polyfunctional furo[3,2-*c*]coumarin scaffolds, it is hampered by a limited substrate scope, with only a small number of examples reported. This highlights the need for the development of new methods.

Reported protocols for the synthesis of pyranocoumarins scaffolds

Due to the significant biological applications of pyranocoumarins, there is a strong demand for the synthesis of these derivatives. In 1988, Majumdar *et al.* demonstrated the synthesis of pyranochromenes from 4-propargyloxycoumarin through a [3,3] sigmatropic rearrangement as depicted in Scheme 16.[31]

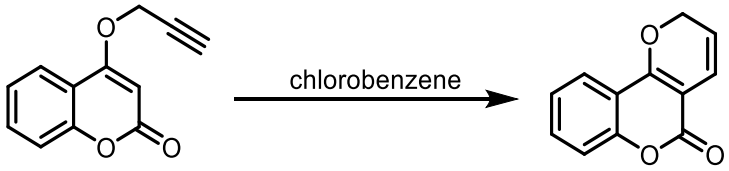

Scheme 16

In 2001, Cravotto and his team reported a method for synthesizing pyranocoumarin derivatives from 4-hydroxycoumarin using α,β-unsaturated iminium salts, as illustrated in Scheme 17.[32]

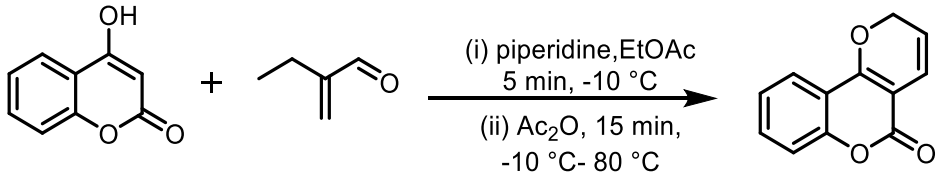

Scheme 17

Traditional methods employed for the synthesis of furocoumarin derivatives encounter significant environmental and economic challenges, as well as substrate scope. These conventional techniques frequently utilize hazardous reagents and produce toxic by-products, posing severe risks to human health and the environment. Moreover, many of these methods rely on using rare earth metal catalysts, hazardous catalysts, and solvents, which are not only prohibitively expensive but also contribute to substantial environmental waste. Using such metals incurs high operational costs and leads to considerable waste management and disposal issues, exacerbating environmental contamination concerns.

Reason for choosing a research topic

A comprehensive review of the existing literature reveals a striking limitation in the number of effective methodologies for synthesizing various substituted furocoumarins derivatives. Specifically, there are only a few established and widely recognized methods for the synthesis of different classes of furocoumarins derivatives, including 2-aryl furocoumarins, tetrahydro coumestan, polyfunctional furocoumarins, and pyranocoumarins. While these methods offer certain advantages, they are inherently flawed by a range of significant drawbacks. Common issues include the reliance on hazardous acids and expensive catalysts, the necessity for high reaction temperatures, extended reaction times, and often, suboptimal yields with a restricted substrate scope. These limitations severely restrict the practical applicability and efficiency of these traditional methods in a broad range of chemical synthesis contexts.

Given the escalating demand for sustainable and eco-friendly practices in the field of organic synthesis, there is an urgent and critical need to develop new, innovative methodologies that can effectively address these challenges. The advancement of novel synthetic approaches that minimize the use of hazardous chemicals, reduce energy consumption, and decrease the generation of waste is not just a theoretical ideal but a practical necessity for improving the

efficiency of quinoline synthesis. It is essential to explore and implement greener synthetic routes that align with modern environmental and economic standards.

In response to these challenges, significant efforts are currently being devoted to the development of new, more sustainable synthetic methodologies. These efforts are focused on creating innovative approaches that offer several key improvements over traditional methods. Such improvements include the reduction or elimination of hazardous reagents, the use of cost-effective and versatile catalysts, the implementation of milder reaction conditions, and the achievement of high yields across a broader range of substrates. These new methodologies are designed to enhance the efficiency of furocoumarins synthesis while also addressing critical environmental concerns.

Reasons for Choosing hydrated ferric(III) chloride ($FeCl_3$) as catalyst:

For several compelling reasons, Iron(III) chloride ($FeCl_3$) is considered one of the best catalysts for organic reactions in synthetic methodologies. As a strong Lewis acid, $FeCl_3$ readily accepts electron pairs, effectively catalyzing a wide range of organic reactions, such as Friedel-Crafts alkylations and acylations, by activating electrophiles and facilitating their reaction with nucleophiles. Its versatility is notable, being applicable in various reactions including oxidations, chlorinations, and polymerizations, making it a valuable catalyst in synthetic organic chemistry. $FeCl_3$ is commercially available, inexpensive, and easy to handle, making it a cost-effective choice for both academic and industrial applications. Its widespread availability ensures it can be easily sourced for large-scale reactions. Soluble in many organic solvents as well as in water, $FeCl_3$ can be used in diverse reaction media, enhancing its utility in various environments. Environmentally, $FeCl_3$ is relatively less toxic and more benign compared to other metal catalysts, posing fewer health risks. It often provides high catalytic efficiency, requiring only small amounts to accelerate reactions and achieve high yields, while enhancing selectivity and reducing unwanted side products. $FeCl_3$'s thermal stability allows it to be used in reactions requiring elevated temperatures, maintaining consistent catalytic activity. Additionally, $FeCl_3$ can be easily removed from reaction mixtures through simple filtration or aqueous workup, facilitating purification.[33] Overall, the combination of strong Lewis acidity, versatility, availability, cost-effectiveness, solubility, environmental friendliness, efficiency, selectivity, thermal stability, and easy removal makes $FeCl_3$ a highly effective and preferred catalyst in various organic synthetic methodologies.[34]

The forthcoming Chapter II of Part B of this thesis will delve into these advancements in detail. This chapter will systematically explore a range of new synthetic methods that represent significant strides forward in the quest for greener and more efficient chemical processes. It will highlight methods that offer numerous benefits, including ease of handling, high regioselectivity, the use of readily available and cost-effective metal triflate catalysts, mild reaction conditions, and short reaction times. Furthermore, it will emphasize how these methods achieve high yields and accommodate a wide substrate scope, thereby expanding the possibilities for the synthesis of diverse quinoline derivatives. Through this exploration, **Chapter II of Part B aims to provide a comprehensive overview of how modern advancements are shaping the future of organic synthesis and meeting the evolving demands of the field.**

Part B

Chapter II: Section A

Synthesis of furo[3,2-*c*]coumarins

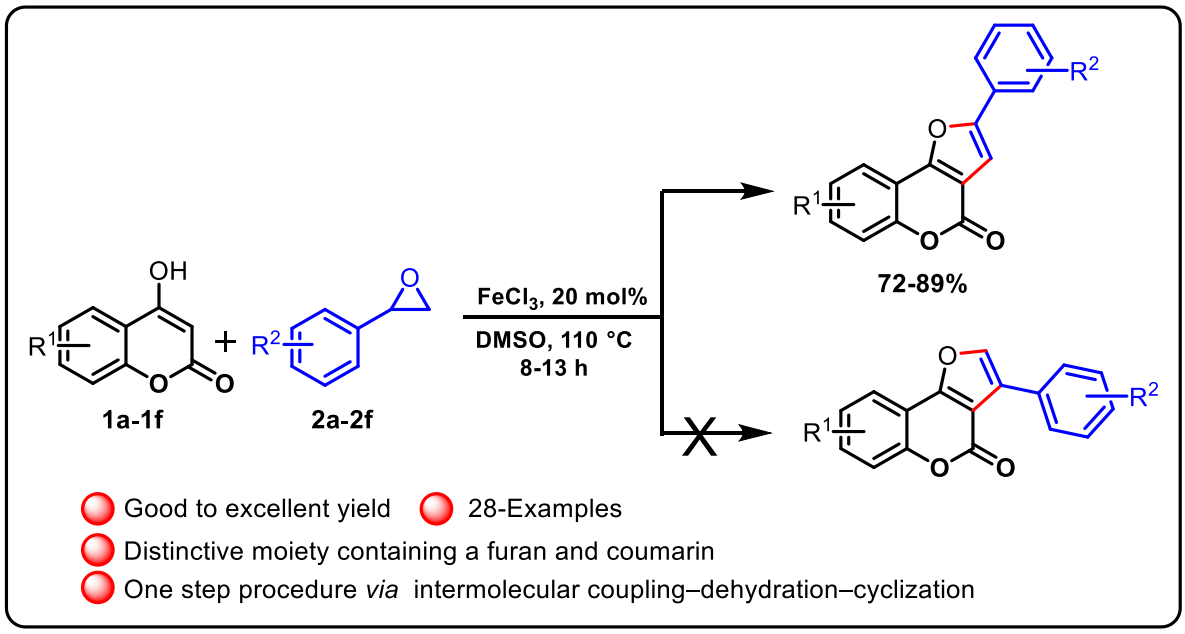

RESULT AND DISCUSSION

EXPERIMENTAL SECTION

Results and Discussion

In Chapter I of Part B, the importance of 2-arylfurocoumarins and their reported methods have been discussed. This section of the chapter explores the regioselective synthesis of furo[3,2-*c*]coumarins derivatives from 4-hydroxycoumarin and aryl oxirane in the presence of 20 mol% $FeCl_3$ catalysts at temperature 110 ^oC (Scheme **18)**. The product formation occurs through a regioselective ring-opening of the aryl oxirane at the less hindered side, followed by dehydration and cyclization. The salient features of the present method are easy handling, cost-effectiveness, shorter reaction time, good to excellent yields, step- and atom economy, broad substrates scope, regioselectivity, and non-requirement of dry solvents, co-catalysts, ligands, or any other additives and inert atmospheric reaction conditions.

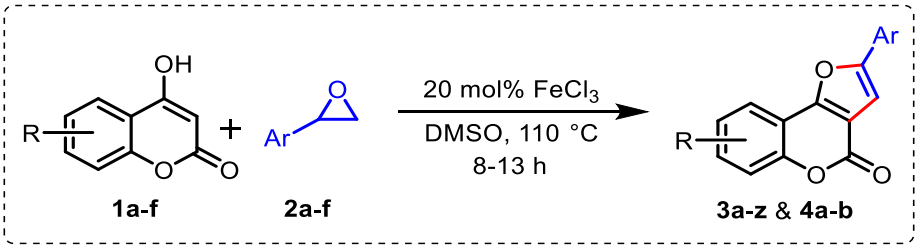

Scheme 18. Synthetic protocol for the synthesis of 2-aryl furo[3,2-*c*]coumarins.

The model substrates were chosen 4-hydroxy-6-methylcoumarin **1a**, and styrene oxide **2a** were chosen as the model substrates to achieve the optimal reaction conditions. Initially, the reaction was examined without a catalyst at room temperature and gradually increased temperature to 120 °C in DMSO as a solvent (Table 1, Entry 1). No desired product was obtained. To find out the role of the catalyst, a similar reaction was scrutinized in the presence of 5 mol% $FeCl_3$ at room temperature for 24 h (Table 1, Entry 2), but there was no progress in the reaction. Next, the same reaction mixture was placed in a pre-heated oil bath at 60 °C and was heated for 15 h (Table 1, Entry 3), and product **3a** was isolated in a 15% yield. The product **3a** was confirmed from IR, ^1H & ^{13}C NMR spectra, and HRMS. In the ^1H NMR spectrum, the characteristic peak at δ 5.6 ppm for the H–3 of the reactant **1a** and the peaks at δ 3.82, δ 3.09, and δ 2.76 for the protons in the epoxide disappeared, and a new peak has appeared at δ 7.18 for the H–3 of the desired product **3a**. In the ^{13}C-NMR spectrum, the peaks δ 51.9 and δ 50.8 for the epoxide carbon disappeared. In addition, the HRMS value of product **3a** gives 277.0859 (expected value of 277.0860) further indicating the formation of the desired product **3a**. After that, the role of temperature was examined to improve the yield of the desired product.

Table 1. Optimization Table [a,b]

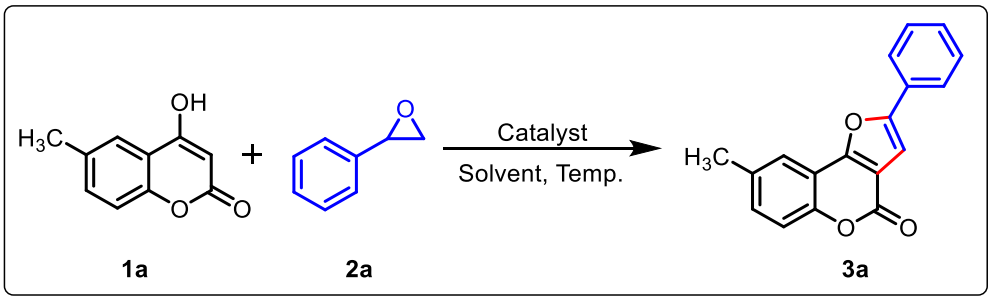

Entry	Catalyst	Mol%	Solvent	Time (h)	Temp (°C)	Yield[b](%)
1[c]	-	-	DMSO	24	RT→120	ND
2[c]	$FeCl_3$	5	DMSO	24	RT	ND
3	$FeCl_3$	5	DMSO	15	60	15
4	$FeCl_3$	5	DMSO	15	80	32
5	$FeCl_3$	5	DMSO	13	100	45
6	$FeCl_3$	5	DMSO	10	110	62
7	$FeCl_3$	5	DMSO	10	120	59
8	$FeCl_3$	10	DMSO	9	110	72
9	**$FeCl_3$**	**20**	**DMSO**	**8**	**110**	**89**
10	$FeCl_3$	30	DMSO	8	110	88
11	$FeCl_3$	20	DMF	8	110	56
12	$FeCl_3$	20	Toluene	8	110	22
13	$FeCl_3$	20	Methanol	8	110	18
14	$CoCl_2$	20	DMSO	10	110	45
15	$CuCl_2$	20	DMSO	10	110	23
16	CSA(±)	20	DMSO	10	110	ND

[a]Reaction conditions: All the reactions were performed using 4-hydroxy-6-methylcoumarin (**1a**, 1.0 mmol), styrene oxide (**2a**, 1.0 mmol). [b]Isolated yield. [c]Reaction performed at room temperature. ND: No Desired Product.

The yield of product **3a** significantly increased 110 °C, as we increased the temperature and **3a** was obtained with a 62% yield (Table 1, Entries 4-7). Further, increasing the temperature, the yield of the desired product did not improve. It is also observed that the yield was drastically reduced above 140 °C and provided an inseparable mixture of products, which may be due to decomposition. Next, the amount of catalysts required was scrutinized, and the reaction was carried out with 10%, 20%, and 30 mol%, respectively (Table 1, Entries 8-10). The above result

revealed that the reaction proceeded very well at 20 mol% of the catalysts, and the desired product was isolated in 89% yield (Table 1, Entry 9). To examine the suitability of other solvents, the reactions were carried out in DMF, toluene, and methanol (Table 1, Entries 11-13), and among all these solvents, it was found that DMSO is the best solvent in terms of reaction time and yield. Motivated by these results, we have carried out a reaction with other metal chloride catalysts such as $CoCl_2$, and $CuCl_2$, and the yield was obtained 45%, and 23%, respectively (Table 1, Entries 14-15). However, no desired product was obtained in the presence of (±) CSA (Table 1, Entry 16). After examining all the parameters, it was concluded that 20 mol% $FeCl_3$ is the most effective catalyst at 110 °C in DMSO for this protocol.

Table 2. The substrate scope of furocoumarin scaffolds[a,b]

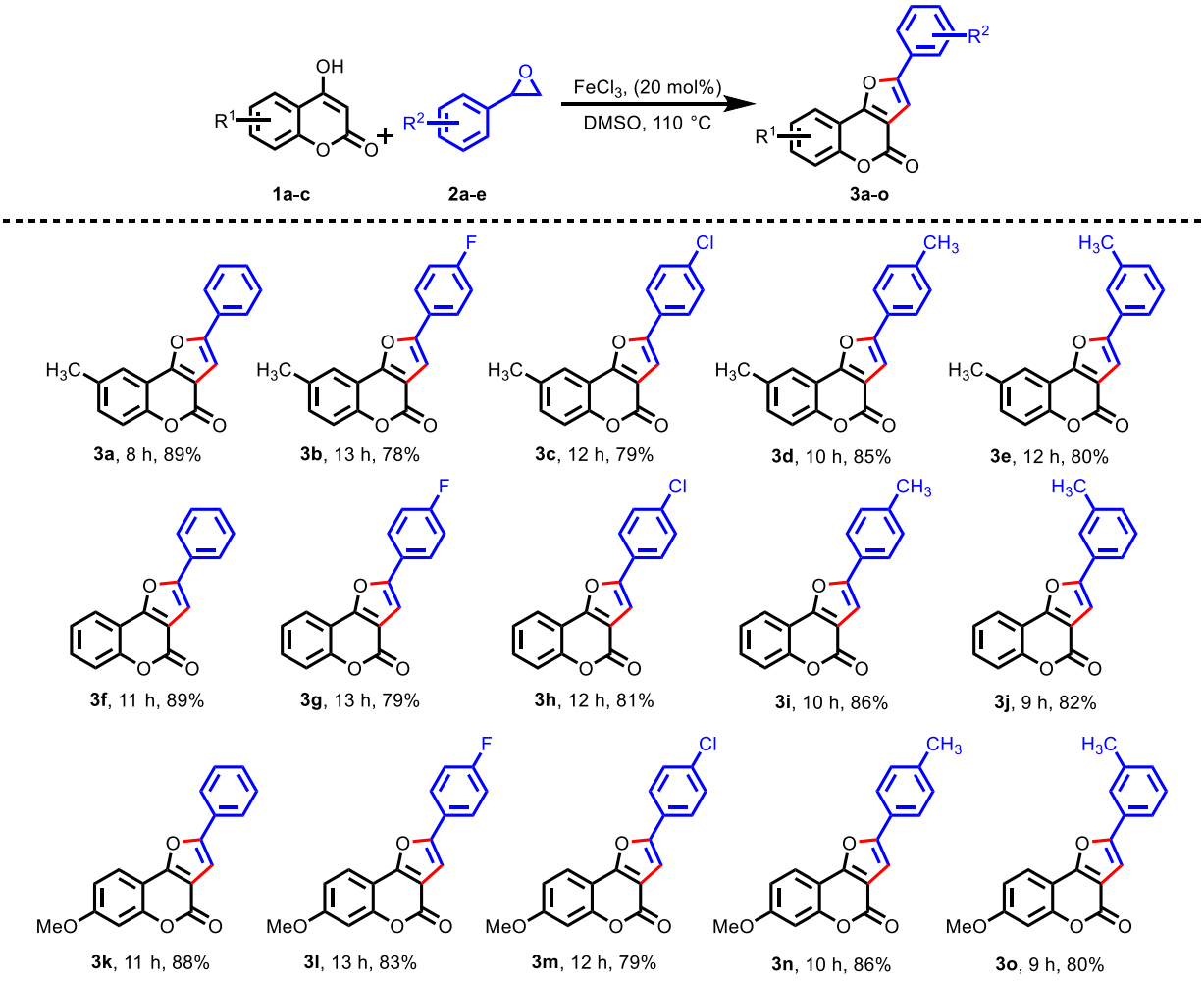

[a]Reaction conditions: All the reactions were performed using 4-hydroxycoumarins (**1a-c**, 1.0 mmol), and styrene oxides (**2a-e**, 1.0 mmol) in the presence of $FeCl_3$ in 2 mL DMSO at 110 °C. [b]Isolated yield.

After determining the optimal reaction conditions, the scope and practicability of the above reaction procedure were examined with various substituted 4-hydroxycoumarins and styrene oxides, as shown in Table 2.

Next, the substrate scope of electron-rich 4-hydroxy-6-methylcoumarin **1a** was investigated with readily available 4-fluoro styrene oxide **2b** and 4-chloro styrene oxide **2c**, and the expected products **3b** and **3c** were obtained in 78% and 79% yield, respectively.

Table 3. The substrate scope of furocoumarin scaffolds[a,b]

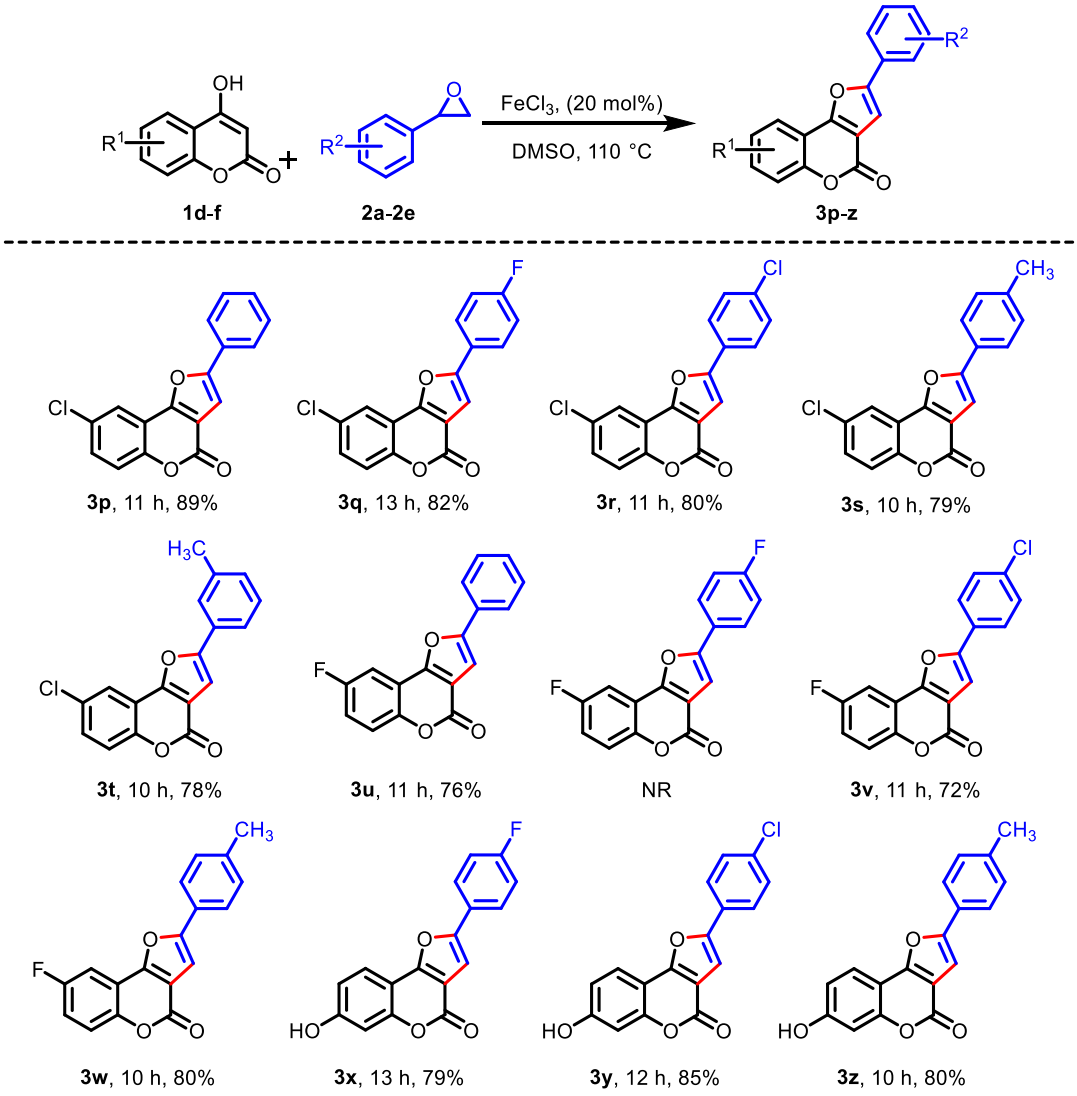

[a]Reaction conditions: All the reactions were performed using substituted 4-hydroxycoumarin (**1d-f**, 1.0 mmol), and substituted styrene oxide (**2a-e**, 1.0 mmol) in the presence of $FeCl_3$ in 2 mL DMSO at 110 °C. [b]Isolated Yield. NR: No Reaction.

Subsequently, the reactions were carried out with 4-hydroxy-6-methylcoumarin **1a** with the prepared styrene oxides **2d** and **2e** under identical reaction conditions, and the desired products **3d** and **3e** were isolated in good yields. It is important to mention that the styrene oxides having

electron-withdrawing groups at the *para*-position, such as fluoro **2b** and chloro **2c**, gave the expected cyclized products **3b** and **3c** in good to excellent yields. Likewise, the styrene oxide containing electron-donating methyl group at the *para* **2d** and o*rtho* **2e** positions provided the desired products **3d** and **3e** in good yields. To examine the generality of the present method, similar reactions were performed with 4-hydroxy coumarin (**1b**) with the five different styrene oxides **2a-e** and furnishes the desired products **3f-j** in 89% to 79% yields. Likewise, 4-hydroxy-7-methoxycoumarin **1c** proceeded well with the styrene oxides (**2a-e**) to provide the corresponding expected products **3k-3o** in 79%-88% yield, respectively.

Subsequently, the cyclization reaction was carried out with 4-hydoxycoumarin having electron-withdrawing at the sixth position, such as chloro **1d** and fluoro **1e,** under similar reaction conditions, and the desired products **3p-3s** and **3t-3w** were obtained in fairly good yields, as shown in Table 3. To enrich the diversity in products, the reactions were also scrutinized with 4,7-dihydroxy coumarin **1f** and substituted styrene oxides **2b**, **2c**, and **2d,** and the corresponding desired products **3x**, **3y**, and **3z** were obtained in 79%, 85%, and 80% yields. To further check the practicability of the present method, the reaction was examined with polyaromatic 2-naphthyl oxirane **2f** and 4-hydroxycoumarin **1b**, and the desired product was isolated **4a** in 80% yield.

Table 4. The substrate scope of furocoumarin scaffolds[a,b]

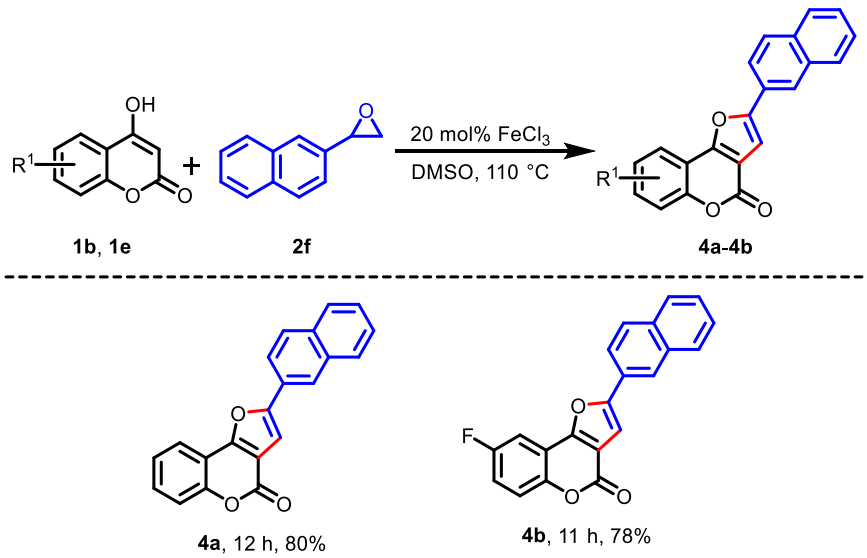

[a]Reaction conditions: All the reactions were performed using substituted 4-hydroxycoumarin (**1b** & **1e**, 1.0 mmol), and 2-naphthyl oxirane (**2f**, 1.0 mmol) in the presence of $FeCl_3$ in 2 mL DMSO at 110 °C. [b]Isolated Yield.

Likewise, the reaction between **2f** and 6-fluoro-4-hydroxycoumarin **1e**, furnished the desired product **4b** in 78% yield under identical reaction conditions. as depicted in Table 4.

All the products were characterized using IR, ^{1}H-NMR, and ^{13}C-NMR spectra, as well as HRMS. To confirm the regioselective opening of the styrene oxide, the product **3h** was also confirmed with a single XRD data. The ORTEP diagram of compound **3h** having CCDC no. 2286699 is shown below.

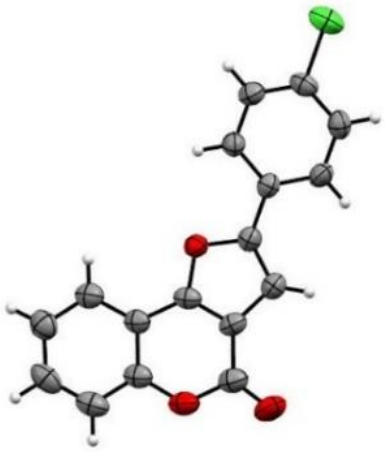

Figure 2. The ORTEP diagram of the product **3h**.

To ascertain whether the reaction proceeds via a radical pathway or not, a control experiment was performed with 6-methyl-4-hydroxycoumarin **1a** and styrene oxide **2a** in the presence of radical inhibitor 2,2,6,6-tetramethylpiperidin-1-yl)oxyl (TEMPO, 1 equiv.), which is depicted in Scheme 19.

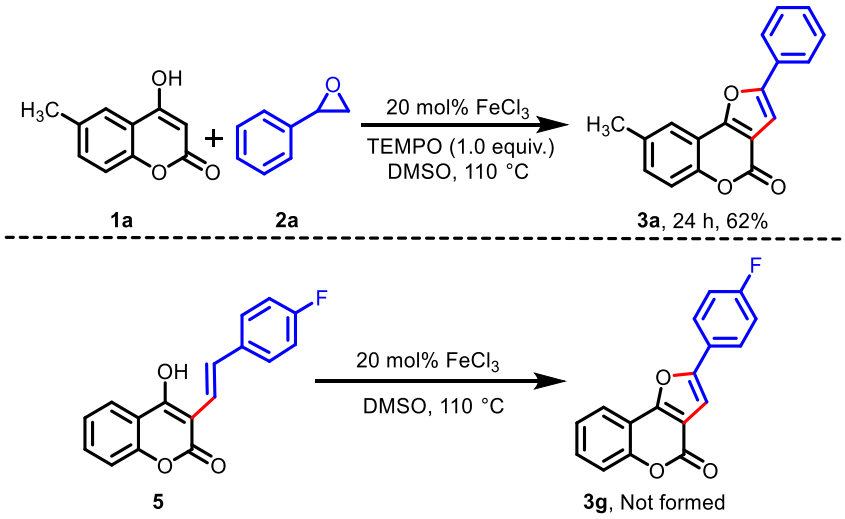

Scheme 19. Control experiment.

From the experimental results, it was observed that product **3a** was formed in 62% yield. Next, we synthesized substrate **5** from another route, and it was examined for the cyclization reaction under identical reaction conditions in the presence of 20 mol% $FeCl_3$ catalyst. However, we did not obtain the expected desired cyclized product **3g**, From these two observations, we concluded that the reaction is not going through the radical pathway nor going through the intermediate **5**.

The plausible mechanism for the formation of the product can be explained as follows: In 1964, Swanson and Laurie reported that $FeCl_3$ could undergo disproportionate reaction to provide reactive Lewis acid species $[FeCl_2]^+$, and $[FeCl_4]^-$ in polar solvents such as DMF, pyridine, and DMSO.[21] Later, 2018 Matsubara *et al.* demonstrated that $FeCl_3$ acts as an ion-pairing Lewis acid catalyst for the aza-Diels-Alder reaction.[15d] Based on their observations, we have proposed the mechanism for forming the desired product, depicted in Scheme 20.

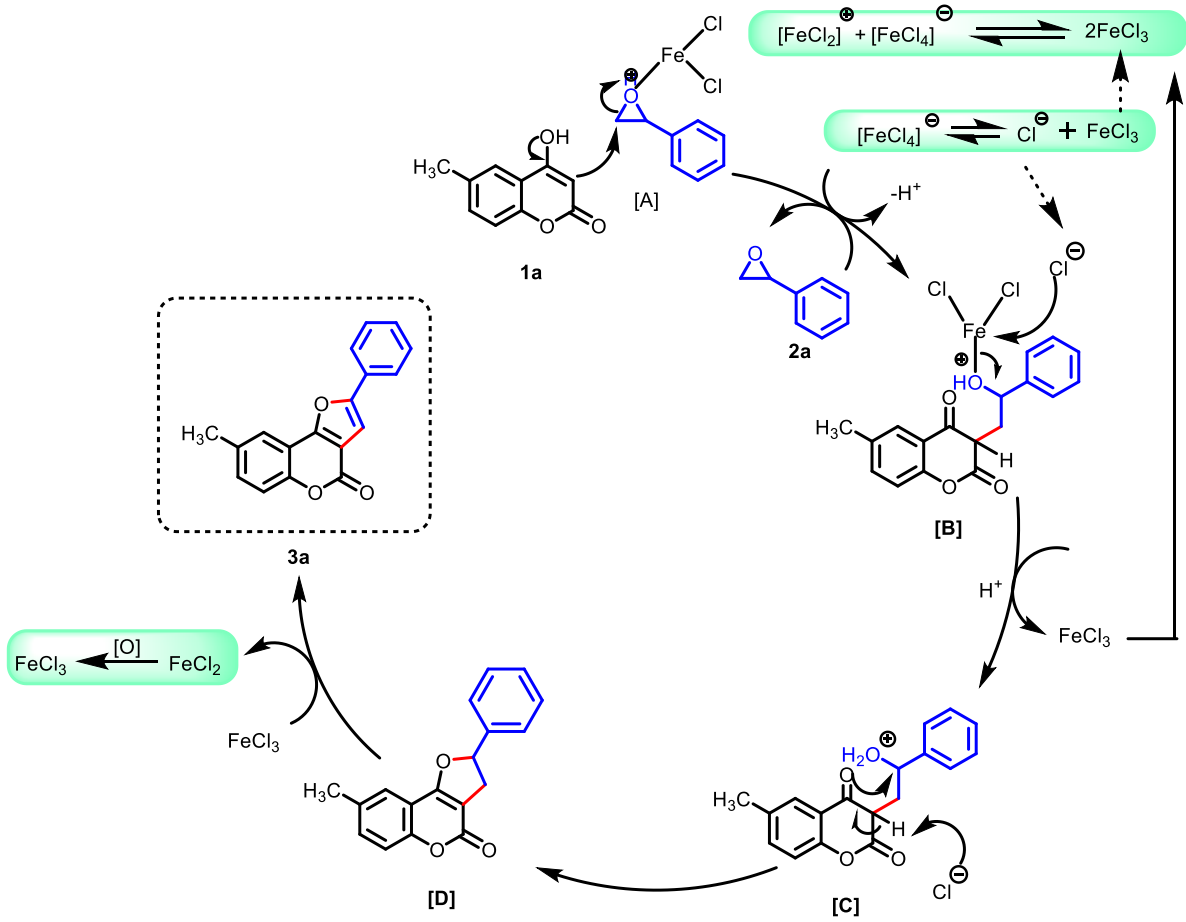

Scheme 20. A plausible mechanism for the synthesis of Furocoumarin derivatives.

Initially, styrene oxide reacts with the reactive species $[FeCl_2]^+$ to give the highly reactive intermediate **A**. Subsequently, the intermediate **A** reacts with 4-hydroxy-6-methylcoumarin **1a**

to furnish intermediate **B** by regioselective epoxide-ring opening at the less hindered site of styrene oxide **2a.**[13–15] Next, the chloride anion (Cl^-), obtained from $[FeCl_4]^-$, assists in the breaking of the Fe–O bond to provide the intermediate **C**. Then, Cl^- removes the hydrogen atom from intermediate **C,** which generates the negatively charged oxygen atom, which further facilitates the cyclization of intermediate **C** by eliminating a molecule of water to provide the cyclized intermediate **D**. Finally, the cyclized intermediate **D** undergoes oxidation by $FeCl_3$ to form the desired product **3a**. At the same time, the reduced $FeCl_2$ will undergo aerial oxidation to $FeCl_3$, and it will again participate in the catalytic cycle. The unsuccessful result of the reaction between **1e** and **2c** may not occur probably because of the presence of an electron-withdrawing group on both rings, as cyclization of the intermediate **C** is not facilitated when both rings contain an electron-withdrawing group as a lone pair of oxygen is not readily available to attack the carbon atom to cyclize.

Conclusion

In summary, we have developed a new method for the synthesis of 2-aryl-4*H*-furo[3,2-*c*]coumarin derivatives by regioselective ring-opening of aryl oxirane with 4-hydroxycoumarins. Here, the catalyst $FeCl_3$ has unique features it acts as a Lewis acid and exists in an ion-pair form in a solvent. The formation of the product is proceeding through *C*–*C* bond formation between H–3 C of 4-hydroxycoumarin and the less hindered site of the styrene oxide, followed by concomitant cyclization with the elimination of the water molecules. The formation of the product goes through a cascade reaction such as intermolecular coupling–dehydration–cyclization. The salient feature of this protocol is no need for derivatization of 4-hydroxycoumarin required for incorporation of arylacetylene at the *C*–3 position, high regioselectivity, non-requirement of any additive, easy handling, mild reaction conditions, and no need for any additives or ligands. In addition, diverse furocoumarins have been developed by the protocol. This novel synthetic approach could draw interest from the pharmaceutical and fine chemicals industries and may be regarded as a more environmentally friendly strategy compared to previously reported methods.

General Procedure for the Synthesis of aryl oxirane (2d and 2f).

In a 100 mL dry round-bottomed flask, the corresponding substituted styrene (5 mmol) was taken in 25 mL dichloromethane, and the reaction flask was placed in an ice bath temperature of 0-5 ^{o}C. Then, the *m*-chloroperbenzoic acid (*m*-CPBA) was added in portions for a period of 30 minutes at ice-bath temperature. After 2 h of stirring at 0-5 ^{o}C, the reaction was brought slowly to room temperature and stirred for another 6 h. After that, the resulting mixture was passed through a filter paper. The solvent was concentrated at the rotatory evaporator, and the crude residue was separated by column chromatography (silica gel 60-120 mesh).

General Procedure for the Synthesis of Furocoumarins Derivatives 3a-3z & 4a-4b.

In a dry 25 mL round-bottomed flask, 4-hydroxycoumarin (**1**, 1.0 mmol) and styrene oxide (**2**, 1.0 mmol) were dissolved in 2 mL of DMSO. Next, 20 mol% $FeCl_3$ catalysts were added to the reaction mixture and placed in a pre-heated oil bath at 110 ^{o}C with constant stirring under an air atmosphere. The progress of the reaction was monitored by checking TLC from time to time. After the completion of the reaction, the colour of the reaction mixture became Castleton green colour. Then, it was brought to room temperature, and the resulting mixture was diluted with 10 mL DCM. The organic layer was washed with brine solution (5 mL x 2). The organic extract was dried over anhydrous sodium sulfate, and the solvent was removed in a rotary evaporator. Finally, the crude residue was passed through a silica gel column (60-120 mesh) to obtain the pure and desired products.

8-Methyl-2-phenyl-4*H*-furo[3,2-*c*]chromen-4-one (3a) White solid (245.70 mg, 89%) mp

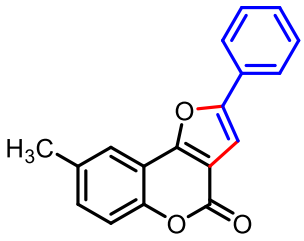

185−186 °C; ^{1}H NMR (600 MHz, $CDCl_3$) δ 7.82 (d, *J* = 7.8 Hz, 2H), 7.75 (s, 1H), 7.48 (t, *J* = 7.6 Hz, 2H), 7.41 – 7.39(m, 1H), 7.34 (q, *J* = 8.6 Hz, 2H), 7.18 (s, 1H), 2.49 (s, 3H); ^{13}C NMR (150 MHz, CDCl3) δ 158.6, 157.1, 156.6, 151.0, 134.6, 131.8, 129.2, 129.1, 129.1, 124.7, 120.6, 117.2, 112.5, 112.5, 102.8, 21.1; IR (KBr)ν_{max}/cm^{-1} 1745 (C=O), 1622 (C=C), 1310 (C–O); HRMS (ESI) Calcd For $C_{18}H_{13}O_3$ 277.0860 (M+H^{+}); Found 277.0859.

2-(4-Fluorophenyl)-8-methyl-4*H*-furo[3,2-*c*]chromen-4-one (3b) White solid (229.37 mg, 78%) mp 215−216 °C; ^{1}H NMR (400 MHz, $CDCl_3$) δ 7.79 (ddd, *J* = 8.8, 5.0, 2.5 Hz, 2H), 7.72 (s, 1H), 7.33 (d, *J* = 2.1 Hz, 2H), 7.17 (t, *J* = 8.6 Hz, 2H), 7.10 (s, 1H), 2.48 (s, 3H); ^{13}C NMR (100 MHz, $CDCl_3$) δ 163.2 (J_{C-F} = 248 Hz), 162.0, 158.5, 157.1, 155.6, 150.9, 134.6, 131.9, 126.6 (J_{C-F} = 8.2 Hz), 125.5 (J_{C-F} = 3.37 Hz), 120.6, 117.3, 116.4, 116.2, 112.5 (J_{C-F} = 8.9 Hz), 102.5 (J_{C-F} = 1.4 Hz), 21.1; ^{19}F NMR (376 MHz, $CDCl_3$) δ -111.12; IR (KBr)ν_{max}/cm^{-1} 1740 (C=O), 1620 (C=C), 1290 (C–O); HRMS (ESI) Calcd For $C_{18}H_{12}FO_3$ 295.0765 ($M+H^+$); Found 295.0765.

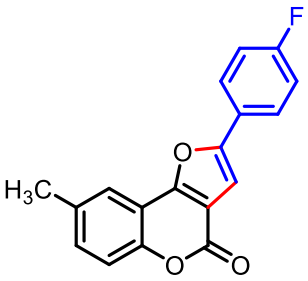

2-(4-Chlorophenyl)-8-methyl-4*H*-furo[3,2-*c*]chromen-4-one (3c) White solid (244.93 mg, 79%) mp 210−212 °C; ^{1}H NMR (600 MHz, $CDCl_3$) δ 7.74 (d, *J* = 8.9 Hz, 3H), 7.45 (d, *J* = 8.3 Hz, 2H), 7.36 – 7.33 (m, 2H), 7.16 (s, 1H), 2.48 (s, 3H); ^{13}C NMR (150 MHz, $CDCl_3$) δ 158.4, 157.2, 155.4, 151.0, 135.1, 134.6, 132.0, 129.4, 127.6, 125.8, 120.6, 117.3, 112.5, 112.4, 103.3, 21.1; IR (KBr)ν_{max}/cm^{-1} 1740 (C=O), 1622 (C=C), 1290 (C–O); HRMS (ESI) Calcd For $C_{18}H_{12}ClO_3$ 311.0470 ($M+H^+$); Found 311.0465.

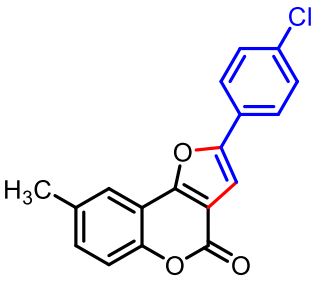

8-Methyl-2-(*p*-tolyl)-4*H*-furo[3,2-*c*]chromen-4-one (3d) White solid (246.58 mg, 85%) mp 185−186 °C; ^{1}H NMR (600 MHz, $CDCl_3$) δ 7.75 (s, 1H), 7.71 (d, *J* = 8.1 Hz, 2H), 7.35 – 7.31 (m, 2H), 7.28 (d, *J* = 8.0 Hz, 2H), 7.11 (s, 1H), 2.48 (s, 3H), 2.42 (s, 3H); ^{13}C NMR (150 MHz, $CDCl_3$) δ 158.7, 156.8, 156.8, 150.9, 139.4, 134.5, 131.6, 129.8, 126.4, 124.6, 120.6, 117.2, 112.6, 112.5, 102.0, 21.5, 21.1; IR (KBr)ν_{max}/cm^{-1} 1735 (C=O), 1600 (C=C), 1280 (C–O); HRMS (ESI) Calcd For $C_{18}H_{13}O_3$ 291.1016 ($M+H^+$); Found 291.1035.

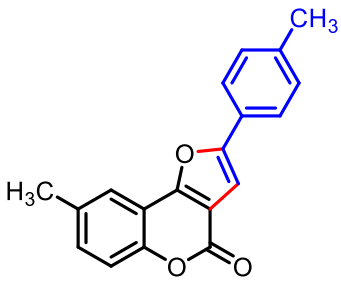

8-Methyl-2-(*m*-tolyl)-4*H*-furo[3,2-*c*]chromen-4-one (3e) White solid (232.07 mg, 80%) mp 238−240 °C; ^{1}H NMR (600 MHz, $CDCl_3$) δ 7.77 (s, 1H), 7.64 – 7.62 (m, 2H), 7.38 – 7.33 (m, 3H), 7.21 (d, *J* = 7.6 Hz, 1H), 7.16 (s, 1H), 2.49 (s, 3H), 2.45 (s, 3H); ^{13}C NMR (100 MHz, $CDCl_3$) δ 167.3, 158.6, 157.0, 156.8, 151.0, 138.9, 134.5, 131.8, 130.0, 129.0, 125.2, 121.9, 120.7, 117.2, 112.6, 112.6, 102.7, 21.6, 21.1; IR

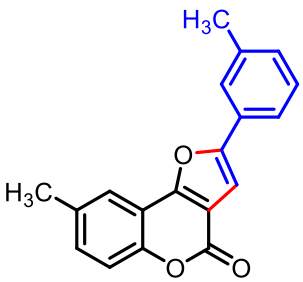

(KBr)ν_{max}/cm^{-1} 1750 (C=O), 1580 (C=C), 1280 (C–O); HRMS (ESI) Calcd For $C_{18}H_{13}O_3$ 291.1016 ($M+H^+$); Found 291.1043.

2-Phenyl-4*H*-furo[3,2-*c*]chromen-4-one (3f) White solid (233.23 mg, 89%) mp 184−185 °C;

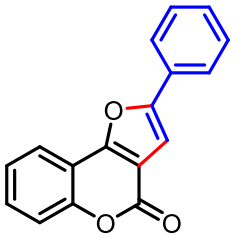

^{1}H NMR (400 MHz, $CDCl_3$) δ 7.98 (dd, *J* = 7.8, 1.4 Hz, 1H), 7.84 – 7.82 (m, 2H), 7.56 – 7.50 (m, 2H), 7.49 – 7.46 (m, 2H), 7.43 – 7.37 (m, 2H), 7.19 (s, 1H); ^{13}C NMR (150 MHz, $CDCl_3$) δ 158.4, 157.0, 156.8, 152.7, 130.7, 129.33, 129.2, 129.1, 124.7, 124.7, 120.9, 117.5, 112.9, 112.6, 102.8; IR (KBr)ν_{max}/cm^{-1} 1742 (C=O), 1622 (C=C), 1250 (C–O); HRMS (ESI) Calcd For $C_{17}H_{11}O_3$ 263.0703 ($M+H^+$); Found 263.0681.

2-(4-Fluorophenyl)-4*H*-furo[3,2-c]chromen-4-one (3g) White solid (221.24 mg, 79%) mp

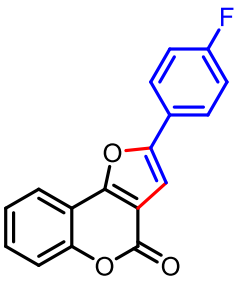

192−196 °C; ^{1}H NMR (600 MHz, $CDCl_3$) δ 7.95 (d, *J* = 7.7 Hz, 1H), 7.80 (dd, *J* = 8.6, 5.2 Hz, 2H), 7.55 – 7.52 (m, 1H), 7.47 (d, *J* = 8.3 Hz, 1H), 7.39 (t, *J* = 7.5 Hz, 1H), 7.18 (t, *J* = 8.6 Hz, 2H), 7.13 (s, 1H); ^{13}C NMR (150 MHz, $CDCl_3$) δ 163.3 (J_{C-F} = 248.7 Hz), 158.3, 157.0, 155.8, 152.7, 130.8, 126.7(J_{C-F} = 8.2 Hz), 125.4 (J_{C-F} = 3.3 Hz), 124.7, 120.9, 117.6, 116.4 (J_{C-F} = 22 Hz), 112.8, 112.6, 102.5 (J_{C-F} = 1.0 Hz); ^{19}F NMR (565 MHz, $CDCl_3$) δ -110.99; IR (KBr)ν_{max}/cm^{-1} 1750 (C=O), 1590 (C=C), 1280 (C–O); HRMS (ESI) Calcd For $C_{17}H_{10}FO_3$ 281.0609 ($M+H^+$); Found 281.0609.

2-(4-Chlorophenyl)-4*H*-furo[3,2-*c*]chromen-4-one (3h) White solid (239.77 mg, 81%) mp

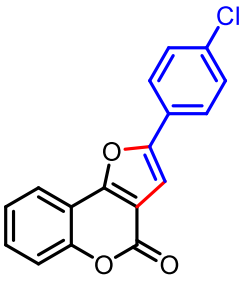

248−250 °C; ^{1}H NMR (600 MHz, $CDCl_3$) δ 7.96 (d, *J* = 7.8 Hz, 1H), 7.75 (d, *J* = 8.4 Hz, 2H), 7.54 (t, *J* = 7.8 Hz, 1H), 7.46 (t, *J* = 7.6 Hz, 3H), 7.39 (t, *J* = 7.5 Hz, 1H), 7.18 (s, 1H); ^{13}C NMR (150 MHz, $CDCl_3$) δ 158.2, 157.2, 155.6, 152.8, 135.2, 131.0, 129.5, 127.6, 125.9, 124.8, 120.9, 117.6, 112.8, 112.7, 103.3; IR (KBr)ν_{max}/cm^{-1} 1736 (C=O), 1620 (C=C), 1280 (C–O); HRMS (ESI) Calcd For $C_{17}H_{10}ClO_3$ 297.0313 ($M+H^+$); Found 297.0313.

2-(*p*-Tolyl)-4*H*-furo[3,2-*c*]chromen-4-one (3i) White solid (237.42 mg, 86%) mp 186−188

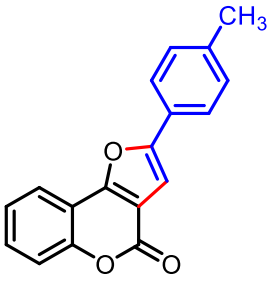

°C; ^{1}H NMR (400 MHz, $CDCl_3$) δ 7.98 – 7.96 (m, 1H), 7.71 (d, *J* = 8.2 Hz, 2H), 7.53 (ddd, *J* = 8.6, 7.2, 1.5 Hz, 1H), 7.48 – 7.45 (m, 1H), 7.40 – 7.36 (m, 1H), 7.29 (d, *J* = 8.0 Hz, 2H), 7.13 (s, 1H), 2.42 (s, 3H); ^{13}C NMR (100 MHz, $CDCl_3$) δ 158.5, 157.0, 156.8, 156.4, 152.7, 139.5, 130.6, 129.8, 126.4, 124.7, 120.9, 117.5, 113.0, 112.6, 102.0, 21.5; IR (KBr)ν_{max}/cm^{-1} 1743 (C=O), 1585 (C=C), 1200 (C–O); HRMS (ESI) Calcd For $C_{18}H_{13}O_3$ 277.0860 ($M+H^+$); Found 277.0860.

2-(*m*-Tolyl)-4*H*-furo[3,2-*c*]chromen-4-one (3j) White solid (226.38 mg, 82%) mp 168−169

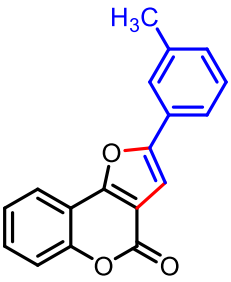

°C; ^{1}H NMR (400 MHz, $CDCl_3$) δ 7.99 (dd, *J* = 7.8, 1.4 Hz, 1H), 7.63 (d, *J* = 8.2 Hz, 2H), 7.56 – 7.51 (m, 1H), 7.48 – 7.46 (m, 1H), 7.41 – 7.35 (m, 2H), 7.22 (d, *J* = 7.3 Hz, 1H), 7.17 (s, 1H), 2.45 (s, 3H); ^{13}C NMR (100 MHz, $CDCl_3$) δ 175.1, 152.7, 138.9, 130.7, 130.7, 130.1, 129.1, 129.0, 128.6, 125.3, 124.7, 121.9, 120.9, 117.5, 112.9, 112.6, 102.7, 21.6; IR (KBr)ν_{max}/cm^{-1} 1743 (C=O), 1585 (C=C), 1200 (C–O); HRMS (ESI) Calcd For $C_{18}H_{13}O_3$ 277.0860 ($M+H^+$); Found 277.0862.

7-Methoxy-2-phenyl-4*H*-furo[3,2-*c*]chromen-4-one (3k) White solid (257.02 mg, 88%) mp

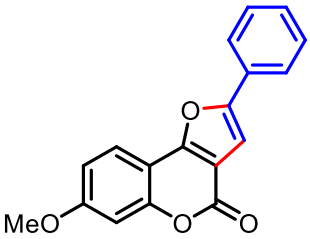

172−173 °C; ^{1}H NMR (600 MHz, $CDCl_3$) δ 7.86 (d, *J* = 9.3 Hz, 1H), 7.81 – 7.79 (m, 2H), 7.47 (t, *J* = 7.7 Hz, 2H), 7.38 (t, *J* = 7.4 Hz, 1H), 7.15 (s, 1H), 6.97 (dq, *J* = 4.0, 2.3 Hz, 2H), 3.91 (s, 3H); ^{13}C NMR (150 MHz, $CDCl_3$) δ 162.1, 158.7, 157.9, 157.8, 155.9, 154.6, 129.3, 129.1, 129.0, 124.5, 121.9, 113.0, 106.3, 102.6, 101.6, 55.9; IR (KBr)ν_{max}/cm^{-1} 1740 (C=O), 1622 (C=C), 1300 (C–O); HRMS (ESI) Calcd For $C_{18}H_{13}O_4$ 293.0809 ($M+H^+$); Found 293.0810.

2-(4-Fluorophenyl)-7-methoxy-4*H*-furo[3,2-*c*]chromen-4-one (3l) White solid (257.35 mg,

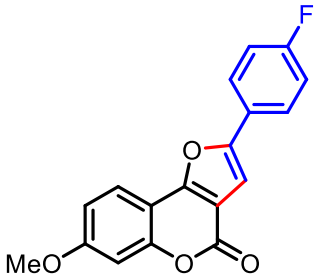

83%) mp 220−221 °C; ^{1}H NMR (400 MHz, $CDCl_3$) δ 7.84 (d, *J* = 9.3 Hz, 1H), 7.79 – 7.76 (m, 2H), 7.17 (t, *J* = 8.7 Hz, 2H), 7.08 (s, 1H), 6.98 – 6.95 (m, 2H), 3.90 (s, 3H); ^{13}C NMR (100 MHz, $CDCl_3$) δ 164.3, 162.1, 158.7, 157.7, 154.9, 154.5, 126.4 (J_{C-F} = 8.26 Hz), 125.6 (J_{C-F} = 1.58 Hz), 121.8, 116.3 (J_{C-F} = 22.1 Hz), 113.1, 110.1, 106.2, 102.3 (J_{C-F} = 1.29 Hz), 101.6, 55.9; ^{19}F NMR (376 MHz,

$CDCl_3$) δ -111.47; IR (KBr)ν_{max}/cm^{-1} 1735 (C=O), 1592 (C=C), 1285 (C–O); HRMS (ESI) Calcd For $C_{18}H_{12}FO_4$ 311.0715 ($M+H^+$); Found 311.0716.

2-(4-Chlorophenyl)-7-methoxy-4*H*-furo[3,2-*c*]chromen-4-one (3m) White solid (257.56 mg, 79%) mp 218−220 °C; ^{1}H NMR (400 MHz, $CDCl_3$) δ 7.86 – 7.84 (m, 1H), 7.74 – 7.71 (m, 2H), 7.46 – 7.43 (m, 2H), 7.14 (s, 1H), 6.97 (dd, *J* = 6.3, 2.4 Hz, 2H), 3.91 (s, 3H); ^{13}C NMR (100 MHz, $CDCl_3$) δ, 162.3, 158.5, 157.9, 154.7, 154.6, 134.8, 129.4, 127.7, 125.7, 121.9, 113.1, 110.1, 106.1, 103.1, 101.6, 55.9; IR (KBr)ν_{max}/cm^{-1} 1735 (C=O), 1592 (C=C), 1285 (C–O); HRMS (ESI) Calcd For $C_{18}H_{12}ClO_4$ 327.0419 ($M+H^+$); Found 327.0419.

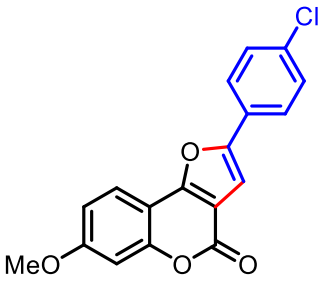

7-Methoxy-2-(*p*-tolyl)-4*H*-furo[3,2-*c*]chromen-4-one (3n) White solid (263.23 mg, 86%) mp 225−226 °C; ^{1}H NMR (600 MHz, $CDCl_3$) δ 7.86 – 7.85 (m, 1H), 7.68 (d, *J* = 8.1 Hz, 2H), 7.28 – 7.26 (m, 2H), 7.08 (s, 1H), 6.96 (dq, *J* = 4.4, 2.3 Hz, 2H), 3.90 (s, 3H), 2.41 (s, 3H); ^{13}C NMR (150 MHz, $CDCl_3$) δ 162.0, 158.8, 157.5, 156.1, 154.4, 139.1, 129.8, 126.5, 124.5, 121.8, 113.0, 110.2, 106.4, 101.8, 101.6, 55.9, 21.5; IR (KBr)ν_{max}/cm^{-1} 1738 (C=O), 1622 (C=C), 1310 (C–O); HRMS (ESI) Calcd For $C_{19}H_{15}O_4$ 307.0965 ($M+H^+$); Found 307.0965.

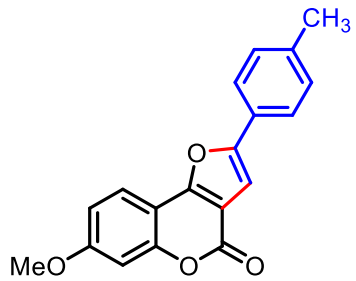

7-Methoxy-2-(*m*-tolyl)-4*H*-furo[3,2-*c*]chromen-4-one (3o) White solid (244.87 mg, 80%) mp 228−230 °C; ^{1}H NMR (600 MHz, $CDCl_3$) δ 7.88 – 7.87 (m, 1H), 7.60 (d, *J* = 11.5 Hz, 2H), 7.36 (t, *J* = 7.6 Hz, 1H), 7.20 (d, *J* = 7.6 Hz, 1H), 7.13 (s, 1H), 6.97 (dq, *J* = 4.3, 2.3 Hz, 2H), 3.90 (s, 3H), 2.44 (s, 3H); ^{13}C NMR (150 MHz, $CDCl_3$) δ 162.1, 158.8, 157.7, 156.0, 154.5, 138.8, 129.8, 129.2, 129.0, 125.1, 121.9, 121.78, 113.0, 110.1, 106.4, 102.5, 101.6, 55.9, 21.6; IR (KBr)ν_{max}/cm^{-1} 1738 (C=O), 1622 (C=C), 1310 (C–O); HRMS (ESI) Calcd For $C_{19}H_{15}O_4$ 307.0965 ($M+H^+$); Found 307.0965.

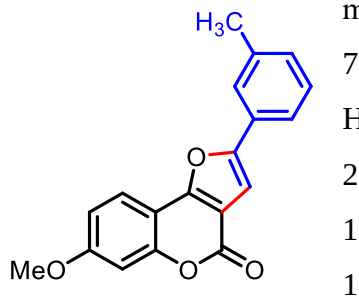

8-Chloro-2-phenyl-4*H*-furo[3,2-*c*]chromen-4-one (3p) White solid (263.46 mg, 89%) mp 215−216 °C; ^{1}H NMR (600 MHz, $CDCl_3$) δ 7.94 (d, *J* = 2.4 Hz, 1H), 7.83 – 7.81 (m, 2H), 7.50 – 7.46 (m, 3H), 7.43 – 7.40 (m, 2H), 7.19 (s, 1H); ^{13}C NMR (150 MHz, $CDCl_3$) δ 157.7, 157.4, 155.6, 151.0, 130.6, 130.3, 129.6, 129.2, 128.8, 124.8, 120.4, 118.9, 113.9, 113.4, 102.9; IR (KBr)ν_{max}/cm^{-1} 1745 (C=O), 1583 (C=C), 1296 (C–O); HRMS (ESI) Calcd For $C_{17}H_{10}ClO_3$ 297.0313 ($M+H^+$); Found 297.0313.

8-Chloro-2-(4-fluorophenyl)-4*H*-furo[3,2-*c*]chromen-4-one (3q) White solid (257.49 mg, 82%) mp 234−235 °C. ^{1}H NMR (400 MHz, $CDCl_3$) δ 7.92 (d, *J* = 2.4 Hz, 1H), 7.82 – 7.79 (m, 2H), 7.48 (dd, *J* = 8.9, 2.4 Hz, 1H), 7.41 (d, *J* = 8.9 Hz, 1H), 7.19 (t, *J* = 8.7 Hz, 2H), 7.13 (s, 1H); ^{13}C NMR (100 MHz, $CDCl_3$) δ 163.4 (J_{C-F} = 249.09 Hz), 157.7, 156.5, 155.6, 151.0, 130.7, 130.3, 126.8 (J_{C-F} = 8.34 Hz), 125.1 (J_{C-F} = 3.37 Hz), 120.4, 119.0, 116.5 (J_{C-F} = 33.12 Hz), 113.8, 113.4, 102.6 (J_{C-F} = 1.44 Hz); ^{19}F NMR (376 MHz, $CDCl_3$) δ -110.45; IR (KBr)ν_{max}/cm^{-1} 1732 (C=O), 1580 (C=C), 1256 (C–O); HRMS (ESI) Calcd For $C_{17}H_9ClFO_3$ 315.0219 ($M+H^+$); Found 315.0213.

8-Chloro-2-(4-chlorophenyl)-4*H*-furo[3,2-*c*]chromen-4-one (3r) White solid (263.98 mg, 80%) mp 262−263 °C; ^{1}H NMR (600 MHz, $CDCl_3$) δ 7.93 (d, *J* = 2.4 Hz, 1H), 7.76 – 7.74 (m, 2H), 7.49 – 7.46 (m, 3H), 7.41 (d, *J* = 8.8 Hz, 1H), 7.18 (s, 1H); ^{13}C NMR (150 MHz, $CDCl_3$) δ 157.6, 156.3, 155.8, 151.1, 135.5, 130.8, 130.4, 129.5, 127.3, 126.0, 120.5, 119.0, 113.8, 113.4, 103.3; IR (KBr)ν_{max}/cm^{-1} 1732 (C=O), 1582 (C=C), 1256 (C–O); HHRMS (ESI) Calcd For $C_{17}H_9Cl_2O_3$ 330.9924 ($M+H^+$); Found 331.0257.

8-Chloro-2-(*p*-tolyl)-4*H*-furo[3,2-*c*]chromen-4-one (3s) White solid (244.93 mg, 79%) mp 212−213 °C; ^{1}H NMR (600 MHz, DMSO-d_6) δ 7.99 (dd, *J* = 8.5, 3.0 Hz, 1H), 7.92 – 7.90 (m, 2H), 7.57 (d, *J* = 3.2 Hz, 1H), 7.41 (d, *J* = 7.9 Hz, 2H), 7.01 (d, *J* = 8.6 Hz, 1H), 6.96 (s, 1H), 2.44 (s, 3H); ^{13}C NMR (100 MHz, DMSO-d_6) δ 160.5, 157.7, 157.2, 155.0, 154.0, 138.6, 129.7, 126.1, 124.2, 122.2, 113.6, 108.8, 104.3, 103.0, 102.2, 21.0; IR (KBr)ν_{max}/cm^{-1} 1745 (C=O), 1622 (C=C), 1310 (C–O); HRMS (ESI) Calcd For $C_{18}H_{12}ClO_3$ 311.0470 ($M+H^+$); Found 311.0708.

8-Chloro-2-(*m*-tolyl)-4*H*-furo[3,2-*c*]chromen-4-one (3t) White solid (241.83 mg, 78%) mp 212−213 °C; ^{1}H NMR (600 MHz, $CDCl_3$) δ 7.95 (d, *J* = 2.3 Hz, 1H), 7.64 – 7.62 (m, 2H), 7.47 (dd, *J* = 8.8, 2.4 Hz, 1H), 7.41 – 7.36 (m, 2H), 7.24 (d, *J* = 7.8 Hz, 1H), 7.17 (s, 1H), 2.45 (s, 3H); ^{13}C NMR (150 MHz, $CDCl_3$) δ 159.6, 157.8, 157.6, 155.6, 151.0, 139.0, 130.6, 130.4, 130.3, 129.1, 128.7, 125.4, 122.0, 120.6, 120.4, 118.9, 102.7, 29.8; IR (KBr)ν_{max}/cm^{-1} 1745 (C=O), 1610 (C=C), 1265 (C–O); HRMS (ESI) Calcd For $C_{18}H_{12}ClO_3$ 311.0470 ($M+H^+$); Found 311.0595.

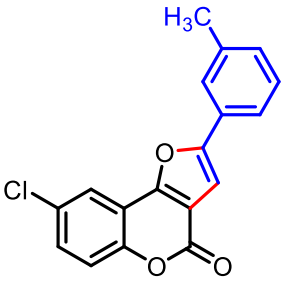

8-Fluoro-2-phenyl-4*H*-furo[3,2-*c*]chromen-4-one (3u) White solid (212.84 mg, 76%) mp 179−180 °C; ^{1}H NMR (600 MHz, $CDCl_3$) δ 7.83 – 7.82 (m, 2H), 7.65 – 7.63 (m, 1H), 7.50 (t, *J* = 7.6 Hz, 2H), 7.46 – 7.41 (m, 2H), 7.25 – 7.23 (m, 1H), 7.20 (s, 1H); ^{13}C NMR (100 MHz, $CDCl_3$) δ 159.2 (J_{C-F} = 243.91 Hz), 157.8, 156.3 (J_{C-F} = 3.9 Hz), 156.2, 148.9, 135.5, 129.5, 127.3, 126.0, 119.3 (J_{C-F} = 8.58 Hz), 118.3 (J_{C-F} = 24.38 Hz), 113.4, 109.9, 106.8 (J_{C-F} = 25.81) 103.4; ^{19}F NMR (377 MHz, $CDCl_3$) δ -116.24; IR (KBr)ν_{max}/cm^{-1} 1732 (C=O), 1580 (C=C), 1260 (C–O); HRMS (ESI) Calcd For $C_{17}H_{10}FO_3$ 281.0609 ($M+H^+$); Found 281.0652.

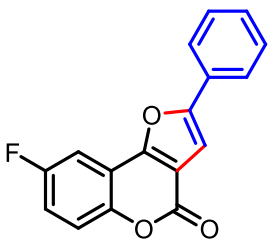

2-(4-Chlorophenyl)-8-fluoro-4*H*-furo[3,2-*c*]chromen-4-one (3v) White solid (226.09 mg, 72%) mp 181−183 °C; ^{1}H NMR (600 MHz, $CDCl_3$) δ 7.76 – 7.74 (m, 2H), 7.62 (dd, *J* = 7.7, 3.0 Hz, 1H), 7.48 – 7.46 (m, 2H), 7.45 – 7.44 (m, 1H), 7.25 – 7.23 (m, 1H), 7.19 (s, 1H); ^{13}C NMR (150 MHz, $CDCl_3$) δ 159.3 (J_{C-F} = 243.72 Hz), 157.9, 156.3 (J_{C-F} = 2.91 Hz), 156.3, 149.0, 135.6, 129.6, 127.4, 126.1, 119.4 (J_{C-F} = 8.55 Hz), 118.4 (J_{C-F} = 24.42 Hz), 113.6, 113.5, 106.9 (J_{C-F} = 25.69 Hz), 103.5; ^{19}F NMR (377 MHz, $CDCl_3$) δ -116.08; IR (KBr)ν_{max}/cm^{-1} 1736 (C=O), 1595 (C=C), 1293 (C–O); HRMS (ESI) Calcd For $C_{17}H_9ClFO_3$ 315.0219 ($M+H^+$); Found 315.0213.

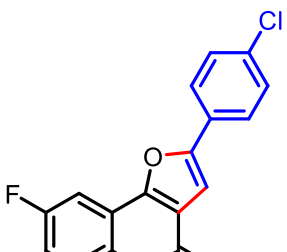

8-Fluoro-2-(*p*-tolyl)-4*H*-furo[3,2-*c*]chromen-4-one (3w) White solid (235.25 mg, 80%) mp 185−186 °C; ^{1}H NMR (600 MHz, $CDCl_3$) δ 7.71 (d, *J* = 8.1 Hz, 2H), 7.62 (dd, *J* = 7.7, 2.9 Hz, 1H), 7.44 (dd, *J* = 9.1, 4.2 Hz, 1H), 7.29 (d, *J* = 8.0 Hz, 2H), 7.23 (td, *J* = 8.7, 2.9 Hz, 1H), 7.13 (s, 1H), 2.42 (s, 3H); ^{13}C NMR (150 MHz, $CDCl_3$) δ 159.1 (J_{C-F} = 243.48 Hz), 158.1, 157.6, 155.8 (J_{C-F} = 2.76 Hz), 148.7 (J_{C-F} = 2.05 Hz), 139.8,

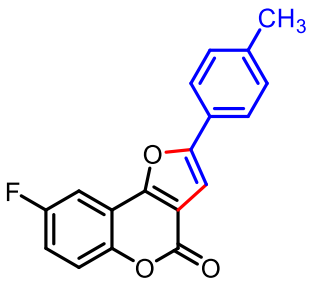

129.9, 126.1, 124.7, 119.2 (J_{C-F} = 8.62 Hz), 117.9 (J_{C-F} = 24.48 Hz), 113.7 (J_{C-F} = 9.87 Hz), 113.4, 106.7 (J_{C-F} = 25.75 Hz), 102.1, 21.5; ^{19}F NMR (565 MHz, $CDCl_3$) δ -116.33; IR (KBr)ν_{max}/cm^{-1} 1745 (C=O), 1622 (C=C), 1310 (C–O); HRMS (ESI) Calcd For $C_{18}H_{12}FO_3$ 295.0765 ($M+H^+$); Found 295.0765.

2-(4-Fluorophenyl)-7-hydroxy-4*H*-furo[3,2-*c*]chromen-4-one (3x) White solid (233.87 mg, 79%) mp 198−199 °C; ^{1}H NMR (600 MHz, DMSO-d_6) δ 7.99 – 7.96 (m, 2H), 7.89 (d, *J* = 8.3 Hz, 1H), 7.54 (s, 1H), 7.35 (t, *J* = 9.0 Hz, 2H), 6.92 (dd, *J* = 8.5, 2.0 Hz, 1H), 6.87 (d, *J* = 2.3 Hz, 1H); ^{13}C NMR (150 MHz, DMSO-d_6) δ 162.2 (J_{C-F} = 246.06 Hz), 160.7, 157.6, 157.4, 154.0, 153.8, 126.5 (J_{C-F} = 8.31 Hz), 125.4 (J_{C-F} = 3.03 Hz), 122.3, 116.2 (J_{C-F} = 21.96 Hz), 113.6, 108.8, 104.2, 103.0, 102.9; ^{19}F NMR (565 MHz, DMSO-d_6) δ -112.06; IR (KBr)ν_{max}/cm^{-1} 3510 (O–H), 1732 (C=O), 1615 (C=C), 1265 (C–O); HRMS (ESI) Calcd For $C_{17}H_{10}FO_4$ 297.0558 ($M+H^+$); Found 297.0743.

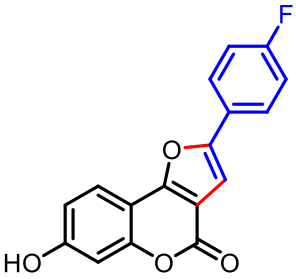

2-(4-Chlorophenyl)-7-hydroxy-4*H*-furo[3,2-*c*]chromen-4-one (3y) White solid (265.21 mg, 85%) mp 288−290 °C; ^{1}H NMR (600 MHz, DMSO-d_6) δ 7.96 (d, *J* = 8.5 Hz, 2H), 7.91 (d, *J* = 8.6 Hz, 1H), 7.65 (s, 1H), 7.58 (d, *J* = 8.5 Hz, 2H), 6.92 (dd, *J* = 8.6, 2.1 Hz, 1H), 6.88 (d, *J* = 2.0 Hz, 1H); ^{13}C NMR (150 MHz, DMSO-d_6) δ 160.7, 157.5, 157.5, 154.1, 153.5, 133.2, 129.1, 127.6, 125.8, 122.3, 113.6, 108.8, 104.1, 103.9, 103.0; IR (KBr)ν_{max}/cm^{-1} 3500 (O–H), 1730 (C=O), 1615 (C=C), 1250 (C–O); HRMS (ESI) Calcd For $C_{17}H_{10}ClO_4$ 313.0263 ($M+H^+$); Found 313.0261.

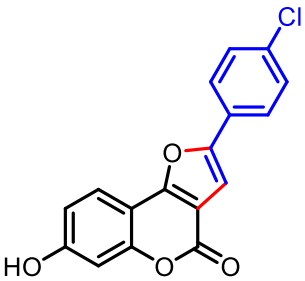

7-Hydroxy-2-(*p*-tolyl)-4*H*-furo[3,2-*c*]chromen-4-one (3z) White solid (233.65 mg, 80%); ^{1}H NMR (600 MHz, DMSO-d_6) δ 7.99 (dd, *J* = 8.5, 3.0 Hz, 1H), 7.92 – 7.90 (m, 2H), 7.57 (d, *J* = 3.2 Hz, 1H), 7.41 (d, *J* = 7.9 Hz, 2H), 7.01 (d, *J* = 8.6 Hz, 1H), 6.97 – 6.96 (s, 1H), 2.44 (s, 3H); ^{13}C NMR (100 MHz, DMSO-d_6) δ 160.5, 157.7, 157.2, 155.0, 154.0, 138.6, 129.7, 126.1, 124.2, 122.2, 113.6, 108.8, 104.3, 103.0, 102.2, 21.0; IR (KBr) ν_{max}/cm^{-1} 3500 (O–H), 1740 (C=O), 1622 (C=C), 1280 (C–O); HRMS (ESI) Calcd For $C_{18}H_{13}O_4$ 293.0809 ($M+H^+$); Found 293.0810.

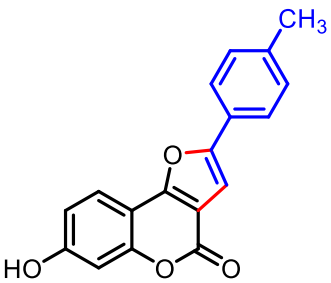

2-(Naphthalen-2-yl)-4*H*-furo[3,2-*c*]chromen-4-one (4a) White solid (249.66 mg, 80%) mp 230−232 °C; ^{1}H NMR (600 MHz, $CDCl_3$) δ 8.32 (s, 1H), 8.05 (dd, *J* = 7.8, 1.4 Hz, 1H), 7.94 (dd, *J* = 8.0, 5.0 Hz, 2H), 7.88 – 7.85 (m, 2H), 7.57 – 7.52 (m, 3H), 7.48 (d, *J* = 8.2 Hz, 1H), 7.43 – 7.40 (m, 1H), 7.30 (s, 1H); ^{13}C NMR (150 MHz, $CDCl_3$) δ 158.4, 157.2, 156.8, 152.8, 133.5, 133.4, 130.8, 129.1, 128.5, 128.0, 127.1, 127.0, 126.3, 124.7, 123.8, 122.3, 121.0, 117.6, 112.9, 112.7, 103.3; IR (KBr) ν_{max}/cm^{-1} 1745 (C=O), 1621 (C=C), 1282 (C–O); HRMS (ESI) Calcd For $C_{21}H_{13}O_3$ 313.0860 ($M+H^+$); Found 313.0870.

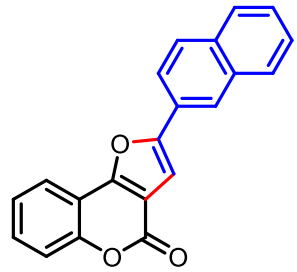

8-Fluoro-2-(naphthalen-2-yl)-4*H*-furo[3,2-*c*]chromen-4-one (4b) White solid (257.45 mg, 78%) mp 238−239 °C; ^{1}H NMR (600 MHz, $CDCl_3$) δ 8.32 (s, 1H), 7.94 (dd, *J* = 8.0, 3.7 Hz, 2H), 7.87 (d, *J* = 7.6 Hz, 1H), 7.85 (dd, *J* = 8.6, 1.7 Hz, 1H), 7.71 (dd, *J* = 7.7, 2.9 Hz, 1H), 7.55 (pd, *J* = 6.8, 1.4 Hz, 2H), 7.46 (dd, *J* = 9.1, 4.3 Hz, 1H), 7.31 (s, 1H), 7.27 – 7.24 (m, 1H); ^{13}C NMR (100 MHz, $CDCl_3$) δ 160.4, 157.9 ($J_{C\text{-}F}$ = 0.93 Hz), 157.4, 156.2 ($J_{C\text{-}F}$ = 2.75 Hz), 148.9 ($J_{C\text{-}F}$ = 2.05 Hz), 133.6, 133.4, 129.1, 128.6, 128.0, 127.2, 127.2, 126.1, 124.0, 122.2, 119.2 ($J_{C\text{-}F}$ = 8.56 Hz), 118.2 ($J_{C\text{-}F}$ = 24.47 Hz), 113.6, ($J_{C\text{-}F}$ = 9.66 Hz), 113.5, 106.9 ($J_{C\text{-}F}$ = 25.64 Hz), 103.43; ^{19}F NMR (376 MHz, $CDCl_3$) δ -116.22; IR (KBr) ν_{max}/cm^{-1} 1740 (C=O), 1615 (C=C), 1280 (C–O); HRMS (ESI) Calcd For $C_{21}H_{12}FO_3$ 331.0765 ($M+H^+$); Found 331.0765.

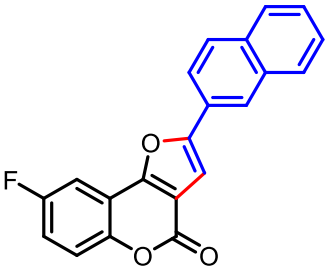

XRD for compound (3h): All the data for the structural analysis of compound **3h** has been deposited to the Cambridge Crystallographic Data Centre, CCDC No. 2286699.

Table 5. Crystal data and structure refinement for compound **3h.**

Entry		**Identification Code**	**Compound 3h**
01		Empirical formula	$C_{17}H_9ClO_3$
02		Formula weight	296.69
03		Temperature	297.00
04		Wavelength	0.71073 Å
05		Radiation type	MoKα
06		Radiation system	Fine-focus sealed tube
07		Crystal system	orthorhombic
08		Space group	$Pna2_1$
09		Cell length	a= 25.055(6) /Å b= 3.8926(9) /Å c= 13.226(3) /Å
10		Cell angle	α=90 β=90(2) γ=90
11		Cell volume	1290.0(5)
12		Density	1.528
13		Completeness to theta	99
14		Absorption correction	multi-scan
15		Refinement method	Full-matrix least-squares on F2
16		Index ranges	$-30 \leq h \leq 30$, $-4 \leq k \leq 4$, $-16 \leq l \leq 16$
17		Reflection number	2527
18		2Θ range	4.478 to 51.982
19		Cell formula units Z	4
20		CCDC no	2286699

^{1}H NMR Spectrum of 8-Methyl-2-phenyl-4*H*-furo[3,2-*c*]chromen-4-one (3a)

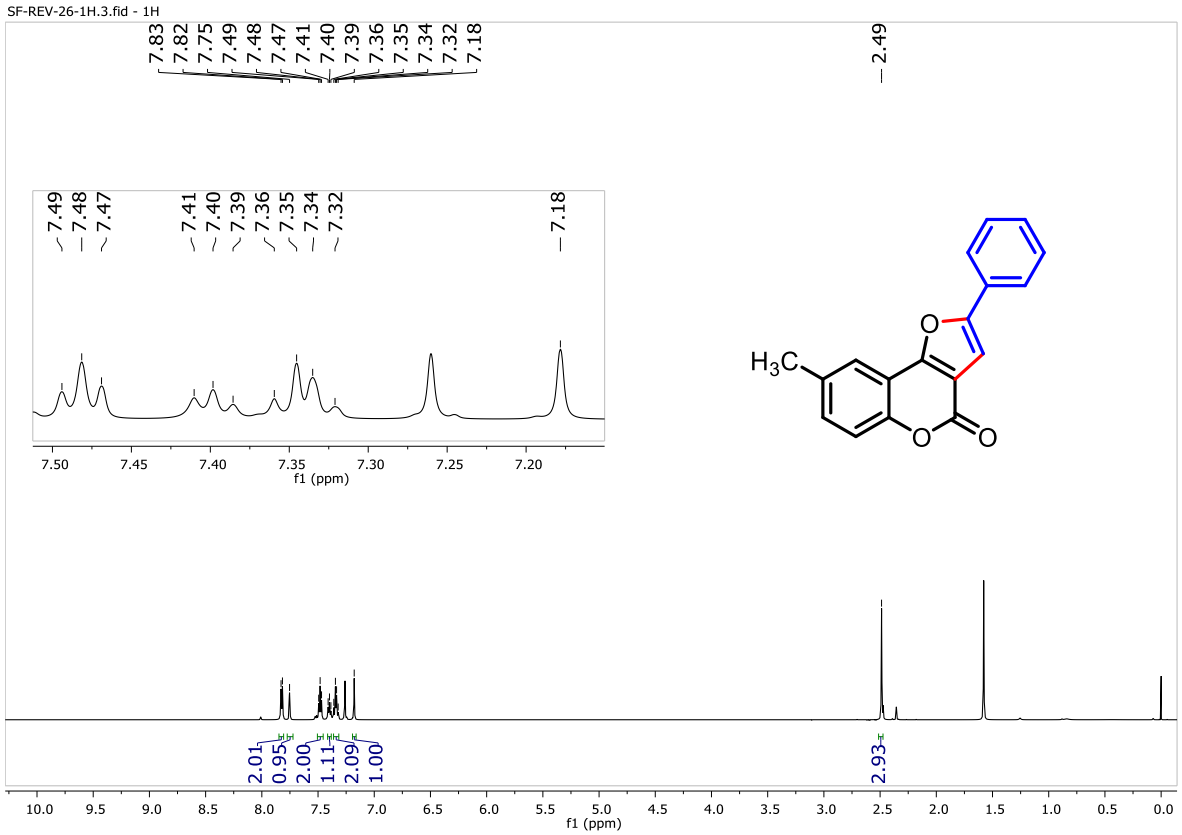

^{13}C NMR Spectrum of 8-Methyl-2-phenyl-4*H*-furo[3,2-*c*]chromen-4-one (3a)

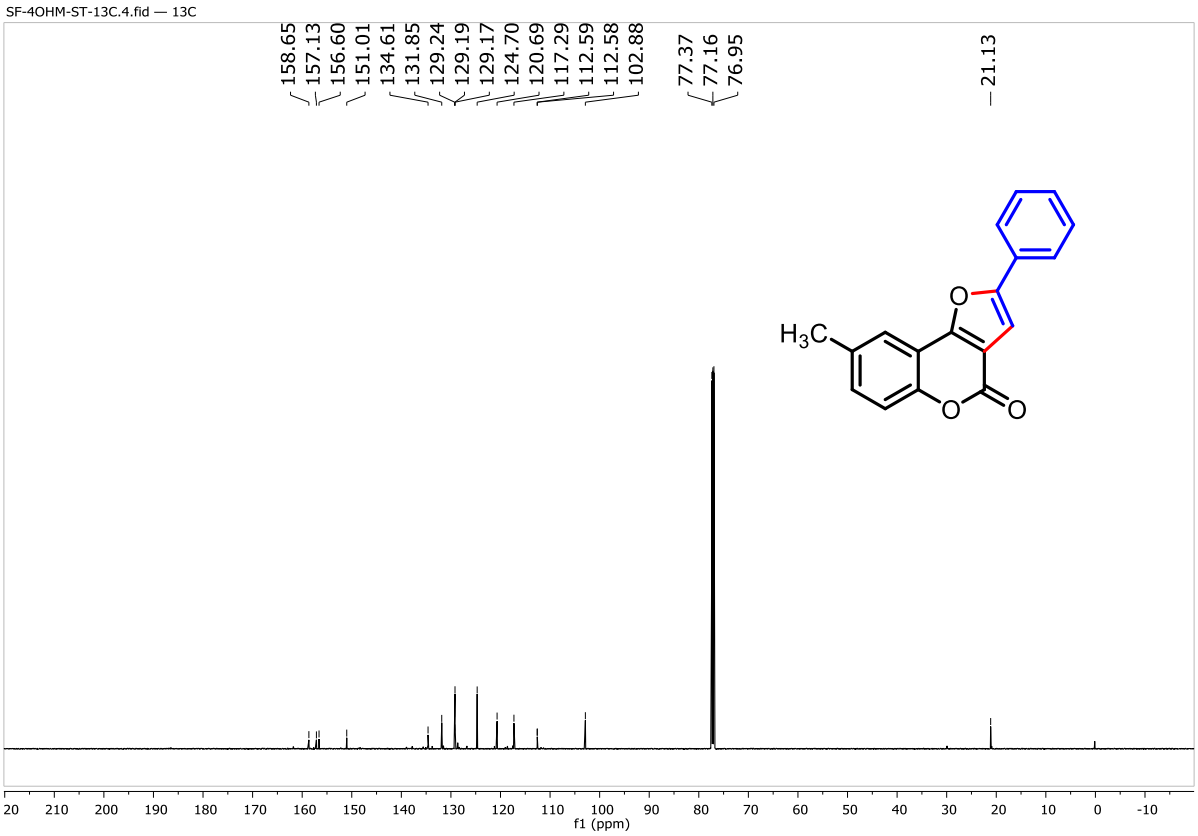

HRMS Spectrum of 8-Methyl-2-phenyl-4*H*-furo[3,2-*c*]chromen-4-one (3a)

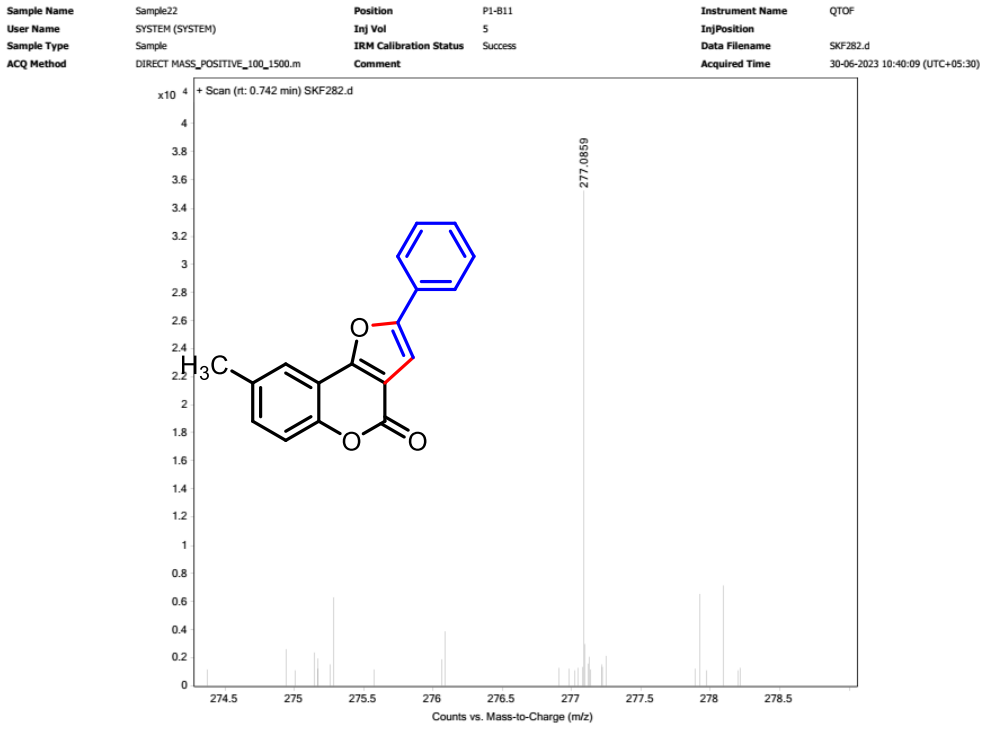

^{1}H NMR Spectrum of 2-(Naphthalen-2-yl)-4*H*-furo[3,2-*c*]chromen-4-one (4a)

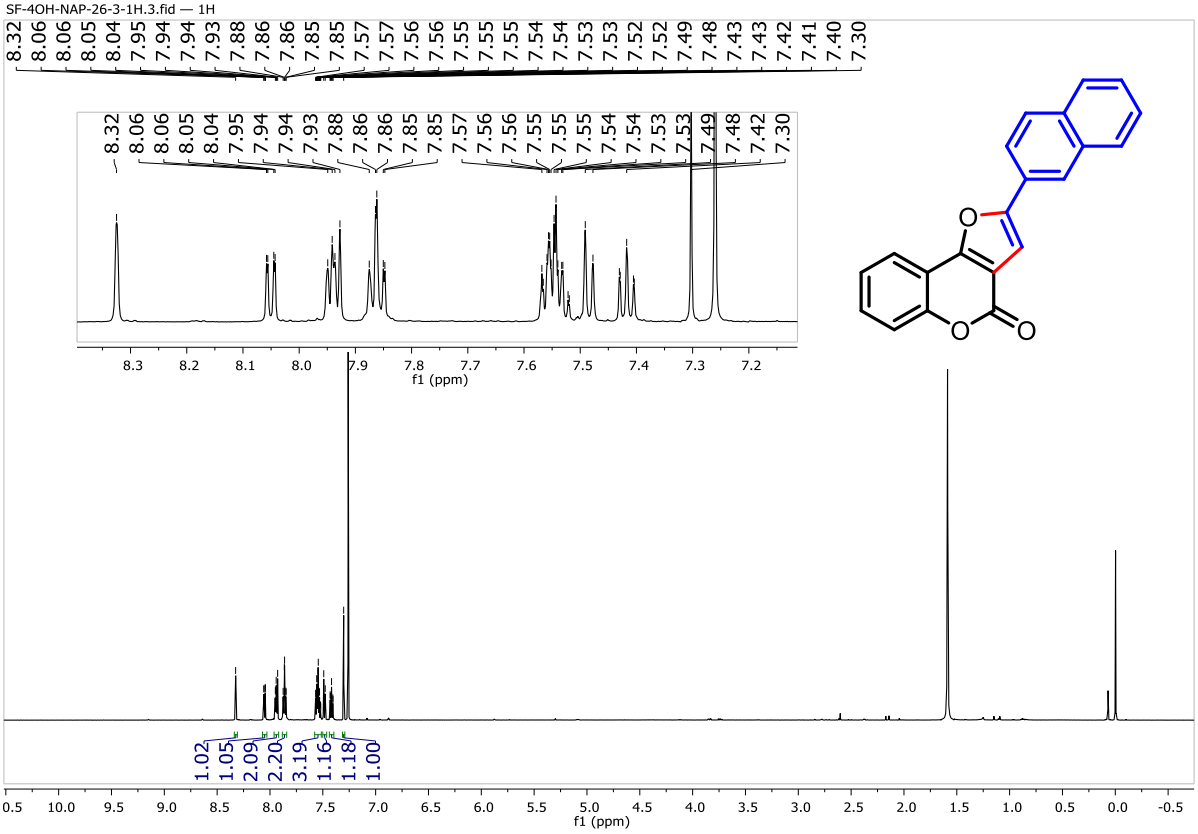

^{13}C NMR Spectrum of 2-(Naphthalen-2-yl)-4*H*-furo[3,2-*c*]chromen-4-one (4a)

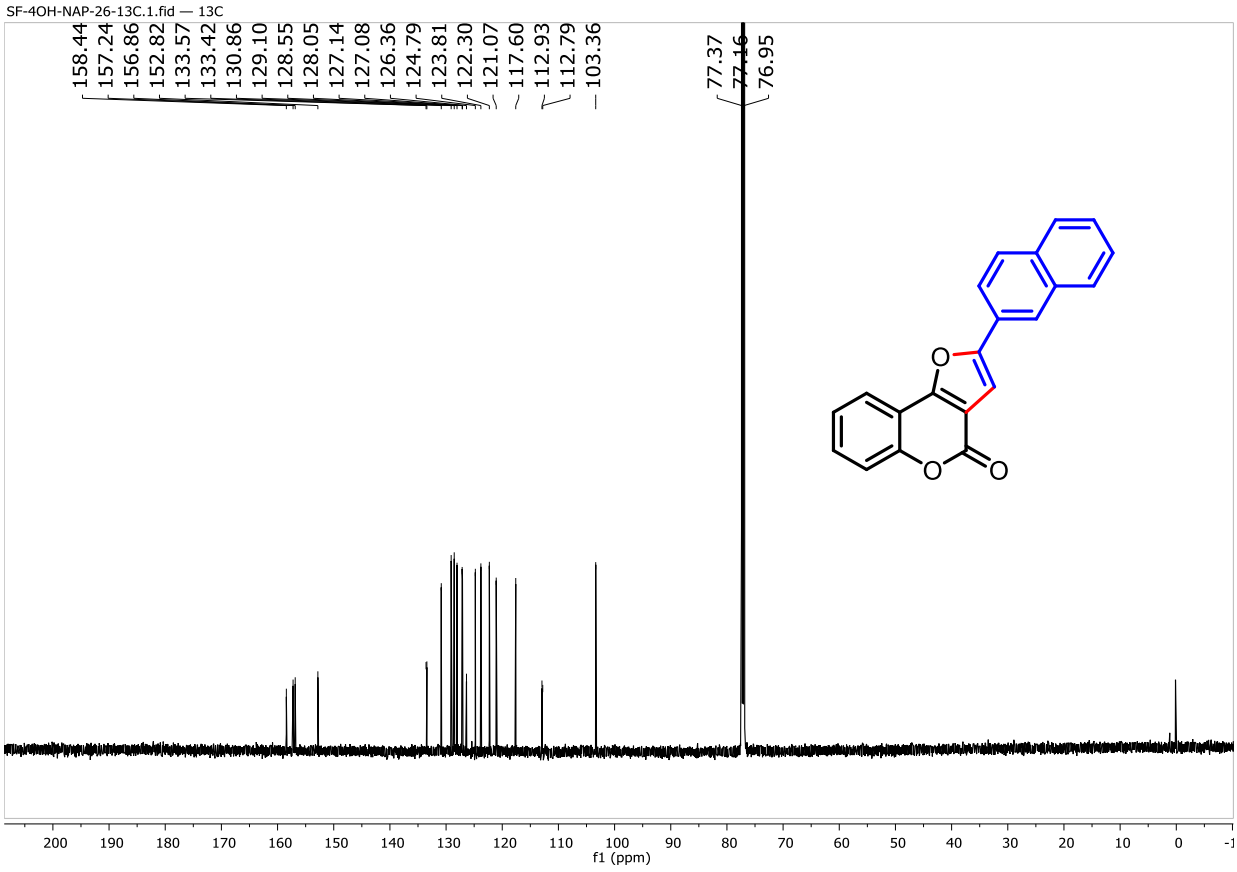

HRMS Spectrum of 2-(Naphthalen-2-yl)-4*H*-furo[3,2-*c*]chromen-4-one (4a)

Sample Name	Sample2	**Position**	P1-A2	**Instrument Name**	QTOF
User Name	SYSTEM (SYSTEM)	**Inj Vol**	5	**InjPosition**	
Sample Type	Sample	**IRM Calibration Status**	Success	**Data Filename**	SF28RJ6.d
ACQ Method	DIRECT MASS_POSITIVE_01_1.m	**Comment**		**Acquired Time**	13-10-2023 14:48:25 (UTC+05:30)

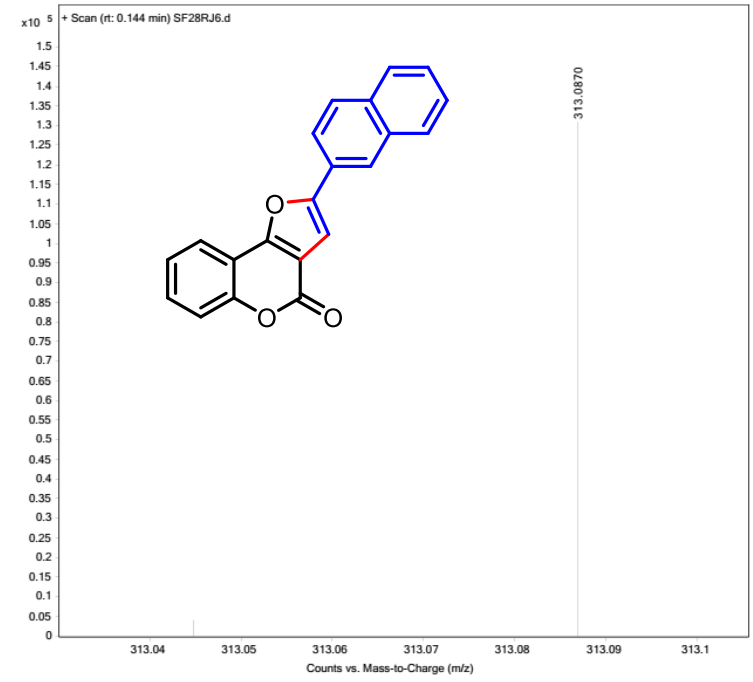

Part B

Chapter II: Section B

Synthesis of 9-substituted tetrahydro coumestan derivatives and synthesis of some naturally occurring coumestan derivatives

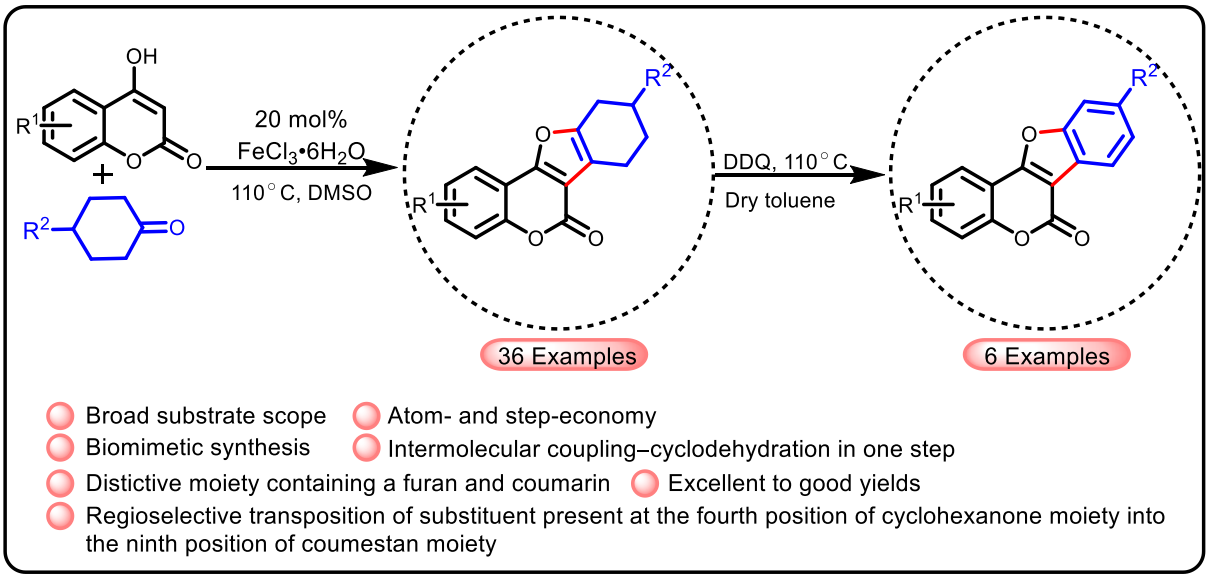

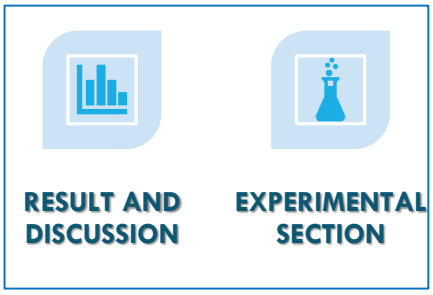

Results and Discussion

In Chapter I of Part B, the importance of coumestan and their reported methods have been thoroughly discussed. This Section of the chapter describes the biomimetic synthesis of substituted tetrahydro coumestan derivatives from 4-hydroxycoumarins and cyclohexanone derivatives using 20 mol% $FeCl_3$•$6H_2O$ catalysts in DMSO as a solvent at 110 ^oC as shown in Scheme 21. Further, coumestan derivatives (**9**) were synthesized from the corresponding tetrahydro coumestan derivatives by dehydrogenation with DDQ in dry toluene at 110 ^oC. The advantages of the present method are mild reaction conditions, easy to handle, readily available starting materials, non-requirement of dry solvents and additives, no need for inert atmospheric reaction conditions, high atom economy, broad substrate scope, and good to excellent yields. Moreover, by this strategy synthesis of naturally occurring coumestan, coumestrol dimethyl ether, and 4-*O*-Methyl coumestrol validated the two-step synthetic route.

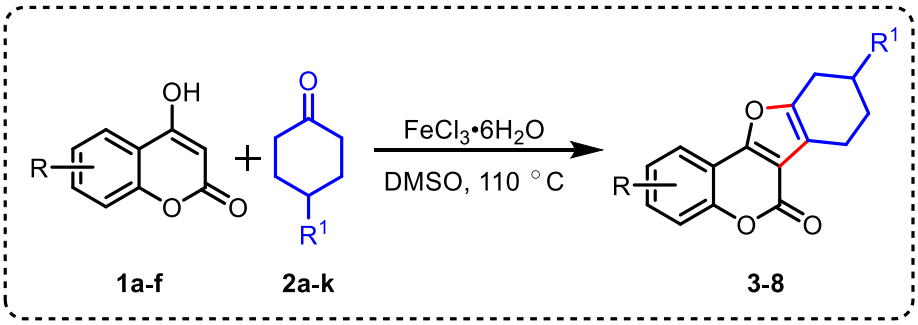

Scheme 21. Synthetic method for the synthesis of tetrahydro coumestan.

To determine the optimized reaction conditions for synthesizing tetrahydro coumestan derivative 4- hydroxycoumarin **1a** and 4-methylcyclohexanone **2a** were chosen as a model substrate. Numerous reactions were carried out with 1 mmol of 4-hydroxycoumarin **1a** and 4-methylcyclohexanone **2a**, and their results are summarized in Table 6. In addition, similar reactions are also scrutinized with other catalysts and solvents. First, the reaction was carried out without a catalyst at room temperature to 110 °C in DMSO as a solvent (Table 6, Entry 1). The reaction did not proceed. After that, 10 mol% of $FeCl_3$•$6H_2O$ in DMSO at RT was added (Table 6, Entry 2). Unfortunately, again, the reaction did not proceed. Next, the same reaction was heated at 60 °C in a pre-heated oil bath, and the desired product **3a** was obtained in 35% yield in 12 h (Table 6, Entry 3). The product **3a** was characterized using IR, ^1H & ^{13}C NMR Spectra, and HRMS. Different temperatures were investigated to further increase the yield of the desired product, and 110 °C came out as the best reaction temperature as desired product **3a** was isolated in 65 % (Table 6, Entries 4-9). Markedly, it was observed that increasing the

temperature above 140 °C resulted in drastically lower yield as bi-products (2'-hydroxyacetophenone) were isolated. The reaction condition was consequently screened to improve the yield of the desired product further. To our delight, the yield of the desired product **3a** was significantly increased to 89% as 20 mol% of $FeCl_3$•$6H_2O$ was added at 110 °C (Table 6, Entry 10). Further, increasing the catalyst amount does not affect the yield significantly. Next, we checked the catalytic activity of other metal catalysts such as $CoCl_2$, and non-metal catalysts such as I_2 and *p*-TSA•H_2O (Table 6, Entries 12-14). Surprisingly, the reactions with non-metal catalysts such as I_2 and *p*-TSA•H_2O furnished the desired product at 69% and 72%, respectively. However, $FeCl_3$•$6H_2O$ emerged as the best catalyst because it is cheaper and provides the best yield of 89%.

Table 6. Optimization studies[a,b]

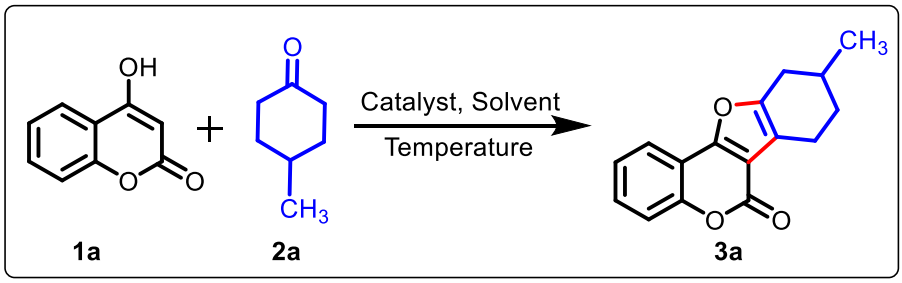

Entry	Catalyst	Mol%	Solvent	Temp (°C)	Time (h)	Yield (%)[b]
1[c]	-	-	DMSO	RT →110	24	ND
2	$FeCl_3$•$6H_2O$	10	DMSO	RT	24	ND
3	$FeCl_3$•$6H_2O$	10	DMSO	60	15	35
4	$FeCl_3$•$6H_2O$	10	DMSO	70	15	42
5	$FeCl_3$•$6H_2O$	10	DMSO	80	15	51
6	$FeCl_3$•$6H_2O$	10	DMSO	90	12	56
7	$FeCl_3$•$6H_2O$	10	DMSO	100	10	62
8	$FeCl_3$•$6H_2O$	10	DMSO	110	10	66
9	$FeCl_3$•$6H_2O$	10	DMSO	120	10	63
10	**$FeCl_3$•$6H_2O$**	**20**	**DMSO**	**110**	**8**	**89**
11	$FeCl_3$•$6H_2O$	30	DMSO	110	8	86
12	$CoCl_2$	20	DMSO	110	8	35
13	I_2	20	DMSO	110	8	69
14	*p*-TSA•H_2O	20	DMSO	110	8	72

15	$FeCl_3•6H_2O$	20	DMF	110	8	28
16	$FeCl_3•6H_2O$	20	Dioxane	110	8	49

[a]Reaction conditions: All the reactions were performed using 4-hydroxycoumarin (**1a**, 1.0 mmol), and 4-methyl cyclohexanone (**2a**, 1.0 mmol). [b]Isolated yield. [C]Reaction performed at room temperature. ND: No desired product.

The reactions were examined with other solvents, such as DMF and 1,4-dioxane, under identical reaction conditions, and the desired product **3a** was isolated at 42% and 69%, respectively (Table 6, Entries 15-16).

After getting the optimal reaction condition in hand, the reactivity and substituent effect on the cyclohexanone derivative with 4-hydroxycoumarin **1a** were investigated (Table 7). First, we scrutinized the practical utility of cyclohexanone **2b** with 4-hydroxycoumarin **1a** and isolated the desired product **3b** in 85%. Afterward, various electron-rich cyclohexanones such as 4-ethyl **2c**, 4-*iso*-propyl **2d**, 4-*tert* butyl **2e**, and **2f** were examined with 4-hydroxycoumarin **1a** to afford the desired tetrahydro coumestan scaffolds **3c**, **3d**, **3e**, and **3f** in 86%, 80%, 92%, and 82%, respectively, in good yields.

Table 7 Substrate scope with different types of substituted cyclohexanone.[a,b]

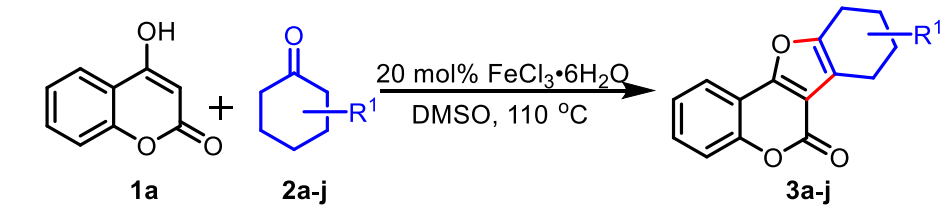

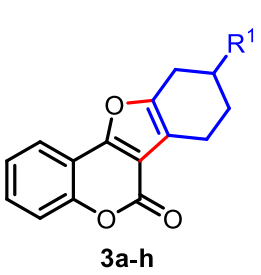

3a, R^1 = Me, 8.0 h, 89%
3b, R^1 = H, 8.0 h, 85%
3c, R^1 = Et, 9.5 h, 86%
3d, R^1 = ^{i}Pr, 7.0 h, 80%
3e, R^1 = ^{t}Bu, 8.5 h, 92%
3f, R^1 = OMe, 8.5 h, 82%
3g, R^1 = CO_2Et, 8.5 h, 78%
3h, R^1 = Ph, 8.5 h, 81%

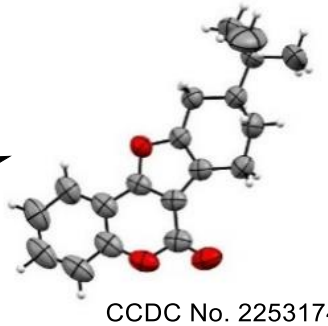

CCDC No. 2253174

[a]Reaction conditions: All the reactions were performed using 4-hydroxycoumarin (**1a**, 1.0 mmol) and substituted cyclohexanone (**2a-h**, 1.0 mmol) $FeCl_3•6H_2O$ in 2 mL DMSO at 110 °C. [b]Isolated yield.

The single XRD structure of compound **3e** was further ascertained that the substituent *tert*-butyl group is located at the 9th position of tetrahydro coumestan backbone, coming from the 4th position of cyclohexanone scaffolds. Likewise, the cyclohexanone derivatives having electron-withdrawing groups, such as CO_2Et (**2g**) and 4-phenyl cyclohexanone (**2h**), also

reacted very well to provide the desired product **3g** and **3h** in 78% and 81%, respectively. To determine the practicability and generality of our synthetic strategy, various substituted 4-hydroxy coumarins were scrutinized with a different type of 4-substituted cyclohexanones to further evaluate the efficacy, as shown in Table 8.

Table 8. Substrate scope with different types of substituted cyclohexanones.[a,b]

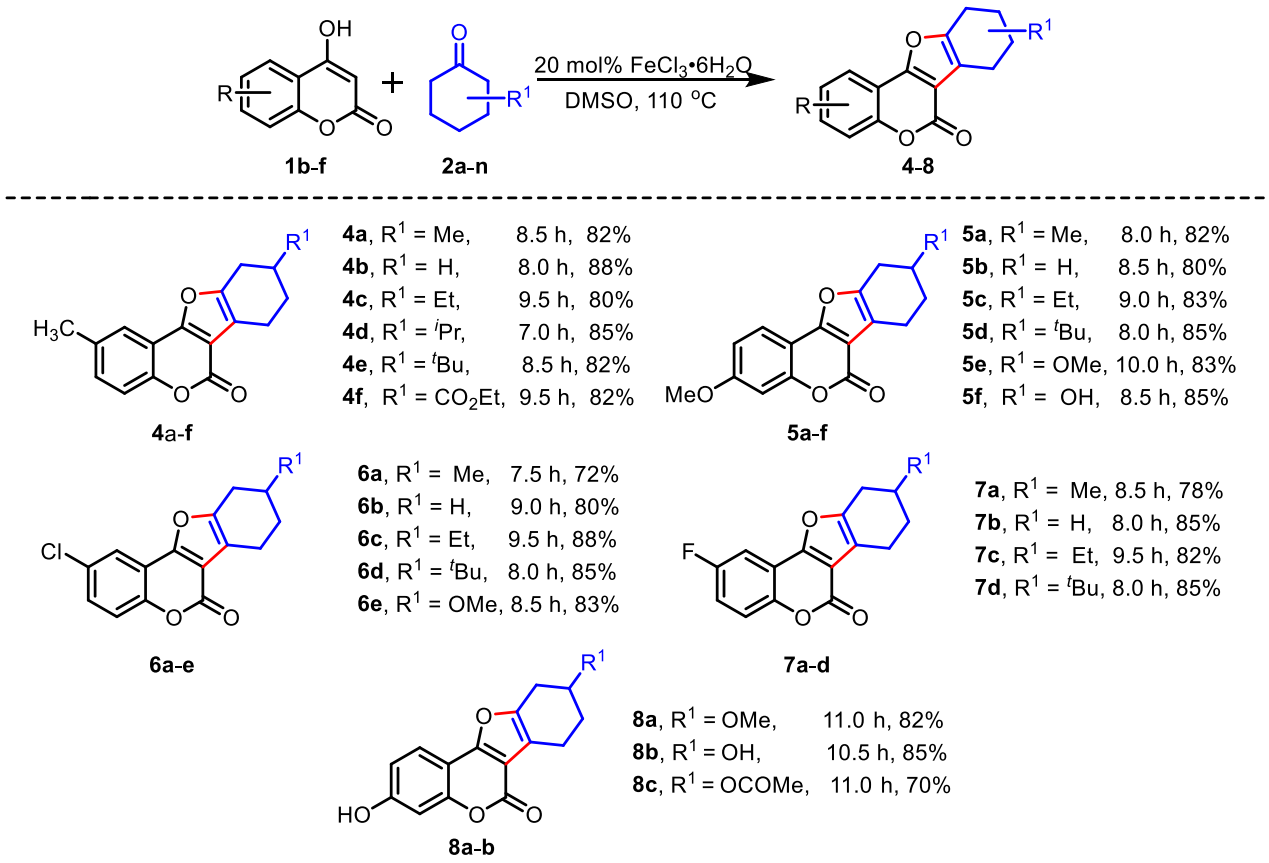

[a]Reaction conditions: All the reactions were performed using 4-hydroxycoumarin (**1b-f**, 1.0 mmol) and substituted cyclohexanone (**2a-n**, 1.0 mmol) in 2 mL DMSO at 110 °C. [b]Isolated yield.

Interestingly, both electron-donating, namely 6-methyl-4-hydroxycoumarin **1b**, 7-methoxy-4-hydroxycoumarin **1c,** and electron-withdrawing such as 6-chloro-4-hydroxycoumarin **1d,** and 6-fluoro-4hydroxycoumarin **1e** also provide the corresponding desired products **4-7** in good to excellent yields (88%-72%), as shown in Table 8.

To verify the reaction on a gram scale, the reaction was carried out with 4-hydroxycoumarin, **1a** (1.0 g, 6.17 mmol) and 4-methyl cyclohexanone **2a** (0.691 g, 6.17 mmol) in the presence of 20 mol% $FeCl_3$•$6H_2O$ (0.333 g) at 110 °C, the desired product **3a** was isolated in 1.410 g (90%) yield.

Motivated by these successful results, we put forward our efforts to synthesize the precursors of naturally occurring 4'-*O*-methyl coumestrol (**III**) and coumestrol (**II**) derivatives. Considering this goal, the reaction was examined with 4,7-dihydroxycoumarin **1f** and 4-methoxy-cyclohexanone **2f** under identical conditions, and the desired product **8a** was obtained with an 82 % yield. Similarly, the reaction was executed with 4,7-dihydroxycoumarin and 4-hydroxy cyclohexanone **2m**. The desired product **8b** was isolated in 85% yield. From all these successful results, we conclude that the substituents have no electronic and steric effects on the reactivity of different cyclohexanone with various 4-hydroxycoumarins. Indeed, the scope concerning cyclohexanone was found to be excellent.

Table 9. Substrates scope. [a,b]

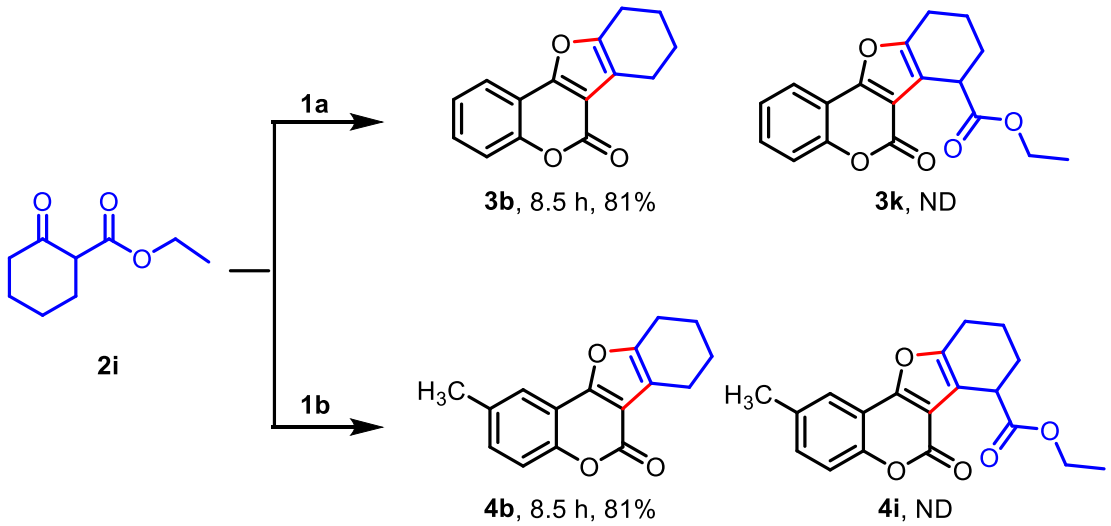

[a]Reaction conditions: All the reactions were performed using 4-hydroxycoumarin (**1a-b**, 1.0 mmol) and substituted cyclohexanone (**2i**, 1.0 mmol) in 2 mL DMSO at 110 °C. [b]Isolated yield. ND: No desired product.

Notably, it was observed while carrying out the reaction of ethyl-2-oxocyclohexanecarboxylate **2i** with 4-hydroxycoumarin **1a** and 6-methyl-4-hydroxycoumarin **1b**, the cyclized products **3b** and **4b** were obtained with the elimination of the ester group by hydrolysis followed by decarboxylation, instead of the expected products **3k** and **4i**, respectively as depicted in Table 9.

Furthermore, 3-methyl cyclohexanone **2j** was scrutinized with **1a** and **1b** under similar reaction conditions; the desired products **3i** and **4g** were isolated in 83% and 80% yield, respectively. As expected the substituent at the 3rd position of cyclohexanone was transposed at the 10th of the tetrahydro coumestan scaffold.

Likewise, polycyclic cyclohexanone, such as β-tetralone **2k** examined with 4-hydroxy coumarin **1a** and 6-methyl-4-hydroxy coumarin **1b**, also provide the corresponding product **3j** and **4h** in 72% and 82% yield under similar reaction conditions as shown in Table 10. Unfortunately, it is observed that the reaction did not give the product when the reaction was performed with 2-methyl cyclohexanone **2l** and **1a** under similar reaction conditions.

Table 10. Substrate scope [a,b]

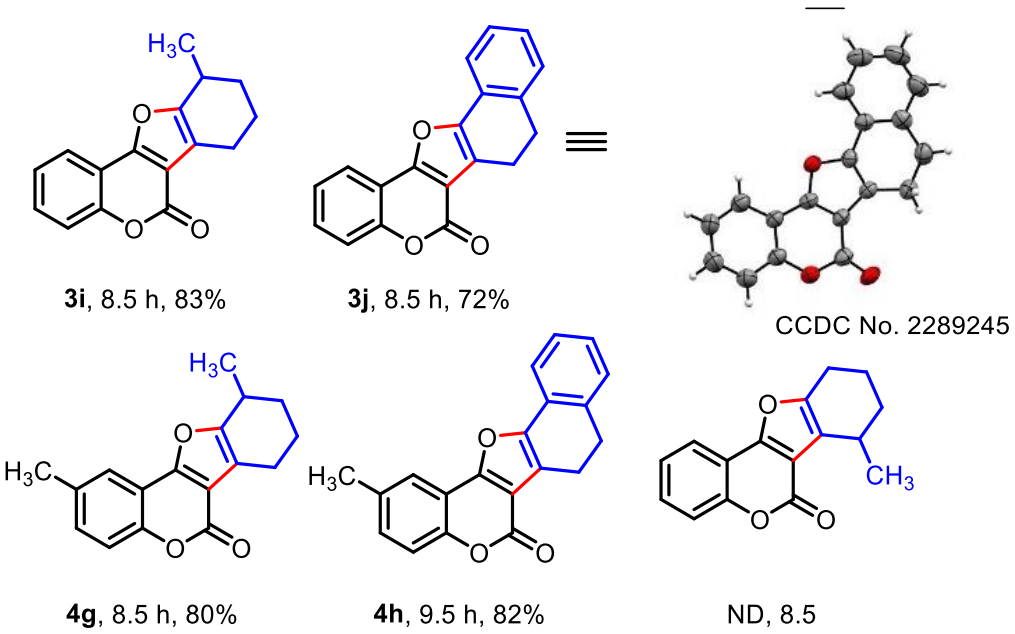

[a]Reaction conditions: All the reactions were performed using 4-hydroxycoumarin (**1a-b**, 1.0 mmol) and substituted cyclohexanone (**2j-l**, 1.0 mmol) in 2 mL DMSO at 110 °C. [b]Isolated yield. ND: No desired product.

After synthesizing different 9 and 10 substituted tetrahydro coumestan derivatives, we paid our attention to accomplishing the synthesis of naturally occurring coumestan (**I**), coumestrol dimethyl ether (**II**), 4-*O*-methyl coumestrol (**III**) and coumestrol (**IV**), respectively. The corresponding tetrahydro coumestan derivatives **3b**, **5e**, and **8a** were aromatized using DDQ in dry toluene under reflux conditions to furnish coumestan (**9a=I**), coumestrol dimethyl ether (**9b=II**), and 4-*O*-methyl coumestrol (**9e=III**) in 85%, 82% and 72% yields, respectively. ^{1}H NMR and ^{13}C NMR Spectral data of compounds **9a**, **9b,** and **9e** were compared with the earlier reported data. In addition, we have achieved the formal synthesis of coumestrol (**9c=IV**) since it is already known[6d] that the compound **9c** can be converted into coumestrol **9b** after the demethylation using BBr_3. Next, we aim to synthesize coumestrol (**9c=IV**) without a protection approach from the corresponding tetrahydro coumestan derivative **8b**. The dehydrogenation reactions were examined under different conditions such as by employing DDQ in dry toluene and Pd\C in diphenyl ether. Unfortunately, we did not get the expected naturally occurring

coumestrol **9c**; instead, we isolated the product **9d**, obtained after eliminating the OH group from the 9th position.

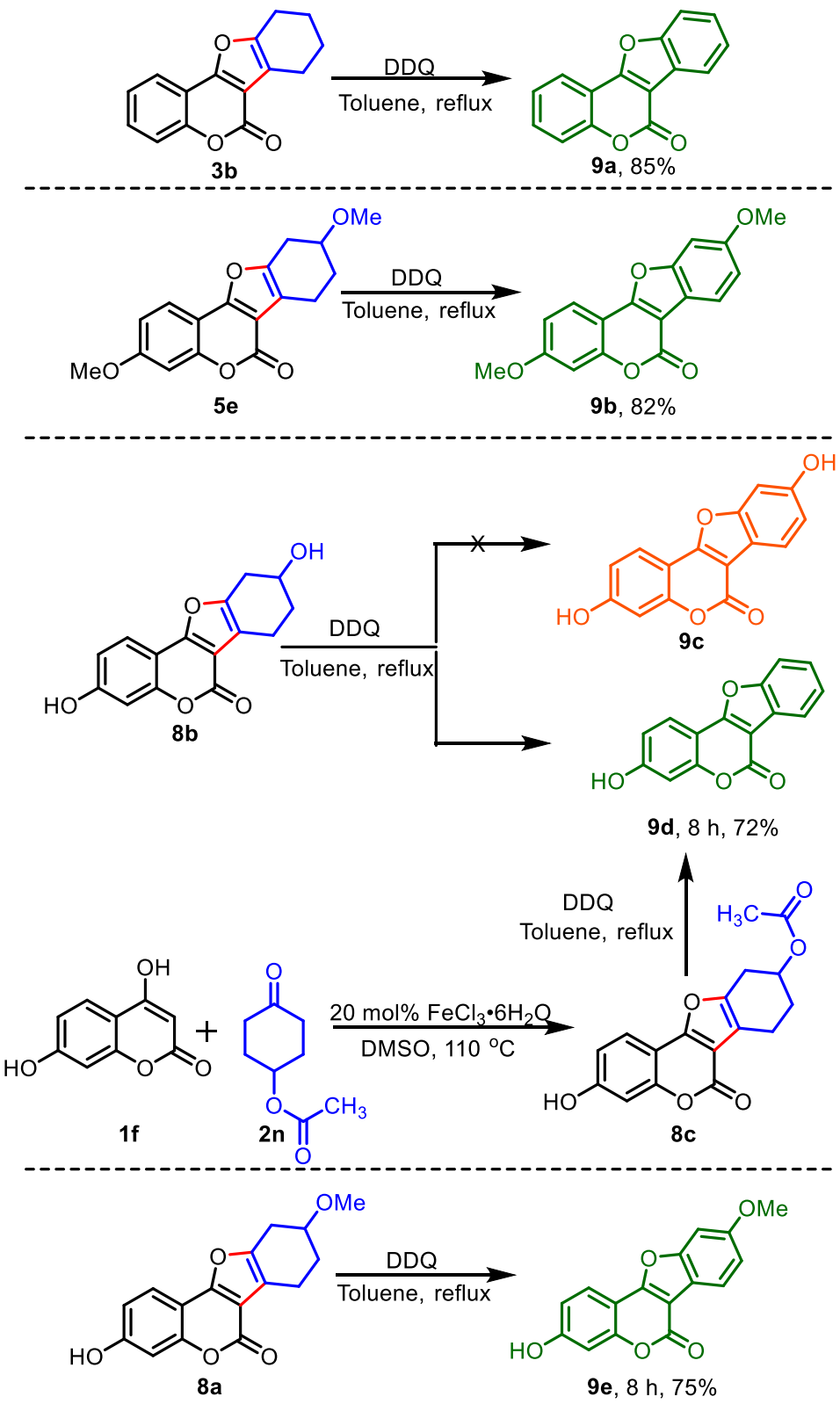

Scheme 22. Strategy to synthesize coumestan **9a**, coumestrol dimethyl ether **9b**, coumestrol **9c**, and 4-*O*-methyl coumestrol **9e**.

Therefore, we thought it might be achievable to synthesize coumestrol by protecting the OH group as acetate. With this goal in mind, 4-hydroxy cyclohexanone **2m** was converted into 4-oxo cyclohexyl acetate **2n,** and its tetrahydro analogue **8c** was prepared by following the identical reaction conditions. Unfortunately, when compound **8c** was tried for aromatization, it again provided compound **9d** after the elimination of the acetate group as depicted in scheme 22.

However, to further check the applicability, new coumestans **9f** and **9g** were synthesized by aromatization from the corresponding tetrahydro coumestan derivatives, as demonstrated in Scheme 23.

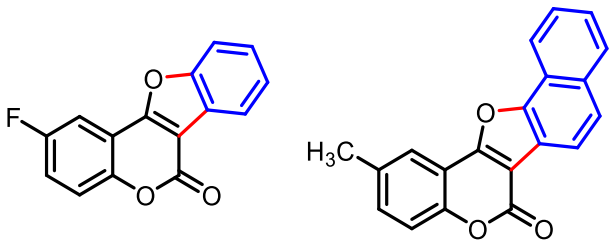

9f, 9.5 h, 81% **9g**, 6.5 h, 82%

Scheme 23. Novel analogue of coumestan derivatives.

Based on the experimental results and from the previous literature reports, we proposed the probable mechanism for the formation of tetrahydro coumestan derivatives as shown in Scheme 24. It is reported in the literature that $FeCl_3$•$6H_2O$ can undergo a disproportionate reaction to give reactive Lewis acid species $[FeCl_2]^+$ and $[FeCl_4]^-$ in polar solvents such as DMSO.[6b,e] First, cyclohexanone derivatives **2** react with the reactive Lewis acid intermediate $[FeCl_2]^+$ to increase the electrophilicity of the cyclohexanone, and subsequently, it reacts with 4-hydroxycoumarin **1** to give the intermediate [**A**]. Next, the intermediate [**A**] undergoes enolization to provide the intermediate [**B**]. As expected, the Knoevenagel intermediate [**A'**] did not form during the reaction. After that, the chloride anion (Cl^-) from the ion-pair intermediate $[FeCl_4]^-$assists in the breaking of the Fe–O bond to give the intermediate [**C**], and parallelly, the H ion protonates OH. Next, water is eliminated from the intermediate [**C'**] to provide the intermediate [**D**]. Again, $[FeCl_2]^+$ activates the double bond of intermediate [**D**] that facilitates the attack of a lone pair of OH groups to provide the next cyclized intermediate [**E**]. Like the previous step, the chloride ion (Cl^-) again assists the cleavage of the Fe–O bond to form the intermediate [**F**]. At last, the intermediate [**F**] undergoes oxidation by $FeCl_3$ to give the desired products (**3-8**). To ascertain the oxidation of the intermediate [**F**] by $FeCl_3$, we performed a reaction under inert atmospheric conditions with 4-hydroxycoumarin **1a** and

cyclohexanone **2b** in the presence of 20 mol% $FeCl_3 \cdot 6H_2O$ and the desired product **3b** obtained an 80% yield.

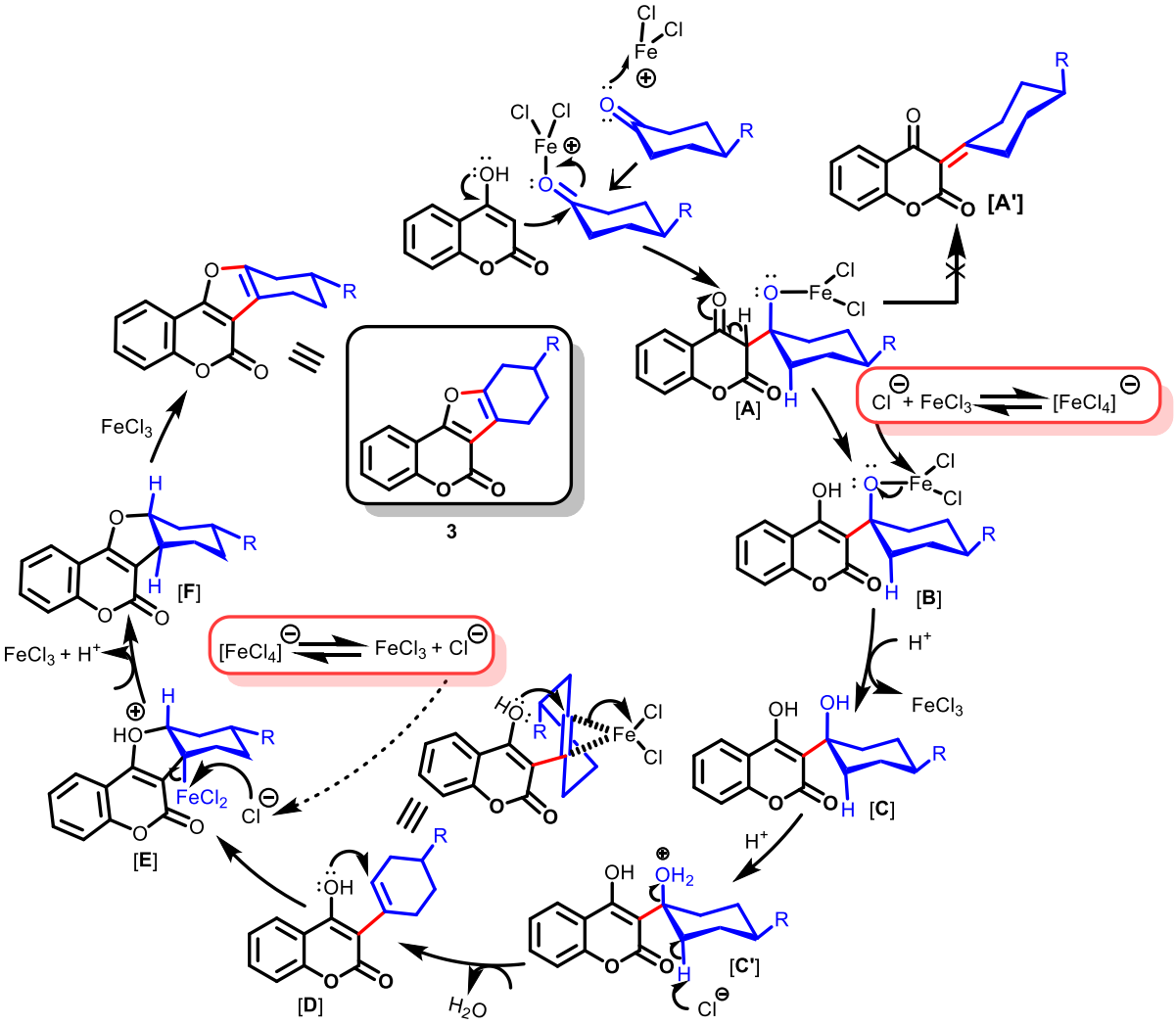

Scheme 24. A plausible mechanism for the formation of tetrahydro coumestan scaffolds.

Conclusions

In summary, we developed a simple, reliable, efficient, and straightforward biomimetic synthetic route for synthesizing 9-substituted tetrahydro coumestan derivatives from readily available 4-hydroxycoumarin and cyclohexanone derivatives in a step and atom economic manner. The novel strategy represents a high atom-economic, easy handling, good yield, broad substrate scope, and excellent functional group tolerance. Moreover, these derivatives can be converted into different coumestan derivatives by aromatization. Our approach also accomplished both naturally occurring coumestan, coumestrol dimethyl ether, and 4-*O*-Methyl coumestrol. The manipulation of various alkyl groups present at the 9th position in the ring can

be converted to novel coumestan derivatives, and by applying this method many more (Lucernol, and psoralidin) coumestan derivatives can be synthesized.

Experimental Section

General Procedure for the Synthesis of Tetrahydro Coumestan Derivatives (3)

In a 25 mL round-bottomed flask, a mixture of 4-hydroxycoumarin derivative (1, 1.0 mmol) and substituted cyclohexanone (2, 1.0 mmol) were taken in 2 mL of DMSO. Then, the catalyst ferric chloride $FeCl_3$•$6H_2O$ (54 mg, 0.020 mmol) was added to the reaction mixture, and the reaction flask was placed in a pre-heated oil bath at 110 ^oC with constant stirring. The progress of the reaction was monitored by checking TLC from time to time. After the completion of the reaction, it was brought to room temperature, and the resulting mixture was diluted with 10 mL DCM. The organic layer was washed with brine solution (5 mL x 2). After that, the organic extract was dried over anhydrous sodium sulfate, and the solvent was removed in a rotary evaporator. Finally, the crude residue was purified through a silica gel (60-120 mesh) to obtain the pure product. The desired product was eluted with ethyl acetate and hexane mixture (5:95) except the product **8**.

General Procedure for the Synthesis of Coumestan Analogue (9)

In a 25 ml round-bottomed flask, a mixture of tetrahydro coumestan (**3**, 1.0 mmol) and DDQ (2.0 mmol) were dissolved in 2 mL of dry toluene, and the reaction flask was placed in a pre-heated oil bath at 110 ^oC with constant stirring under an inert atmosphere. The progress of the reaction was monitored by checking TLC from time to time. After the completion of the reaction, it was brought to room temperature, and the resulting mixture was diluted with 10 mL of ethyl acetate. The organic layer was washed with brine solution (5 mL x 2). After that, dried with anhydrous sodium sulfate, the solvent was removed in a rotary evaporator, and the crude residue was passed through a silica gel (60-120 mesh) column to get the pure product.

9-Methyl-7,8,9,10-tetrahydro-6*H*-benzofuro[3,2-*c*]chromen-6-one (3a) Yield 89% (226.30 mg) Rose pink solid, mp 168–169 °C. ^{1}H NMR (600 MHz, $CDCl_3$) δ 7.82 (dd, *J* = 7.8, 1.4 Hz, 1H), 7.45 (td, *J* = 7.8, 7.2, 1.5 Hz, 1H), 7.42 – 7.40 (m, 1H), 7.32 – 7.30 (m, 1H), 2.93 – 2.84 (m, 2H), 2.72 (ddt, *J* = 13.9, 8.5, 3.0 Hz, 1H), 2.36 (ddt, *J* = 16.6, 9.3, 2.4 Hz, 1H), 2.08 – 2.04 (m, 1H), 1.95 – 1.91 (m, 1H), 1.48 – 1.44 (m, 1H), 1.15 (d, *J* = 6.7 Hz, 3H); ^{13}C NMR (150 MHz, $CDCl_3$) δ 158.9, 156.3, 154.3, 152.4, 129.9, 124.4, 120.6, 117.3, 116.5, 113.5, 110.5, 31.3, 30.7, 29.4, 21.4, 20.4; IR (KBr)ν_{max}/cm^{-1} 3027 (C–H), 1655 (C=O), 1372 (C–O); HRMS (ESI) Calcd For $C_{16}H_{15}O_3$ 255.1016 ($M+H^+$); Found 255.1010.

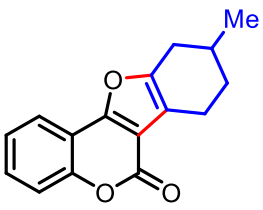

7,8,9,10-Tetrahydro-6*H*-benzofuro[3,2-*c*]chromen-6-one (3b) Yield 85% (204.21 mg)

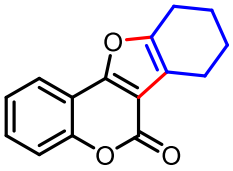

White solid, mp 190–191 °C (lit. mp. 190-191 °C)[6e]. ^{1}H NMR (600 MHz, $CDCl_3$) δ 7.81 (d, *J* = 7.6 Hz, 1H), 7.45 (t, *J* = 7.7 Hz, 1H), 7.41 (d, *J* = 8.2 Hz, 1H), 7.31 (t, *J* = 7.4 Hz, 1H), 2.79 (t, *J* = 6.0 Hz, 2H), 2.76 (t, *J* = 6.2 Hz, 2H), 1.93 (dd, *J* = 7.6, 4.0 Hz, 2H), 1.83 (dd, *J* = 7.5, 4.0 Hz, 2H); ^{13}C NMR (150 MHz, $CDCl_3$) δ 158.9, 156.1, 154.4, 152.3, 129.9, 124.4, 120.5, 117.3, 116.9, 113.4, 110.5, 23.3, 22.6, 22.4, 21.1; IR (KBr)ν_{max}/cm^{-1} 3020 (C–H), 1661 (C=O), 1301 (C–O); HRMS (ESI) Calcd For $C_{15}H_{13}O_3$ 241.0860 ($M+H^+$); Found 241.0860.

9-Ethyl-7,8,9,10-tetrahydro-6*H*-benzofuro[3,2-*c*]chromen-6-one (3c) Yield 86% (230.74

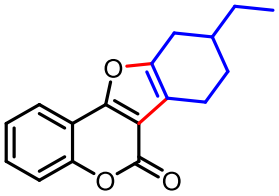

mg) White solid, mp 138–139 °C. ^{1}H NMR (600 MHz, $CDCl_3$) δ 7.82 (d, *J* = 7.8 Hz, 1H), 7.47 – 7.41 (m, 2H), 7.31 (t, *J* = 7.4 Hz, 1H), 2.93 – 2.87 (m, 2H), 2.69 (t, *J* = 13.4 Hz, 1H), 2.37 (dd, *J* = 16.4, 9.5 Hz, 1H), 1.99 (d, *J* = 13.2 Hz, 1H), 1.83 – 1.82 (m, 1H), 1.52 (dd, *J* = 14.1, 7.1 Hz, 1H), 1.45 – 1.43 (m, 2H), 1.01 (t, *J* = 7.4 Hz, 3H); ^{13}C NMR (150 MHz, $CDCl_3$) δ 159.0, 156.3, 154.5, 152.3, 129.9, 124.4, 120.5, 117.3, 116.8, 113.5, 110.5, 36.2, 29.2, 28.7, 28.6, 20.5, 11.7; IR (KBr)ν_{max}/cm^{-1} 3021 (C–H), 1650 (C=O), 1290 (C–O); HRMS (ESI) Calcd For $C_{17}H_{17}O_3$ 269.1173 ($M+H^+$); Found 269.1169.

9-*Iso*propyl-7,8,9,10-tetrahydro-6*H*-benzofuro[3,2-*c*]chromen-6-one (3d) Yield 80%

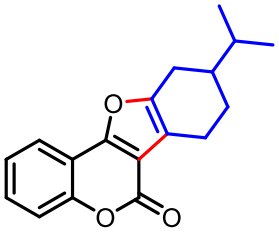

(225.86 mg) light Yellow liquid. ^{1}H NMR (600 MHz, $CDCl_3$) δ 7.69 – 7.67 (m, 1H), 7.38 – 7.36 (m, 1H), 7.31 (d, *J* = 8.3 Hz, 1H), 7.22 (t, *J* = 7.9 Hz, 1H), 2.88 – 2.84 (m, 1H), 2.70 (dd, *J* = 16.4, 4.4 Hz, 1H), 2.58 – 2.53 (m, 1H), 2.40 – 2.35 (m, 1H), 1.95 – 1.92 (m, 1H), 1.63 (dq, *J* = 12.6, 6.3 Hz, 2H), 1.37 (td, *J* = 12.7, 12.1, 5.2 Hz, 1H), 0.95 – 0.93 (m, 6H); ^{13}C NMR (150 MHz, $CDCl_3$) δ 158.6, 156.1, 154.7, 152.2, 129.7, 124.3, 120.4, 117.1, 116.6, 113.2, 110.2, 40.9, 32.0, 26.4, 26.3, 20.8, 20.2, 19.5; IR (KBr)ν_{max}/cm^{-1} 3025 (C–H), 1656 (C=O), 1300 (C–O); HRMS (ESI) Calcd For $C_{18}H_{19}O_3$ 283.1329 ($M+H^+$); Found 283.1321.

9-(*tert*-Butyl)-7,8,9,10-tetrahydro-6*H*-benzofuro[3,2-*c*]chromen-6-one (3e) Yield 92%

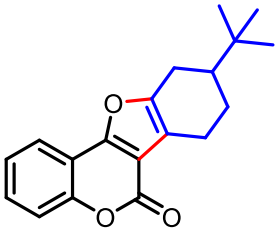

(272.65 mg) White solid, mp 141–142 °C. ^{1}H NMR (600 MHz, $CDCl_3$) δ 7.79 (d, *J* = 7.7 Hz, 1H), 7.45 (t, *J* = 7.7 Hz, 1H), 7.40 (d, *J* = 8.2 Hz, 1H), 7.30 (t, *J* = 7.4 Hz, 1H), 2.98 (dd, *J* = 16.5, 4.3 Hz, 1H), 2.81 (dd, *J* = 16.3, 4.6 Hz, 1H), 2.60 – 2.58 (m, 1H), 2.49 (t, *J* = 13.8 Hz, 1H), 2.10 – 2.07 (m, 1H), 1.64 – 1.61 (m, 1H), 1.35 (qd, *J* = 12.4, 5.4 Hz, 1H), 0.99 (s, 9H); ^{13}C NMR (150 MHz, $CDCl_3$) δ 158.9, 156.4, 155.3, 152.3, 129.8, 124.4, 120.5, 117.3, 116.7, 113.4, 110.3, 45.1, 32.6, 27.4, 25.0, 24.2, 21.4; IR (KBr)ν_{max}/cm^{-1} 3031 (C–H), 1649 (C=O), 1291 (C–O); HRMS (ESI) Calcd For $C_{19}H_{21}O_3$ 297.1486 ($M+H^+$); Found 297.1486.

9-Methoxy-7,8,9,10-tetrahydro-6*H*-benzofuro[3,2-*c*]chromen-6-one (3f) Yield 82%

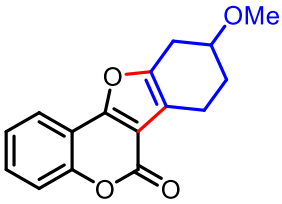

(221.62 mg) White solid, mp 135–136 °C. ^{1}H NMR (600 MHz, $CDCl_3$) δ 7.81 (dd, *J* = 7.8, 1.3 Hz, 1H), 7.46 (td, *J* = 7.9, 7.3, 1.5 Hz, 1H), 7.41 (d, *J* = 7.8 Hz, 1H), 7.33 – 7.30 (m, 1H), 3.84 (p, *J* = 5.5 Hz, 1H), 3.45 (s, 3H), 3.10 (dd, *J* = 16.5, 4.8 Hz, 1H), 2.94 – 2.90 (m, 1H), 2.85 – 2.80 (m, 2H), 2.01 (dt, *J* = 9.6, 4.7 Hz, 2H); ^{13}C NMR (150 MHz, $CDCl_3$) δ 158.8, 156.9, 152.4, 151.8, 130.1, 124.5, 120.6, 117.3, 116.5, 113.3, 110.3, 75.3, 56.5, 29.7, 26.9, 17.7; IR (KBr)ν_{max}/cm^{-1} 3025 (C–H), 1660 (C=O), 1300 (C–O); HRMS (ESI) Calcd For $C_{16}H_{15}O_4$ 271.0965 ($M+H^+$); Found 271.0982.

Ethyl 6-oxo-7,8,9,10-tetrahydro-6*H*-benzofuro[3,2-*c*]chromene-9-carboxylate (3g) Yield

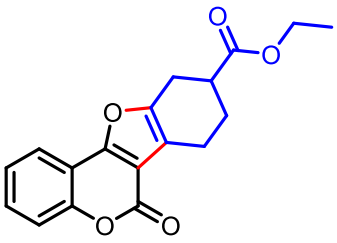

(243.60 mg) White solid, mp 110–111 °C. ^{1}H NMR (600 MHz, $CDCl_3$) δ 7.83 (dd, *J* = 7.8, 1.3 Hz, 1H), 7.49 – 7.46 (m, 1H), 7.43 – 7.41 (m, 1H), 7.34 – 7.31 (m, 1H), 4.21 (qd, *J* = 7.1, 3.6 Hz, 2H), 3.08 – 3.03 (m, 2H), 2.94 (ddd, *J* = 27.3, 14.0, 7.4 Hz, 2H), 2.82 – 2.77 (m, 1H), 2.26 (dq, *J* = 13.0, 4.8 Hz, 1H), 1.98 – 1.92 (m, 1H), 1.30 (t, *J* = 7.1 Hz, 3H); ^{13}C NMR (150 MHz, $CDCl_3$) δ 174.1, 158.7, 156.7, 152.5, 152.5, 130.2, 124.5, 120.7, 117.4, 116.4, 113.3, 110.3, 61.1, 39.6, 25.6, 25.4, 20.0, 14.3; IR (KBr)ν_{max}/cm^{-1} 3022 (C–H), 1660 (C=O), 1305 (C–O); HRMS (ESI) Calcd For $C_{18}H_{17}O_5$ 313.1071 ($M+H^+$); Found 313.1090.

9-Phenyl-7,8,9,10-tetrahydro-6*H*-benzofuro[3,2-*c*]chromen-6-one (3h) Yield 81% (256.24 mg) Whitish yellow solid, mp 195–196 °C. ^{1}H NMR (500 MHz, $CDCl_3$) δ 7.74 (d, *J* = 7.7 Hz, 1H), 7.41 – 7.37 (m, 1H), 7.34 (d, *J* = 8.3 Hz, 1H), 7.28 – 7.17 (m, 6H), 3.08 – 2.91 (m, 3H), 2.84 – 2.75 (m, 2H), 2.12 – 2.09 (m, 1H), 1.89 (dt, *J* = 12.3, 5.3 Hz, 1H); ^{13}C NMR (125 MHz, $CDCl_3$) δ 157.8, 155.5, 152.9, 151.4, 143.9, 129.0, 127.8, 125.9, 125.8, 123.4, 119.6, 116.3, 115.7, 112.3, 109.4, 39.5, 30.0, 29.1, 19.9; IR (KBr)ν_{max}/cm^{-1} 3020 (C–H), 1662 (C=O), 1295 (C–O); HRMS (ESI) Calcd For $C_{21}H_{17}O_3$ 317.1173 ($M+H^+$); Found 317.1145.

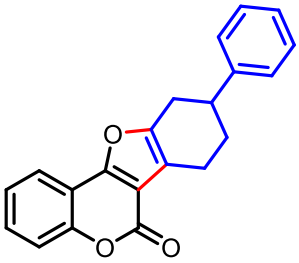

10-Methyl-7,8,9,10-tetrahydro-6*H*-benzofuro[3,2-*c*]chromen-6-one (3i) Yield 83% (211.05 mg) White solid, mp 160–161 °C. ^{1}H NMR (600 MHz, $CDCl_3$) δ 7.82 (dd, *J* = 7.8, 1.3 Hz, 1H), 7.46 (td, *J* = 7.8, 7.2, 1.5 Hz, 1H), 7.42 – 7.41 (m, 1H), 7.32 – 7.30 (m, 1H), 2.98 (dd, *J* = 16.5, 4.9 Hz, 1H), 2.83 – 2.77 (m, 2H), 2.35 (ddt, *J* = 16.4, 9.4, 2.5 Hz, 1H), 1.97 (dt, *J* = 33.5, 9.1 Hz, 2H), 1.62 – 1.58 (m, 1H), 1.12 (d, *J* = 6.7 Hz, 3H); ^{13}C NMR (150 MHz, $CDCl_3$) δ 158.9, 156.4, 154.2, 152.4, 129.9, 124.4, 120.5, 117.3, 116.7, 113.5, 110.5, 30.7, 29.1, 29.0, 22.8, 21.1; IR (KBr)ν_{max}/cm^{-1} 3031 (C–H), 1660 (C=O), 1372 (C–O); HRMS (ESI) Calcd For $C_{16}H_{15}O_3$ 255.1016 ($M+H^+$); Found 255.1032.

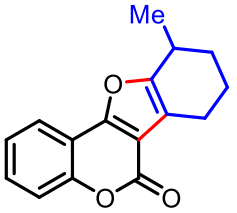

7,8-Dihydro-6*H*-naphtho[2',1':4,5]furo[3,2-*c*]chromen-6-one (3j) Yield 72% (207.57 mg) White solid, mp 205–206 °C. ^{1}H NMR (600 MHz, $CDCl_3$) δ 7.95 (d, *J* = 7.8 Hz, 1H), 7.63 (d, *J* = 7.5 Hz, 1H), 7.50 (td, *J* = 7.9, 7.3, 1.4 Hz, 1H), 7.44 (d, *J* = 8.3 Hz, 1H), 7.37 (t, *J* = 7.5 Hz, 1H), 7.31 (t, *J* = 7.2 Hz, 1H), 7.26 (d, *J* = 5.3 Hz, 1H), 7.25 – 7.22 (m, 1H), 3.14 (dd, *J* = 8.7, 5.6 Hz, 2H), 3.09 (dd, *J* = 11.8, 4.7 Hz, 2H); ^{13}C NMR (150 MHz, $CDCl_3$) δ 158.7, 156.8, 152.6, 152.6, 135.5, 130.4, 128.4, 128.3, 127.1, 126.6, 124.6, 120.8, 120.1, 117.8, 117.4, 113.3, 110.9, 28.5, 19.6; IR (KBr)ν_{max}/cm^{-1} 3021 (C–H), 1622 (C=O), 1311 (C–O); HRMS (ESI) Calcd For $C_{19}H_{13}O_3$ 289.0860 ($M+H^+$); Found 289.0886.

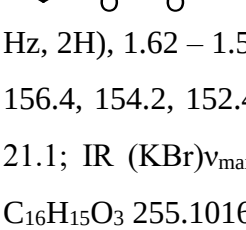

2,9-Dimethyl-7,8,9,10-tetrahydro-6*H*-benzofuro[3,2-*c*]chromen-6-one (4a) Yield 82% (220.01 mg) White solid, mp 171–172 °C. ^{1}H NMR (500 MHz, $CDCl_3$) δ 7.60 (s, 1H), 7.29 (d, *J* = 8.4 Hz, 1H), 7.24 (s, 1H), 2.92 – 2.82 (m, 2H), 2.72 – 2.69 (m, 1H), 2.43 (s, 3H), 2.35 (dd, *J* = 16.0, 9.4 Hz, 1H), 2.04 (s, 1H), 1.92 (d, *J* = 12.4 Hz, 1H), 1.45 (ddt,

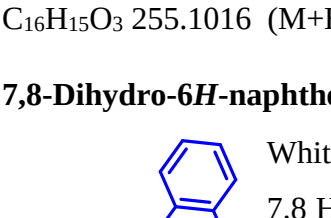

J = 15.4, 10.9, 5.7 Hz, 1H), 1.14 (d, *J* = 6.6 Hz, 3H); ^{13}C NMR (100 MHz, $CDCl_3$) δ 159.1, 156.4, 154.1, 150.5, 134.2, 130.9, 120.3, 117.0, 116.5, 113.1, 110.3, 31.2, 30.7, 29.3, 21.4, 21.0, 20.4; IR (KBr)ν_{max}/cm^{-1} 3019 (C–H), 1655 (C=O), 1305 (C–O); HRMS (ESI) Calcd For $C_{17}H_{17}O_3$ 269.1173 ($M+H^+$); Found 269.1173.

2-Methyl-7,8,9,10-tetrahydro-6*H*-benzofuro[3,2-*c*]chromen-6-one (4b) Yield 88% (223.76 mg) White solid, mp 185–186 °C. ^{1}H NMR (600 MHz, $CDCl_3$) δ 7.59 (s, 1H), 7.29 (d, *J* = 8.5 Hz, 1H), 7.24 (dd, *J* = 8.5, 1.8 Hz, 1H), 2.78 (td, *J* = 6.0, 1.8 Hz, 2H), 2.74 (td, *J* = 6.2, 1.8 Hz, 2H), 2.43 (s, 3H), 1.94 – 1.90 (m, 2H), 1.82 (dp, *J* = 8.6, 2.7 Hz, 2H); ^{13}C NMR (150 MHz, $CDCl_3$) δ 159.0, 156.2, 154.2, 150.5, 134.2, 130.9, 120.3, 117.0, 116.8, 113.0, 110.4, 23.3, 22.6, 22.4, 21.1, 21.0; IR (KBr)ν_{max}/cm^{-1} 3022 (C–H), 1660 (C=O), 1301 (C–O); HRMS (ESI) Calcd For $C_{16}H_{15}O_3$ 255.1016 ($M+H^+$); Found 255.1038.

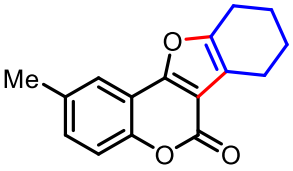

9-Ethyl-2-methyl-7,8,9,10-tetrahydro-6*H*-benzofuro[3,2-*c*]chromen-6-one (4c) Yield 80% (225.86 mg) White solid, mp 142–143 °C. ^{1}H NMR (600 MHz, $CDCl_3$) δ 7.61 (s, 1H), 7.30 (d, *J* = 8.4 Hz, 1H), 7.25 (s, 1H), 2.93 – 2.86 (m, 2H), 2.68 (d, *J* = 13.8 Hz, 1H), 2.44 (s, 3H), 2.36 (dd, *J* = 15.8, 9.5 Hz, 1H), 1.98 (d, *J* = 12.7 Hz, 1H), 1.82 (d, *J* = 4.5 Hz, 1H), 1.48 (ddd, *J* = 28.2, 14.0, 7.1 Hz, 3H), 1.01 (t, *J* = 7.4 Hz, 3H); ^{13}C NMR (150 MHz, $CDCl_3$) δ 159.2, 156.4, 154.3, 150.6, 134.2, 130.9, 120.3, 117.0, 116.8, 113.1, 110.4, 36.2, 29.2, 28.7, 28.6, 21.1, 20.5, 11.7; IR (KBr)ν_{max}/cm^{-1} 3021 (C–H), 1655 (C=O), 1292 (C–O); HRMS (ESI) Calcd For $C_{18}H_{19}O_3$ 283.1329 ($M+H^+$); Found 283.1333.

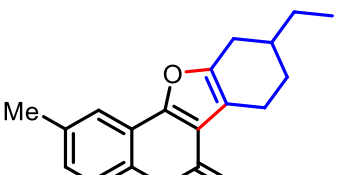

9-*Iso*propyl-2-methyl-7,8,9,10-tetrahydro-6*H*-benzofuro[3,2-*c*]chromen-6-one (4d) Yield 85% (251.90 mg) White solid, mp 135–136 °C; ^{1}H NMR (600 MHz, $CDCl_3$) δ 7.57 (s, 1H), 7.28 (d, *J* = 8.5 Hz, 1H), 7.23 (dd, *J* = 8.5, 1.7 Hz, 1H), 2.95 – 2.92 (m, 1H), 2.78 (dd, *J* = 16.3, 4.3 Hz, 1H), 2.65 – 2.59 (m, 1H), 2.48 – 2.44 (m, 1H), 2.43 (s, 3H), 2.01 – 1.98 (m, 1H), 1.72 – 1.66 (m, 2H), 1.43 (dq, *J* = 11.3, 6.1 Hz, 1H), 1.00 (dd, *J* = 10.4, 6.5 Hz, 6H); ^{13}C NMR (150 MHz, $CDCl_3$) δ 159.0, 156.4, 154.6, 150.5, 134.1, 130.8, 120.2, 117.0, 116.7, 113.1, 110.3, 41.0, 32.1, 26.5, 26.4, 21.0, 20.9, 20.2, 19.5; IR (KBr)ν_{max}/cm^{-1} 3025 (C–H), 1665 (C=O), 1301 (C–O); HRMS (ESI) Calcd For $C_{19}H_{21}O_3$ 297.1486 ($M+H^+$); Found 297.1466.

9-(*tert*-Butyl)-2-methyl-7,8,9,10-tetrahydro-6*H*-benzofuro[3,2-*c*]chromen-6-one (4e)

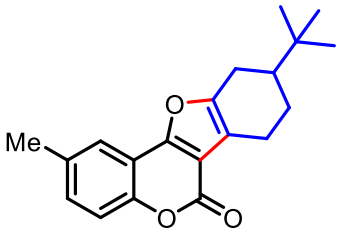

Yield 82% (254.51 mg) White solid, mp 151–153 °C. ^{1}H NMR (600 MHz, $CDCl_3$) δ 7.58 (s, 1H), 7.29 (d, *J* = 8.5 Hz, 1H), 7.24 (dd, *J* = 8.5, 1.7 Hz, 1H), 2.97 (dd, *J* = 16.5, 5.0 Hz, 1H), 2.80 (dd, *J* = 16.3, 5.1 Hz, 1H), 2.59 (dd, *J* = 16.7, 12.0 Hz, 1H), 2.48 (t, *J* = 14.7 Hz, 1H), 2.43 (s, 3H), 2.08 (dd, *J* = 13.0, 3.6 Hz, 1H), 1.64 (dd, *J* = 5.1, 2.1 Hz, 1H), 1.35 (tt, *J* = 12.4, 6.2 Hz, 1H), 0.98 (s, 9H); ^{13}C NMR (150 MHz, $CDCl_3$) δ 159.1, 156.5, 155.1, 150.6, 134.2, 130.9, 120.2, 117.0, 116.7, 113.1, 110.3, 45.1, 32.6, 27.4, 25.0, 24.2, 21.4, 21.0; IR (KBr)ν_{max}/cm^{-1} 3011 (C–H), 1650 (C=O), 1299 (C–O); HRMS (ESI) Calcd For $C_{20}H_{23}O_3$ 311.1642 ($M+H^+$); Found 311.1642.

Ethyl 2-methyl-6-oxo-7,8,9,10-tetrahydro-6*H*-benzofuro[3,2-*c*]chromene-9-carboxylate

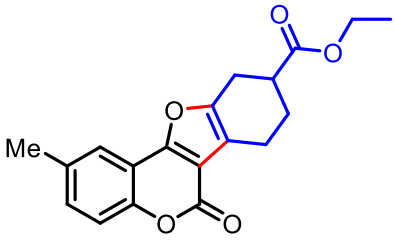

(4f) Yield 82% (267.59 mg) White solid, mp 158–159 °C. ^{1}H NMR (400 MHz, $CDCl_3$) δ 7.62 (s, 1H), 7.30 (d, *J* = 8.5 Hz, 1H), 7.28 (d, *J* = 1.7 Hz, 1H), 4.21 (qd, *J* = 7.1, 2.6 Hz, 2H), 3.04 (dd, *J* = 12.5, 3.8 Hz, 2H), 2.93 – 2.89 (m, 2H), 2.79 (ddd, *J* = 14.1, 9.0, 4.4 Hz, 1H), 2.44 (s, 3H), 2.28 – 2.23 (m, 1H), 1.99 – 1.90 (m, 1H), 1.30 (t, *J* = 7.1 Hz, 3H); ^{13}C NMR (125 MHz, $CDCl_3$) δ 174.2, 158.9, 156.8, 152.3, 150.7, 134.3, 131.2, 120.4, 117.1, 116.4, 112.9, 110.2, 61.1, 39.7, 25.5, 25.5, 21.0, 20.0, 14.3; IR (KBr)ν_{max}/cm^{-1} 3021 (C–H), 1665 (C=O), 1293 (C–O); HRMS (ESI) Calcd For $C_{19}H_{19}O_5$ 327.1227 ($M+H^+$); Found 327.1236.

2,10-Dimethyl-7,8,9,10-tetrahydro-6*H*-benzofuro[3,2-*c*]chromen-6-one (4g) Yield 80%

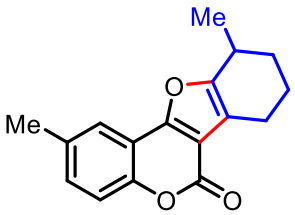

(241.64 mg) White solid, mp 143–145 °C. ^{1}H NMR (400 MHz, $CDCl_3$) δ 7.61 (d, *J* = 1.8 Hz, 1H), 7.30 (d, *J* = 8.5 Hz, 1H), 7.24 (d, *J* = 1.8 Hz, 1H), 2.97 (dd, *J* = 16.4, 4.8 Hz, 1H), 2.77 (dd, *J* = 9.3, 3.0 Hz, 2H), 2.44 (s, 3H), 2.34 (ddt, *J* = 16.5, 9.3, 2.5 Hz, 1H), 1.97 (ddd, *J* = 19.6, 13.9, 4.9 Hz, 2H), 1.63 – 1.59 (m, 1H), 1.12 (d, *J* = 6.6 Hz, 3H); ^{13}C NMR (100 MHz, $CDCl_3$) δ 159.2, 156.5, 154.0, 150.5, 134.2, 130.9, 120.3, 117.0, 116.7, 113.1, 110.4, 30.7, 29.1, 29.0, 22.8, 21.1, 21.1; IR (KBr)ν_{max}/cm^{-1} 3019 (C–H), 1650 (C=O), 1299 (C–O); HRMS (ESI) Calcd For $C_{17}H_{17}O_3$ 269.1173 ($M+H^+$); Found 269.1172.

2-Methyl-7,8-dihydro-6*H*-naphtho[2',1':4,5]furo[3,2-*c*]chromen-6-one (4h) Yield 82%

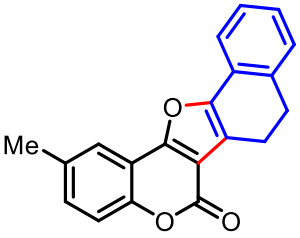

(247.90 mg) White solid, mp 161–162 °C. ^{1}H NMR (600 MHz, $CDCl_3$) δ 7.74 (s, 1H), 7.64 (d, *J* = 7.4 Hz, 1H), 7.34 – 7.29 (m, 3H), 7.27 – 7.22 (m, 2H), 3.15 – 3.12 (m, 2H), 3.08 (dd, *J* = 8.7, 5.3 Hz, 2H), 2.48 (s, 3H); ^{13}C NMR (150 MHz, $CDCl_3$) δ 158.9, 156.9, 152.5, 150.8, 135.5, 134.5, 131.4, 128.4, 128.2, 127.0, 126.7, 120.6, 120.0, 117.8, 117.2, 112.9, 110.8, 28.5, 21.1, 19.6; IR (KBr)ν_{max}/cm^{-1} 3022 (C–H), 1662 (C=O), 1291 (C–O); HRMS (ESI) Calcd For $C_{20}H_{15}O_3$ 303.1016 ($M+H^+$); Found 303.1015.

3-Methoxy-9-methyl-7,8,9,10-tetrahydro-6*H*-benzofuro[3,2-*c*]chromen-6-one (5a) Yield

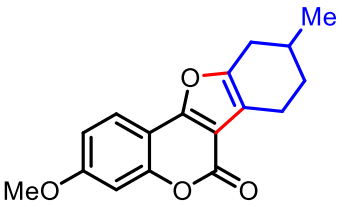

82% (233.13 mg) White solid, mp 171–172 °C. ^{1}H NMR (600 MHz, $CDCl_3$) δ 7.68 (d, *J* = 8.6 Hz, 1H), 6.90 (d, *J* = 2.4 Hz, 1H), 6.88 (dd, *J* = 8.7, 2.4 Hz, 1H), 3.86 (s, 3H), 2.89 – 2.85 (m, 1H), 2.81 (dd, *J* = 16.4, 5.2 Hz, 1H), 2.69 (dt, *J* = 11.4, 6.6 Hz, 1H), 2.35 – 2.30 (m, 1H), 2.04 – 2.00 (m, 1H), 1.91 (ddd, *J* = 13.2, 5.3, 2.7 Hz, 1H), 1.47 – 1.40 (m, 1H), 1.13 (d, *J* = 6.7 Hz, 3H); ^{13}C NMR (150 MHz, $CDCl_3$) δ 161.4, 159.1, 157.0, 154.0, 153.2, 121.5, 116.1, 112.6, 108.0, 106.9, 101.4, 55.8, 31.2, 30.7, 29.4, 21.4, 20.4; IR (KBr)ν_{max}/cm^{-1} 3021 (C–H), 1655 (C=O), 1301 (C–O); HRMS (ESI) Calcd For $C_{17}H_{17}O_4$ 285.1122 ($M+H^+$); Found 285.1122.

3-Methoxy-7,8,9,10-tetrahydro-6*H*-benzofuro[3,2-*c*]chromen-6-one (5b) Yield 80%

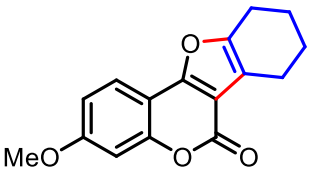

(216.22 mg) White solid, mp 160–161 °C. ^{1}H NMR (600 MHz, $CDCl_3$) δ 7.70 (d, *J* = 8.7 Hz, 1H), 6.92 (d, *J* = 2.3 Hz, 1H), 6.89 (dd, *J* = 8.7, 2.4 Hz, 1H), 3.87 (s, 3H), 2.77 (td, *J* = 6.0, 1.9 Hz, 2H), 2.73 (ddt, *J* = 6.2, 4.5, 1.9 Hz, 2H), 1.94 – 1.90 (m, 2H), 1.81 (ddt, *J* = 8.6, 6.0, 2.7 Hz, 2H); ^{13}C NMR (150 MHz, $CDCl_3$) δ 161.5, 159.2, 156.8, 154.1, 153.3, 121.5, 116.5, 112.6, 108.2, 106.9, 101.5, 55.8, 23.2, 22.6, 22.5, 21.1; IR (KBr)ν_{max}/cm^{-1} 3021 (C–H), 1620 (C=O), 1303 (C–O); HRMS (ESI) Calcd For $C_{16}H_{15}O_4$ 271.0965 ($M+H^+$); Found 271.0956.

9-Ethyl-3-methoxy-7,8,9,10-tetrahydro-6*H*-benzofuro[3,2-*c*]chromen-6-one (5c) Yield

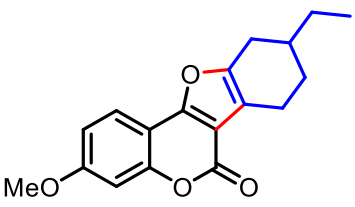

83% (247.61 mg) White solid, mp 138–139 °C. ^{1}H NMR (600 MHz, $CDCl_3$) δ 7.70 (d, *J* = 8.7 Hz, 1H), 6.92 (d, *J* = 2.3 Hz, 1H), 6.90 (dd, *J* = 8.7, 2.4 Hz, 1H), 3.87 (s, 3H), 2.90 – 2.84 (m, 2H), 2.70 – 2.65 (m, 1H), 2.34 (ddt, *J* = 14.4, 9.5, 2.4 Hz, 1H),

1.99 – 1.96 (m, 1H), 1.80 (dt, *J* = 9.4, 4.6 Hz, 1H), 1.52 – 1.43 (m, 3H), 1.00 (t, *J* = 7.4 Hz, 3H); ^{13}C NMR (100 MHz, $CDCl_3$) δ 161.4, 159.2, 157.1, 154.0, 153.4, 121.5, 116.4, 112.6, 108.1, 107.0, 101.4, 55.8, 36.2, 29.1, 28.7, 28.7, 20.5, 11.7; IR (KBr)ν_{max}/cm^{-1} 3020 (C–H), 1660 (C=O), 1291 (C–O); HRMS (ESI) Calcd For $C_{18}H_{19}O_4$ 299.1278 ($M+H^+$); Found 299.1278.

9-(*tert*-butyl)-3-Methoxy-7,8,9,10-tetrahydro-6*H*-benzofuro[3,2-*c*]chromen-6-one (5d)

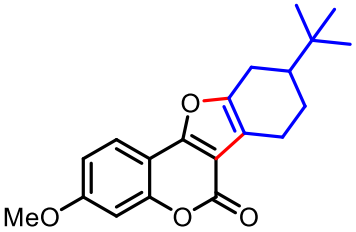

Yield 85% (277.43 mg) White solid, mp 159–161 °C. ^{1}H NMR (600 MHz, $CDCl_3$) δ 7.68 (d, *J* = 8.6 Hz, 1H), 6.91 (d, *J* = 2.3 Hz, 1H), 6.89 (dd, *J* = 8.7, 2.3 Hz, 1H), 3.86 (s, 3H), 2.95 (dd, *J* = 16.5, 5.0 Hz, 1H), 2.78 (dd, *J* = 16.2, 5.0 Hz, 1H), 2.60 – 2.55 (m, 1H), 2.47 (t, *J* = 14.6 Hz, 1H), 2.07 (dd, *J* = 13.0, 3.7 Hz, 1H), 1.63 – 1.58 (m, 1H), 1.35 (dt, *J* = 12.5, 6.2 Hz, 1H), 0.98 (s, 9H); ^{13}C NMR (100 MHz, $CDCl_3$) δ 161.4, 159.2, 157.1, 154.2, 154.0, 121.4, 116.3, 112.6, 107.9, 106.9, 101.4, 55.8, 45.1, 32.6, 27.4, 24.9, 24.2, 21.4; IR (KBr)ν_{max}/cm^{-1} 3020 (C–H), 1660 (C=O), 1305 (C–O); HRMS (ESI) Calcd For $C_{20}H_{23}O_4$ 327.1591 ($M+H^+$); Found 327.1609.

3,9-Dimethoxy-7,8,9,10-tetrahydro-6*H*-benzofuro[3,2-*c*]chromen-6-one (5e) Yield 83%

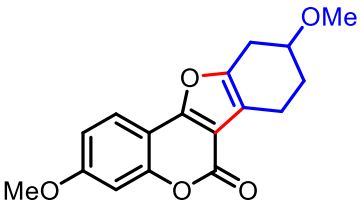

(249.25 mg) White solid, mp 168–169 °C. ^{1}H NMR (400 MHz, $CDCl_3$) δ 7.70 (d, *J* = 8.5 Hz, 1H), 6.92 – 6.88 (m, 2H), 3.87 (s, 3H), 3.83 – 3.80 (m, 1H), 3.44 (s, 3H), 3.07 (dd, *J* = 16.6, 4.9 Hz, 1H), 2.92 – 2.86 (m, 1H), 2.82 – 2.77 (m, 2H), 1.99 (dt, *J* = 13.1, 6.4 Hz, 2H); ^{13}C NMR (100 MHz, $CDCl_3$) δ 161.6, 159.0, 157.6, 154.1, 150.7, 121.5, 116.1, 112.7, 107.9, 106.8, 101.5, 75.4, 56.5, 55.8, 29.6, 27.0, 17.7; IR (KBr)ν_{max}/cm^{-1} 3019 (C–H), 1650 (C=O), 1305 (C–O); HRMS (ESI) Calcd For $C_{17}H_{17}O_5$ 301.1071 ($M+H^+$); Found 301.1072.

9-Hydroxy-3-methoxy-7,8,9,10-tetrahydro-6*H*-benzofuro[3,2-*c*]chromen-6-one (5f) Yield

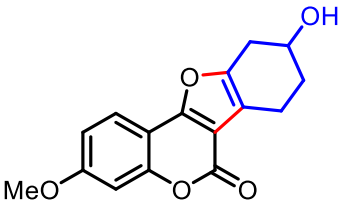

85% (243.33 mg) White solid, mp 168–169 °C. ^{1}H NMR (500 MHz, $CDCl_3$) δ 7.70 (d, *J* = 8.6 Hz, 1H), 6.92 – 6.89 (m, 2H), 4.35 (s, 1H), 3.87 (s, 3H), 3.11 (dd, *J* = 16.4, 4.8 Hz, 1H), 2.94 (dt, *J* = 16.9, 6.0 Hz, 1H), 2.85 – 2.75 (m, 2H), 2.04 – 1.99 (m, 1H), 1.94 (dd, *J* = 13.6, 6.4 Hz, 1H), 1.79 (s, 1H); ^{13}C NMR (125 MHz, $CDCl_3$) δ 161.7, 159.0, 157.8, 154.2, 150.5, 121.6, 115.8, 112.7, 107.8, 106.8, 101.5, 66.8, 55.8, 32.5, 30.6, 17.6; IR

(KBr)ν_{max}/cm^{-1} 3018 (C–H), 1655 (C=O), 1301 (C–O); HRMS (ESI) Calcd For $C_{16}H_{15}O_5$ 287.0914 ($M+H^+$); Found 287.0913.

2-Chloro-9-methyl-7,8,9,10-tetrahydro-6*H*-benzofuro[3,2-*c*]chromen-6-one (6a) Yield

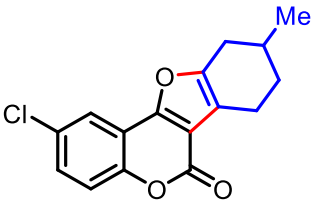

72% (207.88 mg) White solid, mp 158–160 °C. ^{1}H NMR (600 MHz, $CDCl_3$) δ 7.74 (d, *J* = 2.4 Hz, 1H), 7.37 (dd, *J* = 8.8, 2.4 Hz, 1H), 7.32 (d, *J* = 8.8 Hz, 1H), 2.90 – 2.82 (m, 2H), 2.72 – 2.66 (m, 1H), 2.37 – 2.32 (m, 1H), 2.07 – 2.03 (m, 1H), 1.94 – 1.91 (m, 1H), 1.48 – 1.42 (m, 1H), 1.14 (d, *J* = 6.7 Hz, 3H); ^{13}C NMR (150 MHz, $CDCl_3$) δ 158.2, 155.1, 154.9, 150.5, 129.9, 129.7, 120.0, 118.6, 116.7, 114.4, 111.1, 31.2, 30.6, 29.3, 21.3, 20.3; IR (KBr)ν_{max}/cm^{-1} 3029 (C–H), 1662 (C=O), 1291 (C–O); HRMS (ESI) Calcd For $C_{16}H_{14}ClO_3$ 289.0626 ($M+H^+$); Found 289.0612.

2-Chloro-7,8,9,10-tetrahydro-6*H*-benzofuro[3,2-*c*]chromen-6-one (6b) Yield 80% (219.76

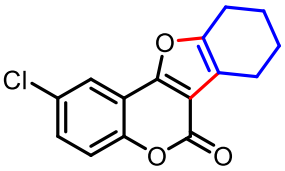

mg) White solid, mp 173–175 °C. ^{1}H NMR (600 MHz, $CDCl_3$) δ 7.78 (d, *J* = 2.4 Hz, 1H), 7.39 (dd, *J* = 8.8, 2.4 Hz, 1H), 7.34 (d, *J* = 8.8 Hz, 1H), 2.77 (dtd, *J* = 16.3, 6.2, 1.9 Hz, 4H), 1.95 – 1.92 (m, 2H), 1.82 (ddd, *J* = 9.1, 7.2, 4.5 Hz, 2H); ^{13}C NMR (150 MHz, $CDCl_3$) δ 158.3, 155.2, 154.8, 150.6, 129.9, 129.8, 120.1, 118.7, 117.2, 114.4, 111.2, 23.3, 22.5, 22.3, 21.0; IR (KBr)ν_{max}/cm^{-1} 3012 (C–H), 1662 (C=O), 1301 (C–O); HRMS (ESI) Calcd For $C_{15}H_{12}ClO_3$ 275.0470 ($M+H^+$); Found 275.0456.

2-Chloro-9-ethyl-7,8,9,10-tetrahydro-6*H*-benzofuro[3,2-*c*]chromen-6-one (6c) Yield 88%

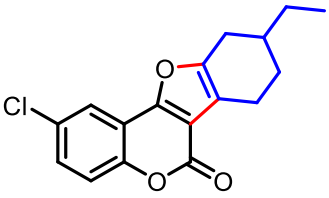

(266.42 mg) White solid, mp 178–179 °C. ^{1}H NMR (600 MHz, $CDCl_3$) δ 7.78 (d, *J* = 2.4 Hz, 1H), 7.39 (dd, *J* = 8.8, 2.4 Hz, 1H), 7.34 (d, *J* = 8.8 Hz, 1H), 2.92 – 2.86 (m, 2H), 2.71 – 2.65 (m, 1H), 2.36 (ddt, *J* = 16.4, 9.6, 2.2 Hz, 1H), 2.01 – 1.98 (m, 1H), 1.84 – 1.80 (m, 1H), 1.48 (ddt, *J* = 26.8, 12.7, 6.4 Hz, 3H), 1.01 (t, *J* = 7.4 Hz, 3H); ^{13}C NMR (100 MHz, $CDCl_3$) δ 158.3, 155.3, 155.0, 150.6, 129.9, 129.8, 120.1, 118.7, 117.0, 114.5, 111.1, 36.1, 29.2, 28.6, 28.5, 20.4, 11.6; IR (KBr)ν_{max}/cm^{-1} 3012 (C–H), 1655 (C=O), 1372 (C–O); HRMS (ESI) Calcd For $C_{17}H_{16}ClO_3$ 303.0783 ($M+H^+$); Found 303.785.

9-(*tert*-Butyl)-2-chloro-7,8,9,10-tetrahydro-6*H*-benzofuro[3,2-*c*]chromen-6-one (6d)

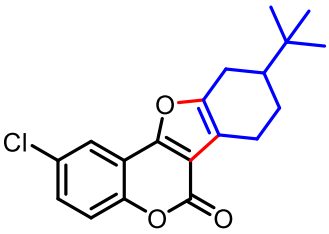

Yield 85% (281.18 mg) White solid, mp 168–169 °C. ^{1}H NMR (400 MHz, $CDCl_3$) δ 7.78 (d, *J* = 2.3 Hz, 1H), 7.39 (dd, *J* = 8.9, 2.3 Hz, 1H), 7.35 (d, *J* = 8.8 Hz, 1H), 2.98 (dd, *J* = 16.4, 5.1 Hz, 1H), 2.82 (dd, *J* = 16.4, 5.2 Hz, 1H), 2.63 – 2.46 (m, 2H), 2.09 (dd, *J* = 13.6, 4.7 Hz, 1H), 1.43 – 1.25 (m, 2H), 0.99 (s, 9H); ^{13}C NMR (100 MHz, $CDCl_3$) δ 158.4, 157.7, 156.1, 155.1, 150.6, 130.0, 129.8, 120.1, 118.7, 117.0, 114.5, 45.0, 32.6, 27.4, 25.0, 24.2, 21.3; IR (KBr)ν_{max}/cm^{-1} 3022 (C–H), 1652 (C=O), 1312 (C–O); HRMS (ESI) Calcd For $C_{19}H_{20}ClO_3$ 331.1096 ($M+H^+$); Found 331.1172.

2-Chloro-9-methoxy-7,8,9,10-tetrahydro-6*H*-benzofuro[3,2-*c*]chromen-6-one (6e) Yield

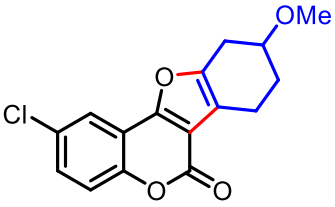

83% (252.91 mg) White solid, mp 172–173 °C. ^{1}H NMR (600 MHz, $CDCl_3$) δ 7.77 (d, *J* = 2.4 Hz, 1H), 7.39 (dd, *J* = 8.8, 2.4 Hz, 1H), 7.34 (d, *J* = 8.8 Hz, 1H), 3.85 (dt, *J* = 10.3, 5.2 Hz, 1H), 3.44 (s, 3H), 3.08 (dd, *J* = 16.6, 4.9 Hz, 1H), 2.91 – 2.89 (m, 1H), 2.82 – 2.77 (m, 2H), 2.02 – 1.98 (m, 2H); ^{13}C NMR (150 MHz, $CDCl_3$) δ 158.1, 155.4, 152.6, 150.6, 130.0, 130.0, 120.1, 118.7, 116.7, 114.3, 110.9, 75.0, 56.5, 29.6, 26.8, 17.5; IR (KBr)ν_{max}/cm^{-1} 3019 (C–H), 1652 (C=O), 1305 (C–O); HRMS (ESI) Calcd For $C_{16}H_{14}ClO_4$ 305.0576 ($M+H^+$); Found 305.0575.

2-Fluoro-9-methyl-7,8,9,10-tetrahydro-6*H*-benzofuro[3,2-*c*]chromen-6-one (7a) Yield

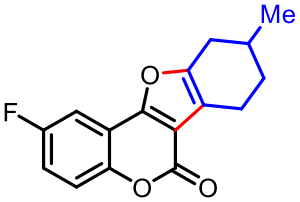

78% (212.36 mg) White solid, mp 188–189 °C. ^{1}H NMR (600 MHz, $CDCl_3$) δ 7.44 (dd, *J* = 7.9, 3.0 Hz, 1H), 7.36 (dd, *J* = 9.1, 4.3 Hz, 1H), 7.14 (td, *J* = 8.7, 3.0 Hz, 1H), 2.91 – 2.83 (m, 2H), 2.73 – 2.66 (m, 1H), 2.35 (dd, *J* = 16.5, 9.3 Hz, 1H), 2.08 – 2.02 (m, 1H), 1.93 (ddd, *J* = 13.3, 5.2, 2.6 Hz, 1H), 1.45 (ddt, *J* = 16.0, 10.5, 5.5 Hz, 1H), 1.14 (d, *J* = 6.7 Hz, 3H); ^{13}C NMR (150 MHz, $CDCl_3$) δ 159.0 ($J_{C\text{-}F}$ = 242.80 Hz), 158.4, 155.4 ($J_{C\text{-}F}$ = 2.82 Hz), 155.0, 148.4 ($J_{C\text{-}F}$ = 1.9 Hz), 118.9 ($J_{C\text{-}F}$ = 8.55 Hz), 117.1 ($J_{C\text{-}F}$ = 24.43 Hz), 116.7, 114.1 ($J_{C\text{-}F}$ = 9.61 Hz), 111.1, 106.3 ($J_{C\text{-}F}$ = 25.6 Hz), 31.3, 30.6, 29.3, 21.3, 20.3; ^{19}F NMR (471 MHz, $CDCl_3$) δ -116.89; IR (KBr)ν_{max}/cm^{-1} 3023 (C–H), 1655 (C=O), 1291 (C–O); HRMS (ESI) Calcd For $C_{16}H_{14}FO_3$ 273.0922 ($M+H^+$); Found 273.0922.

2-Fluoro-7,8,9,10-tetrahydro-6*H*-benzofuro[3,2-*c*]chromen-6-one (7b) Yield 85% (219.50 mg) White solid, mp 145–146 °C. ^{1}H NMR (600 MHz, $CDCl_3$) δ 7.45 (dd, *J* = 7.9, 2.9 Hz, 1H), 7.37 (dd, *J* = 9.1, 4.3 Hz, 1H), 7.15 (td, *J* = 8.6, 3.0 Hz, 1H), 2.77 (dtd, *J* = 16.9, 6.2, 1.9 Hz, 4H), 1.95 – 1.91 (m, 2H), 1.83 (ddt, *J* = 8.6, 5.9, 2.7 Hz, 2H); ^{13}C NMR (150 MHz, $CDCl_3$) δ 159.0 (J_{C-F} = 242.77 Hz), 158.5, 155.2 (J_{C-F} = 2.82 Hz), 155.1, 148.4 (J_{C-F} = 1.99 Hz), 118.9 (J_{C-F} = 8.65 Hz), 117.3, 117.1 (J_{C-F} = 4.51 Hz), 114.1 (J_{C-F} = 9.76 Hz), 111.2, 106.4 (J_{C-F} = 25.56 Hz), 23.3, 22.5, 22.3, 21.0; ^{19}F NMR (565 MHz, $CDCl_3$) δ -116.89; IR (KBr)ν_{max}/cm^{-1} 3023 (C–H), 1661 (C=O), 1289 (C–O); HRMS (ESI) Calcd For $C_{15}H_{12}FO_3$ 259.0765 ($M+H^+$); Found 259.0765.

9-Ethyl-2-fluoro-7,8,9,10-tetrahydro-6*H*-benzofuro[3,2-*c*]chromen-6-one (7c) Yield 82% (234.76 mg) White solid, mp 155–156 °C. ^{1}H NMR (600 MHz, $CDCl_3$) δ 7.45 (dd, *J* = 7.9, 3.0 Hz, 1H), 7.37 (dd, *J* = 9.1, 4.3 Hz, 1H), 7.15 (td, *J* = 8.6, 3.0 Hz, 1H), 2.92 – 2.86 (m, 2H), 2.71 – 2.65 (m, 1H), 2.36 (ddt, *J* = 16.5, 9.5, 2.4 Hz, 1H), 1.99 (ddt, *J* = 11.8, 5.2, 2.6 Hz, 1H), 1.84 – 1.80 (m, 1H), 1.48 (ddt, *J* = 28.6, 13.7, 7.4 Hz, 3H), 1.01 (t, *J* = 7.5 Hz, 3H); ^{13}C NMR (150 MHz, $CDCl_3$) δ 159.0 (J_{C-F} = 242.73 Hz), 158.5, 155.4 (J_{C-F} = 2.76 Hz), 155.2, 148.4 (J_{C-F} = 1.96 Hz), 118.9 (J_{C-F} = 8.64zz Hz), 117.2, 117.0 (J_{C-F} = 9.42 Hz), 114.2 (J_{C-F} = 9.72 Hz), 111.1, 106.4 (J_{C-F} = 25.62 Hz), 36.1, 29.2, 28.6, 28.5, 20.4, 11.6; ^{19}F NMR (471 MHz, $CDCl_3$) δ -116.89; IR (KBr)ν_{max}/cm^{-1} 3020 (C–H), 1650 (C=O), 1301 (C–O); HRMS (ESI) Calcd For $C_{17}H_{16}FO_3$ 287.1078 ($M+H^+$); Found 287.1083.

9-(*tert*-Butyl)-2-fluoro-7,8,9,10-tetrahydro-6*H*-benzofuro[3,2-*c*]chromen-6-one (7d) Yield 85% (267.19 mg) White solid, mp 168–169 °C. ^{1}H NMR (600 MHz, $CDCl_3$) δ 7.46 (dd, *J* = 7.9, 2.9 Hz, 1H), 7.38 (dd, *J* = 9.1, 4.3 Hz, 1H), 7.16 (td, *J* = 8.7, 3.0 Hz, 1H), 2.98 (dd, *J* = 16.6, 5.1 Hz, 1H), 2.83 (dd, *J* = 16.4, 5.1 Hz, 1H), 2.63 – 2.58 (m, 1H), 2.53 – 2.48 (m, 1H), 2.09 (dd, *J* = 12.1, 2.8 Hz, 1H), 1.63 (tdd, *J* = 12.3, 5.1, 2.0 Hz, 1H), 1.36 (tt, *J* = 12.3, 6.2 Hz, 1H), 0.99 (s, 9H); ^{13}C NMR (150 MHz, $CDCl_3$) δ 159.0 (J_{C-F} = 242.59 Hz), 158.5, 156.1, 156.0, 155.5 (J_{C-F} = 2.74 Hz), 148.4 (J_{C-F} = 2.04 Hz), 118.9 (J_{C-F} = 8.62 Hz), 117.3, 117.0 (J_{C-F} = 16.60 Hz), 114.2 (J_{C-F} = 9.6 Hz), 111.1, 106.3 (J_{C-F} = 25.65 Hz), 45.1, 32.6, 27.4, 25.0, 24.2, 21.4; ^{19}F NMR (377 MHz, $CDCl_3$) δ -116.87; IR (KBr)ν_{max}/cm^{-1}

3019 (C–H), 1665 (C=O), 1305 (C–O); HRMS (ESI) Calcd For $C_{19}H_{20}FO_3$ 315.1391 ($M+H^+$); Found 315.1338.

3-Hydroxy-9-methoxy-7,8,9,10-tetrahydro-6*H*-benzofuro[3,2-*c*]chromen-6-one (8a)

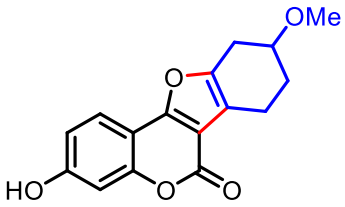

Yield 82% (234.75 mg) White solid, mp 162–163 °C. ^{1}H NMR (600 MHz, DMSO-d_6) δ 10.49 (s, 1H), 7.62 (d, *J* = 8.6 Hz, 1H), 6.83 (dd, *J* = 8.6, 2.1 Hz, 1H), 6.79 (d, *J* = 2.1 Hz, 1H), 3.78 (d, *J* = 5.1 Hz, 1H), 3.31 (s, 3H), 3.02 (dd, *J* = 16.4, 4.6 Hz, 1H), 2.70 (d, *J* = 5.5 Hz, 1H), 2.61 (d, *J* = 6.7 Hz, 2H), 1.91 – 1.82 (m, 2H); ^{13}C NMR (151 MHz, DMSO-d_6) δ 160.0, 157.7, 156.9, 153.5, 150.6, 121.6, 115.0, 113.4, 106.2, 104.6, 102.9, 74.3, 55.5, 28.6, 26.3, 17.1; IR (KBr)ν_{max}/cm^{-1} 3022 (C–H), 1650 (C=O), 1291 (C–O); HRMS (ESI) Calcd For $C_{16}H_{15}O_5$ 287.0914 ($M+H^+$); Found 287.0911. (Purified by 15:85 of ethyl acetate: hexane).

3,9-Dihydroxy-7,8,9,10-tetrahydro-6*H*-benzofuro[3,2-*c*]chromen-6-one (8b) Yield 85%

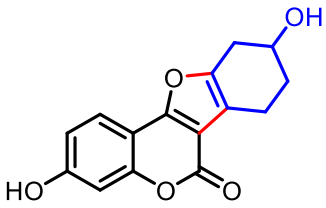

(231.41 mg) White solid, mp 169–171 °C. ^{1}H NMR (600 MHz, DMSO-d_6) δ 10.49 (s, 1H), 7.69 – 7.67 (m, 1H), 6.85 – 6.84 (m, 1H), 6.82 (s, 1H), 5.05 (d, *J* = 3.9 Hz, 1H), 4.10 (s, 1H), 2.98 (dd, *J* = 14.9, 5.1 Hz, 1H), 2.71 – 2.68 (m, 1H), 2.59 (dd, *J* = 15.9, 5.8 Hz, 2H), 1.86 – 1.82 (m, 1H), 1.74 (dq, *J* = 13.1, 7.0 Hz, 1H); ^{13}C NMR (150 MHz, DMSO-d_6) δ 160.4, 158.3, 157.4, 154.0, 151.6, 122.1, 115.3, 113.8, 106.8, 105.1, 103.4, 65.2, 32.4, 30.5, 17.8; IR (KBr)ν_{max}/cm^{-1} 3020 (C–H), 1655 (C=O), 160 (C–O); HRMS (ESI) Calcd For $C_{15}H_{13}O_5$ 273.0758 ($M+H^+$); Found 273.0759. (Purified by 20:80 of ethyl acetate: hexane).

3-Hydroxy-6-oxo-7,8,9,10-tetrahydro-6*H*-benzofuro[3,2-*c*]chromen-9-yl acetate (8c)

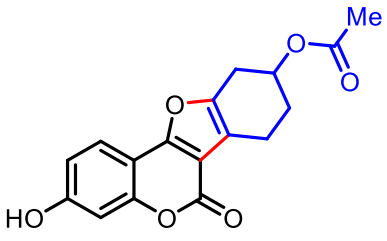

Yield 70% (219.85 mg) White solid, mp 188-190 °C. ^{1}H NMR (600 MHz, DMSO-*d6*) δ 10.49 (s, 1H), 7.49 (d, *J* = 8.5 Hz, 1H), 6.78 (d, *J* = 8.5 Hz, 1H), 6.73 (s, 1H), 5.22 (s, 1H), 3.07 (d, *J* = 13.7 Hz, 1H), 2.76 – 2.73 (m, 1H), 2.63 (s, 2H), 2.01 (s, 3H), 1.95 (dd, *J* = 13.4, 7.1 Hz, 1H), 1.90 – 1.88 (m, 1H); ^{13}C NMR (150 MHz, DMSO-d_6) δ 170.0, 160.1, 157.6, 156.9, 153.5, 149.5, 121.5, 114.9, 113.3, 106.1, 104.4, 102.8, 68.0, 28.5, 26.1, 21.0, 16.9; IR (KBr)ν_{max}/cm^{-1} 3028 (C–H), 1650 (C=O), 1600 (C–O); HRMS (ESI) Calcd For $C_{17}H_{15}O_6$ 315.0864 ($M+H^+$); Found 315.0868. (Purified by 20:80 of ethyl acetate: hexane).

6*H*-benzofuro[3,2-*c*]chromen-6-one (9a) Yield 85% (200.80 mg) White solid, mp 180-182 °C (lit. mp. 181-182 °C °C)[6c]. ^{1}H NMR (600 MHz, $CDCl_3$) δ 8.18 – 8.16 (m, 1H), 8.08 – 8.05 (m, 1H), 7.69 (d, *J* = 7.6 Hz, 1H), 7.65 – 7.62 (m, 1H), 7.50 (ddt, *J* = 15.0, 13.2, 7.9 Hz, 3H), 7.43 (t, *J* = 7.5 Hz, 1H); ^{13}C NMR (100 MHz, $CDCl_3$) δ 159.1, 157.2, 154.6, 152.8, 131.0, 127.2, 125.9, 124.3, 123.8, 122.6, 121.0, 116.6, 111.8, 110.9, 105.0; IR (KBr)ν_{max}/cm^{-1} 3027 (C–H), 1655 (C=O), 1295 (C–O); HRMS (ESI) Calcd For $C_{15}H_9O_3$ 237.0547 ($M+H^+$); Found 237.0548.

3,9-Dimethoxy-6*H*-benzofuro[3,2-*c*]chromen-6-one (9b) Yield 82% (242.95 mg) White solid, mp 198–199 °C (lit. mp.197.6–198.8)[6g]. ^{1}H NMR (500 MHz, $CDCl_3$) δ 7.95 (d, *J* = 8.6 Hz, 1H), 7.87 (d, *J* = 8.4 Hz, 1H), 7.17 (d, *J* = 2.1 Hz, 1H), 7.04 (dd, *J* = 8.6, 2.2 Hz, 1H), 6.99 – 6.97 (m, 2H), 3.91 (d, *J* = 2.0 Hz, 6H); ^{13}C NMR (125 MHz, $CDCl_3$) δ 162.7, 160.2, 159.4, 158.6, 156.6, 155.3, 122.6, 121.7, 116.8, 113.3, 113.2, 106.3, 103.6, 101.5, 97.0, 56.0, 55.9; IR (KBr)ν_{max}/cm^{-1} 3022 (C–H), 1660 (C=O), 1305 (C–O); HRMS (ESI) Calcd For $C_{17}H_{13}O_5$ 297.0758 ($M+H^+$); Found 297.0758.

3-Hydroxy-6*H*-benzofuro[3,2-*c*]chromen-6-one (9d) Yield 72% (181.60 mg) White solid, mp 268-169 °C (lit. mp. 270-272)[6h]. ^{1}H NMR (600 MHz, DMSO-d_6) δ 10.89 (s, 1H), 7.95 – 7.93 (m, 2H), 7.86 – 7.84 (m, 1H), 7.53 – 7.48 (m, 2H), 6.97 (dd, *J* = 8.6, 2.2 Hz, 1H), 6.94 (d, *J* = 2.2 Hz, 1H); ^{13}C NMR (151 MHz, DMSO-d_6) δ 162.0, 160.8, 157.6, 155.4, 154.6, 126.4, 125.4, 123.4, 123.2, 120.5, 114.0, 112.1, 103.9, 103.2, 101.8; IR (KBr)ν_{max}/cm^{-1} 3025 (C–H), 2928 (C–H), 1621 (C=C), 1368 (C–O); HRMS (ESI) Calcd For $C_{15}H_9O_4$ 253.0496 ($M+H^+$); Found 253.0498. (Purified by 15:85 of ethyl acetate: hexane).

3-Hydroxy-9-methoxy-6*H*-benzofuro[3,2-*c*]chromen-6-one (9e) Yield 75% (211.68 mg) White solid, mp 325-328 °C. ^{1}H NMR (400 MHz, DMSO-d_6) δ 10.78 (s, 1H), 7.88 (d, *J* = 8.5 Hz, 1H), 7.79 (d, *J* = 8.6 Hz, 1H), 7.49 (d, *J* = 2.1 Hz, 1H), 7.10 (dd, *J* = 8.6, 2.2 Hz, 1H), 6.96 (dd, *J* = 8.6, 2.2 Hz, 1H), 6.92 (d, *J* = 2.1 Hz, 1H), 3.86 (s, 3H); ^{13}C NMR (150 MHz, DMSO-d_6) δ 161.4, 160.0, 158.9, 157.6, 155.9, 154.8, 122.9, 120.6, 115.9, 113.9, 113.5, 104.1, 103.1, 101.9, 97.4, 55.9; IR (KBr)ν_{max}/cm^{-1} 3028 (C–H), 2928 (C–H), 1621 (C=C), 1368 (C–O); HRMS (ESI) Calcd For $C_{16}H_{11}O_5$ 283.0601 ($M+H^+$); Found 283.0601. (Purified by 25:75 of ethyl acetate: hexane).

2-Fluoro-6*H*-benzofuro[3,2-*c*]chromen-6-one (9f) Yield 81% (205.91 mg) White solid, mp

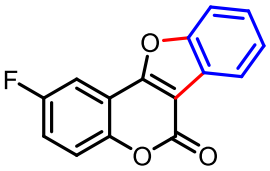

169–170 °C. ^{1}H NMR (400 MHz, $CDCl_3$) δ 8.18 – 8.15 (m, 1H), 7.70 (td, *J* = 7.6, 2.4 Hz, 2H), 7.55 – 7.46 (m, 3H), 7.33 (ddd, *J* = 9.1, 8.1, 3.0 Hz, 1H); ^{13}C NMR (100 MHz, $CDCl_3$) δ 160.3, 159.2 (J_{C-F} = 2.88 Hz), 157.8 (J_{C-F} = 2.45 Hz), 155.8, 149.9 (J_{C-F} = 2.15 Hz), 127.3, 125.6, 123.4, 122.2, 119.5 (J_{C-F} = 30.99 Hz), 119.4 (J_{C-F} = 1.88 Hz), 113.5 (J_{C-F} = 9.48 Hz), 112.0, 107.8 (J_{C-F} = 25.53 Hz), 106.7; ^{19}F NMR (376 MHz, $CDCl_3$) δ -115.96; IR (KBr)ν_{max}/cm^{-1} 3022 (C–H), 1655 (C=O), 1291 (C–O); HRMS (ESI) Calcd For $C_{15}H_8FO_3$ 255.0452 ($M+H^+$); Found 255.0453.

2-Methyl-6*H*-naphtho[2',1':4,5]furo[3,2-*c*]chromen-6-one (9g) Yield 82% (246.25 mg)

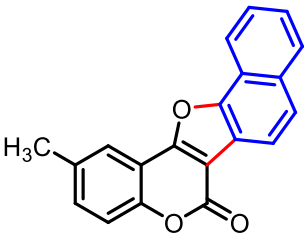

White solid, mp 189–190 °C. ^{1}H NMR (400 MHz, $CDCl_3$) δ 8.46 (d, *J* = 8.3 Hz, 1H), 8.20 (d, *J* = 8.5 Hz, 1H), 8.03 (d, *J* = 8.2 Hz, 1H), 7.98 – 7.96 (m, 1H), 7.89 (d, *J* = 8.8 Hz, 1H), 7.71 (ddd, *J* = 8.2, 7.1, 1.0 Hz, 1H), 7.61 (ddd, *J* = 8.1, 7.0, 1.2 Hz, 1H), 7.43 (d, *J* = 1.9 Hz, 2H), 2.54 (s, 3H); ^{13}C NMR (100 MHz, $CDCl_3$) δ 204.4, 134.7, 132.7, 132.7, 130.7, 128.8, 127.3, 126.5, 126.1, 121.4, 121.0, 120.1, 119.1, 118.1, 117.4, 112.7, 110.9, 107.1, 104.0, 21.1; IR (KBr)ν_{max}/cm^{-1} 3020 (C–H), 1665 (C=O), 1291 (C–O); HRMS (ESI) Calcd For $C_{20}H_{13}O_3$ 301.0860 ($M+H^+$); Found 301.0755.

XRD for compounds (3e and 3j): All the data for the structural analysis of compounds **3e** and **3j** has been deposited to the Cambridge Crystallographic Data Centre, CCDC No. 2253174 and 2289245.

Table 11. Crystal data and structure refinement for compound **3e**

Entry	**Identification Code**	**Compound 3e**
01	Empirical formula	$C_{19}H_{20}O_3$
02	Formula weight	296.369
03	Temperature	298.00
04	Wavelength	0.71073
05	Radiation type	Mo Kα
06	Radiation system	Fine-focus sealed tube
07	Crystal system	orthorhombic
08	Space group	Pbca
09	Cell length	a=14.8561(10) b=7.4709(5) c=28.931(2)
10	Cell angle	α=90 β=90 γ=90
11	Cell volume	3211.0(4)
12	Density	1.226
13	Completeness to theta	99
14	Absorption correction	multi-scan
15	Refinement method	Full-matrix least-squares on F2
16	Index ranges	$-17 \leq h \leq 17$, $-8 \leq k \leq 8$, $-34 \leq l \leq 34$
17	Reflection number	37896
18	2Θ range for data collection/°	5.48 to 49.98
19	Cell formula units Z	8
20	CCDC no	2253174

Table 12. Crystal data and structure refinement for compound **3j**

Entry	**Identification Code**	**Compound 3j**
01	Empirical formula	$C_{19}H_{12}O_3$
02	Formula weight	288.29
03	Temperature	288.29
04	Wavelength	0.71073
05	Radiation type	MoKα
06	Radiation system	Fine-focus sealed tube
07	Crystal system	orthorhombic
08	Space group	$P2_12_12_1$
09	Cell length	a=7.028(3) (10) b=13.206(4) c=13.206(4)
10	Cell angle	α=90 β=90 γ=90
11	Cell volume	1365.8(8)
12	Density	1.402
13	Completeness to theta	99
14	Absorption correction	multi-scan
15	Refinement method	Full-matrix least-squares on F2
16	Index ranges	$-8 \leq h \leq 8$, $-16 \leq k \leq 16$, $-18 \leq l \leq 18$
17	Reflection number	28563
18	2Θ range for data collection/°	4.144 to 52.91
19	Cell formula units Z	4
20	CCDC no	2289245

^{1}H NMR Spectrum of 9-Methyl-7,8,9,10-tetrahydro-6*H*-benzofuro[3,2-*c*]chromen-6-one (3a)

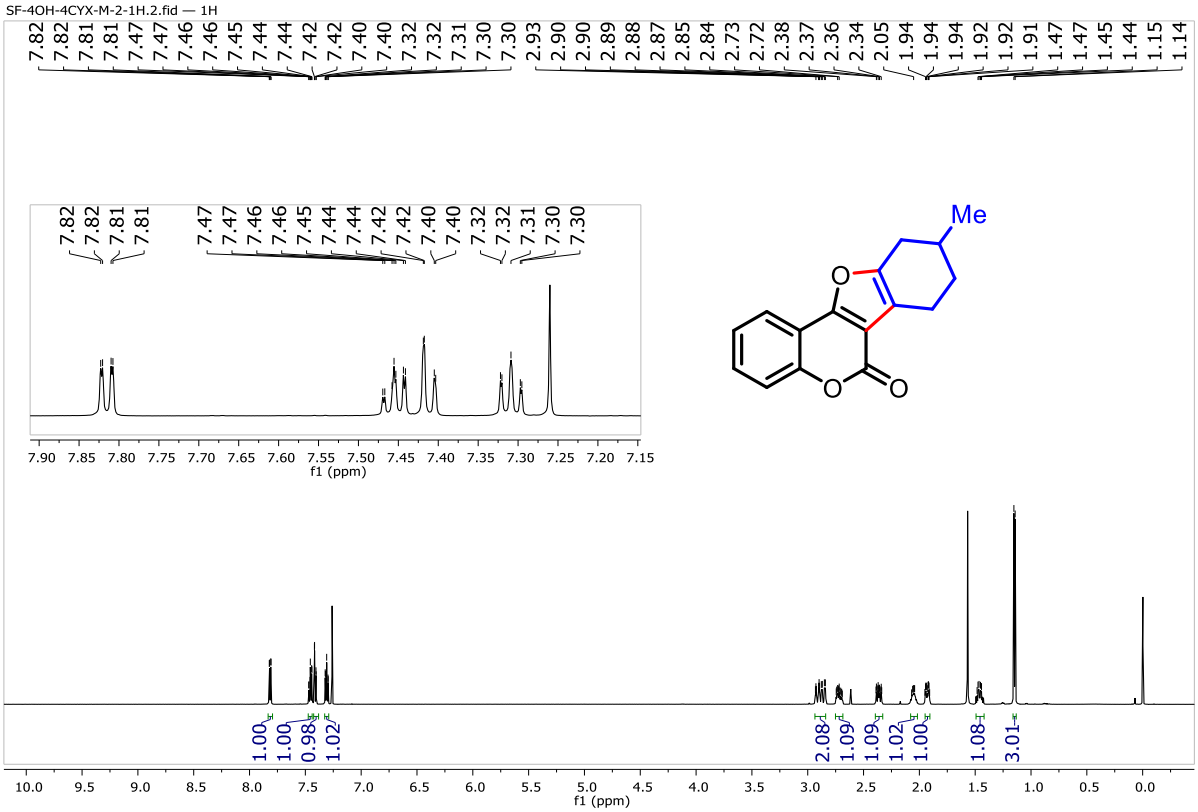

^{13}C NMR Spectrum of 9-Methyl-7,8,9,10-tetrahydro-6*H*-benzofuro[3,2-*c*]chromen-6-one (3a)

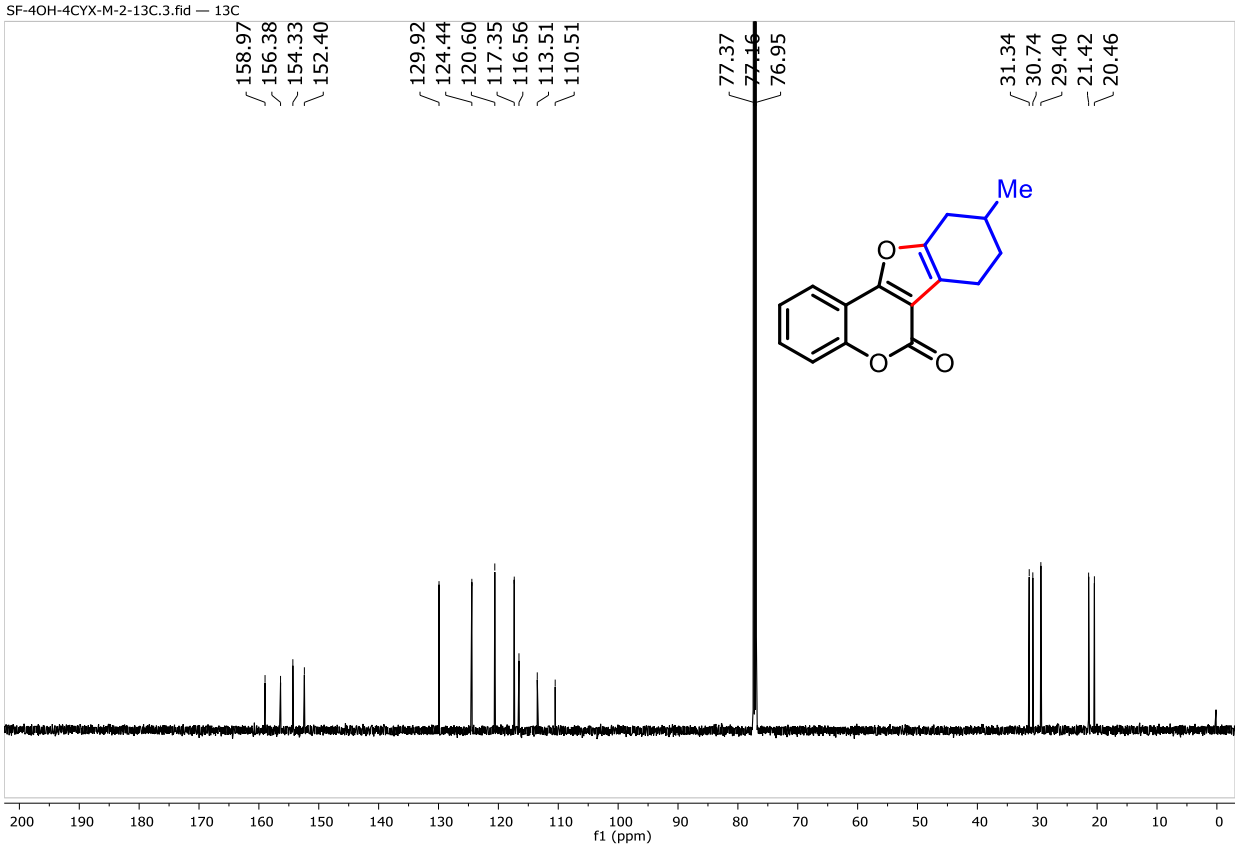

HRMS Spectrum of 9-Methyl-7,8,9,10-tetrahydro-6*H*-benzofuro[3,2-*c*]chromen-6-one (3a)

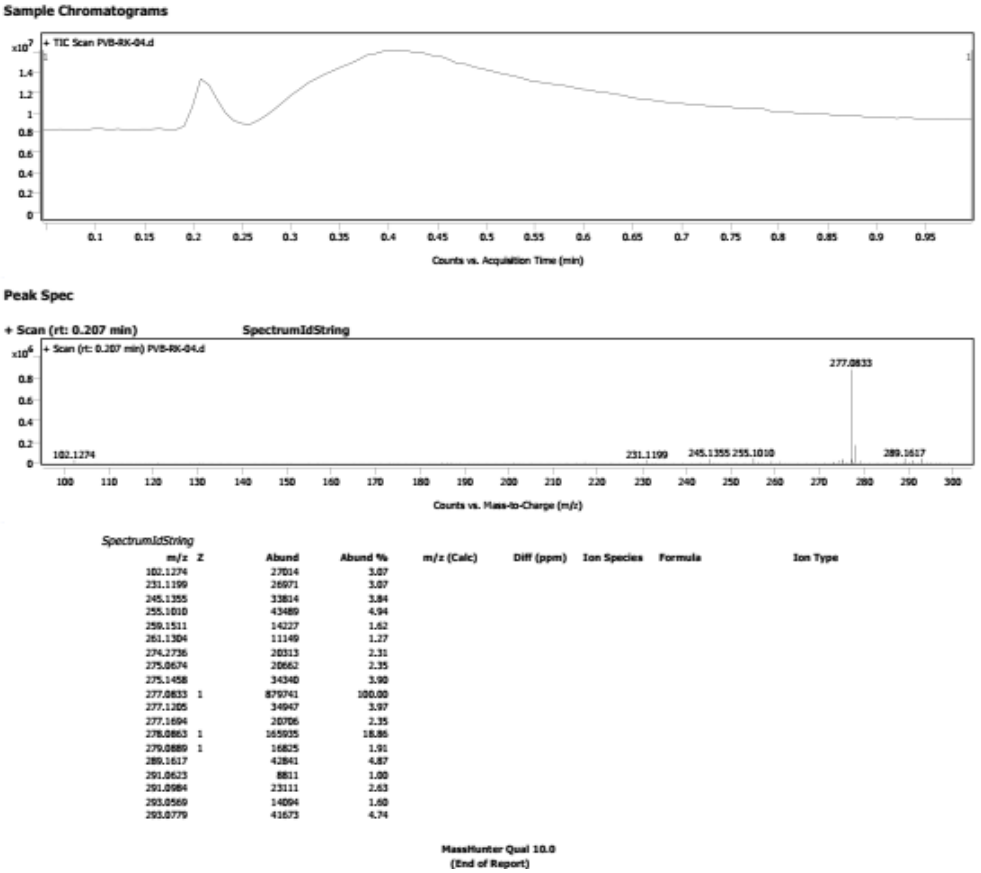

^{1}H NMR Spectrum of 6*H*-benzofuro[3,2-*c*]chromen-6-one (9a)

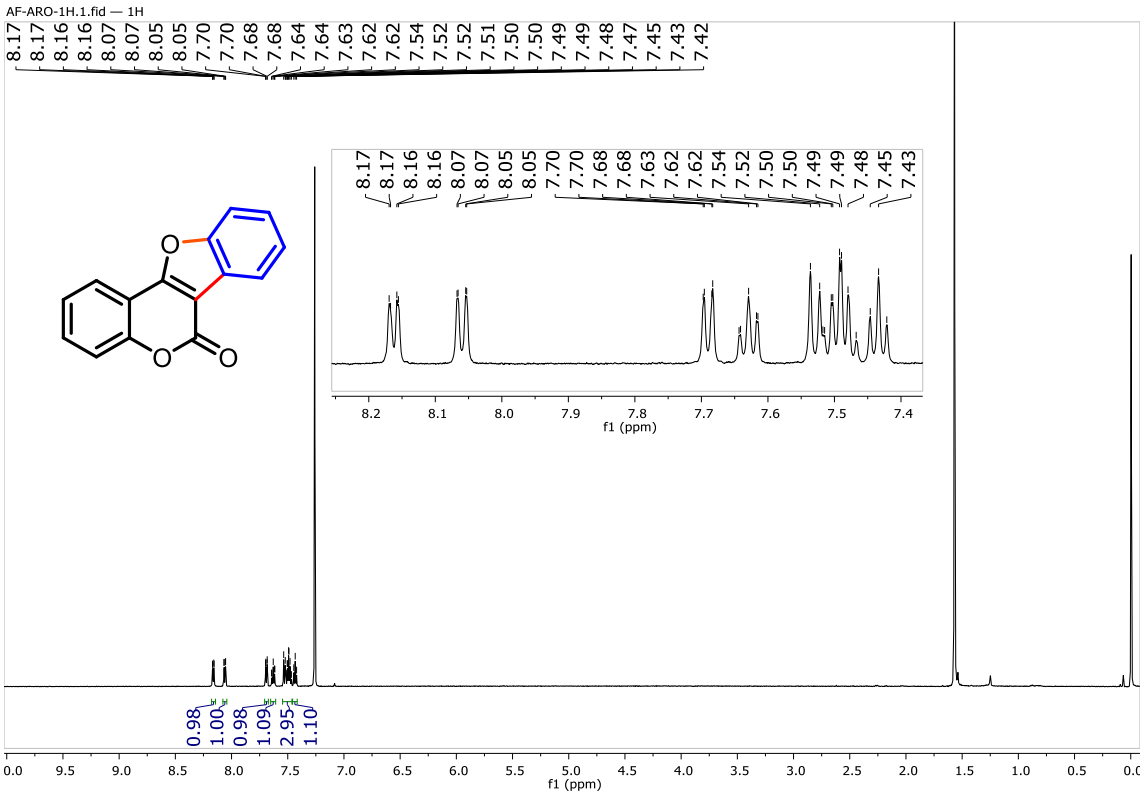

^{13}C NMR Spectrum of 6*H*-benzofuro[3,2-*c*]chromen-6-one (9a)

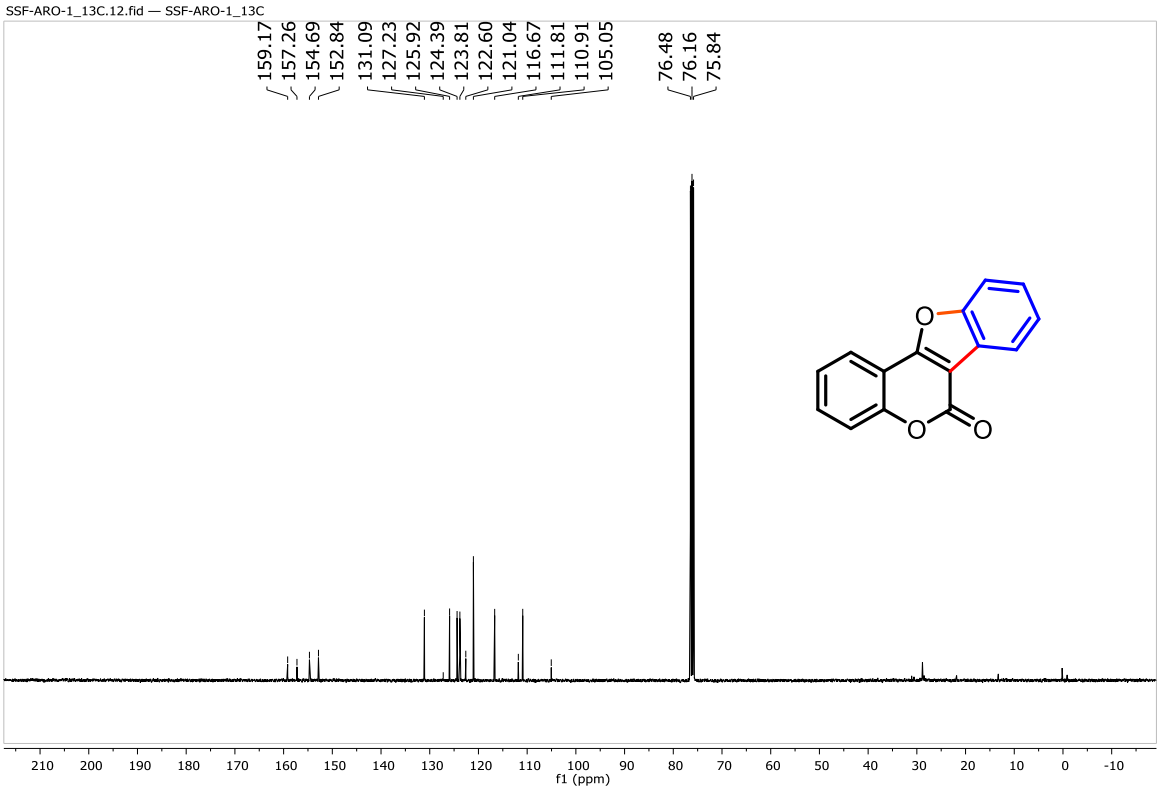

HRMS Spectrum of 6*H*-benzofuro[3,2-*c*]chromen-6-one (9a)

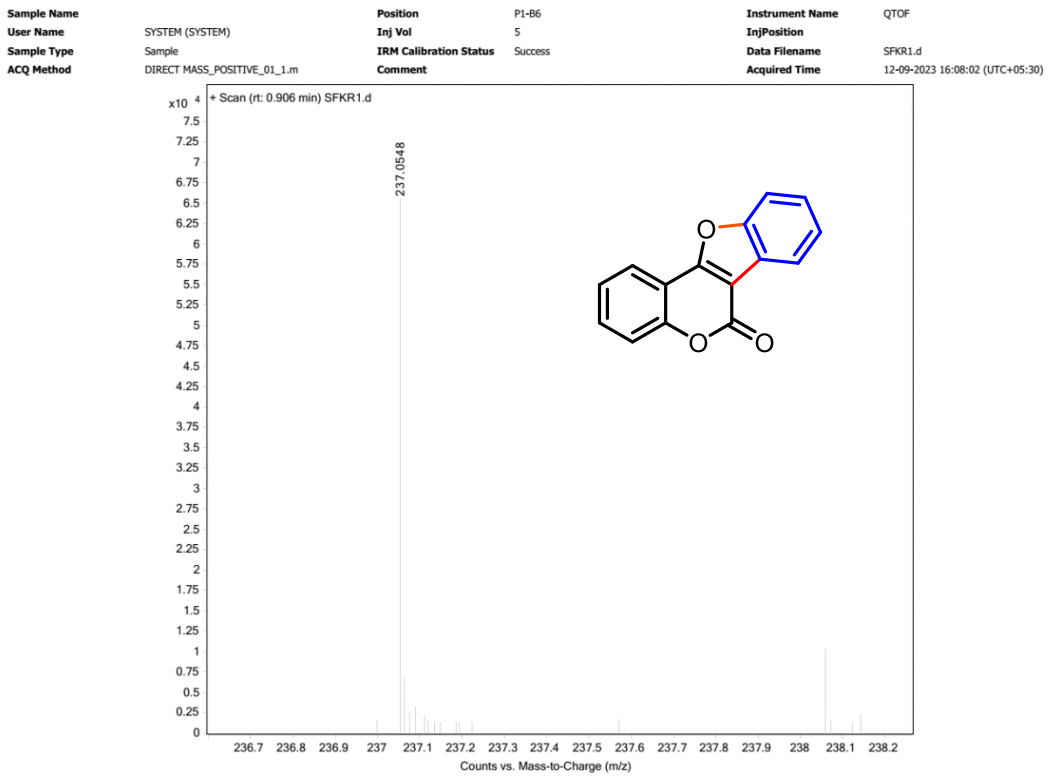

^{1}H NMR Spectrum of 3,9-Dimethoxy-6*H*-benzofuro[3,2-*c*]chromen-6-one (9b)

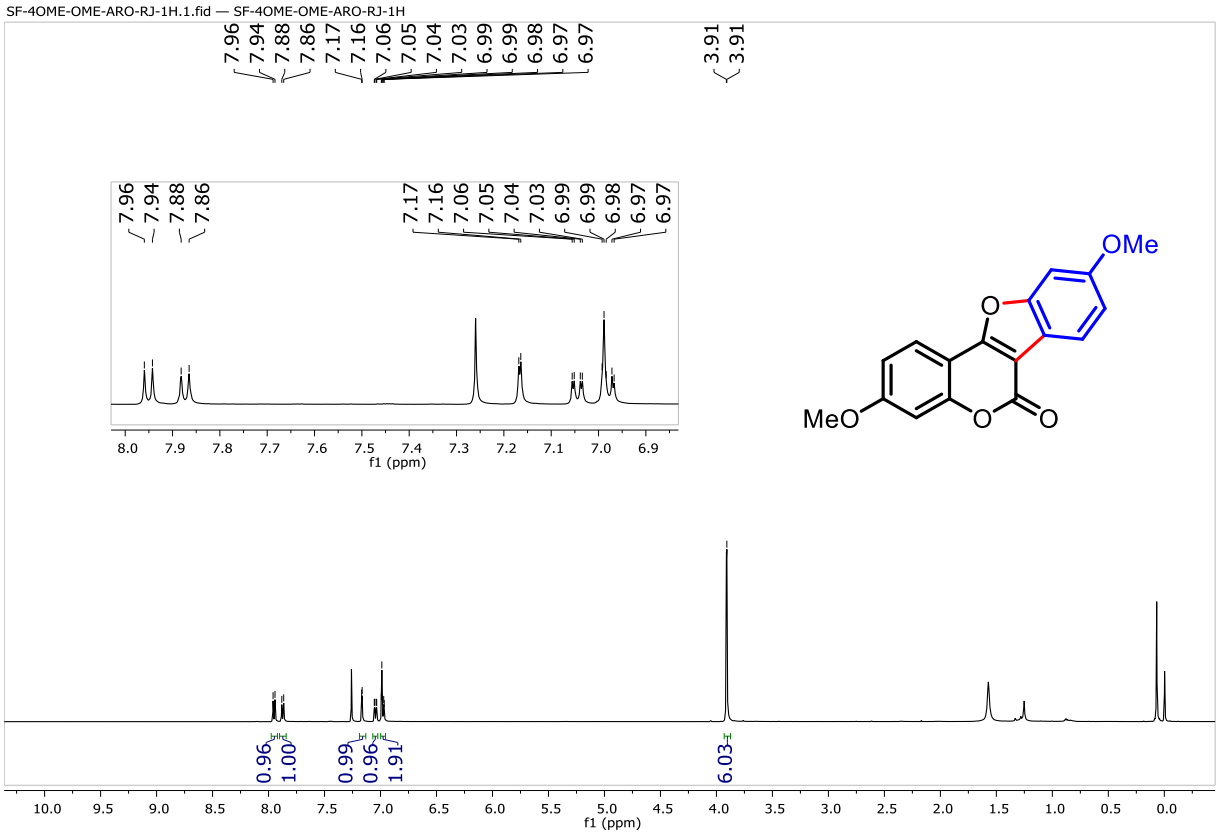

^{13}C NMR Spectrum of 3,9-Dimethoxy-6*H*-benzofuro[3,2-*c*]chromen-6-one (9b)

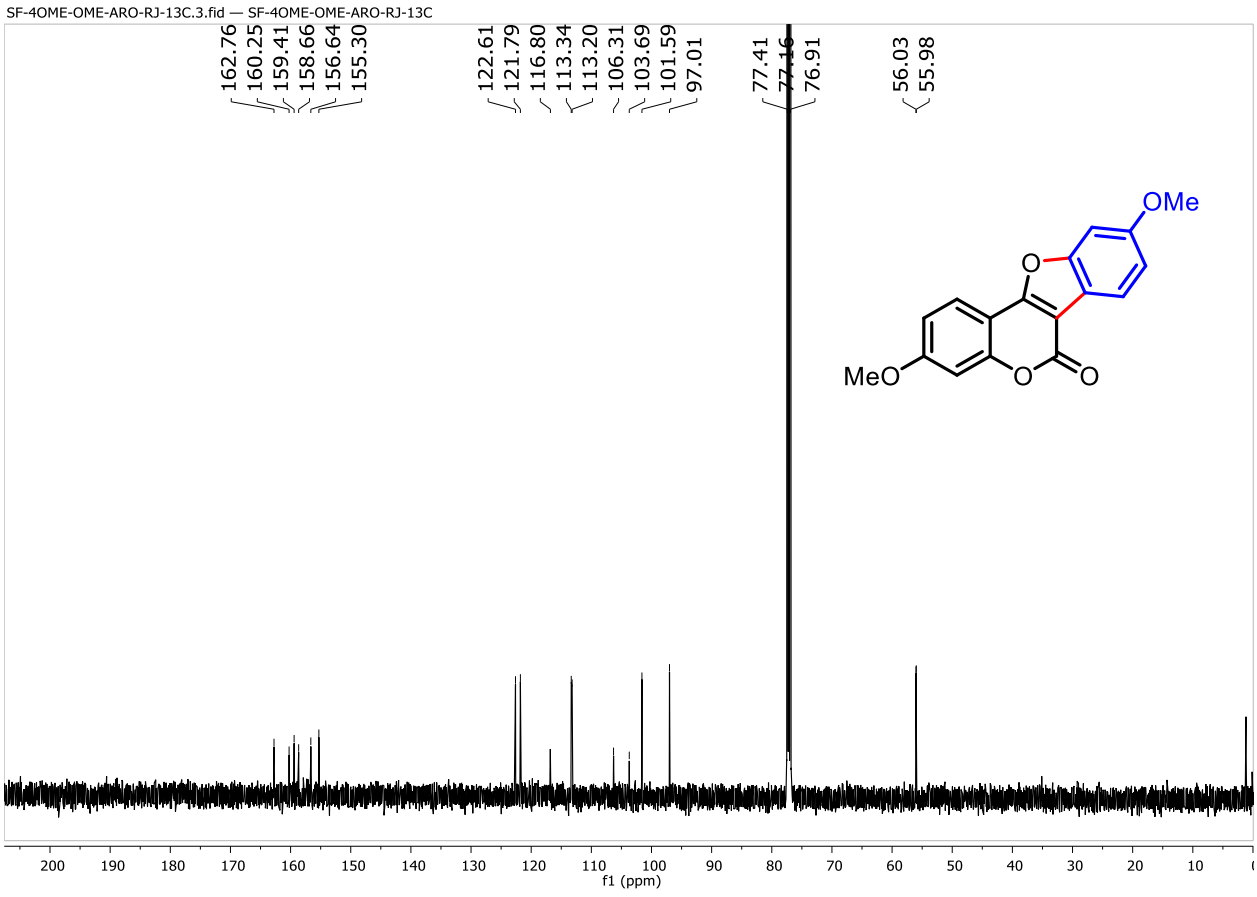

HRMS Spectrum of 3,9-Dimethoxy-6*H*-benzofuro[3,2-*c*]chromen-6-one (9b)

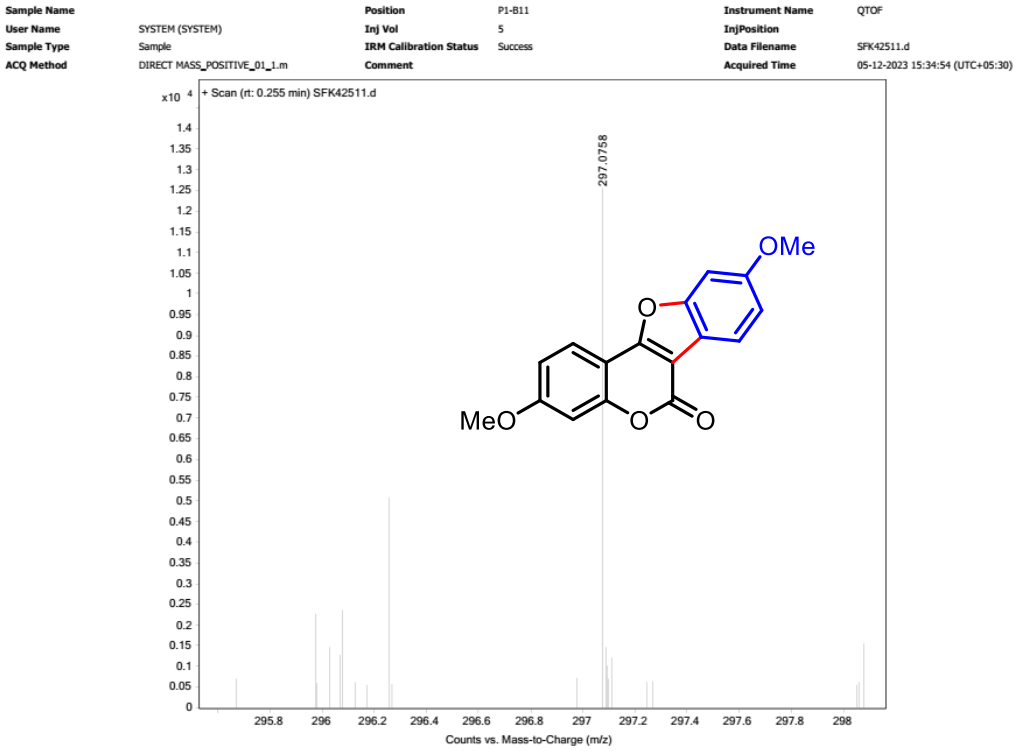

^{1}H NMR Spectrum of 3-Hydroxy-9-methoxy-6*H*-benzofuro[3,2-*c*]chromen-6-one (9e)

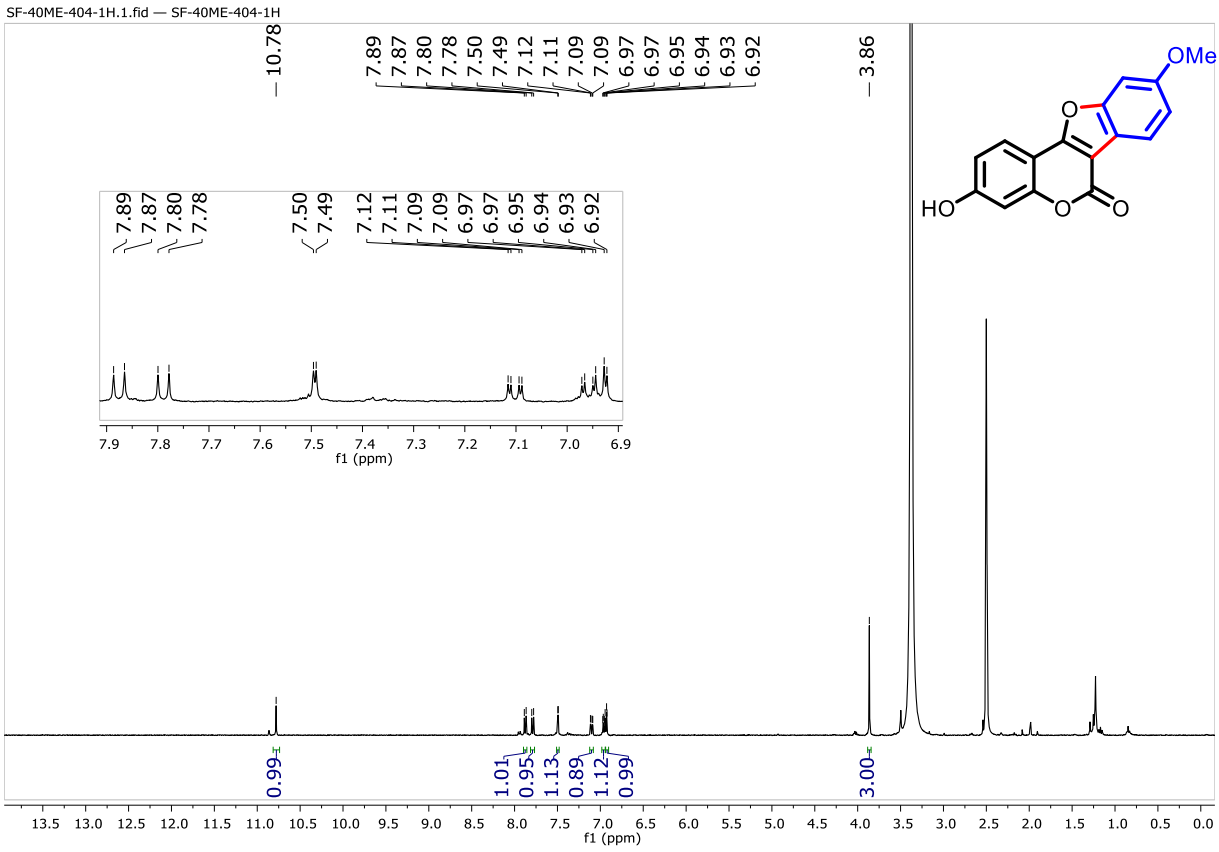

^{13}C NMR Spectrum of 3-Hydroxy-9-methoxy-6*H*-benzofuro[3,2-*c*]chromen-6-one (9e)

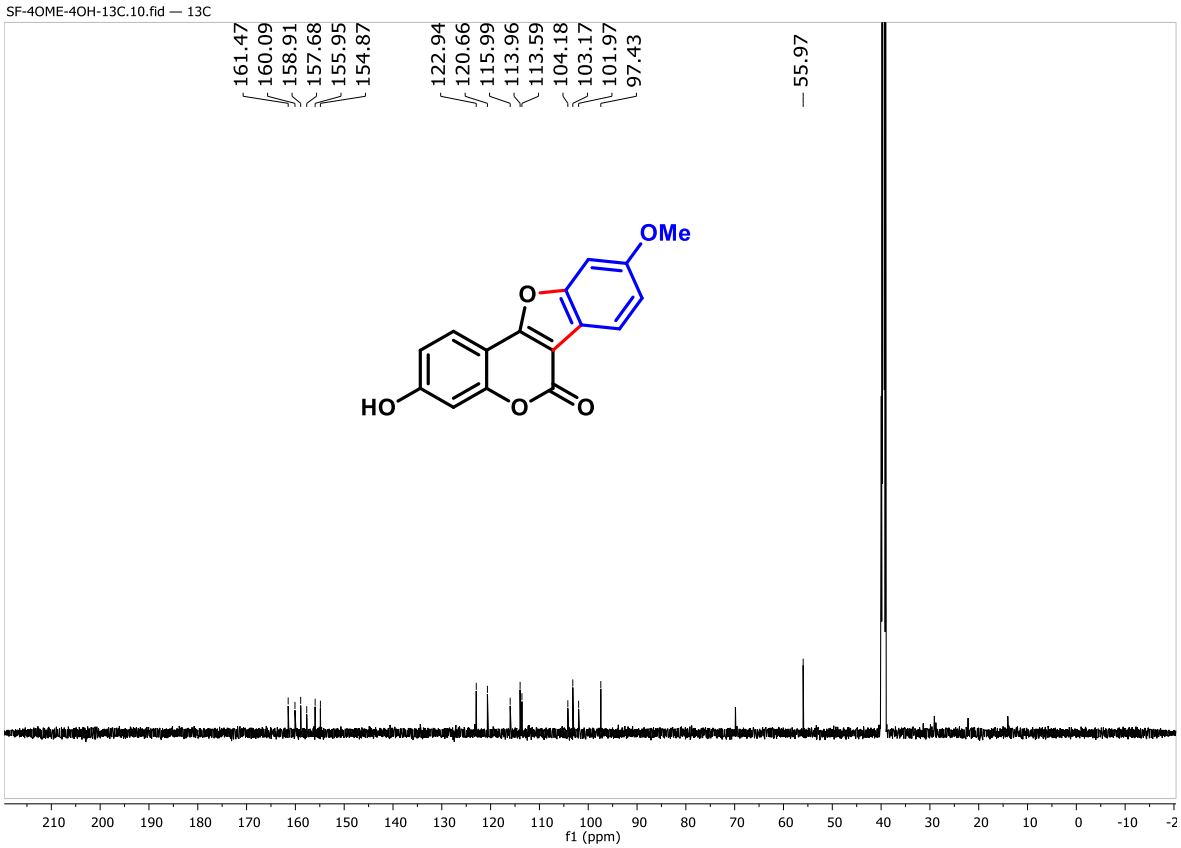

HRMS Spectrum of 3-Hydroxy-9-methoxy-6*H*-benzofuro[3,2-*c*]chromen-6-one (9e)

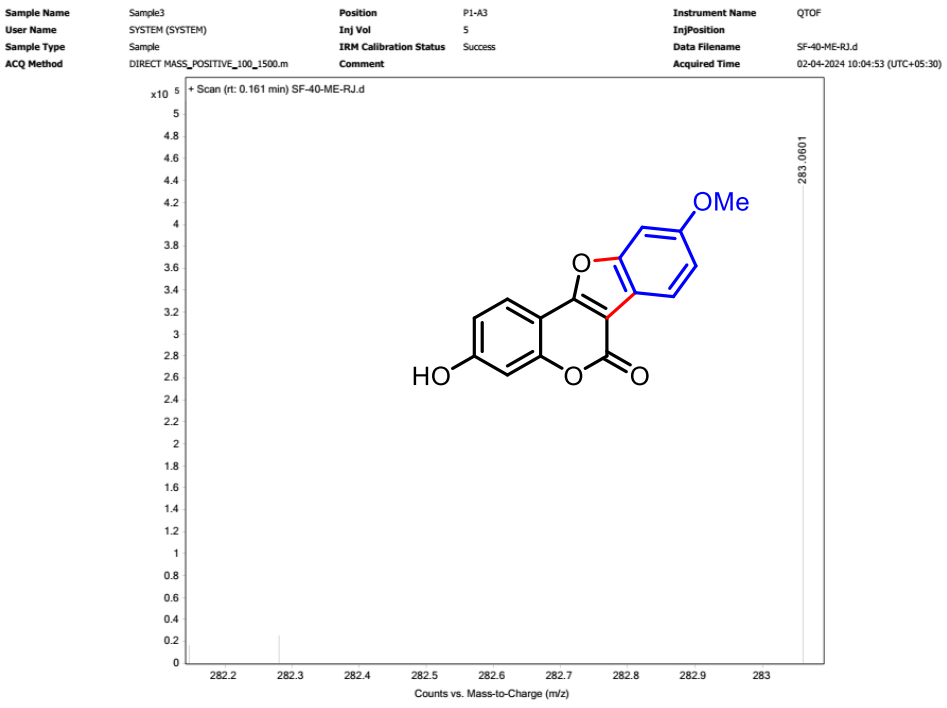

Part B

Chapter II: Section C

Synthesis of dinaphthofuran and furocoumarin derivatives

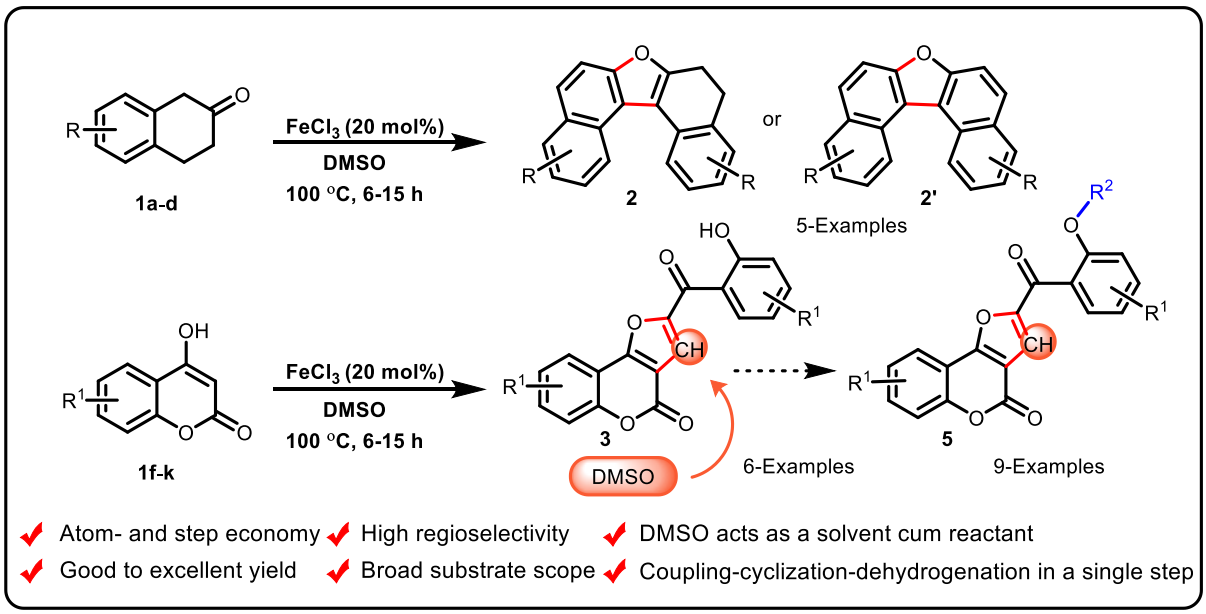

RESULT AND DISCUSSION
EXPERIMENTAL SECTION

Results and Discussion

Chapter I of Part B thoroughly discusses the importance of dinaphthofuran and furocoumarin and their synthetic reported methods. Section C of Chapter II describes a straightforward and eco-friendly protocol for the synthesis of functionalized dinaphthofurans **2** from β-tetralone **1a-e** *via* an intermolecular cross-coupling, cyclization, dehydrogenation in a single step using 20 mol% ferric chloride catalyst in DMSO as a solvent as depicted in Scheme 25a. Likewise, the synthesis of highly functionalized furocoumarins **3** was achieved from various 4-hydroxycoumarins **1f-k** under identical reaction conditions through the formation of dicoumarol intermediate by insertion of methylene group at the 3-position from DMSO solvent followed by reacting with another molecule of 4-hydroxycoumarins as shown in Scheme 25b. The intermediate dicoumarol undergoes simultaneous ring-opening followed by cyclization and dehydrogenation provided furocoumarin derivatives **3** in good yields. The reaction condition is mild and easily handled without the involvement of additives, any oxidants, and an inert atmosphere. Later on, the OH group present in product **3** was explored to synthesize the new class of ether derivative **5** with the goal in mind to synthesize new triazole derivatives and new heterocyclic entity. The perk of this protocol is that it has a broad substrate scope, good to excellent yield, polyfunctional scaffolds, and products that have more than one pharmaceutically important motif.

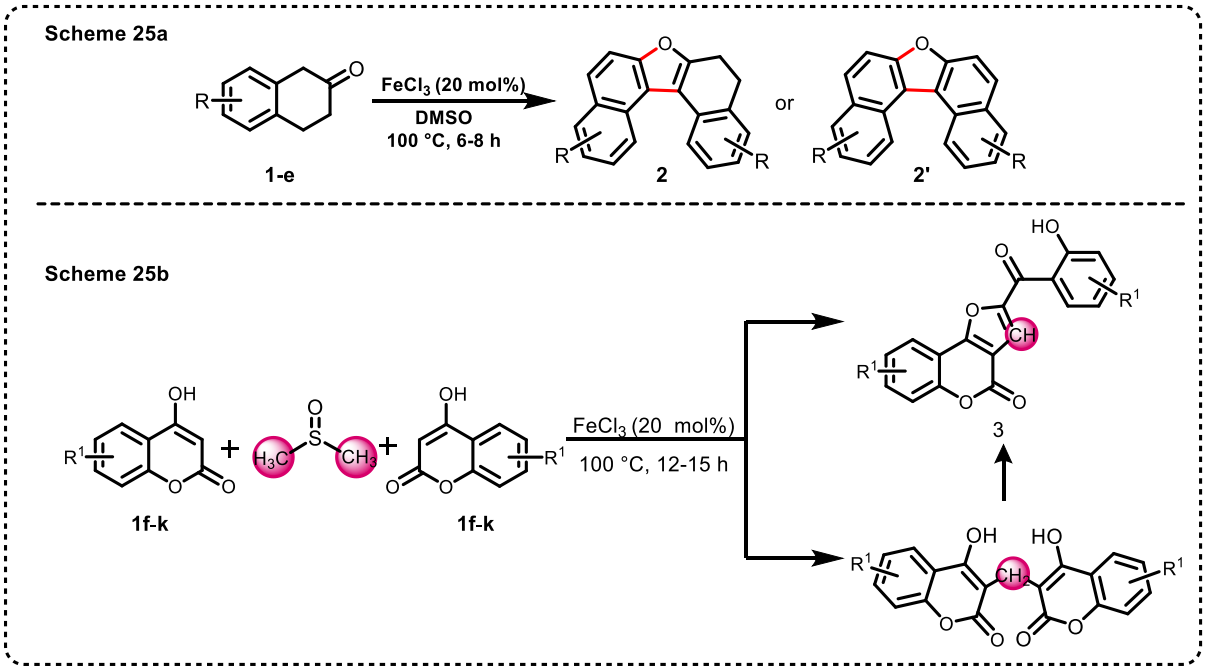

Scheme 25. Synthetic protocol for the synthesis of dinaphthofuran and furocoumarin.

To get the optimized reaction conditions, β-tetralone **1a** was chosen as the model substrate, as depicted in Table 13. Initially, the reaction was examined without a catalyst at room temperature, and progressively temperature was increased to 110 °C in DMSO as a solvent. In both cases, the desired product was not obtained. Next, the reaction was carried out with 5 mol% $FeCl_3$ at room temperature. Unfortunately, again the reaction did not take place. After that, the same reaction was scrutinized at a 60 °C pre-heated oil bath for 18 h and got the desired product **2a** with a 20% yield. The product **2a** was ascertained by spectra (IR, ^1H, and ^{13}C NMR) and HRMS. In the IR spectrum, the carbonyl stretching frequency of aldehydic group of β-tetralone at 1716 cm^{-1} disappeared, and in ^1H, NMR spectrum, the characteristic singlet peak of H-1 of β-tetralone at δ 3.6 ppm ^1H, NMR spectrum, the characteristic singlet peak of H-1 of β-tetralone at δ 3.6 ppm disappeared from the product, disappeared from the product. On the other hand, stretching frequency at 1235 cm^{-1} appeared. In ^1H NMR spectra of product **2a**, two triplets appeared at δ 3.14 and 3.02 ppm.

Table 13. Optimization Table[a,b]

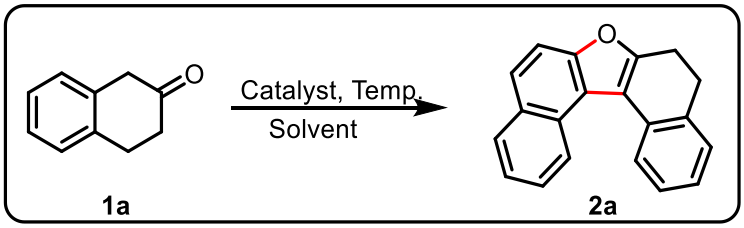

Entry	Catalyst	Mol%	Solvent	Time(h)	Temp.(°C)	Yield[b](%)
1[c]	-	-	DMSO	24	RT→110	NR
2[c]	$FeCl_3$	5	DMSO	24	RT	NR
3	$FeCl_3$	5	DMSO	18	60	20
4	$FeCl_3$	5	DMSO	15	80	32
5	$FeCl_3$	5	DMSO	13	100	48
6	$FeCl_3$	5	DMSO	10	110	46
7	$FeCl_3$	10	DMSO	10	100	58
8	$FeCl_3$	15	DMSO	9	100	69
9	**$FeCl_3$**	**20**	**DMSO**	**6**	**100**	**83**
10	$FeCl_3$	30	DMSO	8	100	80
11	$FeCl_3$	20	DMF	8	100	56
12	$FeCl_3$	20	Methanol	8	100	22

14	$CoCl_2$	20	DMSO	10	100	45
15	$CuCl_2$	20	DMSO	10	100	23

[a]Reaction conditions: All the reactions were performed using β-tetralone (**1a**, 1.0 mmol). [b]Isolated yield. [c]Reaction performed at room temperature. NR: No Reaction.

Additionally, the HRMS value of product **2a** was 271.1120 (expected value of 271.1118), further indicating the formation of the desired product **2a**. To speed up the process with more efficiency, the temperature was scrutinized from 80 °C to 110 °C and it was observed that at 110 °C, the maximum yield of 48% was obtained. Next, the amount of catalyst loading was examined to increase the yield further, and at 20 mol%, an 83% yield of the desired product was obtained. Notably, it was found that as we increased the amount of catalyst, the reaction time was also reduced. Further increasing the amount of catalyst did not increase the yield of the desired product. Thereafter, the efficacy of other solvents, such as dimethyl formamide and methanol, was scrutinized, but the yield of the desired product was not satisfactory.

Table 14. Substrate scope of dinaphthofurans[a,b]

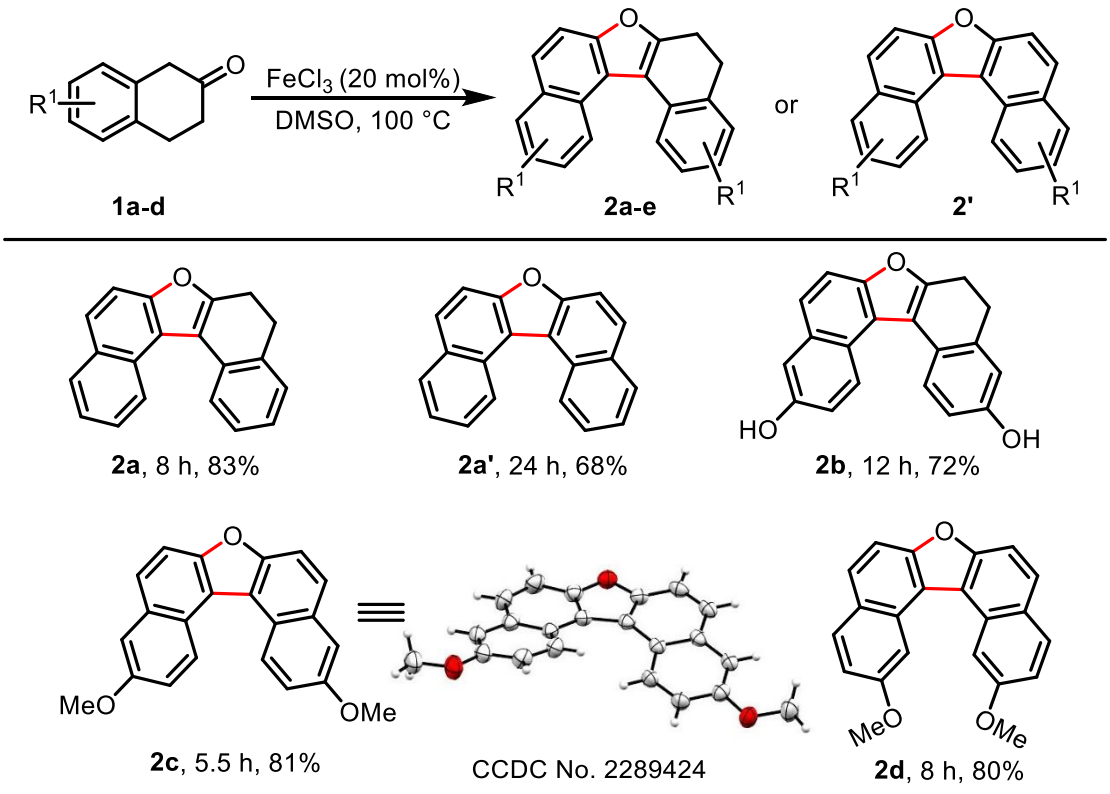

[a]Reaction conditions: All the reactions were performed using β-tetralones (**1a-e**, 1.0 mmol) in the presence of $FeCl_3$ in 2 mL DMSO at 100 °C. [b]Isolated yield.

Motivated by these results, the reaction was also carried out with metal catalysts $CoCl_2$ and $CuCl_2$, and got the desired product at 45% and 23%, respectively. After investigating all the

parameters, it was concluded that $FeCl_3$ is the most effective catalyst at 110 °C in DMSO as a solvent for this reaction.

After getting the optimal reaction condition in hand, we scrutinized the practicability and influence of substitution variation at β-tetralone. The positive outcome demonstrated that the reaction proceeds smoothly and effectively, yielding the desired products **2a** and **2b** in high to moderate yields with high regioselectivity, as depicted in Table 14. Interestingly, it was found that fully aromatized dinaphtofurans **2c** & **2d** were obtained in 81% and 80%, respectively, in a single step if the methoxy group was present at the 7thand 8th position of β-tetralone **1c** & **1d**. Subsequently, we tried to aromatize the **2a** & **2b** and observed that **2a** got aromatized **2a'** when the reaction time was increased from 8 h to 18 h, but for **2b**, the product was decomposed when we increased the reaction time. Unfortunately, β-tetralone having an electron-withdrawing group such as 6-bromo-2-tetralone **1e** did not furnish the expected product under similar reaction conditions. The reason for the failure of the reaction is probably due to the instability of the enolate ion generated from the β-tetralone derivative because of the presence of the bromo group at the 6th position.

To establish the mechanism for the formation of dinaphthofurans, whether the reaction is going through a radical pathway or not, the following experiment was done as shown in Scheme 26.

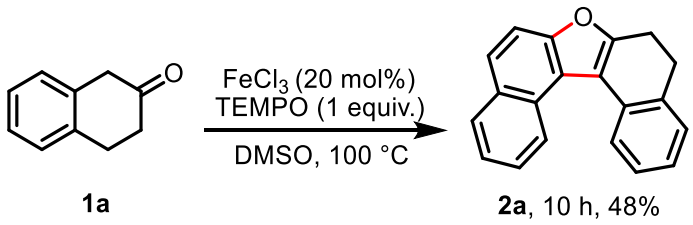

Scheme 26. Preliminary experiment.

On the basis of previous literature reports and preliminary experiments as shown in Scheme 26, a plausible mechanism for the formation of product is shown in Scheme 27. In the presence of $FeCl_3$, β-tetralones exist in their tautomer form keto and enol. The enol form of β-tetralones attacks the other molecule of β-tetralones at 1st position to form the intermediate [**A**]. In the presence of the $FeCl_3$, the OH group of intermediate undergoes keto to form the next intermediate [**B**]. A lone pair of OH of the enol form of intermediate [**B**] attacks the ketone carbon to form the cyclized intermediate. Next, dehydration takes place from intermediate [**D**] to form the intermediate [**E**]. Finally, oxidation takes place by $FeCl_3$ to form the desired product

2. At last, $FeCl_2$ undergoes aerial oxidation and again $FeCl_3$ is generated which is involved in the catalytic cycle.

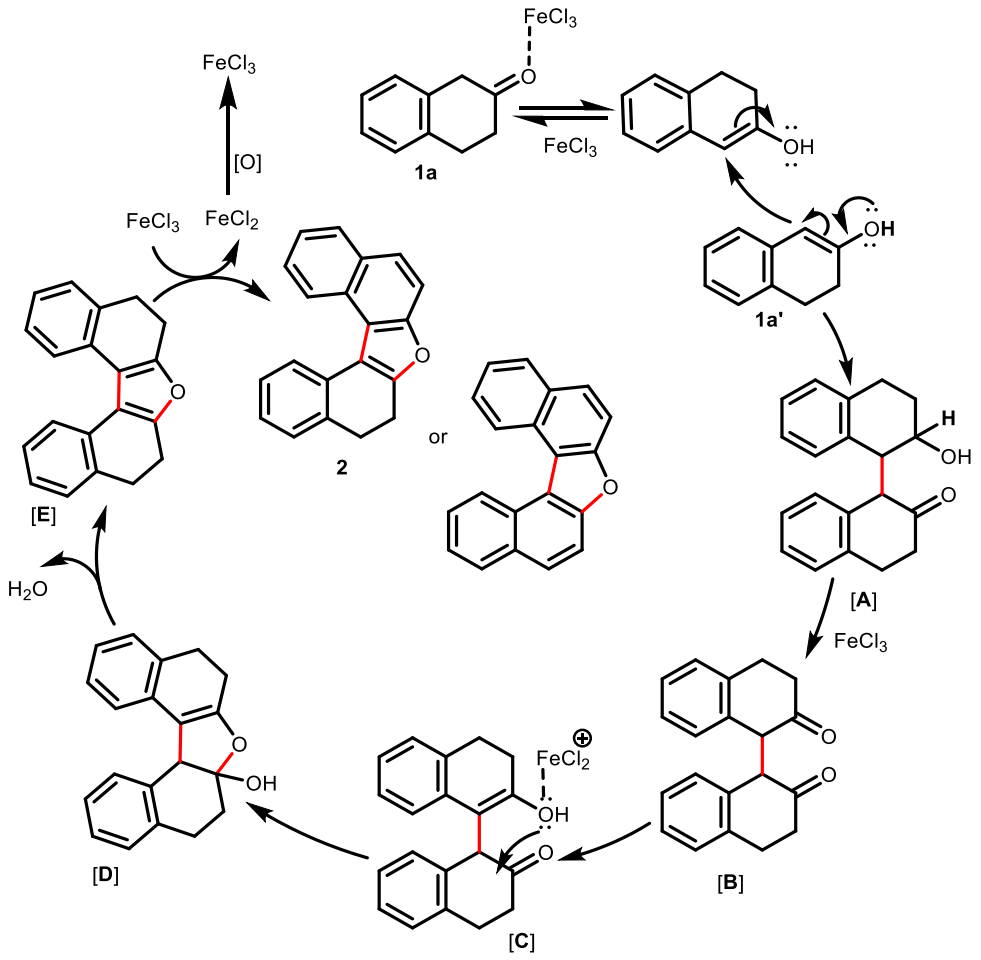

Scheme 27. A plausible mechanism for the formation of dinaphthofurans **2**.

Next, we target to synthesize different dicoumarol derivatives via a CH_2 insertion from DMSO under the same reaction conditions. Interestingly we have isolated polyfunctional furocoumarins derivatives **3**, which are obtain through decarboxylation, cyclization, and dehydrogenation.

Subsequently, to check the electronic and steric effect of the substitute variation at 4-hydroxycoumarin, first, electron-rich 6-methyl **1g**, 7-methoxy **1h,** and 7-hydroxy **1i** were examined under the same reaction condition. To our delight, the desired products **3b**, **3c**, and **3d** were isolated in 89%, 85%, and 81% yields, respectively.

Surprisingly, electron-withdrawing 4-hydroxycoumarin 6-chloro **1j** and 6-fluoro **1k** also reacted very well to provide the desired products **3e** and **3f** in a 78% and 90% yield as depicted in Table 15. It is important to mention that C-3 carbon in polyfunctional furocoumarin is

coming from the solvent DMSO. Due to polyfunctionality in a molecule, a wide range of potential reactions can be carried out to access new chemical entities.

Table 15. The substrate scope of furocoumarins[a,b]

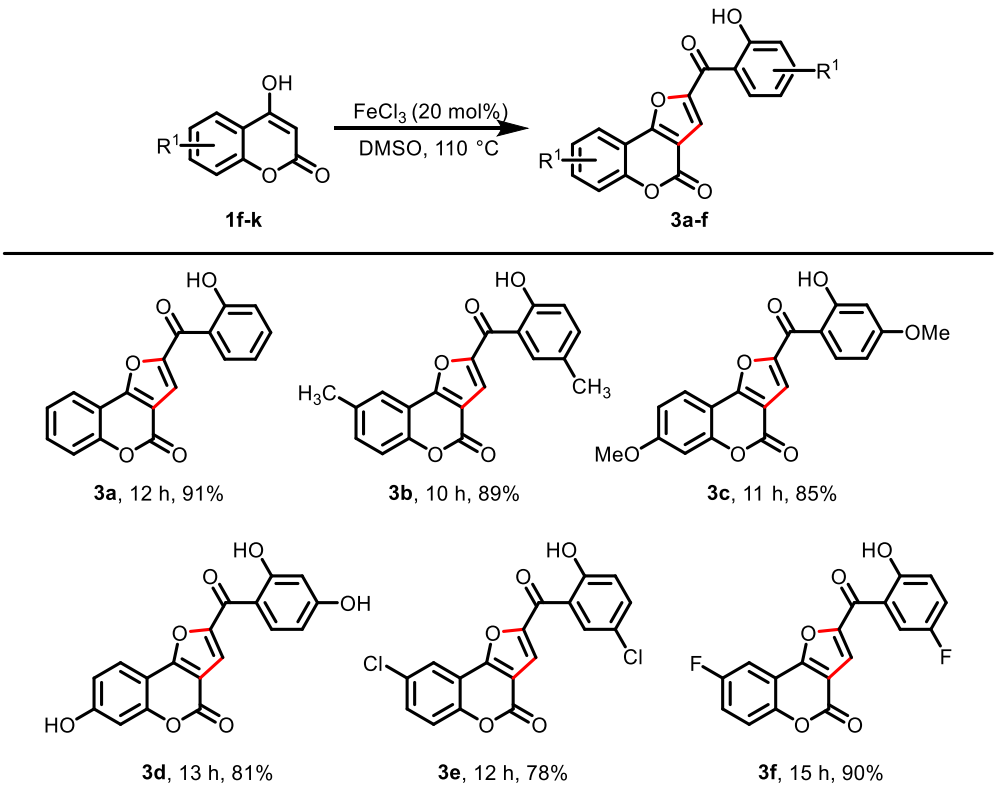

[a]Reaction conditions: All the reactions were performed using 4-hydroxycoumarins (**1f-k**, 1.0 mmol) in the presence of $FeCl_3$ in 2 mL DMSO at 100 °C. [b]Isolated yield.

To check the substrate scope of the product **3,** it was further transformed into various ether derivatives using alkyne/allyl/aryl bromide in the presence of K_2CO_3 in dry acetone at room temperature. The successful results depicted that product **3** has a broad substrate scope, and the substitution patterns on aromatic rings were well tolerated and uniformly furnished the desired product in 68 to 85% yield (Table 16). Later, acetylation of product **3a** was also executed to check the reactivity additionally, and as expected, it gave the desired product with an 80% yield as demonstrated in Table 16.

Table 16. The substrate scope of products 3[a,b]

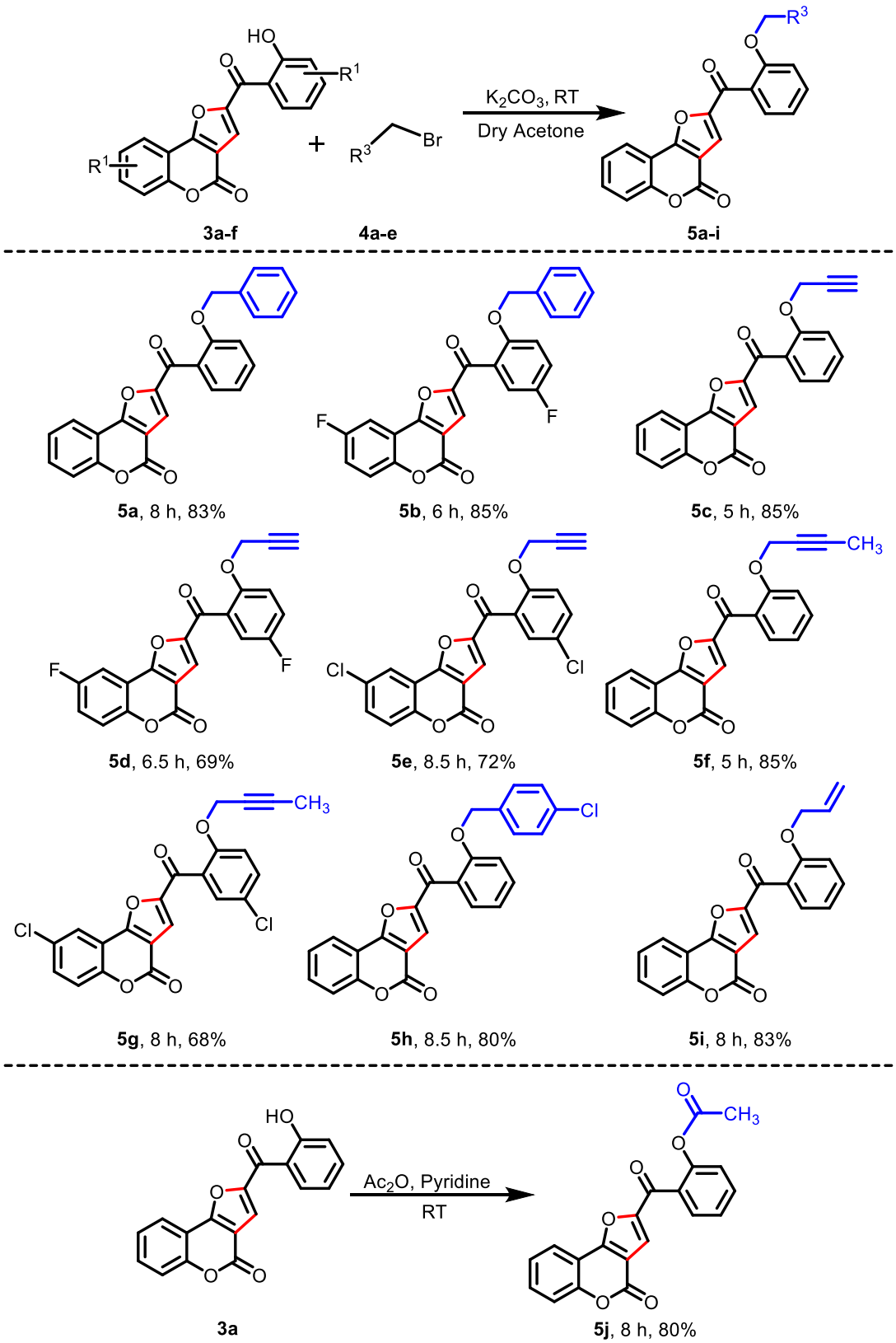

[a]Reaction conditions: All the reactions were performed using polyfunctional furocoumarins (**3**, 1.0 mmol) and alkyne/allyl/aryl bromide (**4a-e**, 1.0 mmol) in the presence of K_2CO_3 in dry acetone at room temperature. [b]Isolated yield.

Next, to obtain the expected product **6a** from product **5c,** the sigmatropic rearrangement was executed as shown in Scheme 28a. Unfortunately, we did not obtain the expected product **6a** instead of that the starting material was recovered **3a** by the clevage of the propargyl ether.

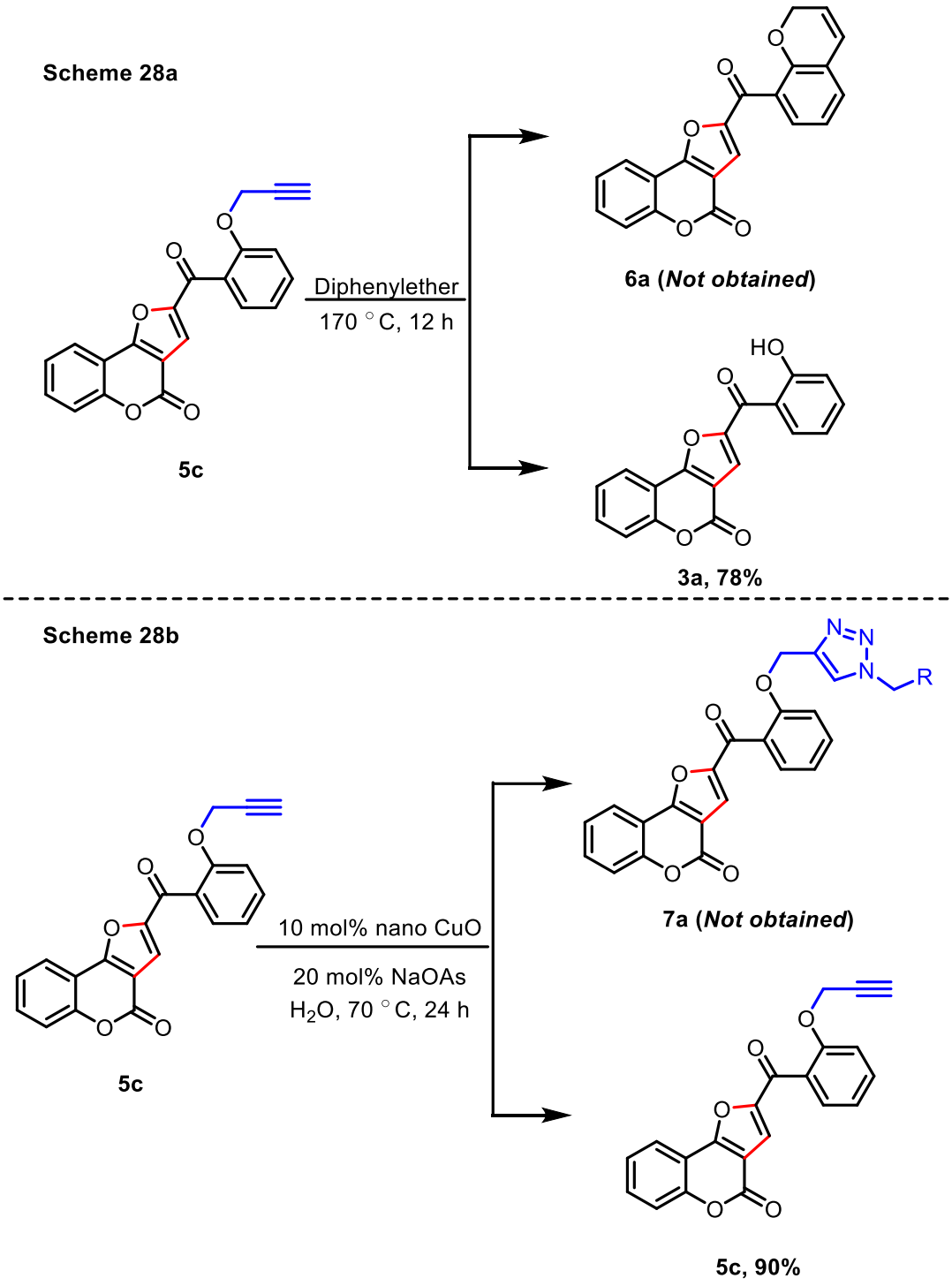

Scheme 28 Experiments towards the synthesis of **6a** and **7a**.

Next, we put forward our synthetic effort towards the synthesis of triaole derivative **7a** as depicted in Scheme 28b. Despite our effort we could not obtain the expected product **7a.5**

Based on preliminary experiments depicted in Scheme 29 and previous literature reports,[20] a proposed mechanism is illustrated in Scheme 30. Initially, sulfenium is generated from DMSO in the presence of $FeCl_3$. After that, 4-hydroxycoumarin **1f** attacks the sulfenium ion to generate an intermediate [**A**]. Next, another molecule of 4-hydroxycoumarin **1f** attacks the intermediate [**A**] and releases the methanethiol to generate the intermediate [**B**]. $FeCl_3$ in DMSO solvent undergoes a disproportionation reaction to give reactive Lewis-acid species $[FeCl_2]^+$ and $[FeCl_4]^-$. $[FeCl_2]^+$ coordinates with the lactone ring's oxygen, facilitating the tautomerization of the enol form to the keto form [**D**].

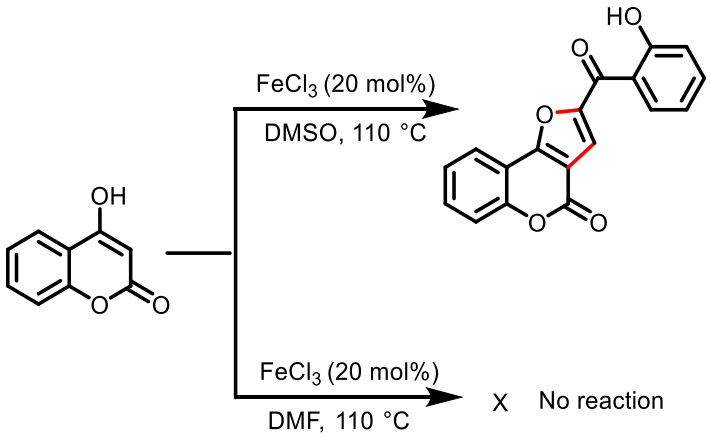

Scheme 29. Preliminary experiment.

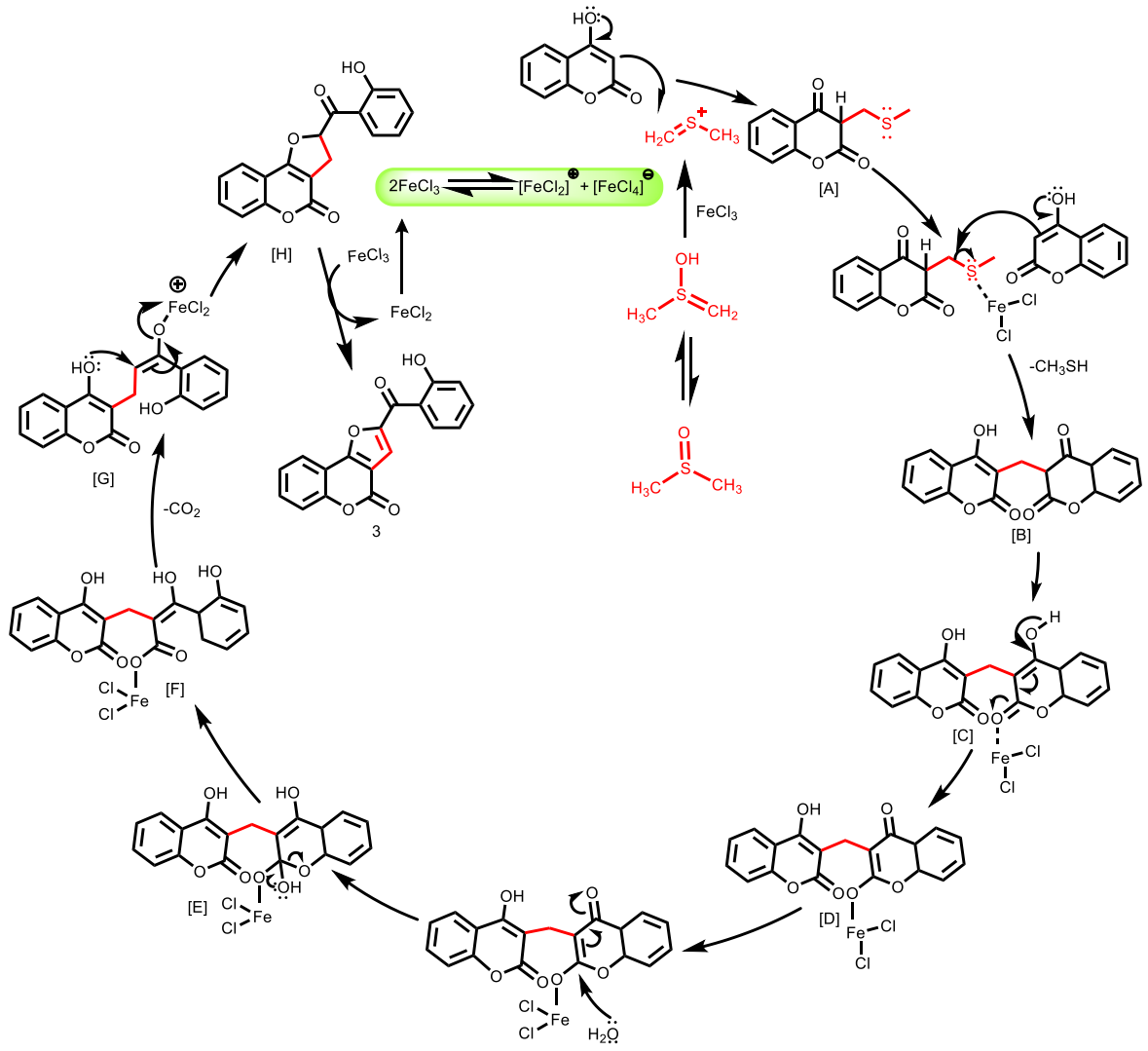

Scheme 30. A plausible mechanism for the formation of polyfunctional furocoumarins **3**

Next, the water molecule attacks the intermediate [**D**] to form the intermediate [**E**]. Intermediate [**F**] is formed due to the ring opening of intermediate [**E**]. Finally, decarboxylation occurs, and a lone pair of oxygen attacks the double bond to form the cyclic intermediate [**H**]. At last, $FeCl_3$ oxidizes the intermediate [**H**] to form the desired product **3a**. The reduced $FeCl_2$ undergoes aerial oxidation to form the $FeCl_3$ and is again involved in the catalytic cycle.

Conclusion

In summary, the synthesis of dinaphthofurans and polyfunctional furocoumarins has been achieved using $FeCl_3$ in DMSO as a solvent at 100 °C. Later, the substrate scope of product **3** was further explored to synthesize novel ether so that it can be further converted into triazoles or undergo a [3-3] sigmatropic rearrangement though both reactions are unsuccessful. In the synthesis of dinaphthofurans, intermolecular cross-coupling, cyclization, and dehydrogenation

occur in a single step, whereas in the case of polyfunctional furocoumarins-solvent act as a reactant, intermolecular coupling, decarboxylation, cyclization, and dehydrogenation occurs in a single step. The advantages of this method are that the reactions are well tolerated with the substitution pattern, high regioselectivity, good yield, and non-requirement of any ligand, additive, or co-catalyst. Here DMSO acts as a solvent cum reaction for the formation of product **3**, making this protocol more interesting.

General Procedure for the Synthesis of Dinaphthofurans 2.

In a dry 25 mL round-bottomed flask, β-tetralones (**1a-1e**, 1.0 mmol) were dissolved in 2 mL of DMSO. Then, 20 mol% $FeCl_3$ catalysts were mixed with the reaction mixture and placed in a 100 ^oC pre-heated oil bath with constant stirring under an air atmosphere. The progress of the reaction was monitored by checking TLC from time to time. After the completion of the reaction, the color of the reaction mixture became Dark reddish. Then, it was brought to room temperature, and the resulting mixture was diluted with 10 mL DCM. The organic layer was washed with brine solution (5 mL x 2). The organic layer was extracted and dried over anhydrous sodium sulfate, and the solvent was removed in a rotary evaporator. At last, the crude residue was passed through a silica gel column (60-120 mesh) to obtain the pure and desired products.

General Procedure for the Synthesis of Furocoumarins 3.

In a dry 25 mL round-bottomed flask, 4-hydroxycoumarin (**1f-1k**, 1.0 mmol) was dissolved in 2 mL of DMSO. Next, 20 mol% $FeCl_3$ catalysts were added to the reaction mixture and placed in a 100 ^oC pre-heated oil bath with constant stirring under an air atmosphere. The progress of the reaction was monitored by checking TLC from time to time. After the completion of the reaction, the reaction mixture became a Dark reddish color. Then, it was brought to room temperature, and the resulting mixture was diluted with 10 mL DCM. The organic layer was washed with brine solution (5 mL x 2). The organic layer was washed with brine solution (5 mL x 2). The organic layer was extracted and dried over anhydrous sodium sulfate, and the solvent was removed in a rotary evaporator. At last, the crude residue was passed through a silica gel column (60-120 mesh) to obtain the pure and desired products.

General Procedure for the Synthesis of Product 5.

In a dry 25 mL round-bottomed flask, furocoumarins (**3**, 1.0 mmol) and allyl/aryl bromide (**4a-e**, 1.0 mmol) were dissolved in 2 mL of dry acetone. Then, 2 equiv. of K_2CO_3 was added to the reaction mixture and placed at RT with constant stirring under an inert atmosphere. The progress of the reaction was monitored by checking TLC from time to time. After the completion of the reaction, the solvent from the reaction mixture was evaporated; the resulting mixture was diluted with 10 ml of ethyl acetate and was washed with water (2 x 10 ml). The organic layer was dried over anhydrous sodium sulfate, and the solvent was removed in a rotary

evaporator. Finally, the crude residue was passed through a silica gel column (60-120 mesh) to obtain the pure and desired products.

5,6-Dihydrodinaphtho[2,1-*b*:1',2'-*d*]furan (2a) White solid (112.09 mg, 83%) mp 118−120 °C. ^{1}H NMR (600 MHz, $CDCl_3$) δ 8.75 (d, *J* = 8.4 Hz, 1H), 8.09 (d, *J* = 7.6 Hz, 1H), 7.99 (d, *J* = 8.1 Hz, 1H), 7.75 (d, *J* = 8.8 Hz, 1H), 7.67 (d, *J* = 8.8 Hz, 1H), 7.60 – 7.57 (m, 1H), 7.52 – 7.50 (m, 1H), 7.40 (t, *J* = 7.5 Hz, 1H), 7.36 (d, *J* = 7.2 Hz, 1H), 7.25 – 7.22 (m, 1H), 3.14 (t, *J* = 7.4 Hz, 2H), 3.02 (t, *J* = 7.6 Hz, 2H); ^{13}C NMR (150 MHz, Chloroform-*d*) δ 157.8, 153.0, 135.0, 132.3, 131.3, 129.2, 128.3, 128.0, 127.0, 126.0, 125.6, 125.2, 125.1, 124.9, 124.4, 120.2, 116.4, 112.5, 30.4, 22.9; IR (KBr)ν_{max}/cm^{-1} 1750, 1580, 1280; HRMS (ESI) Calcd For $C_{20}H_{15}O$ 271.1118 ($M+H^+$); Found 271.1096.

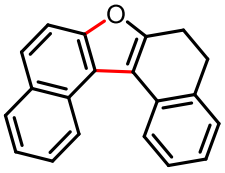

Dinaphtho[2,1-b:1',2'-d]furan (2a') White solid (112.09 mg, 83%) mp 122−123 °C. ^{1}H NMR (600 MHz, $CDCl_3$) δ 9.17 (d, *J* = 8.5 Hz, 1H), 8.08 (d, *J* = 8.0 Hz, 1H), 7.97 (d, *J* = 8.8 Hz, 1H), 7.86 (d, *J* = 8.8 Hz, 1H), 7.76 (t, *J* = 7.6 Hz, 1H), 7.60 (t, *J* = 7.4 Hz, 1H); ^{13}C NMR (150 MHz, $CDCl_3$) δ 154.5, 131.3, 129.6, 128.7, 128.4, 126.3, 125.7, 124.5, 119.5, 112.9; IR (KBr)ν_{max}/cm^{-1} 1580, 1280; HRMS (ESI) Calcd For $C_{20}H_{13}O$ 269.0961 ($M+H^+$); Found 269.0933.

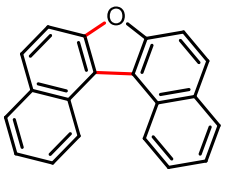

5,6-Dihydrodinaphtho[2,1-*b*:1',2'-*d*]furan-3,11-diol (2b) White solid (108.75 mg, 72%) mp 138−139 °C. ^{1}H NMR (600 MHz, DMSO-*d6*) δ 11.87 (s, 1H), 11.49 (s, 1H), 7.92 (t, *J* = 8.4 Hz, 2H), 7.61 (t, *J* = 7.6 Hz, 1H), 7.51 (t, *J* = 7.7 Hz, 1H), 7.38 – 7.35 (m, 2H), 6.97 – 6.92 (m, 2H), 3.25 – 3.23 (m, 2H), 2.88 – 2.86 (m, 2H); ^{13}C NMR (150 MHz, $CDCl_3$) δ 205.5, 162.8, 160.6, 160.3, 151.9, 136.1, 131.8, 130.7, 124.0, 123.2, 120.2, 119.7, 119.6, 119.2, 117.7, 116.3, 116.2, 103.6, 37.5, 19.1; IR (KBr)ν_{max}/cm^{-1} 1750, 1580, 1280; HRMS (ESI) Calcd For $C_{20}H_{15}O_3$ 303.1016 ($M+H^+$); Found 303.1019.

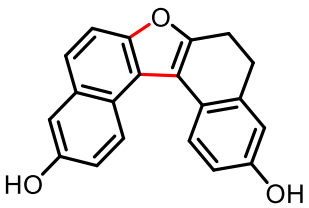

3,11-Dimethoxydinaphtho[2,1-*b*:1',2'-*d*]furan (2c) White solid (132.8 mg, 81%) mp 116−118 °C. ^{1}H NMR (500 MHz, $CDCl_3$) δ 9.01 (d, *J* = 8.8 Hz, 2H), 7.85 – 7.78 (m, 4H), 7.41 (d, *J* = 8.7 Hz, 4H), 4.00 (s, 6H); ^{13}C NMR (150 MHz, $CDCl_3$) δ 156.4, 153.4, 132.6, 127.2, 127.0, 123.7, 119.6, 117.9, 113.2, 108.5, 55.5; IR (KBr)ν_{max}/cm^{-1} 1750, 1580, 1280; HRMS (ESI) Calcd For $C_{22}H_{17}O_3$ 329.1173 ($M+H^+$); Found 329.1175.

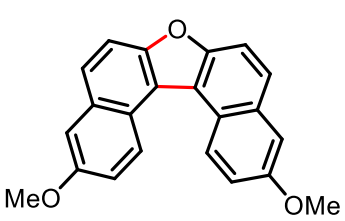

2,12-Dimethoxydinaphtho[2,1-*b*:1',2'-*d*]furan (2d) White solid (131.2 mg, 80%) mp 122−123 °C. 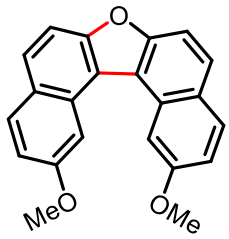

^{1}H NMR (500 MHz, $CDCl_3$) δ 8.50 (s, 2H), 7.99 (d, *J* = 8.8 Hz, 2H), 7.88 (d, *J* = 8.7 Hz, 2H), 7.69 (d, *J* = 8.7 Hz, 2H), 7.25 (d, *J* = 3.2 Hz, 2H), 4.05 (s, 6H); ^{13}C NMR (125 MHz, $CDCl_3$) δ 158.1, 154.9, 131.1, 129.9, 127.9, 126.4, 118.8, 115.1, 110.4, 107.3, 55.9; IR (KBr)ν_{max}/cm^{-1} 1750, 1580, 1280; HRMS (ESI) Calcd For $C_{22}H_{17}O_3$ 329.1173 ($M+H^+$); Found 329.0806.

2-(2-Hydroxybenzoyl)-4*H*-furo[3,2-*c*]chromen-4-one (3a) Light yellow solid (139.23 mg, 91%) mp 238−240 °C. 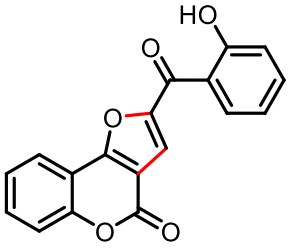

^{1}H NMR (600 MHz, $CDCl_3$) δ 11.70 (s, 1H), 8.16 (d, *J* = 8.0 Hz, 1H), 8.07 (d, *J* = 7.8 Hz, 1H), 7.82 (s, 1H), 7.66 (t, *J* = 7.8 Hz, 1H), 7.59 (t, *J* = 7.7 Hz, 1H), 7.51 (d, *J* = 8.4 Hz, 1H), 7.45 (t, *J* = 7.6 Hz, 1H), 7.11 (d, *J* = 8.4 Hz, 1H), 7.04 (t, *J* = 7.6 Hz, 1H); ^{13}C NMR (150 MHz, $CDCl_3$) δ 184.6, 163.5, 159.9, 157.3, 153.9, 152.1, 137.2, 132.9, 130.9, 125.2, 122.1, 119.6, 119.0, 118.6, 118.3, 117.9, 112.0, 111.7; IR (KBr)ν_{max}/cm^{-1} 175, 1580, 1280; HRMS (ESI) Calcd For $C_{18}H_{11}O_5$ 307.0601 ($M+H^+$); Found 307.0576.

2-(2-Hydroxy-5-methylbenzoyl)-8-methyl-4*H*-furo[3,2-*c*]chromen-4-one (3b) Light yellow solid (148.6 mg, 89%) mp 232−233 °C. 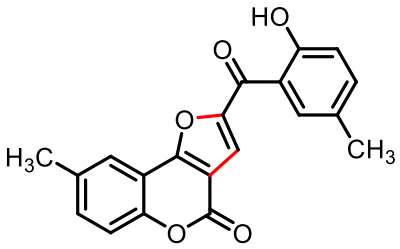

^{1}H NMR (600 MHz, $CDCl_3$) δ 11.45 (s, 1H), 7.84 (d, *J* = 17.3 Hz, 2H), 7.76 (s, 1H), 7.44 (d, *J* = 8.4 Hz, 1H), 7.38 (t, *J* = 10.6 Hz, 2H), 6.99 (d, *J* = 8.5 Hz, 1H), 2.49 (s, 3H), 2.38 (s, 3H); ^{13}C NMR (150 MHz, $CDCl_3$) δ 184.6, 161.3, 160.0, 157.6, 152.1, 151.7, 138.2, 135.3, 134.0, 130.4, 128.8, 121.7, 118.7, 118.3, 118.2, 117.5, 111.6, 111.6, 21.0, 20.8; IR (KBr)ν_{max}/cm^{-1} 1750, 1580, 1280; HRMS (ESI) Calcd For $C_{20}H_{15}O_5$ 335.0914 ($M+H^+$); Found 335.0896.

2-(2-Hydroxy-4-methoxybenzoyl)-7-methoxy-4*H*-furo[3,2-*c*]chromen-4-one (3c) Light yellow solid (155.55 mg, 85%) mp 255−256 °C. 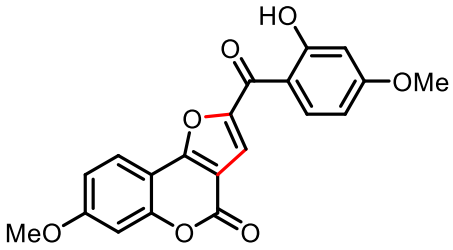

^{1}H NMR (600 MHz, $CDCl_3$) δ 12.50 (s, 1H), 8.11 (d, *J* = 9.0 Hz, 1H), 7.94 (d, *J* = 8.7 Hz, 1H), 7.74 (s, 1H), 7.01 (dd, *J* = 8.7, 2.3 Hz, 1H), 6.98 (d, *J* = 2.3 Hz, 1H), 6.57 (dd, *J* = 9.0, 2.5 Hz, 1H), 6.53 (d, *J* = 2.5 Hz, 1H), 3.93 (s, 3H), 3.90 (s, 3H); ^{13}C NMR (150 MHz, $CDCl_3$) δ 166.9, 163.6, 157.8, 155.8, 151.8, 132.6, 128.9,

123.1, 120.4, 117.5, 113.6, 112.5, 109.3, 108.6, 105.6, 105.3, 101.8, 101.4, 56.1, 55.9; IR (KBr)ν_{max}/cm^{-1} 1750, 1580, 1280; HRMS (ESI) Calcd For $C_{20}H_{15}O_7$ 367.0813 ($M+H^+$); Found 367.0818.

2-(2,4-Dihydroxybenzoyl)-7-hydroxy-4*H*-furo[3,2-*c*]chromen-4-one (3d) Light yellow solid (136.89 mg, 81%) mp 206−208.; ^{1}H NMR (600 MHz, DMSO-*d*6) δ 12.60 (s, 1H), 7.94 – 7.93 (m, 1H), 7.75 (d, *J* = 8.8 Hz, 1H), 7.37 – 7.30 (m, 2H), 6.99 (s, 1H), 6.86 (d, *J* = 7.9 Hz, 1H), 6.37 (dd, *J* = 8.8, 2.3 Hz, 1H), 6.24 (d, *J* = 2.3 Hz, 1H); ^{13}C NMR (150 MHz, DMSO-*d*6) δ 202.7, 164.2, 159.7, 155.9, 155.2, 150.9, 133.7, 128.1, 123.2, 114.3, 112.8, 111.2, 110.6, 108.1, 102.2, 78.7; IR (KBr)ν_{max}/cm^{-1} 1750, 1580, 1280; HRMS (ESI) Calcd For $C_{18}H_{11}O_7$ 339.0500 ($M+H^+$); Found 339.0503.

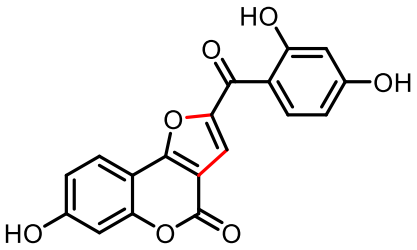

8-Chloro-2-(5-chloro-2-hydroxybenzoyl)-4*H*-furo[3,2-*c*]chromen-4-one (3e) Light yellow solid (146.25 mg, 78%) mp 210−212 °C. ^{1}H NMR (600 MHz, DMSO-*d*$_6$) δ 10.59 (s, 1H), 8.03 (d, *J* = 2.5 Hz, 1H), 7.79 (s, 1H), 7.77 (dd, *J* = 8.9, 2.5 Hz, 1H), 7.64 (d, *J* = 8.9 Hz, 1H), 7.51 – 7.48 (m, 2H), 7.03 (d, *J* = 8.7 Hz, 1H); ^{13}C NMR (150 MHz, DMSO-*d*$_6$) δ 181.3, 158.0, 156.4, 155.2, 153.0, 152.0, 133.2, 132.7, 129.4, 129.1, 126.0, 122.9, 121.1, 119.6, 118.9, 118.0, 113.1, 112.4; IR (KBr)ν_{max}/cm^{-1} 1750, 1580, 1280; HRMS (ESI) Calcd For $C_{18}H_9Cl_2O_5$ 374.9822 ($M+H^+$); Found 374.3035.

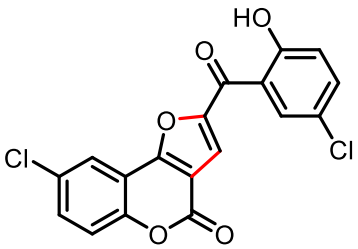

8-Fluoro-2-(5-fluoro-2-hydroxybenzoyl)-4*H*-furo[3,2-*c*]chromen-4-one (3f) Light yellow solid (154.01 mg, 90%) mp 215−216 °C. ^{1}H NMR (600 MHz, $CDCl_3$) δ 11.50 (s, 1H), 7.88 (q, *J* = 4.2, 3.6 Hz, 2H), 7.73 (dd, *J* = 7.3, 2.9 Hz, 1H), 7.50 (dd, *J* = 9.1, 4.2 Hz, 1H), 7.40 – 7.34 (m, 2H), 7.09 (dd, *J* = 9.2, 4.6 Hz, 1H); ^{13}C NMR (150 MHz, $CDCl_3$) δ 183.5 ($J_{C\text{-}F}$ = 2.65 Hz), 160.0 ($J_{C\text{-}F}$ = 0.9 Hz), 159.2 ($J_{C\text{-}F}$ = 245.62 Hz), 159.1 ($J_{C\text{-}F}$ = 2.89 Hz), 156.7, 155.2 ($J_{C\text{-}F}$ = 238.29 Hz), 152.4, 150.1 ($J_{C\text{-}F}$ = 2.13 Hz), 125.1 ($J_{C\text{-}F}$ = 23.53 Hz), 120.6 ($J_{C\text{-}F}$ = 24.43 Hz), 120.5 ($J_{C\text{-}F}$ = 7.26 Hz), 119.8 ($J_{C\text{-}F}$ = 8.44 Hz), 118.5, 117.7 ($J_{C\text{-}F}$ = 6.69 Hz), 115.8 ($J_{C\text{-}F}$ = 24.33 Hz), 112.6 ($J_{C\text{-}F}$ = 9.72 Hz), 112.4, 107.9 ($J_{C\text{-}F}$ = 25.78 Hz); ^{19}F NMR (565 MHz, $CDCl_3$) δ -114.71, -122.58; IR (KBr)ν_{max}/cm^{-1} 1750, 1580, 1280; HRMS (ESI) Calcd For $C_{18}H_9F_2O_5$ 343.0413 ($M+H^+$); Found 343.0400.

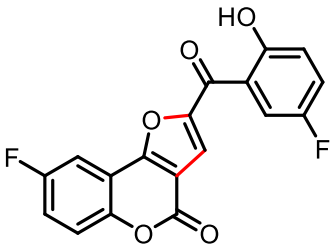

2-(2-(Benzyloxy)benzoyl)-4*H*-furo[3,2-*c*]chromen-4-one (5a) Light yellow solid (164.50 mg, 83%) mp 238−240 °C. ^{1}H NMR (600 MHz, $CDCl_3$) δ 7.97 (d, *J* = 7.7 Hz, 1H), 7.60 (t, *J* = 7.8 Hz, 1H), 7.55 – 7.51 (m, 2H), 7.47 (s, 1H), 7.45 (d, *J* = 8.4 Hz, 1H), 7.38 (t, *J* = 7.7 Hz, 1H), 7.20 – 7.17 (m, 5H), 7.10 (t, *J* = 8.6 Hz, 2H), 5.09 (s, 2H); ^{13}C NMR (150 MHz, $CDCl_3$) δ 182.9, 159.5, 157.5, 157.0, 153.9, 153.7, 136.0, 133.4, 132.5, 130.1, 128.5, 128.0, 127.6, 127.1, 125.0, 122.1, 121.1, 117.6, 117.4, 113.3, 112.1, 111.6, 70.7; IR (KBr)ν_{max}/cm^{-1} 1750, 1580, 1280; HRMS (ESI) Calcd For $C_{25}H_{17}O_5$ 397.1071 ($M+H^+$); Found 397.1071.

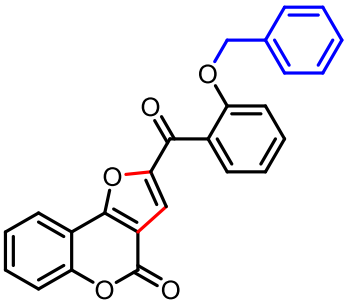

2-(2-(Benzyloxy)-5-fluorobenzoyl)-8-fluoro-4*H*-furo[3,2-*c*]chromen-4-one (5b) White solid Yield (183.6 mg, 85%) mp 216−218 °C. ^{1}H NMR (600 MHz, $CDCl_3$) δ 7.59 (dd, *J* = 7.5, 2.8 Hz, 1H), 7.51 (s, 1H), 7.43 (dd, *J* = 9.1, 4.2 Hz, 1H), 7.33 – 7.30 (m, 1H), 7.23 (dd, *J* = 9.3, 6.3 Hz, 2H), 7.17 – 7.14 (m, 5H), 7.05 (dd, *J* = 9.0, 3.9 Hz, 1H), 5.05 (s, 2H); ^{13}C NMR (150 MHz, $CDCl_3$) δ 181.4 (J_{C-F} = 1.03 Hz), 159.0 (J_{C-F} = 244.98 Hz), 158.6 (J_{C-F} = 2.68 Hz), 156.9 (J_{C-F} = 240.87 Hz), 156.9, 153.8, 153.2 (J_{C-F} = 2.07 Hz), 149.9 (J_{C-F} = 1.9 Hz), 135.7, 128.5, 128.3 (J_{C-F} = 6.52 Hz), 128.2, 127.1, 120.2, 120.0 (J_{C-F} = 5.34 Hz), 119.8, 119.5 (J_{C-F} = 8.47 Hz), 117.2, 116.7 (J_{C-F} = 24.45 Hz), 114.9 (J_{C-F} = 7.59 Hz), 112.7 (J_{C-F} = 9.66 Hz), 112.2, 107.8 (J_{C-F} = 25.75 Hz), 71.6; ^{19}F NMR (565 MHz, $CDCl_3$) δ -115.25, -121.73; IR (KBr)ν_{max}/cm^{-1} 1750, 1580, 1280; HRMS (ESI) Calcd For $C_{25}H_{15}F_2O_5$ 433.0883 ($M+H^+$); Found 433.0882.

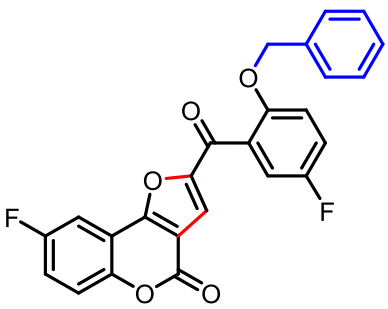

2-(2-(Prop-2-yn-1-yloxy)benzoyl)-4*H*-furo[3,2-*c*]chromen-4-one (5c) White solid Yield 85% (146.33 mg, 85%) mp 212−213 °C. ^{1}H NMR (600 MHz, $CDCl_3$) δ 8.04 (dd, *J* = 7.8, 1.3 Hz, 1H), 7.63 – 7.60 (m, 1H), 7.57 – 7.54 (m, 1H), 7.53 – 7.51 (m, 2H), 7.46 (d, *J* = 8.3 Hz, 1H), 7.41 – 7.38 (m, 1H), 7.18 (d, *J* = 8.4 Hz, 1H), 7.14 (t, *J* = 7.5 Hz, 1H), 4.72 (d, *J* = 2.4 Hz, 2H), 2.49 (t, *J* = 2.4 Hz, 1H); ^{13}C NMR (150 MHz, $CDCl_3$) δ 182.5, 159.9, 157.5, 155.4, 153.8, 153.6, 133.1, 132.7, 130.1, 127.8, 125.1, 122.3, 121.8, 118.3, 117.7, 113.4, 112.2, 111.8, 77.8, 76.5, 56.3; IR (KBr)ν_{max}/cm^{-1} 1750, 1580, 1280; HRMS (ESI) Calcd For $C_{21}H_{13}O_5$ 345.0758 ($M+H^+$); Found 345.0758.

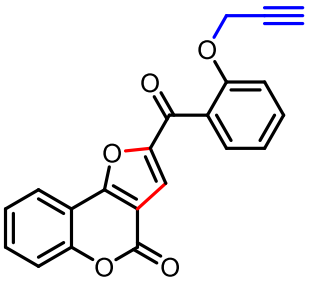

8-Fluoro-2-(5-fluoro-2-(prop-2-yn-1-yloxy)benzoyl)-4*H*-furo[3,2-*c*]chromen-4-one (5d)

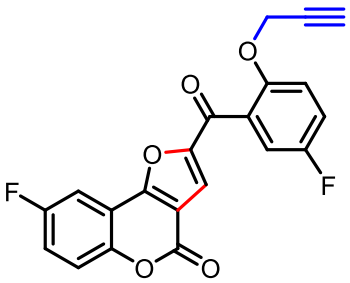

White solid (131.1 mg, 69%) mp 258−259 °C. ^{1}H NMR (400 MHz, $CDCl_3$) δ 7.71 (dd, *J* = 7.5, 2.9 Hz, 1H), 7.57 (s, 1H), 7.46 (dd, *J* = 9.2, 4.2 Hz, 1H), 7.36 – 7.27 (m, 2H), 7.25 – 7.23 (m, 1H), 7.16 (dd, *J* = 8.9, 4.0 Hz, 1H), 4.69 (d, *J* = 2.4 Hz, 2H), 2.52 (t, *J* = 2.4 Hz, 1H); ^{13}C NMR (100 MHz, $CDCl_3$) δ 181.0, 176.5, 157.0, 153.6, 151.5 (J_{C-F} = 2.49 Hz), 150.1, 120.3 (J_{C-F} = 24.41 Hz), 119.7, 119.6, 119.5 (J_{C-F} = 3.88 Hz), 118.1, 116.9, 116.7, 115.2 (J_{C-F} = 7.44 Hz), 114.9 (J_{C-F} = 3.23 Hz), 112.9, 112.5, 108.1 (J_{C-F} = 25.73 Hz), 77.3, 76.8, 57.0; ^{19}F NMR (376 MHz, $CDCl_3$) δ -115.24, -120.87; IR (KBr)ν_{max}/cm^{-1} 1750, 1580, 1280; HRMS (ESI) Calcd For $C_{21}H_{11}F_2O_5$ 381.0570 ($M+H^+$); Found 381.0570.

8-Chloro-2-(5-chloro-2-(prop-2-yn-1-yloxy)benzoyl)-4*H*-furo[3,2-*c*]chromen-4-one (5e)

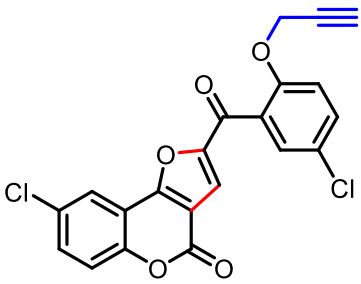

White solid (148.68 mg, 72%) mp 252−253 °C. ^{1}H NMR (400 MHz, DMSO-d_6) δ 8.06 (d, *J* = 2.4 Hz, 1H), 7.80 (s, 1H), 7.78 (dd, *J* = 8.9, 2.5 Hz, 1H), 7.69 (dd, *J* = 9.0, 2.7 Hz, 1H), 7.66 – 7.63 (m, 1H), 7.60 (d, *J* = 2.7 Hz, 1H), 7.34 (d, *J* = 9.0 Hz, 1H), 4.88 (d, *J* = 2.4 Hz, 2H), 3.54 (t, *J* = 2.4 Hz, 1H); ^{13}C NMR (100 MHz, DMSO-*d*6) δ 180.4, 156.1, 153.9, 152.9, 151.8, 132.6, 132.5, 129.3, 128.4, 125.2, 121.2, 121.1, 119.4, 118.5, 118.0, 115.8, 112.9, 112.2, 78.9, 78.3, 69.7; IR (KBr)ν_{max}/cm^{-1} 1750, 1580, 1280; HRMS (ESI) Calcd For $C_{21}H_{11}Cl_2O_5$ 412.9979 ($M+H^+$); Found 412.9973.

2-(2-(But-2-yn-1-yloxy)benzoyl)-4*H*-furo[3,2-*c*]chromen-4-one (5f) White solid (152.15

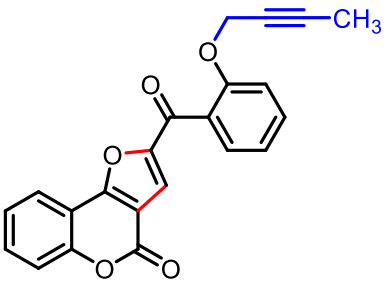

mg, 85%) mp 218−220 °C. ^{1}H NMR (600 MHz, $CDCl_3$) δ 8.06 (dd, *J* = 7.8, 1.3 Hz, 1H), 7.62 (ddd, *J* = 8.7, 7.5, 1.6 Hz, 1H), 7.56 – 7.51 (m, 3H), 7.47 (d, *J* = 8.1 Hz, 1H), 7.42 – 7.39 (m, 1H), 7.17 (d, *J* = 8.4 Hz, 1H), 7.13 – 7.11 (m, 1H), 4.67 (q, *J* = 2.2 Hz, 2H), 1.81 (t, *J* = 2.3 Hz, 3H); ^{13}C NMR (150 MHz, $CDCl_3$) δ 182.7, 159.8, 157.6, 155.8, 153.8, 153.8, 133.1, 132.6, 130.0, 127.8, 125.1, 122.3, 121.4, 118.2, 117.7, 113.5, 112.2, 111.8, 84.7, 73.4, 56.9, 3.7; IR (KBr)ν_{max}/cm^{-1} 1750, 1580, 1280; HRMS (ESI) Calcd For $C_{22}H_{15}O_5$ 359.0914 ($M+H^+$); Found 359.0915.

2-(2-(But-2-yn-1-yloxy)-5-chlorobenzoyl)-8-chloro-4*H*-furo[3,2-*c*]chromen-4-one (5g)

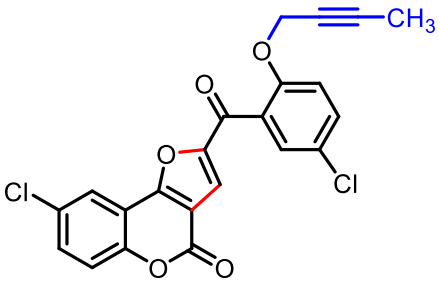

White solid (145.18 mg, 68%) mp 208−210 °C. ^{1}H NMR (400 MHz, $CDCl_3$) δ 8.01 (d, *J* = 2.4 Hz, 1H), 7.58 – 7.55 (m, 2H), 7.52 – 7.48 (m, 2H), 7.42 (d, *J* = 8.9 Hz, 1H), 7.13 (d, *J* = 8.7 Hz, 1H), 4.65 (q, *J* = 2.3 Hz, 2H), 1.83 (t, *J* = 2.3 Hz, 3H); ^{13}C NMR (100 MHz, $CDCl_3$) δ 181.2, 158.5, 156.8, 154.3, 153.8, 152.2, 132.9, 132.7, 130.8, 129.7, 128.8, 126.8, 121.7, 119.2, 117.9, 115.1, 113., 112.4, 83.3, 72.9, 57.2, 3.7; IR (KBr)ν_{max}/cm^{-1} 1750, 1580, 1280; HRMS (ESI) Calcd For $C_{22}H_{13}Cl_2O_5$ 427.0135 ($M+H^+$); Found 427.0133.

2-(2-((4-Chlorobenzyl)oxy)benzoyl)-4*H*-furo[3,2-*c*]chromen-4-one (5h) White solid (172 mg, 80%), mp 212−213 °C. ^{1}H NMR (500 MHz, $CDCl_3$) δ 8.08 (d, *J* = 7.8 Hz, 1H), 7.72 (t, *J* = 7.9 Hz, 1H), 7.64 – 7.61 (m, 2H), 7.57 (t, *J* = 4.2 Hz, 2H), 7.51 – 7.47 (m, 2H), 7.42 (td, *J* = 8.9, 4.6 Hz, 2H), 7.36 (s, 1H), 7.21 (t, *J* = 7.5 Hz, 1H), 7.16 (d, *J* = 8.2 Hz, 1H), 5.16 (s, 2H); ^{13}C NMR (125 MHz, $CDCl_3$) δ 182.7, 159.7, 157.4, 156.7, 153.8, 134.6, 133.9, 133.4, 132.6, 130.5, 130.1, 128.7, 128.5, 127.6, 125.0, 122.1, 121.4, 117.7, 117.7, 113.4, 112.1, 111.6, 70.1; IR (KBr)ν_{max}/cm^{-1} 1750, 1580, 1280; HRMS (ESI) Calcd For $C_{25}H_{16}ClO_5$ 431.0681 ($M+H^+$); Found 431.0681.

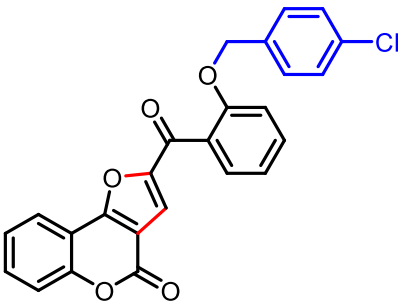

2-(2-(Allyloxy)benzoyl)-4*H*-furo[3,2-*c*]chromen-4-one (5i) White solid (143.59 mg, 83%) mp 251−252 °C. ^{1}H NMR (600 MHz, $CDCl_3$) δ 8.03 (dd, *J* = 7.8, 1.2 Hz, 1H), 7.63 – 7.60 (m, 1H), 7.53 – 7.50 (m, 3H), 7.47 (d, *J* = 8.3 Hz, 1H), 7.40 (t, *J* = 7.6 Hz, 1H), 7.09 (t, *J* = 7.4 Hz, 1H), 7.03 (d, *J* = 8.7 Hz, 1H), 5.87 (ddd, *J* = 22.3, 10.4, 5.1 Hz, 1H), 5.25 – 5.22 (m, 1H), 5.15 – 5.13 (m, 1H), 4.57 (d, *J* = 5.1 Hz, 2H); ^{13}C NMR (150 MHz, $CDCl_3$) δ 182.8, 159.7, 157.6, 156.7, 153.8, 153.8, 133.3, 132.6, 132.3, 130.0, 127.4, 125.1, 122.2, 121.0, 117.9, 117.8, 117.7, 113.1, 112.2, 111.7, 69.4; IR (KBr)ν_{max}/cm^{-1} 1750, 1580, 1280; HRMS (ESI) Calcd For $C_{21}H_{15}O_5$ 347.0914 ($M+H^+$); Found 347.0922.

2-(4-Oxo-4*H*-furo[3,2-*c*]chromene-2-carbonyl)phenyl acetate (5j) Cream whitish solid (139.2 mg, 80%) mp 255−256 °C. ^{1}H NMR (600 MHz, $CDCl_3$) δ 8.05 (dd, *J* = 7.8, 1.3 Hz, 1H), 7.72 (dd, *J* = 7.6, 1.4 Hz, 1H), 7.64 (t, *J* = 7.9 Hz, 2H), 7.59 (s, 1H), 7.48 (d, *J* = 8.4 Hz, 1H), 7.41 (q, *J* = 7.2 Hz, 2H), 7.27 (d, *J* = 6.6 Hz, 1H), 2.21 (s, 3H); ^{13}C NMR (150 MHz, $CDCl_3$) δ 180.7, 169.3, 160.3, 157.3, 153.9, 152.7, 149.0, 133.4, 133.0, 130.0, 129.8, 126.0, 125.2, 123.9, 122.4, 118.8, 117.8, 111.9, 111.7, 20.9; IR (KBr)ν_{max}/cm^{-1} 1750, 1580, 1280; HRMS (ESI) Calcd For $C_{20}H_{13}O_6$ 349.0707 ($M+H^+$); Found 349.0709.

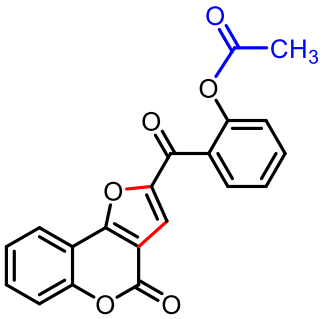

XRD for compound (2c): All the data for the structural analysis of compound **2c** has been deposited to the Cambridge Crystallographic Data Centre, CCDC No. 2289424.

Table 17. Crystal data and structure refinement for compound **2c**

Entry	Identification Code	Compound 2c
01	Empirical formula	$C_{22}H_{16}O_3$
02	Formula weight	328.35
03	Temperature	298.00
04	Wavelength	0.71073 Å
05	Radiation type	MoKα
06	Radiation system	Fine-focus sealed tube
07	Crystal system	orthorhombic
08	Space group	$P2_12_12_1$
09	Cell length	a= 5.8970(4) /Å b= 11.2252(8) /Å c= 23.7345(16) /Å
10	Cell angle	α=90 β=90 γ=90
11	Cell volume	1571.11(19)
12	Density	1.388
13	Completeness to theta	99
14	Absorption correction	multi-scan
15	Refinement method	Full-matrix least-squares on F2
16	Index ranges	$-7 \leq h \leq 7$, $-14 \leq k \leq 14$, $-29 \leq l \leq 29$
17	Reflection number	41161
18	2Θ range	3.432 to 52.776
19	Cell formula units Z	4
20	CCDC no	2289424

^{1}H NMR Spectrum of 5,6-Dihydrodinaphtho[2,1-*b*:1',2'-*d*]furan (2a)

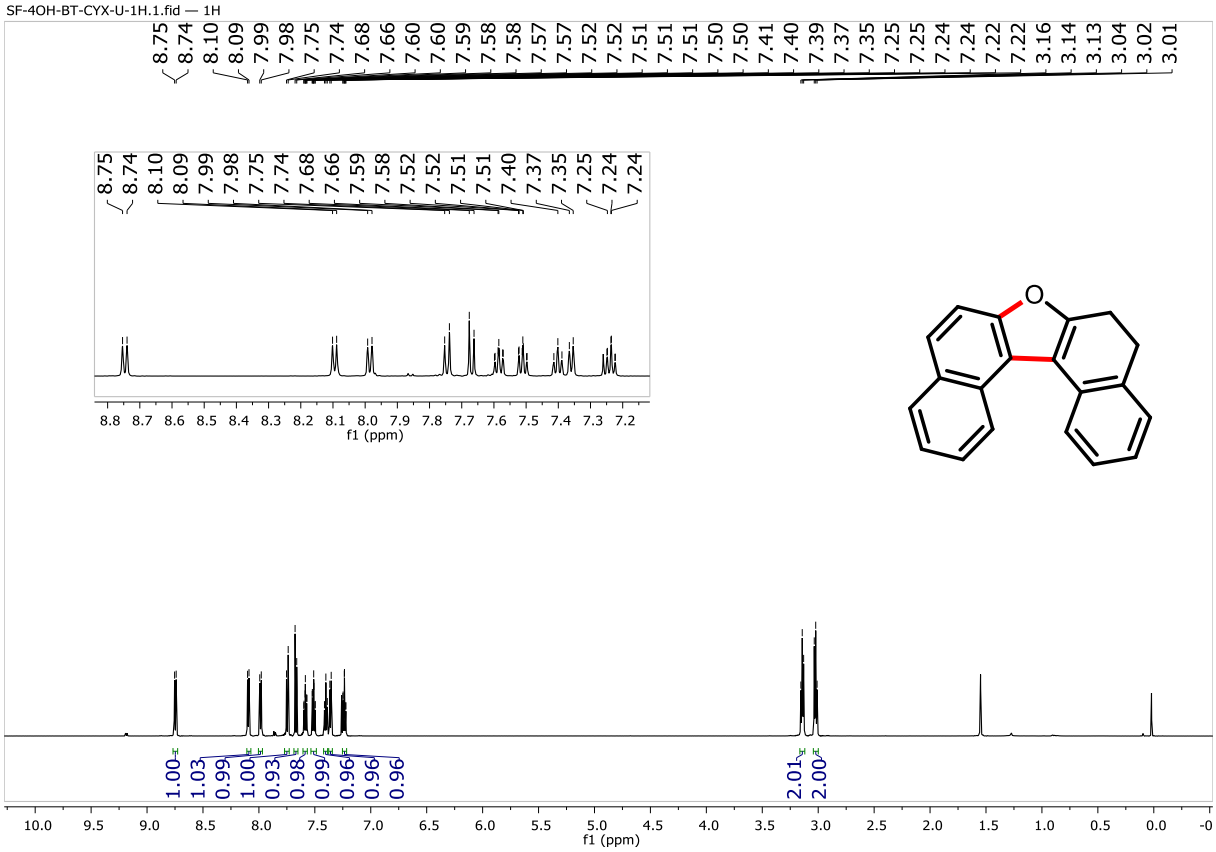

^{13}C NMR Spectrum of 5,6-Dihydrodinaphtho[2,1-*b*:1',2'-*d*]furan (2a)

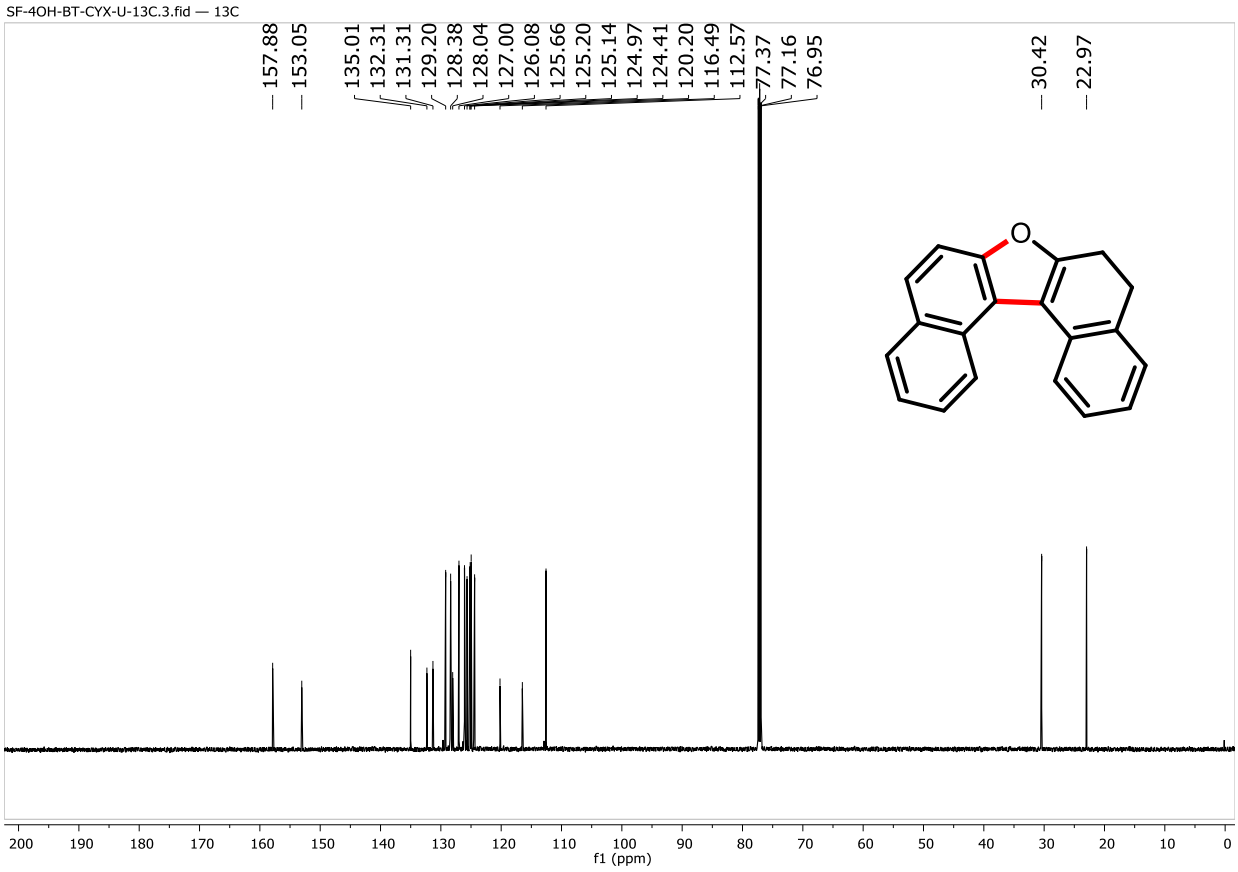

HRMS Spectrum of 5,6-Dihydrodinaphtho[2,1-*b*:1',2'-*d*]furan (2a)

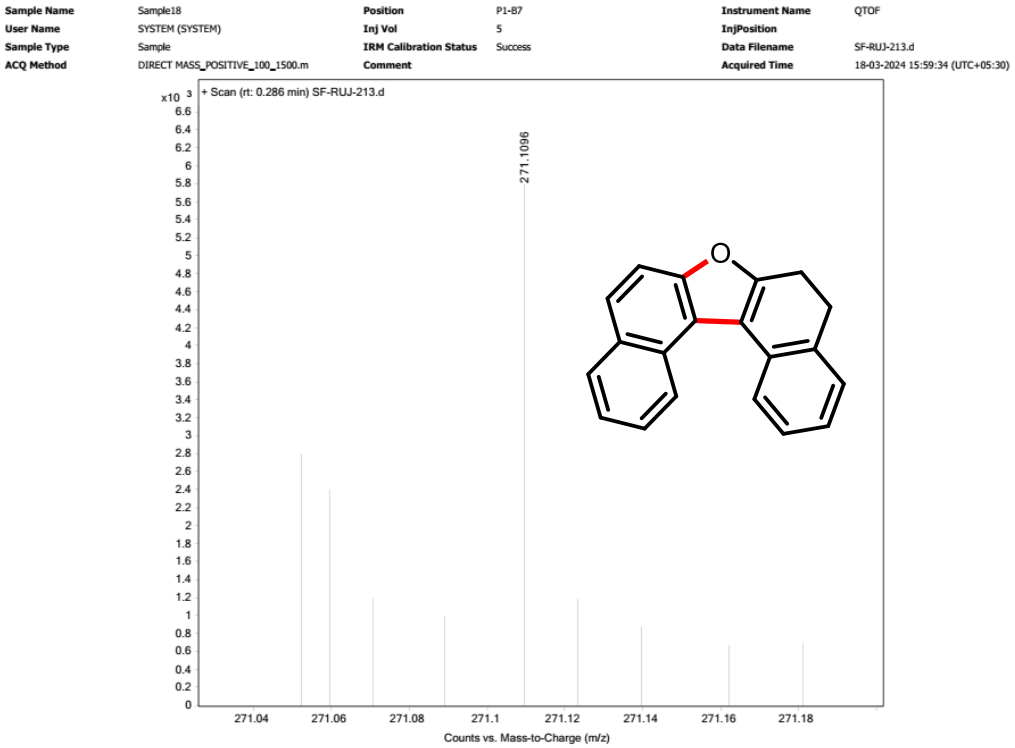

^{1}H NMR Spectrum of 2-(2-Hydroxybenzoyl)-4*H*-furo[3,2-*c*]chromen-4-one (3a)

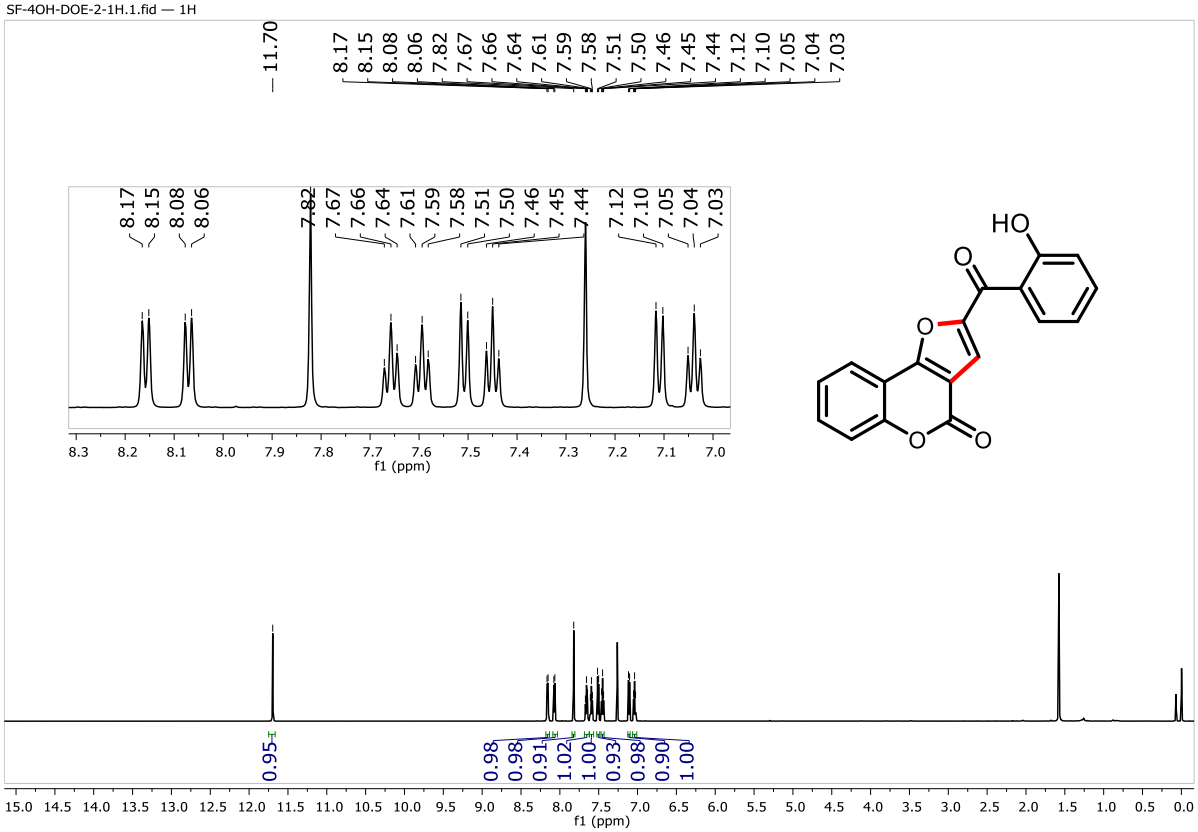

^{13}C NMR Spectrum of 2-(2-Hydroxybenzoyl)-4*H*-furo[3,2-*c*]chromen-4-one (3a)

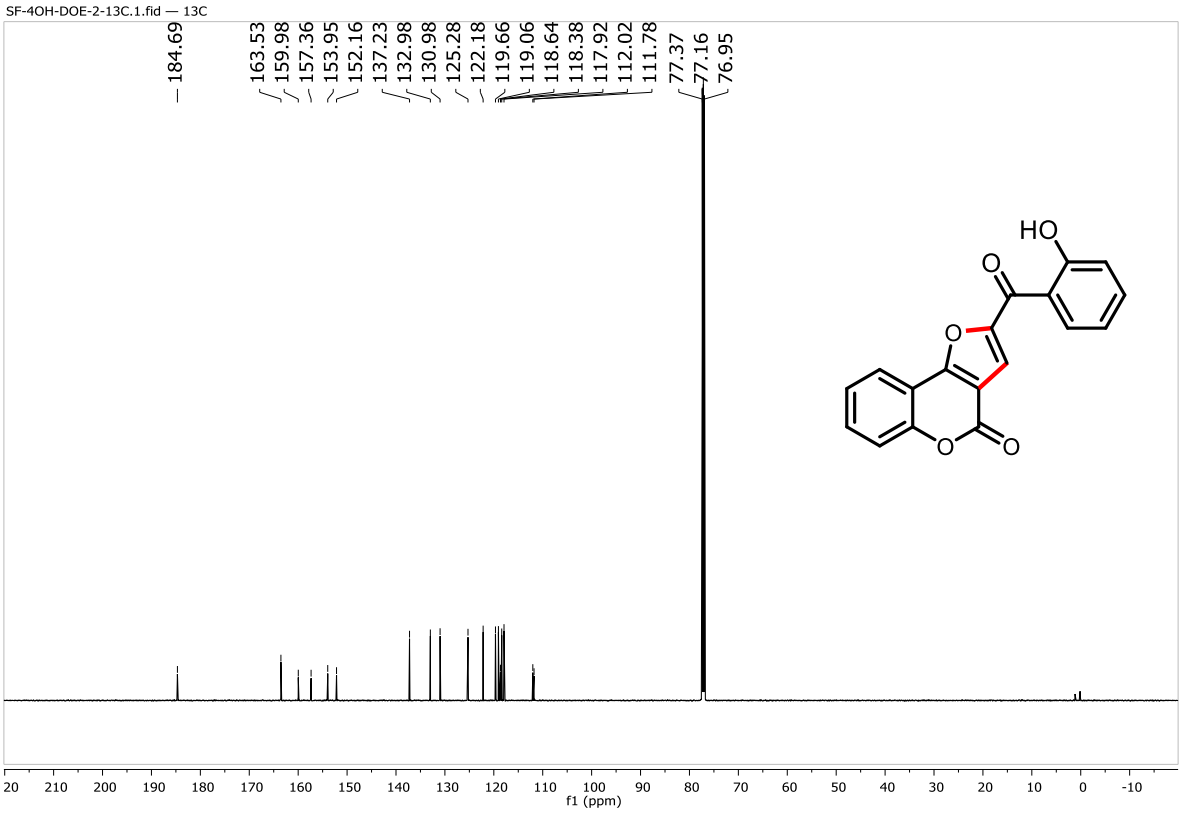

HRMS Spectrum of 2-(2-Hydroxybenzoyl)-4*H*-furo[3,2-*c*]chromen-4-one (3a)

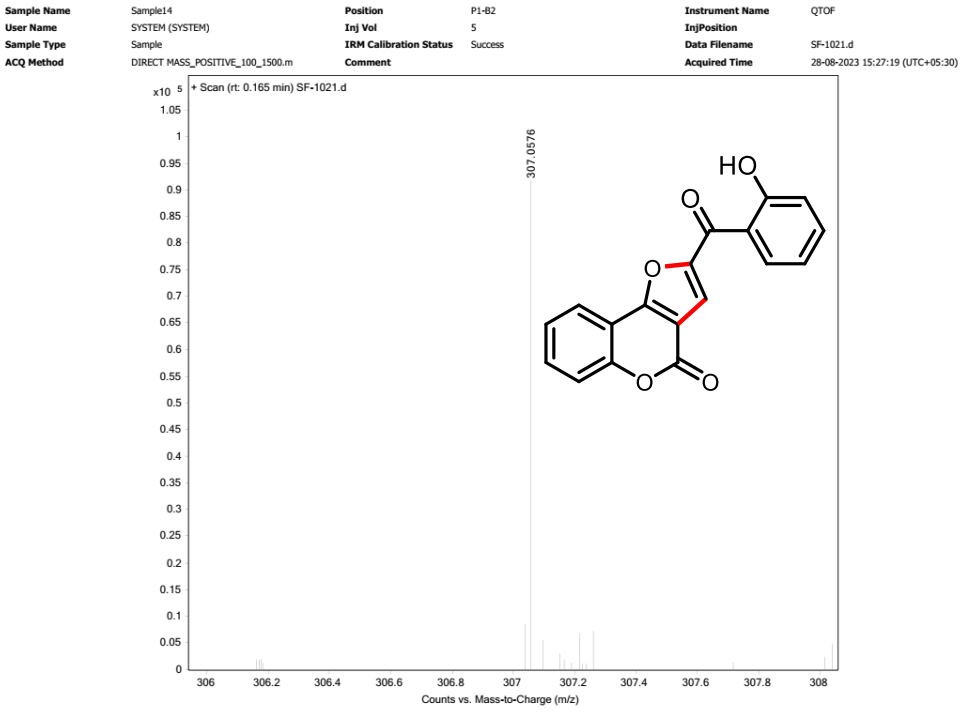

^{1}H Spectrum of 2-(2-(Benzyloxy)benzoyl)-4*H*-furo[3,2-*c*]chromen-4-one (5a)

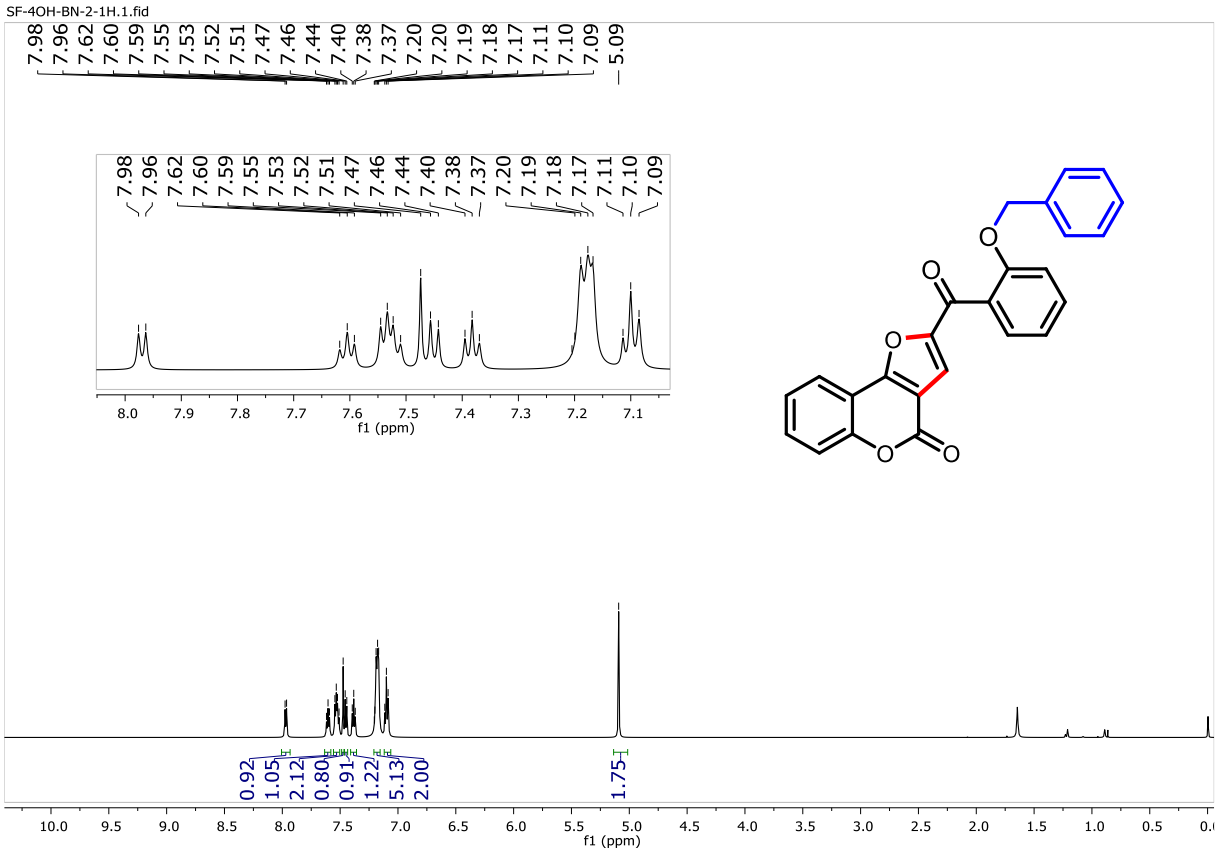

^{13}C NMR Spectrum of 2-(2-(Benzyloxy)benzoyl)-4*H*-furo[3,2-*c*]chromen-4-one (5a)

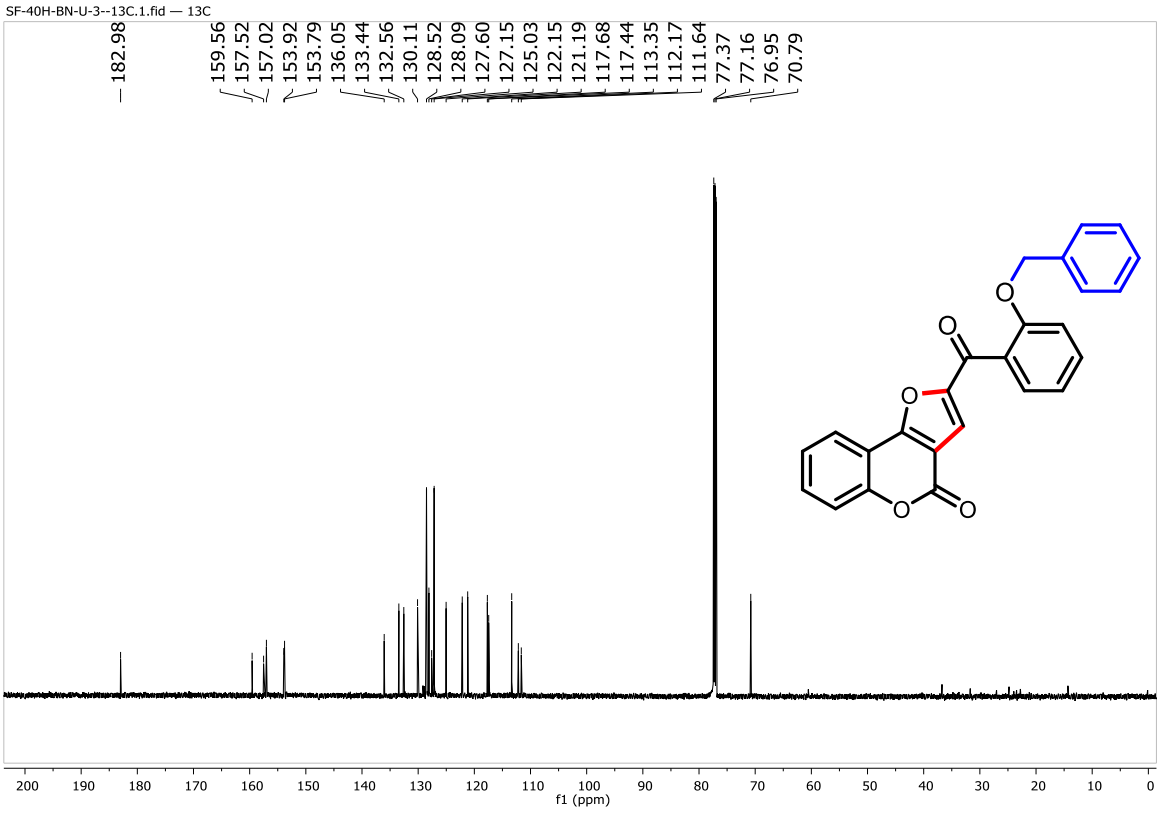

HRMS Spectrum of 2-(2-(Benzyloxy)benzoyl)-4*H*-furo[3,2-*c*]chromen-4-one (5a)

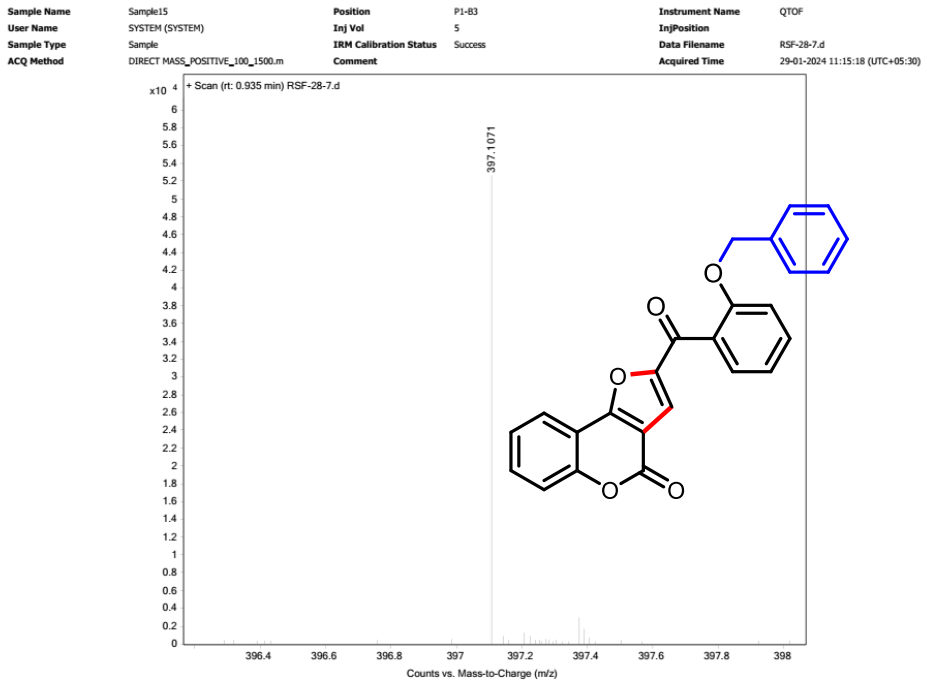

Part B

Chapter II: Section D

Synthesis of pyranocoumarin, furocoumarin, and 4-hydroxy-3-styryl coumarin

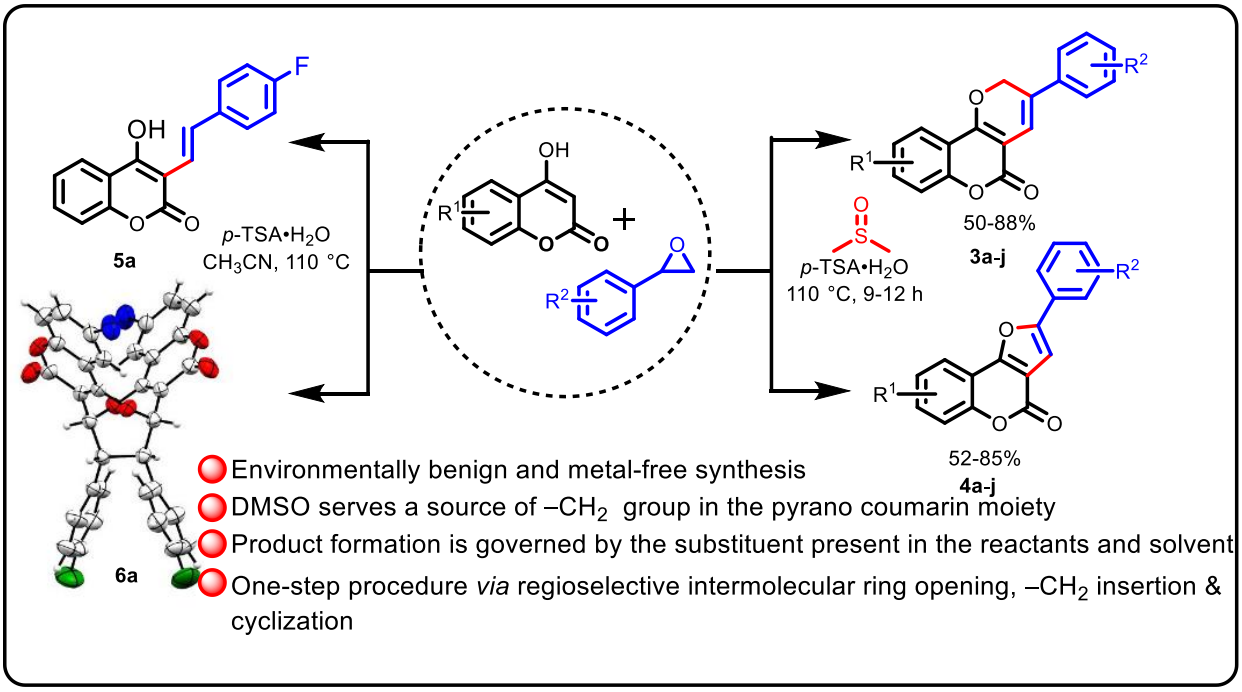

RESULT AND DISCUSSION

EXPERIMENTAL SECTION

Results and Discussion

Chapter I of Part B already explores the relevance of pyranocoumarins and furocoumarin, along with a detailed account of the synthetic methods reported in the literature. Section D of Chapter II illustrates the synthesis of 3-aryl-2*H*,5*H*-pyrano[3,2-*c*]chromen-5-ones **3** from 4-hydroxycoumarin, styrene oxide, and DMSO in the presence of *p*-TSA•H_2O at 110 °C via a three-component reaction in which the CH_2 of the pyrano moiety is inserted from DMSO. On the contrary, the reaction between 4-hydroxycoumarin and styrene oxide in the presence of DMSO under identical reaction conditions provided 2-aryl-4*H*-furo[3,2-*c*]chromen-4-one **4** depending upon the substituent present either on the 4-hydroxycoumarins or styrene oxides. It is important to point out that the solvent DMSO is not involved in the reaction as a reactant in the formation of furocoumarins. The advantages of the present method are easy handling, metal-free, inexpensive, commercially available starting material, environmentally benign, and high atom economy. Surprisingly, by changing the solvent from DMSO to CH_3CN, the novel monomeric product 4-hydroxy-3-styryl-2*H*-chromen-2-one **5** was obtained instead of the expected furocoumarins from 4-hydroxycoumarins and styrene oxides. Moreover, some novel monomeric product (*E*)-6-chloro-3-(4-fluorostyryl)-4-hydroxy-2*H*-chromen-2-one underwent unexpected cyclization to provide a more interesting and complex novel tricyclic product **6**.

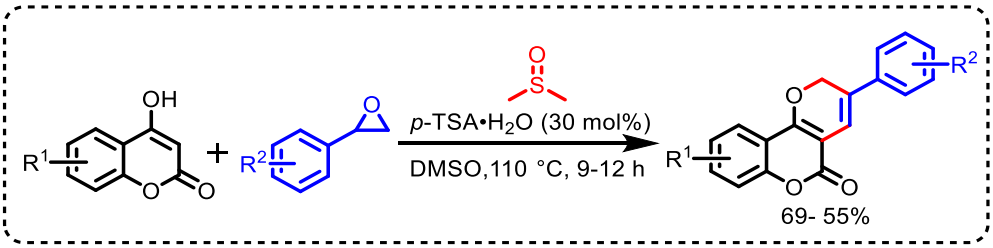

Scheme 31. Strategy for the synthesis of pyranocoumarins.

For optimization, we choose commercially available 4-hydroxycoumarin **1a** and styrene oxide **2a** as the model substrates. Initially, the reaction was scrutinized at room temperature to 110 °C without a catalyst, and the reaction did not take place as demonstrated in Table 18 (Entry 1). Next, the reaction was examined with 5 mol % *p*-TSA•H_2O at room temperature (Table 18, Entry 2). Unfortunately, no reaction took place. After that, the same reaction mixture was heated at 80°C, and the desired product **3a** was obtained with a 15% yield (Table 18, Entry 3), characterized by recording IR, ^{1}H NMR, ^{13}C NMR spectra, and HRMS. In the ^{1}H NMR spectrum, the peaks for the OH of proton 4-hydroxycoumarin at δ 12.6 and H-3 proton at δ 5.64 have disappeared, on the other hand, two new characteristic peaks appeared as a doublet

for two hydrogens at δ 5.4 with a coupling constant, J = 1.4 Hz, and a triplet for one hydrogen at δ 7.07 with a same coupling constant value, J = 1.4 Hz. Furthermore, a characteristic peak at δ 68.77 has appeared in the ^{13}C NMR spectrum for -OCH_2 carbon. Moreover, a total of 16 signals are present in the ^{13}C NMR spectrum, indicating that DMSO participated in the reaction. To increase the yield of the desired product **3a**, the reaction was examined at various temperatures such as 90 °C, 100 °C, 110 °C, and 120 °C; the best yield was obtained at 32% at 110°C (Table 18, Entries 4-8). It was observed that the yield of the desired product **3a** did not improve much with the increase in temperature. Subsequently, the reaction conditions were screened further to improve the yield of the desired product.

Table 18. Optimization Table[a,b]

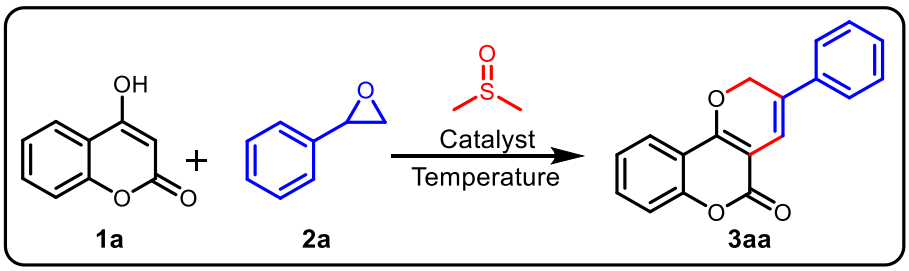

Entry	Catalyst	Mol(%)	Time(h)	Temperature(°C)	Yield[b](%)
1[c]	-	-	24	RT	NR
2[c]	*p*-TSA•H_2O	5	24	RT →120	NR
3	*p*-TSA•H_2O	5	24	60	NR
4	*p*-TSA•H_2O	5	15	80	15
5	*p*-TSA•H_2O	5	15	90	18
6	*p*-TSA•H_2O	5	15	100	26
7	*p*-TSA•H_2O	5	15	110	32
8	*p*-TSA•H_2O	5	15	120	30
9	*p*-TSA•H_2O	10	13	110	38
10	*p*-TSA•H_2O	20	11	110	48
11	***p*-TSA•H_2O**	**30**	**9**	**110**	**69**
12	MsOH	30	10	120	NR
13	CSA (±)	30	10	120	NR

[a]Reaction conditions: All the reactions were performed using 4-hydroxycoumarin (**1a**, 1.0 mmol), and styrene oxide (**2a**, 1.0 mmol) in 2 mL DMSO. [b]Isolated Yield. [c]Reaction at Room temperature. NR: No Reaction.

Next, the catalyst loading was increased, and the reaction was carried out with 10%, 20%, and 30 mol% catalysts; the yield was improved from 32% to 69% (Table 18, Entries 9-11). It is worthwhile that as we increase the catalyst amount the reaction time was also reduced from 15 h to 9 h. Various reactions were scrutinized with 30 mol% methane sulfonic acid and CSA (±) to examine the effectiveness of other catalysts. Unfortunately, the reaction did not occur in both catalysts' presence (Table 18, Entries 12 and 13). After investigating all the parameters, it was concluded that 30 mol% *p*-TSA•H_2O is the most effective and efficient catalyst at 110 °C under ambient air for this strategy.

The substrate scope was explored with the optimal reaction conditions, as depicted in Table 19. Initially, the influence of substitution variation at styrene oxide was scrutinized with 4-hydroxycoumarin **1a**. The successful results illustrate that the reaction went smoothly with styrene oxide containing electron-withdrawing groups 4-Cl (**2b**) and 4-F (**2c**), providing the desired product **3ab** and **3ac** in 63% and 63%, respectively, with high regioselectivity. To further investigate the scope of this protocol, the substrate 6-chloro-4-hydroxycoumarin **1b**, having an electron-withdrawing group at the 6th position, was carried out with styrene oxide **2a**, 4-chloro styrene oxide **2b**, and 4-fluoro styrene oxide **2c** respectively under similar reaction conditions. As expected, it also furnishes the desired products, such as **3ba**, **3bb**, and **3bc**, in 68%, 61, and 65% yields. To investigate the generality further, the substrate having an electron-withdrawing group, such as 6-fluoro-4-hydroxycoumarin **1c**, was carried out with styrene oxide **2a** and 4-chloro styrene oxide **2b** under identical reaction conditions**.** As speculated, the desired products **3ca** and **3cb** were obtained in 76 % and 62% yield.

Subsequently, the reaction scope was also carried out with the substrate having an OH groupat the 7th position, namely 4,7-dihydroxy coumarin **1d** with styrene oxide **2a**. The desired product **3da** was isolated with a 55% yield**.** Moreover, when the reaction was performed with 6-methyl-4-hydroxycoumarin **1e** and styrene oxide **2a**, a mixture of the products, pyranocoumarin (**3ea**) was obtained in 50 % yield along with furocoumarin **4ea** in 20% yield.

On the other hand, when the reaction was examined with 7-methoxy-4-hydroxycoumarin **1f** and styrene oxide **2a** under identical reaction conditions, the furanocoumarin derivative **4fa** was obtained with 82% yield instead of the expected pyranocoumarin scaffolds. We recently demonstrated the $FeCl_3$-catalyzed synthesis of furocoumarins with 4-hydroxycoumarin and

styrene oxide.[19] Here, furocoumarins are formed under metal-free conditions but the product is governed by the substituents on reactants, and the reaction follows an ionic mechanism. After that, a reaction was carried out between **1f** and styrene oxides **2b** & **2c**, having an electron-withdrawing group.

Table 19. The Substrate scope of pyranocoumarin[a,b]

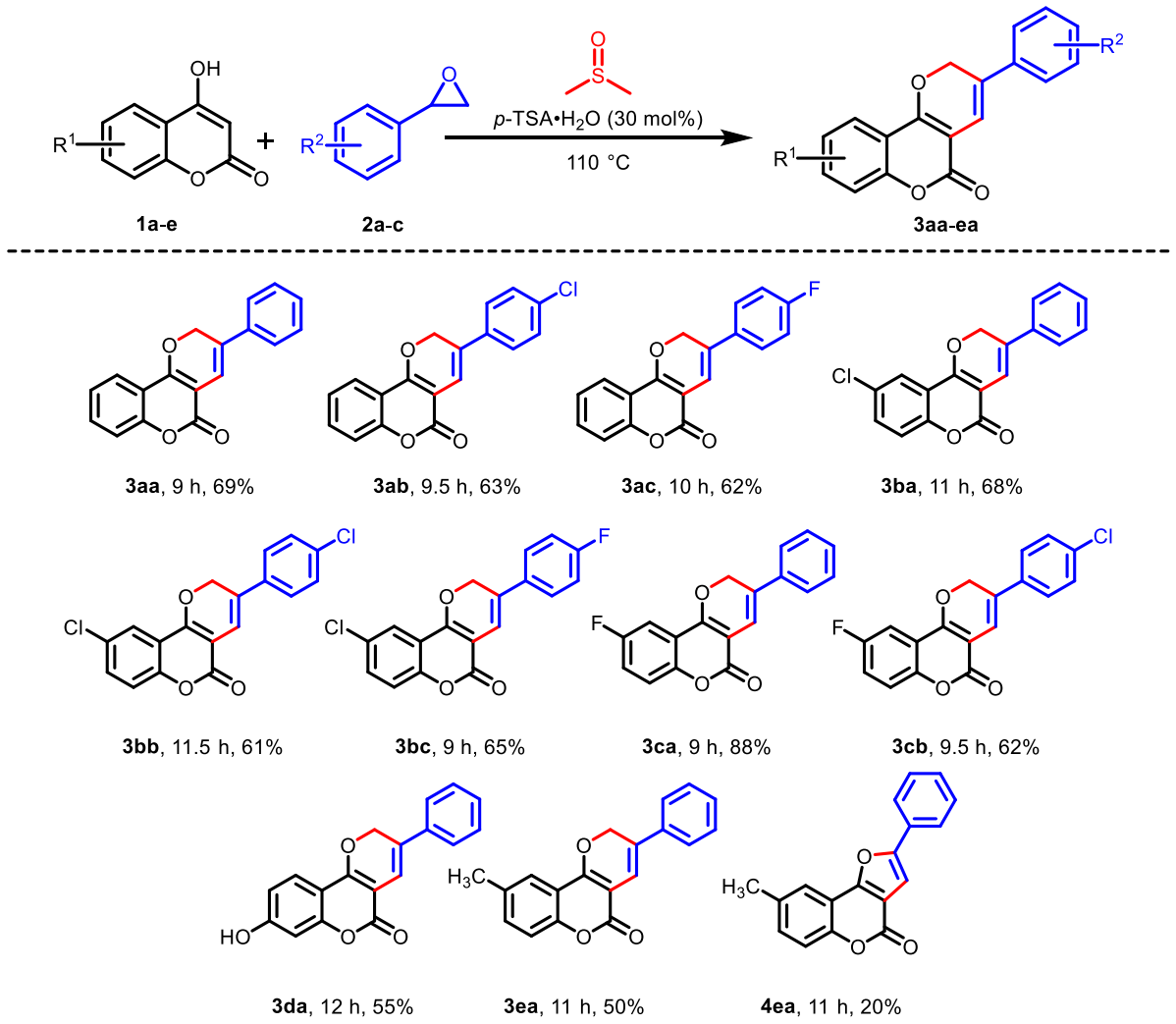

[a]Reaction conditions: All the reactions were performed using substituted 4-hydroxycoumarin (**1a-e**, 1.0 mmol), and substituted styrene oxide (**2a-c**, 1.0 mmol) in the presence of *p*-TSA•H_2O in 2 mL DMSO at 110 °C. [b]Isolated Yield.

The products furocoumarins **4fb** and **4fc** were obtained with a good yield. To examine the electron-donating effect of styrene oxide, methyl-substituted styrene oxides were prepared and various reactions were examined with 4-methyl-styrene oxide **2d** and 7-methoxy-4-hydroxycoumarin **1f**, 4-hydroxycoumarin **1a,** 6-fluoro-4-hydroxycoumarin **1c** and 6-methyl-4-hydroxycoumarin **1e**, respectively under identical reaction conditions. The furocoumarin derivatives **4fd-ed** were isolated with moderate to good yields (56%-85%). To further ascertain

the electronic effect on styrene oxide, the reactions were performed with 4-hydroxycoumarin **1a** as well as 7-methoxy-4-hydroxycoumarin **1f** and styrene oxide **2e**, having a methyl at the *meta* position. In both cases, the furocoumarin derivatives **4ae** and **4fe** were isolated in good yield. To check the reactivity of polyaromatic styrene oxide, the reaction was scrutinized with 4-hydroxycoumarin **1a** and 2-naphthyl oxirane **2f** under identical reaction conditions, and the furocoumarin derivative **4af** was obtained in a 69% yield as depicted in **Table 20**. Unexpectedly, despite having an electron-withdrawing group on both the reactants, between (**1c**) and (**2c**) provided furocoumarin **4cc** in 68% yield instead of the pyranocoumarin.

Table 20. The substrate scope of furocoumarins scaffolds[a,b]

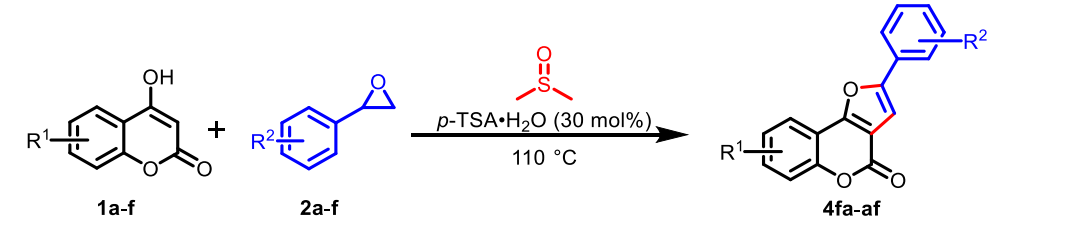

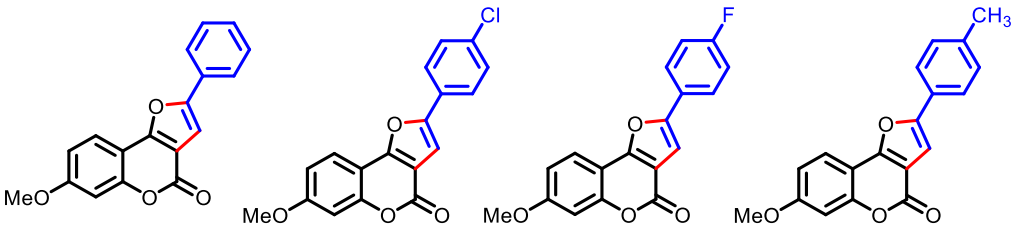

4fa, 8 h, 82% **4fb**, 8.5 h, 79% **4fc**, 9 h, 79% **4fd**, 9 h, 85%

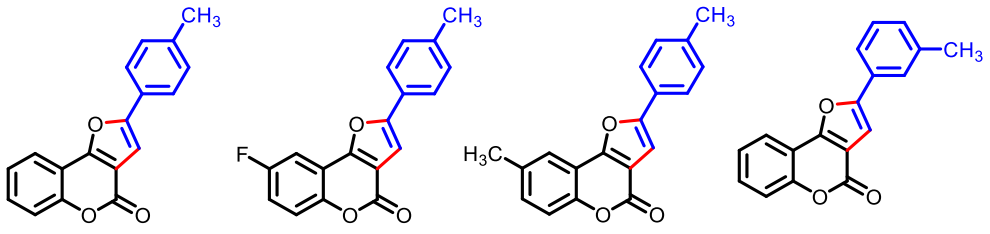

4ad, 8 h, 80% **4cd**, 9 h, 65% **4ed**, 9 h, 56% **4ae**, 9.5 h, 62%

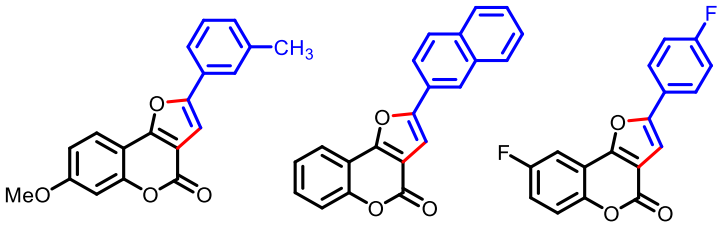

4fe, 9.5 h, 81% **4af**, 9.5 h, 69% **4cc**, 9.0 h, 68%

[a]Reaction conditions: All the reactions were performed using substituted 4-hydroxycoumarin (**1a-f**, 1.0 mmol), and substituted styrene oxide (**2a-f**, 1.0 mmol) in the presence of *p*-TSA•H_2O in 2 mL DMSO at 110 °C. [b]Isolated Yield.

To further check the applicability of the reaction, a gram scale reaction was carried out by taking 5 mmol 4-hydroxy coumarin **1a** with 5 mmol styrene oxide **2a** in the presence of 30 mol% *p*-TSA•H_2O at 110 °C, as expected desired product **3aa** was obtained in 65% yield (Scheme 32).

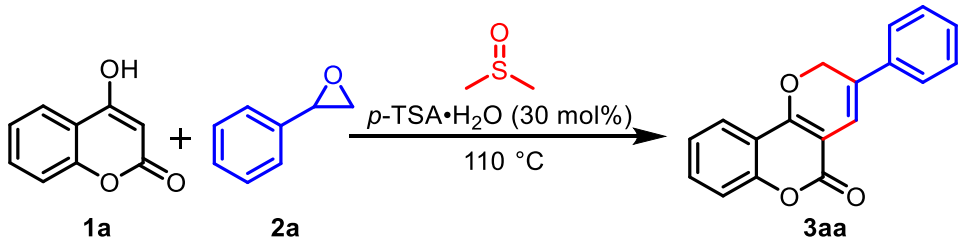

Scheme 32. A gram-scale reaction.

From the control experiment, plausible mechanisms for the formation of the desired product pyranocoumarins **3** are depicted in **Scheme 33**. Firstly, 4-hydoxycoumarin (**1**) attacks on the less hindered site of styrene oxide (**2a**) in the presence of *p*-TSA•H_2O to form the intermediate **A**. Next, the intermediate **A** undergoes dehydration to form intermediate **B**. Then the *p*-toluenesulfonate anion extracts the acidic hydrogen from intermediate **B** and generates an anion intermediate **C**, which exists in the resonating form **D**. At the same time in the reaction, the reactive intermediate sulfenium ion is generated from DMSO in the presence of *p*-TSA•H_2O that reacts with the intermediate **D** to form the next intermediate **E**.[35] From intermediate **E**, the *p*-toluenesulfonate anion extracts hydrogen and releases the methanethiol gas to form intermediate **F**, followed by electrocyclic ring closure of intermediate **F** and form the desired product **3**.

To further establish the proposed reaction mechanism, we explore the energy profile by choosing a model substrate 4-hydroxycoumarin **1a** and styrene oxide **2a** of all the steps, quantum chemical analysis of each step of the mechanism shown in **Scheme 33 (*Pathway I*)** has been performed using B3LYP/6-31+G(d,p) level. The energy released during the formation of pyranocoumarin is -58.51 kcal/mol, which is highly exergonic, and for the formation of furocoumarin, it is -93.72 kcal/mol. The first step of the reaction is epoxide ring opening by 4-hydroxycoumarin to give intermediate **A**, exergonic by 14.8 kcal/mol. After that, two pathways are proposed from intermediate **A**. Pathway **I** lead to the formation of pyranocoumarin. Intermediate **A** converts to intermediate **B** by water elimination, exergonic by 3.1 kcal/mol. Intermediate **B** gives intermediate **C** which can convert to its other resonating form intermediate **D**. DMSO converts to dimethylsulfinic acid **D1**, this step requires 22.7

kcal/mol energy. After that, **D1** converts to **D2**, endergonic by 78.6 kcal/mol. intermediate **D** and **D2** react to give intermediate **E**. This step is highly exergonic by 120.8 kcal/mol, because of electrostatic interactions between cation **D2** and anion **D**. Intermediate **E** gives intermediate **F** by releasing methylsulfide anion, which releases methanethiol in the reaction. Intermediate **F** undergoes electrocyclic ring closure to give **3**, pyranocoumarin, releasing 10.9 kcal/mol. **TS-1** is traced for the electro-cyclisation step with one imaginary frequency, with E_a=10.88 kcal/mol.

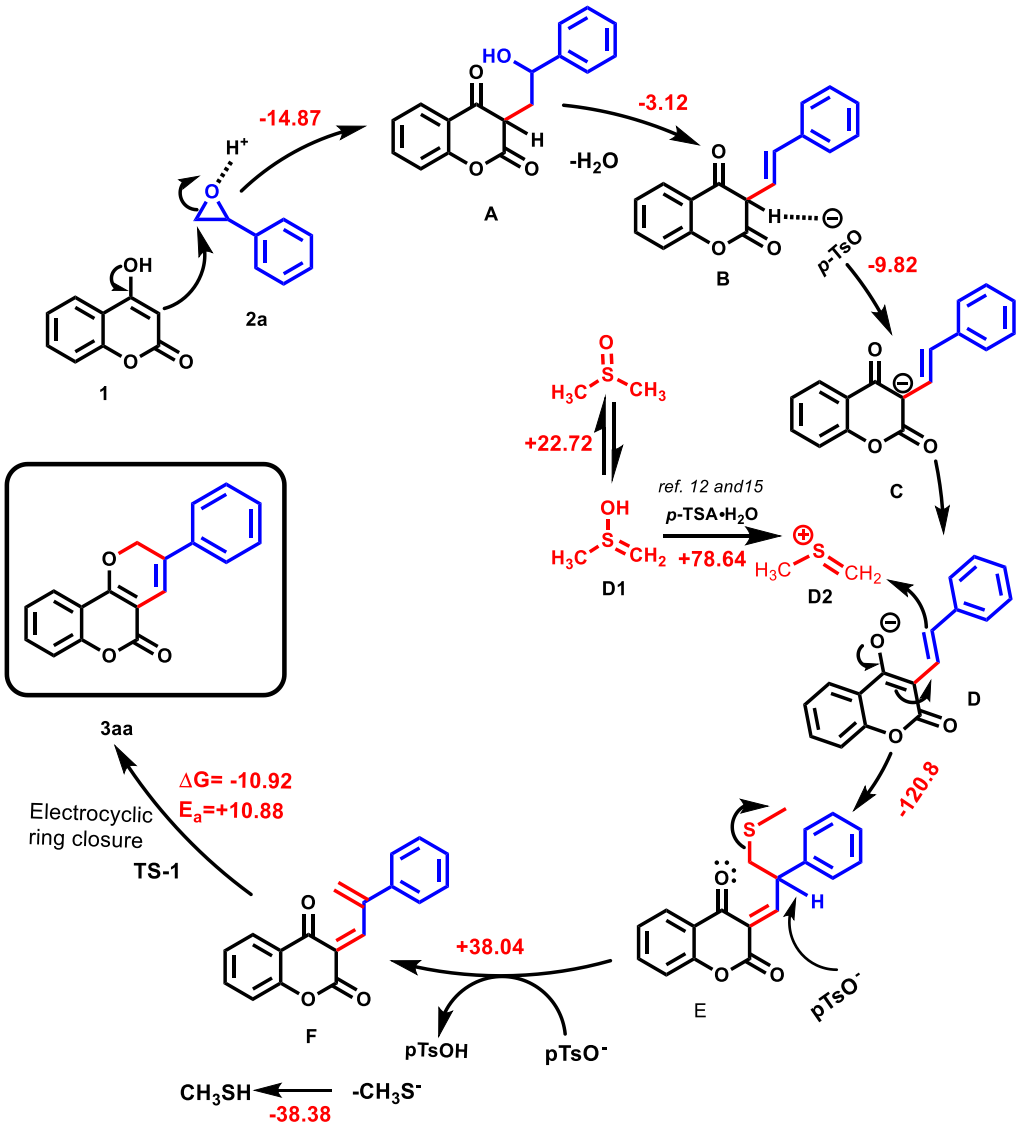

Scheme 33 (*Pathway I*). A plausible reaction mechanism for the formation of pyranocoumarin **3aa**. The calculations were carried out using B3LYP/6-31+G(d,p) level of DFT. All the energy values are estimated using the free energy (G) values. The relative energies of the reaction path are provided in kcal/mol.

On the other hand, if 4-hydroxy coumarin (**1a**) contains a strong electron donation group (OMe **1f**) or styrene oxide (*meta*-CH_3 **1d** and *para*-CH_3 **1e**) having an electron-donating group, the reaction follows pathway II as depicted in **Scheme 34**. Like the previous mechanism here, 7-methoxy-4-hydroxycoumarin (**1f**) also attacks the less hindered site of styrene oxide in the presence of *p*-TSA•H_2O to form the intermediate **A**. Then, the oxygen anion attacks the **D2** to form the intermediate **G**. Intermediate **G** converts to its other tautomeric form, **G′** (enol form). **G′** with the removal of DMSO forms intermediate **H**. At last, aerial oxidation occurs in intermediate **H**, and the desired product furocoumarin **4aa** is formed, as shown in **Scheme 34**.

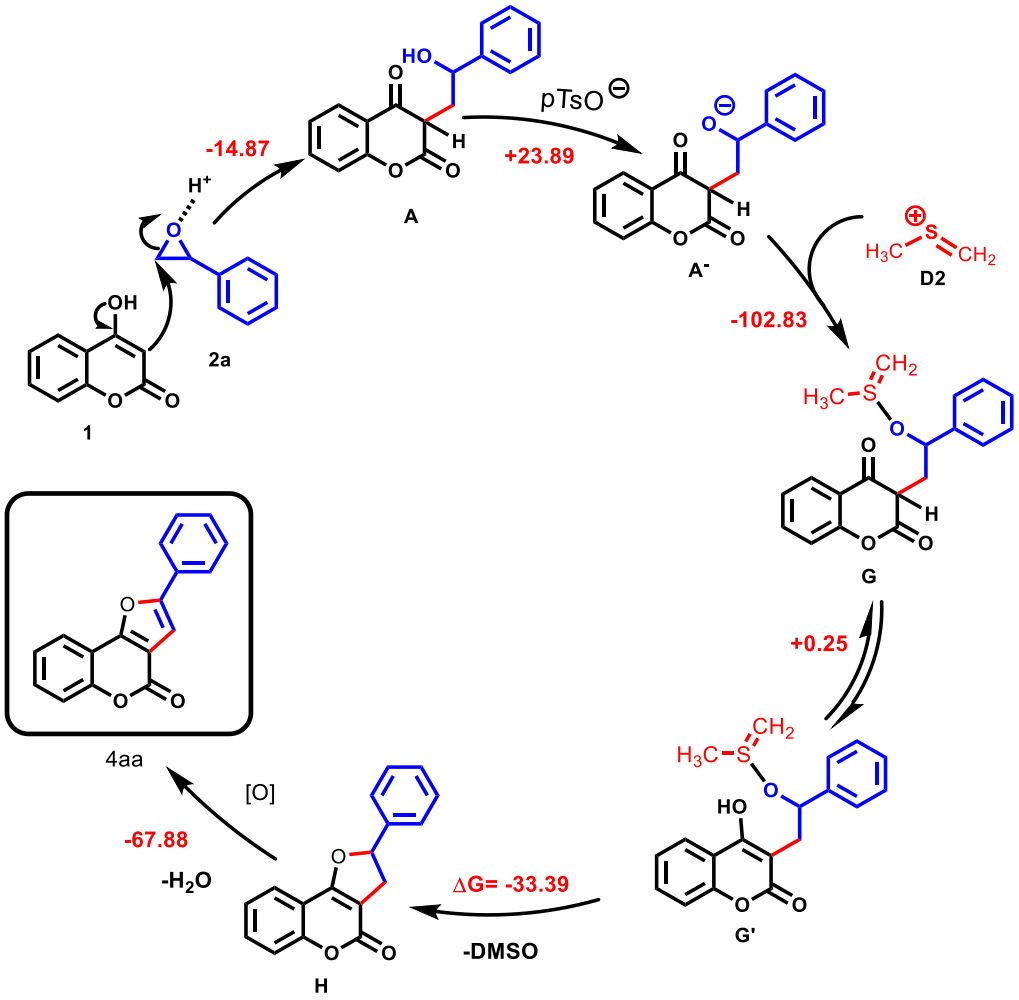

Scheme 34 (*Pathway II*). A plausible reaction mechanism for the formation of furocoumarin **4aa.** The calculations were carried out using the B3LYP/6-31+G(d,p) level of DFT. All the energy values are estimated using the free energy (G) values. The relative energies of the reaction path are provided in kcal/mol.

We believe from the present study that the pyranocoumarin (**3**) is formed because the intermediate **D** is stabilized due to the electron-withdrawing group at the 6th position. On the

other hand, intermediate **D** is destabilized due to the presence of an alkyl group or methoxy at the 6th and 7th position of 4-hydroxycoumarin, respectively, leading to the formation of **4**.

For the formation of furocoumarins by choosing a model substrate 4-hydroxycoumarin **1a** and styrene oxide **2a** quantum chemical analysis of each step of the mechanism shown in **Scheme 34 (*Pathway II*)** has been performed using B3LYP/6-31+G(d,p) level. First, an anion of intermediate **A** by $pTsO^-$ is generated, endergonic by 23.89 kcal/mol.

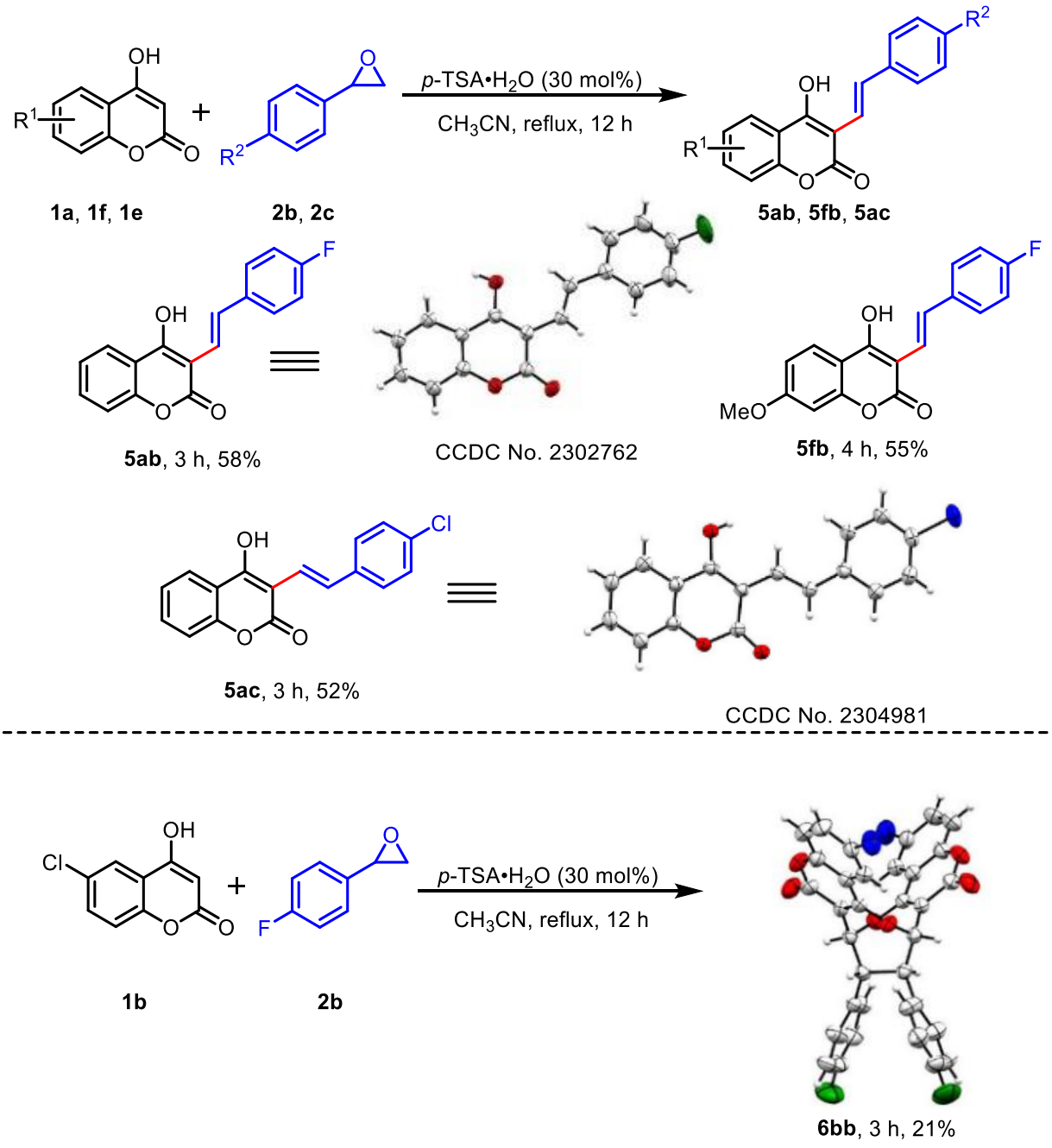

Scheme 35. Reaction in the presence of CH_3CN as a solvent.

The oxygen of intermediate **A**$^-$ attacks the **D2** (generated from DMSO) to form intermediate **G**, exergonic by 102.83 kcal/mol. Intermediate **G** converts to its enol tautomer **G′** with a small energy change (0.25 kcal/mol endergonic). Release of DMSO from **G′** facilitates the formation of product **H** directly with an energy release of -33.39 kcal/mol. Intermediate **H** undergoes aerial oxidation by releasing 67.88 kcal/mol, to give water and **4**, furocoumarins.

We subsequently directed our efforts towards whether the furocoumarins can be synthesized exclusively irrespective of substituents present in the 4-hydroxycoumarin and styrene oxides under metal-free conditions since using the solvent, DMSO, provided puzzling results, such as, in some cases, pyranocoumarin formed by $–CH_2$ group insertion, or in some cases, furocoumarin, without a $–CH_2$ insertion. With this goal in mind, the solvent DMSO was replaced with CH_3CN and carried out a similar reaction with 4-hydroxycoumarin **1a** with 4-fluorostyrene oxide **b** and 4-chlorostyrene oxide **2c**, respectively using 30 mol% *p*-toluenesulfonic acids under reflux conditions. The non-cyclized products 4-hydroxy-3-styryl-2*H*-chromen-2-one derivatives **5ab** and **5ac** were obtained in good yields.

Notably, we did not observe the formation of furocoumarin derivatives and it indicates that the solvent DMSO has an important role. Similarly, 7-methoxy-4-hydroxycoumarin **1f** on reaction with 4-fluorostyrene oxide **2b** also provided a non-cyclized product **5fb** in good yield. In some cases, an interesting novel complex structure 6 was isolated by reacting 2 molecules of 6-chloro-4-hydroxycoumarin **1b** and 2 molecules of 4-fluoro styrene oxide (**2b)** in 41% yield under identical reaction conditions as illustrated in Scheme 35. It is interesting to point out that the complex molecules are connected uniquely and it is an insoluble crystal, the structure of the product is only ascertained from a single XRD data. In which the 4-Fluorostyrene **2b** oxide was connected with the 4th position of one 6-chloro-4-hydroxycoumarin **1b** and the 3rd position of other molecules of 6-chloro-4-hydroxycoumarin. Similarly, the second molecule of 4-fluoro styrene oxide was connected with 6-chloro-4-hydroxycoumarin and formed two 7-membered rings and one 8-membered ring, as shown in Scheme 36.

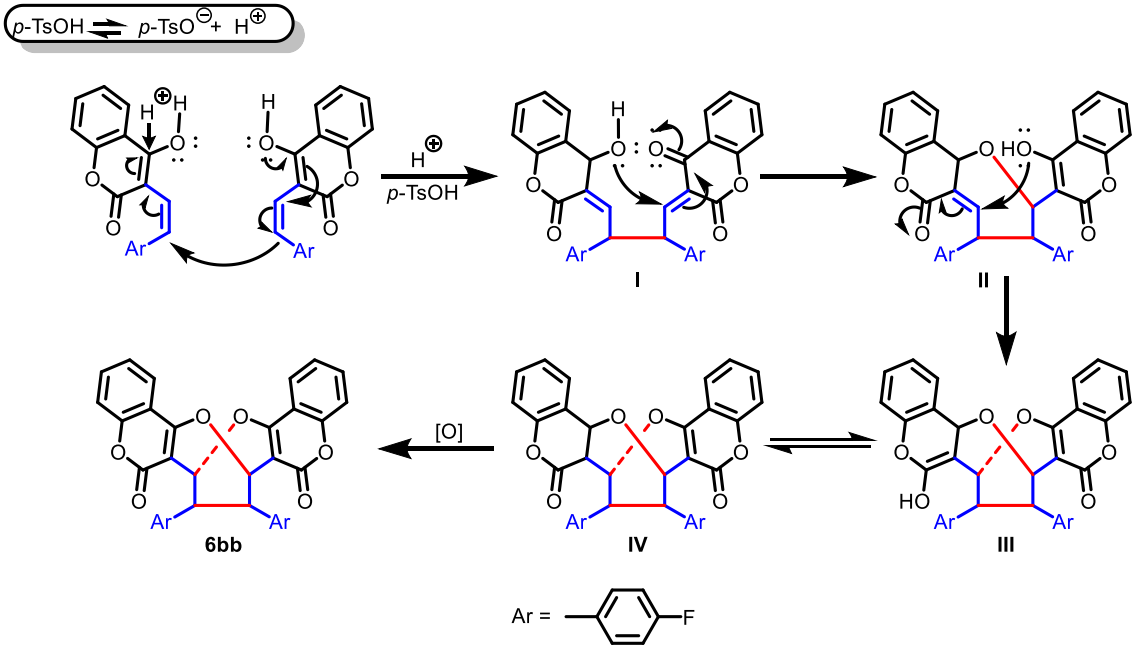

Scheme 36. A Plausible mechanism for the formation of tricyclic product **6bb**.

The plausible mechanism for the formation of tricyclic product is demonstrated in Scheme 5. First, the reaction starts with the attack of a proton from *p*-TSA•H_2O on one monomer unit that triggers another monomer unit to react and form intermediate **A**. The next two times, intramolecular Michael addition takes place to form the next intermediate **B** and **C**. Intermediate **C** tautomerizes to its keto form. Finally, aerial oxidation takes place to form the product **6bb**.

In conclusion, we developed a reliable, straightforward, and operationally simple protocol for synthesizing novel pyranocoumarin and furocoumarin. Interestingly sulfenium ion is generated from DMSO in the presence of *p*-TSA•H_2O and acts as a reagent cum solvent. In the presence of acetonitrile, 4-hydroxy-3-styryl coumarin as a non-cyclic product confirms the role of solvent DMSO in forming a cyclic product. The salient feature is the substrate-dependent formation of a 5-or-6-membered ring, making this protocol more interesting. Moreover, solvents also play an important role in forming the 4-hydroxy-3-styryl coumarin and unique tricyclic product. The perks of this method are easy handling, high atom economy, metal-free, and low-cost catalyst. Furthermore, this protocol does not require any additive, oxidant, or inert atmospheric conditions.

General Procedure for the Synthesis of Pyranocoumarins 3 and Furocoumarins 4 Derivatives.

A mixture of 4-hydroxycoumarin (**1**, 1.0 mmol) and styrene oxide (**2**, 1.0 mmol) was dissolved in 2 mL DMSO in a 25 mL round-bottomed flask. Next, 30 mol% *p*-TSA•H_2O was added to the reaction mixture as a catalyst, and it was kept in a pre-heated oil bath at 110 ^oC with constant stirring under an air atmosphere. The progress of the reaction was monitored by checking TLC from time to time. After the completion of the reaction, it was brought to room temperature, and the resulting mixture was diluted with 10 mL of dichloromethane. The organic layer was washed with brine solution (5 mL x 2). After that, the organic extract was dried with anhydrous sodium sulfate, the solvent was removed using a rotary evaporator, and the crude residue was purified through a silica gel (60–120 mesh) column chromatography.

General Procedure for the Synthesis of Hydroxy-3-styryl coumarin 5 and Tricyclic product 6.

4-Hydroxycoumarins (**1**, 1.0 mmol) and styrene oxides (**2**, 1.0 mmol) were dissolved in 2 mL of CH_3CN in a 25 mL round-bottomed flask. Then, the catalyst 30 mol% *p*-TSA•H_2O was added, and the reaction flask was placed in a pre-heated oil bath at 110 ^oC with constant stirring under an air atmosphere. The progress of the reaction was monitored by checking TLC from time to time. After the completion of the reaction, it was brought to room temperature, and a white crystal appeared that was filtered with Whatman filter paper and washed with 10 mL acetone. The product was dried in the rotary evaporator and then placed in a high vacuum.

3-Phenyl-2*H*,5*H*-pyrano[3,2-*c*]chromen-5-one (3aa) Yellow solid (190.49 mg, 69%) mp

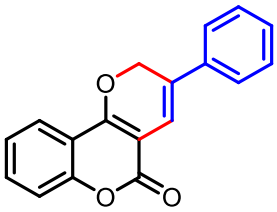

133−135 °C. ^1H NMR (600 MHz, $CDCl_3$) δ 7.81 (dd, *J* = 7.9, 1.4 Hz, 1H), 7.55 (ddd, *J* = 8.7, 7.4, 1.6 Hz, 1H), 7.47 – 7.45 (m, 2H), 7.41 (t, *J* = 7.7 Hz, 2H), 7.34 (t, *J* = 7.8 Hz, 2H), 7.32 – 7.29 (m, 1H), 7.07 (t, *J* = 1.4 Hz, 1H), 5.48 (d, *J* = 1.4 Hz, 2H); ^{13}C NMR (150 MHz, $CDCl_3$) δ 161.0, 159.0, 153.1, 135.6, 132.3, 129.0, 128.6, 127.1, 124.8, 124.3, 122.8, 116.9, 114.9, 114.1, 102.7, 68.7; IR (KBr)ν_{max}/cm^{-1} 1745 (C=O), 1622 (C=C), 1310 (C–O); HRMS (ESI) Calcd For $C_{18}H_{13}O_3$ 277.0860 ($M+H^+$); Found 277.0860.

3-(4-chlorophenyl)-2*H*,5*H*-pyrano[3,2-*c*]chromen-5-one (3ab) Yellow solid (195.76 mg, 63%) mp 128−130 °C. ^{1}H NMR (500 MHz, $CDCl_3$) δ 7.80 (d, *J* = 7.65 Hz, 1H), 7.55 (d, *J* = 7.1 Hz, 1H), 7.48 – 7.45 (m, 1H), 7.38 (s, 3H), 7.35 – 7.29 (m, 2H), 7.06 – 7.05 (m, 1H), 5.43 (d, *J* = 1.25 Hz, 2H); ^{13}C NMR (125 MHz, $CDCl_3$) δ 160.9, 159.1, 153.2, 134.4, 134.0, 132.5, 129.5, 129.2, 126.0, 124.4, 122.9, 117.0, 114.8, 114.7, 102.5, 68.5; IR (KBr)ν_{max}/cm^{-1} 1748 (C=O), 1625 (C=C), 1305 (C–O); HRMS (ESI) Calcd For $C_{18}H_{12}ClO_3$ 311.0470 (M+H$^+$); Found 311.0467.

3-(4-Fluorophenyl)-2*H*,5*H*-pyrano[3,2-*c*]chromen-5-one (3ac) Yellow solid (182.45 mg, 62%) mp 145−146 °C. ^{1}H NMR (600 MHz, $CDCl_3$) δ 7.80 (d, *J* = 7.8 Hz, 1H), 7.55 (t, *J* = 7.8 Hz, 1H), 7.43 (dd, *J* = 8.0, 5.7 Hz, 2H), 7.34 – 7.29 (m, 2H), 7.10 (t, *J* = 8.5 Hz, 2H), 7.00 (s, 1H), 5.43 (s, 2H); ^{13}C NMR (150 MHz, $CDCl_3$) δ 162.8 ($J_{C\text{-}F}$ = 247.45 Hz), 161.0, 158.9, 153.1, 132.4, 131.8, 131.8, 126.5 ($J_{C\text{-}F}$ = 8.01 Hz), 124.3, 122.8, 117.0, 116.1 ($J_{C\text{-}F}$ = 21.67 Hz), 114.8, 114.0 ($J_{C\text{-}F}$ = 1.62 Hz), 102.5, 68.6; ^{19}F NMR (565 MHz, $CDCl_3$) δ -112.34; IR (KBr)ν_{max}/cm^{-1} 1750 (C=O), 1620 (C=C), 1305 (C–O); HRMS (ESI) Calcd For $C_{18}H_{12}FO_3$ 295.0765 (M+H$^+$); Found 295.0756.

9-Chloro-3-phenyl-2*H*,5*H*-pyrano[3,2-*c*]chromen-5-one (3ba) Yellow solid (211.29 mg, 68%) mp 122−125 °C. ^{1}H NMR (400 MHz, $CDCl_3$) δ 7.77 (d, *J* = 2.5 Hz, 1H), 7.49 – 7.42 (m, 6H), 7.36 (d, *J* = 6.9 Hz, 1H), 7.04 (s, 1H), 5.48 (d, *J* = 1.3 Hz, 2H); ^{13}C NMR (100 MHz, $CDCl_3$) δ 160.5, 157.7, 151.4, 135.3, 132.2, 129.9, 129.2, 129.0, 128.9, 127.9, 124.8, 122.3, 118.4, 116.0, 113.7, 68.9; IR (KBr)ν_{max}/cm^{-1} 1735 (C=O), 1622 (C=C), 1315 (C–O); HRMS (ESI) Calcd For $C_{18}H_{12}ClO_3$ 311.0470 (M+H$^+$); Found 311.0707.

9-Chloro-3-(4-fluorophenyl)-2*H*,5*H*-pyrano[3,2-*c*]chromen-5-one (3bb) Yellow solid (213.60 mg, 65%) mp 143−144 °C. ^{1}H NMR (600 MHz, $CDCl_3$) δ 7.76 – 7.74 (m, 2H), 7.49 – 7.46 (m, 2H), 7.37 (d, *J* = 2.0 Hz, 3H), 7.02 (s, 1H), 5.43 (d, *J* = 1.02 Hz, 2H); ^{13}C NMR (150 MHz, $CDCl_3$) δ 160.4, 157.0 ($J_{C\text{-}F}$ = 231.28 Hz), 151.4, 134.2 ($J_{C\text{-}F}$ = 149.64 Hz), 132.4, 129.5, 129.3, 126.6, 126.0, 126.0, 122.3, 120.4, 119.0, 118.4, 115.9, 114.2, 103.2 ($J_{C\text{-}F}$ = 30.73 Hz), 68.6; ^{19}F NMR (565

MHz, $CDCl_3$) δ -121.88; IR (KBr)ν_{max}/cm^{-1} 1735 (C=O), 1615 (C=C), 1310 (C–O); HRMS (ESI) Calcd For $C_{18}H_{11}ClFO_3$ 329.0376 ($M+H^+$); Found 329.0359.

9-Chloro-3-(4-chlorophenyl)-2*H*,5*H*-pyrano[3,2-*c*]chromen-5-one (3bc) Yellow solid

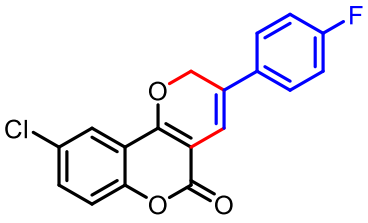

(210.55 mg, 61%) mp 118−121 °C. ^{1}H NMR (600 MHz, $CDCl_3$) δ 7.77 – 7.76 (m, 1H), 7.51 – 7.46 (m, 2H), 7.40 (d, *J* = 9.0 Hz, 1H),7.38 (d, *J* = 2.2 Hz, 3H), 7.27 (d, *J* = 8.9 Hz, 1H), 7.02 (s, 1H), 5.44 (d, *J* = 1.4 Hz, 2H); ^{13}C NMR (150 MHz, $CDCl_3$) δ 157.7, 151.3, 134.6, 133.6, 132.3, 130.7, 129.8, 129.4, 129.1, 126.5, 125.9, 122.2, 118.3, 114.1, 103.2, 68.5; IR (KBr)ν_{max}/cm^{-1} 1725 (C=O), 1630 (C=C), 1310 (C–O); HRMS (ESI) Calcd For $C_{18}H_{11}Cl_2O_3$ 345.0080 ($M+H^+$); Found 345.0081.

9-Fluoro-3-phenyl-2*H*,5*H*-pyrano[3,2-*c*]chromen-5-one (3ca) Yellow solid (258.96 mg, 88%) mp 130−132 °C. ^{1}H NMR (600 MHz, $CDCl_3$) δ 7.46 – 7.44 (m, 3H), 7.41 (t, *J* = 7.6 Hz, 2H), 7.35 (t, *J* = 7.2 Hz, 1H), 7.30 (dd, *J* = 9.0, 4.3 Hz, 1H), 7.26 – 7.23 (m, 1H), 7.04 (t, *J* = 1.4 Hz, 1H), 5.48 (d, *J* = 1.4 Hz, 2H); ^{13}C NMR (150 MHz, $CDCl_3$) δ 160.7,158.9 (J_{C-F} = 242.86 Hz), 158.0 (J_{C-F} = 2.80 Hz), 149.1 (J_{C-F} = 1.62 Hz), 135.3, 129.0, 128.8, 127.8, 124.8, 119.8 (J_{C-F} = 24.61 Hz), 118.5 (J_{C-F} = 8.29 Hz), 115.8, (J_{C-F} = 9.10 Hz), 113.7, 108.4 (J_{C-F} = 25.26 Hz), 103.2, 68.8; ^{19}F NMR (565 MHz, $CDCl_3$) δ -116.80; IR (KBr)ν_{max}/cm^{-1} 1745 (C=O), 1625 (C=C), 1315 (C–O); HRMS (ESI) Calcd For $C_{18}H_{12}FO_3$ 295.0765 ($M+H^+$); Found 295.0765.

3-(4-Chlorophenyl)-9-fluoro-2*H*,5*H*-pyrano[3,2-*c*]chromen-5-one (3cb) Yellow solid

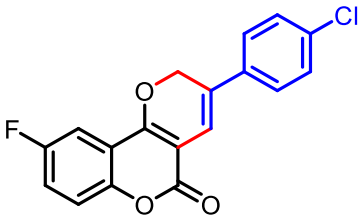

(203.80 mg, 62%) mp 128−130 °C. ^{1}H NMR (600 MHz, $CDCl_3$) δ 7.48 (dt, *J* = 8.0, 4.1 Hz, 1H), 7.41 (s, 3H), 7.34 (dd, *J* = 9.0, 4.3 Hz, 1H), 7.30 (d, *J* = 3.0 Hz, 1H), 7.27 (d, *J* = 3.1 Hz, 1H), 7.06 (s, 1H), 5.47 (d, *J* = 1.2 Hz, 2H); ^{13}C NMR (150 MHz, $CDCl_3$) δ 160.6, 158.9 (J_{C-F} = 237.99 Hz), 158.1 (J_{C-F} = 2.29 Hz), 149.2, 134.2 (J_{C-F} = 138.57 Hz), 129.5, 129.3, 126.6, 126.0, 120.0 (J_{C-F} = 24.49 Hz), 118.6 (J_{C-F} = 8.22 Hz), 115.7 (J_{C-F} = 9.15 Hz)114.3, 108.5 (J_{C-F} = 25.23 Hz), 103.1, 68.6; ^{19}F NMR (565 MHz, $CDCl_3$) δ -116.67; IR (KBr)ν_{max}/cm^{-1} 1750 (C=O), 1625 (C=C), 1305 (C–O); HRMS (ESI) Calcd For $C_{18}H_{11}ClFO_3$ 329.0376 ($M+H^+$); Found 329.0360.

8-Hydroxy-3-phenyl-2*H*,5*H*-pyrano[3,2-*c*]chromen-5-one (3da) White solid (160.75 mg, 55%) mp 115−116 °C. ^{1}H NMR (600 MHz, DMSO-d_6) δ 7.63 (d, J = 8.7 Hz, 1H), 7.54 (d, J = 7.5 Hz, 2H), 7.41 (t, J = 7.7 Hz, 2H), 7.33 (t, J = 7.3 Hz, 1H), 6.88 (s, 1H), 6.83 (dd, J = 8.7, 2.2 Hz, 1H), 6.74 (d, J = 2.1 Hz, 1H), 5.49 (s, 2H); ^{13}C NMR (150 MHz, DMSO-d_6) δ 162.3, 160.5, 159.8, 154.7, 135.4, 129.1, 128.5, 126.2, 124.8, 124.4, 113.8, 113.3, 106.3, 102.6, 98.8, 68.3; IR (KBr)ν_{max}/cm^{-1} 1755 (C=O), 1630 (C=C), 1301 (C–O); HRMS (ESI) Calcd For $C_{18}H_{13}O_4$ 293.0809 (M+H$^+$); Found 293.0808.

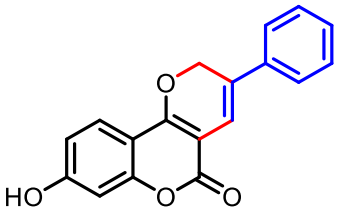

9-Methyl-3-phenyl-2*H*,5*H*-pyrano[3,2-*c*]chromen-5-one (3ea) Yellow solid (145.15 mg, 50%) mp 118−120 °C. ^{1}H NMR (600 MHz, $CDCl_3$) δ 7.75 (d, J = 8.6 Hz, 1H), 7.58 (s, 1H), 7.45 (dd, J = 8.5, 2.5 Hz, 1H), 7.37 (s, 3H), 7.35 (s, 1H), 7.22 (d, J = 8.4 Hz, 1H), 7.05 (s, 1H), 5.41 (d, J = 1.5 Hz, 2H), 2.42 (s, 3H); ^{13}C NMR (150 MHz, $CDCl_3$) δ 160.4, 151.4, 134.4, 134.2, 133.6, 130.8, 129.4, 129.2, 126.0, 125.9, 125.0, 122.5, 116.8, 114.9, 102.4, 68.4, 21.0; IR (KBr)ν_{max}/cm^{-1} 1755 (C=O), 1622 (C=C), 1310 (C–O); HRMS (ESI) Calcd For $C_{19}H_{15}O_3$ 291.1016 (M+H$^+$); Found 291.1015.

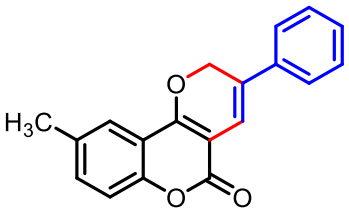

7-Methoxy-2-phenyl-4*H*-furo[3,2-*c*]chromen-4-one (4fa) White solid (239.67 mg, 82%) mp 172−173 °C. ^{1}H NMR (600 MHz, $CDCl_3$) δ 7.86 (d, J = 9.4 Hz, 1H), 7.79 (d, J = 7.7 Hz, 2H), 7.47 (t, J = 7.7 Hz, 2H), 7.38 (t, J = 7.4 Hz, 1H), 7.14 (s, 1H), 6.97 (d, J = 7.3 Hz, 2H), 3.90 (s, 3H); ^{13}C NMR (150 MHz, $CDCl_3$) δ 162.1, 158.7, 157.7, 155.8, 154.5, 129.2, 129.1, 129.0, 124.5, 121.9, 113.0, 110.1, 106.3, 102.6, 101.6, 55.9; IR (KBr)ν_{max}/cm^{-1} 1755 (C=O), 1645 (C=C), 1309 (C–O); HRMS (ESI) Calcd For $C_{18}H_{13}O_4$ 293.0809 (M+H$^+$); Found 293.0786.

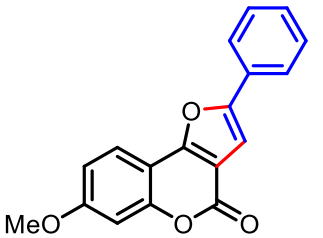

2-(4-Chlorophenyl)-7-methoxy-4*H*-furo[3,2-*c*]chromen-4-one (4fb) White solid (258.11 mg, 79%) mp 218−220 °C. ^{1}H NMR (600 MHz, $CDCl_3$) δ 7.86 – 7.84 (m, 1H), 7.72 (d, J = 8.5 Hz, 2H), 7.44 (d, J = 8.6 Hz, 2H), 7.14 (s, 1H), 6.97 (dd, J = 7.1, 2.2 Hz, 2H), 3.91 (s, 3H); ^{13}C NMR (150 MHz, $CDCl_3$) δ 162.3, 158.5, 157.9, 154.7, 154.6, 134.8, 129.4, 127.7, 125.7, 121.9, 113.1, 110.1, 106.1, 103.1, 101.6, 55.9;

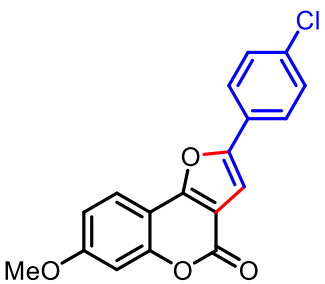

IR (KBr)ν_{max}/cm^{-1} 1750 (C=O), 1635 (C=C), 1319 (C–O); HRMS (ESI) Calcd For $C_{18}H_{12}ClO_4$ 327.0419 ($M+H^+$); Found 327.0415.

2-(4-Fluorophenyl)-7-methoxy-4*H*-furo[3,2-*c*]chromen-4-one (4fc) White solid (245.12 mg, 79%) mp 220−221 °C. ^{1}H NMR (600 MHz, $CDCl_3$) δ 7.85 (d, *J* = 8.6 Hz, 1H), 7.78 (dd, *J* = 8.6, 5.2 Hz, 2H), 7.17 (t, *J* = 8.6 Hz, 2H), 7.08 (, 1H), 6.98 (d, *J* = 7.9 Hz, 2H), 3.90 (s, 3H); ^{13}C NMR (150 MHz, $CDCl_3$) δ 164.3, 162.1, 161.8, 158.7, 157.7, 154.9, 154.5, 126.4 (J_{C-F} = 12.36 Hz), 125.6 (J_{C-F} = 5.01 Hz), 121.8, 116.3 (J_{C-F} = 33 Hz), 113.1, 110.1, 106.2, 102.3 (J_{C-F} = 2.19 Hz), 101.6, 55.9; IR (KBr)ν_{max}/cm^{-1} 1755 (C=O), 1655 (C=C), 1319 (C–O); HRMS (ESI) Calcd For $C_{18}H_{12}FO_4$ 311.0715 ($M+H^+$); Found 311.0715.

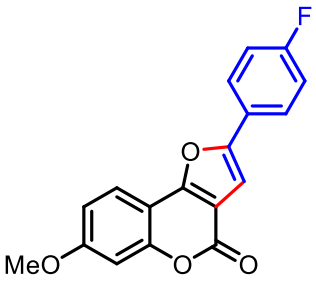

7-Methoxy-2-(*p*-tolyl)-4*H*-furo[3,2-c]chromen-4-one (4fd) White solid (260.36 mg, 85%) mp 225−226 °C. ^{1}H NMR (400 MHz, $CDCl_3$) δ 7.85 (d, *J* = 9.3 Hz, 1H), 7.69 (d, *J* = 8.2 Hz, 2H), 7.27 (d, *J* = 6.0 Hz, 2H), 7.08 (s, 1H), 6.96 (dq, *J* = 5.4, 2.4 Hz, 2H), 3.90 (s, 3H), 2.41 (s, 3H); ^{13}C NMR (100 MHz, $CDCl_3$) δ 162.0, 158.8, 157.5, 156.2, 154.5, 139.2, 129.8, 126.6, 124.5, 121.9, 113.0, 110.2, 106.4, 101.8, 101.6, 55.9, 21.5; IR (KBr)ν_{max}/cm^{-1} 1755 (C=O), 1630 (C=C), 1301 (C–O); HRMS (ESI) Calcd For $C_{19}H_{15}O_4$ 307.0965 ($M+H^+$); Found 307.0965.

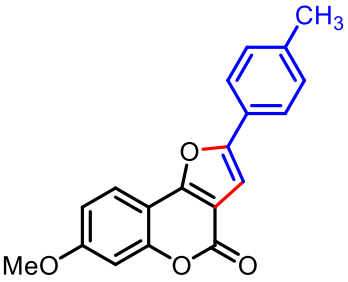

2-(*p*-Tolyl)-4*H*-furo[3,2-*c*]chromen-4-one (4ad) White solid (221.03 mg, 80%) mp 186−188 °C. ^{1}H NMR (600 MHz, $CDCl_3$) δ 7.97 (dd, *J* = 7.8, 1.3 Hz, 1H), 7.71 (d, *J* = 8.1 Hz, 2H), 7.52 (ddd, *J* = 8.7, 7.3, 1.5 Hz, 1H), 7.47 – 7.46 (m, 1H), 7.38 (dd, *J* = 15.0, 1.0 Hz, 1H), 7.29 (d, *J* = 7.9 Hz, 2H), 7.13 (s, 1H), 2.42 (s, 3H); ^{13}C NMR (150 MHz, $CDCl_3$) δ 158.5, 157.1, 156.8, 156.4, 152.7, 139.5, 130.6, 129.8, 126.4, 124.7, 120.9, 117.5, 113.0, 112.7, 102.0, 21.5; IR (KBr)ν_{max}/cm^{-1} 1749 (C=O), 1635 (C=C), 1301 (C–O); HRMS (ESI) Calcd For $C_{18}H_{13}O_3$ 277.0860 ($M+H^+$); Found 277.0836.

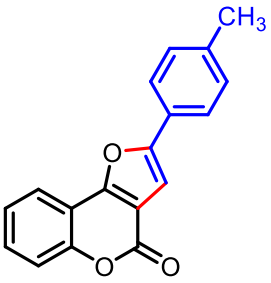

8-Fluoro-2-(*p*-tolyl)-4*H*-furo[3,2-*c*]chromen-4-one (4cd) White solid (191.28 mg, 65%) mp 185−186 °C.

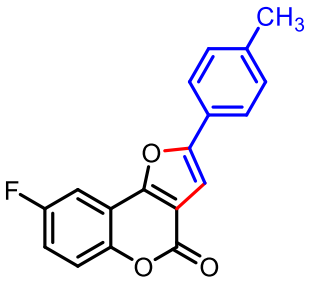

^{1}H NMR (400 MHz, $CDCl_3$) δ 7.72 – 7.70 (m, 2H), 7.63 (dd, *J* = 7.8, 2.9 Hz, 1H), 7.44 (dd, *J* = 9.1, 4.3 Hz, 1H), 7.29 (d, *J* = 8.0 Hz, 2H), 7.25 – 7.20 (m, 1H), 7.13 (s, 1H), 2.42 (s, 3H); ^{13}C NMR (100 MHz, $CDCl_3$) δ 159.2 (J_{C-F} = 228.74 Hz), 157.9, 157.7, 155.8 (J_{C-F} = 2.95 Hz), 148.7, 139.8, 129.9, 126.1, 124.8, 119.2 (J_{C-F} = 8.6 Hz), 117.9 (J_{C-F} = 24.48 Hz), 113.7 (J_{C-F} = 9.69 Hz), 113.4, 106.7 (J_{C-F} = 25.71 Hz), 102.1, 21.5; ^{19}F NMR (376 MHz, $CDCl_3$) δ -116.36; IR (KBr)ν_{max}/cm^{-1} 1750 (C=O), 1635 (C=C), 1310 (C–O); HRMS (ESI) Calcd For $C_{18}H_{12}FO_3$ 295.0765 ($M+H^+$); Found 295.0765.

8-Methyl-2-(*p*-tolyl)-4*H*-furo[3,2-*c*]chromen-4-one (4ed) White solid (162.58 mg, 56%) mp 185−186 °C.

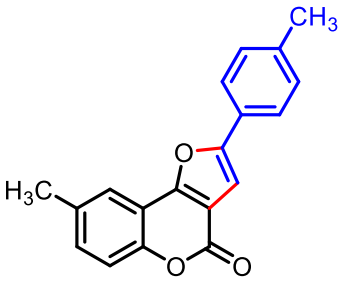

^{1}H NMR (600 MHz, $CDCl_3$) δ 7.75 (s, 1H), 7.71 (d, *J* = 8.1 Hz, 2H), 7.36– 7.33 (m, 2H), 7.28 (d, *J* = 7.9 Hz, 2H), 7.12 (s, 1H), 2.48 (s, 3H), 2.42 (s, 3H); ^{13}C NMR (150 MHz, $CDCl_3$) δ 158.7, 156.8, 156.8, 150.9, 139.4, 134.5, 131.6, 129.8, 126.4, 124.6, 120.6, 117.2, 112.6, 112.5, 102.0, 21.5, 21.1; IR (KBr)ν_{max}/cm^{-1} 1745 (C=O), 1622 (C=C), 1310 (C–O); HRMS (ESI) Calcd For $C_{19}H_{15}O_3$ 291.1016 ($M+H^+$); Found 291.1013.

2-(*m*-Tolyl)-4*H*-furo[3,2-*c*]chromen-4-one (4ae) White solid (171.30 mg, 62%) mp 168−169 °C.

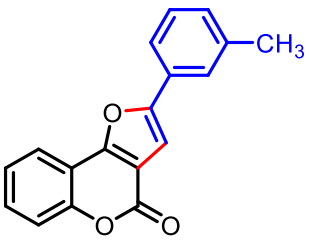

^{1}H NMR (400 MHz, $CDCl_3$) δ 7.98 (dd, *J* = 7.8, 1.5 Hz, 1H), 7.62 (d, *J* = 8.2 Hz, 2H), 7.53 (ddd, *J* = 8.6, 7.2, 1.5 Hz, 1H), 7.46 (d, *J* = 8.3 Hz, 1H), 7.41 – 7.35 (m, 2H), 7.22 (d, *J* = 7.5 Hz, 1H), 7.17 (s, 1H), 2.45 (s, 3H); ^{13}C NMR (100 MHz, $CDCl_3$) δ 158.4, 157.0, 156.9, 152.7, 138.9, 130.7, 130.1, 129.1, 129.0, 125.3, 124.7, 121.9, 120.9, 117.5, 112.9, 112.6, 102.7, 21.6; IR (KBr)ν_{max}/cm^{-1} 1740 (C=O), 1632 (C=C), 1291 (C–O); HRMS (ESI) Calcd For $C_{18}H_{13}O_3$ 277.0860 ($M+H^+$); Found 277.0832.

7-Methoxy-2-(*m*-tolyl)-4*H*-furo[3,2-*c*]chromen-4-one (4fe) White solid (248.11 mg, 81%) mp 228−230 °C.

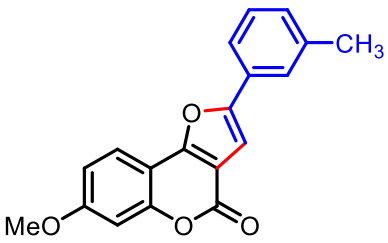

^{1}H NMR (400 MHz, $CDCl_3$) δ 7.88 (d, *J* = 9.3 Hz, 1H), 7.60 (d, *J* = 8.3 Hz, 2H), 7.36 (t, *J* = 7.6 Hz, 1H), 7.20 (d, *J* = 7.5 Hz, 1H), 7.13 (s, 1H), 6.97 (dq, *J* = 4.9, 2.4 Hz, 2H), 3.90 (s, 3H), 2.44 (s, 3H); ^{13}C NMR (100 MHz, $CDCl_3$) δ 162.1, 158.7, 157.7, 156.1, 154.5, 138.8, 129.8,

129.2, 129.0, 125.1, 121.9, 121.7, 113.0, 110.2, 106.4, 102.5, 101.6, 55.9, 21.6; IR (KBr)ν_{max}/cm^{-1} 1740 (C=O), 1630 (C=C), 1301 (C–O); HRMS (ESI) Calcd For $C_{19}H_{15}O_4$ 307.0965 ($M+H^+$); Found 307.0963.

2-(Naphthalen-2-yl)-4*H*-furo[3,2-*c*]chromen-4-one (4af) White solid (215.50 mg, 69%) mp 230−232 °C. ^{1}H NMR (400 MHz, $CDCl_3$) δ 8.32 (s, 1H), 8.05 (dd, *J* = 7.8, 1.4 Hz, 1H), 7.94 (dd, *J* = 9.1, 3.0 Hz, 2H), 7.88 – 7.84 (m, 2H), 7.57 – 7.53 (m, 3H), 7.48 (d, *J* = 7.6 Hz, 1H), 7.43 – 7.39 (m, 1H), 7.30 (s, 1H); ^{13}C NMR (100 MHz, $CDCl_3$) δ 158.4, 157.2, 156.8, 152.8, 133.5, 133.4, 130.8, 129.1, 128.5, 128.0, 127.1, 127.0, 126.3, 124.7, 123.8, 122.3, 121.0, 117.6, 112.9, 112.8, 103.3; IR (KBr)ν_{max}/cm^{-1} 1748 (C=O), 1620 (C=C), 1309 (C–O); HRMS (ESI) Calcd For $C_{21}H_{13}O_3$ 313.0860 ($M+H^+$); Found 313.0861.

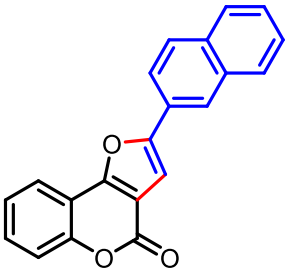

8-Fluoro-2-(4-fluorophenyl)-4*H*-furo[3,2-*c*]chromen-4-one (4cc) White solid (202.8 mg, 68%) mp 192−193 °C. ^{1}H NMR (600 MHz, $CDCl_3$) δ 7.93 (dd, *J* = 8.6, 5.2 Hz, 2H), 7.74 (dd, *J* = 7.7, 2.8 Hz, 1H), 7.57 (dd, *J* = 9.1, 4.2 Hz, 1H), 7.37 (dt, *J* = 8.9, 4.4 Hz, 1H), 7.32 (t, *J* = 8.5 Hz, 2H), 7.26 (s, 1H); ^{13}C NMR (100 MHz, $CDCl_3$) δ 163.4 ($J_{C\text{-}F}$ = 248.82 Hz), 160.3, 157.9, 157.4 ($J_{C\text{-}F}$ = 151.59 Hz), 156.1, 148.8 ($J_{C\text{-}F}$ = 2.01 Hz), 126.8 ($J_{C\text{-}F}$ = 8.34 Hz), 125.1 ($J_{C\text{-}F}$ = 3.38 Hz), 119.3 ($J_{C\text{-}F}$ = 8.66 Hz), 118.2 ($J_{C\text{-}F}$ = 24.52 Hz), 116.4 ($J_{C\text{-}F}$ = 22.05 Hz), 113.5 ($J_{C\text{-}F}$ = 9.73 Hz), 113.3, 106.8 ($J_{C\text{-}F}$ = 25.6 Hz), 102.6 ($J_{C\text{-}F}$ = 1.15 Hz); ^{19}F NMR (376 MHz, $CDCl_3$) δ -110.48, -116.11; IR (KBr)ν_{max}/cm^{-1} 1745 (C=O), 1622 (C=C), 1303 (C–O); HRMS (ESI) Calcd For $C_{21}H_{13}O_3$ 299.0515 ($M+H^+$); Found 299.0515.

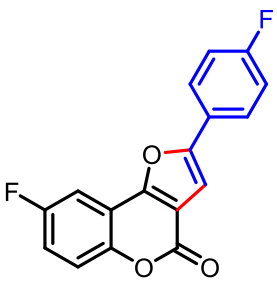

(E)-3-(4-Fluorostyryl)-4-hydroxy-2*H*-chromen-2-one (5ab) Whitish yellow solid (163.71 mg, 58%) mp 230−232 °C. ^{1}H NMR (600 MHz, DMSO-d_6) δ 8.03 (d, *J* = 7.9 Hz, 1H), 7.77 (d, *J* = 16.1 Hz, 1H), 7.65 – 7.60 (m, 3H), 7.40 – 7.35 (m, 3H), 7.21 (t, *J* = 8.7 Hz, 2H); ^{13}C NMR (150 MHz, DMSO-d_6) δ 161.6 ($J_{C\text{-}F}$ = 243.22 Hz), 161.1, 160.8, 151.8, 134.7 ($J_{C\text{-}F}$ = 3.06 Hz), 132.3, 129.8, 128.1 ($J_{C\text{-}F}$ = 8.05 Hz), 124.1, 123.7 118.6, 116.2, 116.2, 115.6 ($J_{C\text{-}F}$ = 21.3 Hz) 102.2; IR (KBr)ν_{max}/cm^{-1} 1758 (C=O), 1615 (C=C), 1312 (C–O); HRMS (ESI) Calcd For $C_{17}H_{12}FO_3$ 283.0765 ($M+H^+$); Found 283.0765.

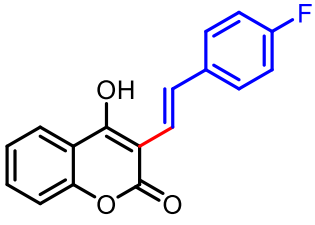

(*E*)-3-(4-Fluorostyryl)-4-hydroxy-7-methoxy-2*H*-chromen-2-one (5fb) Whitish yellow solid (171.76 mg; 55%) mp 236−238 °C. ^{1}H NMR (600 MHz, DMSO-d_6) δ 7.93 (d, J = 9.5 Hz, 1H), 7.70 (d, J = 16.0 Hz, 1H), 7.57 (dd, J = 8.6, 5.6 Hz, 2H), 7.31 (d, J = 16.1 Hz, 1H), 7.18 (t, J = 8.8 Hz, 2H), 6.96 – 6.95 (m, 2H), 3.85 (s, 3H); ^{13}C NMR (125 MHz, DMSO-d_6) δ 162.8, 161.4, 161.1, 153.7, 134.9, 128.8, 128.2, 128.0 ($J_{C\text{-}F}$ = 7.87 Hz), 125.3 ($J_{C\text{-}F}$ = 71.53 Hz), 118.7, 115.6 ($J_{C\text{-}F}$ = 21.31 Hz), 112.2, 109.2, 100.2, 100.0, 56.0; ^{19}F NMR (565 MHz, DMSO-d_6) δ -114.96. IR (KBr)ν_{max}/cm^{-1} 1748 (C=O), 1620 (C=C), 1309 (C–O); HRMS (ESI) Calcd For $C_{18}H_{14}FO_4$ 313.0871 ($M+H^+$); Found 313.0868.

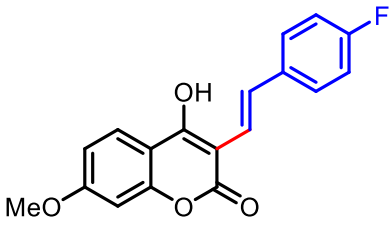

(*E*)-3-(4-Chlorostyryl)-4-hydroxy-2*H*-chromen-2-one (5ac)

Yield: 155.33 mg, 52%. white crystal; mp > 300 °C. Due to the non-solubility of the compound in any deuterated solvents, we are unable to record ^{1}H NMR.

2,10-Dichloro-17,18-bis(4-fluorophenyl)-6*H*,7*H*,14*H*,15*H*-7,15-ethano[1]benzopyrano[4',3':6,7][1,5]dioxocino[3,2-*c*][1]benzopyran-6,14-dione (6bb)

Yield: 132.59 mg, 21%. white crystal; mp > 300 °C. Due to the non-solubility of the compound in any deuterated solvents, we cannot record ^{1}H NMR.

XRD for compounds (5ab, 5ac, and 6bb): All the data for the structural analysis of compounds **5ab, 5ac, and 6bb** has been deposited to the Cambridge Crystallographic Data Centre, CCDC No. 2302762, 2304981, and 2304980.

Table 21. Crystal data and structure refinement for compound **5a**

Entry	**Identification Code**	**Compound 5a**
01	Empirical formula	$C_{34}H_{22}F_2O_6$
02	Formula weight	564.51
03	Temperature	298.00
04	Wavelength	0.71073 Å
05	Radiation type	MoKα
06	Radiation system	Fine-focus sealed tube
07	Crystal system	Triclinic
08	Space group	P-1
09	Cell length	a= 7.4841(9) /Å b= 11.7620(13) /Å c= 14.9185(17) /Å
10	Cell angle	α=87.072(3) β=85.251(3) γ=83.981(3)
11	Cell volume	1300.3(3)
12	Density	1.442
13	Completeness to theta	99
14	Absorption correction	multi-scan
15	Refinement method	Full-matrix least-squares on F2
16	Index ranges	$-8 \leq h \leq 8$, $-13 \leq k \leq 13$, $0 \leq l \leq 17$
17	Reflection number	4356
18	2Θ range	3.486 to 49.17
19	Cell formula units Z	2
20	CCDC no	2302762

Table 22. Crystal data and structure refinement for compound **5c**

Entry	Identification Code	Compound 5c
01	Empirical formula	$C_{19}H_{17}ClO_4S$
02	Formula weight	376.83
03	Temperature	294.00
04	Wavelength	0.71073
05	Radiation type	MoKα
06	Radiation system	Fine-focus sealed tube
07	Crystal system	triclinic
08	Space group	P-1
09	Cell length	a= 9.3800(14) /Å b= 9.5121(14) /Å c= 11.3170(17) /Å
10	Cell angle	α=81.866(4) β=66.266(3) γ=70.102(3)
11	Cell volume	869.1(2)
12	Density	1.440
13	Completeness to theta	99
14	Absorption correction	multi-scan
15	Refinement method	Full-matrix least-squares on F2
16	Index ranges	$-12 \leq h \leq 12$, $-12 \leq k \leq 12$, $-15 \leq l \leq 15$
17	Reflection number	23770
18	2Θ range	4.554 to 56.812
19	Cell formula units Z	2
20	CCDC no	2304981

Table 23. Crystal data and structure refinement for compound **6**

Entry	Identification Code	Compound 6
01	Empirical formula	$C_{34}H_{18}Cl_2F_2O_6$
02	Formula weight	631.38
03	Temperature	297.00
04	Wavelength	0.71073
05	Radiation type	MoKα
06	Radiation system	Fine-focus sealed tube
07	Crystal system	monoclinic
08	Space group	C2/c
09	Cell length	a= 17.444(2) /Å b= 10.1928(12) /Å c= 17.067(2) /Å
10	Cell angle	α=90 β=116.435(3) γ=90
11	Cell volume	2717.2(6)
12	Density	1.543
13	Completeness to theta	99
14	Absorption correction	multi-scan
15	Refinement method	Full-matrix least-squares on F2
16	Index ranges	$-20 \leq h \leq 20$, $-12 \leq k \leq 12$, $-20 \leq l \leq 20$
17	Reflection number	20479
18	2Θ range	4.772 to 50.136
19	Cell formula units Z	8
20	CCDC no	2304980

^{1}H NMR Spectrum of 3-Phenyl-2*H*,5*H*-pyrano[3,2-*c*]chromen-5-one (3aa)

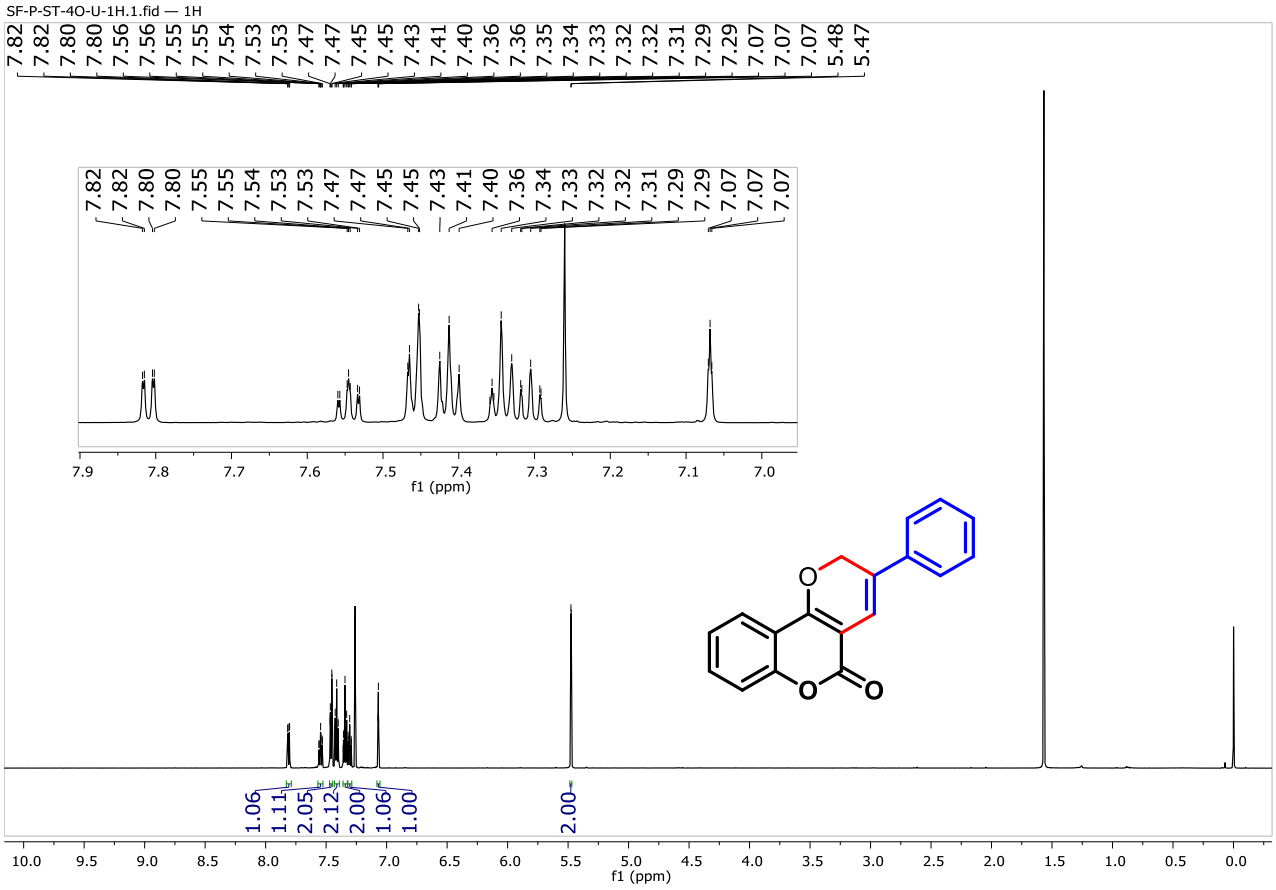

^{13}C NMR Spectrum of 3-Phenyl-2*H*,5*H*-pyrano[3,2-*c*]chromen-5-one (3aa)

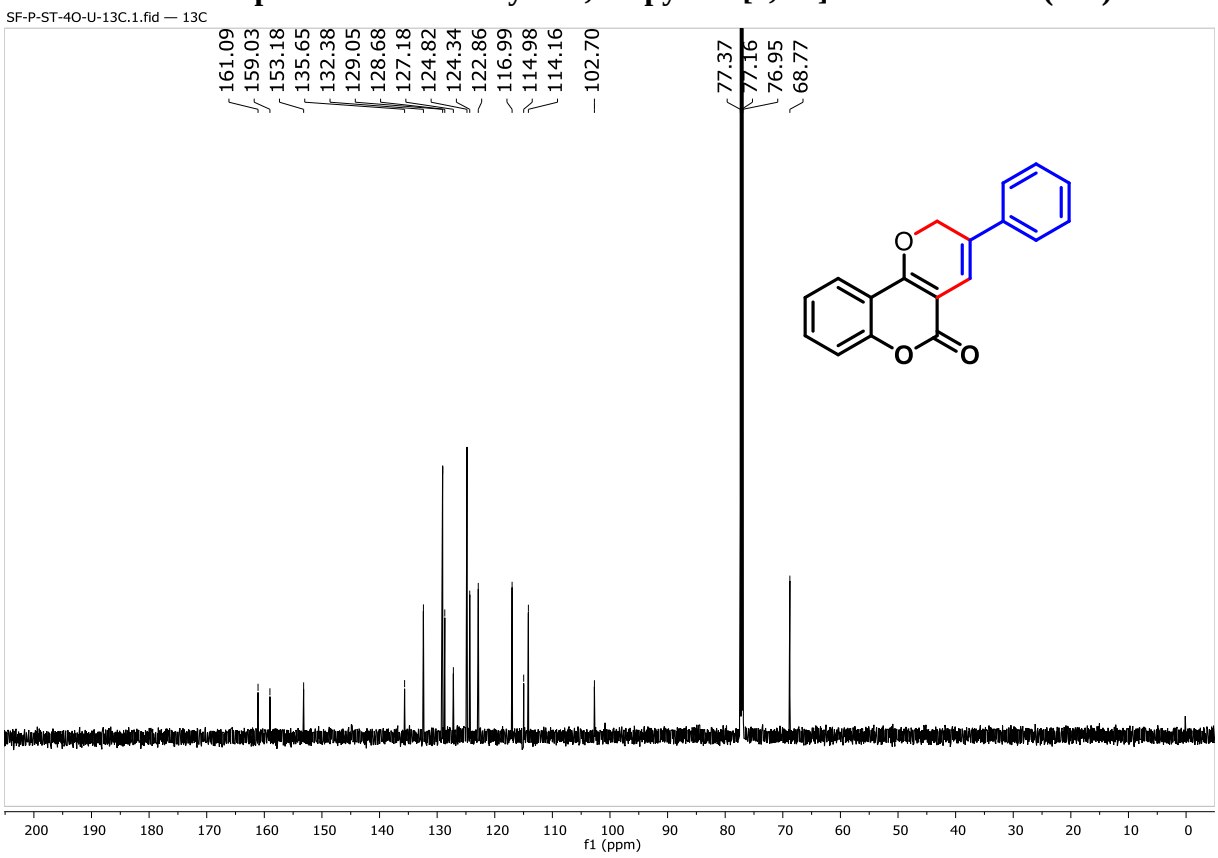

HRMS Spectrum of 3-Phenyl-2*H*,5*H*-pyrano[3,2-*c*]chromen-5-one (3aa)

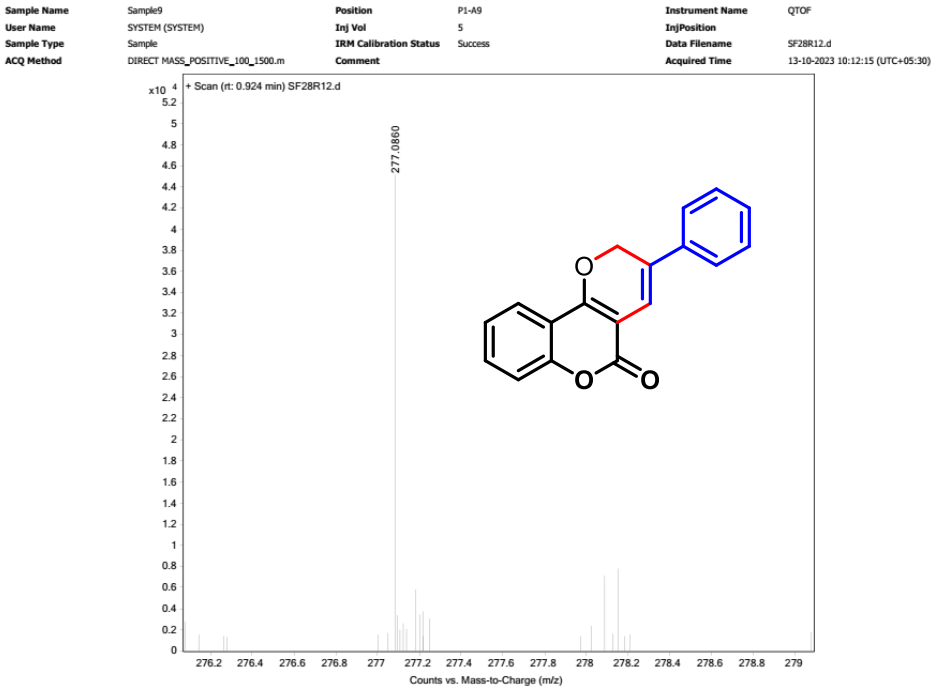

^{1}H NMR (600 MHz, $CDCl_3$) Spectrum of (*E*)-3-(4-Fluorostyryl)-4-hydroxy-7-methoxy-2*H*-chromen-2-one (5fc)

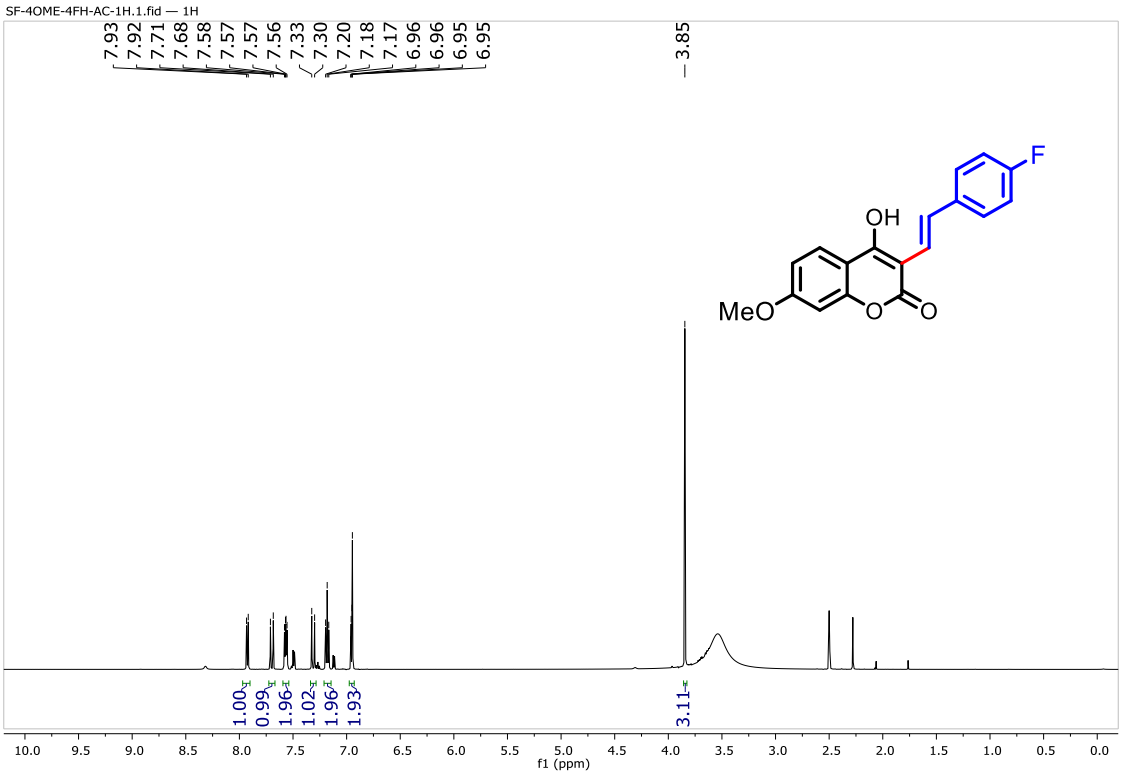

^{13}C {^{1}H} NMR (125 MHz, $CDCl_3$) NMR Spectrum of (*E*)-3-(4-Fluorostyryl)-4-hydroxy-7-methoxy-2*H*-chromen-2-one (5fc)

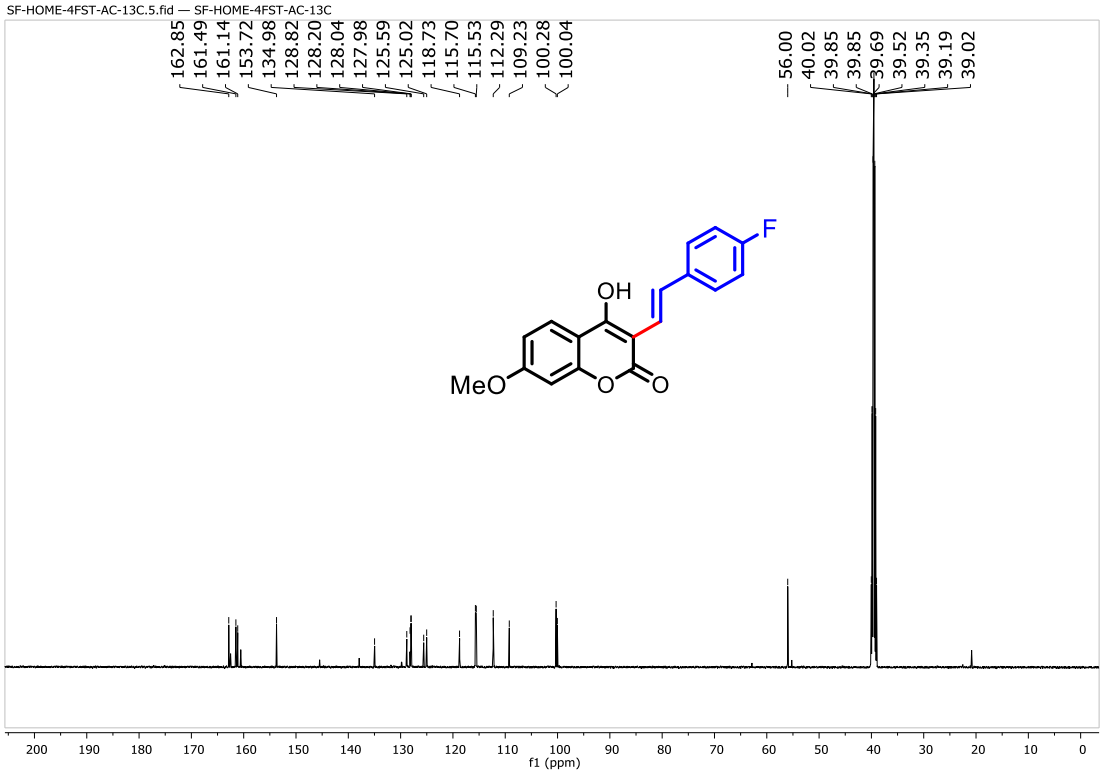

^{19}F\{^{1}H, ^{13}C\} NMR (565 MHz, $CDCl_3$)Spectrum of (*E*)-3-(4-Fluorostyryl)-4-hydroxy-7-methoxy-2*H*-chromen-2-one (5fc)

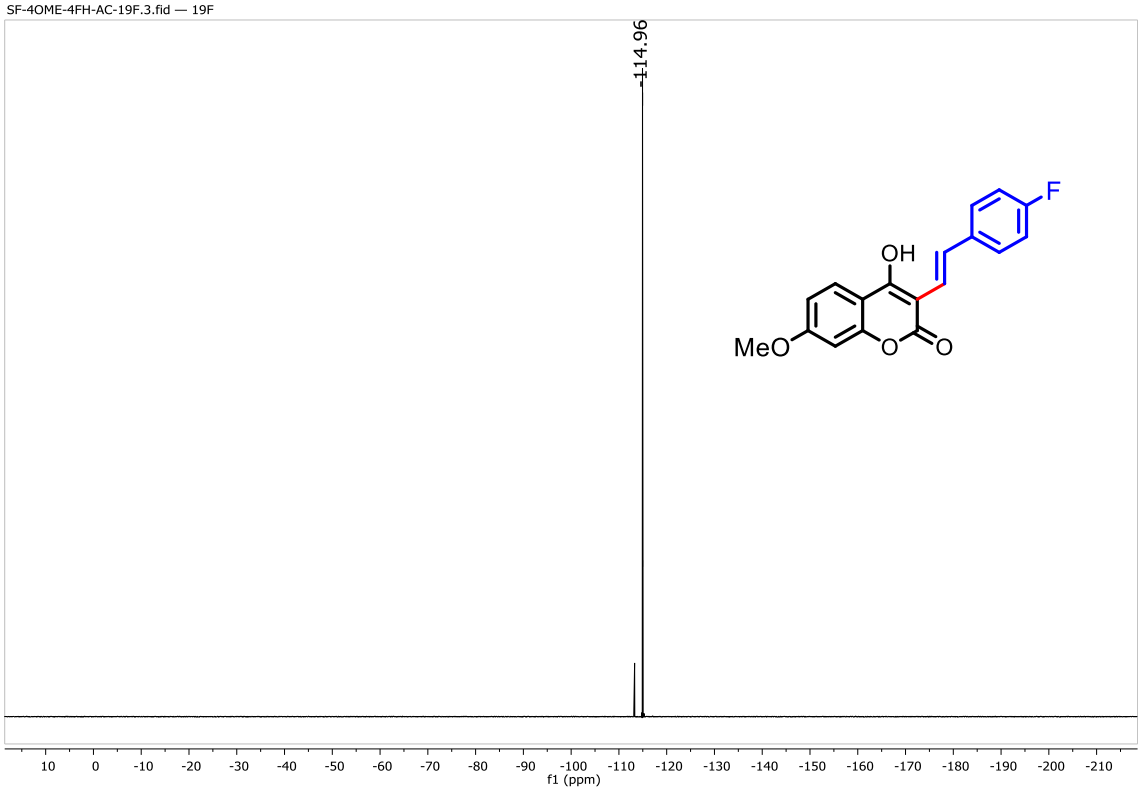

HRMS Spectrum of (*E*)-3-(4-Fluorostyryl)-4-hydroxy-7-methoxy-2*H*-chromen-2-one (5fc)

Sample Name	Sample9	**Position**	P1-A8	**Instrument Name**	QTOF
User Name	SYSTEM (SYSTEM)	**Inj Vol**	5	**InjPosition**	
Sample Type	Sample	**IRM Calibration Status**	Success	**Data Filename**	SF-201-RF-32.d
ACQ Method	DIRECT MASS_POSITIVE_100_1500.m	**Comment**		**Acquired Time**	06-11-2023 09:57:19 (UTC+05:30)

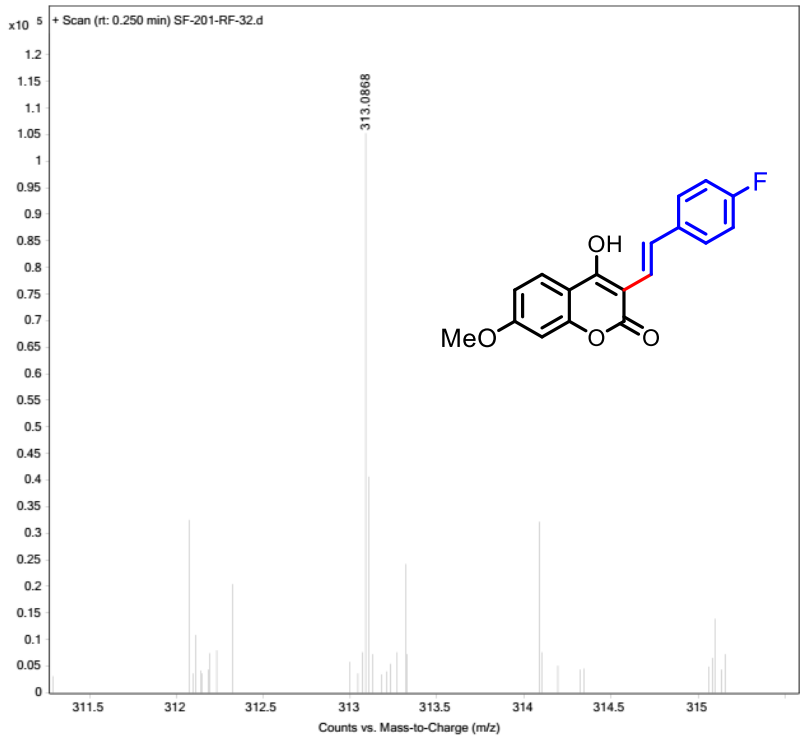

References:

1. M. M. Melough, E. Cho and O. K. Chun, *Food Chem. Toxicol.*, 2018, **113**, 99–107; (b) M. M. Melough, S. G. Lee, E. Cho, K. Kim, A. A. Provatas, C. Perkins, M. K. Park, A. Qureshi and O. K. Chun, *J. Agric. Food Chem.*, 2017, **65**, 5049–5055.
2. (a) E. J. Lee, M. C. Song, and C.-S. Rha, *Front Plant Sci*, 2022, **13**, 923163; (b) E. M. Bickoff, A. N. Booth, R. L. Lyman, A. L. Livingston, C. R. Thompson and F. DeEds, *Science*, 1957, **126**, 969–970.
3. (a) R. O'Kennedy and R. Zhorenes, Coumarins: Biology, Applications, Mode of Action, Wiley, Chichester, 1997; (b) Y. Tu, Y. Yang, Y. Li and C. He, *Pharmacol. Res.*, 2021, **169**, 105615.
4. (a) Z.-I. Rhew and Y. Han, *Arch. Pharm. Res.*, 2016, **39**, 1482–1489; (b) J. Sumorek-Wiadro, A. Zając, A. Maciejczyk and J. Jakubowicz-Gil, *Fitoterapia*, 2020, **142**, 104492; (c) U. Shahab, M. Faisal, A. A. Alatar and S. Ahmad, *IUBMB Life*, 2018, **70**, 547–552; (d) G. Montero, F. Arriagada, G. Günther, S. Bollo, F. Mura, E. Berríos and J. Morales, *Int. J. Pharm.*, 2019, **562**, 86–95; (e) S.-N. Kim, S.-Y. Ahn, H.-D. Song, H.-J. Kwon, A. Saha, Y. Son, Y. K. Cho, Y.-S. Jung, H. W. Jeong and Y.-H. Lee, *J. Nutr. Biochem.*, 2020, **76**, 108300; (f) H. Y. Song, A. Jo, J. Shin, E. H. Lim, Y. E. Lee, D. E. Jeong and M. Lee, *Molecules*, 2019, **24**, 4088; (g) G. Murphy and H. Nagase, *Nat. Clin. Pract. Rheumatol.*, 2008, **4**, 128–135; (h) E. M. Bickoff, A. L. Livingston and A. N. Booth, *Arch. Biochem. Biophys.*, 1960, **88**, 262–266; (i) W.-L. Hung, J. H. Suh and Y. Wang, *J. Food Drug Anal.*, **25**, 71–83; (j) E. S. Andina, A. A. Kyagova, N. N. Yurikova, M. B. Neklyukova, A. Ya. Potapenko, W. Adam and C. R. Saha-Möller, in *Biologic Effects of Light 1998: Proceedings of a Symposium Basel, Switzerland November 1–3, 1998*, eds. M. F. Holick and E. G. Jung, Springer US, Boston, MA, 1999, pp. 213–216.
5. V. Di Noto, L. D. Via, O. Gia, A. M. Onori, L. Cellai and S. M. Magno, *J. Phys. Chem. B*, 2000, **104**, 4992–4999.
6. T. Nehybova, J. Smarda and P. Benes, *Anticancer Agents Med. Chem.*, 2014, **14**, 1351–1362.
7. K. P. Beena and G. S. Pooja, *Chem. Asian J.*, 2022, **15**, 176–181.
8. (a) A. M. Rayar, N. Lagarde, F. Martin, F. Blanchard, B. Liagre, C. Ferroud, J.-F. Zagury, M. Montes and M. Sylla-Iyarreta Veitía, *Eur. J. Med. Chem.*, 2018, **146**, 577–587; (b) Y. Jacquot, B. Refouvelet, L. Bermont, G. L. Adessi, G. Leclercq and

A. Xicluna, *Pharmazie*, 2002, **57**, 233–237; (c) L. Li, J. Li, M. Khanna, I. Jo, J. P. Baird and S. O. Meroueh, *ACS Med Chem. Lett.*, 2010, **1**, 229–233; (d) P. Magiatis, E. Melliou, A.-L. Skaltsounis, S. Mitaku, S. Léonce, P. Renard, A. Pierré and G. Atassi, *J. Nat. Prod.*, 1998, **61**, 982–986; (e) T. Smyth, V. N. Ramachandran and W. F. Smyth, *Int. J. Antimicrob. Agents*, 2009, **33**, 421–426; (f) S. J. Min, H. Lee, M.-S. Shin and J. W. Lee, *Int. J. Mol. Sci.*, 2023, **24**, 10026.

9. A. H. F. Abdelwahab and S. A. H. Fekry, *Eur. J. Chem.*, 2021, **12**, 340–359.
10. N. W. Mazlan, C. Clements and R. Edrada-Ebel, *Marine Drugs*, 2020, **18**, 661.
11. S. Ali, K. Kaur and J. Agarwal, *J. Mol. Liq.*, 2023, **374**, 121256.
12. J. Jamalis, F. S. M. Yusof, S. Chander, R. Abd. Wahab, D. P. Bhagwat, M. Sankaranarayanan, F. Almalki and T. Ben Hadda, *Antiinflamm Antiallergy Agents Med. Chem.*, 2020, **19**, 222–239.
13. Y. Zou, M. Lobera and B. B. Snider, *J. Org. Chem.*, 2005, **70**, 1761–1770.
14. S. Borthakur, P. P. Kaishap and S. Gogoi, *Asian J. Org. Chem.*, 2018, **7**, 918–921.
15. J. Kim, K. Lee and P. H. Lee, *Bull. Korean Chem. Soc.*, 2020, **41**, 709–718.
16. V. V. Pelipko, R. I. Baichurin, K. A. Lyssenko, V. V. Dotsenko and S. V. Makarenko, *Mendeleev Commun.*, 2022, **32**, 454–456.
17. G. Cheng and Y. Hu, *Chem. Commun.*, 2007, 3285–3287.
18. L. Chen, Y. Li and M.-H. Xu, *Org. Biomol. Chem.*, 2010, **8**, 3073–3077.
19. D. Zha, H. Li, S. Li and L. Wang, *Adv. Synth. Catal.*, 2017, 359, 467–475.
20. A. Dey and A. Hajra, *Org. Biomol. Chem.*, 2017, 15, 8084–8090.
21. X. Chang, P. Zeng and Z. Chen, *Eur. J. Org. Chem.*, 2019, 6478–6485.
22. A. Jana, D. Ali, P. Bhaumick and L. H. Choudhury, *J. Org. Chem.*, 2022, 87, 7763–7777.
23. Y. R. Lee, J. Y. Suk and B. S. Kim, *Org. Lett.*, 2000, **2**, 1387–1389.
24. R. Zhang, Z. Xu, W. Yin, P. Liu and W. Zhang, *Synth. Commun.*, 2014, **44**, 3257–3263.
25. Q. T. Pham, P. Q. Le, H. V. Dang, H. Q. Ha, H. T. D. Nguyen, T. Truong and T. M. Le, *RSC Adv.*, 2020, **10**, 44332–44338.
26. (a) A. R. Kapdi, A. Karbelkar, M. Naik, S. Pednekar, C. Fischer, C. Schulzkec and M. Tromp, *RSC Adv.*, 2013, **3**, 20905; (b) M.-T. Nolan, L. M. Pardo, A. M. Prendergast and G. P. McGlacken, *J. Org. Chem.*, 2015, **80**, 10904; (c) L. Tang, Y. Pang, Q. Yan, L. Shi, J. Huang, Y. Du and K. Zhao, *J. Org. Chem.*, 2011, **76**, 2744; (d) C. Cheng, W.-W. Chen, B. Xu and M.-H. Xu, *Org. Chem. Front.*, 2016, **3**, 1111–

1115; (e) J. Sheng, T. Xu, E. Zhang, X. Zhang, W. Wei and Y. Zou, *J. Nat. Prod.*, 2016, **79**, 2749–2753; (f) N. Takeda, O. Miyata and T. Naito, *Eur. J. Org. Chem.*, 2007, 1491–1509; (g) A. Fürstner, E. K. Heilmann and P. W. Davies, *Angew. Chem. Int. Ed.*, 2007, **46**, 4760–4763; (h) J. Liu, Y. Liu, W. Du, Y. Dong, J. Liu and M. Wang, *J. Org. Chem.*, 2013, **78**, 7293–7297.

27. M. Hori, J.-D. Guo, T. Yanagi, K. Nogi, T. Sasamori and H. Yorimitsu, *Angew. Chem. Int. Ed. Engl.*, 2018, **57**, 4663–4667.
28. K. Nakanishi, D. Fukatsu, K. Takaishi, T. Tsuji, K. Uenaka, K. Kuramochi, T. Kawabata and K. Tsubaki, *J. Am. Chem. Soc.*, 2014, **136**, 7101–7109.
29. P. Biswas, J. Ghosh, T. Sarkar, S. Maiti and C. Bandyopadhyaya, *J. Chem. Res.*, 2012, **36**, 623–625.
30. M. Maiti, J. Ghosh, T. Tapas Sarkar, C. Bandyopadhyay, *J. Indian Chem. Soc*. 2013, **90**, 1497–1499.
31. K. C. Majumdar, A. T. Khan, and R. N. De, *Synth. Commun.*, 1988, **18**, 1589–1595.
32. G. Cravotto, G. M. Nano, S. Tagliapietra, *Synthesis*, 2001, **1**, 49-51.
33. D. D. Diaz, P. O. Miranda, J. I. Padron and V. S. Martin, *Curr. Org. Chem.*, **10**, 457–476.
34. M. Tajbakhsh, M. Heidary, R. Hosseinzadeh and M. A. Amiri, *Tetrahedron Lett.*, 2016, **57**, 141–145.
35. S. Yashmin, R. Ali, S. Mondal and A. T. Khan, *Chem. Commun.*, 2022, **58**, 5853–5856.

Appendix

- Thesis Conclusion
- Future Perspectives
- List of Publications

THESIS CONCLUSION

During my Ph. D. tenure, the research works were mainly focused on the synthesis of substituted quinoline such as 4-arylquinolines, 2,3-dialkylquinolines, 2,4-diarylquinolines, 2-benzyl-3-phenylquinolines using aryl amine as the key starting material hydrated *p*-toluene sulphonic acid as a catalyst. In addition, the synthesis of 2-aryl furocoumarins, tetrahydro coumestan, coumestan, dinaphthofurans, polyfunctional furocoumarins, and pyranocoumarins were achieved utilizing 4-hydroxycoumarin as the key starting material. The summarized results are shown below schematically.

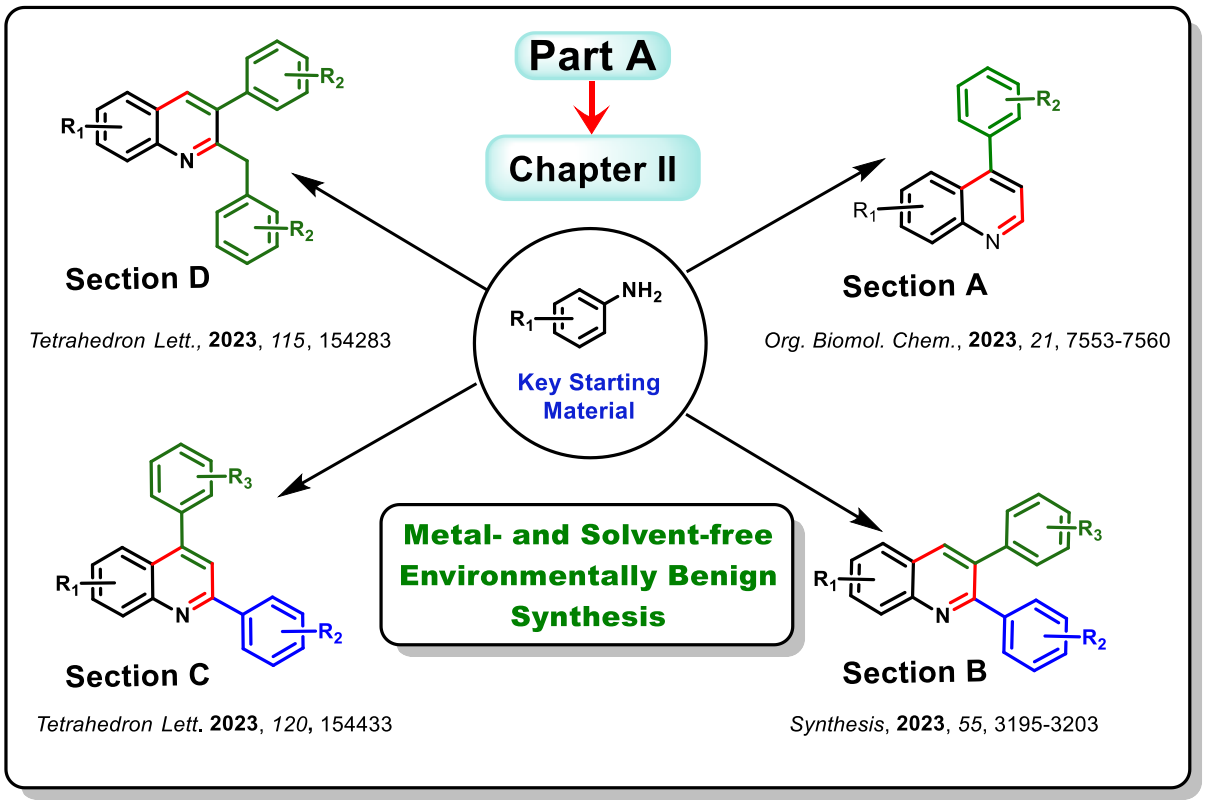

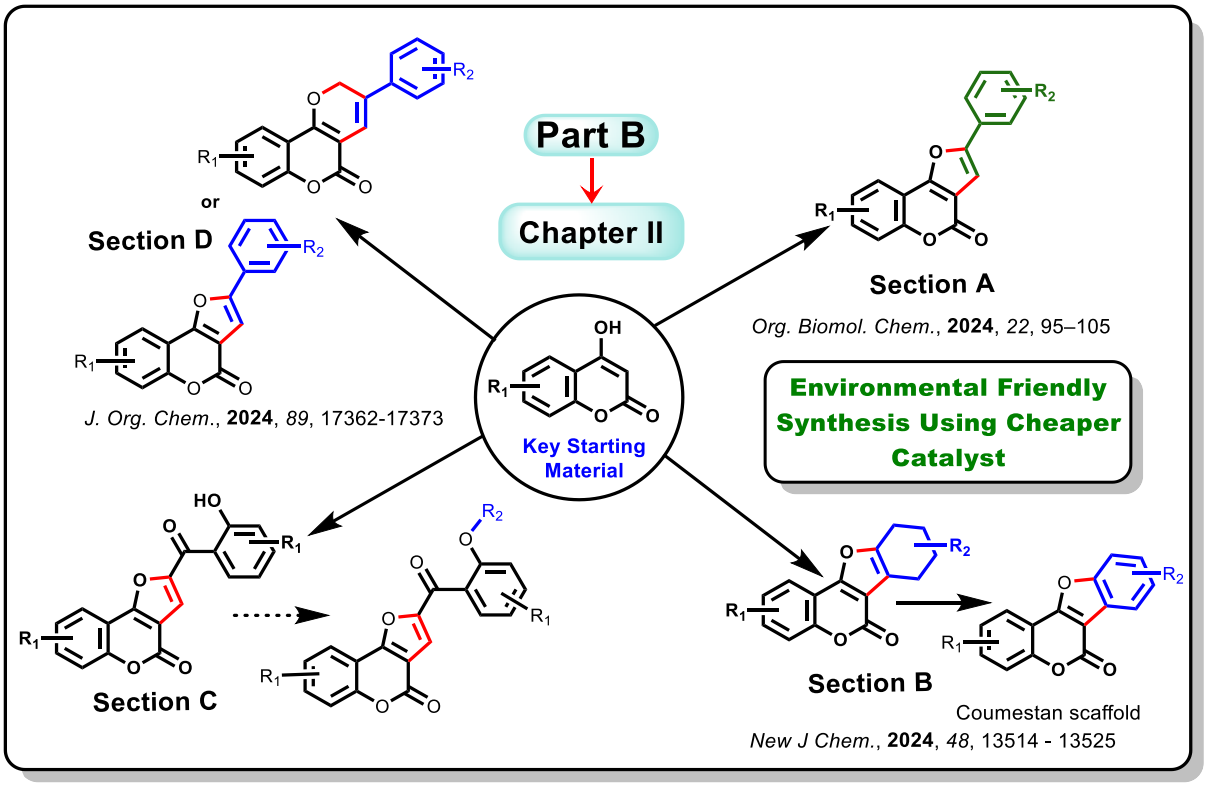

FUTURE PERSPECTIVES

New synthetic methodologies will be developed to accomplish new chemical entities of biological importance using hydrated *p*-toluene sulfonic acid and ferric(III) chloride as catalysts. Moreover, the key starting materials, aryl amines and 4-hydroxycoumarins, will be explored to synthesize new molecules, and their biological study will be carried out. The future perspectives are shown in a schematic manner below.

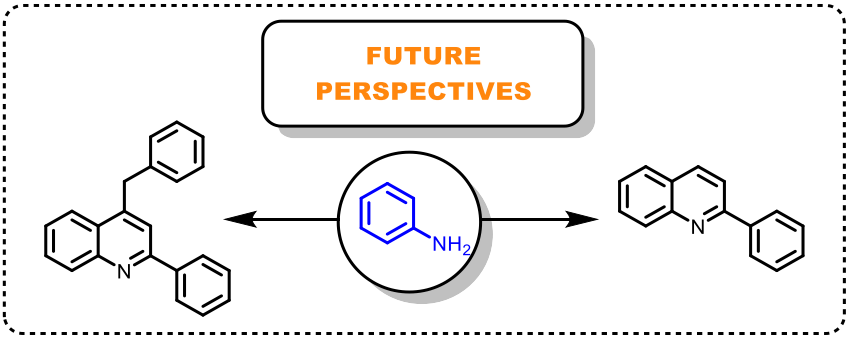

Figure 3a. The schematic diagram for future perspective.

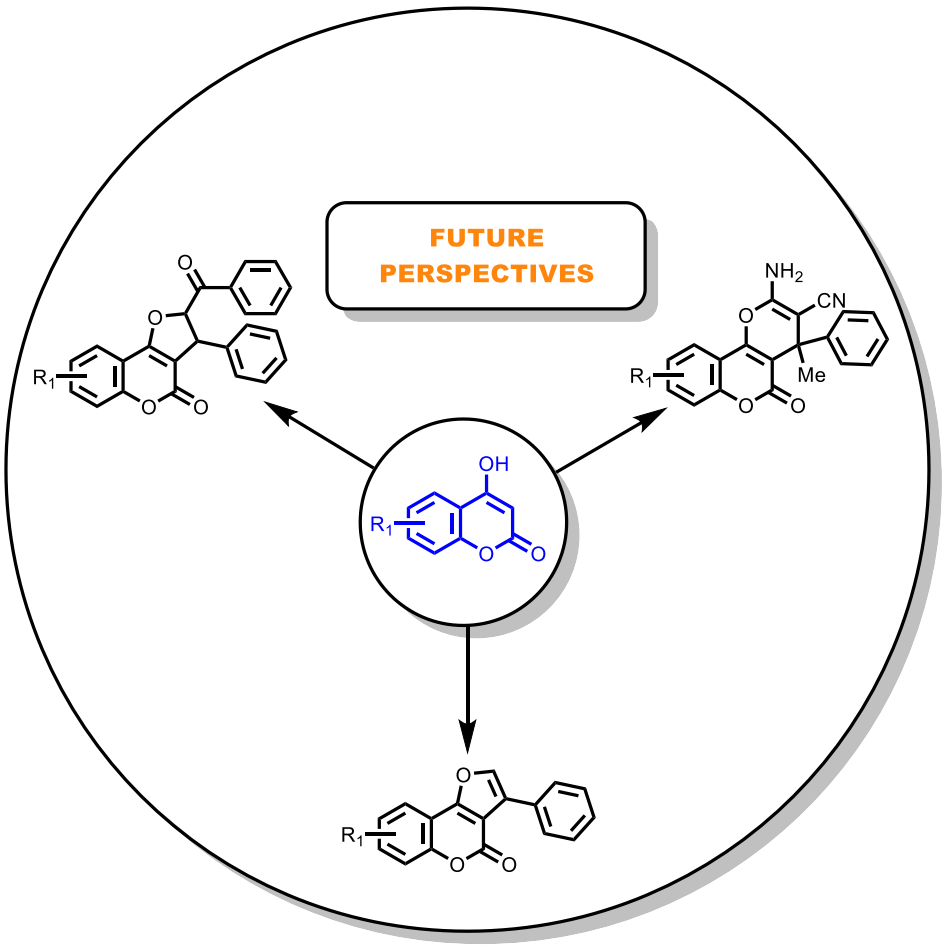

Figure 3b. The schematic diagram for future perspective.

LIST OF PUBLICATIONS FROM THE THESIS WORK

1. **S. Faraz** and A. T. Khan, *p*-TSA·H_2O catalyzed metal-free and environmentally benign synthesis of 4-aryl quinolines from arylamine, acetylene, and dimethyl sulfoxide. *Org. Biomol. Chem.*, **2023**, *21*, 7553-7560.
2. **S. Faraz** and A. T. Khan, *p*-TSA·H_2O catalyzed synthesis of 2,3-diarylquinoline derivatives via one-pot-three-component reaction. *Synthesis*, **2023**, *55*, 3195-3203.
3. **S. Faraz,** S. Yashmin, M. D. Marathe, and A. T. Khan, Environmentally benign synthesis of 2,4-diarylquinolines under metal- & solvent-free conditions. *Tetrahedron Lett*. **2023**, *120*, 154433.
4. **S. Faraz**, M. Kumar, A. T. Khan, S. Ponneganti, R. P., Metal- and solvent-free synthesis of 2-benzyl-3-arylquinoline using a pseudo-three-component reaction. *Tetrahedron Lett.*, **2023**, *115*, 154283.
5. **S. Faraz,** A. Ali and A. T. Khan, $FeCl_3$ catalyzed regioselective ring-opening of aryl oxirane with 4-hydroxycoumarin for the synthesis of furo[3,2-*c*]coumarins. *Org. Biomol. Chem.*, **2024**, *22*, 95–105.
6. **S. Faraz** and A. T. Khan, A short and elegant synthetic approach for 9-substituted tetrahydro coumestan derivatives and synthesis of some naturally occurring coumestan derivatives. *New J. Chem.*, **2024**, *48*, 13514–13525.
7. **S. Faraz**, K. Mehta, P. V Bharatam, and A. T. Khan, A three-component new synthetic approach for the synthesis of pyranocoumarin: Modulation of this approach as a function of substituent effect forms the furocoumarin and 4-hydroxy-3-styryl coumarin as a function of solvent effect. *J. Org. Chem.*, **2024**, *89*, 17362-17373.
8. **S. Faraz** and A. T. Khan, One-pot synthesis of dinaphthofuran and furo[3,2-*c*] coumarin derivatives catalyzed by hydrated ferric chloride. *(Manuscript under revision)*

RESEARCH PAPERS THAT ARE NOT INCLUDED IN THE THESIS

1. A. Ali, **S. Faraz**, and A. T. Khan, L-Proline-catalysed synthesis of 2-2ryl-2*H*,5*H*-thiopyrano[2,3-*b*] thiochromen-5-ones from 4-hydroxydithiocoumarins and cinnamaldehyde derivatives. *Org. Biomol. Chem.* **2024**, *22*, 1426–1433.

2. **S. Faraz**, H. Khatun, S Dutta, and A. T. Khan, *p*-TSA•H_2O–Catalyzed synthesis of novel functionalized dihydro furocoumarins via a pseudo-three-component reaction. *Org. Biomol. Chem.* **2025**, *00*, 0000–0000. *(Manuscript under revision)*
3. **S. Faraz** and A. T. Khan, Novel synthesis of pyranocoumarins under metal- and solvent-free conditions. *Org. Biomol. Chem.* **2025**, *00*, 0000–0000. *(Manuscript under preparation)*
